Brain immune response as therapeutic target in the treatment of Parkinson's disease

Neus Rabaneda Lombarte

Doctoral thesis

BRAIN IMMUNE RESPONSE AS THERAPEUTIC TARGET IN THE TREATMENT OF PARKINSON'S DISEASE

Neus Rabaneda Lombarte

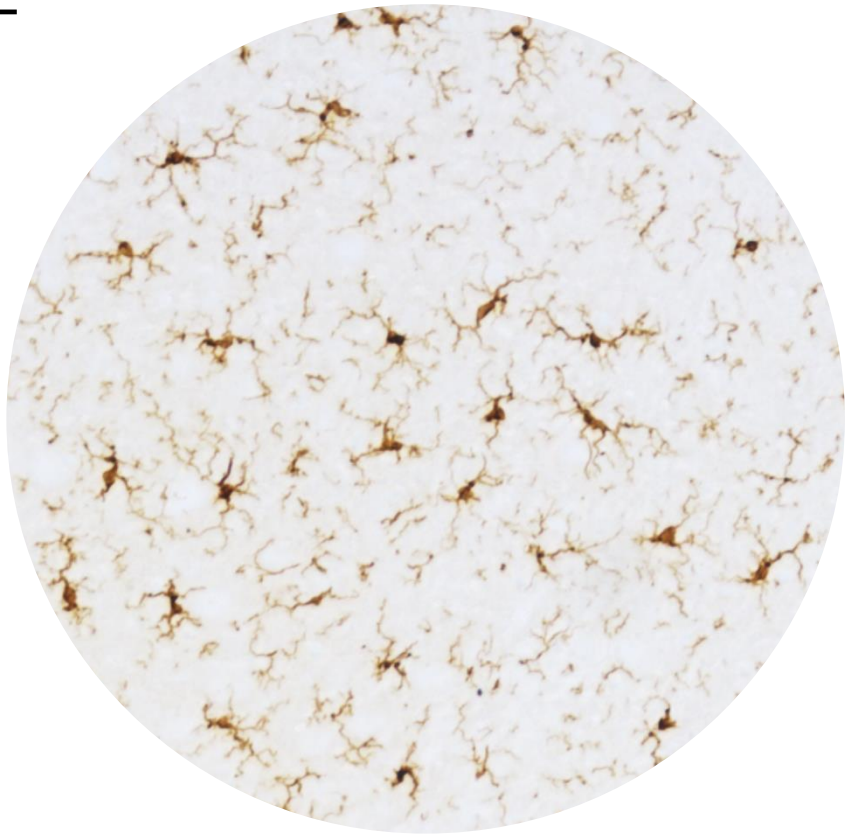

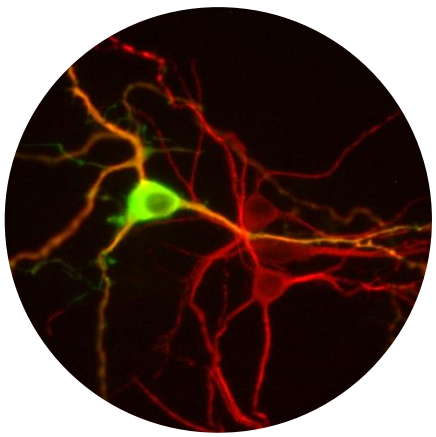

Universitat de Barcelona
2019

fusioDoctoral program in Biomedicine
Universitat de Barcelona

Brain immune response as therapeutic target in the treatment of Parkinson's disease

Thesis presented by

Neus Rabaneda Lombarte

To obtain the degree of

Doctor of Philosophy (PhD) in Biomedicine
by Universitat de Barcelona


This PhD thesis was performed at the
Department of Brain Ischemia and Neurodegeneration, Institut d'Investigacions Biomèdiques de Barcelona (IIBB - CSIC) and the
Department of Biomedical Science, Facultat de Medicina, Universitat de Barcelona.
Institut d'Investigacions Biomèdiques August Pi i Sunyer (IDIBAPS)

PhD candidate,
Neus Rabaneda Lombarte

Director,
Dr. Carme Solà Subirana

Director,
Dr. Josep Saura Martí

Tutor,
Dr. Josep Saura Martí

Barcelona, 2019

Als meus pares,

Acknowledgments

Abans de res voldria expressar la meva gratitud a totes les persones que han format part d'aquest camí, abans de res que és després de tot, perquè després de tot te n'adones que no ets tu, que ets tu amb els altres i sense els altres tu no ets i aquesta tesi no seria.

Carme i Jou, directors excel·lents i millors persones. Veu embarcar-vos en aquesta, diria jo, boja aventura que com que no sabíem que era impossible ho hem aconseguit. **Carme**, gràcies per la infinita paciència, per saber lidiar amb els meus emails interminables y converses caòtiques, per tenir-ho tot tan controlat i ben classificat, que la teva taula a priori és un desastre però tu saps exactament on ho tens tot i es que busques un article del 1900 i t'aixeques directe al carpesano que toca, i m'al·lucina, admiro el teu perfeccionisme i la teva ciència més que exacte, gràcies per les converses científiques fins les nou de la nit, per discutir cada detall, cada inquietud o dubte que em quedava les vegades que fes falta, per deixar esplaiar-me i sobretot per ser TAN bona persona, i tenir el do de fer sentir a qualsevol tan bé que a vegades penso que tan de bo se m'hagi encomanat la teva manera de ser. **Jou**, les meves sinceres gràcies per fer-ho tan fàcil, per aplanar el camí, pel teu input científic sempre encertat, el teu esperit crític i docent tan característic i per tenir sempre, sempre la porta oberta. No ha sigut fàcil, però sense la teva implicació no hagués pogut ser possible. Gràcies per coincidir en aquell màster i obrir-me la porta a un món, que en aquell moment ni intuïa què significaria per mi. **Joan**, gràcies per ser tan bona persona, disposat sempre a ajudar, per explicar-ho tot tan bé, pel teu suport, els teus savis consells, per tenir paciència quan a vegades sóc massa impacient i tinc tan que aprendre. Per cert... acabo de recordar que no sé si queden algunes cèl·lules per contar... com vaig riure! **Jose**, per tot el que m'has ensenyat sobre genètica, per oferir la teva ajuda en tot i per parlar tan! **Tony**, el post-doc que m'ho va ensenyar tot durant els primers anys, gràcies per assentar les bases per poder començar a ser independent al laboratori, per copiar-me el dia de cumple i fer-ne 42 quan jo en feia 24. **Marta**, gràcies per ser la meva referent, que després de tu anava jo i havia d'estar a l'alçada.

A tots els meus estudiants, que han pintat etapes de colors vius. **Lídia**, gràcies per compartir la incertesa del principi, el fet de no saber ben bé què fèiem al laboratori i ni tan sols amb les nostres vides. **Efren**, el meu primer estudiant, perquè el primer mai s'oblida, pels "lo limitant són les columnes", per pensar-te que ets el "preferit" de la Carme, pels canvis de medi, pels comptatges infinits del Hoechst després de dinar, pels teus consells científics i els altres, per compartir més que la poyata i per cada llàgrima que m'ha caigut dels ulls rient al teu costat. **Lucas**, gracias por dejarme ser tu jefa superiora preferida, por revolucionarme el laboratorio como si fuera primavera todo el año, por llevarte con todos, por hacerme creer que trabajaba con Van Gogh, por luchar

por dedicarte a la neurociencia molecular aún y haber estudiado psicología, porque eres un científico que además es psicólogo. **Andrés**, por tus “ups”, por tus camisas con guitarras y el color burdeos, tu no sé qué que nos hace reír tanto, tu inocencia y tus dudas, nuestras conversaciones de metabolismo y qPCRs interminables, por aguantar mis “¿Andrés? ¿Qué haces? Venga, venga!”. **Laura**, gràcies per compartir la última fase d’aquest viatge, per quedar-te, perquè des de que estàs tots els imprevistos passen divendres a les set de la tarda, per riure’t quan faig mil coses al lab a la vegada, per despedir-te al migdia perquè saps que no sortiré fins les nou parlant amb la Carme.

Al **Miquel Vila**, gràcies per donar-me la oportunitat de col·laborar amb el vostre grup i aprendre tan, per ser tan amables i confiar en mi. **Annabel**, por enseñarme las immunos, ese trabajo chino que sólo tú sabes hacer tan bien, por ser tan amigable y por tu acento tan gracioso. **Thais**, per totes les injeccions i les hores al quarto de dissecció, **Celine**, por enseñarme a diseccionar y por tu interès. **Albert i Sandra**, gràcies per compartir penes i glories del doctorat, i a tots els membres de l’equip, per deixar que us ocupés el microscopi fins i tot els caps de setmana o quan tothom marxava, als **Jordis**, les **Ariadnes**, la **Bea**, la **Iria**, la **Marta**, a tots, per rebrem sempre amb un somriure i perquè ha sigut com si formés part de vosaltres.

Rita, gracias por París, por acogerme con los brazos abiertos y tu pasión por la ciencia, **Sabah,** qu'est-ce que j'aurais fait sans toi? you got involved in my project as it was yours, we went together to the lab even in bank holiday, thank you for all I learnt from you and pour nos aventures avec l‘α-synuclein! **Jérémy**, because you may be the only french being able to suddenly sing “Els Segadors” while I’m reading a plate in the spectrophotometer, pour les cookies et pour le maudite CellRox!, Ah! et je pense I forgot to buy quelques souvenir avec la Tour Effiel! **Luciana**, gracias por crear “tan buena onda” en el lab y tu generosidad. **Etienne,** thank you for let me be part of your team, **Patrick** and **Stéphane**, thank you for your scientific conversations, and thank you to **Julia, David, Cansu, Dominique, Jaime, Déborah, Jérémie** and all the people at ICM that made me feel like home.

A tothom de l’IIBB, UB, Hospital Clínic i IDIBAPS que d’alguna manera o altra han col·laborat en el camí d’aquesta tesi. **Ana Cámara**, gràcies per totes les extraccions de sang pels cultius de microglia-like, **Valerie**, gracias por compartir dudas científicas y también por todas las esperas a la hora de comer con Carme! **Paqui**, gracias por enseñarme el genotipaje, **Anaïs**, **Carla**, **Gerard** i **Clara**, per coordinar els cultius de microglia-like. **Elisa**, por compartir las peripecias con las nanopartículas y por ser tan fan de Jou como yo, **Júlia**, per ser tan divertida parlant de ciència, **Annita**, que hem compartit uni i lab, la paciència personificada amb les meves preguntes i guia del camí i salvavides en els moments d’histèria, **Vicente**, porque nunca me he reído tanto con un tapÓN, **Cristina**, por tus chistes malos, **Blanca**, per les nostres “charles” i compartir laboratori, **Clara**, perquè quan estaves no podia parar de riure, **Aynara**, por las fiestas, **Estefanía**, por enseñarme que reírse de uno mismo puede ser aún más divertido y gracias por tu trato fácil y tu

alegría. **Edu i Rafa**, gràcies per totes les vostres solucions informàtiques i ser els informàtics més enrotllats. També donar les gràcies a l'**Anna Planas, Coral, Lupe, Pablo, Artigues** i a tots els membres dels vostres grups, per estar tan a prop i ser propers a la vegada… gràcies a tots els companys de l'IIBB, també a tots els membres del Departament de Biomedicina de la UB i a tot el personal de l'Estabulari, en especial a en **Pep Marimón**, per les teves recomanacions de veterinari amb la colònia.

A les de la uni: **Marta, Annita, Míriam i Marta**, pel suport i els ànims, per entendre un "no puc quedar", pels estius a Begur i per aguantar-me ja fa més de 10 anys. **Míriam**, la meva crossa indispensable, per tenir sempre totes les respostes, gràcies per saber-ho tot i estar-hi sempre i salvar-me en els moments de crisi, que n'han sigut molts. A les psicòlogues: **Júlia, Anna, Laura** i **Olga**, per compartir experiències de doctorat i **Anna**, per haver enfrontat el mateix repte que jo amb Medicina. Recordo la frase que em veu regalar: "*Ama lo que haces, haz lo que amas*". To **Jony**, thank you for all your scientific and english comments. A la **Paula**, porque des de l'insti nos vamos siguiendo. A l'**Alba**, per aporta la dosi d'aventura a la tesi. A l'**Annabel**, la **Clara** i el **Pol,** per ser els millors companys de classe de Medicina i informar-me de tot quan jo no hi podia ser.

Xavi, gràcies per compartir el mateix input per créixer, perquè menjar-nos el món se'ns queda petit, per admirar-me, per fer-me sentir que el que faig té un gran valor, per entendre totes les vegades que no ens hem pogut veure, per esperar i esperar, perquè tot i així aquí estem, perquè junts volem més alt i per ser... la meva millor casualitat.

Gràcies a tota la meva família. A la **Marta**, a la **Gemma** i a **l'Enric**, tan petit i ja saps més que jo de virus i bacteris, potser encara no te n'adones però la teva vitalitat extraordinària fa sentir a absolutament tothom tan especial que, pensar que quan començava aquest projecte encara no hi eres se'm fa molt estrany, gràcies per ser tan carinyós i fer-te estimar tan. A l'**Àdam**, el més petit de la família i el més gran, per encendre'ns una espelma d'enorme il·lusió.

Als meus **pares**, què dir-vos? Si no hi ha paraules... que m'emociono quan penso en tot l'esforç vostre que hi ha darrera. Sense vosaltres què faria? Gràcies per tot el suport indispensable que em doneu i per permetre que treballés i estudiés sempre en les millor condicions. Gràcies per ajudar-me absolutament en tot i estar sempre pel que faci falta. I a la meva **àvia**, gràcies per estar tan orgullosa de la teva néta, vostè diu que sóc una estudiant més que excel·lent, però vostè m'ensenya tots els deures que fa per la memòria i jo penso: ho hauré heretat d'ella? Iaia, gràcies per tot el que fa per mi, Iaia, jo de gran vull ser com vostè.

Table of contents

Abbreviations

6-OHDA	6-hidroxi-dopamine
ANOVA	Analysis of variance
Arg1	Arginase 1
ATP	Adenosine triphosphate
BDNF	Brain-derived neurotrophic factor
bp	Base pair
BSA	Bovine serum albumin
C/EBPβ	CCAAT/enhancer-binding protein β
Carkl	Carbohydrate kinase-like protein
CD	Cluster of differentiation
CD200full	Full-length CD200
CD200tr	Truncated CD200
CD200R	CD200 receptor
cDNA	Complementary DNA
CNS	Central nervous system
COX2	Cyclooxygenase 2
Ct	Threshold cycle
DAMPs	Damage-associated molecular patterns
DAPI	4',6-diamidino-2-phenylindol
DIV	Days *in vitro*
DMEM-F12	Dulbecco's modified Eagle medium-F12
DMSO	Dimethyl sulfoxide
DNA	Deoxyribonucleic acid
EAE	Experimental autoimmune encephalomyelitis
ELISA	Enzyme-Linked Immuno Sorbent Assay
FAO	Fatty acid oxidation
FBS	Fetal bovine serum
Fc	Fusion protein
Fizz1	Found in inflammatory zone 1
GDNF	Glial cell-derived neurotrophic factor
Gfap	Glial fibrillary acidic protein
Glut1	Glucose transporter 1
GAPDH	Glyceraldehyde-3-phosphate dehydrogenase
gp91phox	Catalytic subunit of NADPH oxidase
Hif1α	Glycolysis activator hypoxia-inducible factor 1α
Hk1	Hexokinase 1

HLA	Human leukocyte antigen
HRP	Horseradish peroxidase
Iba1	Ionized calcium binding adaptor molecule 1
IFN	Interferon
Ig	Immunoglobulin
IL	Interleukin
IL1ra	Interleukin 1 receptor antagonist
Iso	Isotype
iNOS	Inducible nitric oxide synthase
kDa	kiloDalton(s)
LBs	Lewy bodies
LP	Lewy-pathology
LPS	Lipopolysaccharide
MAP2	Microtubule-associated protein 2
MPP+	1-methyl-4-phenylpyridinium
MPTP	1-methyl-4-phenyl-1,2,3,6-tetrahydropyridine
MTT	3-(4,5dimethylthiazol-2-yl)-2,5-diphenyl tetrazolium bromide
MR	Mannose receptor
NADPH	Nicotinamide adenine dinucleotide phosphate
NF-κB	Nuclear factor kappa-light-chain-enhancer of activated B cells
NFT	Neurofibrillary tangles
NO	Nitric oxide
NO_2^-	Nitrite ion
NP	Degeneration and neuritic plaques
Nrf2	Nuclear factor erythroid 2-related factor 2
OD	Optical density
PAMPs	Pathogen-associated molecular patterns
PBS	Phosphate buffer
PCR	Polymerase chain reaction
PD	Parkinson’s disease
PEI	Polycation polyethyleneimine
PET	Positron emission tomography
PFA	Paraformaldehyde
Pfkp	Phosphofructokinase, platelet
Pgc1β	Peroxisome proliferator-activated receptor gamma coactivator 1β
PI	Propidium iodide
PPARγ	Peroxisome proliferator activated receptor γ
Rn18s	18S ribosomal RNA
PRR	Pattern recognition receptors
RNA	Ribonucleic acid

ROS	Reactive oxygen species
SDS	Sodium dodecyl sulphate
SN	Substantia nigra
SNpc	Substantia nigra pars compacta
SNpr	Substantia nigra pars reticulata
TBS	Tris-Buffered Saline
TGFβ	Transforming growth factor β
TH	Tyrosine hydroxylase
TLR	Toll-like receptor
TNFα	Tumor necrosis factor α
TREM2	Triggering receptor expressed on myeloid cells 2
V	Variant
Ym1	Chitinase 3-like 3

Summary

Neuroinflammation is present in practically all neurological disorders. Microglial cells, the main representatives of the endogenous immune system of the brain, play a key role in neuroinflammation, although peripheral immune cells can also be involved. In the last years, a considerable effort has been focused on the study of the modulation of the inflammatory response as a possible therapeutic strategy in neurological diseases. Parkinson's disease (PD) is the second most common neurodegenerative disease and is mainly characterized by a loss of dopaminergic neurons in the substantia nigra pars compacta (SNpc) and an abnormal intracellular accumulation of α-synuclein protein, known as Lewy bodies. Mounting evidence suggests that dopaminergic cell death is influenced by the innate immune system. Activated microglia has been described in the *post-mortem* brains of PD patients; however, the pathogenic role of the immune system in PD remains enigmatic. In the present thesis, we have studied one of the inhibitory mechanisms suggested to be involved in the control of the inflammatory response in microglial cells: CD200 ligand (mainly expressed in neurons and astrocytes) - CD200R1 receptor (mainly microglial) interaction.

The aim of this thesis was to study the involvement of the microglial inhibitory immune receptor CD200R1 in the modulation of neuroinflammation and its potential as therapeutic target in PD.

In vitro, the disruption of the CD200-CD200R1 system potentiated the pro-inflammatory response of glial cells. Mesencephalic cultures from CD200-deficient mice showed a higher microglial proportion and increased sensitivity of dopaminergic neurons to the neurotoxin 1-methyl-4-phenylpyridinium (MPP+). The parkinsonian neurotoxins MPP+ and rotenone impaired the immune response of glial cells to pro- and anti-inflammatory stimuli and changed CD200 and CD200R1 expression.

In vivo, in the 1-methyl-4-phenyl-1,2,3,6-tetrahydropyridine (MPTP) experimental mouse model of PD dopaminergic neurodegeneration and glial activation were associated to changes in CD200 and CD200R1 expression: mainly a transient increase in striatal CD200R1 and a sustained decrease in CD200full in the ventral midbrain. When we potentiated the CD200-CD200R1 system by administering a CD200R1 agonist, we observed partial protection in dopaminergic neurons of the SNpc, which was accompanied by an attenuated microglial activation. On the contrary, CD200-deficient mice showed a more reactive microglial phenotype at early stages after MPTP administration, although it was not associated to an exacerbated neurodegeneration.

Post-mortem brain samples from substantia nigra, frontal cortex and hippocampus of PD patients had particular changes in the expression of the mRNA variants and protein isoforms of the CD200-CD200R1 system.

In conclusion, these results suggest that the CD200-CD200R1 system is a potential target to control microglial activation in PD, and that the mechanisms of control of microglial activation may be used to modulate microglial activation and its potential neurotoxicity on neurodegenerative diseases.

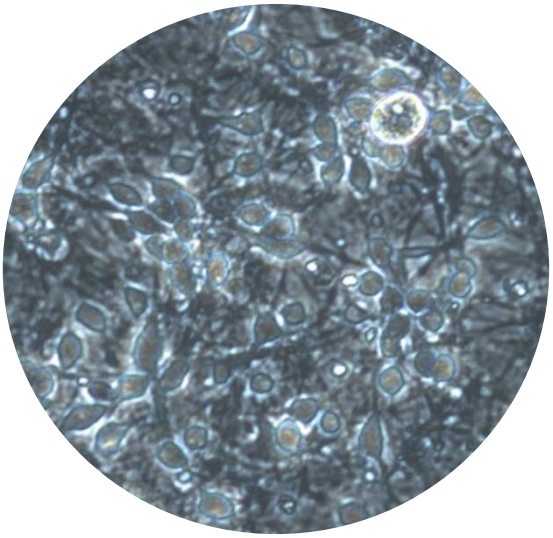

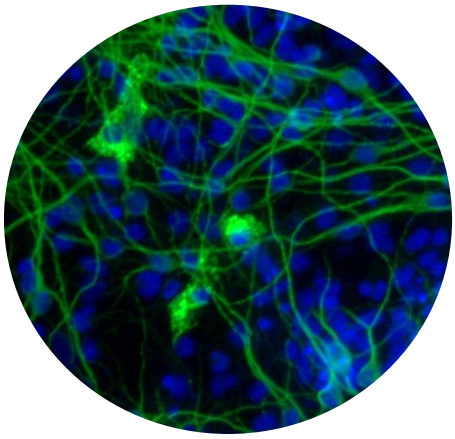

Introduction

1 Neuroinflammation and neurodegenerative diseases

Neuroinflammation is a complex cascade of self-defensive response to injurious stimuli in the nervous system and it is present in practically all neurological disorders (Dendrou, McVean, and Fugger 2016). Neurological disorders are diseases of the central and peripheral nervous system and include dementia (e.g. Alzheimer's disease); autoimmune diseases (e.g. multiple sclerosis); Parkinson's disease (PD); motor neuron diseases (e.g. amyotrophic lateral sclerosis); cerebrovascular diseases (e.g. stroke); neuropsychiatric disorders (e.g. schizophrenia); headache disorders (e.g. migraines); sleep disorders (e.g. narcolepsy); epilepsy; neuroinfections; traumatic brain injuries; brain tumours and others (WHO 2006). Their prevalence is increasing and currently affect around 1 billion people worldwide (Cottler et al. 2015). The disability associated with these diseases affects not only the patient but also the family and community, representing ~7% of the total global burden of disease measured in disability-adjusted life years, across all causes and ages (Chin and Vora 2014). Neuroinflammation is emerging as a key process in these conditions, either as a causative factor or as a secondary response, and considering its ubiquity, it represents an important avenue to address therapeutic approaches (Dendrou, McVean, and Fugger 2016).

Specifically, neurodegenerative diseases are a heterogeneous group of neurological disorders characterized by chronic, progressive and selective loss of neurons that leads to deficits in specific functions performed by the affected neurons (Kovacs 2016). Primary neurodegenerative diseases include Alzheimer's disease, PD, amyotrophic lateral sclerosis, Huntington's disease, and Creutzfeldt-Jakob disease, among others, and their neuropathological features involve intracellular and/or extracellular protein aggregation (e.g. proteopathies) and, although they are not considered to be primarily inflammatory, activation of glial cells is a well-established hallmark of these diseases. Neuroinflammation in primary neurodegenerative diseases is a chronic inflammatory process of unknown origin, in which activated glial cells, mainly microglia, play an important role, and it is suggested to contribute to the progress of neuronal damage (Glass et al. 2010). This neuroinflammation is principally typified by the innate immunity, mediated by central nervous system (CNS)-resident cells and accompanied by low to moderate levels of inflammatory mediators in the parenchyma, although the role of the adaptive immunity and changes in the permeability of the blood-brain barrier (BBB) are gradually gaining interest (Fig. 1) (Zlokovic 2008; Mosley et al. 2012). In contrast to primary neurodegenerative diseases, in other degenerative diseases considered primarily inflammatory, such as multiple sclerosis, neuroinflammation is characterized by an important infiltration of the CNS parenchyma by lymphocytes and monocyte-derived macrophages, as well as a drastic loss of BBB integrity and glial reactivity (Fig. 1) (Ransohoff 2016).

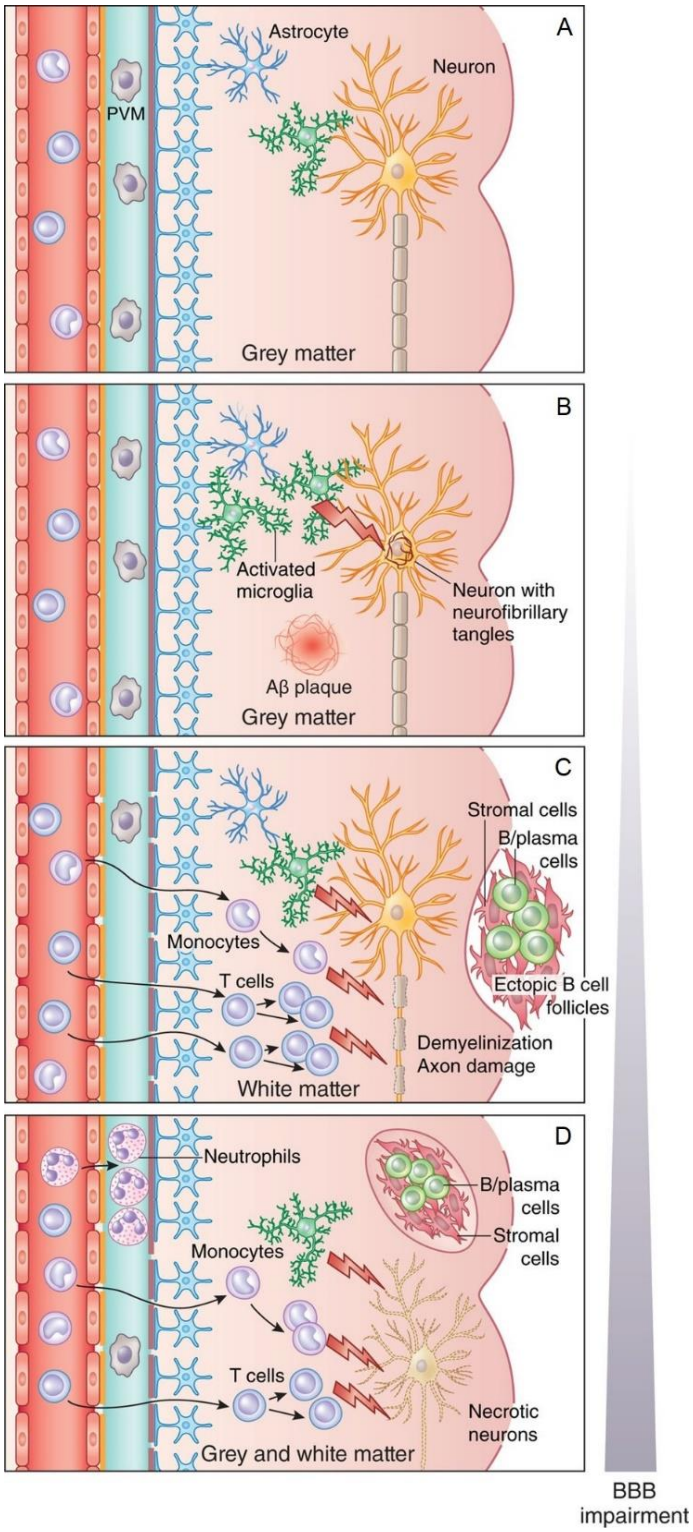

Figure 1. The immune system in neurological diseases. In physiological conditions, the blood-brain barrier (BBB) prevents blood cell engraftment (**A**). In primary neurodegenerative diseases, such as Alzheimer's disease (**B**), activation of glial cells is a hallmark. In contrast, in multiple sclerosis (**C**) and stroke (**D**), a considerable leakage of the BBB and T- and B-cell, neutrophil, and monocyte infiltrates are typical. Aβ: amyloid β-peptide (Prinz and Priller 2017).

Some authors support the idea that the concept of neuroinflammation should be used only when there is an important involvement of the adaptive immune system including the presence of T and B lymphocytes and other hematopoietic cells within the CNS. This is a typical feature of multiple sclerosis and encephalitis. In contrast, primary neurodegenerative diseases should be considered innate immune reactions (Prinz and Priller 2017). However, neuroinflammation has gradually become a general term that includes all types of immune reactions in the CNS.

Neuroinflammation is a protective response to initiate a healing process by removing harmful stimuli and cellular debris, releasing neurotrophic factors, promoting tissue repair and regrowth, secreting reactive oxygen species (ROS), proteases and cytokines to restore homeostasis. However, uncontrolled neuroinflammation can become harmful, because an excessive and prolonged reaction leads to the accumulation of potential neurotoxic factors such as ROS and pro-inflammatory cytokines. In addition, the beneficial effects of neuroinflammation seem to be ineffective in neurodegenerative diseases (Gao and Hong 2008).

2 The immune system in the CNS

The immune system that protects the CNS is comprised of cells that reside within the CNS and cells that traffic into the CNS with disease (Prinz and Priller 2017).

2.1 MICROGLIA: THE MAIN COMPONENT OF THE IMMUNE SYSTEM OF THE CNS

Under homeostatic conditions, the immune system within the CNS is comprised mainly of innate immune cells and consists of the microglia in the CNS parenchyma, and meningeal macrophages, perivascular macrophages and choroid plexus macrophages in CNS-periphery interfaces between parenchyma and the circulation (Li and Barres 2018; Prinz and Priller 2017). In the CNS parenchyma, astrocytes can also participate in neuroinflammation (Sofroniew 2015).

As microglial cells represent the principal component of the endogenous immune system of the brain, these cells will be explained below.

Microglial cells are generated during early development from yolk sac primitive macrophages. The microglial population in the CNS is maintained by local self-renewal in physiological conditions, with no requirement for influx of circulating progenitors from the blood or bone marrow (Figs. 2A and 3A) (Ajami et al. 2007; Ginhoux et al. 2010; Mildner et al. 2007; Madore, Baufeld, and Butovsky 2017). Microglia remains self-proliferating at turnover rates that depend on the region. In mice, hippocampus and olfactory bulb, niches of cell proliferation, there are subpopulations of microglia with increased self-renewal (Tay et al. 2017). Under acute neurodegeneration or CNS inflammation such as nerve axotomy or amyotrophic lateral sclerosis model, microglia expand clonally without recruitment of blood monocytes (Figs. 2B and 3B) (Ajami

et al. 2007). When there is resolution of the damage, the original microglia network is restored by apoptosis of excess cells (Fig. 2C) (Tay et al. 2017; Madore, Baufeld, and Butovsky 2017).

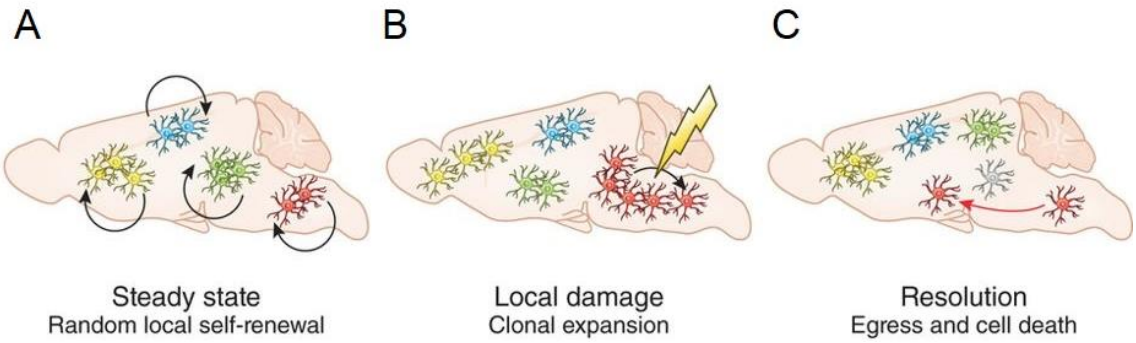

Figure 2. Microglial network regulation in health and disease. A In steady-state conditions, there is random local self-renewal of microglia. **B** Local damage induces microgliosis through clonal expansion. **C** Resolution involves egress (red arrow) and apoptosis (grey cell) of excess cells. From: Madore, Baufeld et al. 2017.

Experimental studies showed that after exposure mice to irradiation, the integrity of the BBB is compromised and allows entry of blood cells; however, recruited monocytes, although contributing to inflammation, are unable to persist in the CNS and do not contribute to the resident microglial population (Fig. 3C) (Ajami et al. 2011; Ginhoux and Garel 2018). These short-lived monocytes recruited when BBB is disrupted, although not contributing to microglia pool, may have important roles in disease. This is the case of multiple sclerosis and the experimental mouse model of autoimmune encephalomyelitis (EAE), where there is disruption of the BBB and recruitment of short-lived monocytes that do not contribute to microglial pool but are essential drivers of disease severity (Ajami et al. 2011).

The contribution of circulating cells to the microglial pool has been described after irradiation plus a bone marrow transplantation, when there is disruption of the BBB in conjunction with circulating bone marrow hematopoietic progenitors (Fig. 3D). In this unique circumstance, the early hematopoietic progenitors enter the CNS and can give rise to microglial-like cells that are able to persist long time in CNS and do contribute to the microglial pool. However, this is a non-physiological state because early hematopoietic progenitors are not normally found in peripheral blood (Ajami et al. 2007; Ginhoux and Garel 2018; Ajami et al. 2011).

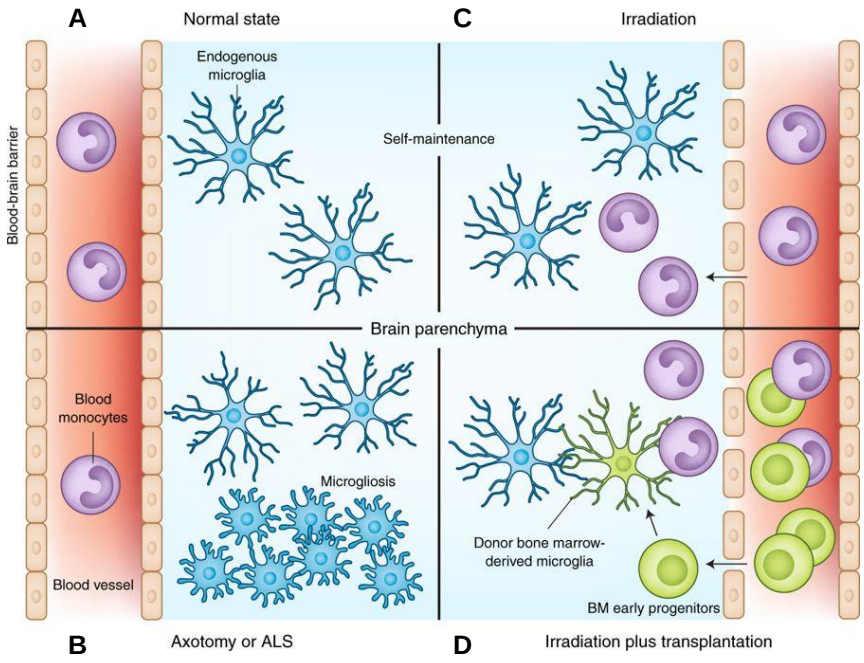

Figure 3. Participation of microglia and blood monocytes in different adulthood scenarios. ALS: amyotrophic lateral sclerosis BM: bone marrow. From: Ginhoux and Garel 2018.

In conclusion, circulating precursors do not contribute to the microglial pool, neither to maintain microglial population in healthy brain nor to microgliosis seen in axotomy or amyotrophic lateral sclerosis model. Recent studies support similar ideas for Alzheimer's disease, prion disease or stroke. In Alzheimer's disease, microglial population is increased without contribution of bone marrow-derived cells, and interestingly microglia and bone marrow-derived phagocytes may have distinct roles (Bolmont et al. 2008; Martin et al. 2017; Mildner et al. 2011); in stroke, microglia and infiltrating circulating cells represent two distinct populations of cells with different functions (ElAli and Jean LeBlanc 2016; Li et al. 2013); in prion disease, circulating progenitors contribute to the perivascular macrophages population but not to microglial population (Gomez-Nicola, Schetters, and Perry 2014). In other neurodegenerative diseases where there is also microgliosis such as PD, bone marrow cells may infiltrate the brain but its contribution to the expansion of parenchymal microglial population remains to be elucidated (Gomez-Nicola and Perry 2015).

Meningeal macrophages, perivascular macrophages and choroid plexus macrophages also participate in the immune system within the CNS and, as in the case of microglia, arise from embryonic yolk sac precursors (Fig. 4A) (Prinz, Erny, and Hagemeyer 2017). Under steady-state conditions, microglia, meningeal macrophages and perivascular macrophages maintain their populations by self-renewal, and only choroid plexus macrophages population receive input from circulating monocytes (Fig 4B). Each immune cell is localized in a specific niche and has its own expression signature, which is related to its function. Only under certain disease states or experimental manipulations (e.g. irradiation), monocytes can infiltrate the brain parenchyma (Fig.

4B) (Li and Barres 2018; Prinz and Priller 2017). Little evidence is available about the possible contribution of choroid plexus macrophages, meningeal macrophages and perivascular macrophages to the expansion of the microglial population in the diseased brain (Gomez-Nicola and Perry 2015).

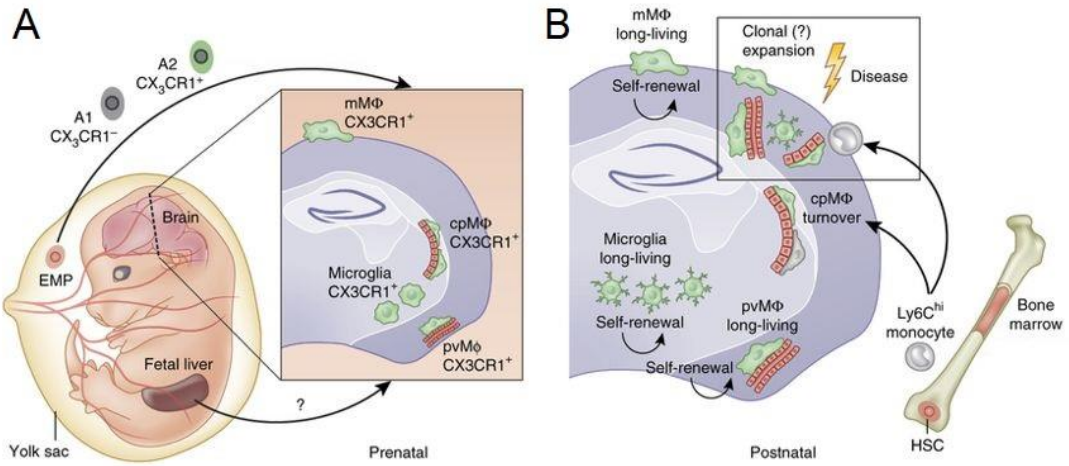

Figure 4. Origen and turnover of macrophages in the CNS. A In mice, at E7.0-E8.0, there is a transient early wave of myeloid cell development called “primitive hematopoiesis”, in which erythromyeloid precursor (EMP) cells from the yolk sac proliferate, differentiate and migrate to several tissues including the brain. In the brain, these precursors differentiate into microglia, perivascular macrophages (pvMΦ), meningeal macrophages (mMΦ) and choroid-plexus macrophages (cpMΦ). At E12.5, myelopoiesis takes place by progenitor cells in the fetal liver and maturing myeloid cells continue to engraft in all tissues beyond E14.5-E15.5; however, due to the BBB, the microglia, pvMΦ, mMΦ and cpMΦ are thought to be excluded from this fetal contribution. **B** At birth, myelopoiesis is restricted to bone marrow. In the healthy adult brain, microglia, pvMΦ and mMΦ have extreme longevity and self-renewal potential and only cpMΦ have a contribution from bone-marrow progenitors. Under disease conditions or following irradiation, bone-marrow cells can enter the CNS. HSC: hematopoietic stem cell. From: Prinz, Erny et al. 2017.

2.2 OTHER COMPONENTS OF THE IMMUNE SYSTEM OF THE CNS

Several layers protect the surface of the brain, including the skull, the dura mater and the leptomeninges composed by the arachnoid and the pia mater. The pia mater covers the brain and the intracerebral vascular system (Fig. 5), surrounding the arteries entering the brain (Engelhardt, Vajkoczy, and Weller 2017). The arachnoid mater establishes a barrier between the dura mater and the cerebrospinal fluid and it is impermeable to fluids and expresses efflux pumps (Engelhardt, Vajkoczy, and Weller 2017). The pia mater is permeable to solutes and immune cells, but not to erythrocytes (Hutchings and Weller 1986).

The cerebrospinal fluid is produced as a filtrate of the fenestrated blood vessels in the choroid plexus of ventricles and flows in the subarachnoid space, between the arachnoid and the pia maters and the ventricular system (Fig. 5). It provides buoyancy to the CNS and transports

cytokines, neurotransmitters and hormones (Whedon and Glassey 2009). In homeostatic conditions, the cerebrospinal fluid also contains, although in low quantities, antigen-presenting cells, monocytes and CD4+ T lymphocytes (Fig. 5), most of them effector-memory T cells that can produce immediate effector functions without the need for further differentiation (Ransohoff and Engelhardt 2012; Kivisakk et al. 2006).

Under homeostatic conditions, it is nowadays believed that the CNS parenchyma is devoid of leukocytes (granulocytes, T and B cells and monocytes), both in human and mouse brain, although it is an ongoing research topic in neuroscience today (Prinz and Priller 2017; Prinz, Erny, and Hagemeyer 2017). Moreover, in the CNS parenchyma there are not classical dendritic cells, the cells that present antigens to T naïve cells. However, memory T cells in the cerebrospinal fluid monitor the CNS and can encounter meningeal, perivascular and choroid plexus macrophages that can function as antigen-presenting cells upon activation, and this provides CNS immune surveillance under homeostasis (Ransohoff and Cardona 2010). Meningeal, perivascular and choroid plexus macrophages may modulate immune cells entry and phenotype during inflammation (Brendecke and Prinz 2015).

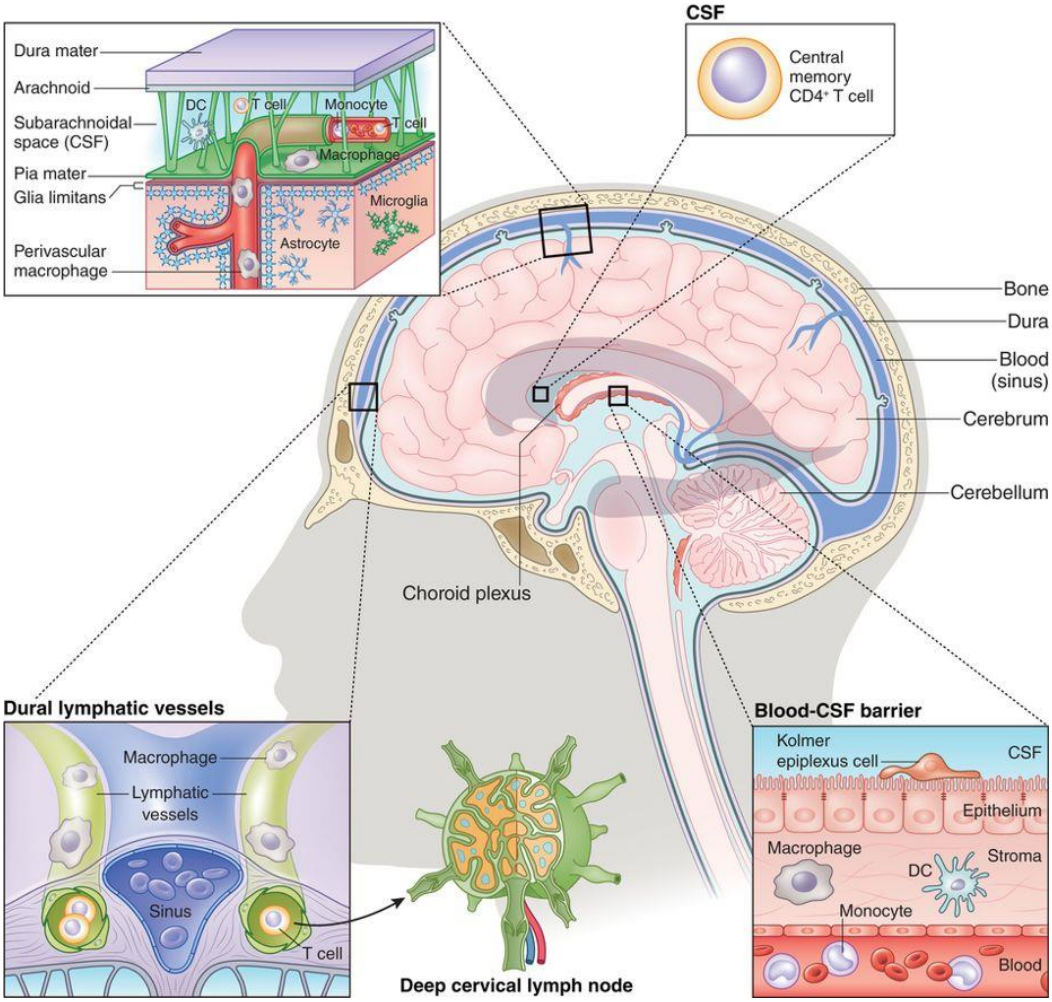

Figure 5. Anatomy of the immune system of the CNS during homeostasis. CSF: cerebrospinal fluid, DC: dendritic cell. From: Prinz and Priller 2017.

Two extracellular systems exist in the CNS, the cerebrospinal fluid, which occupies the subarachnoid space and the ventricular system, and the interstitial fluid (Kida, Pantazis, and Weller 1993), which is found in the CNS parenchyma (Carare et al. 2008). The cerebrospinal fluid in the subarachnoid space can drain through arachnoid villi into venous sinuses (Upton and Weller 1985), but the cerebrospinal fluid and soluble antigens therein can also drain to cervical and lumbar lymph nodes via cribriform plate, dural lymphatic vessels and spinal nerve roots (Kida, Pantazis, and Weller 1993; Aspelund et al. 2015; Louveau et al. 2015). Immune cells including CD4+ T cells in the cerebrospinal fluid, dendritic cells and monocytes, can use this pathway to reach the lymph nodes (Cserr, Harling-Berg, and Knopf 1992; Goldmann et al. 2006; Kaminski et al. 2012). In contrast, interstitial fluid and soluble antigens in the CNS parenchyma drain to lymph nodes along the walls of cerebral capillaries and arteries. This pathway does not allow immune-cell trafficking (Carare et al. 2008). A direct interconnection between cerebrospinal fluid and interstitial fluid at the surface of the brain, named glymphatic system, has been recently proposed (Iliff et al. 2012).

The main brain barriers that prevent from the entry of peripheral immune cells into the CNS parenchyma are the glia limitans, the BBB and the choroid plexus (Engelhardt, Vajkoczy, and Weller 2017). Compacted astrocyte foot processes compose the glia limitans, a barrier at the surface of the CNS parenchyma and around blood vessels (Fig. 5). The BBB is a barrier between the blood and the CNS parenchyma and is composed of specialized endothelial cells, astroglial end-feet and pericytes. It regulates the passage of immune cells, which have to cross the BBB and the glia limitans to reach the CNS parenchyma (Owens, Bechmann, and Engelhardt 2008). The choroid plexus epithelial cells also establish a barrier in the ventricles between the blood and the cerebrospinal fluid, because the choroid plexus stroma contains a microvascular network that does not have a BBB (Spector, Robert Snodgrass, and Johanson 2015; Engelhardt et al. 2016).

3 The biology of microglia

3.1 STRUCTURE AND GENERAL MICROGLIAL FUNCTIONS IN HOMEOSTASIS

The concept of microglia was introduced by Pio del Rio-Hortega in 1932 (Rio-Hortega 1932). Microglial cells are the resident macrophages of the brain parenchyma and are considered the main effector of immune brain function (Ransohoff and Perry 2009; Manich et al. 2019). They represent approximately 10% of the adult brain cell population (Salter and Stevens 2017).

3.1.1 Microglial morphology

In homeostatic conditions, microglial cells have a highly ramified morphology and are composed by a multitude of fine and exceptionally motile processes emanating from a small cell body (Fig. 6). The cell soma has a relative fixed position whereas processes have high degree of motility and are constantly surveying the surrounding microenvironment (Nimmerjahn, Kirchhoff, and Helmchen 2005). Microglia are ubiquitously distributed in the CNS parenchyma and each cell has its own territory, but their density varies depending on the region, being less abundant in the cerebellum and more abundant in the substantia nigra (SN) (Lawson, Perry, and Gordon 1992; Perry 2016). In rodents, microglia show higher densities in grey matter, whereas in humans they are denser in white matter (Mittelbronn et al. 2001).

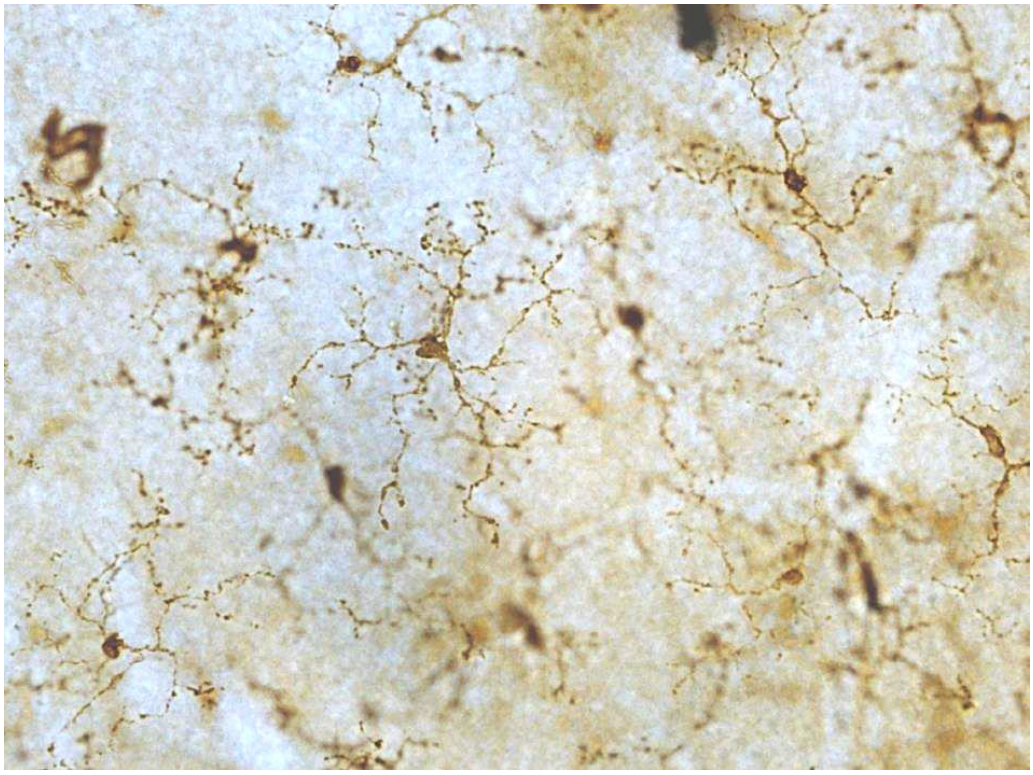

Figure 6. Microglial morphology. The branching of the processes in microglial cells and the territory occupied by each cell in the outer plexiform layer of the mouse retina is shown. From: Perry 2016.

3.1.2 Microglial functions

Microglial cells participate in different functions in the healthy CNS.

Microglial surveillance and monitoring

In physiological conditions, microglia actively scan the extracellular space and cellular neighbourhood with their motile processes. They continuously detect, transduce, integrate and

respond to environmental signals to maintain brain homeostasis and transform to executive states of activation when required (Heneka, Kummer, and Latz 2014; Kettenmann et al. 2011; Salter and Stevens 2017). Microglia scan the entire volume of the brain over a course of a few hours (Nimmerjahn, Kirchhoff, and Helmchen 2005).

Developmental synaptic pruning

During development, microglia contribute to synaptic pruning by engulfing and eliminating axons and dendritic spines (Paolicelli et al. 2011; Tremblay, Lowery, and Majewska 2010). An aberrant microglial pruning leads to defects in synaptic development and abnormal wiring, which could contribute to neurodevelopmental disorders including schizophrenia or autism (Schafer et al. 2012; Sekar et al. 2016)). Classical-complement cascade and chemokine (C-X3-C motif) ligand (CX3CL)1 - CX3C chemokine receptor (CX3CR)1 system, among others, are involved in microglial synaptic pruning (Paolicelli et al. 2011; Schafer et al. 2012; Stevens et al. 2007; Lui et al. 2016).

Neuronal programmed cell death

Microglial cells act as scavengers and phagocyte neuronal debris after programmed neuronal cell death. Neuronal apoptosis occurs in the healthy brain to eliminate the excess of neurons generated during development (Brown and Neher 2014; Marin-Teva et al. 2011). Moreover, microglia can have a more active role by inducing the neuronal apoptosis during development. Superoxide ions, nerve growth factors, tumor necrosis factor (TNF) and cell-surface receptor CR3 have been implicated in this process (Frade and Barde 1998; Marin-Teva et al. 2011; Sedel et al. 2004; Wakselman et al. 2008).

Synaptic plasticity in the adult

Not only during development but also in the healthy adult brain, microglia remove synapses in the context of neuronal plasticity. While microglia are scanning the environment by constantly extending and retracting their processes in homeostatic conditions, some processes can rest for several minutes and make direct contact with neuronal synapses. Preferentially, the less active inputs are removed by the microglia (Hong et al. 2016; Kettenmann, Kirchhoff, and Verkhratsky 2013) Activated microglia can also affect synaptic transmission, for instance through toll-like receptor (TLR)4 (Pascual et al. 2012). Microglia are crucial regulators of learning and memory, adult neurogenesis and activity-triggered synaptic plasticity (Gemma and Bachstetter 2013; Parkhurst et al. 2013; Sipe et al. 2016; Salter and Stevens 2017).

3.2 MICROGLIAL ACTIVATION

Any disturbance in the CNS environment is sensed by microglial cells and induces their activation. Microglial activation is defined as the triggering of rapid and profound morphological, gene

expression and functional changes in microglia after sensing any loss of brain homeostasis (Kettenmann et al. 2011). Activated microglia shorten their processes, increase their cellular size and finally adopt an amoeboid morphology. In addition, activated microglia rearrange surface molecules, change intracellular enzymes, proliferate and move to the side of lesion following chemotactic gradients and release multiple factors with inflammatory effects. They can also phagocyte tissue debris, damaged cells or microbes and produce neurotrophic factors. Activated microglial release chemoattractive molecules to recruit immune cell populations to CNS, and present antigens to T cells (Heneka, Kummer, and Latz 2014; Kettenmann et al. 2011; Salter and Stevens 2017).

3.2.1 Phenotypes of microglial activation

The term microglial activation comprises a range of different “activated” stages (Cherry, Olschowka, and O'Banion 2014b). A classical classification based on the M1/M2 polarisation described in macrophages was adopted as the standard designation for microglial activation profiles (Fig. 7) (Heneka, Kummer, and Latz 2014; Wolf, Boddeke, and Kettenmann 2017).

The termed **M1 or classically activated state** is induced *in vitro* by treating primary microglial cultures with lipopolysaccharide (LPS) and interferon (IFN)γ and is typified by the production of ROS and pro-inflammatory molecules including interleukin (IL)1β, IL2, IL6, IFNγ, CXCL9, CXCL10, inducible nitric oxide synthase (iNOS), cyclooxygenase (COX)2 or TNFα (Chhor et al. 2013; Fenn et al. 2012; Varnum and Ikezu 2012). *In vivo*, the M1 phenotype is induced by IL1β, TNFα or a high concentration of adenosine triphosphate (ATP) (Davalos et al. 2005; Ransohoff and Perry 2009). M1 cells are involved in antigen presentation, killing of intracellular pathogens and cytotoxicity, induction of Th1 and Th17 cells, which in turn mediate inflammation (Cherry, Olschowka, and O'Banion 2014b; Franco and Fernandez-Suarez 2015).

In the **M2 or alternative activated state**, microglial cells acquire an anti-inflammatory phenotype and are involved in the resolution of inflammation, wound repair and debris clearance. In turn, M2 microglial cells are divided into three different subtypes that are induced by different environmental factors.

The treatment of cultured microglial cells with IL4 or IL13, closely related cytokines that signal through IL4Rα, leads to the **M2a** phenotype and is characterized by the expression of anti-inflammatory molecules including Arg1, found in inflammatory zone (Fizz)1, mannose receptor (MR), insulin growth factor 1 (IGF1), transforming growth factor (TGF)β or Chitinase 3-like 3 (Ym1), inhibition of nuclear factor kappa-light-chain-enhancer of activated B cells (NF-κB) and the expression of receptors for phagocytosis (Gadani et al. 2012; Sica and Mantovani 2012). The main function of M2a phenotype is the suppression of inflammation, phagocytosis of cellular debris and tissue repair promotion (Cherry, Olschowka, and O'Banion 2014b; Chhor et al. 2013).

After ligation of immunoglobulin Fcγ receptors by immune complexes on LPS- or IL1β-primed microglia, the **M2b** phenotype is acquired by microglial cells. M2b microglia express $IL10^{high}$, $IL12^{low}$, MHCII and CD86, suggesting the ability to induce Th2 T cells and the capability to initiate the M2 response in general (Mantovani et al. 2013; Mosser and Edwards 2008; Filardy et al. 2010).

The treatment of cultured microglial cells with IL10 and glucocorticoid hormones or TGFβ leads to the **M2c** phenotype and it is typified by the expression of anti-inflammatory molecules as CXCL13, sphingosine kinase and suppressor of cytokine signalling 3 (Chhor et al. 2013; Mantovani et al. 2004; Fenn et al. 2012; Hu et al. 2012; Varnum and Ikezu 2012). The M2c phenotype is involved in tissue remodelling and matrix deposition after inflammation has been down-regulated (Mantovani et al. 2004).

The existence of an **M0** phenotype is in debate (Cherry, Olschowka, and O'Banion 2014a) and it would correspond to microglia in homeostatic conditions displaying the functions required for the maintenance of healthy environment including debris clearance, plasticity, production of insulin growth factor (IGF1) and brain-derived neurotrophic factor (BDNF), among others (Fig. 7).

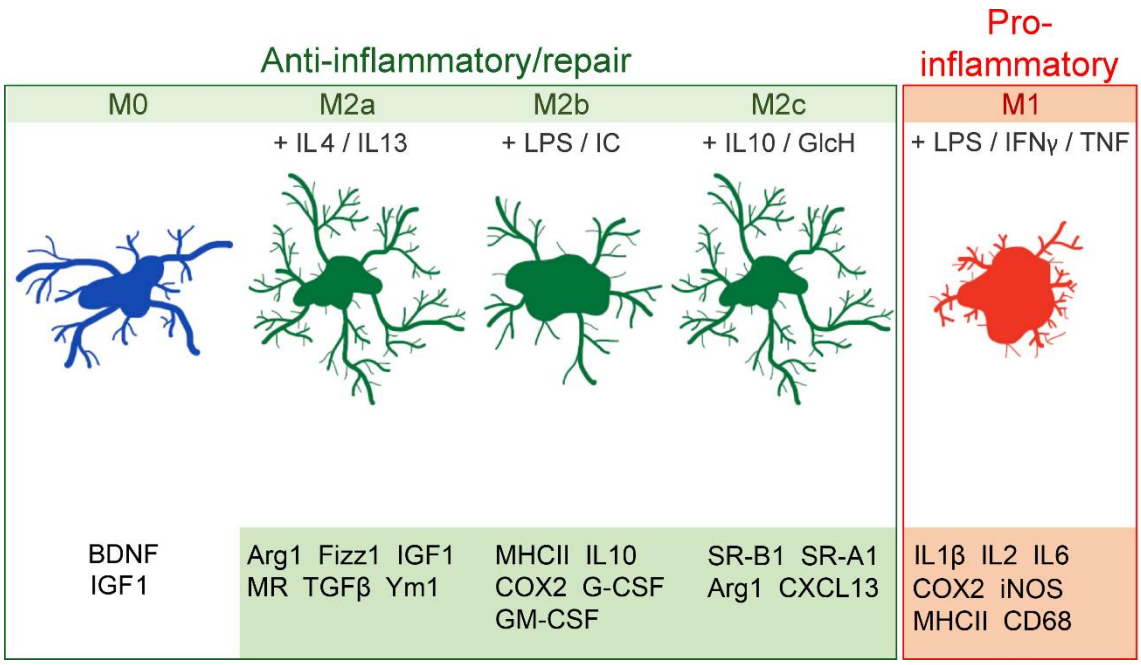

Figure 7. Activated states of microglia based on M1/M2 classification. The M1 phenotype is implicated in the pro-inflammatory response, the M2a, M2b and M2c phenotypes are implicated in the anti-inflammatory/repair response and the M0 phenotype is present in homeostasis and it may be included in the M2 polarised cell group. The molecules that induce each state (top), the microglial morphology acquired in each state (middle) and some molecules expressed by each polarised cell (down) are indicated. Arg1: arginase1, BDNF: brain-derived neurotrophic factor, CD68: cluster of differentiation 68, COX2: cyclooxygenase 2, CXCL13: chemokine (C-X-C motif) ligand 13, Fizz1: found in inflammatory zone 1, G-CSF: granulocyte colony-stimulating factor, GlcH: glucocorticoid hormones, GM-CSF: granulocyte-macrophage colony-stimulating factor, IC: immune complexes, IFNγ: interferon gamma, IGF1: insulin growth factor, IL: interleukin, iNOS: inducible nitric oxide synthase, LPS: lipopolysaccharide, MHCI: major histocompatibility complex type I receptor, MHCII: major histocompatibility complex type II receptor, SR-A1: scavenger receptor class A1, SR-B1: scavenger receptor class B1, TGFβ: transforming growth factor beta, Ym1: chitinase 3-like 3. Adapted from: Franco and Fernandez-Suarez 2015.

This classification of microglial activation as M1/M2 categories has its limitations, as it was defined *in vitro* following exposure to one or two stimuli, and most likely does not represent the complexity of all *in vivo* subtypes (Cherry, Olschowka, and O'Banion 2014b). An extensive diversity of microglial phenotypes upon activation has been described in transcriptomic and single-cell assay studies (Ransohoff 2016; Wes et al. 2016; Gosselin et al. 2017). Moreover, different microglial activated subtypes may coexist *in vivo*, together with a combination of infiltrating macrophages (Franco and Fernandez-Suarez 2015).

Neither the morphological changes that undergo activated microglia nor the cell-surface markers known to be expressed by these cells are enough to specifically define which particular state of activation is occurring in microglia in a given CNS disease state (Perry, Nicoll, and Holmes 2010; Salter and Stevens 2017). Transcriptomic, proteomic, and epigenomic features of microglia in specific contexts are a current issue of study (Salter and Stevens 2017).

3.2.2 Microglial activation/dysfunction and neurodegenerative diseases

In the human CNS, microglia are rapidly activated after an acute injury to adopt one of many diverse phenotypes depending on the stimuli, disease type, stage of the disease and the age of the individual (Fig. 8) (Nimmerjahn, Kirchhoff, and Helmchen 2005; Perry, Nicoll, and Holmes 2010). Activated microglia have beneficial functions for neuron survival including innate immunity, debris clearance, repair facilitation though neurogenesis and migration guidance of stem cells to the injury site. However, overactivated and dysregulated microglia can become dysfunctional and ellicit detrimental effects for neurons by producing an excess of cytotoxic factors such as reactive nitrogen and oxygen species and pro-inflammatory cytokines. In neurodegenerative diseases, a chronic state of neuroinflammation has been described with an activated microglia, although the beneficial or detrimental effects of the overactivated microglia and whether or not microglial activation is a consequence of neuronal damage is poorly understood. In neurodegenerative diseases, misfolded proteins, aggregates, degeneration of neurons and environmental toxins, such as rotenone, have been proposed to participate in the persistent activation of microglia, which probably acquire a different phenotype from that found after an acute insult (Fig. 8) (Block, Zecca, and Hong 2007; Perry, Nicoll, and Holmes 2010; Heneka 2019; Song and Colonna 2018; Hickman et al. 2018). Interestingly, age is the main risk factor for many neurodegenerative diseases and microglial cells become dysregulated with aging. An aging of microglia could, therefore, contribute to age-associated brain changes (von Bernhardi, Eugenin-von Bernhardi, and Eugenin 2015).

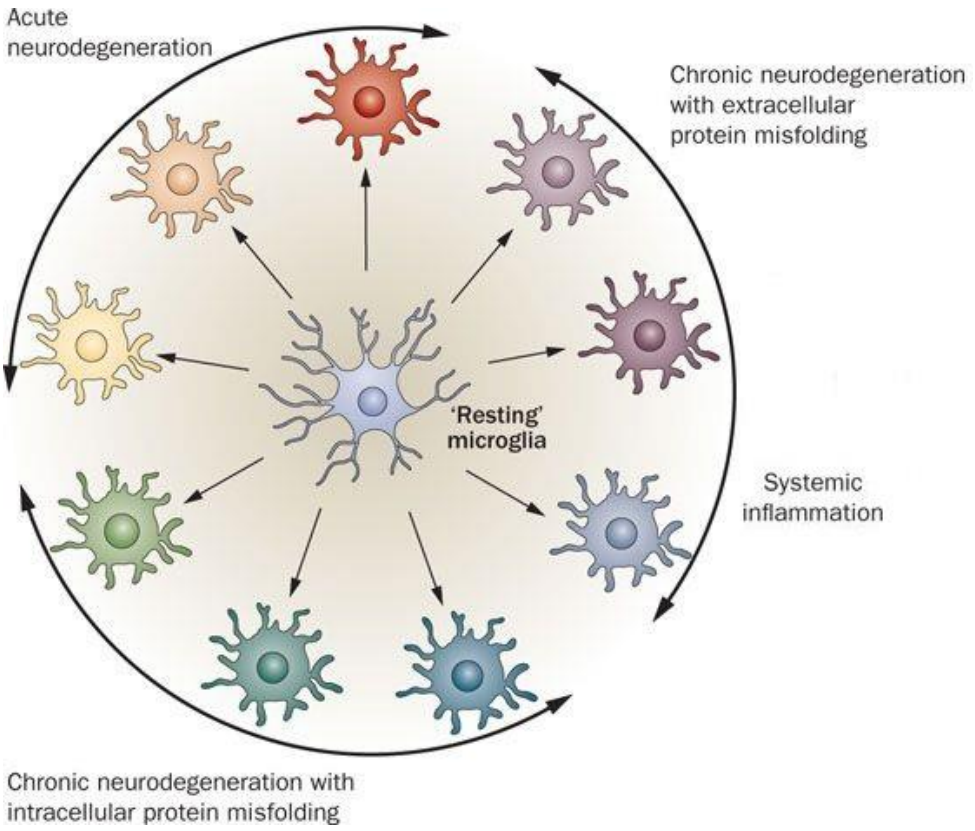

Figure 8. Multiple microglial phenotypes. Depending on the stimuli, disease type, stage of the disease, chronification of the disease or age of the individual microglial acquire different phenotypes of activation. From: Perry, Nicoll et al. 2010.

3.2.3 Mechanisms of control of microglial activation

In microglia, the transition between surveillance and activated states is triggered by the loss of existing constitutive inhibitory signals termed “off signals” or by the presence of “on signals” (Block, Zecca, and Hong 2007; Hanisch and Kettenmann 2007).

“Off signals” maintain a persisting signalling to keep microglia in a surveillance state and its interruption activates microglia (Kettenmann et al. 2011). Many of them are produced by neurons (Ransohoff and Cardona 2010). In contrast to “on signals”, “off signals” allow microglia to react to unknown signs of danger (Fig. 9) (Kettenmann et al. 2011). “Off signals” can be divided into:

- **Membrane-bound molecules** including CD200-CD200R1, CX3CL1-CX3CR1 and SIRPα(CD172a)-CD47 systems (Brooke et al. 2004; Hernangomez et al. 2014).
- **Soluble mediators** including TGFβ, IL34 and CSF1 (Wohleb 2016).
- **Neurotransmitters** including glutamate, GABA, acetylcholine and noradrenaline, suggesting that neuronal activity also controls microglial function (Pocock and Kettenmann 2007).

"On signals" are signalling molecules that appear in the brain upon homeostatic disturbance and are sensed by microglial cells triggering their activation (Kettenmann et al. 2011). "On signals" can be divided into:

- **Soluble factors** including cytokines, chemokines and trophic factors, whose receptors are expressed by activated microglia (Kettenmann et al. 2011). ATP is one of the main soluble "on signals" and is released by injured cells. Excessive neuronal activity can constitute also an "on signal" through increased concentration of neurotransmitters (Burnstock 2016; Kettenmann et al. 2011).
- Microglial **membrane-bound receptors** whose counter-receptors are expressed by damaged neurons (Manich et al. 2019). This mechanism includes Triggering receptor expressed on myeloid cells (TREM)2, whose microglial expression increases in various CNS neurodegenerative diseases such as Alzheimer's disease (Krasemann et al. 2017; Yeh, Hansen, and Sheng 2017). CD22-CD45 and CD172α-CD47 are also included in this class (Manich et al. 2019; Mott et al. 2004).
- **Infectious agents.** Bacterial or viral structures constitute the pathogen-associated molecular patterns (PAMPs) sensed by microglia through pattern recognition receptors (PRR), such as the TLRs (Kettenmann et al. 2011; Wolf, Boddeke, and Kettenmann 2017).
- **Damaged endogenous molecules** including cellular debris, nucleic acids, aggregated, biochemically-altered or misfolded proteins such as β-amyloid, α-synuclein, mutant huntingtin and superoxide dismutase 1. All these altered endogenous molecules are observed in neurodegenerative diseases and can act as damage-associated molecular patterns (DAMPs) and activate PRRs, such as TLR4 and 6, leading to the sustained production of neuroinflammatory factors (Kettenmann et al. 2011; Manich et al. 2019; Wolf, Boddeke, and Kettenmann 2017).

The loss of specific "off signals" or the presence of certain "on signals" will determine the phenotype of microglial activation (Manich et al. 2019). Furthermore, the surveillance features, the receptors repertoire, the interpretation of environmental signals and the signalling outcomes may differ among microglial populations in different CNS regions, since each area has specific properties and microglia may display distinct reactive options (Kettenmann et al. 2011).

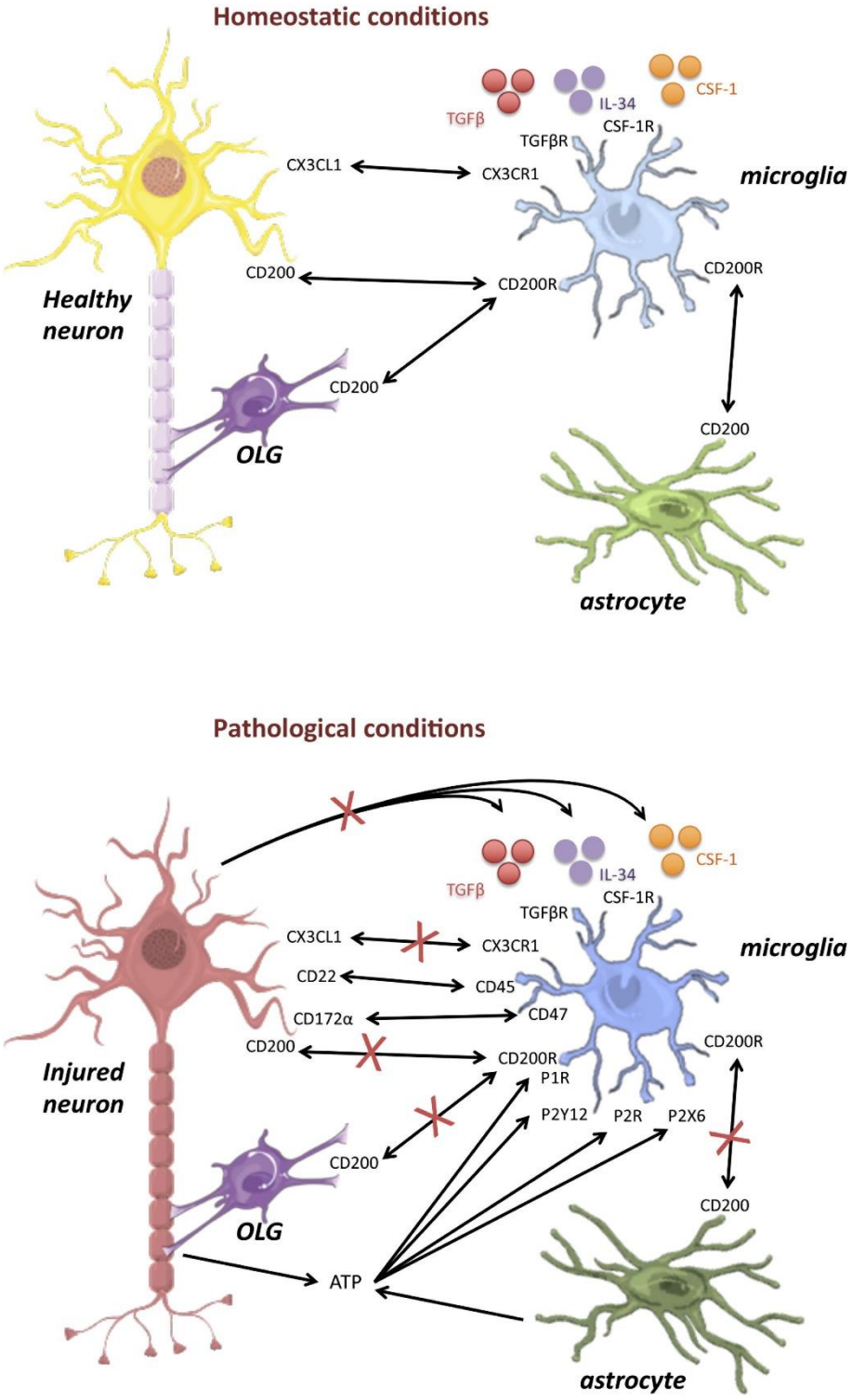

Figure 9. Principal "Off signals" and "On signals" regulating microglial activation. Neurons, astrocytes and oligodendrocytes maintain microglia in homeostatic conditions by expressing constitutive "off signals", including CD200 ligand that interacts with the microglial CD200R1 receptor. When these communications are altered or "on signals" appear, microglial activation is induced. (↔ binding; → release). ATP: adenosine triphosphate, CD: cluster of differentiation, CSF-1: colony stimulating factor 1, CX3CL1: chemokine (C-X3-C motif) ligand 1, CX3CR1: chemokine (C-X3-C motif) receptor 1, IL34: interleukin, OLG: oligodendrocyte, P1R P2R P2X6 and P2Y12: purinergic receptors, R: receptor, TGFβ: transforming growth factor. From: Manich, Recasens et al. 2019.

3.2.4 Microglial metabolism

In macrophages, M1/M2 polarisation is associated with a metabolic reprogramming and this has been extensively studied (O'Neill and Hardie 2013; Pearce and Pearce 2013). M1 macrophages increase glycolysis by increasing 6-phosphofructo-2-kinase/fructose-2,6-bisphosphatase-3 (PFKFB3) expression (Fig 10A i) (Rodriguez-Prados et al. 2010). High rates of glycolysis allow macrophages to quickly trigger microbicidal activity and have energetic advantages in hypoxic microenvironments (Nizet and Johnson 2009). M1 macrophages also activate the hypoxia-inducible factor (HIF)1α, which regulates glycolysis (Palazon et al. 2014) and increases IL1β expression (Tannahill et al. 2013). To increase phagocytic activity, phospholipid synthesis is increased and fatty acid oxidation (FAO) is not modified (Fig 10A iii) (Ecker et al. 2010). M1 macrophages produce large quantities of ROS by nicotinamide adenine dinucleotide phosphate (NADPH) oxidase and reactive nitrogen species including nitric oxide (NO) by iNOS (Fig 10A vii). NADPH is necessary for both enzymes and is produced in the pentose phosphate pathway flux (Fig 10A ii) and by the metabolism of citrate, a tricarboxylic acid (TCA) cycle intermediate (Fig 10A v) (O'Neill and Hardie 2013). Glutamine metabolism generates intermediate metabolites to fuel the TCA cycle (Fig 10A iv). The TCA cycle intermediate *cis*-aconitate (CAC) is converted into itaconic acid by the up-regulated immune-responsive gene 1 (IRG1) to generate also mitochondrial ROS (Fig 10A vi) (Michelucci et al. 2013). In order to protect themselves, M1 macrophages also generate the antioxidant glutathione (GSH) via pentose phosphate pathway flux (Fig 10A ii).

M2 state is energetically demanding and can be long-lasting. In contrast to M1 macrophages, M2 macrophages have low glycolysis rates but rely on oxidative metabolism, a pathway that provides sustained energy for tissue remodelling and repair. For this purpose, FAO and oxidative phosphorylation are increased in M2 macrophages (Fig. 10B i) (Biswas et al. 2012; Ghesquiere et al. 2014; O'Neill and Hardie 2013). IL4 induces M2 phenotype and up-regulates peroxisome proliferator-activated receptor gamma coactivator (PGC)1β, which enhance mitochondrial biogenesis and the switch to FAO (Vats et al. 2006). Carbohydrate kinase-like protein (CARKL) catalyses the formation of sedoheptulose-7-phosphate to inhibit pentose phosphate pathway flux (Fig. 10B iii) (Haschemi et al. 2012). Glutamine metabolism generates polyamines and TCA cycle intermediates (Fig. 10B ii). Finally, Arginase activity is potentiated instead of iNOS pathway (Fig. 10B iv) (Ghesquiere et al. 2014).

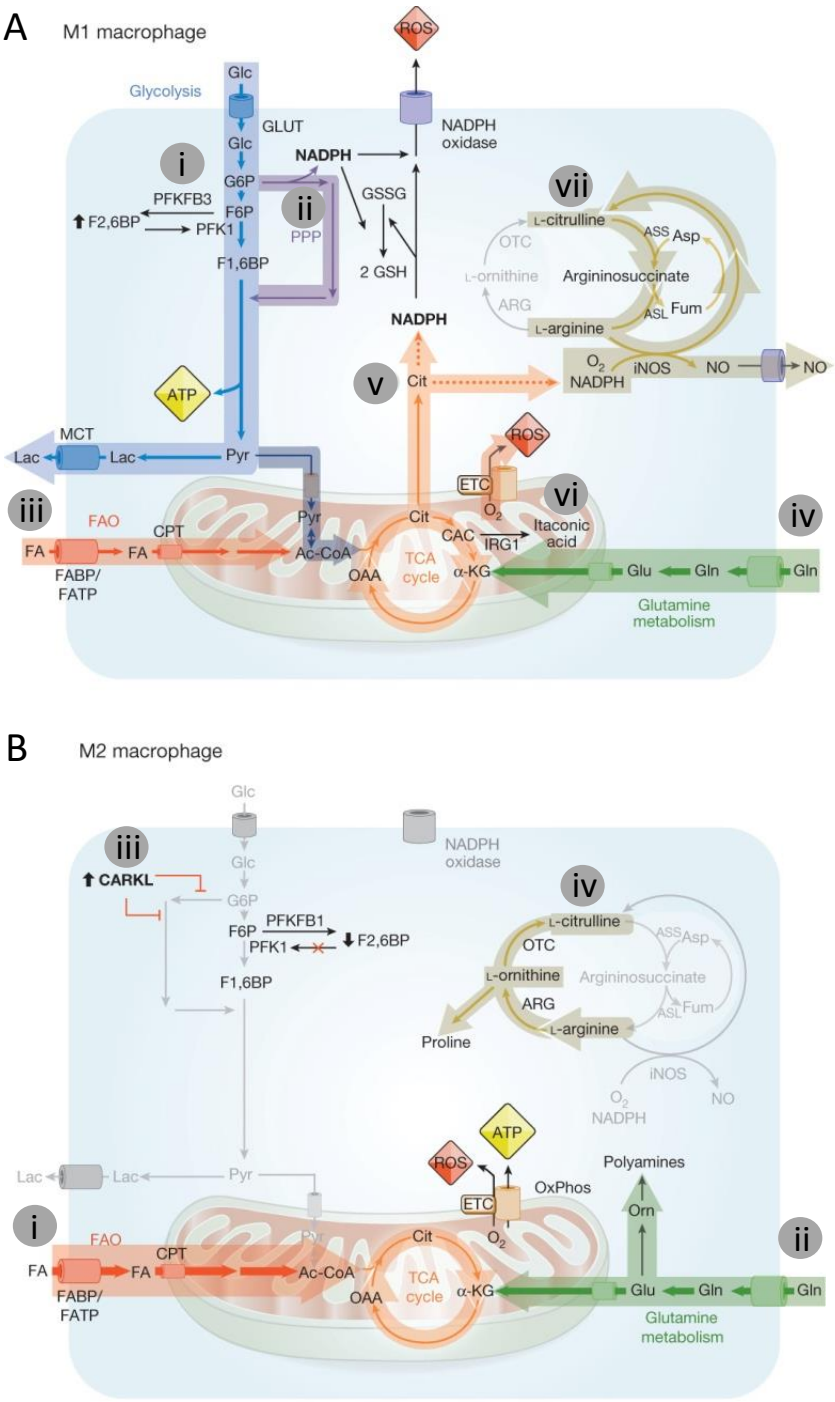

Figure 10. Macrophage metabolism. Metabolic reprogramming in M1 (**A**) and M2 (**B**) macrophages. Key steps are indicated in roman numerals. α-KG: α-ketoglutarate, Ac-CoA: acetyl-coenzyme A, ARG: arginase, ASL: argininosuccinate lyase; Asp: aspartate, ASS: argininosuccinate synthase, CARKL: carbohydrate kinase-like protein, Cit: citrate, CPT: carnitine palmitoyltransferase, GSH: reduced glutathione, ETC: electron transport chain, F1,6BP: fructose 1,6-bisphosphate, F2,6BP: fructose 2,6 bisphosphate, F6P: fructose 6-phosphate, FA; fatty acid, FABP: fatty acid binding protein; FAO: fatty acid oxidation, FATP: fatty acid transfer protein; Fum, fumarate; G6P, glucose 6-phosphate, Glc: glucose, Gln: glutamine, Glu: glutamate, GLUT: glucose transporter, GSSG: oxidized glutathione, iNOS: inducible nitric oxide synthase; IRG1: immunoresponsive gene 1, Lac: lactate, MCT: monocarboxylate transporter, NADPH, nicotinamide adenine dinucleotide phosphate, NO: nitric oxide, OAA: oxaloacetate, Orn: ornithine; OTC: ornithine transcarbamylase, OxPhos: oxidative phosphorylation, PFK1: phosphofructokinase-1, PFKFB1: 6-phosphofructo-2-kinase/fructose-2,6-bisphosphatase-1, PFKFB3: 6-phosphofructo-2-kinase/fructose-2,6-bisphosphatase-3, PPP: pentose phosphate pathway, Pyr: pyruvate, ROS: reactive oxygen species, TCA: tricarboxylic acid. From: Ghesquiere et al. 2014.

Most of the studies describing the metabolic changes during polarisation of immune cells have been performed in peripheral cells (O'Neill and Hardie 2013; Pearce and Pearce 2013) and little is known about metabolic states in microglial cells (Durafourt et al. 2012; Orihuela, McPherson, and Harry 2016; Moss and Bates 2001; Chenais, Morjani, and Drapier 2002; Bernhart et al. 2010; Volobоueva et al. 2013; Gimeno-Bayon et al. 2014; Sohn 2012). Similar to macrophages, microglial cells increase glycolysis rates after an M1 stimulus. However, after an M2 stimulus, mitochondrial oxygen consumption is not altered in microglial cells, in contrast to the increased mitochondrial oxidative metabolism reported in macrophages (Orihuela, McPherson, and Harry 2016). Furthermore, microglial cells are more reluctant to adopt an M2 phenotype than macrophages (Durafourt et al. 2012).

4 The CD200-CD200R1 system

Microglial activation is controlled by different mechanisms. Among them, the CD200-CD200R1 system constitutes an “off signal” to keep microglia in a surveillance state. In the CNS, the surface molecule CD200 is mainly expressed in neurons, astrocytes and oligodendrocytes (Barclay et al. 2002). Its receptor, CD200R1, is mainly expressed in macrophages including microglia. CD200-CD200R1 interaction leads to the inhibition of the production of pro-inflammatory signals in microglial cells (Hoek et al. 2000; Manich et al. 2019; Biber et al. 2007). Its powerful immunoregulatory functions confer to CD200-CD200R1 system an interesting potential to explore.

4.1 CD200 GENE IN MOUSE AND HUMAN

The mouse CD200 gene is located on chromosome 16, whereas the human CD200 gene is located on chromosome 3 (Wright et al. 2003). The CD200 gene is highly conserved across humans and rodents, showing a high degree of sequence and structural similarity (Borriello et al. 1998; Wright et al. 2003).

4.1.1 Mouse CD200 gene

In mice, the CD200 gene is composed of six exons and five introns and can generate two different transcripts by alternative splicing, termed full-length CD200 (CD200full) mRNA variant and truncated CD200 (CD200tr) mRNA variant (Chen et al. 2008; McCaughan, Clark, and Barclay 1987).

CD200full variant is considered the canonical transcript and it encodes de CD200full isoform. **CD200tr variant** is originated by alternative splicing and it lacks exon 2 (Fig. 11A Grey box). In 1998, Borriello and collaborators described that the absence of exon 2 results in a translation frameshift and a premature stop codon 10 nt from the 5' end of exon 3 (Fig. 11A Red box) (Borriello et al. 1998). They concluded that the resulting transcript would originate a translated product of only 7 amino acids and therefore, unlikely to be a functional protein (Fig. 11A Orange box) (Borriello et al. 1998). However, Chen and collaborators carried out a detailed examination of the cDNA sequence and revealed the existence of another consensus Kozak start sequence 116 nt downstream of this stop codon (Fig. 11A Blue box), which corrects the frameshift from the alternative splicing and results in the expression of an N-terminal deleted truncated protein, the CD200tr (Fig. 11A) (Chen et al. 2008; Chen et al. 2010). Despite missing the N-terminal, CD200tr has the same frameshift as CD200full. Therefore, CD200tr protein has the same protein structure as CD200full protein but it lacks the N-terminal region.

4.1.2 Human CD200 gene

In humans, CD200 gene can generate ten different transcripts by alternative splicing, termed CD200 variant 1 to 10, according to the NCBI database (May 2019). On the one hand, two of the CD200 mRNA variants are termed truncated CD200 (CD200tr) mRNA variants for the analogy to mouse CD200tr mRNA variant (Fig. 11). Human CD200tr protein lacks the N-terminal region, as in mice. On the other hand, eight of the CD200 mRNA variants are termed full-length CD200 (CD200full) mRNA variants (Borriello et al. 1998; Chen et al. 2008; McCaughan, Clark, and Barclay 1987). There are no studies regarding the possible functional relevance of each CD200full and CD200tr variant.

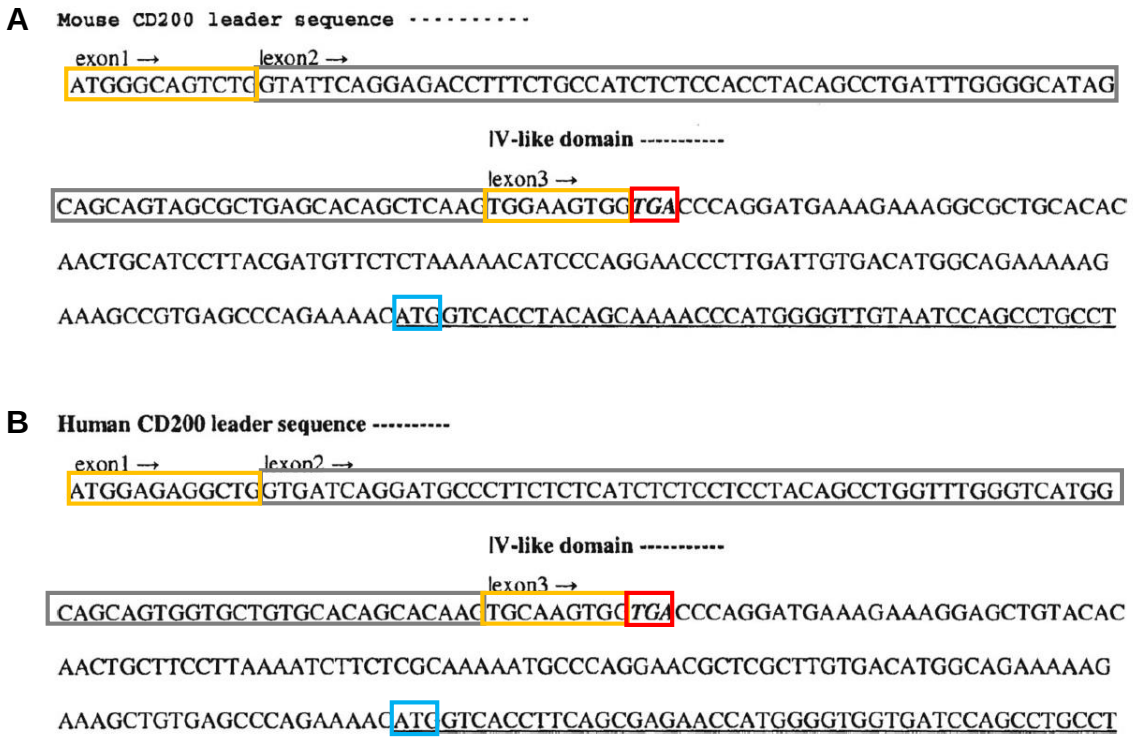

Figure 11. Murine and human CD200 cDNA sequence. Representation of murine (**A**) and human (**B**) CD200full cDNA corresponding to the initial region of the coding sequence (CDS). Notice that the completed CDS is not represented, as the 3' end of exon 3, as well as exons 4 and 5 are not shown (exon 6 is not part of the CDS). Colour boxes highlight important regions in the generation of CD200tr. **Orange box:** sequence encoding a 7 amino acids peptide unlikely to be functional, generated when exon 2 is missing by alternative splicing in the production of CD200tr. **Grey box:** exon 2, spliced in CD200tr. **Red box:** premature stop codon 10 nt from the 5' end of exon 3 (the V-region). **Blue box:** consensus Kozak start sequence 116 nt downstream of the stop codon. Underlined: sequence codifying N-terminal deleted truncated protein, CD200tr. Modified from: Chen et al. 2008.

4.2 CD200 PROTEIN STRUCTURE

Comparing the murine CD200 protein with the rat or human CD200 protein homologs reveals 92-100% (Clark et al. 1985) and 71-79% (McCaughan, Clark, and Barclay 1987) overall conservation, respectively. This high degree of homology between mouse, rat and human CD200 proteins, suggests conservation of function (Walker and Lue 2013). Remarkably, CD200 has a high content of potential N-linked glycosylation sites, both in mouse and human (Khatri 2012).

Mouse and human CD200full

CD200full, previously known as OX2, is a ~32 kDa type-1 transmembrane-anchored glycoprotein with two immunoglobulin superfamily domains arranged in a typical V/C2 set with an extracellular domain composed by the N-terminal tail, a transmembrane domain and a short cytoplasmic domain (Clark et al. 1985; McMaster and Williams 1979) (UniProtKB - P41217 and UniProtKB - O54901). CD200full is devoid of any known intracellular signalling motifs and is a ligand for CD200R1 (Preston et al. 1997; Wright et al. 2000). In humans, eight mRNA variants of CD200full are described in the NCBI database, but only three protein isoforms have been described so far (UniProtKB - P41217).

Mouse and human CD200tr

CD200tr is a transmembrane protein lacking part of the N-terminal region of the CD200full isoform. The N-terminal region is important for the interaction with CD200R1. In consequence, CD200tr binds to CD200R1 but it blocks CD200full function in a competitive fashion, making CD200tr a physiologic antagonist of CD200full (Chen et al. 2008; Chen et al. 2010).

Mouse and human sCD200

A soluble form of CD200 (**sCD200**) has also been described in mouse serum (Gorczynski et al. 2010) and in human plasma (Wong et al. 2012; Wong et al. 2010). Although the structure and function of mouse sCD200 are not clear, it is suggested to be generated by proteolytic cleavage of cell surface CD200 (Gorczynski et al. 2013) and to have an immunosuppressive function (Gorczynski et al. 2013). In humans, sCD200 is also thought to be generated by proteolytic cleavage of cell surface CD200, as in mice (Wong et al. 2012; Wong et al. 2010). Although it is able to signal through CD200R1 (Wong et al. 2016), its function is unclear. It is suggested to have

immunosuppressive functions, especially in cancer (Kacerovsky et al. 2013; Wong et al. 2012; Wong et al. 2010), but also to promote inflammation in skin and allergic diseases (Akman-Karakas et al. 2014; Tural Onur et al. 2015). However, little is known about the presence of sCD200 in the brain. Previous reports in mouse and human suggest a localization for CD200 in the brain exclusively in membranes (Costello et al. 2011; Walker et al. 2009; Walker and Lue 2013).

Human CD200$_{c\text{-}tail}$

In humans, the cleavage of the cytoplasmic tail of CD200 by a consensus γ-secretase generating the human **CD200$_{c\text{-}tail}$**, has recently been described. CD200$_{c\text{-}tail}$ translocates to the nucleus and binds to DNA regions encoding transcription factors implicated in the regulation of cell proliferation in human chronic lymphocytic leukemia cells (Chen et al. 2018). CD200$_{c\text{-}tail}$ may be important in cancer growth; however, whether it has also implications in non-cancer cells including neurons, astrocytes or B and T cells, remains to be elucidated (Chen et al. 2018).

Table 1. CD200 gene, proteins and function in *Mus musculus*.

Species: *Mus musculus*		
Gene	**Protein**	**Function**
CD200 (Borriello et al. 1998)	**CD200full** (Borriello et al. 1998)	Ligand of CD200R1 (Preston et al. 1997).
	CD200tr Generated by alternative mRNA splicing. (Chen et al. 2008).	Ligand of CD200R1 (Chen et al. 2008).
	sCD200 Generated probably by protein cleavage (Gorczynski et al. 2013; Gorczynski et al. 2010).	Immunosuppressive (Gorczynski et al. 2013).

Table 2. CD200 gene, proteins and function in *Homo sapiens.*

Species: *Homo sapiens*		
Gene	**Protein**	**Function**
CD200 (McCaughan, Clark, and Barclay 1987)	**CD200full** (McCaughan, Clark, and Barclay 1987)	Ligand of CD200R1 isoform 4 (Vieites et al. 2003).
	CD200tr Generated by alternative mRNA splicing (Chen et al. 2008).	Ligand of CD200R1 isoform 4 (Chen et al. 2008).
	sCD200 Generated by protein cleavage (Wong et al. 2010, 2012, 2016).	Unclear (Akman-Karakas et al. 2014; Kacerovsky et al. 2013; Wong et al. 2010).
	CD200$_{c\text{-}tail}$ Generated by protein cleavage. (Chen et al. 2018).	Cancer growth (Chen et al. 2018).

4.3 CD200R GENE FAMILY IN MOUSE AND HUMAN

CD200 receptor (CD200R) family is a paired receptor family. Paired receptors are families of membrane proteins that are characterized by i) being encoded by different genes, but located as a gene cluster on a given chromosome, ii) having similar extracellular regions, iii) being expressed on overlapping immune populations, and iv) being conformed by members with activating potential and also members with inhibitory potential (Yamada and McVicar 2008). Although their extracellular regions typically have about 90% amino acid sequence identity, paired receptors can produce opposite type of signalling due to different cytoplasmic regions or to different ligand specificities.

Mouse CD200R gene family

The mouse CD200R family is located as a gene cluster on chromosome 16 region B5, within ~400 kbp of the CD200 gene (Fig. 12) (Gorczynski, Chen, Clark, et al. 2004). The mouse CD200R family is composed by one inhibitory member termed CD200R1, and five members termed CD200R-like a, (CD200RLa), CD200R-like b (CD200RLb), CD200R-like c (CD200RLc), CD200R-like d (CD200RLd) (Wright et al. 2003) and CD200R-like e (CD200RLe) (Hatherley et al. 2005). CD200RLd is presumably a pseudogene (Wright et al. 2003). CD200RLa,b,c,e are also termed CD200R4,3,2,5 as synonyms, respectively (Gorczynski, Chen, Kai, et al. 2004). Most of the authors use the nomenclature “RL” meaning “receptor-like” rather than “R” meaning “receptor” because they are not considered receptors for CD200 (Hatherley et al. 2005; Hatherley et al. 2013; Wright et al. 2003)

CD200R1 is a receptor for CD200 and the binding leads to an inhibitory transduction signal (Preston et al. 1997; Wright et al. 2000). Gorczynski and collaborators had reported that all members of CD200R family described until then (CD200R1, CD200La,b,c) could bind to CD200 ligand (Gorczynski, Chen, Clark, et al. 2004); however, this was later rejected (Hatherley et al. 2005; Hatherley et al. 2013; Wright et al. 2003).

The ligands of CD200RLa, CD200RLb, CD200Lc and CD200RLe are unknown but pathogen components are a possibility (Hatherley et al. 2005). There are contradictory data regarding whether CD200RLc binds to CD200 ligand (Hatherley et al. 2013; Hayakawa, Wang, and Lo 2016; Khatri 2012). The functional and biological significance of these receptors remains unknown. CD200RLa and CD200RLb products pair with the adaptor protein, DAP12, and are expected to cause an activating signal transduction, in contrast to the inhibitory signal produced by CD200R1 (Wright et al. 2003; Voehringer, Shinkai, and Locksley 2004). CD200RLc and CD200RLe are predicted to be associated with DAP12 creating also the potential for activating signal transduction (Hatherley et al. 2005).

Whereas CD200R1 gene is detected in all mouse strains analysed (Akkaya and Barclay 2010), most mouse strains have only three of the CD200R activating genes, either the combination of CD200RLa, Lb and Lc or CD200RLa, Lb and Le. The CD200RLc and CD200RLe genes are mutually exclusive (Akkaya and Barclay 2010). CD200RLe is found in CD1 and NOD1 mouse strains but not in CD57B/L6 (Voehringer, Shinkai, and Locksley 2004).

Human CD200R family

The human CD200R gene family is located on chromosome 3 (Fig. 12) (Gorczynski, Chen, Clark, et al. 2004) and is composed by one inhibitory member termed CD200R1, and one member termed CD200R-like a (CD200RLa) (Wright et al. 2003) or as a synonym CD200R2 (Gorczynski, Chen, Kai, et al. 2004). CD200R1 and CD200La are located as a gene cluster on chromosome 3q12-13 (Fig. 12) (Vieites et al. 2003). CD200La might be a non-functional gene, as no expression have been detected (Wright et al. 2003).

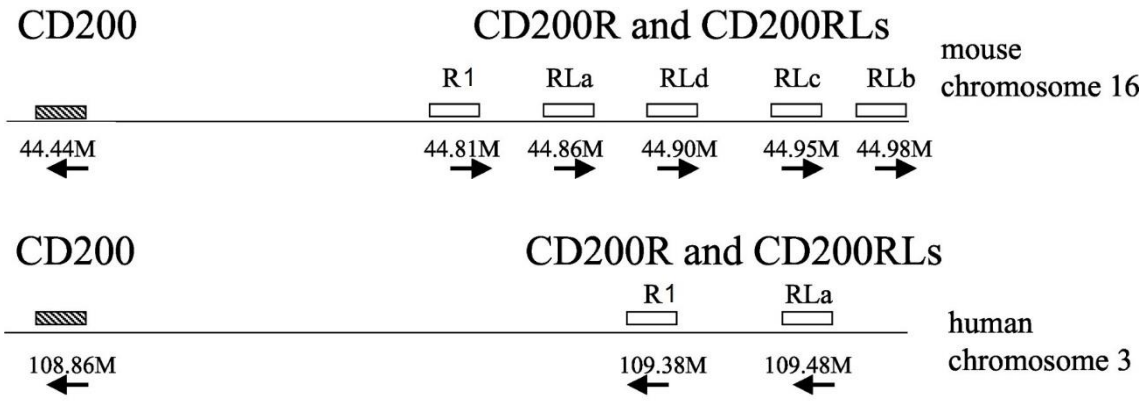

Figure 12. Organization of CD200 and CD200R genes in the mouse and human genomes. The approximate position on the genome of CD200, CD200R1, CD200RLa, CD200RLb, CD200RLc and CD200RLd genes is shown as oblongs. The numbers indicate the bases and the arrows the direction of transcription. From: Wright et al. 2003. CD200RLe is not shown because it was described later by Hatherley and collaborators (Hatherley et al. 2005).

The CD200R gene is highly conserved across humans and rodents (Wright et al. 2003). CD200R family members have been generated by extensive gene duplication of the CD200R gene (Wright et al. 2003).

4.3.1 Human CD200R1 gene

In humans, the inhibitory receptor CD200R1 gene comprises nine exons and can generate four different transcripts by alternative splicing, termed CD200R1 variant 1 (V1 CD200R1), variant 2 (V2 CD200R1), variant 3 (V3 CD200R1) and variant 4 (V4 CD200R1) (Fig. 13). Alternative splicing involves i) the insertion of exon 5 which creates a frameshift leading to a premature stop codon that produces mRNA variants encoding soluble proteins and/or ii) splicing of exon 2 which

produces the deletion of 23 amino acids. The insertion of exon 5 is observed in variants 2 and 3. The splicing of exon 2 is observed in variants 3 and 4 (Fig. 13) (Vieites et al. 2003).

In this way, the mRNA termed **V1 CD200R1** is composed by exons 1, 2, 3, 4, 6, 7, 8 and 9 (exon 5 functions as an intron in this variant), and encodes a transmembrane protein named CD200R1 isoform 1. When insertion of exon 5 occurs, the resulted mRNA is termed **V2 CD200R1** and it is composed by exons 1, 2, 3, 4, 5 and 6, and encodes a soluble protein named CD200R1 isoform 2. When both insertion of exon 5 and splicing of exon 2 occur, the resulting mRNA is termed **V3 CD200R1** and it is composed by exons 1, 3, 4, 5 and 6 and encodes a soluble protein named CD200R1 isoform 3. When only splicing of exon 2 occurs, the resulted mRNA is termed **V4 CD200R1** and it is composed by exons 1, 3, 4, 6, 7, 8 and 9 and encodes a transmembrane protein named CD200R1 isoform 4 (Fig. 13) (Vieites et al. 2003).

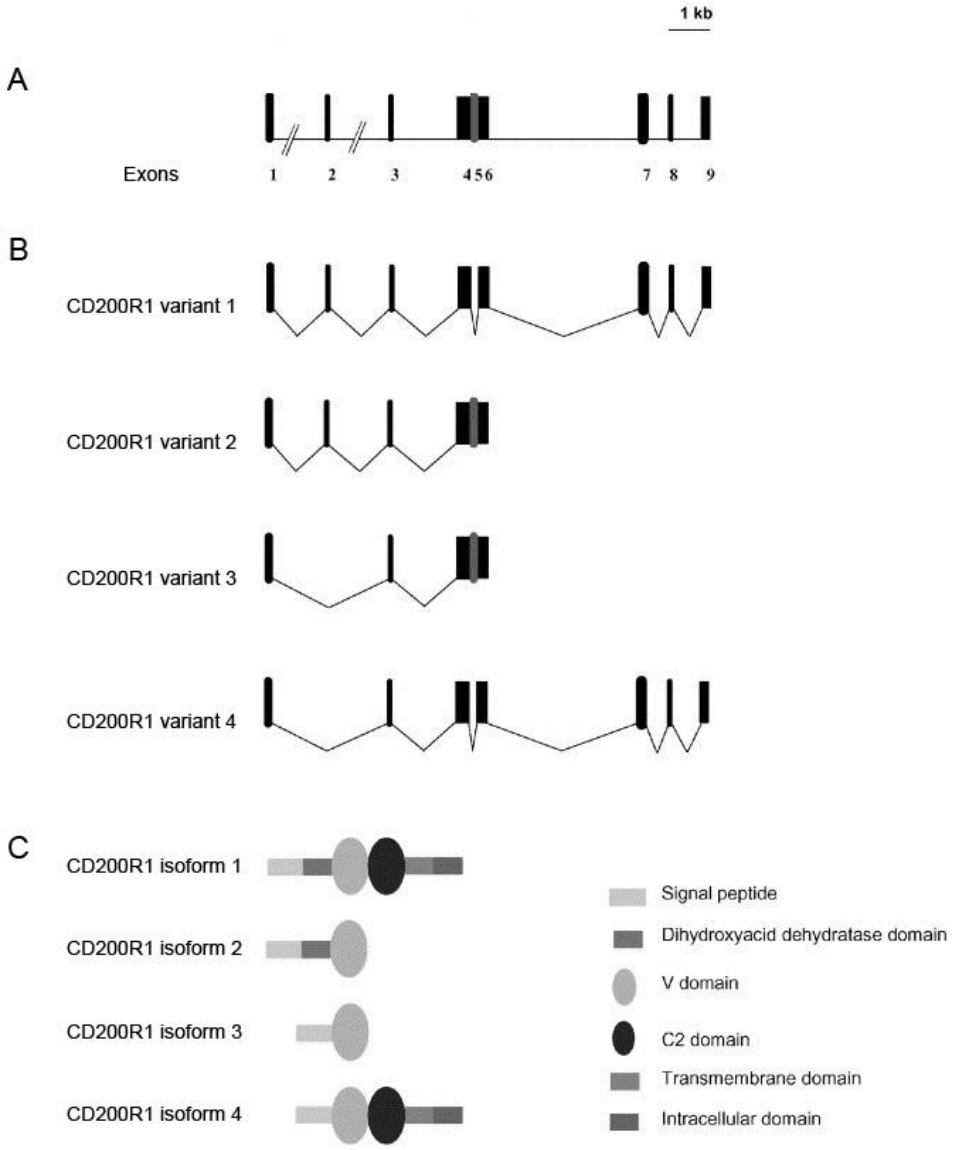

Figure 13. Genomic organization, splicing pattern and protein structure of human CD200R1. A Genomic structure of the human CD200R1 gene. Exons are depicted on scale as black boxes and introns as thin lines. **B** The mRNA variants produced by the human CD200R gene. Exon 5 functions as an intron (thin line) or exon (grey box). **C** Domain structure of CD200R1 isoforms. Modified from Vieites et al. 2003.

Since this thesis is focused on CD200R1, I have dedicated the next sections to this protein.

4.4 CD200R1 PROTEIN STRUCTURE

In mice, **CD200R1** protein (~35 kDa UniProtKB - Q9ES57) is a type I transmembrane-anchored glycoprotein with an extracellular domain composed by the N-terminal tail, a transmembrane domain and a cytoplasmic domain, containing two immunoglobulin superfamily domains in a V/C2 set arrangement.

In humans, **CD200R1 isoform 4** (~36.6 kDa, UniProtKB - Q8TD46) is the canonical sequence. It has a 52% amino acid sequence identity with mouse CD200R1 (Vieites et al. 2003). CD200R1 isoform 4 is also a transmembrane glycoprotein with an extracellular domain composed by the N-terminal tail, a transmembrane domain and a cytoplasmic domain, containing two immunoglobulin fold-family domains in a typical V/C2 set arrangement. It has a peptide cleavage site between positions 24-25 and nine potential N-linked and one potential O-linked glycosylation sites (Vieites et al. 2003).

Both in mouse and human, CD200 has a minimal cytoplasmic domain and does not activate an intracellular signalling pathway. In contrast, CD200R1 has a larger cytoplasmic domain and is capable of down-regulating the activity of the immune system (Walker and Lue 2013).

In humans, apart from CD200R1 isoform 4, three more CD200R1 isoforms exist:

CD200R1 isoform 1 (~39 kDa, UniProtKB - Q8TD46) is encoded by human V1 CD200R1 mRNA. V1 CD200R1 has the same mRNA sequence as V4 CD200 except for the presence of exon 2. Exon 2 encodes 23 amino acids at position 23 of the protein, which are not present in mouse CD200R1. These amino acids generate a putative dihydroxyacid dehydratase domain in CD200R1 isoform 1. However, structural evidence suggests that CD200R is not a dihydroxyacid dehydratase enzyme. The implications of this domain are unknown, whether it allows the binding to CD200 ligand remains to be elucidated and thus, the function of CD200R1 isoform 1 has not been described (Vieites et al. 2003).

CD200R1 isoform 2 and isoform 3 (~21.3 kDa and ~18.8 kDa, respectively, UniProtKB - Q8TD46) are soluble proteins found in humans. This is a unique feature of human CD200R gene expression, as soluble CD200R1 proteins are not described in mouse. The function of soluble CD200R1 isoforms 2 and 3 is unknown (Vieites et al. 2003). In this regard, CD200R1 isoform 3 might bind to CD200 ligand blocking its function. In contrast, CD200R1 isoform 2 contains the 23 amino acids encoded by exon 2, and it is not known whether it binds to CD200 ligand.

Kos and collaborators reported a soluble form of CD200R1 (**sCD200R1**) in human plasma (Kos et al. 2014). This soluble form could correspond to the soluble CD200R1 isoform 2 or 3; however, it could also be generated from the cleavage of the transmembrane CD200R1 isoform 1 or 4. Neither the origin nor the function of this soluble form of CD200R1 are known.

A remarkable feature of CD200R1, as in the case of CD200, is the high content of potential N-linked glycosylation sites, both in mouse and human (Khatri 2012).

Table 3. CD200R family genes, proteins, function and receptor ligands in *Mus musculus*.

Species: *Mus musculus*			
Gene	**Protein**	**Function**	**Ligand**
CD200R1 (Wright et al. 2003)	**CD200R1** (Preston et al. 1997; Wright et al. 2003)	Inhibitor (Wright et al. 2000).	CD200full CD200tr (Preston et al. 1997).
CD200RLa = CD200R4 (Wright et al. 2003)	**CD200RLa = CD200R4** (Wright et al. 2003)	Activator (Voehringer, Shinkai, and Locksley 2004; Wright et al. 2003).	Unknown
CD200RLb = CD200R3 (Wright et al. 2003)	**CD200RLb = CD200R3** (Wright et al. 2003)	Activator (Voehringer, Shinkai and Locksley 2004; Wright et al. 2003).	Unknown
CD200RLc = CD200R2 (Wright et al. 2003)	**CD200RLc= CD200R2** (Wright et al. 2003)	Probably activator (Hatherley et al. 2005).	Unclear (Hatherley et al. 2013; Khatri 2012; Hatherley et al. 2005).
CD200RLd (Wright et al. 2003)	Pseudogene (Wright et al. 2003).		
CD200RLe = CD200R5 (Hatherley et al. 2005)	**CD200RLe = CD200R5** (Hatherley et al. 2005)	Probably activator (Hatherley et al. 2005).	Unknown

Table 4. CD200R family genes, proteins, protein function and receptor ligands in *Homo sapiens*.

Species: *Homo sapiens*			
Gene	**Protein**	**Function**	**Ligand**
CD200R1 (Vieites et al. 2003; Wright et al. 2003)	**CD200R1 isoform 1** (Vieites et al. 2003) **CD200R1 isoform 2** (Vieites et al. 2003) **CD200R1 isoform 3** (Vieites et al. 2003) **CD200R1 isoform 4** (Vieites et al. 2003)	Unknown Unknown Unknown Inhibitory (Vieites et al. 2003)	Unknown Unknown Unknown CD200full and CD200tr (Vieites et al. 2003)
	sCD200R1 Unknown origin; it could be CD200R1 isoform 2 or 3, or generated by cleavage of CD200R1 isoform 1 or 4. (Kos et al. 2014).	Bone loss marker (Kos et al. 2014)	
CD200RLa = **CD200R2** (Wright et al. 2003)	Pseudogene (Wright et al. 2003).		

4.5 CELLULAR CD200 AND CD200R1 EXPRESSION

CD200 is highly expressed in neurons but also in endothelial cells, astrocytes and oligodendrocytes, dendritic cells, thymocytes, T and B lymphocytes, osteoblasts and trophoblasts (Lee et al. 2006; Webb and Barclay 1984; Dick et al. 2001; Rosenblum et al. 2004; Dorfman and Shahsafaei 2011; Clark et al. 2003; Koning et al. 2009). In the brain, CD200 expression is widespread with higher levels in grey matter than in white matter (Webb and Barclay 1984). In physiological conditions, CD200tr is expressed in brain but at very low levels (almost negligible) compared with CD200full (Chen et al. 2008); however, CD200tr expression can increase in pathological conditions (Moertel et al. 2014; Valente et al. 2017).

CD200R1 expression is restricted to myeloid cells: dendritic cells, mast cells, eosinophils, basophils, neutrophils, macrophages, lymphoid cells (T, B cells, natural killer) and osteoclasts (Kos et al. 2014; Lee et al. 2006; Masocha 2009; Rijkers et al. 2008; Wright et al. 2003). In the CNS, CD200R1 expression has been reported mainly in microglia. There are two publications from the same research group showing CD200R1 expression in astrocytes and oligodendrocytes in mouse but at levels much lower than that of microglial CD200R1 (Chitnis et al. 2007; Liu et al. 2010).

4.6 CD200 AND CD200R1 INTERACTION AND FUNCTION IN THE CNS

4.6.1 CD200 and CD200R1 signalling

Both CD200full and CD200tr bind CD200R1 but whereas CD200full produces the activation of a signalling pathway, CD200tr does not (Chen et al. 2008; Chen et al. 2010; Clark et al. 1985; McMaster and Williams 1979). In the text below the function of CD200R1 signalling pathway is described and the term CD200 is used to refer to CD200full.

CD200 interacts with CD200R1 in adjacent cells. Unlike most of the inhibitory receptors, CD200R1 does not contain ITIM motifs (Daeron et al. 2008; Mihrshahi and Brown 2010). In the cytoplasmic region, CD200R1 contains three tyrosine residues, the most distal tyrosine residue being part of an NPxY motif which is able to interact with PTB domains (Fig. 14) (Wright et al. 2000). The binding of CD200 to CD200R1 results in the phosphorylation of these tyrosine residues in CD200R1. Dok2 binds to the third phosphotyrosine in the cytoplasmic tail of CD200R1 via its PTB domain. Then, Dok2 is phosphorylated and recruits, through an SH2 (Src homology2) domain, the Ras/GAP (Ras GTPase-activating protein), which suppresses Ras-ERK (Ras-extracellular signal-regulated kinases) and Ras-PI3K (Ras-phosphoinositide 3-kinases) signalling pathways. This results in the inhibition of macrophage activation, the decrease in iNOS activity and the down-regulation of the synthesis of pro-inflammatory cytokines such as TNFα, IFNγ, IL1,

IL17, IL6, IL8, IP10 (IFNγ-induced protein 10 kDa) and MIG (monokine induced by IFNγ) (Fig. 14). A down-regulation of NF-κB presumably contributes to CD200R1-inhibition of pro-inflammatory signals, although other pathways may be involved (Fig. 14) (Holmannova et al. 2012; Jenmalm et al. 2006; Lyons et al. 2012; Mihrshahi, Barclay, and Brown 2009; Mihrshahi and Brown 2010; Walker and Lue 2013; Zhang et al. 2004; Manich et al. 2019). Dok1 negatively regulates Dox2-mediated CD200R1 signalling through the recruitment of CrkL (CT10 sarcoma oncogene cellular homologue-like) (Fig. 14) (Mihrshahi and Brown 2010).

In the CNS, CD200 and CD200R1 expression is regulated by the transcription factors C/EBPβ (CCAAT/enhancer-binding protein β) and PPARγ (peroxisome proliferator-activated receptor γ), both involved in inflammatory processes (Dentesano et al. 2014; Dentesano et al. 2012; Hayakawa, Wang, and Lo 2016; Frank et al. 2018). Moreover, CD200 treatment induces the mRNA expression of CD200R1 in microglia *in vitro* (Varnum et al. 2015).

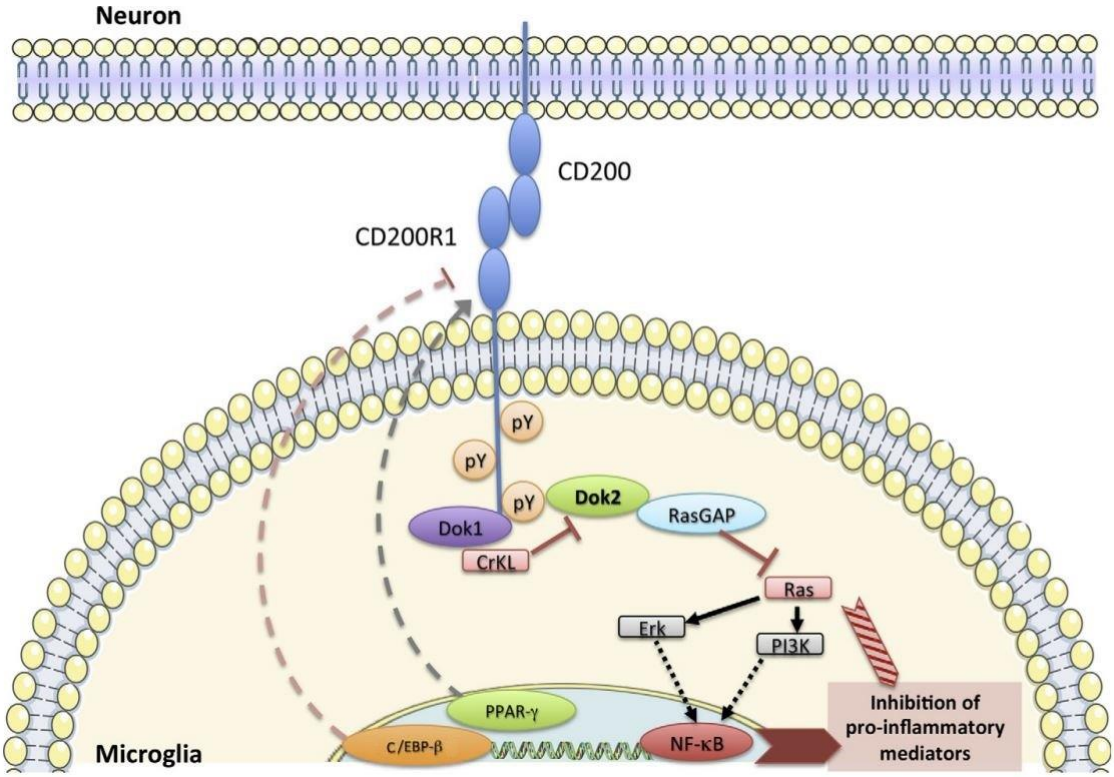

Figure 14. Intracellular signalling pathway after CD200-CD200R1 interaction. When CD200 binds CD200R1, Dok2 is phosphorylated leading to the inhibition of Ras-PI3K and Ras-ERK pathways which results in inhibition of pro-inflammatory signals, presumably through the down-regulation of NK-κB. Dok1 negatively regulates CD200R1-signaling through CrkL. C/EBPβ and PPARγ control the expression of CD200R1. C/EBPβ: CCAAT/enhancer-binding protein-β, CrkL: CT10 sarcoma oncogene cellular homologue-like, NF-κB: nuclear factor kappa-light-chain-enhancer of activated B cells, PPARγ: peroxisome proliferator-activated receptor γ, PI3K: phosphoinositide 3-kinases, Ras-ERK Ras-extracellular signal-regulated kinases, Ras-PI3K Ras-phosphoinositide 3-kinases. From: Manich et al. 2019.

4.6.2 CD200 and CD200R1 functions

Some authors refer to the inhibitory CD200 receptor as CD200R instead of CD200R1. We have maintained this nomenclature when we have cited their work. Similarly, CD200full and CD200tr are not distinguished in some reports and we have referred as “CD200” in these cases.

In the CNS, the best characterized function of the CD200-CD200R1 system is the inhibition of the pro-inflammatory microglial activation, especially in the presence of LPS or IFNγ (Copland et al. 2007; Costello et al. 2011; Cox et al. 2012; Denieffe et al. 2013; Meuth et al. 2008). Furthermore, the inhibition of CD200-CD200R1 interaction produces microglial priming by increasing the expression of PAMP and DAMP receptors (Costello et al. 2011; Deckert et al. 2006; Denieffe et al. 2013; Hoek et al. 2000), which leads to a more disinhibited and vigilant microglial phenotype that will produce an exacerbated response to a secondary inflammatory stimulus (Perry and Holmes 2014). Aging, peripheral immune challenges as well as chronic neurodegenerative diseases have been related to primed microglia (Perry and Holmes 2014).

Under inflammatory conditions, potentiation of CD200-CD200R1 interaction is also associated with down-regulation of antigen-presenting capacity (Cox et al. 2012; Liu et al. 2010), inhibition of microglial migration (Carter and Dick 2004) and contradictory data have been found regarding phagocytosis (Bilkei-Gorzo 2014; Varnum et al. 2015; Lyons et al. 2017). In homeostatic conditions, stimulation of CD200-CD200R interaction does not modify microglial migration (Carter and Dick 2004) and the link between the CD200-CD200R1 system and the capability of antigen-resenting, phagocytosis and proliferation is unclear (Costello et al. 2011; Deckert et al. 2006; Denieffe et al. 2013; Broderick et al. 2002).

As a consequence of its inhibitory effect on pro-inflammatory microglial activation, CD200-CD200R1 interaction confers tissue protection. Neuroprotective effects of the potentiation of CD200-CD200R interaction have been described *in vitro* (Meuth et al. 2008; Yi et al. 2016) and *in vivo* in multiple sclerosis (Chitnis et al. 2007), optic nerve crush (Huang et al. 2018) and uveoretinitis (Banerjee and Dick 2004) experimental models. Furthermore, CD200-CD200R1 interaction also participates in tissue repair and homeostasis recovery after injury (Lago et al. 2018; Mecha et al. 2013; Hernangomez et al. 2012; Procaccini et al. 2015; Cohen et al. 2017) and CD200 treatment enhances the expression of glial cell-derived neurotrophic factor (GDNF) and promotes neuronal maturation *in vitro* (Varnum et al. 2015). Some studies show the capability of CD200 to bind to the fibroblast growth factor receptor (FGFR) and have neuritogenic and survival-promoting effects (Pankratova et al. 2016; Turner et al. 2016). In addition, FGFR activation inhibits inflammation and it is associated with an increased CD200 expression (Cox et al. 2012).

The CD200-CD200R1 interaction also promotes a pro-reparative microglial activation. For instance, potentiation of the CD200-CD200R1 system increases IL10 and decreases IL6 expression in *in vivo* nerve injury and multiple sclerosis experimental models (Chitnis et al. 2007; Hernangomez et al. 2016; Huang et al. 2018). Also, the suppression of CD200 expression decreases the expression of the pro-reparative markers IL4R, dectin and MR after spinal cord injury (Cohen et al. 2017) and prevents the induction of an anti-inflammatory phenotype upon IL4 treatment *in vitro* (Yi et al. 2016).

Although inhibition of the pro-inflammatory response is the most studied effect of the CD200-CD200R1 system, the CD200R1-signalling also induces the expression of the anti-inflammatory markers IL10 and Arg1 in microglial cells (Yi et al. 2016; Hernangomez et al. 2012). After the anti-inflammatory IL4 stimulus, there is an up-regulation of CD200 expression in neurons (Lyons et al. 2007; Lyons et al. 2009; Varnum et al. 2015; Yi et al. 2012). In contrast, contradictory effects have been reported regarding the up-regulation of neuronal CD200 expression after IL10 stimulation (Hernangomez et al. 2014; Hernangomez et al. 2012; Varnum et al. 2015). With regard to CD200R expression, up-regulation after IL4 or IL13 treatment has been reported in human (Koning et al. 2009; Walker et al. 2009) but not in mouse (Koning et al. 2009; Yi et al. 2016) microglia.

Another function for CD200-CD200R interaction is the contribution to CNS development (Shrivastava, Gonzalez, and Acarin 2012). Thus, the CD200-CD200R system has been suggested to play a role during development in synapse formation and refinement process, axogenic sprouting and elongation, spine density and migration of myeloid precursors (Bartolome, Ibanez-Olias, and Gil-Loyzaga 2002; Loh et al. 2016; Shrivastava, Gonzalez, and Acarin 2012). These processes are known to be regulated by microglial cells. During development, the CD200R1 mRNA expression in the mouse brain increases with time reaching a peak at the first week postnatal and decreases progressively until the low levels found in the adult brain (Manich et al. 2019). In contrast, CD200 mRNA expression is kept at moderate levels throughout adulthood (Manich et al. 2019).

4.7 CD200 AND CD200R1 IN AGING AND AUTOIMMUNE DISEASES

Aging is characterised by an enhancement of the pro-inflammatory environment in the brain. Although microglial CD200R expression is preserved in aging, CD200 expression in neurons progressively decreases, which suggest an involvement of this system in the establishment of age-related neuroinflammation (Cao et al. 2010; Frank et al. 2006; Cox et al. 2012; Walker et al. 2009; Wang et al. 2011). In addition, decreased CD200 expression in aging has been related with alterations in neuronal function (Cox 2012, Ojo 2012) and the potentiation of the CD200-CD200R1 system in aged animals results in reduced neuroinflammation (Cox et al. 2012).

Because of its immunoregulatory function, the CD200-CD200R1 system plays a role in autoimmune diseases and its potentiation displays a protective effect and ameliorates the symptomatology and the tissue preservation (Manich et al. 2019). In experimental models of multiple sclerosis (Chitnis et al. 2007; Hoek et al. 2000; Liu et al. 2010; Meuth et al. 2008; Valente et al. 2017; Hernangomez et al. 2012), uveoretinitis (Broderick et al. 2002; Banerjee and Dick 2004; Copland et al. 2007) and rheumatoid arthritis (Gorczynski et al. 2002; Hoek et al. 2000) CD200-CD200R1 modulation modifies the course and severity of the disease. Furthermore, CD200-CD200R1 modulation not only exerts its effect on microglia/macrophages but also on peripheral immune cell infiltration in EAE and autoimmune uveoretinitis experimental models (Banerjee and Dick 2004; Chitnis et al. 2007; Copland et al. 2007; Hoek et al. 2000; Liu et al. 2010; Meuth et al. 2008; Broderick et al. 2002).

4.8 CD200 AND CD200R1 IN NEURODEGENERATIVE DISEASES

While the contribution of the CD200-CD200R1 system to autoimmune diseases is well established, this is still a current issue of study in neurodegenerative diseases. Age is the major risk factor for PD and Alzheimer's disease and aging has been related to neuroinflammation, that can be modulated by the CD200-CD200R1 system (Cox et al. 2012). Therefore, the CD200-CD200R1 system may also play a role in the neuroinflammation observed in PD (Tansey and Goldberg 2010; Wang, Liu, and Zhou 2015) and Alzheimer's disease (Calsolaro and Edison 2016; Heneka et al. 2015). Furthermore, in the SN (Wang et al. 2011) and hippocampus (Walker et al. 2009), the most affected areas in PD and Alzheimer's disease, respectively, decreased CD200 expression has been observed in aged mice.

Regarding Alzheimer's disease, hippocampus and inferior temporal gyrus of Alzheimer's disease patients have decreased CD200 and CD200R expression (Walker et al. 2009). Moreover, activation of the CD200-CD200R1 system in Alzheimer's disease experimental models has shown a reduction in neuroinflammation, hippocampal amyloid β-plaque accumulation and restoration of neurogenesis (Lyons et al. 2012; Varnum et al. 2015).

In contrast, in experimental models of amyotrophic lateral sclerosis, a disease where neuroinflammation is also present (Liu and Wang 2017), an up-regulation of CD200R1 mRNA expression from pre-symptomatic stages has been observed (Chen et al. 2004), suggesting a different contribution of the CD200-CD200R1 system in this pathology. Patients diagnosed with neurovascular age-related macular degeneration have a higher proportion of CD11b+/CD200+ monocytes in the blood. This has been suggested to be a peripheral mechanism to attenuate central microglial activation and it highlights the importance of peripheral-central immune communication (Singh et al. 2013)

4.8.1 CD200 and CD200R1 in Parkinson's disease

Due to the presence of neuroinflammation in PD, it has been proposed that the CD200-CD200R1 system may play a role in its pathogenesis or progression by modulating not only microglial activation but also peripheral inflammation (Liu, Gao, and Hong 2003).

Post-mortem studies have shown no alterations in the expression of CD200 protein in temporal cortex and cingulate cortex of PD patients, but patient stratification by LB stage showed decreased CD200 protein expression in the temporal cortex of cases with an early stage (I and IIb) and in the cingulate cortex of stage I cases (Walker et al. 2017). However, no information is provided regarding which CD200 isoform was analysed in this study.

In vivo studies have demonstrated a down-regulation of CD200 and CD200R expression in MPTP-injected mouse brain (Ren, Ye, et al. 2016). In a 6-hydroxydopamine (6-OHDA) PD rat model, administration of an anti-CD200R blocking antibody aggravated the symptomatology, increased the dopaminergic neurodegeneration and dopamine loss and increased microglial activation and expression of pro-inflammatory markers (Zhang, Wang, et al. 2011).

In vitro studies, where the CD200-CD200R1 axis is modulated, also provide evidence of the role of this system on dopaminergic neurodegeneration in the PD context. On the one hand, CD200-treated microglial cultures show enhanced GDNF gene expression, a survival factor for dopaminergic neurons (Varnum et al. 2015). On the other hand, disruption of CD200-CD200R interaction with an anti-CD200R blocking antibody selectively increases the susceptibility of dopaminergic neurons to neurotoxicity induced by rotenone in mesencephalic cultures (Wang et al. 2011). Moreover, CD200-treated microglial cultures show inhibition of MPP+-induced INFγ, TNFα and IL1β release (Ren, Ye, et al. 2016).

Peripheral immunity dysfunction has been suggested to also participate in the development of PD (Sampson et al. 2016; Qin et al. 2007). Macrophages derived from blood monocytes of PD patients show an impaired CD200R expression in response to stimuli (LPS, conditioned medium from healthy or dying differentiated PC12 cells, co-culture with healthy or dying differentiated PC12 cells for 24 h), suggesting an intrinsic abnormality in these cells in PD (Luo et al. 2010). Apart from exerting an effect on microglial function, the CD200-CD200R1 system also influences the communication between the peripheral immune system and the CNS (Xie et al. 2017). In this sense, intraperitoneal injection of LPS in rats induces peripheral inflammation which is propagated to the CNS and results in dopaminergic neuronal loss, microglial activation and increased pro-inflammatory cytokines (Xie et al. 2017). The presence of microglia and monocytes is essential for this propagation. Although intraperitoneal LPS administration is also associated with increased CD200 and CD200R1 expression in the SN, activation of the CD200-CD200R1 system attenuated the dopaminergic neurodegeneration in this model whereas blockade of the

CD200-CD200R1 system aggravated it (Xie et al. 2017). Therefore, the CD200-CD200R1 signalling is also critical in regulating the transmission of inflammation from the periphery to the CNS (Xie et al. 2017).

5 Parkinson's disease

In 1817, James Parkinson described for the first time in his publication 'Essay on the Shaking Palsy' the motor and non-motor features of a syndrome he termed 'Shaking Palsy' or 'Paralysis Agitans', although components of possible PD can be found in earlier documents (Parkinson 2002). Five decades after the publication of the Shaking Palsy, Jean-Martin Charcot first used the term 'Maladie de Parkinson' and he was particularly influential in refining and expanding this early description (Goetz 2011). Today, about 200 years after the first clear medical description, the main goal of PD research remains the same: finding strategies for a cure.

5.1 EPIDEMIOLOGY

PD is the second-most common neurodegenerative disorder, after Alzheimer's disease, and it affects 2 - 3% of the population ≥65 years of age. PD is a chronic, progressive, incurable disease (Poewe and Mahlknecht 2009). Meta-analysis of the worldwide data showed a rising prevalence of PD with age (all per 100000): 41 in 40 to 49 years; 107 in 50 to 59 years; 173 in 55 to 64 years; 428 in 60 to 69 years; 425 in 65 to 74 years; 1087 in 70 to 79 years; and 1903 in older than age 80 (Pringsheim et al. 2014). Age is considered the main risk factor for PD (de Lau and Breteler 2006) and the number of people with PD is expected to double between 2005 and 2030, alongside the increased longevity of the human population (Dorsey et al. 2007). Differences in prevalence by geographic location and sex can be detected. PD is twice as common in men than in women and this may be explained by sex hormones, sex-associated genetics or sex-related differences in the exposure to environmental risk factors (Van Den Eeden et al. 2003). In Asia, there is a significantly lower prevalence of PD than in North America, Europe, and Australia in the 70- to 79-year-old population (Pringsheim et al. 2014).

Worldwide incidence estimates of PD range from 5 to >35 new cases per 100000 individuals yearly (Twelves, Perkins, and Counsell 2003). The incidence seems to vary depending on the race, ethnicity, genotype or environment. However, geography and race are often related, and it might be difficult to determine the relative contribution of each to the risk of developing PD.

Mortality does not increase during the first decade after disease onset, although it increases from then on doubling that of the general population (Pinter et al. 2015). Years lived with disability due to this disease are expected to increase in the future.

5.2 CLINICAL FEATURES AND DIAGNOSIS

The average age of PD onset is in the late fifties. Age of onset before 45 years is considered an early onset and may have genetic basis (Alcalay et al. 2010; Marder 2010). PD is clinically defined by the presence of bradykinesia in combination with rest tremor, rigidity, or both; as well as additional supporting and exclusionary criteria. Motor symptoms appearing as the disease progresses include abnormal posture, postural instability and motor blocks. The majority of patients also present non-motor symptoms, which can antedate the onset of classic motor symptoms, and include depression, pain, cognitive impairment (dementia, hallucinosis, memory deficits), sensory symptoms (hyposmia, impaired colour vision), sleep disturbance (idiopathic rapid eye movement (REM)-sleep behaviour disorder) and autonomic dysfunction (constipation, bladder hyperreflexia, erectile dysfunction, orthostatic hypotension) (Schapira, Chaudhuri, and Jenner 2017). Non-motor symptoms increase in prevalence as the disease advances and become a major determinant for quality of life and disability. A particularly prevalent and disabling non-motor symptom is dementia which is present in 83% of patients after 20 years of disease duration (Poewe et al. 2017).

For the diagnosis of PD, firstly, parkinsonism syndrome has to be diagnosed (as bradykinesia in combination with either rest tremor, rigidity, or both) (Postuma et al. 2015). PD is the most common cause of parkinsonism, accounting for ~80% of cases (Dauer and Przedborski 2003). However, there are other etiologies that present parkinsonism and must be considered as differential diagnoses: multiple system atrophy, dementia with Lewy Bodies, progressive supranuclear palsy, corticobasal syndrome; as well as secondary causes of parkinsonism as drug-induced parkinsonism (Keener and Bordelon 2016). Once parkinsonism has been diagnosed, MDS-PD criteria are applied to determine whether PD is the cause of this parkinsonism (Movement Disorder Society - Clinical diagnostic criteria for PD (MDS-PD Criteria), 2015 (Postuma et al. 2015). Two distinct levels of diagnostic can be defined:

1) Clinically established PD requires all the following three parameters (Postuma et al. 2015):
    a) Absence of absolute exclusion criteria: evidence of alternate unrelated cause.
    b) at least two of the following supportive criteria: L-DOPA responsiveness, L-DOPA-induced dyskinesia, rest tremor and the presence of either olfactory loss or cardiac sympathetic denervation on metaiodobenzylguanidine scintigraphy.

c) no red flags: no presentation of unusual features even though they are not absolutely exclusionary for PD.

2) Diagnosis of clinically probable PD requires (Postuma et al. 2015):
   a) absence of absolute exclusion criteria.
   b) presence of red flags counterbalanced by supportive criteria.

Full diagnostic certainty is impossible during life and diagnosis can only be confirmed on autopsy. Error rates for clinical diagnosis can be as high as 24% (Poewe et al. 2017). Parkinsonian symptoms, used in clinical diagnosis, are estimated to appear only after dopamine levels have declined by approximately 80% and SNpc dopaminergic neurons are greatly lost (~30-60%) (Burke and O'Malley 2013; Dauer and Przedborski 2003). Therefore, the inaccuracy of the diagnosis and its delay represents a major barrier for a treatment aimed to prevent neuronal death. For this reason, one of the greatest current challenges is to develop diagnostic tests and biomarkers not only for diagnostic confidence but particularly for early diagnosis. In this regard, some complementary tests are: imaging techniques, such as positron emission tomography (PET), single photon emission computed tomography (SPECT) or magnetic resonance imaging (MRI), that help to differentiate between PD and clinical mimics without loss of SNpc neurons; genetic testing that, although not being part of the routine diagnostic process, is used in patients with suggestive family history or specific clinical features; cerebrospinal fluid and blood test that have suboptimal sensitivities and specificities and are currently not clinically useful; and finally, non-motor prodromal symptoms for screening and prevention that are in study (Poewe et al. 2017). The MDS has recently published diagnostic criteria for prodromal and early PD (Berg et al. 2018; Berg et al. 2015).

5.3 MANAGEMENT

Currently, there is no cure for PD and the therapies are symptomatic treatments that do not prevent or stop the progression of the disease. Treatment of PD is currently based on pharmacological substitution of striatal dopamine. The gold standard since more than 50 years ago is the systemic administration of the dopamine-precursor amino acid L-DOPA, despite the development of a wearing-off effect of shorter duration responses and motor complications with the chronic use of this dopaminergic drug. Other therapies aimed to replace striatal dopamine are catechol-O-methyltransferase inhibitors, monoamine oxidase type B inhibitors and dopamine agonists (Poewe et al. 2017). Non-motor symptoms may not respond to dopamine replacement therapy or can even be aggravated or precipitated by this treatment. There are numerous non-dopaminergic approaches to address both motor and non-motor symptoms, some of them previously approved for another indication (anticholinergics for tremor, amantadine for L-DOPA-induced dyskinesia, safinamide for motor fluctuations and parkinsonism, cholinesterase inhibitors for cognitive disturbances, clozapine for psychotic symptoms, pro-kinetic drugs such as macrogol

for constipation, among others) (Poewe et al. 2017). Deep brain stimulation (DBS) of the subthalamic nucleus is a valid option for patients with advanced PD who experience intractable L-DOPA-related motor complications. DBS of the globus pallidus internus is an alternative target for the treatment of motor complications (Poewe et al. 2017). An increasing number of studies report exercise as a beneficial adjunct to pharmacologic therapy (Ahlskog 2011; Palmer et al. 1986). Experimental therapies including targeting α-synuclein aggregation and transport, gene-based approaches, fetal cell transplantation and stem cells have tried to restore striatal dopamine. Future clinical trials focused on patients at the prodromal or preclinical phase of disease could have a greater likelihood of success as pathology is less-advanced (Poewe et al. 2017).

5.4 RISK FACTORS

Longitudinal studies have reported factors associated with the risk of developing PD. Specifically, the following items have been associated with an increased risk of PD: male sex, family history of PD, exposure to pesticides, genetic factors, history of melanoma, traumatic brain injury and consumption of dairy products as high milk intake. Nevertheless, other factors have been associated with a reduced risk of PD: smoking, caffeine consumption, generic variants, higher serum urate concentrations, physical activity and use of the non-steroidal anti-inflammatory drug (NSAID) ibuprofen (Ascherio and Schwarzschild 2016). Although sporadic PD is the most common type, 10% of PD patients have familial forms (Klein and Westenberger 2012).

Anti-inflammatory drugs as protective factors and neurotoxins as contributors to the development of PD are presented below, since this thesis is focused on neuroinflammation and the experimental models used in this thesis are based on the exposure to neurotoxins.

5.4.1 Anti-inflammatory drugs

Several studies have reported an association between the use of anti-inflammatory drugs and PD. Meta-analysis support that regular use of ibuprofen is associated with a reduction in PD risk, whereas no association is found for other NSAIDs. This suggests that ibuprofen has specific protective properties, possibly by activating PPARγ. Interestingly, Ibuprofen is also more strongly associated with lower risk of Alzheimer's disease than other NSAIDs (Ascherio and Schwarzschild 2016). Recently, evidence of an association between immunosuppressants, such as corticosteroids and inosine monophosphate dehydrogenase inhibitors, with a lower risk of PD has been described (Racette et al. 2018). Neuroinflammation may play a role in the pathogenesis of PD and these pharmacoepidemiological studies provide additional evidence for the potential of the immune system as a pharmacological target for PD.

5.4.2 Neurotoxins

Exposure to neurotoxic agents may contribute to the development of some neurodegenerative diseases (Mostafalou and Abdollahi 2013). In 1982, the accidental exposure to the neurotoxin 1-methyl-4-phenyl1,2,3,6-tetrahydropyridine (MPTP) in drug abusers caused parkinsonism (Langston et al. 1983). Epidemiological studies show that the exposure to the pesticides rotenone and paraquat, which are functional and structural analogs of MPTP respectively, as well as to other pesticides, is a risk factor for PD (Goldman 2014; Kamel et al. 2014; Tanner et al. 2011). MPTP and its analogs impair mitochondrial respiration by inhibiting complex I of the electron transport chain, and it has been suggested that mitochondrial dysfunction is involved in the induction of oxidative damage in dopaminergic neurons in parkinsonism (Goldman 2014). Experimental models of PD have been developed by exposing neuronal cell cultures or laboratory animals to these agents (Bove and Perier 2012). These models are useful for studying mechanisms of dopaminergic neuronal cell degeneration and testing potential therapeutic approaches.

5.5 PATHOLOGY

The characteristic features of PD include the loss of the nigrostriatal dopaminergic neurons, the presence of gliosis and the presence of intraneuronal protein (α-synuclein) accumulation (Fig. 1) (Gelb, Oliver, and Gilman 1999; Poewe et al. 2017). α-synuclein accumulates in neuronal perikarya and in neuronal processes, termed Lewy bodies (LBs) and Lewy neurites (LNs), respectively. Classical LBs are round eosinophilic cytoplasmic protein aggregates that stain strongly for α-synuclein and have a hyaline appearance on haematoxylin and eosin staining (Dickson 2012). Although most of them are intraneuronal, α-synuclein immunoreactive glia, particularly oligodendroglia, can be also detected (Wakabayashi et al. 2000; Wakabayashi and Takahashi 1997). LBs are composed also of neurofilament, ubiquitin and ubiquitin binding protein p62 (Dickson 2012).

According to Braak staging model, Lewy-pathology follows a spatio-temporal pattern and spreads caudal-to-rostrally from peripheral and enteric autonomic nervous system, through the medulla oblongata and pontine tegmentum (stage 1-2), midbrain and basal prosencephalon (stage 3-4) to neocortex (stage 5-6) (Braak et al. 2003; Braak et al. 2004; Dickson et al. 2009).

Neither the loss of pigmented dopaminergic neurons in the SN nor the presence of LBs is specific for PD (Poewe et al. 2017). Neuronal loss in the SNpc is found in a wide range of parkinsonian disorders, which can be classified as those with and without α-synuclein pathology (Dickson et al. 2009; Iacono et al. 2015). In the same manner, LBs can be found in a variety of diseases including dementia with Lewy bodies, multiple system atrophy or Alzheimer's disease, or even in

people of advanced age without clinical neurodegenerative disease (Gibb and Lees 1988; Halliday, Lees, and Stern 2011).

Nigrostriatal neurons contain the pigment neuromelanin and their loss is responsible for the classic macroscopic finding of SNpc depigmentation (Fig. 15). The cell bodies of these neurons are located in the SNpc and project primarily to the putamen, being the dorsolateral putamen the striatal component with the highest dopamine depletion when SNpc dopaminergic neurons die. Caudate, the other striatal component, is more preserved than putamen because it is mainly innervated by mesolimbic dopaminergic neurons from the ventral tegmental area, which are less affected in PD (Fig. 15). The dopaminergic neuronal loss is progressive. In early stages, cell loss is restricted to the ventrolateral SN but spreads to other midbrain dopaminergic neurons as the disease progresses. The depletion of dopamine in the striatum exceeds the dopaminergic neuronal loss in the SNpc at the onset of symptoms (~80% dopamine depletion in the putamen and ~30-60% of SNpc dopaminergic neuronal loss) (Burke and O'Malley 2013; Dauer and Przedborski 2003). Neuropathological studies in humans reported that the loss of dopaminergic markers in the dorsal putamen occurs rapidly and is virtually complete by four years after PD diagnosis (Kordower et al. 2013). This suggests that degeneration occurs first in the striatal dopaminergic nerve terminals and that neuronal death may result from a “dying back” process. Moreover, growing evidence supports that axon degeneration takes the initial brunt of injury and that the molecular mechanism of axon degeneration is distinct from the soma destruction (Cheng, Ulane, and Burke 2010). As the disease progresses, other neurons are affected including noradrenergic (locus coeruleus), serotonergic (raphe) and cholinergic (nucleus basalis of Meynert, dorsal motor nucleus of vagus) systems and areas as cerebral cortex, olfactory bulb and autonomic nervous system (Kalia and Lang 2015).

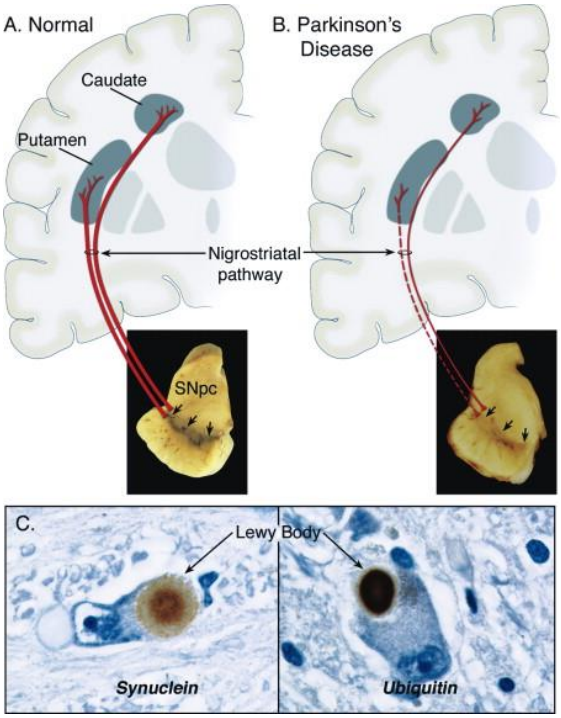

Figure 15. Neuropathology of PD. A Schematic representation of the normal nigrostriatal pathway. Dopaminergic neurons, which have the cell bodies in the substantia nigra pars compacta (SNpc), project to the basal ganglia and synapse in the putamen and caudate nucleus. **B** Schematic representation of the degenerated nigrostriatal pathway in PD. There is a marked loss of dopaminergic neurons that project to the putamen and a modest loss of the ones projecting to the caudate. The photograph shows the depigmentation of the SNpc in PD. **C** α-synuclein and ubiquitin immunostainings reveal Lewy bodies in the dopaminergic neurons of the SNpc. From: Dauer and Przedborski 2003.

The motor symptoms in PD are due to nigrostriatal dopaminergic degeneration (Hornykiewicz 2008). SNpc forms part of the basal ganglia, a group of subcortical nuclei that control voluntary movements. When neuronal loss occurs in the SNpc, the ultimate result is the inhibition of the thalamus, and this leads to an inhibition of motor cortex that results in bradykinesia (Fig. 16) (Burch and Sheerin 2005).

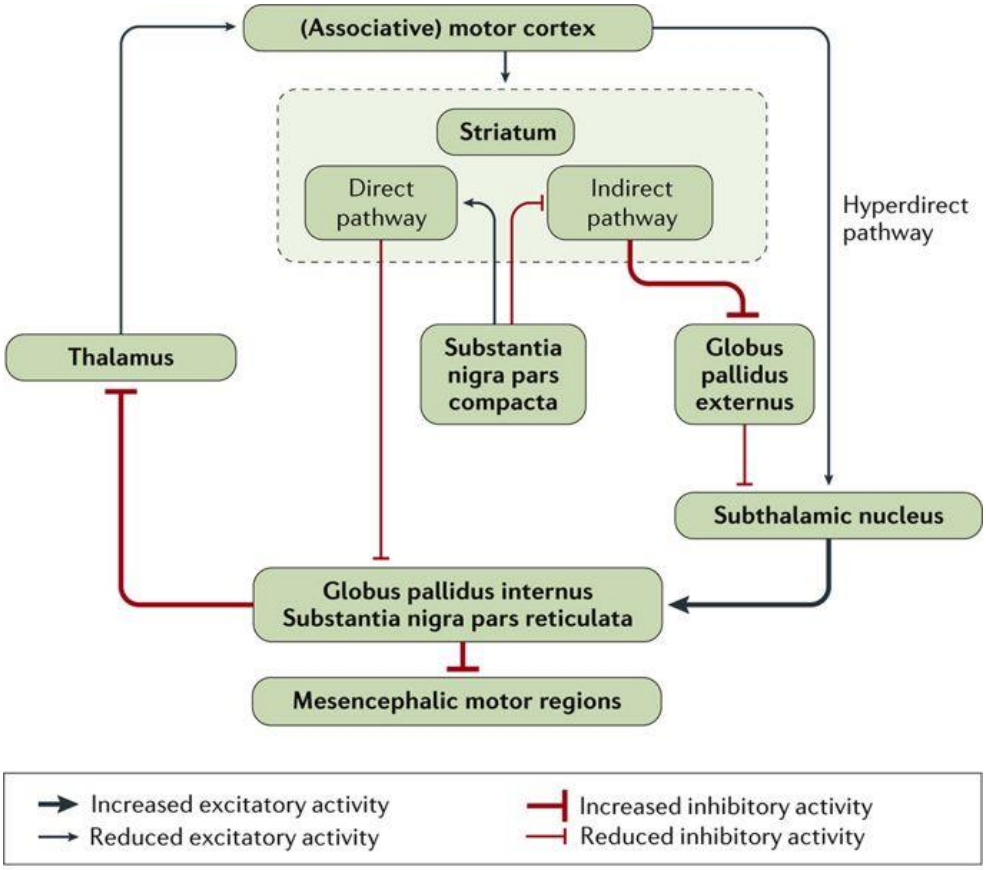

Figure 16. Motor cortex circuitry activity changes in PD. The motor circuit consists of corticostriatal projections from the primary motor cortex, supplementary motor area, cingulate motor cortex and premotor cortex to the striatum. The hyperdirect pathway has direct glutamatergic connectivity from the motor cortex to the subthalamic nucleus. The striatal projections to globus pallidus internus and the substantia nigra pars reticulate (SNpr) are divided into 'direct' and 'indirect' pathways. The direct pathway originates from striatal neurons that express dopamine D1 receptors, which project to the GABAergic neurons in the globus pallidus internus and the SNpr. The 'indirect' pathway originates from striatal neurons that express D2 receptors, which project to the globus pallidus externus, and reaches the globus pallidus internus via the subthalamic nucleus as a glutamatergic relay. Through these two pathways, the striatal dopaminergic tone regulates the GABAergic output activity of the basal ganglia. As indicated, parkinsonism is associated with changes in these relays, resulting in the net effect of a strong increase in the firing rate of GABAergic basal ganglia output neurons, which over-inhibit downstream thalamocortical and brainstem areas. From: Poewe et al. 2017.

Recently, neuromelanin levels in the SN have been related with the development of PD. Neuromelanin accumulation increases with age and when reaches a threshold it may initiate the development of PD. Laboratory animals commonly used in research lack neuromelanin but the overexpression of tyrosinase in the SN of rats leads to neuromelanin accumulation. When

neuromelanin levels reach a threshold, parkinsonian phenotype, LBs and nigrostriatal neurodegeneration are observed in these animals (Carballo-Carbajal et al. 2019).

5.6 EXPERIMENTAL MODELS OF PD

5.6.1 Experimental *in vivo* models of PD: MPTP

In order to investigate processes thought to be involved in PD and to evaluate and select drug candidates, experimental models have been created. Experimental models of PD can be divided in neurotoxin models (6-OHDA, MPTP), pesticide/herbicide models (rotenone, paraquat), inflammation models (acute and chronic LPS) and genetic models (Jackson-Lewis, Blesa, and Przedborski 2012; Meredith, Sonsalla, and Chesselet 2008). These models have been developed in a large number of organism such as yeast, *C.elegans*, zebrafish, flies, snails, rodents, or non-human primates (Cooper and Van Raamsdonk 2018; Tenreiro et al. 2017; Emborg 2007; Makhija and Jagtap 2014; Whitworth 2011; Maasz et al. 2017; Zeng, Geng, and Jia 2018). None of the models captures all the clinical and pathological features of PD (Jackson-Lewis, Blesa, and Przedborski 2012). Therefore, the experimental model should be selected depending on the hypothesis being asked.

5.6.1.1 MPTP mouse model

The MPTP experimental model was established after the observation, in 1982, that accidental exposure to MPTP in young drug abusers caused an acute, severe and irreversible parkinsonism syndrome characterized by all of the cardinal features of PD (Langston et al. 1983). The MPTP mouse model of PD recapitulates the nigrostriatal dopaminergic degeneration, oxidative stress, ROS, energy failure, and inflammation observed in PD. It is considered the gold standard model of PD but some drawbacks have to be considered: neuronal death is not gradual and LBs are not present, although in old MPTP-injected monkeys proteinaceous inclusions have been described (Forno et al. 1986).

Primates and mice are the most popular species where this model is applied. Remarkably, depending on the strain of mice, the sensitivity to MPTP changes. Not only different levels of nigrostriatal damage but also different rates of mortality due to peripheral toxicity are observed (Muthane et al. 1994; Smeyne and Jackson-Lewis 2005).

MPTP is lipophilic and, after systemic administration, it rapidly crosses the BBB (Markey et al. 1984). Then, MPTP, which is a pro-toxin, is oxidized to 1-methyl-4-phenyl-2,3-dihydropyridinium (MPDP+) by monoaminase oxidase B (MAO-B) in cells having this enzyme: astrocytes (Ransom

et al. 1987) and serotonergic neurons (Shen et al. 1985). Next, it is converted to the active metabolite MPP+ probably by spontaneous oxidation, and released from the cells by an unknown mechanism. MPP+, a polar molecule, enters the cells through dopamine transporters (DAT), but also through serotonin and norepinephrine transporters (Fig. 17) (Javitch et al. 1985; Mayer, Kindt, and Heikkila 1986). DAT does not explain the specificity of MPTP-induced dopaminergic neurodegeneration because MPP+ accumulates in all monoaminergic neurons producing biochemical alterations; however, degeneration is most prominent in dopaminergic neurons. (Burns et al. 1983; Hallman, Olson, and Jonsson 1984; Ovadia, Zhang, and Gash 1995; Rose et al. 1993; Wallace et al. 1984) Moreover, not all dopaminergic neurons show the same sensitivity to MPTP-induced neuronal loss, dopaminergic neurons in the SNpc being the ones most affected (Dauer and Przedborski 2003). Strikingly, after MPTP administration the highest levels of MPP+ are found in the adrenal medulla but no cytotoxicity of chromaffin cells is observed (Reinhard et al. 1987).

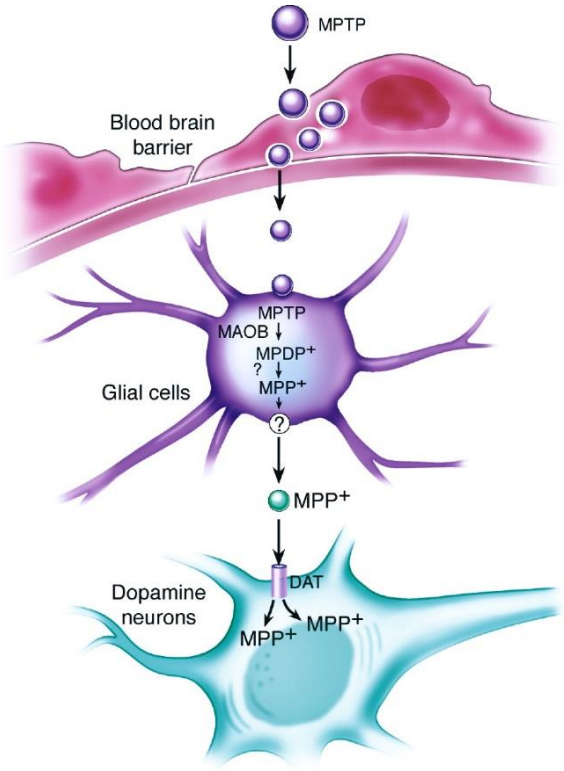

Figure 17. MPTP metabolism. Pro-toxin MPTP crosses the blood-brain barrier and it is converted into its active metabolite MPP+ in astrocytes and serotonergic neurons (not shown). MPP+ enters dopaminergic neurons through DAT. From: Dauer and Przedborski 2003.

Once inside dopaminergic neurons, MPP+ 1) interact with cytosolic enzymes, 2) is partly internalized in vesicles, which may prevent from its damage, and 3) is concentrated in the mitochondria where it inhibits the complex I of the mitochondrial electron transport chain causing an inhibition of oxidative phosphorylation. This results in a decreased ATP production, particularly in the striatum and ventral midbrain (Chan et al. 1991; Fabre et al. 1999), and in an increased production of free radicals causing oxidative stress and activation of programmed cell death molecular pathways. *In vitro* and *in vivo* studies also demonstrate that MPP+ induces a massive dopamine release from vesicles to cytosol causing an increase in intracellular ROS levels by dopamine autoxidation (Fig. 18) (Chang and Ramirez 1986; Pileblad, Nissbrandt, and Carlsson 1984)

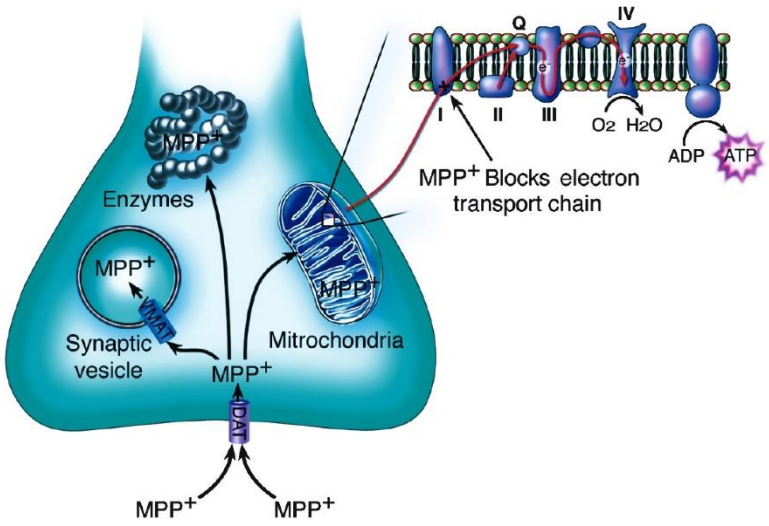

Figure 18. MPP+ intracellular pathways. MPP+ is concentrated into mitochondria where it blocks complex I. This interrupts the transfer of electrons decreasing ATP synthesis and enhancing ROS production. MPP+ can also interact with cytosolic enzymes or be sequestered into synaptic vesicles. From: Dauer and Przedborski 2003.

The MPTP mouse model is useful to study mechanisms of dopaminergic neuronal degeneration and to test potential therapeutic approaches (Dauer and Przedborski 2003; Vila and Przedborski 2003). Three different MPTP regimens of administration have been widely used in mice: acute, sub-acute and chronic.

The acute regimen consists of four intraperitoneal injections of MPTP (20 mg/kg) in saline at 2 hour intervals within a single day (Jackson-Lewis and Przedborski 2007). This causes 90% dopamine depletion in the striatum and 70-80% loss of SNpc dopaminergic neurons by a mechanism mainly involving oxidative stress and a non-apoptotic form of death. Loss of dopaminergic cell bodies in the SN peaks at day 2 after MPTP administration and it remains stable by day 7 after MPTP administration. This regimen is traditionally used to study the implication of oxidative stress in the pathogenic process (Jackson-Lewis and Przedborski 2007; Przedborski 2001). The sub-acute regimen consists of one intraperitoneal injection of MPTP per day (30 mg/kg/day) in saline for 5 consecutive days (Tatton and Kish 1997). This, causes less dopamine depletion in the striatum (40-50%) and less SNpc dopaminergic neuronal loss (30–50%) compared to the acute regimen. The neuronal death is mainly apoptotic, peaks at day 4 after the last MPTP injection and is stable by day 21 after MPTP administration. It is traditionally used to study the molecular pathways of apoptosis (Przedborski 2001). Finally, the chronic regimen consists of ten intraperitoneal injections of MPTP (25 mg/kg) and an adjuvant, probenecid (250 mg/kg in tris-HCl buffer), every 3.5 days for 5 weeks. This is the model that most resembles the human PD pathology as the SNpc dopaminergic loss is more progressive and inflammation more prolonged (Schintu et al. 2009; Meredith et al. 2008). However, the chronic regimen is not as well characterized as the acute and subacute regimens.

Inflammation is present in the MPTP mouse model and it is composed of activated microglia, reactive astrocytes and T lymphocytes. In the acute MPTP mouse model, activation of microglia occurs before astrocytic reactivity and, interestingly, it reaches a maximum before the peak of dopaminergic neuronal death. The astrocytic reaction in the SNpc appears at the same time or after dopaminergic neurodegeneration suggesting that it may be secondary to neuronal death. T lymphocytes infiltration is observed after microglial activation and before astrocytic reactivity (Fig.19). MPTP-injected monkeys show activated microglial cells months and even years after intoxication, whereas in MPTP-injected rodents this is observed only for a few days (Czlonkowska et al. 1996; Hirsch and Hunot 2009; Kohutnicka et al. 1998; Liberatore et al. 1999; Barcia 2013; Przedborski 2001).

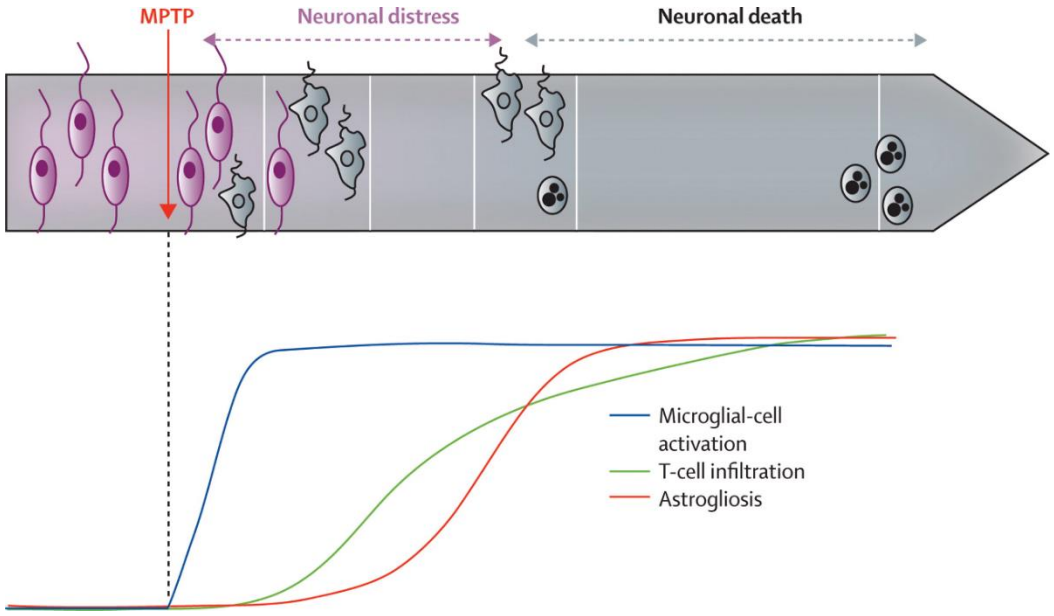

Figure 19. Sequence of cellular events within the substantia nigra in the acute MPTP mouse model of PD. After exposure to MPTP, there is neuronal distress and death but also microglial activation, T-cell infiltration and astrogliosis. From: Hirsch and Hunot 2009.

5.6.2 Experimental *in vitro* models of PD: MPP+ and rotenone

In *in vitro* models, MPP+ and other neurotoxins related to PD including rotenone can be used to treat cellular cultures. Mesencephalic neurons/glia cultures from rodent embryos enriched in dopaminergic neurons are useful for studying cellular alterations induced by these neurotoxins (Chen et al. 2013; Shimohama et al. 2003).

5.7 MOLECULAR PATHOGENESIS: NEUROINFLAMMATION AND PD

The underlying molecular pathogenesis in PD involves alteration in multiple pathways and mechanisms: α-synuclein proteostasis, mitochondrial function, oxidative stress, calcium homeostasis, axonal transport and neuroinflammation (Poewe et al. 2017).

5.7.1 Neuroinflammation and PD

Growing evidence suggests that a neuroinflammatory process is involved in the development of PD. A large number of *post-mortem*, human cerebrospinal fluid and blood, brain imaging, epidemiological, genetic, animal and *in vitro* studies clearly associate inflammation with PD and these are summarized in Figure 20 (Gelders, Baekelandt, and Van der Perren 2018). However, the understanding of the contribution of neuroinflammation in the pathogenesis of PD is still to be elucidated, as well as whether this inflammatory process is a cause or a consequence of the neuronal degeneration.

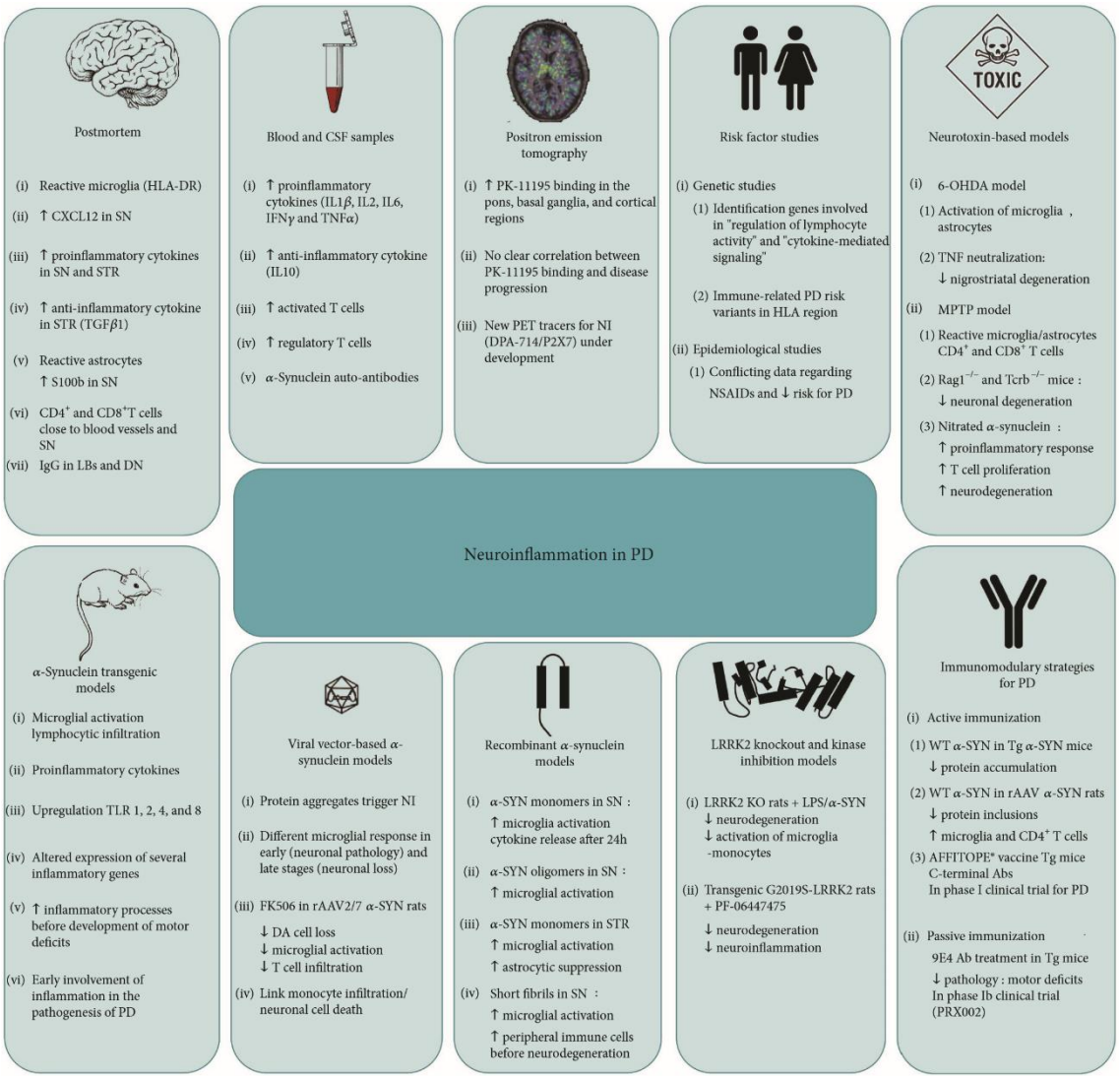

Figure 20. Overview of clinical and preclinical evidence linking neuroinflammation to neurodegeneration in PD. CSF: cerebrospinal fluid, DN: dopaminergic neurons, KO: knock-out, LBs: Lewy bodies, NI: neuroinflammation, STR: striatum, α-SYN: α-synuclein, Tg: transgenic, TLR: toll-like receptor. From: Gelders, Baekelandt, and Van der Perren 2018.

The first evidence of neuroinflammation in PD came from the evaluation of *post-mortem* brain tissue from PD. In 1988, the presence of activated microglia, expressing high levels of human leukocyte antigen D-related (HLA-DR), in the SNpc of PD *post-mortem* samples was first reported (McGeer et al. 1988). This was interpreted as the presence of an innate immune response with inflammatory profile that could contribute to the neurodegenerative process (Mosley et al. 2012). Subsequent *post-mortem* studies reported the presence of a spectrum of cytokines such as IL1β, IL6, TNFα, TGFβ, CXCR4 or CXCL12, and different immune cells such as activated microglial and astroglial cells and infiltrated T cells, in the SN and other affected brain regions associated with α-synuclein aggregation (Bartels et al. 2010; Boka et al. 1994; Gerhard et al. 2006; Imamura et al. 2003; McGeer et al. 1988; Mogi et al. 1995; Mogi, Harada, Kondo, et al. 1994; Mogi, Harada, Riederer, et al. 1994; Shimoji et al. 2009). The increase in both pro- and anti-inflammatory

cytokines suggests different microglial phenotypes in affected areas. Importantly, neurons express receptors for these cytokines, highlighting that they are sensitive to these inflammatory mediators. These findings in human *post-mortem* tissue indicate that PD patients undergo a neuroinflammatory state in the affected brain areas, both at cellular and molecular level.

In accordance with the *post-mortem* data, studies of serum, plasma and cerebrospinal fluid also support the presence of neuroinflammation in PD. Pro- (e.g. IL1β, TNFα, IL6, IL2, IFNγ) (Blum-Degen et al. 1995; Mogi et al. 1996; Nagatsu et al. 2000) and anti- (e.g. TGFβ, IL4) (Mogi et al. 1995; Mogi et al. 1996) inflammatory cytokines have been observed in serum, plasma or cerebrospinal fluid from PD patients. These findings are of relevance because they indicate that inflammation in PD goes beyond the brain. These cytokines are probably released by microglia, astroglia, macrophages and lymphocytes (Barcia 2013; Mount et al. 2007; Van Eldik et al. 2007). Their specific function in PD is unclear. Initially, the purpose of increased cytokine levels may be the restoration of damaged tissue, but a perpetuated inflammatory state may be detrimental as there is evidence that pro-inflammatory cytokines have deleterious consequences for remnant neurons (Barcia 2013; Hirsch et al. 2003; McGeer and McGeer 1998). High levels of TNFα and IFNγ, but not of IL1β, IL6 and TGFβ have been described in plasma of chronic parkinsonian monkeys suggesting that TNFα and IFNγ maintain the long-term inflammatory response (Barcia et al. 2011). As microglial and astroglial activation, the increased circulating cytokines in MPTP-injected mice are transient and return to the basal levels when neurodegeneration is stabilized (Hebert et al. 2003; Luchtman, Shao, and Song 2009), whereas, in human or non-human primates, cytokines levels in serum and brain remain elevated years after the MPTP insult (Barcia et al. 2011).

PET-scan analysis with PK-11195 have also revealed microglial activation in pons, basal ganglia and cortical regions of PD patients (Gerhard et al. 2006), indicating the presence of microglial activation not only in late stages, but also in early stages of the disease (Bartels et al. 2010; Edison et al. 2013; Gerhard et al. 2006; Iannaccone et al. 2013; Ouchi et al. 2005). Patients followed for 2 years after the original PET scan did not show fluctuations in microglial activation, suggesting a plateau or a limitation of the technique (Edison et al. 2013; Gerhard et al. 2006; Iannaccone et al. 2013). However, the specificity of PK-11195 for M1 or M2 microglia binding is not clear, therefore it can be concluded that microglia are activated but not in which state (M1 or M2 phenotype). These *in vivo* studies in patients indicate the presence of an ongoing inflammatory process throughout the course of the disease.

Risk factors studies provide support to the hypothesis that neuroinflammation is not only associated with the progression of the disease but also directly involved in the pathogenesis. PD onset has been reported following incidental bacterial or viral infection in susceptible humans (Jang et al. 2009; Niehaus and Lange 2003). The search for susceptibility genes has reported polymorphisms in inflammatory genes associated with increased risk of developing PD (Hirsch

and Hunot 2009), such as genes encoding TNF, TNF receptor 1, IL1β, IL1 receptor antagonist, CD14 (Hirsch and Hunot 2009) and TREM2 (Rayaprolu et al. 2013). Recent genome-wide association studies (GWAS) have revealed the association of a large amount of loci with PD and, interestingly, several of them are implicated in immunity such as the HLA region or LRRK2 (Dzamko, Geczy, and Halliday 2015). Furthermore, epidemiological studies have associated the anti-inflammatory drug ibuprofen with a reduction in PD risk supporting also a role of neuroinflammation in the progression of PD (Ascherio and Schwarzschild 2016).

Both cellular and molecular features described in PD patients have been reproduced in a diversity of PD animal models, including inflammation (Chesselet et al. 2012; Cicchetti et al. 2002; Kurkowska-Jastrzebska et al. 1999). Several evidence from PD animal models support that neuroinflammation is involved in the death of dopaminergic neurons (Hirsch and Hunot 2009).

At the cellular level, the role of microglia, astrocytes, oligodendrocytes and T cells in the pathology of PD is unclear. Regarding **microglia**, it is unclear whether their presence and activation are a cause or a consequence of dopaminergic damage (Barcia 2013; Block, Zecca, and Hong 2007; Perry, Nicoll, and Holmes 2010). Microglial activation is found in the SN, putamen, hippocampus, transentorhinal cortex, cingulate cortex and temporal cortex of PD patients (Imamura et al. 2003). Direct role of microglial activation in neuronal degeneration is supported by animal studies showing that inhibition of microglial activation prevents neuronal degeneration (Brochard et al. 2009; Liberatore et al. 1999; Wu et al. 2002). Importantly, injection of inflammatory agonists, such as bacterial LPS (Herrera et al. 2000; Qin et al. 2007) or viral pathogens (Jang et al. 2009; Ogata et al. 1997) to experimental animals, activates glial cells and selectively kills dopaminergic neurons, illustrating that activation of microglia can indeed induce neurotoxicity in dopaminergic neurons. In addition, a PD animal model based on the intraperitoneal injection of LPS has been described (Liu and Bing 2011). A study also showed that the administration of LPS in combination with MPTP is synergistic and exacerbates both MPTP-induced glial activation and neurodegeneration (Gao et al. 2003c). However, evidence has also shown that glial cells can be potentially beneficial for dopaminergic neurons by providing trophic factors (BDNF, GDNF) (Batchelor et al. 2002; Kirschner et al. 1996; Tomac et al. 1995) or by phagocytosing debris from apoptotic cells (McGeer et al. 1988).

Astrocytes become reactive and also participate in the neuroinflammatory process in PD. Evidence in animal models indicate that astrocytic reaction occurs in parallel or after neuronal cell death (Barcia 2013; Przedborski 2001). In general, astrocyte reactivity is considered a neuroprotective process (Escartin and Bonvento 2008) by releasing factors that contribute to tissue repair (Chen, Yung, and Chan 2005; Lin et al. 1993), scavenging toxic compounds released by dying neurons, reducing oxidative stress by metabolizing dopamine, protecting from NO neurotoxicity (Chen, Yung, and Chan 2005; Hirsch et al. 1998), regulating macrophage and lymphocyte infiltration (Cardona, Gonzalez, and Teale 2003; Carrillo-de Sauvage et al. 2012) or

eliminating debris (Iliff et al. 2012). Furthermore, the most vulnerable area affected in PD, the SNpc, is a region with a low density of astrocytes (Hirsch et al. 1998).

Nevertheless, astrocytes can release pro-inflammatory cytokines contributing to the inflammatory and neurodegeneration process (Barcia 2013). It has been reported that neuroinflammation induces a type of reactive astrocytes termed A1, whereas ischemia induces A2 reactive astrocytes. This terminology is analogue to M1 and M2 microglial/macrophage nomenclature and astrocytes might have, as well, more than two states of polarisation. A1 reactive astrocytes up-regulate genes (e.g. complement genes) involved in synapse destruction suggesting that A1 astrocytes may have a "harmful" effect. In contrast, A2 reactive astrocytes up-regulate genes involved in synapse repair, survival and neuronal growth (e.g. thrombospondins, neurotrophic factors genes) suggesting a "helpful" phenotype (Liddelow and Barres 2017). Complement component 3 (C3) is one of the most characteristically up-regulated genes in A1 astrocytes and is not expressed by A2 reactive astrocytes, hence, it is used as a marker for A1 state. Interestingly, the presence of abundant C3-positive A1 reactive astrocytes has been recently described in *post-mortem* brain regions of a variety of neurodegenerative diseases including PD (Liddelow et al. 2017). Furthermore, M1 activated microglia can induce A1 reactive astrocytes, both *in vitro* and *in vivo*, by secreting IL1α, TNF and C1q (Liddelow et al. 2017). Surprisingly, it has been also reported that, besides many complement components inductors of synaptic degeneration, A1 reactive astrocytes can also secrete a soluble yet-to-be-identified neurotoxin that rapidly induces apoptosis of neurons and oligodendrocytes. Therefore, although reactive astrocytes are generally considered part of a neuroprotective process (Barcia 2013), it is important to consider which astrocytic state is playing the major role. It is unknown whether inflammation is secondary to neurodegeneration but the presence of both M1 phenotype activated microglia and A1 phenotype activated astrocytes in PD might contribute the neurodegeneration.

Another evidence of the detrimental role of astrocytes is that it is unclear whether microglia are sufficient by themselves to induce neuronal death. Some studies show microglial toxicity (Boje and Arora 1992; Burguillos et al. 2011) but these are *in vitro* studies that do not recapitulate *in vivo* microglia phenotypes (Bohlen et al. 2017). Liddelow and collaborators reported that activated microglia were insufficient by themselves to kill neurons, but they strongly induce A1 astrocytes, which could drive neurodegeneration by secreting not only multiple complement components but also a yet-to-be-identified neurotoxin (Liddelow et al. 2017).

The role of **oligodendroglia** in PD is still to be elucidated. In the SN of *post-mortem* PD tissue, complement-activated oligodendroglia is an early sign of neurodegenerative change and it has been suggested that complement opsonizes damaged oligodendroglia for microglial phagocytosis and (Yamada 1991). Moreover, inclusions of α-synuclein have been reported in oligodendroglia of PD patients (Wakabayashi et al. 2000) and oligodendroglia appear increased in number and with a reactive phenotype in PD models (Annese et al. 2013).

Both innate and adaptive immune responses are implicated in the pathophysiology of PD. The presence of **CD8+ and CD4+ T lymphocytes** in the SN of *post-mortem* PD tissue has been reported, although no B cells or natural killer cells have been described so far (Brochard et al. 2009). The localization of these cells is thought to be specific to damaged areas, as no CD8+ or CD4+ T lymphocytes have been detected in the red nucleus, an area not affected in PD. α-synuclein has been postulated as a plausible antigen, which would support the hypothesis of an autoimmune disease (Appel, Beers, and Henkel 2010). Infiltration of CD4+ T lymphocytes has been reported to contribute to neurodegeneration in a mouse model of PD (Brochard et al. 2009). Infiltration of peripheral cells suggests changes in BBB function in these patients. Regarding this, the normal contacts between nigral neurons and capillary are lost in the early stages of the disease in PD patients (Farkas et al. 2000). Increased density of endothelial cells in the SN (Farkas et al. 2000), pathological changes in the microanatomy of capillaries (Faucheux et al. 1999) and BBB dysfunction have been shown in PD brain (Zlokovic 2008).

There are several hypotheses about which mechanisms are responsible for the induction of the neuroinflammation observed in PD. α-synuclein has been postulated as one of the triggers of the M1 phenotype. α-synuclein can be secreted to the extracellular space by exocytosis from neurons but it may also be released from dying cells. In the extracellular space, α-synuclein is phagocytosed by microglial cells, what can induce microglial activation, increase the expression of pro-inflammatory enzymes and cytokines, as well as increase NO and ROS production (Zhang et al. 2005) contributing to dopaminergic neuronal death progression (Hirsch and Hunot 2009), due to the sensitivity of dopaminergic neurons to oxidative damage (Gao et al. 2003b). It has been reported a correlation between α-synuclein deposition and the number of MHCII-positive cells (M1 activation state marker) in *post-mortem* PD brain (Croisier et al. 2005). MHCII deficiency prevented α-synuclein-induced microglial activation and dopaminergic neurodegeneration *in vivo* (Harms et al. 2013). In addition, it has been suggested that α-synuclein aggregation induces both innate and adaptive immunity in PD and that neuroinflammation can also promote α-synuclein misfolding (Gao et al. 2008; Hirsch and Hunot 2009; Ferreira and Romero-Ramos 2018). Another microglial activation trigger is extracellular neuromelanin released from damaged dopaminergic neurons (Viceconte et al. 2015; Zecca et al. 2008; Zhang, Phillips, et al. 2011). Furthermore, there is evidence supporting the hypothesis that dopaminergic neuronal death is enough to activate microglial cells (Roodveldt, Christodoulou, and Dobson 2008). Neuronal degeneration is associated with the release of signals from early stages that can activate microglia. In this regard, ATP released and calcium waves transmitted from damaged neurons can be sensed by microglial cells, which phagocyte debris and engulf degenerating neurons to restore the tissue (Davalos et al. 2005; Sieger et al. 2012; Barcia et al. 2012).

Increasing evidence suggests that intestinal inflammation is a silent driver of PD pathogenesis (Houser and Tansey 2017). Gastrointestinal dysfunction often precedes the onset of motor

symptoms in PD patients and it has been proposed that PD originates in the intestine and progresses to the brain through the spreading of inflammation. In susceptible individuals, intestinal tissue damage or exposure to inflammatory triggers such as aggressive pathogens can provoke the activation of the immune system in the gut, which increases α-synuclein aggregation. The α-synuclein aggregates may be transmitted from the gut to the brain via the vagus nerve. Ultimately, chronic intestinal inflammation becomes systemic and promotes neuroinflammation, which drives neurodegeneration (Forsyth et al. 2011; Hawkes, Del Tredici, and Braak 2007; Holmqvist et al. 2014; Houser and Tansey 2017; Weller et al. 2005). Moreover, a distinct microbial community in the gut of PD patients has been described and also a role of gut microbiota in promoting motor deficits and microglial activation in mice with overexpression of α-synuclein (Sampson et al. 2016).

Regarding the molecular pathways linking neuroinflammation with dopaminergic neuronal death in PD, it has been suggested that activated glial cells can create a toxic oxidative environment that damages dopaminergic neurons. Specifically, activated microglial cells can induce enzymatic systems including iNOS (Hunot et al. 1996) and NADPH oxidase (Fig. 21) (Wu et al. 2003). iNOS leads to an increase in the levels of NO· free radicals, whereas NADPH oxidase leads to an increase in superoxide free radicals ($O_2{\cdot}^-$). NO· and $O_2{\cdot}^-$ free radicals react and form the highly reactive nitrogen species peroxynitrite ($ONOO^-$), which can induce oxidative damage to proteins in dopaminergic neurons such as tyrosine hydroxylase decreasing its enzymatic activity (Ara et al. 1998), and α-synuclein potentiating its aggregation (Przedborski, Chen, et al. 2001; Schildknecht et al. 2013). Furthermore, $O_2{\cdot}^-$ can be dismutated into H_2O_2, which reacts with free ferrous iron producing the highly reactive hydroxyl free radical (·OH) that contribute to the oxidative damage in dopaminergic neurons. Reactive astrocytes, usually associated with protective properties, can also participate in oxidative damage by inducing the expression of myeloperoxidase (Giasson et al. 2000), which produces hypochlorous acid (HOCl) from H_2O_2 and Cl^-. HOCl can produce oxidative damage to dopaminergic neurons directly or indirectly when combined with $O_2{\cdot}^-$ to generate ·OH radicals. Moreover, non-reactive nitrites (NO_2^-), an end product of NO free radicals, can be converted into reactive $NO_2{\cdot}^-$ free radicals by myeloperoxidase contributing also to oxidative damage in dopaminergic neurons. In addition, dopaminergic neurons can also contribute to the formation of ROS through COX2 expression (Fig. 21).

Supporting this hypothesis, increased expression of iNOS, NADPH oxidase and MPO have been described in the SN in both PD patients and animal models of PD (Knott, Stern, and Wilkin 2000; Choi et al. 2005; Hunot et al. 1996; Wu et al. 2003). Furthermore, SN is highly enriched in iron content and in both animal models of PD and PD patients shows increased COX2 expression in dopaminergic neurons (Hirsch 2006).

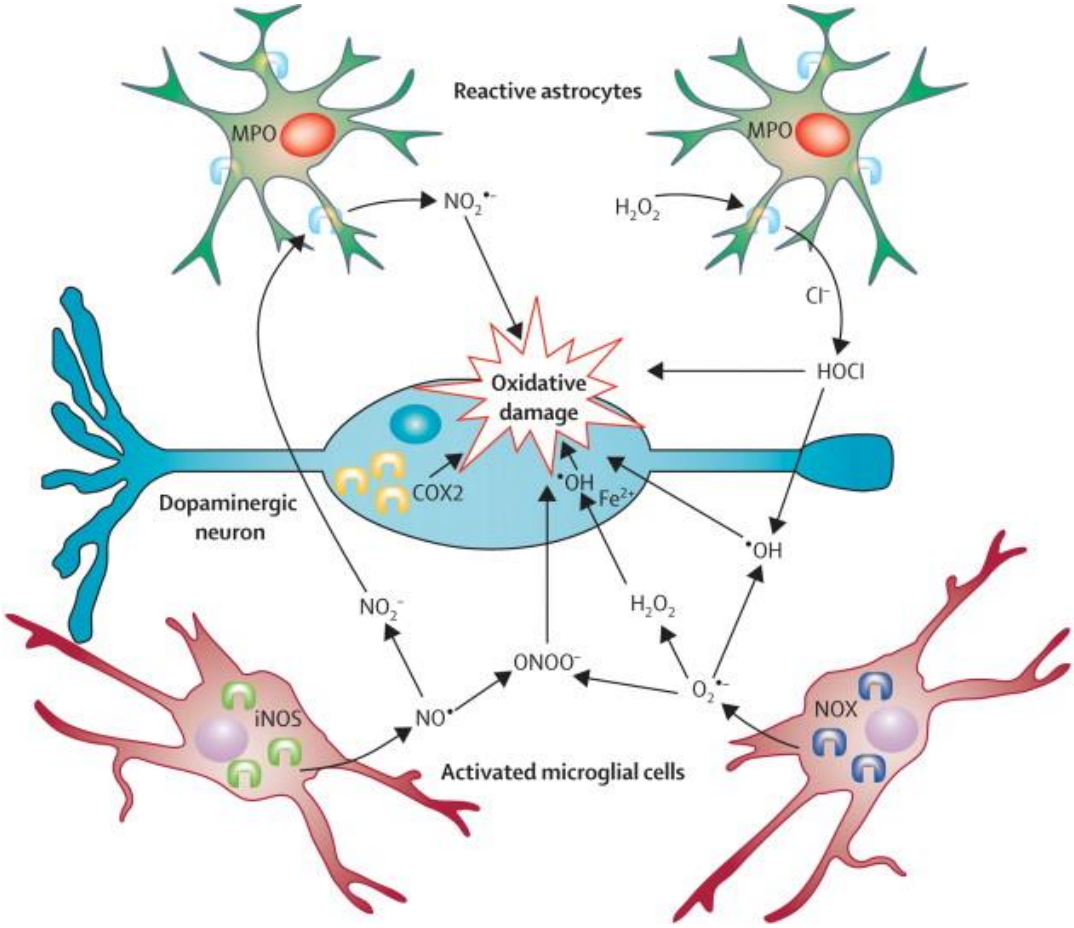

Figure 21. Possible link between neuroinflammatory processes and oxidative damage to dopaminergic neurons in PD. COX2: cyclooxygenase 2, iNOS: inducible nitric oxide synthase, NOX: NADPH oxidase, MPO: myeloperoxidase. From: Hirsch and Hunot 2009.

Neuroinflammation might contribute to dopaminergic cell death also through pro-inflammatory cytokines released by activated microglia, including TNFα, IL1β, and IFNγ. All these cytokines can have a direct effect (Fig. 22, only TNFα is shown) on dopaminergic neurons by interacting with their neuronal receptors, which can activate intracellular death pathways (NFκB, JNK, p38). These cytokines can also have an indirect effect (Fig. 22) by inducing iNOS expression through CD23 receptor in microglial cells leading to the production of NO free radicals. Furthermore, Fas ligand derived from CD4+ T cells might have a direct effect on dopaminergic neurons by interacting with its receptor and activating death pathways, or an indirect effect by increasing the release of additional inflammatory factors in microglial cells (Fig. 22) (Hirsch and Hunot 2009). Both in PD patients and in MPTP-injected mice, Fas expression is increased (Ferrer et al. 2000; Hayley et al. 2004).

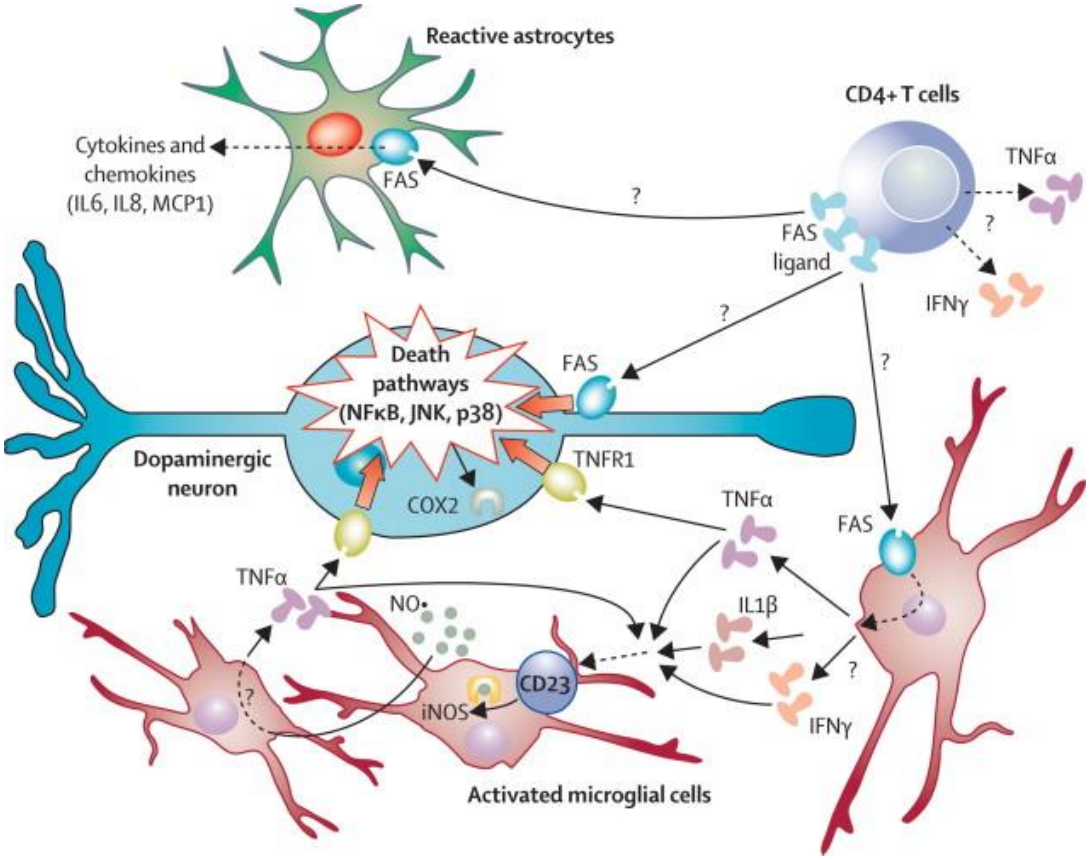

Figure 22. Possible mechanisms underlying the deleterious consequences of neuroinflammatory processes in PD. COX2: cyclooxygenase 2, IL: interleukin, iNOS: inducible nitric oxide synthase. MCP: monocyte chemoattractant protein, NF-κB: nuclear factor kappa-light-chain-enhancer of activated B cells, NO: nitric oxide, TNF: tumour necrosis factor, TNFR: tumour necrosis factor receptor. From: Hirsch and Hunot 2009.

In summary, the role of innate and adaptive immune responses in PD has not yet been fully established, but internal and external factors that influence inflammation may affect the physiology of innate immune cells in the brain and thus influence disease progression.

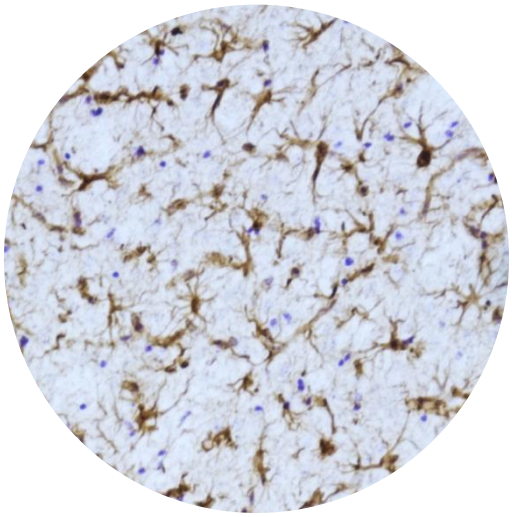

Objectives

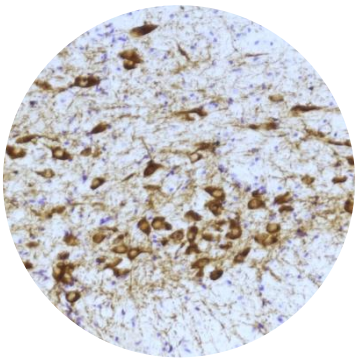

Objectives

The aim of this thesis is to study the involvement of the microglial inhibitory immune receptor CD200R1 in the modulation of neuroinflammation and its potential as a therapeutic target in Parkinson's disease. The specific objectives are:

1. To study the effect of CD200-CD200R1 alterations on glial activation and dopaminergic neurodegeneration using *in vitro* approaches.

1.1 To determine the effect of an anti-CD200 blocking antibody on glial activation in mixed glial cultures.

1.2 To evaluate the effect of the disruption of the CD200-CD200R1 system on glial activation in mixed glial and microglial cultures from CD200 knock-out mice.

1.3 To study the effect of the disruption of the CD200-CD200R1 system on dopaminergic neurodegeneration in mesencephalic cultures from CD200 knock-out mice.

2 To determine the effect of parkinsonian neurotoxins on glial activation and on the CD200-CD200R1 system in primary mixed glial and microglial cultures.

2.1 To analyse the effect of MPP+ and rotenone on the pro-inflammatory response of glial cells.

2.2 To study the effect of MPP+ and rotenone on the anti-inflammatory response of glial cells.

2.3 To assess the effect of MPP+ and rotenone on the CD200-CD200R1 system.

3 To evaluate the effect of CD200-CD200R1 modulation in the acute MPTP mouse model of PD.

3.1 To characterize the temporal pattern of neuroinflammation, dopaminergic neurodegeneration and CD200 and CD200R1 expression changes.

3.2 To determine the effect of the potentiation of the CD200-CD200R1 system using a CD200R1 agonist.

3.3 To study the effect of the disruption of the CD200-CD200R1 system using CD200 knock-out mice.

4 To determine the expression of the CD200-CD200R1 system in human samples.

4.1 To analyse the expression of CD200R1 mRNA variants in human monocytes and microglia-like cells.

4.2 To evaluate the expression of CD200R1 mRNA variants in microglia-like cells in response to different stimuli.

4.3 To study the CD200 and CD200R1 expression in *post-mortem* brain tissue of PD patients.

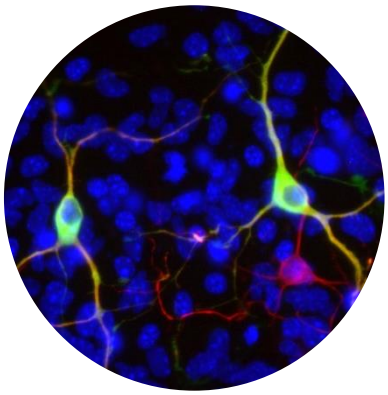

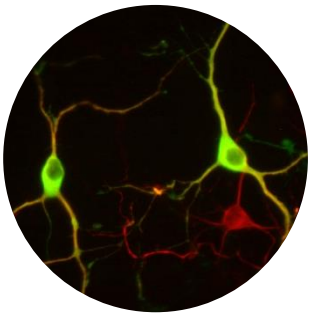

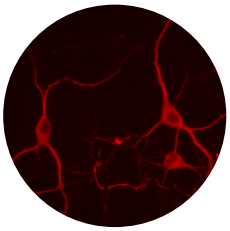

Materials and methods

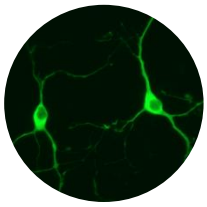

1 Animals

We used C57BL/6 mice from Charles River (Lyon, France) and from a CD200-deficient mice colony (Hoek et al. 2000). Animals were housed under controlled conditions (22ºC ± 1ºC; 12h light/dark cycle) with food and water available *ad libitum* and maintained under veterinary supervision. Experiments were carried out in accordance with European Union directives (86/609/EU) and Spanish regulations (BOE 67/8509-12, 1988) on the use of laboratory animals, and were approved by the Ethics and Scientific Committees of University of Barcelona and Consejo Superior de Investigaciones Científicas (CSIC). All the animal procedures and methods carried out at Vall d'Hebron Research Institute (VHIR) followed the Guide for the Care and Use of Laboratory Animals (Guide, 8th edition, 2011, NIH) and European (2010/63/UE), Spanish (RD53/2013) and Catalan (Decret 214/97) legislation. All the procedures had been approved by the Vall d'Hebron Research Institute Animal Ethical Experimental Committee.

1.1 CD200-DEFICIENT MICE

We received CD200-deficient mice from Dr. David Copland (University of Bristol, United Kingdom). CD200-deficient mice (CD200 knock-out, CD200 -/-) on the C57BL/6 background were generated at DNAX (Palo Alto, CA) (Hoek et al. 2000) using C57BL/6 embryonic stem cells.

2 *In vitro* experiments

2.1 PRIMARY GLIAL CULTURES

2.1.1 Primary mixed glial cultures

Mouse primary mixed glial cultures were prepared from 1- or 2-day-old neonatal C57BL/6 mice (Charles River, Lyon, France). The culture medium used consisted of Dulbecco's modified Eagle medium (DMEM)-F12 nutrient mixture (Invitrogen, Ref. 31330-038) supplemented with 10% heat-inactivated fetal bovine serum (FBS) (Invitrogen, Ref. 10270-106; Inactivation: 30 minutes at 60ºC), 20 U/mL penicillin - 20 µg/mL streptomycin (Invitrogen, Ref. 15140-114) and 0.5 µg/mL amphotericin B (Invitrogen, Ref. 15290-018).

For each culture, 5 to 8 cerebral cortices were dissected, placed in a petri dish with cold phosphate buffer (PBS) and carefully stripped of their meninges. In sterile conditions, the tissue was minced with a scalpel and transferred to a 50-mL tube for centrifugation (3 minutes at 200 g). The supernatant was discarded and the pellet was resuspended in 12 mL of warm 0.25% trypsin (Life Technologies, Ref. 25200-072) and transferred to a glass bottle with width base to improve the enzymatic digestion process. It was incubated in a shaking water bath for 25 min at 37ºC (100 rpm). Trypsinization was stopped by adding an equal volume of culture medium and the solution was transferred to a 50-mL tube. To avoid aggregation of cells by released sticky DNA from disrupted cells, 0.02% deoxyribonuclease I was added and mixed by inversion 6 to 8 times. The solution was gently dispersed by pipetting up and down 25 times with a 10 mL serologic pipette and centrifuged for 7 minutes at 200 g. The supernatant was discarded and the pellet was resuspended in 30 mL of warm culture medium. The cell suspension was filtered through a 100-µm-pore mesh. Cells were counted using a Neubauer chamber, seeded at a density of 350000 cells/mL in multi-well culture plates and cultured at 37ºC in a 5% CO2 humidified atmosphere. The working volume was 100, 300, 500 µL or 2.5 mL per well of 96-, 48-, 24- or 6-well plates, respectively. Medium was replaced every 7 days and cultures were used at 21 days *in vitro* (DIV). At this point, they are composed of 75% astrocytes and 25% microglia (Fig. 23). We usually obtained 4-5x10^6 cells/pup.

To obtain CD200 +/+ and CD200 -/- cultures, homozygous female and male mice from the CD200 knock-out colony (see section “3.4.1 Colony formation”) were crossed. CD200 +/+ and CD200 -/- cultures were obtained in parallel.

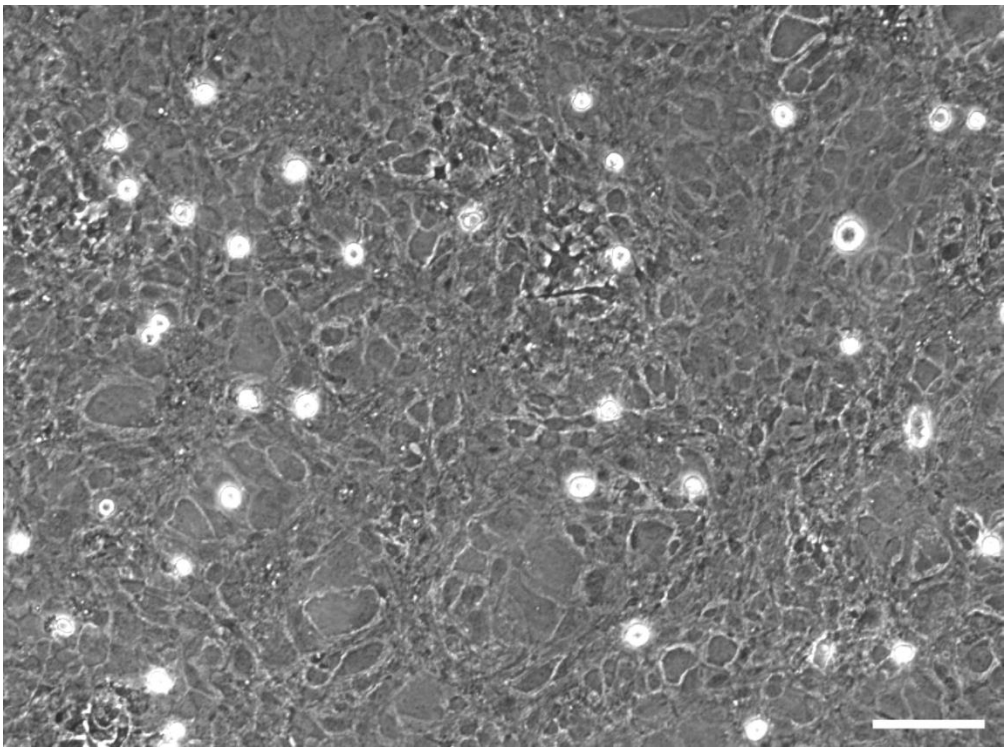

Figure 23. Primary mixed glial culture at 21 DIV. Phase-contrast image. Scale bar: 100 µm.

2.1.2 Primary microglial cultures

2.1.2.1 Mild trypsinization method

Mouse primary microglial cultures were prepared from mouse primary mixed glial cultures by the mild trypsinization method previously described in our group (Saura, Tusell, and Serratosa 2003). After 21 DIV, conditioned medium from mixed glial cultures was removed from plates and kept at 37ºC. Cultures were washed once with DMEM-F12 (Life technologies, Ref. 31330-038). Then, cultures were incubated for 30 min at 37ºC with trypsin (0.25% Trypsin-EDTA solution, Life Technologies, Ref. 25200-072) diluted 1:4 in DMEM-F12. This results in the detachment of an upper layer of cells in one piece containing astrocytes, leaving a population of cells firmly attached to the well identified as >98% microglia (Fig. 24). Trypsinization was stopped by adding an equal volume of serum-containing DMEM-F12. The medium containing the detached layer of cells was removed and conditioned medium was returned to the plates. Microglial cultures were used 24 h after isolation by this procedure.

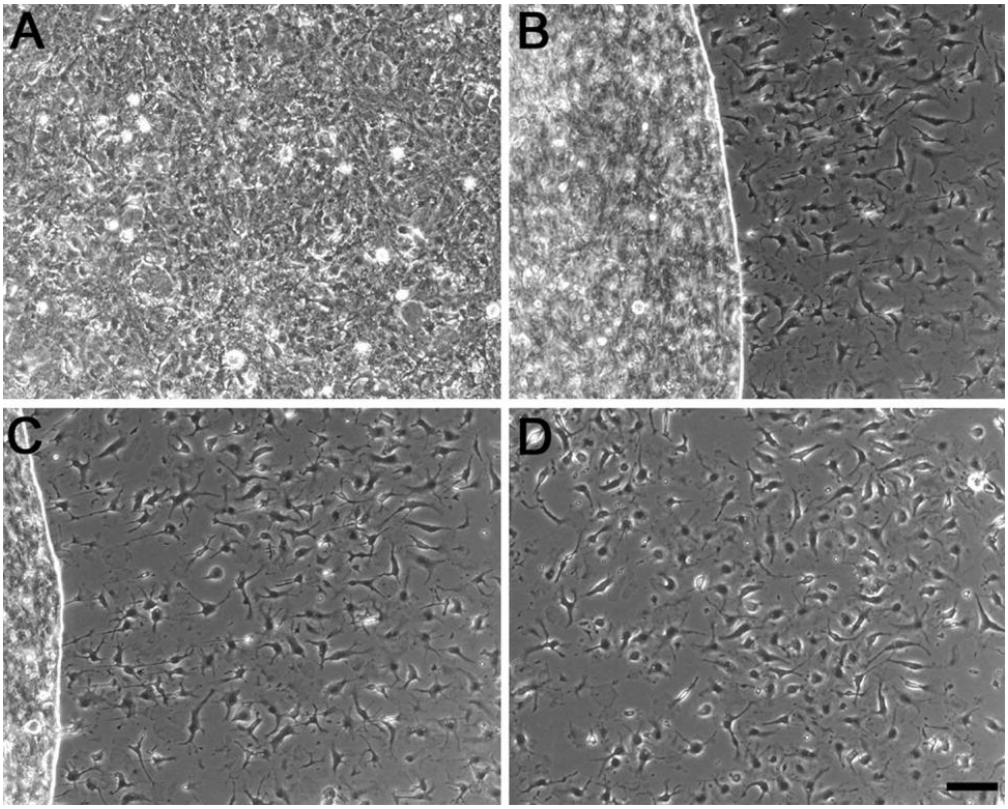

Figure 24. Microglial cultures obtained by the mild trypsinization method of mixed glial cultures. A-D Phase-contrast images. Detachment of the upper layer of cells containing astrocytes, leaving microglial cells attached. Scale bar: 40 μm**.** From: Saura et al. 2003.

2.1.2.2 PEI method

A simplified approach for high-yield isolation of microglial cells described by Dr. Raisman-Vozari and Dr. Michel's research team (Sepulveda-Diaz et al. 2016) was established in our laboratory after a short-term stage in their laboratory (Experimental therapeutics of Parkinson's disease laboratory, headed by Dr. Hirsch; *Institut du Cerveau et de la Moelle Epinière*, Paris). Microglial cells in culture were obtained from the brain of 1-day-old neonatal C57BL/6 mice (Charles River, Lyon, France). Before starting the culture procedure, polycation coating solution consisting of 2 mg/mL polycation polyethyleneimine (PEI, Fluka, Ref. P3143) diluted in a pH 8,3 borate buffer was applied (8 mL) to T-75 culture flasks (Corning, Ref. 430641U) for at least 30 minutes at 37ºC. Then, four washes with PBS (8 mL each) were done before cell seeding. The culture medium used consisted of 1X DMEM (Gibco, Ref. 31885-023) supplemented with 10% heat-inactivated FBS (Biowest, Ref S1820-500; Inactivation: 30 minutes at 60ºC) and 1% penicillin/streptomycin (Gibco, Ref. 15140-122) filtered using a 0.2-µm filter (Thermo Scientific, Ref. CASE 00186 00202A).

For each culture, 5 to 8 brains were dissected, placed in a petri dish with cold PBS and carefully stripped of their meninges. Brains were placed in a 15-mL tube containing 3 mL of cold L15 Leibovitz medium (Gibco, Ref. L11415-049) and, in sterile conditions, cells where mechanically dissociated by repeated pipetting (10 strokes plus 60 times up and down carefully) using a 1 mL sterile tip fitted to a Gilson pipette set to 900 µL. Culture medium was added to dissociated cells to complete a total volume of 12 mL. Cells were gently mixed by inversion and debris allowed to settle down for 10 minutes at room temperature. Then, the supernatant containing dissociated cells in suspension was carefully transferred to a 50-mL tube, while tissue pieces that remained not dissociated at this stage were taken for another round of trituration. The final supernatant was then centrifuged at 1000 rpm for 6 min at 4ºC. The resulting pellet was resuspended before plating at a density of 2 brains/12 mL and cultured at 37ºC in humidified 5% CO_2/95% air. The working volume was 12 mL per PEI-coated Corning T-75 flask. Over time, astrocytes die and progressively detach while microglial cells remain attached and proliferate (Fig. 25A,B). When astrocytes have totally disappeared (16-18 DIV, Fig. 25C), cultures are ready to use. If not used, 1 mL of medium/day has to be added (for maximum 10 days from that day). If medium is added too early when some astrocytes still remain in the flask, astrocytes proliferate and we will not obtain a pure microglial culture, whereas if medium is added too late microglia will die. Therefore, regular observation of cultures is extremely important.

Once astrocytes had totally disappeared, flasks were washed three times with 10 mL of serum free-DMEM and incubated with 5 mL of trypsin (0.05%)-EDTA (2 mM) solution (Gibco, Ref: 25300-054) 5-10 minutes at 37ºC for microglial cell detachment. Then, 10 mL of culture medium was added to neutralize the trypsin solution. Cells recovered by centrifugation at 1000 rpm for 6 min at 4ºC were counted using a Neubauer chamber and seeded at a density of 100000 and 250000 cells in a volume of 500 and 1000 µL per 48 and 24-well plate, respectively. At 20 DIV

(Fig. 25D) we usually obtained $4x10^6$ cells/T-75 flask. Cells were cultured at 37ºC in 5% CO_2 humidified atmosphere and used at 24 h *in vitro.*

To obtain CD200 +/+ and CD200 -/- cultures, homozygous female and male from the CD200 knock-out colony (see section “3.4.1 Colony formation”) were crossed. CD200 +/+ and CD200 -/- cultures were obtained in parallel.

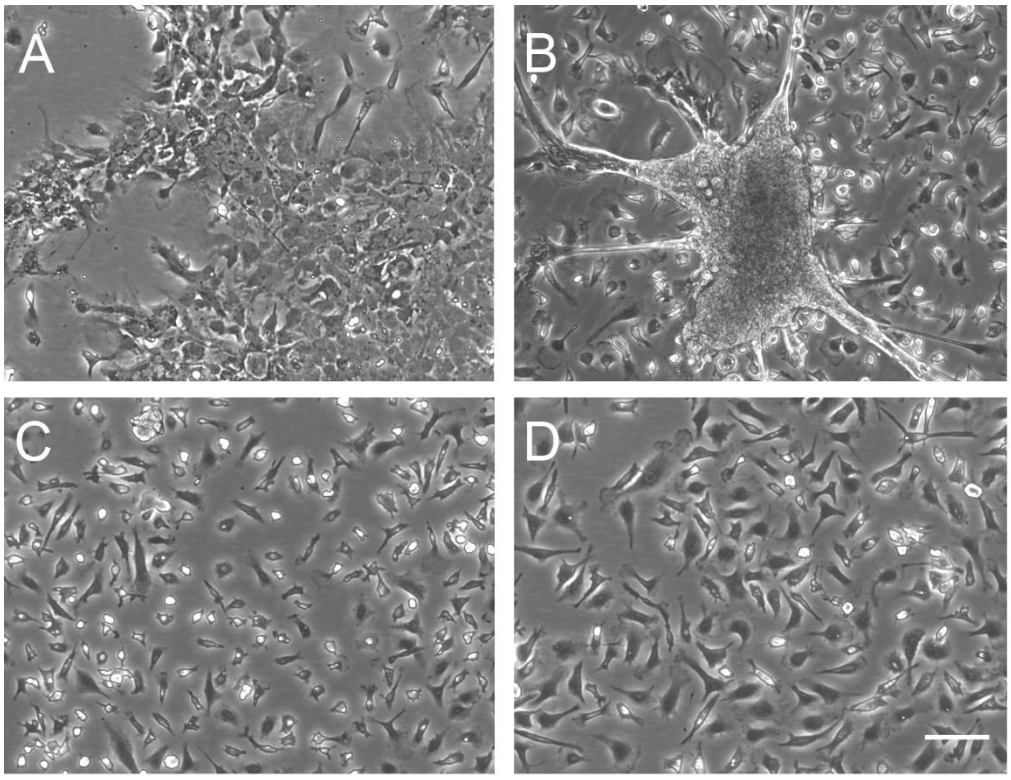

Figure 25. Primary microglial cultures following PEI method. Phase-contrast images. Detachment of the astrocytes over time, leaving microglial cells attached. Culture in a T-75 flask at 6 DIV (**A**), 12 DIV (**B**), 16 DIV (+1 mL of medium added) (**C**) and 20 DIV (**D**) ready for trypsinization. Scale bar: 50 µm.

2.2 PRIMARY MESENCEPHALIC NEURON-GLIA CULTURES

Mouse ventral mesencephalic neuron-glia cultures were established following the protocol described by Professor J.S. Hong (Research Triangle Park, NC, USA) (Chen, Oyarzabal, and Hong 2013), with some modifications. Ventral mesencephalic tissue was carefully dissected from gestational age 13/14 days C57BL/6 mouse embryos. Simultaneously pregnant CD200 -/- females and CD200 +/+ females from the CD200 knock-out colony (see section ““3.4.1 Colony formation”) were used to obtain CD200 -/- and CD200 +/+ embryos and cultures were done in parallel.

Before starting the culture procedure, 48-well plates (Thermo Scientific, Nunc™ 150687), were coated with poly-D-lysine (300 µL/well, 25 mg/L in H_2O, Sigma-Aldrich, Ref. 27964-99-4) for at least 2 h at 37ºC.

The culture medium was freshly prepared. 12,5 mL of DMEM (Millipore, Ref. F0455) were diluted in 112,5 mL of miliQ water and, once adjusted to pH 7, it was supplemented with 147.88 mg of D-glucose (Sigma-Aldrich, Ref. G6152) and 275 mg of $NaHCO_3$ (Sigma-Aldrich, Ref. S8875). Then, 12.5 mL of this medium were discarded and 0.125 mL of 4-aminobenzoic acid (Sigma-Aldrich, Ref. A9878), 0.25 mL of penicillin G (Sigma-Aldrich, Ref. P3032), 0.438 mL of insulin (Sigma-Aldrich, Ref. I5500) and 3.87 mg of L-glutamine (Sigma-Aldrich, Ref. G8540) were added. The medium was filtered using 0.2 µm syringe filter (TPP, Ref. 99722) and supplemented with 12.5 mL of heat-inactivated FBS (Life Technologies, Ref. 10270-106. Inactivation: 30 minutes at 60ºC).

For each culture, two pregnant females were used. Embryos were removed from the amniotic membrane, transferred into a petri dish with cold PBS for a rinse and transferred into a new petri dish with cold PBS. Under the microscope, the ventral mesencephalic region was dissected (Fig. 26) and placed in a petri dish with cold culture medium. Figure 26 illustrates the procedure for mesencephalic isolation. In sterile conditions, midbrain tissue was transferred into a 50-mL tube and PBS was added up to 7 mL. Mechanical dissociation was done by slowly passing 15 times the tissue through a 10 mL serological pipette. Then, 1 mL pipette tip was fitted to the end of a 5 mL serological pipette and the tissue was passed through it 10 times. Finally, a 200 µL pipette tip was fitted to the end of a 5 mL serological pipette and tissue was passed through it 5 times. After centrifugation (430 g for 6 minutes at 4ºC) supernatant was discarded and the pellet was resuspended in 10 mL of warm culture medium.

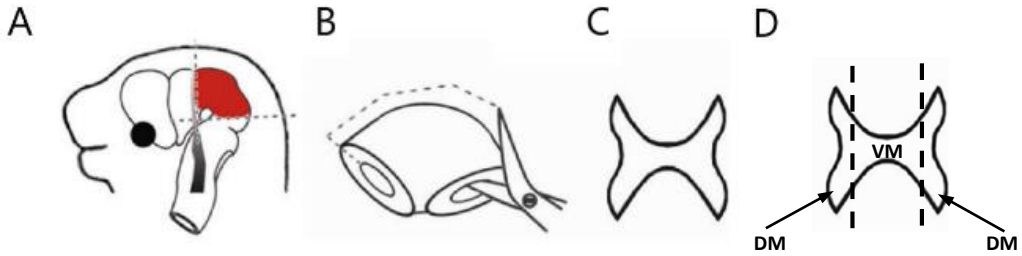

Figure 26. Illustration of the steps to isolate the mesencephalic region. Under the microscope (**A**) separate the rostral forebrain (use the traverse sinus as hallmark) and the caudal hindbrain from the mesencephalic region as indicated by the dotted lines. **B** Butterfly the tissue by inserting the microdissection scissors through the inside of the mesencephalic region of the neural tube and slicing open the tissue along the dorsal midline. **C** Remove the meninges from the butterflied mesencephalic tissue. **D** In order to increase the proportion of dopaminergic neurons, make two horizontal cuts to remove the dorsal mesencephalon (DM) from the ventral mesencephalon (VM). Modified from: Chen, Oyarzabal, and Hong 2013.

.

The cell suspension was filtered through a 70-µm-pore mesh. Using trypan blue stain, viable cells were counted in a Neubauer chamber and seeded at a density of 1 x 10^6 cells/mL in poly-D-

lysine-coated 48-well plates and cultured at 37ºC in a 5% CO2 humidified atmosphere (Fig. 27). The working volume was 300 µL per well of 48-well plate. Cultures were used at 10 DIV. We usually obtained 0.8-1.5x10^6 cells/pup.

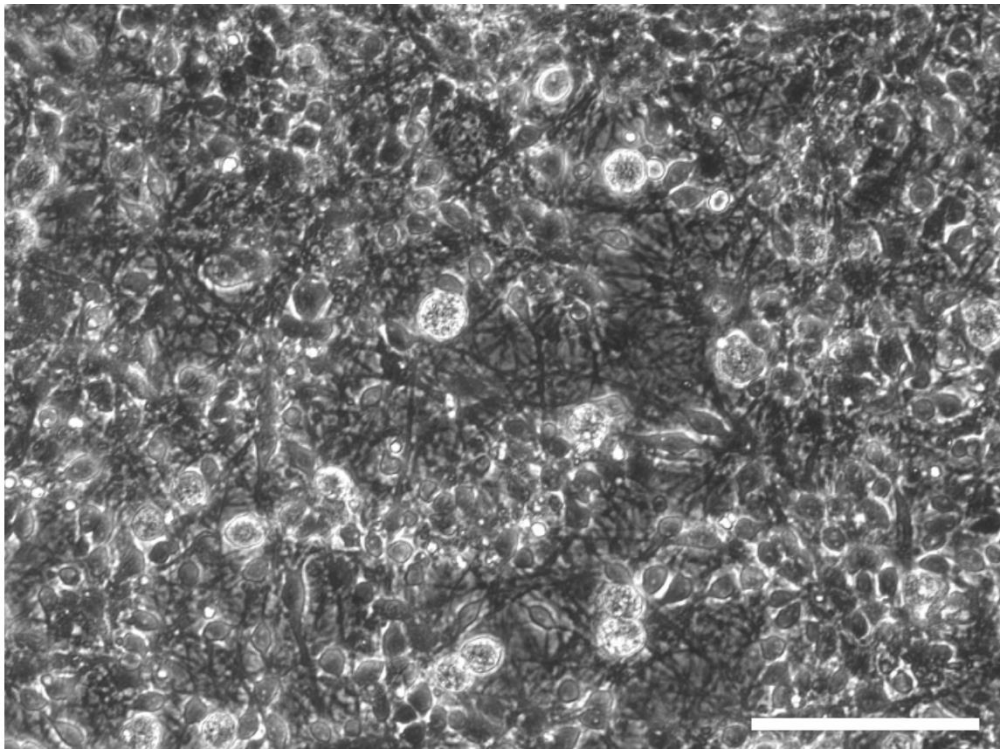

Figure 27. Primary mesencephalic culture. Phase-contrast image of mesencephalic culture at 10DIV. Scale bar: 100 µm.

2.3 HUMAN MONOCYTE AND MICROGLIA-LIKE CELL CULTURES

Monocyte cultures were prepared from peripheral blood cells of healthy adult volunteers. To this end, 60 mL of peripheral blood were collected in collaboration with the Neurology Unit, Hospital Clinic de Barcelona using 18 mg EDTA tubes (BD Biosciences, Ref. 367525). Peripheral blood mononuclear cells were isolated by Histopaque-1077 (Sigma-Aldrich, Ref. 10771) density gradient centrifugation following the manufacturer's protocol. Three 50-mL tubes were filled with 20 mL of Histopaque-1077 each and brought to room temperature. 20 mL of blood were gently layered onto the Histopaque-1077. This step was done very carefully to avoid mixing the two liquids. The samples were centrifuged at 400 g for 30 minutes at room temperature. During centrifugation, erythrocytes aggregate and rapidly sediment, granulocytes become slightly hypertonic resulting in pelleting at the bottom of the tube, and lymphocytes and other mononuclear cells band at the interface between Histopaque-1077 and plasma (Fig. 28).

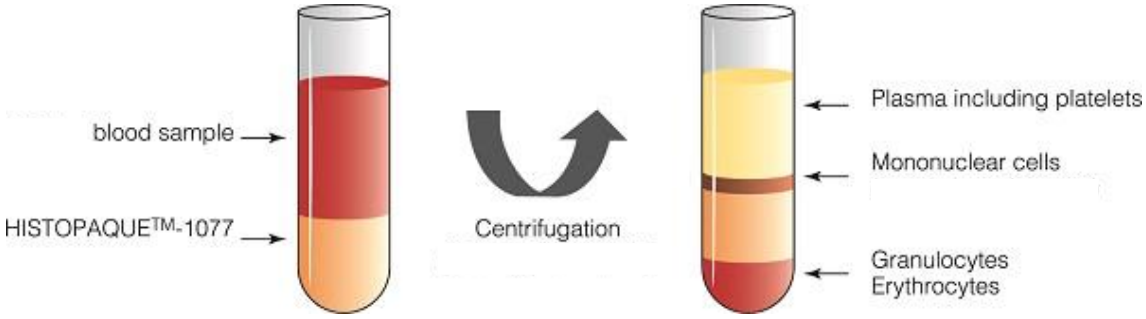

Figure 28. Histopaque-1077 density gradient centrifugation (Sigma-Aldrich, Ref. 10771).

After centrifugation, the opaque interface containing the mononuclear cells (approximately 4 mL) was carefully transferred from each 50-mL tube into three clean 15-mL tubes and washed three times by adding 10 mL of culture medium and centrifuging at 250 g for 10 minutes. In the last wash, the 3 pellets were collected in a single 15-mL tube. The culture medium consisted of RPMI-1640 Glutamax (Invitrogen, Ref. 61870-044) supplemented with 10% heat-inactivated FBS (Life Technologies, Ref. 10270-106. Inactivation: 30 minutes at 60ºC), 100 U/mL penicillin - 100 µg/mL streptomycin (Life Technologies, Ref. 15140-122), and 0.25 µg/mL amphotericin B (Life Technologies, Ref. 15290-018). Peripheral blood mononuclear cells were counted using a Neubauer chamber, plated onto 48-well plates (200 µL per well) at a density of 4 x 10^5 cells/mL and cultured at 37ºC in a 5% CO2 humidified atmosphere. The next day, culture medium and non-adherent cells were aspirated. The remaining adherent cells correspond to monocytes and at this time point were used.

To obtain human induced microglia-like cells, these monocyte cultures were used, following the protocol described by Ohgidani and collaborators (Fig. 29) (Ohgidani et al. 2014). The monocyte cultures described above were cultured with RPMI-1640 Glutamax supplemented with 100 U/mL penicillin - 100 µg/mL streptomycin, 0.25 µg/mL amphotericin B and a mixture of cytokines: recombinant human GM-CSF (10 ng/mL; R&D Systems, Ref. RYD-215-GM-010) and recombinant human IL34 (100 ng/mL; Peprotech (Bionova), Ref. 200-34) in order to obtain induced microglia-like cells (Ohgidani et al. 2014). After 7 DIV the medium containing cytokines was changed for medium without cytokines and at 14 DIV cultures were used.

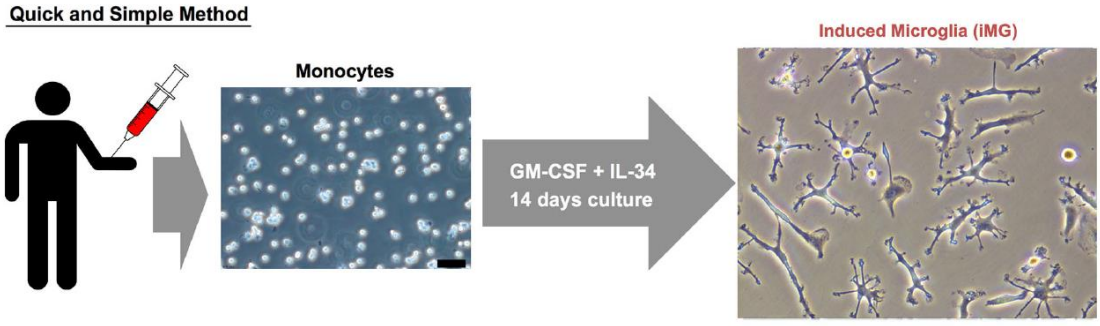

Figure 29. Induced microglia-like cells from human peripheral blood cells. From: Ohgidani et al. 2014.

2.4 TREATMENTS

2.4.1 Pro-inflammatory stimuli

Lipopolysaccharide and interferon-γ (LPS/IFNγ)

Cultures were treated with LPS from *Escherichia coli* 026:B6 (100 ng/mL diluted in medium; Sigma-Aldrich, Ref. L8274) plus recombinant mouse IFNγ produced by *Escherichia coli* (0.1, 1 or 30 ng/mL diluted in medium; Sigma-Aldrich, Ref. I4777) for different lengths of time.

2.4.2 Anti-inflammatory stimulus

Interleukin (IL)4

Cultures were treated with recombinant mouse IL4 produced by CHO Cells (50 ng/mL diluted in medium; Creative BioMart, Ref. 297M) for different lengths of time.

2.4.3 CD200-CD200R1 modulation

Anti-CD200 blocking antibody

Rat anti-mouse CD200 (0.1, 0.5, 1, 5 µg/mL diluted in medium; Bio-Rad, Ref. MCA1958GA) or its corresponding isotype control (rat IgG2a) (0.1, 0.5, 1, 5 µg/mL diluted in medium; AbD, Bio-Rad, Ref. MCA1212) was added to the culture medium 30 minutes prior to LPS/IFNγ treatment.

2.4.4 Parkinsonian neurotoxins

1-methyl-4-phenylpyridinium (MPP+) and rotenone

Glial cultures were treated with 10, 25, 50 or 100 µM MPP+ (Sigma-Aldrich, Ref. D048) or 20, 40, 100 or 150 nM rotenone (Sigma-Aldrich, Ref. R8875) for different lengths of time, in the absence or presence of LPS/IFNγ or IL4. MPP+ or rotenone, and LPS/IFNγ or IL4 were added simultaneously to the culture medium. Mesencephalic cultures were treated with 0.1, 1, 5 or 10 µM MPP+ (Sigma-Aldrich, Ref. D048) or 0.1, 1, 5 or 10 nM rotenone (Sigma-Aldrich, Ref. R8875) for different lengths of time. Stock solutions of 50 mM MPP+ in milliQ H_2O and 10 mM rotenone in dimethyl sulfoxide (DMSO) were freshly prepared on the day of treatment and diluted in medium. DMSO in the cell cultures was always below 1/1000.

2.5 CELL VIABILITY

2.5.1 MTT assay

Despite being used to determine cell metabolic activity, the 3-(4,5-dimethylthiazol-2-yl)-2,5-diphenyl tetrazolium bromide (MTT) assay is also used to estimate cell viability. MTT is converted to water-insoluble MTT-formazan of dark blue colour by mitochondrial dehydrogenases of living cells. The blue crystals are solubilized with DMSO and the intensity is measured colorimetrically at a wavelength of 570 nm. 96-well plates of mixed glial or microglial cultures were treated in quadruplicate. After 24 h of treatment, MTT (5 mg/mL; Sigma-Aldrich, Ref. M2128) was added to each well and plates were incubated for 30 (mixed glial cultures) or 90 minutes (microglial cultures) at 37ºC and 5% CO_2. Then, the medium was removed and 200 µL (mixed glial cultures) or 100 µL (microglial cultures) of DMSO (Scharlau, Ref. SU01581000) were added. Finally, the reduction of MTT was estimated by optical density at 570 and 650 nm using a microplate reader (Multiskan Spectrum, Thermo Electron Corporation, Waltham, CA). The results were expressed as percentage of control.

2.5.2 Propidium iodide/Hoechst 33342 staining

Propidium iodide/Hoechst 33342 double staining was performed to detect dead cells. Propidium iodide (PI) is a red-fluorescent nuclear and chromosome counterstain that is not permeant to live cells. It binds to DNA by intercalating between the bases, with no sequence preference, of those cells that have lost their membrane integrity. On the contrary, Hoechst 33342 is a cell-permeant nuclear counterstain. It emits blue fluorescence when bound to dsDNA, regardless of whether cells have lost their membrane integrity or not. 96-well plates of mixed glial cultures or microglial cultures were treated in duplicate. After 24 h of treatment, PI (7.5 µg/mL; Molecular Probes, Ref. P-1304) and Hoechst 33342 (3 µg/mL; Molecular Probes, Ref. H21492) were added to each well and plates were incubated for 10 minutes. Two images were taken per well under a fluorescence microscope with 4X (microglial cultures) or 10X objectives (mixed glial cultures) using an Olympus IX70 microscope (Olympus, Okoya, Japan) and a digital camera (CC-12, Olympus Soft Imaging Solutions GmbH, Hamburg, Germany). The results were expressed as percentage of dead cells [(PI+ cells/Hoechst+ cells) x 100].

2.6 NITRIC OXIDE PRODUCTION

Nitric oxide (NO) production was assessed by measuring the accumulation of nitrite ion (NO_2^-) in culture supernatants using the colorimetric Griess reaction. Culture supernatants were collected 24 and 48 h after treatment. Fifty µL of each experimental sample and 50 µL of each point of a

sodium nitrate standard curve (100, 50, 25, 12.5, 6.25, 3.13, 0 µM of $NaNO_2$) were added to a 96-well plate in duplicate. Then, 50 µL of Griess reagent [25 µL of 0.1% N-(1-naphthyl)ethylenediamine dihydrochloride (Sigma-Aldrich, Ref. N5889) in Milli-Q water and 25 µL of 1% sulfanilamide (Sigma-Aldrich, Ref. S9251) in 5% phosphoric acid and Milli-Q water] were dispensed to all wells containing experimental samples or standards. After 10 minutes of incubation at room temperature, optical density at 540 nm was determined using a microplate reader (*Multiskan Spectrum*, Thermo Fisher Scientific, Vantaa, Finland). Nitrite concentration was determined from the standard curve.

2.7 GENE EXPRESSION

2.7.1 RNA extraction

Isolation of RNA was performed 6 or 24 h after cell treatments. One well from 6-well plates, or two wells from 6-well plates, or twelve wells from 48-well plates were used per experimental condition for primary mixed glial cultures, primary microglial cultures or monocytes and microglia-like cultures, respectively. Total mRNA was isolated from mixed glial cultures with *High Pure RNA Isolation Kit* (Roche Diagnostics, Ref. 11 828 665 001). For primary microglial, monocyte and microglia-like cultures, samples with small amount of RNA, we used the *PureLink RNA micro kit* (Invitrogen, Ref. 12183-016). RNA was extracted according to the manufacturer's instructions. Total RNA concentration was measured on a Nanodrop 1000 (Thermo Fischer Scientific). The resulting RNA was stored at -80ºC until further use.

2.7.2 Reverse transcription

Before assessing mRNA expression levels, RNA samples were retrotranscribed to complementary DNA (cDNA). To this end, 0.2 - 1 µg of RNA were reverse transcribed with random and oligo(dT) primers by using *qScript™ cDNA Synthesis Kit* (Quanta Biosciences, Ref. 95047) or with gene-specific primers by using *qScript™ Flex cDNA Synthesis Kit* (Quanta Biosciences, Ref. 95049) and according to manufacturer's instructions. The reverse transcription was performed using a thermal cycler under the following protocol: 25ºC for 5 minutes, 42ºC for 30 minutes and 85ºC for 5 minutes (in the case of random and oligo(dT) primers) or 65ºC for 5 minutes, 42ºC for 45 minutes and 85ºC for 5 minutes (in the case of gene-specific primers). The resulting cDNA was stored at -20ºC until used.

2.7.3 Quantitative real-time PCR (qPCR)

To analyse mRNA expression levels quantitatively, 3 ng of cDNA were used. Specific primers (Integrated DNA Technology) for each gene were used (Table 5). qPCR was carried out using *SYBR Green Mix* (PCR Biosystems, Ref. PB20.11-50) in 15 µL of final volume, using an *iCycler MyIQ* apparatus (Bio-Rad Laboratories). Samples were run at 95ºC for 2 minutes to activate the polymerase followed by 40 cycles consisting on denaturation: 95ºC for 15 s; annealing: 60ºC for 30 s; and extension: 72ºC for 15 s. The mRNA levels were quantified using threshold cycle (Ct) obtained using the *CFX Manager software* (Bio-Rad Laboratories). Relative gene expression values were calculated using the $2^{-\Delta\Delta CT}$ method (Livak and Schmittgen 2001). The result obtained is the fold change of the target gene in the test sample relative to the control sample and normalized to the expression of the reference genes (Table 5).

Table 5 Primers used for qPCR.

Species: *Mus musculus*			
Target mRNA	**Accession number**	**Forward primer (5'→3')**	**Reverse primer (5'→3')**
Arg1	NM_007482.3	TTGCGAGACGTAGACCCTGG	CAAAGCTCAGGTGAATCGGC
Carkl	NM_029031.3	CAGGCCAAGGCTGTGAAT	GCCAGCTGCATCATAGGACT
Cd11b	NM_008401.2	AAGCAGCTGAATGGGAGGAC	GAATGACCCCTGCTCTGTCT
Cd200full	NM_010818.3	GGGCATGGCAGCAGTAGCG	TGTGCAGCGCCTTTCTTTC
Cd200tr	NM_001358443.1	GATGGGCAGTCTGTGGAAGTG	GAGAACATCGTAAGGATGCAGTTG
Cd200R1	NM_021325.3	AGGAGGATGAAATGCAGCCTTA	TGCCTCCACCTTAGTCACAGTATC
COX2	NM_011198.4	TGCAGAATTGAAAGCCCTCT	CCCCAAAGATAGCATCTGGA
Fizz1	NM_020509.3	TCCCAGTGAATACTGATGAGA	CCACTCTGGATCTCCCAAGA
Gfap	NM_010277.3	AAGGTCCGCTTCCTGGAA	GGCTCGAAGCTGGTTCAGTT
Glut1	NM_011400.3	CATCCTTATTGCCCAGGTGTTT	GAAGATGACACTGAGCAGCAGA
gp91phox	NM_007807.5	ACTCCTTGGGTCAGCACTGGCT	GCAACACGCACTGGAACCCCT
Hifα	NM_010431.2	ACAAGTCACCACAGGACAG	AGGGAGAAAATCAAGTCG
Hk1	NM_010438.3	GATGGAGGTGAAGAAGAAGC	GGAAACGAGAAGGTGAAGC
Iba1	NM_019467.3	GAAGCGAATGCTGGAGAAAC	AAGATGGCAGATCTCTTGCC
IL10	NM_010548.2	TGAATTCCCTGGGTGAGAAG	ACACCTTGGTCTTGGAGCTT
IL1β	NM_008361.4	TGGTGTGTGACGTTCCCATTA	CAGCACGAGGCTTTTTTGTTG
IL1ra	NM_031167.5	AGGCCCCACCACCAGCTTTGAGTC	TCACCCAGATGGCAGAGGCAACAA
IL4	NM_021283.2	CGAGGTCACAGGAGAAGGG	AAGCCCTACAGACGAGCTCACT
IL6	NM_031168.2	CCAGTTTGGTAGCATCCATC	CCGGAGAGGAGACTTCACAG
iNOS	NM_010927.3	GGCAGCCTGTGAGACCTTTG	GCATTGGAAGTGAAGCGTTTC
MR	NM_008625.2	TCTTTTACGAGAAGTTGGGGTCAG	ATCATTCCGTTCACCAGAGGG
Nrf2	NM_010902.4	GATCCGCCAGCTACTCCCAGGTTG	CAGGGCAAGCGACTCATGGTCATC
Pfkp	NM_019703.4	AAGCTATCGGTGTCCTGACC	TCCCACCCACTTGCAGAAT
Pgc1β	NM_133249.3	TCCAGAAGTCAGCGGCCT	CTGAGCCCGCAGTGTGG
TGFβ	NM_011577.2	TGCGCTTGCAGAGATTAAAA	AGCCCTGTATTCCGTCTCCT
TNFα	NM_013693.3	TGATCCGCGACGTGGAA	ACCGCCTGGAGTTCTGGAA
Ym1	NM_009892.3	GGGCATACCTTTATCCTGAG	CCACTGAAGTCATCCATGTC
Reference genes:			
βactin	NM_007393.5	CAACGAGCGGTTCCGATG	GCCACAGGATTCCATACCCA
Gapdh	NM_008084.3	GGTGAAGGTCGGTGTGAACG	CTCGCTCCTGGAAGATGGTG
Rn18s	NR_003278.3_	GTAACCCGTTGAACCCCATT	CCATCCAATCGGTAGTAGCG

Arg1, arginase 1; Carkl, carbohydrate kinase-like protein; CD11b, cluster of differentiation 11b; CD200full, full-length CD200; CD200tr, truncated CD200; CD200R1, CD200 receptor 1; COX2, cyclooxygenase 2; Fizz1, found in inflammatory zone 1; Gfap, glial fibrillary acidic protein; Glut1, glucose transporter 1; GAPDH, glyceraldehyde-

3-phosphate dehydrogenase; gp91phox, catalytic subunit of NADPH oxidase; Hif1α, glycolysis activator hypoxia-inducible factor 1α; Hk1, hexokinase 1; Iba1, ionized calcium binding adaptor molecule 1; IL10, interleukin 10; IL1β, interleukin 1β; IL1ra, interleukin 1 receptor antagonist; IL6, interleukin 6; iNOS, inducible nitric oxide synthase; MR, mannose receptor; Nrf2, nuclear factor erythroid 2-related factor 2; Pfkp, phosphofructokinase, platelet; Rn18s, 18S ribosomal RNA; TGFβ, transforming growth factor β; TNFα, tumor necrosis factor α; Ym1, chitinase 3-like 3.

Species: *Homo sapiens*			
Target mRNA	**Accession number**	**Forward primer (5'→3')**	**Reverse primer (5'→3')**
CD200full	NM_005944.6	CAGCCTGGTTTGGGTCATG	GCAGAGAGCATTTTAAGGAAGCA
CD200tr	NM_001318828.1	GATGGAGAGGCTGTGCAAGTG	GCAGAGAGCATTTTAAGGAAGCA
For CD200R1 primers see Section "4.1 CD200R1 mRNA expression in human monocytes and microglia-like cells"			
Reference genes:			
GAPDH	NM_002046.7	GAAGGTGAAGGTCGGAGTCA	GTTAAAAGCAGCCCTGGTGA
RPS18	NM_022551.3	GATGGGCGGCGGAAAAT	CTTGTACTGGCGTGGATTCTGC

CD200full, full-length CD200; CD200tr, truncated CD200; CD200R1, CD200 receptor 1; GAPDH, glyceraldehyde-3-phosphate dehydrogenase; RPS18, ribosomal protein S18.

2.7.4 Conventional PCR

The cDNA was diluted 1/10 to perform conventional PCR. Specific primers (Integrated DNA Technology) for each gene were used (Table 4.3 in section "Results: 4 Expression of CD200-CD200R1 system in human samples"). Conventional PCR was carried out using *2x PCRBIO Ultra Mix* (PCR Biosystems, Ref. PB10.32-01) in 20 µL of final volume according to manufacturer's instructions in a thermal cycler under the following protocol: 95ºC for 2 minutes followed by 37 cycles consisting on: 95ºC for 20 s; 60ºC for 35 s; and 72ºC for 30 s. The amplified DNA was loaded onto an agarose gel, together with a DNA ladder (Thermo Scientific, Ref. SM0311). For DNA detection, *Midori green nucleic acid staining solution* was used (Nippon Genetics Europe, Ref. MG04) and images were obtained using a UV Transilluminator (Gel Doc System, Bio-Rad Laboratories).

2.8 PROTEIN EXPRESSION

2.8.1 Protein extraction and western blot

2.8.1.1 Protein extraction and quantification

Protein levels were determined in primary mixed glial and microglial cells 24 or 48 h after treatments. For isolation of total protein, one or two wells from 6-well plates were used per condition for primary mixed glial or microglial cultures, respectively.

After a cold PBS wash, mixed glial or microglial cells were scrapped and recovered in 100 or 25 µL of radioimmunoprecipitation assay (RIPA) buffer (1% Igepal CA-630, 5 mg/mL sodium deoxycholate, 1 mg/mL sodium dodecyl sulphate (SDS) and protease inhibitor cocktail Complete® (Roche, Ref. 1836145) in PBS) per well, respectively. The content of the wells was pooled, sonicated and centrifuged for 5 min at 10400 g at 4ºC. Harvested supernatants were stored at -20°C. Protein concentration was determined using the Bio-Rad Protein assay kit (Bio-Rad Laboratories, Ref. 500-0006), based on the Bradford assay (Bradford 1976).

2.8.1.2 Western blot

To analyse protein levels semi-quantitatively, western-blot technique was used. Thirty µg of protein were loaded per lane. Protein extracts were diluted in Loading Buffer (120 mM Tris HCl pH 6.8, 10% glycerol, 3% SDS, 20 mM dithiothreitol, 0.4% bromophenol blue) and denatured at 100°C for 5 minutes. Following a standard protocol (Mahmood and Yang 2012), the protein solutions were resolved by SDS-poliacrilamide gel electrophoresis (PAGE) on 8 or 12% polyacrylamide gels, together with a molecular weight marker (*PageRuler™ Plus Prestained Protein Ladder*, Thermo Scientific, Ref. 26619). Polyacrylamide gels were composed of a stacking gel (pH 6.8 125 mM Tris, 0.1 % SDS, 4% bis-acrylamide (29:1), 0.1 % PSA, 0.1 % TEMED) and a separating gel (pH 8.8 375 mM Tris, 0.1 % SDS, 8 or 12% bis-acrylamide (29:1), 0.1 % PSA, 0.1 % TEMED). A 90V current for 10 minutes followed by 120V current for 90 minutes was applied through the gel, using a running buffer (25 mM Tris (pH 8.3), 192 mM glycine, 0.1% SDS). Proteins were transferred to polyvinylidene fluoride (PVDF) membranes (Millipore, Ref. IPVH00010) by traditional wet transfer method for 120 minutes at 60V in transfer buffer (pH 8.3 25 mM Tris, 192 mM glycine, 0.02% SDS, 20% methanol).

Membranes were blocked for non-specific interactions with 5% non-fat dry milk in Tris-Buffered Saline (TBS)-Tween-20 (pH 7.5 20 mM Tris, 150 mM NaCl, 0.05% Tween-20) for 1 h at room temperature and incubated overnight at 4ºC with the desired primary antibody (Table 6). Then, the membranes were incubated with the corresponding horseradish peroxidase (HRP)-conjugated secondary antibody for 1 h at room temperature (Table 7), followed by repeated washing with TBS (pH 7.5 20 mM Tris, 150 mM NaCl, 0.2%). The signal was developed with the western blotting detection kit *WesternBrith™ Sirius HRP substrate* (Advansta, Ref. K-12043) and images were obtained using a *VersaDoc System* (Bio-Rad Laboratories). Data are expressed as the ratio between the band intensity of the protein of interest and the loading control protein (βactin or βtubulin).

Table 6. List of primary antibodies used for western blot.

Primary antibodies					
Epitope	**Weight (kDa)**	**Source**	**Dilution**	**Reference**	**Company**
ARG1	38	Goat polyclonal	1/250	sc-18354	Santa Cruz
βactin	42	Mouse monoclonal	1/60000	A1978	Sigma-Aldrich
βtubulin	50	Mouse monoclonal	1/50000	T4026	Sigma-Aldrich

CD200	44	Goat polyclonal	1/500	AF3355	R&D
CD200R1	38	Goat polyclonal	1/250	sc-14392 (M-21)	Santa Cruz
COX2	72	Rabbit polyclonal	1/1000	sc-1747 (M-19)	Santa-Cruz
iNOS	130	Rabbit polyclonal	1/1000	sc-651 (N-20)	Santa-Cruz
MR	190	Rabbit polyclonal	1/1000	ab64693	Abcam

ARG1, arginase 1; CD200R1, CD200 receptor 1; CD68, cluster of differentiation 68; COX2, cyclooxygenase 2; iNOS, inducible nitric oxide synthase; MR, mannose receptor.

Table 7. List of HRP-conjugated secondary antibodies used for western blot.

HRP-conjugated secondary antibodies				
Epitope	**Source**	**Dilution**	**Reference**	**Provider**
Goat immunoglobulins	Rabbit	1/2000	P0449	Dako
Mouse IgG (H+L)	Goat	1/5000	170-6516	Bio-Rad
Rabbit IgG	Donkey	1/5000	NA934V	GE Healthcare

2.8.2 Secreted protein detection: ELISA

The amount of cytokines released into the culture medium in primary mixed glial or microglial cultures was measured using specific Enzyme-linked immuno sorbent assay (ELISA) kits (*mouse IL1β ELISA Ready-SET-GO!, mouse IL6 ELISA Ready-SET-GO! and mouse TNFα ELISA Ready-SET-GO!*, eBioscience - Affimetrix, Ref. 88-7013-88, 88-7064-88, 88-7324-88, respectively) following manufacturer's instructions. Two wells from 48-well plates or one well from 6-well plates were used per experimental condition for primary mixed glial or microglial cultures, respectively. Culture medium was collected 24 h after treatments and stored at -80ºC until assayed for cytokine content. Cytokine concentrations were determined from standard curves.

2.9 IMMUNOCYTOCHEMISTRY

To observe morphological changes, to quantify changes in cell number of a certain cell type or to evaluate the presence or absence of a certain protein in cultured cells, we performed single or double immunofluorescence in 48-well plates. After 24 h of treatment in duplicates, cells were fixed. For microglial cultures, the fixation procedure consisted in aspirating the medium and incubating the cells with 4% paraformaldehyde (PFA) in 0.1 M sodium PBS for 15 minutes at room temperature. For mixed glial cultures, it consisted of three steps: first, 300 µL 4% PFA was added to the culture wells without having removed the culture medium; after 5 minutes, half of the liquid was removed and 300 µL 4% PFA were added to the culture wells; 5 minutes later, the liquid was totally removed and 300 µL 4% PFA were added to the culture wells for 5 minutes. This gradual fixation in mixed glial cultures avoided losing superficial microglial cells not firmly attached to the astrocyte layer. Non-specific interactions were blocked by incubating cells with 10% normal donkey serum (Vector Laboratories) in PBS containing 1% bovine serum albumin (BSA), for 20

minutes at room temperature. After that, cells were incubated overnight at 4°C with one (single immunofluorescence) or two (double immunofluorescence) primary antibodies (Table 8). After rising in PBS, cells were incubated for 1 h at room temperature with the corresponding secondary fluorescent antibodies (Table 9). All antibodies were diluted in 0.1 M PBS, 1% BSA, 10% normal donkey serum. Cell nuclei were stained with 4',6-diamidino-2-fenilindol (DAPI) (Sigma Aldrich, Ref. D9542). After washing carefully with PBS, cells were preserved in 0.1 M PBS and 0.1% Thimerosal. When necessary, cells were permeabilized by adding 0.3% Triton X-100 to the blocking solution and to the primary and secondary antibody solutions. Immunofluorescent samples were immediately assessed under fluorescent microscope or stored at 4ºC protected from light. Images were obtained with an *Olympus IX70* microscope (Olympus, Okoya, Japan) and a digital camera (*CC-12, Olympus Soft Imaging Solutions GmbH*, Hamburg, Germany).

Table 8. List of primary antibodies used for immunocytochemistry.

Primary antibodies				
Epitope	**Source**	**Dilution**	**Reference**	**Company**
CD200R1	Goat polyclonal	1/20	AF2554	R&D
CD200	Goat polyclonal	1/50	AF3355	R&D
CD68	Rat monoclonal	1/1000	MCA1957	Bio-Rad
GFAP	Rabbit polyclonal	1/1000	Z0334	Dako
IBA1	Rabbit polyclonal	1/500	019-19741	Wako
MAP2	Mouse monoclonal	1/2000	M1406	Sigma
TH	Rabbit polyclonal	1/2000	ab112	abcam

CD200R1, CD200 receptor 1; CD68, cluster of differentiation 68; GFAP, glial fibrillary acidic protein; IBA1, ionized calcium binding adaptor molecule 1; MAP2, Microtubule-associated protein 2; TH, tyrosine hydroxylase.

Table 9. List of secondary antibodies used for immunocytochemistry.

Alexa Fluor® conjugated secondary antibodies				
Epitope	**Source**	**Dilution**	**Reference**	**Provider**
Goat IgG (H+L)	Donkey	1/1000	A11055 488	Invitrogen
Mouse IgG (H+L)	Donkey	1/1000	A21203 594	Invitrogen
Mouse IgG (H+L)	Donkey	1/1000	A21202 488	Invitrogen
Rabbit IgG (H+L)	Donkey	1/1000	A21207 594	Invitrogen
Rabbit IgG (H+L)	Donkey	1/1000	A21206 488	Invitrogen
Rat IgG (H+L)	Donkey	1/1000	A21209 594	Invitrogen
Rat IgG (H+L)	Donkey	1/1000	A21208 488	Invitrogen

2.10 *In vitro* CELL COUNTING

For mesencephalic culture characterisation, the percentage of microglia, astrocytes, and dopaminergic neurons was calculated using the total number of cells (DAPI staining) after ionized calcium binding adaptor molecule (IBA)1 + CD68-, glial fibrillary acidic protein (GFAP)- or tyrosine hydroxylase (TH)-immunocytochemistry, respectively. To count microglial and astroglial cells, three 10X fields/well and two wells per experimental condition of four independent experiments were considered. For dopaminergic neuronal loss estimation after MPP+ or rotenone treatment in mesencephalic cultures, cell counting of TH-positive cells was done in nine 4X fields/well and

considering two wells per experimental condition of four independent experiments. To assess the total number of cells, cell counting of DAPI-stained nuclei was done in three 10X fields/well and considering two wells per experimental condition of four independent experiments.

2.11 PHAGOCYTOSIS

To assess the phagocytic activity of microglial cells, fluorescent latex microspheres (FluoSpheres, carboxylate-modified microspheres, 2.0 µm, red fluorescent (580/605), 2% solids; Thermofisher Scientific, Ref. F8826) were added to the medium (1/1000) for 1 h at 37ºC 23 h after treatment. Before addition to the cells, latex microspheres were sonicated to produce a homogeneous suspension. Two or three wells from 48-well plates were used per experimental condition. After incubation with microspheres, microglial cell cultures were washed three times with PBS and fixed with 4% PFA in 0.1 M PBS for 15 minutes at room temperature. Immunofluorescence against IBA1 was performed as described in section “2.9 Immunocytochemistry”. Images of three microscopic fields using a 20X objective were obtained with an *Olympus IX70* microscope (Olympus, Okoya, Japan) and a digital camera (*CC-12, Olympus Soft Imaging Solutions GmbH*, Hamburg, Germany). Two to three wells per experimental condition were processed and each experimental condition was repeated at least four times. Visual counting of microspheres was performed. The percentage of phagocytic cells and the average number of fluorescent microspheres per microglial cell were calculated. To further characterise the phagocytic activity, we also calculated the % of cells showing phagocytic activity lower than control cells and the % of cells showing higher phagocytic activity than control cells.

2.12 INTRACELLULAR ATP LEVELS

The intracellular ATP levels in primary mixed glial and microglial cultures was assessed using the *ATPlite Luminescence kit* (PerkinElmer, Ref. 6016943) according to the manufacturer’s recommendations. Briefly, cells in 96-well plates (mixed glia) or 6-well plates (microglia) were lysed 24 h after treatments and ATP concentration was measured based on the production of light caused by the reaction of ATP with added luciferase and D-luciferin. The emitted light is proportional to the ATP concentration and was measured using a luminometer (*Orion Microplate Luminometer, Berthold Detection System*, Germany). The ATP concentration in the samples was calculated from an ATP standard curve.

3 *In vivo* experiments

3.1 THE ACUTE MPTP MOUSE MODEL OF PD

1-methyl-4-phenyl-1,2,3,6-tetrahydropyridine (MPTP) administration was performed in collaboration with Dr. Miquel Vila's laboratory at Vall d'Hebron Institute of Research (VHIR, Barcelona, Spain). Eleven to 15-week-old mice received MPTP injections following an acute regimen (Jackson-Lewis and Przedborski 2007), which consisted of one intraperitoneal injection of MPTP-HCl (20 or 18 mg/kg, Sigma-Aldrich, Ref. M0896) every 2 hours for a total of 4 doses in one day. Control mice received saline injections. Mice were killed at indicated time points after the last MPTP injection. Each experimental group was composed of an average of 8 mice. Male mice were used in all experiments with the exception of the experiments with CD200-deficient mice, in which females were used in the control group because we did not obtain enough male mice to complete all the experimental groups.

The collection of samples from the MPTP-injected mice was performed in a dedicated procedure room and with personal protection equipment (Przedborski, Jackson-Lewis, et al. 2001). Tissue remains were discarded as hazardous waste. Surfaces and non-disposable instruments were sprayed with 1% bleach.

The following experimental approaches were considered using this model.

3.1.1 Time course experiment

C57BL/6NCrl mice (Charles River, Lyon, France) were administered with MPTP (20 mg/kg) following the acute regimen and killed at 2 hours, 1, 2, 4 and 7 days after the last MPTP injection.

3.1.2 CD200R1 agonist experiment

C57BL/6NCrl mice (Charles River, Lyon, France) were administered with MPTP (20 mg/kg) following the acute regimen. The CD200R1 agonist (CD200 fusion protein (CD200Fc), 1.8 or 3.6 mg/kg, dissolved in PBS) or its corresponding isotype control (1.8 or 3.6 mg/kg, dissolved in PBS) was administered twice, by intraperitoneal injection, 30 minutes before MPTP injections and 24 h after the last MPTP injection. The CD200Fc and its corresponding isotype control were kindly provided by Genentech Inc. The CD200Fc is a fusion protein constituted by the extracellular domain of mouse CD200 and the mouse IgG2a Fc region. Mouse anti-ragweed IgG2a was used as isotype control. Animals were killed at 7 days after the last MPTP injection.

3.1.3 CD200-deficient mice experiments

The genetic background of the mice is important for MPTP sensitivity. Although C57BL/6 mice are usually used in the MPTP model, increased toxicity of MPTP is observed in certain substrains, such as C57BL/6J mice (Jackson-Lewis and Przedborski 2007). We submitted the CD200 knock-out mice to background strain characterisation (Jackson Laboratories).

CD200-deficient mice (67% C57BL/6NJ and 33% C57BL/6J) were administered with MPTP (18 mg/kg) following the acute regimen and killed at 1 or 7 days after the last MPTP injection.

3.1.3.1 Colony formation

We received 5 female and 5 male CD200 knock-out mice from Dr. David Copland (University of Bristol, United Kingdom). We generated a colony by crossing CD200 knock-out mice with wild-type C57BL/6N mice to yield F1 offspring with an enriched C57BL/6N background. Heterozygous (CD200 +/-) male and female mice of the F1 offspring were crossed to obtain CD200 -/-, CD200 +/- and CD200 +/+ genotypes. All genotypes were produced at the expected Mendelian frequency. CD200 -/- and CD200 +/+ mice were used henceforth. CD200 +/- and CD200 -/- mice were grossly normal in appearance, bred normally, exhibited a normal life-span and fertility, and showed no obvious behavioural changes.

3.1.3.2 Genotyping

To evaluate the genotype (CD200 +/+, CD200 +/-, CD200 -/-) of mice, genomic DNA from tail tissue was extracted and amplified with *REDExtract-N-Amp™ Tissue PCR Kit* (Sigma-Aldrich, Ref. XNAT) following the manufacturer's instructions. The amplified DNA was loaded onto an agarose gel, together with a DNA ladder (Thermo Scientific, Ref. SM0311). For DNA detection, *Midori green nucleic acid staining solution* was used (Nippon Genetics Europe, Ref. MG04) and images were obtained using a UV Transilluminator (Gel Doc System, Bio-Rad Laboratories). The primers (Integrated DNA Technology) used are listed in Table 10. The two pairs of primers were used in each reaction because each DNA sample was screened for both the normal and the mutant allele by using a single PCR. DNA from CD200 +/+ mice was amplified by mCD200 primers, producing one band of 506 bp. DNA from CD200 +/- mice was amplified by mCD200 and mNEO primers, producing one band of 506 bp and one band of 596 bp. DNA from CD200 -/- mice was amplified by mNEO primers, producing one band of 596 bp.

Table 10. Primers used for genotyping.

Genotype	Forward 5' → 3'	Reverse 5' → 3'	Amplicon
CD200 +/+	mCD200-Fw GAAGACAAACCTAGCGGAGACATTAC	mCD200-Rv CTCTTCAGCAATATCACGGGTAGC	506 bp
CD200 -/-	mNEO-Fw GGGAGTGGAACTGTAGAAGGGTG	mNEO-Rv AGGCTATTCGGCTATGACTGGG	596 bp

3.2 EVALUATION OF BRAIN INJURY AND GLIAL ACTIVATION

3.2.1 Tissue collection

For histological analysis, mice were intraperitoneally anesthetized with 0.2 mL of 5% pentobarbital sodium and perfused with physiological saline (0.9% NaCl) through the ascending aorta using a peristaltic pump at a flow rate (9 mL/min for 3 minutes), followed by ice-cold 4% PFA (Panreac, Ref. A3697.9010) diluted in 0.2 M PBS containing 0.15 M sodium phosphate dibasic (Sigma-Aldrich, Ref. S0876) and 0.05 M sodium phosphate monobasic (Sigma-Aldrich, Ref. S9638) for 8 minutes. Brains were removed immediately after the perfusion, immersed overnight in the same fixation solution at 4ºC and then 48 h in 30% sucrose (SCHARLAU, Ref. SA00211000) at 4ºC. Finally, brains were frozen on dry ice and kept at -80ºC until sectioning.

In experiments where mRNA expression analysis was performed, mice were perfused with physiological saline (0.9% NaCl) at 9 mL/min for 11 minutes. The two hemispheres of the cerebrum were separated down the longitudinal fissure. The right hemisphere was fixed as described above for histological analysis. Striatum, ventral midbrain and cerebral cortex from the left hemisphere were dissected and frozen on dry ice and kept at -80ºC until analysis.

3.2.2 Immunohistochemistry

Serial coronal brain sections (20 µm thick) containing the striatum or the SN were obtained with a cryostat (Leica CM1950) at -23ºC and collected in 0.1 M PBS containing 0.01% sodium azide (Sigma-Aldrich, Ref. S8032).

To assess glial reactivity in the striatum and SN, four representative sections of each area per animal were immunostained against GFAP, and four against IBA1. Assessment of nigrostriatal integrity was performed in TH-immunostained tissue sections. TH-immunohistochemistry was performed in four representative sections of striatum per animal covering different striatal levels and in every sixth section throughout the entire SNpc, yielding twelve serial sections per animal. In the experiments using CD200-deficient mice, CD200-immunohistochemistry was also performed to corroborate the genotype of mice.

Free-floating sections were first permeabilized in TBS containing 10% methanol and 3% H_2O_2 for 5 minutes, rinsed in PBS and, blocked with 5% normal goat serum (Vector Laboratories, Ref. S100) for 1 h at room temperature. Sections were incubated overnight at 4ºC in agitation with primary antibodies (Table 11) diluted in TBS containing 2% normal goat serum. After rinsed in PBS, the sections were incubated for 1 h at room temperature with the corresponding secondary biotinylated antibodies (Table 12) diluted in TBS with 2% normal goat serum, followed by PBS washes. To amplify signal intensity, tissue sections were incubated with the avidin-biotin complex

(ABC) Reagent (Thermo Fisher, Ref. 32050) for 30 minutes and washed with PBS. For the visualization of peroxidase activity, we used 3,3′-diaminobenzidine (Sigma-Aldrich, Ref. D5637). Sections were mounted on gelatine-coated slides and air dried overnight. TH-immunostained sections of the SN were counterstained with Nissl stain. Briefly, after 10 minutes of incubation with chloroform, sections were rehydrated through 95%, 70% ethanol to distilled water, stained in 0.1% cresyl violet solution for 10 minutes, rinsed quickly in distilled water and differentiated in acetic acid + 70% ethanol (2 drops of glacial acetic acid in 100 mL of 70% ethanol). All sections were dehydrated through 70%, 95%, 100% ethanol to xylene and coverslips were placed over slides using DPX mounting medium.

Table 11. List of primary antibodies used for immunohistochemistry.

Epitope	Source	Dilution	Reference	Company
CD200	Goat	1/100	AF3355	R&D
GFAP	Rabbit	1/2000	Z0334	Dako
IBA1	Rabbit	1/1000	019-19741	Wako
TH	Rabbit	1/5000 (St) 1/2000 (SN)	ab112	abcam

GFAP, glial fibrillary acidic protein; IBA1, ionized calcium binding adaptor molecule 1; TH, tyrosine hydroxylase.

Table 12. List of biotinylated secondary antibodies used for immunohistochemistry.

Epitope	Source	Dilution	Reference	Company
Goat IgG	Horse	1/1000	PI-9500	Vector
Rabbit IgG	Goat	1/1000	BA1000	Vector

3.3 QUANTITATIVE MORPHOLOGY

3.3.1 Striatal TH-positive fibers

The extent of striatal dopaminergic denervation was measured by optical densitometry in four TH-immunostained sections from each animal (Fig. 30), as previously described (Recasens et al. 2014; Perier et al. 2013). Sections were scanned in an *Epson Perfection V750 PRO* scanner and the grey intensity of the staining in the striatum of both hemispheres of each section was measured using *SigmaScan Pro 5.0* software (Systat Software, USA). The measured values were corrected for non-specific background staining by subtracting values obtained from the cortex. The optical density (OD) was assessed with the formula OD=-log(Intensity in the striatum/Intensity in the cortex).

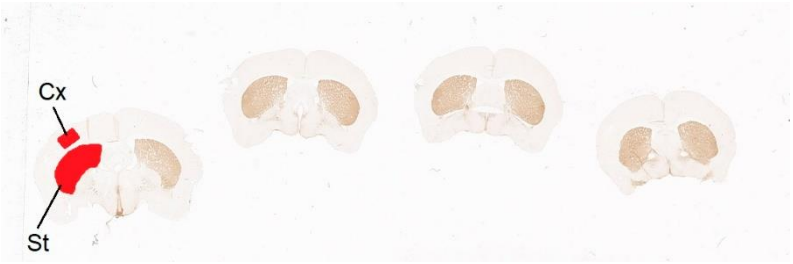

Figure 30. TH-immunohistochemistry in four brain sections corresponding to different striatal levels. The areas of interest, striatum (St) and cortex (Cx), were selected to quantify immunostaining intensity.

3.3.2 SNpc TH-positive neurons

The total number of TH-positive neurons in the SNpc was estimated by stereological quantification using twelve regularly-spaced sections per animal and employing the optical fractionator principle with *Stereoinvestigator Software* (MBF Bioscience, Williston, VT) on a *Zeiss ImagerD1* microscope, as previously described (Recasens et al. 2014; Liberatore et al. 1999). The SNpc was delineated for each section (Fig. 31) and probes for stereological counting were applied to the map obtained (size of counting frame was 50 x 50 µm spaced by 250 x 250 µm). Only TH-positive neurons with their nuclei included within the counting frame were counted.

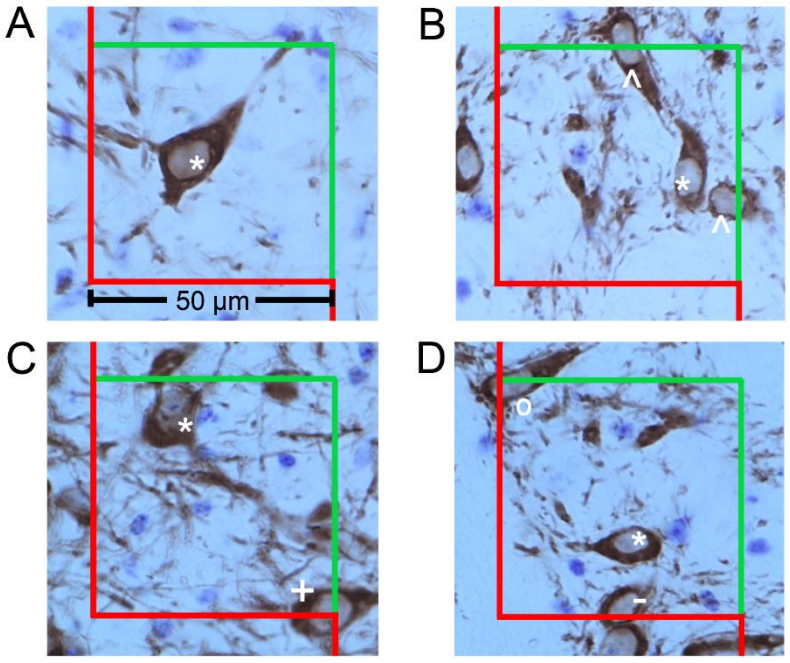

Figure 31. Stereological counting using optical fractionator. Any nucleus of a TH-positive cell inside the counting frame (* in **A-D**) or touching the green line (^ in **B**) was counted, while if it was touching the red line (- in **D**) was excluded. If the nucleus of a TH-positive cell crossed both, green and red lines, the cell was counted only when the nucleus crossed the right bottom vertex (+ in **C**) and not when crossing the left top vertex (º in **D**).

3.3.3 SN IBA1-positive microglia

Microglial reactivity in SN was measured in four IBA1-immunostained sections from each animal. Images of SN of each section using a 4X objective were obtained with an *Olympus IX70* microscope (Olympus, Okoya, Japan) and a digital camera (*CC-12, Olympus Soft Imaging Solutions GmbH*, Hamburg, Germany). Two parameters were measured:

A) IBA1-labelled area:

A grey level threshold was fixed and the area occupied by IBA1-staining in the total SN and SNpc of each animal was measured using *ImageJ* 1.50 software (*National Institutes of Health*) (Fig. 32). Values were expressed as % of area occupied by IBA1-staining in SNpc or total SN. SNpr values were obtained as the difference between total SN and SNpc measurements.

B) IBA1 optical density:

The mean grey intensity in the total SN and SNpc of each section was measured using ImageJ 1.50 software (*National Institutes of Health*) (Fig. 32). Non-specific background staining was obtained from an IBA1-staining free area. The optical density (OD) was assessed with the formula OD=-log(Intensity in SNpc or total SN /Intensity of background area).

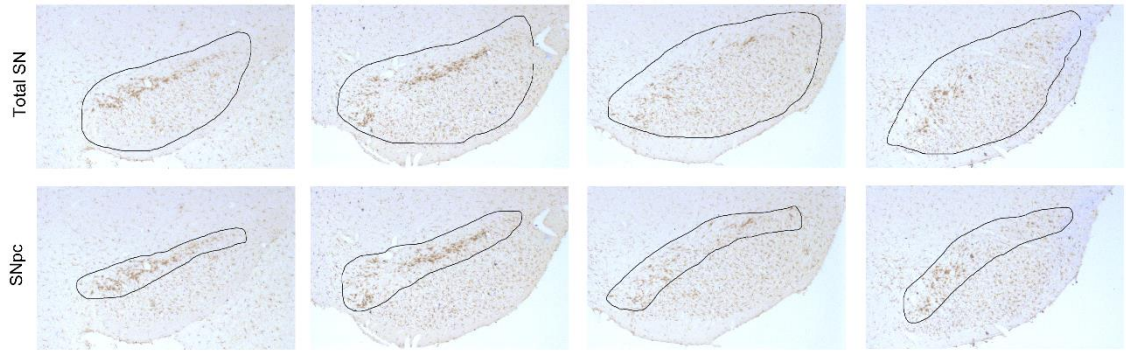

Figure 32. Area selected in the SN to quantify the IBA1-immunohistochemistry. Four brain sections corresponding to different SN anatomical levels from mice 7 days after MPTP administration. Area selected for total SN and SNpc is represented.

3.4 GENE EXPRESSION

Total RNA was extracted at the indicated time points from striatal, ventral midbrain and frontal cortex samples from saline and MPTP-injected mice using the Trizol method (Tri®Reagent, Sigma-Aldrich. Ref. T9424). RNA quantification, reverse transcription and qPCR was performed as described in section “2.7 Gene expression “. One µg of RNA was retrotranscribed and cDNA was diluted 1/30 to perform qPCR.

4 *Post-mortem* human brain analysis

Post-mortem human brain samples were supplied from the *Banc de Teixits Neurològics* (Biobanc, Hospital Clínic de Barcelona, IDIBAPS) in accordance with the Helsinki Declaration, Convention of the Council of Europe on Human Rights and Biomedicine and Ethical Committee of the University of Barcelona. Frozen tissue blocs containing SN, hippocampus and frontal cortex were obtained from 8 control subjects (age range 56 - 90 years, *post-mortem* delay range: 4 - 20 h) and 21 PD patients (age range 50 - 92 years, *post-mortem* delay range: 5 - 18 h).

4.1 GENE EXPRESSION

Total RNA was extracted from frozen tissue samples using the Trizol method (Tri®Reagent, Sigma-Aldrich, Ref. T9424). RNA quantification, everse transcription and qPCR or conventional PCR were performed as previously described in section “2.7 Gene expression “. One µg of RNA was retrotranscribed and cDNA was diluted 1/30 to perform qPCR.

4.2 PROTEIN EXPRESSION

Total tissue protein was isolated in 1x sodium dodecyl sulfate (SDS) - buffer (pH 6.8 0.125 M Tris-HCl, 2% SDS, 10% glycerol, 0.001% bromophenol blue and 5% 2-mercaptoethanol) (Laemmli 1970; Laemmli and Favre 1973). After vortex and incubation for 10 minutes at 70 ºC, samples were centrifuged (16100 g, 10 minutes at room temperature) and the supernatant was collected. Samples were kept at -20ºC until further use. Western blot in *post-mortem* tissue samples was performed as previously described in section “2.8.1.2 Western blot”.

5 Statistical analysis

The results are presented as the mean + or ± standard error of the mean (SEM). At least three independent experiments were performed for analysis. Data were statistically analysed with *GraphPad Prism* software. Statistical analyses when comparing two groups were determined by a two-tailed unpaired Student’s t test or unpaired t test with Welch’s correction. When comparing more than two groups, statistical analyses were performed using one-way analysis of variance

(ANOVA) followed by Newman-Keuls post-test, or two-way ANOVA followed by Bonferroni post-test. Values of $p<0.05$ were considered statistically significant.

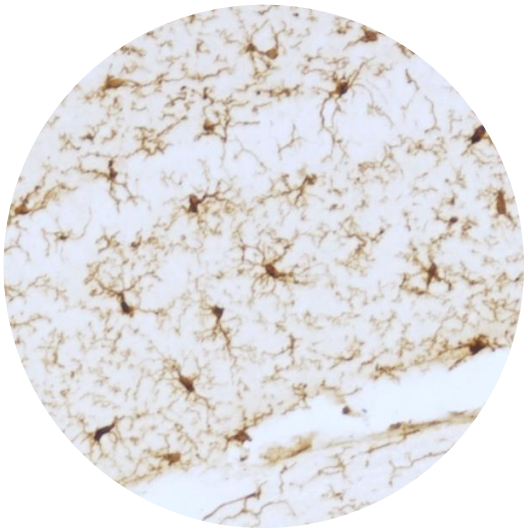

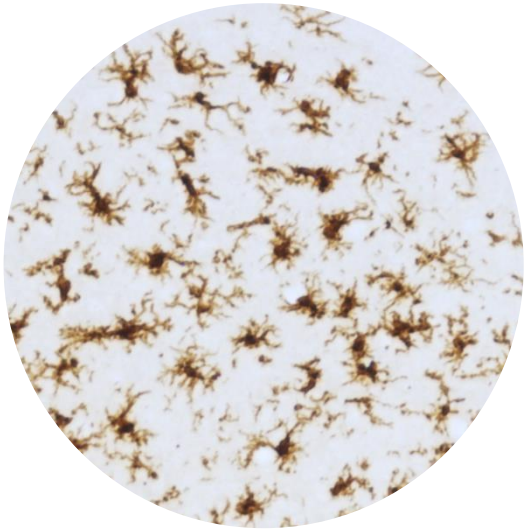

Results

1 Effect of CD200-CD200R1 alterations on glial activation and dopaminergic neurodegeneration using *in vitro* approaches

In the CNS, a decreased expression of CD200 and/or CD200R1 in Alzheimer's disease (Walker et al. 2009) and multiple sclerosis (Koning et al. 2007; Koning et al. 2009) has been described. These alterations in the CD200-CD200R1 system may contribute to the chronic inflammation observed in these diseases. With the aim of further understanding the consequences of this decreased expression, we evaluated the effect of CD200-CD200R1 disruption using two different *in vitro* approaches: anti-CD200 blocking antibody and CD200-deficient mice.

1.1 INHIBITION OF CD200-CD200R1 SYSTEM IN GLIAL CELL CULTURES USING AN ANTI-CD200 BLOCKING ANTIBODY. EFFECT ON GLIAL ACTIVATION

1.1.1 CD200 and CD200R1 are expressed in mixed glial cultures and their expression is modified by LPS/IFNγ treatment

We confirmed that both CD200 and CD200R1 mRNA expression were basally detected in primary mixed glial cultures (composed of 75% astrocytes and 25% microglia) (Fig. 1.1), and that this expression was modified after LPS/IFNγ treatment. LPS/IFNγ induced an increase in CD200tr mRNA expression, the mRNA isoform encoding the truncated form of the protein, 6 h after treatment, while the expression of CD200full mRNA was not modified (Fig. 1.1A). On the contrary, a decrease in CD200R1 mRNA expression was observed 6 h after LPS/IFNγ treatment (Fig. 1.1B). CD200 and CD200R1 expression changes were also detected at protein level 24 h after LPS/IFNγ treatment by immunocytochemistry. Thus, LPS/IFNγ-induced an increase in CD200 (Fig. 1.1C) and a decrease in CD200R1 (Fig. 1.1D) immunostaining 24 h after treatment. CD200 immunostaining was found to colocalize with the astrocyte marker EAAT1 (Fig. 1.1C), while CD200R1 immunostaining colocalized with the microglial cell markers CD68 and Iba1 (Fig. 1.1D). A stranger CD200R1 immunostaining was detected in the microglial cells present above the astrocyte layer than in microglial cells in or below the astrocyte layer (Fig. 1.1D). Note that CD200 antibodies available detect CD200full and probably CD200tr as well.

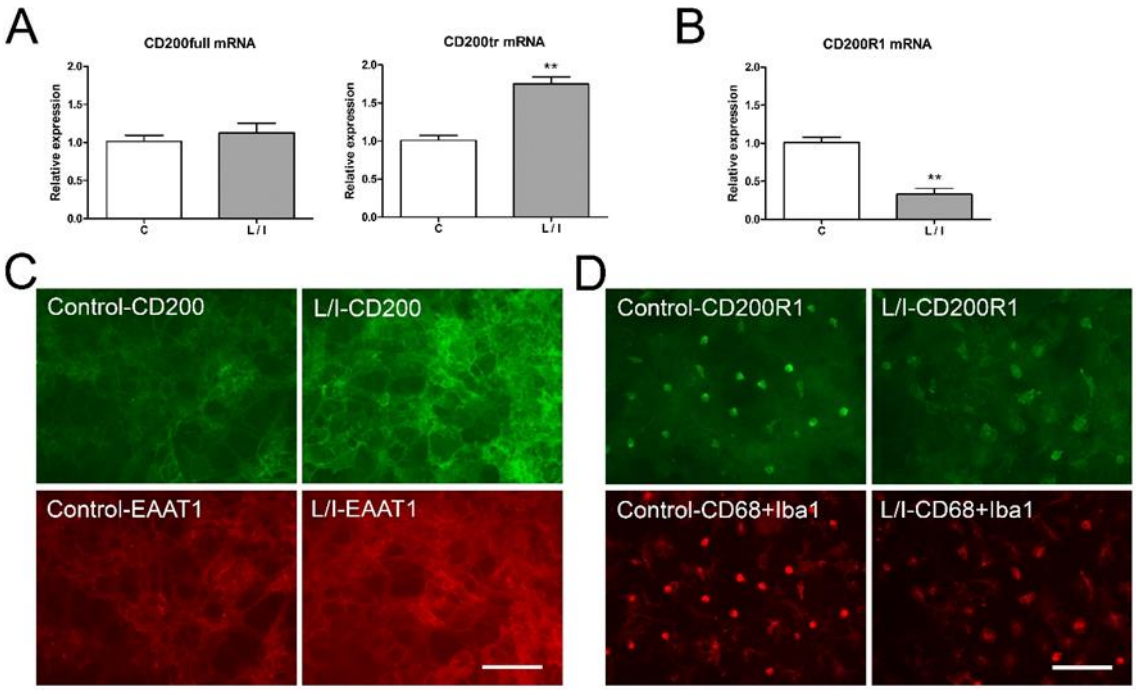

Figure 1.1. LPS/IFNγ treatment induces changes in CD200 and CD200R1 expression in primary mixed glial cultures. CD200full and CD200tr mRNA expression (**A**) and CD200R1 mRNA expression (**B**) in mixed glial cultures 6 h after LPS/IFNγ treatment (L/I, 100 ng/mL LPS + 30 ng/mL IFNγ). Rn18s and βactin were used as genes for normalization. Bars are means + SEM of 3 independent experiments. **p<0.01 vs. C; Student's t test. **C** Cellular localization of CD200 and CD200R1-immunolabelling in control and L/I-treated primary mixed glial cultures 24 h after treatment. Scale bar: 100 µm.

1.1.2 Anti-CD200 blocking antibody does not induce *per se* glial activation

To study whether an anti-CD200 blocking antibody or its corresponding isotype (rat IgG2a, negative control) had *per se* an effect on glial activation, we first determined the expression of pro- and anti-inflammatory molecules in mouse mixed glial cultures treated with these molecules.

In a preliminary study, dose-response experiments were performed in order to select working concentrations of the anti-CD200 blocking antibody and isotype that did not result in significant alterations in cell viability. We evaluated glial cell metabolic activity and viability with the MTT assay and by PI staining, respectively, 24 h after treating mixed glial cultures with increasing concentrations of anti-CD200 blocking antibody or isotype (0.1, 0.5, 1, 5 µg/mL). Anti-CD200 blocking antibody treatment had no effect on MTT reduction (Fig. 1.2A). Surprisingly, all concentrations of isotype used induced a decrease in MTT reduction with the only exception of 0.1 µg/mL isotype (Fig. 1.2A). To determine whether the decrease in MTT reduction was due to cell death and not to a decrease in metabolic activity, PI staining was performed. We observed in cultures treated with 0.5 - 5 µg/mL isotype a tendency to increase the percentage of PI positive cells (Fig. 1.2B,C). The concentration of 0.1 µg/mL was used in subsequent studies for both anti-CD200 blocking antibody and isotype.

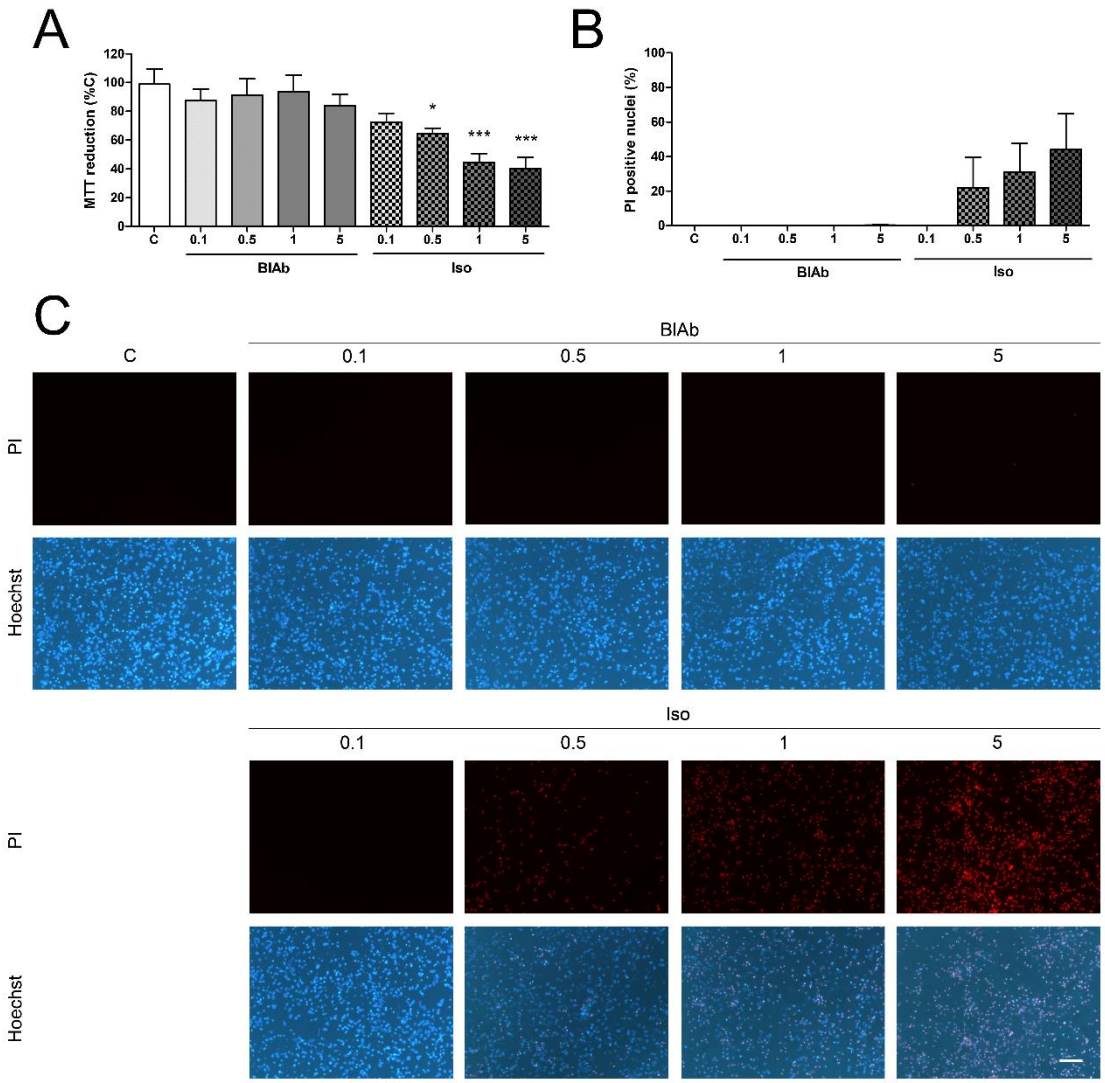

Figure 1.2. Effect of anti-CD200 blocking antibody and isotype on glial cell viability. Primary mixed glial cultures were treated for 24 h with 0.1, 0.5, 1 and 5 µg/mL anti-CD200 blocking antibody (BlAb) or isotype (Iso). **A** MTT reduction expressed as the percentage of control (C). **B** Cell death expressed as the percentage of propidium iodide (PI) positive nuclei in each experimental condition. Bars are means + SEM of 4 independent experiments. *p<0.05 and ***p<0.001 vs. C; one-way ANOVA (repeated measures) and Newman-Keuls post-test. **C** Representative photomicrographs of PI and Hoechst staining of all experimental conditions. Scale bar: 100 µm.

We next evaluated the effect of anti-CD200 blocking antibody treatment on the mRNA levels of the cytokines IL1β, IL6, and TNFα, and the enzymes iNOS and COX2 in primary mixed glial cultures, as markers of a pro-inflammatory response. We also analysed the cytokines IL4, IL10 and TFGβ as markers of an anti-inflammatory response.

The mRNA expression of pro- and anti-inflammatory cytokines (Fig. 1.3A,C) and pro-inflammatory enzymes (Fig. 1.3B) was not modified in mixed glial cultures 6 h after anti-CD200 blocking

antibody treatment. The isotype did not produce any effect on the expression of these markers either (Fig. 1.3).

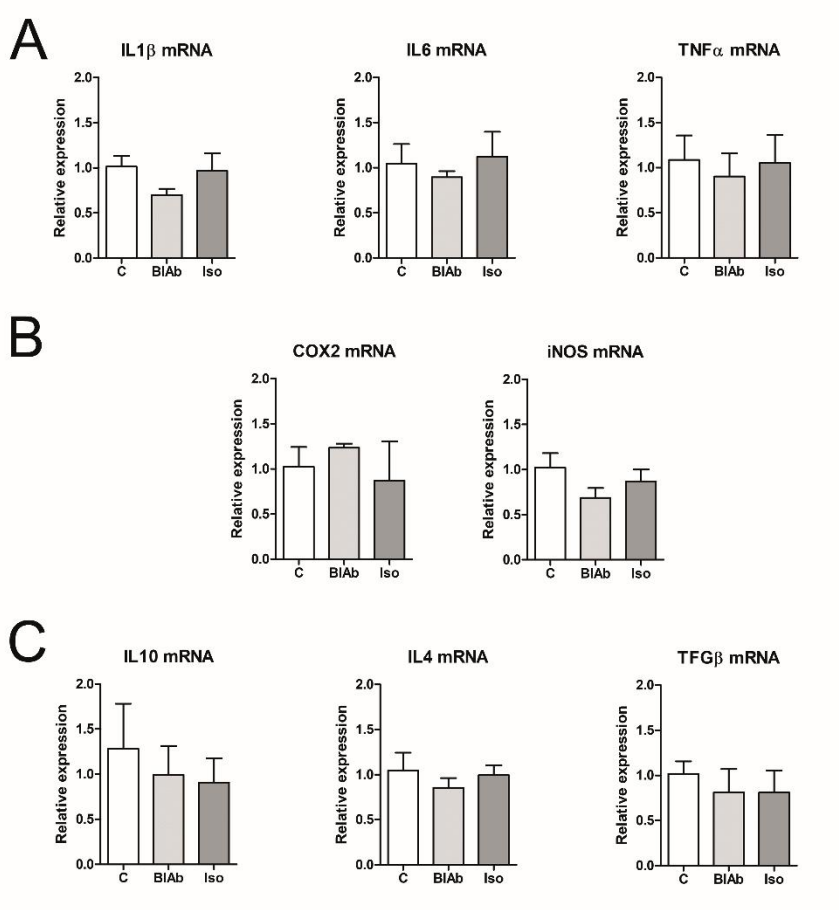

Figure 1.3. Anti-CD200 blocking antibody does not modify the mRNA levels of pro- and anti-inflammatory markers in mixed glial cultures. mRNA levels of (**A**) pro-inflammatory cytokines (IL1β, IL6 and TNFα) and (**B**) enzymes (iNOS, COX2) and (**C**) anti-inflammatory cytokines (IL4, TGFβ, IL10) in primary mixed glial cultures treated for 6 h with anti-CD200 blocking antibody (BlAb, 0.1 µg/mL) or corresponding isotype (Iso, 0.1 µg/mL). Rn18s and βactin were used as reference genes. Bars are means + SEM of 3 independent experiments. One-way ANOVA (repeated measures) and Newman-Keuls post-test.

We also analysed the effect of the CD200-CD200R1 system disruption on NO production and on the protein levels of the pro-inflammatory enzymes iNOS and COX2 in mixed glial cultures. After 24 h of 0.1 µg/mL anti-CD200 blocking antibody treatment, mixed glial cultures showed an increase in NO_2^- accumulation in the culture medium, whereas higher concentrations of anti-CD200 blocking antibody or isotype produced no effect (Fig. 1.4A). COX2 and iNOS protein levels were not modified after 24 h of anti-CD200 blocking antibody (0.1 µg/mL) or isotype (0.1 µg/mL) treatment (Fig. 1.4B).

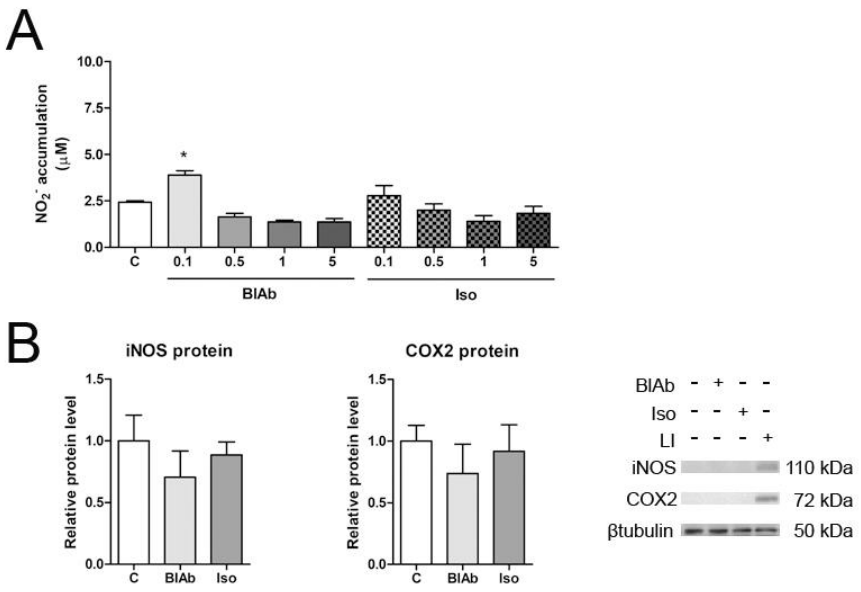

Figure 1.4. Effect of anti-CD200 blocking antibody on NO production and pro-inflammatory enzymes at the protein level. NO_2^- accumulation (**A**) was determined by the Griess method in culture medium of mixed glial cultures 24 h after treatment with anti-CD200 blocking antibody (BlAb, 0.1, 0.5, 1, 5 μg/mL) or isotype (Iso, 0.1, 0.5, 1, 5 μg/mL). Representative immunoblots of COX2 and iNOS protein levels (**B**) in mixed glial cultures 24 h after treatment with BlAb (0.1 μg/mL) or Iso (0.1 μg/mL) or LPS/IFNγ (L/I, 100 ng/mL LPS + 30 ng/mL IFNγ). Data are expressed as fold change to control (C) condition. βtubulin was used as loading control. Treatment with LPS/IFNγ (L/I, 100 ng/mL LPS / 30 ng/mL IFNγ) is shown as positive control. Bars are means + SEM of 4 independent experiments. *p<0.05 vs. C; one-way ANOVA (repeated measures) and Newman-Keuls post-test.

1.1.3 Blocking CD200-CD200R1 interaction potentiates the mRNA expression of pro-inflammatory markers in LPS/IFNγ-treated primary mixed glial cultures

We next studied whether CD200-CD200R1 disruption had an effect on the response of glial cells to an inflammatory stimulus. We determined the expression of pro- and anti-inflammatory molecules after inducing glial activation with LPS/IFNγ in mixed glial cultures, in the absence and the presence of an anti-CD200 blocking antibody.

We first confirmed that concentrations of anti-CD200 blocking antibody and isotype plus LPS/IFNγ did not result in significant alterations in cell viability. We evaluated glial cell viability with the MTT assay and PI staining 24 h after treating the cultures with 100 ng/mL LPS + 30 ng/mL IFNγ in the presence or absence of 0.1 μg/mL anti-CD200 blocking antibody or isotype. Anti-CD200 blocking antibody or isotype was administered 30 minutes before LPS/IFNγ. LPS/IFNγ treatment induced a decrease in MTT reduction (Fig. 1.5A) but did not alter cell viability as assessed by PI assay (Fig. 1.5B,C). Anti-CD200 blocking antibody or isotype did not modify the LPS/IFNγ effect (Fig. 1.5).

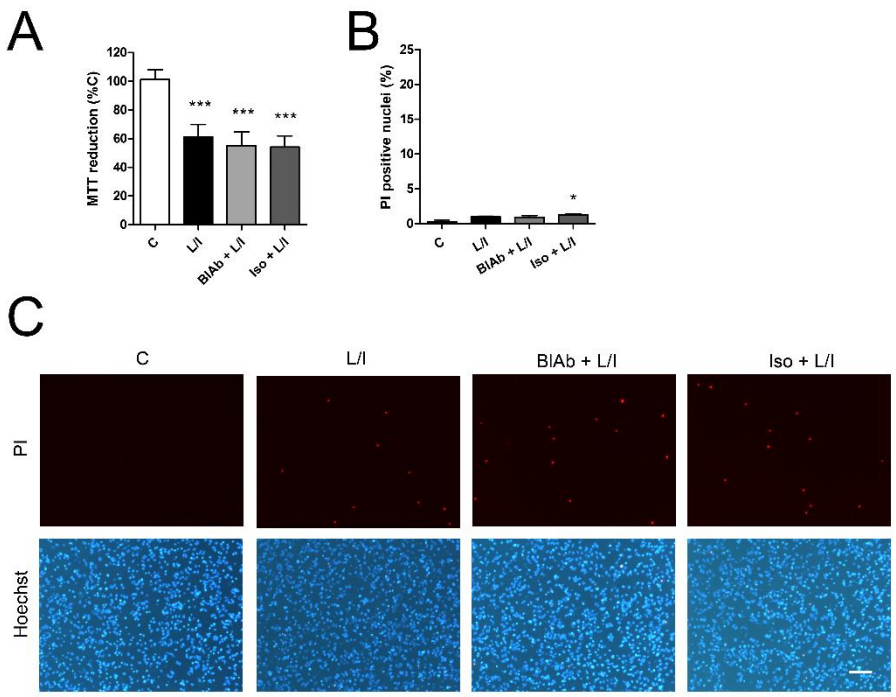

Figure 1.5. Effect of LPS/IFNγ, anti-CD200 blocking antibody and isotype on glial cell viability. Primary mixed glial cultures were treated for 24 h with LPS/IFNγ (L/I, 100 ng/mL LPS + 30 ng/mL IFNγ) in the absence or presence of 0.1 µg/mL anti-CD200 blocking antibody or isotype (BlAb, Iso, 30 minutes before L/I treatment). **A** MTT reduction expressed as the percentage of control (C). **B** Cell death expressed as the percentage of propidium iodide (PI) positive nuclei in each experimental condition. Bars are means + SEM of 4 independent experiments. *p<0.05 and ***p<0.001 vs. C; one-way ANOVA (repeated measures) and Newman-Keuls post-test. **C** Representative photomicrographs of PI and Hoechst staining in mixed glial cells untreated or treated with L/I in the absence or presence of BlAb or Iso. Scale bar: 100 µm.

We then evaluated the effect of anti-CD200 blocking antibody treatment on the mRNA expression of pro-inflammatory (IL1β, IL6, and TNFα, iNOS, COX2) and anti-inflammatory (IL4, IL10 and TFGβ) genes in LPS/IFNγ-treated primary mixed glial cultures. The mRNA expression of all the pro-inflammatory markers studied was clearly induced at 6h in LPS/IFNγ-treated cells (Fig. 1.6A,B). At the same time, mRNA expression of the anti-inflammatory molecules IL10, IL4 and TGFβ was not modified (Fig. 1.6C). When mixed glial cultures were pre-treated with anti-CD200 blocking antibody, a further increase in mRNA expression of IL1β, IL6 and COX2 was detected, while the mRNA expression of the anti-inflammatory markers remained unaltered. Isotype pre-treatment increased IL6 mRNA expression induced by LPS/IFNγ (Fig. 1.6).

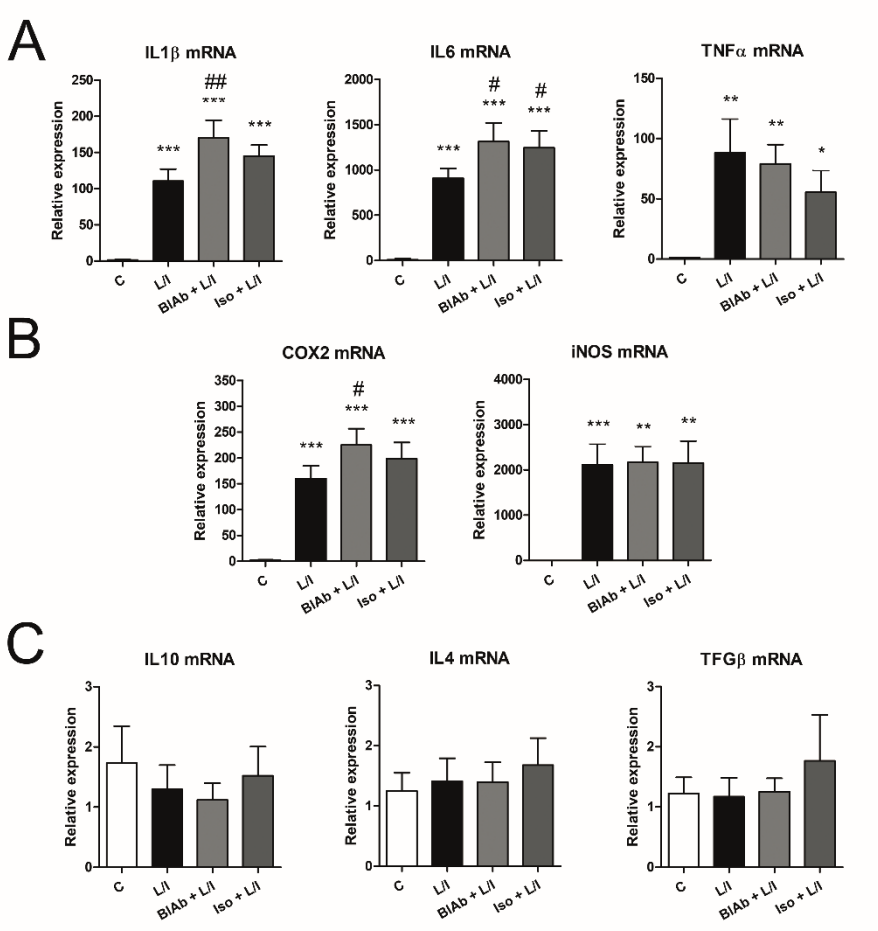

Figure 1.6. Anti-CD200 blocking antibody potentiates the induction of IL1β, IL6 and COX2 mRNA expression in LPS/IFNγ-treated mixed glial cultures. mRNA expression of pro-inflammatory (**A**) cytokines (IL1β, IL6 and TNFα) and (**B**) enzymes (iNOS, COX2) and (**C**) anti-inflammatory cytokines (IL4, TGFβ, IL10) in primary mixed glial cultures treated for 6 h with LPS/IFNγ (L/I, 100 ng/mL LPS + 30 ng/mL IFNγ) in the absence or presence of anti-CD200 blocking antibody or isotype (BlAb, Iso, 0.1 µg/mL, 30 minutes before L/I treatment). Rn18s and βactin were used as reference genes. Bars are means + SEM of 7 independent experiments. *p<0.05, **p<0.01 and ***p<0.001 vs. C; #p<0.05 and ##p<0.01 vs. L/I; one-way ANOVA (repeated measures) and Newman-Keuls post-test.

We also analysed the effect of the disruption of the CD200-CD200R1 system on NO production and pro-inflammatory cytokine (IL1β, TNFα and IL6) and enzyme (iNOS, COX2) protein levels in LPS/IFNγ-treated mixed glial cultures. After LPS/IFNγ treatment, mixed glial cultures showed an increase in NO_2^- accumulation in the culture medium at 24 h, which was not modified by anti-CD200 blocking antibody pre-treatment (Fig. 1.7A). LPS/IFNγ increased TNFα and IL6 extracellular levels after 6h and 24h whereas IL1β levels were increased only after 24 h (Fig. 1.7B). COX2 and iNOS protein levels were increased 24 h after LPS/IFNγ treatment (Fig. 1.7C). Neither cytokine release nor enzyme protein levels induced by LPS/IFNγ were modified by anti-CD200 blocking antibody or isotype pre-treatment (Fig. 1.7B,C).

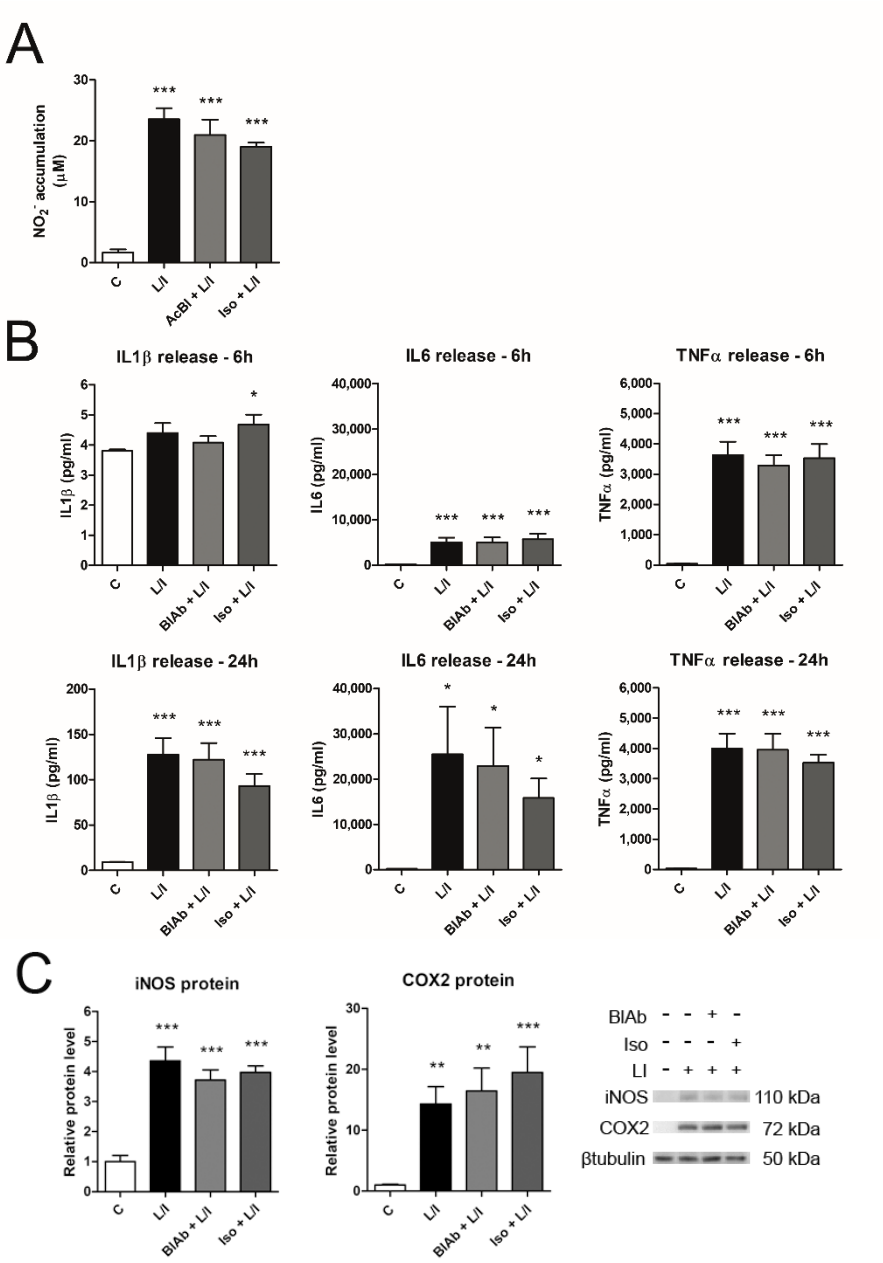

Figure 1.7. Anti-CD200 blocking antibody does not modify pro-inflammatory markers induced by LPS/IFNγ at the protein level. Primary mixed glial cultures were treated for 6 or 24 h with LPS/IFNγ (L/I, 100 ng/mL LPS + 30 ng/mL IFNγ) in the absence and in the presence of anti-CD200 blocking antibody or isotype (BlAb, Iso, 0.1 µg/mL, 30 minutes before L/I treatment). **A** NO_2^- accumulation was determined by the Griess method in culture medium 24 h after treatment. **B** IL1β, IL6 and TNFα release was determined in culture medium 6 and 24 h after treatment. **C** Representative immunoblots of COX2 and iNOS protein levels 24 h after treatment. Data are expressed as fold change to control (C) condition. βtubulin was used as loading control. Bars are means + SEM of 4 - 6 independent experiments. *p<0.05, **p<0.01 and ***p<0.001 vs. C; one-way ANOVA (repeated measures) and Newman-Keuls post-test.

1.2 GLIAL CELL CULTURES FROM CD200-DEFICIENT MICE. EFFECT ON GLIAL ACTIVATION

To further study the role of CD200-CD200R1 interaction in the response of glial cells to a pro-inflammatory stimulus, we determined the expression of pro-inflammatory genes up-regulated by LPS/IFNγ and LPS in mixed glial cultures of CD200 knock-out mice and their corresponding wild-type mice with the same genetic background.

We first confirmed that CD200 was not present in primary mixed glial cultures from CD200 knock-out mice (Fig. 1.8A,B). We observed no differences in the cellular composition between cultures from CD200 knock-out and wild-type mice: 75% astrocytes (GFAP-positive cells) and 25% microglia (IBA1+CD68-positive cells) (Fig. 1.8C). LPS/IFNγ and LPS treatment induced the expression of all pro-inflammatory markers analysed (IL1β, IL6, TNFα, COX2, iNOS and gp91phox (the catalytic subunit of NADPH oxidase)) in mixed glial cultures and surprisingly, no differences were observed between CD200 +/+ and CD200 -/- cultures (Figs. 1.9A and 1.10A). To study whether microglial cells from CD200 knock-out mice had a differential response to pro-inflammatory stimuli, we determined the expression of pro-inflammatory molecules after inducing microglial activation with LPS/IFNγ in microglial cultures from CD200 knock-out and wild-type mice. LPS/IFNγ and LPS treatment induced the expression of all pro-inflammatory markers analysed (IL1β, IL6, TNFα, COX2, iNOS and gp91phox). The increase in TNFα mRNA levels induced by LPS/IFNγ and the increases in TNFα, COX2 and IL10 mRNA levels induced by LPS alone were significantly higher in CD200 -/- than in CD200 +/+ microglial cultures (Figs. 1.9B and 1.10B). We also determined the expression of 0.1 ng/mL IFNγ-induced inflammatory molecules in mixed glial and microglial cultures of CD200 -/- mice and no differences between CD200 -/- and CD200 +/+ mice were obtained (data not shown).

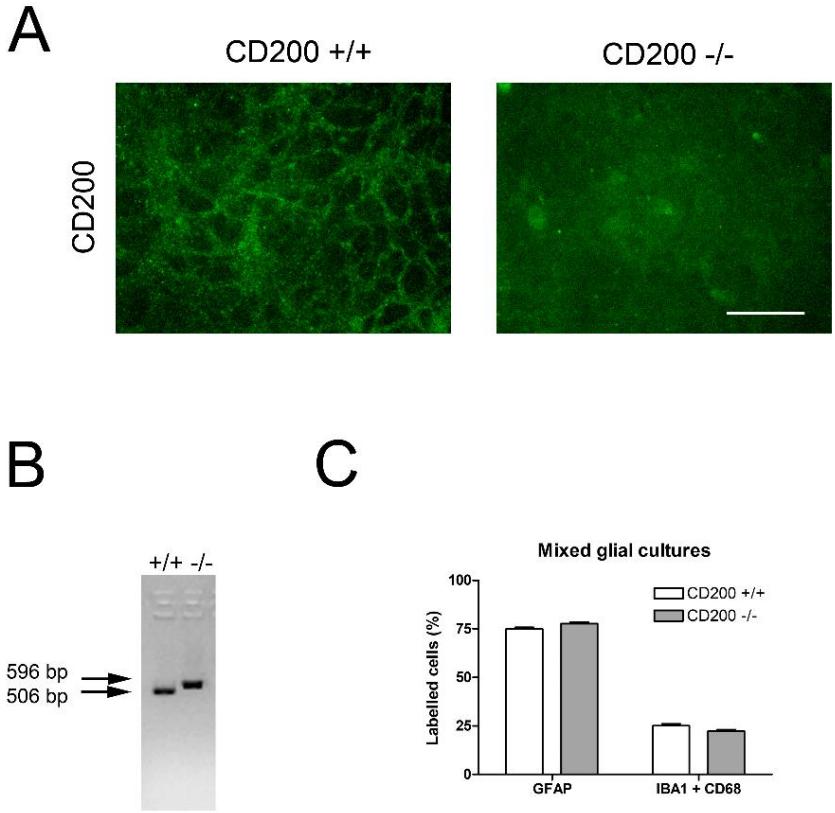

Figure 1.8. CD200 is not present in mixed glial cultures from CD200 -/- mice. Cell composition of mixed glial cultures is the same in CD200 -/- and CD200 +/+ mice with the same genetic background. CD200-immunocytochemistry (**A**) and genotyping (**B**) of CD200 +/+ and CD200 -/- primary mixed glial cultures. Scale bar: 50 µm. **C** Cell composition of mixed glial cultures in CD200 +/+ and CD200 -/-. Bars are means + SEM of 3 independent experiments. $p>0.05$; two-way ANOVA (repeated measures).

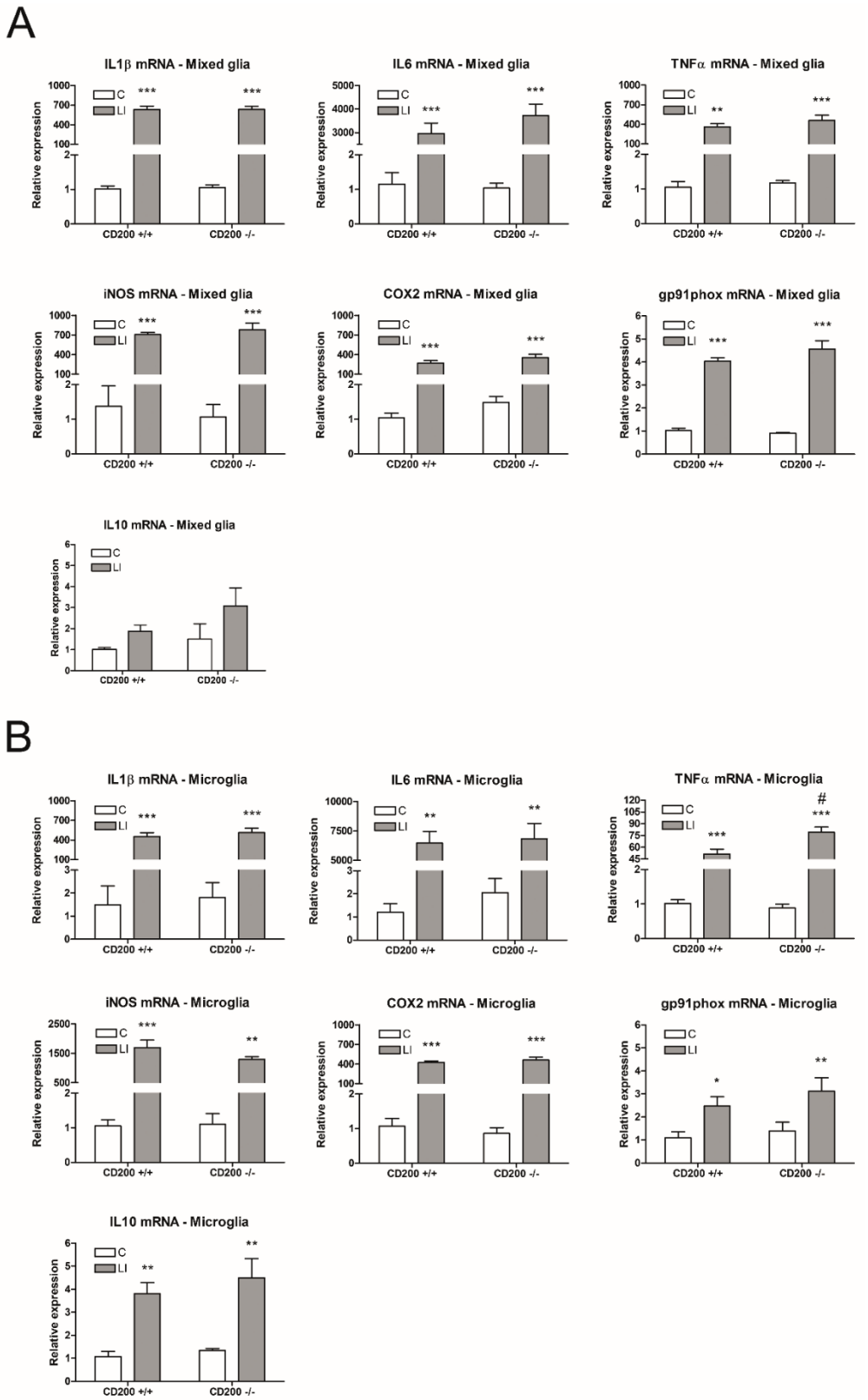

Figure 1.9. Pro-inflammatory response in mixed glial and microglial cultures from CD200-deficient mice treated with LPS/IFNγ. mRNA expression of inflammatory markers (IL1β, IL6, TNFα, COX2, iNOS, gp91phox and IL10) in primary mixed glial (**A**) and microglial (**B**) cultures from CD200 +/+ and CD200 -/- mice treated for 6 h with LPS/IFNγ (LI, 100 ng/mL LPS + 0.1 ng/mL IFNγ). Rn18s and βactin were used as reference genes. Bars are means + SEM of 4 - 5 independent experiments. *p<0.05, **p<0.01 and ***p<0.001 vs. CD200 +/+ control (C); #p<0.05 vs. CD200 +/+ LI; two-way ANOVA (repeated measures) and Newman-Keuls post-test.

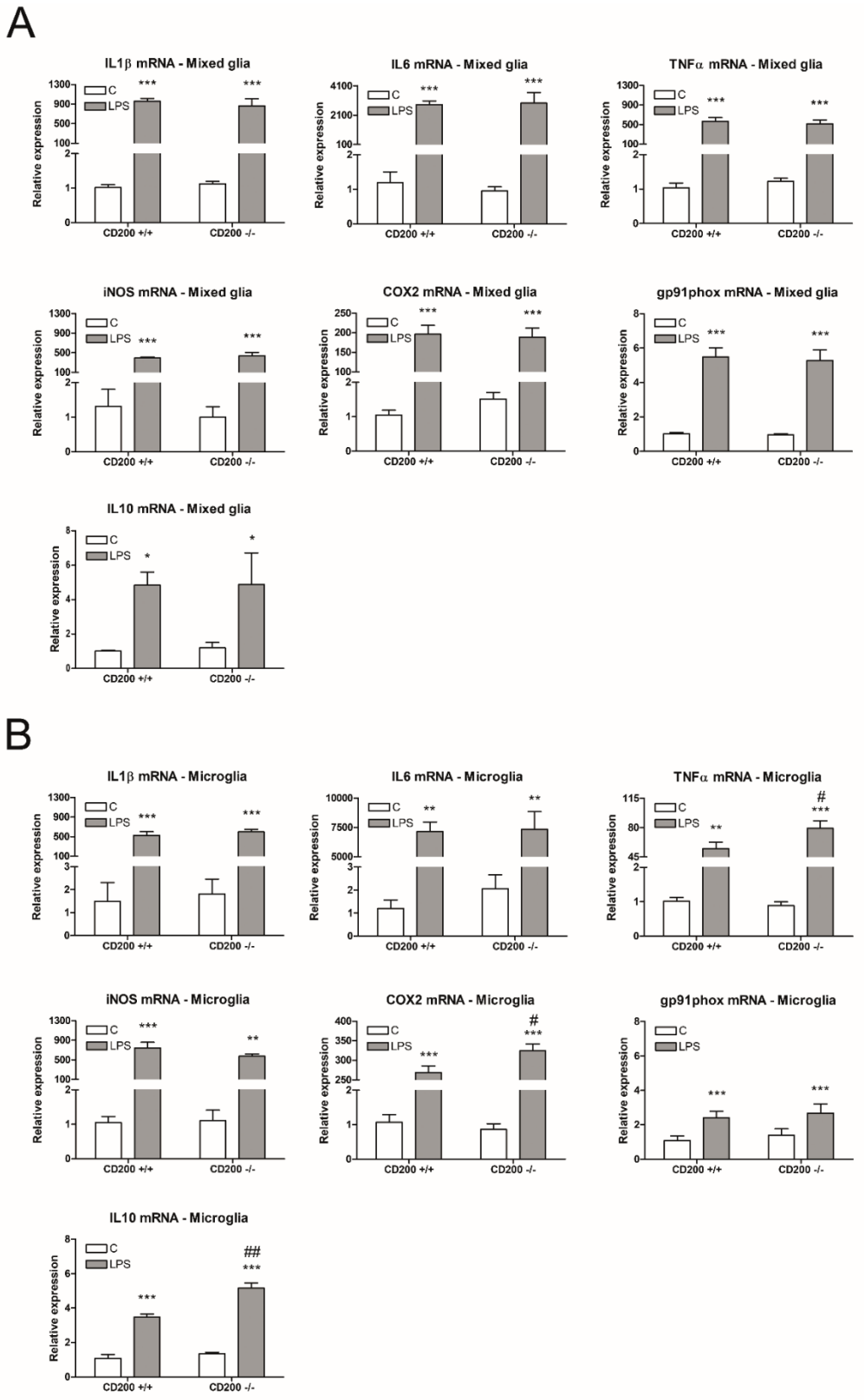

Figure 1.10. Pro-inflammatory response in mixed glial and microglial cultures from CD200-deficient mice treated with LPS alone. mRNA expression of inflammatory markers (IL1β, IL6, TNFα, COX2, iNOS, gp91phox and IL10) in primary mixed glial (**A**) and microglial (**B**) cultures from CD200 +/+ and CD200 -/- mice treated for 6 h with 100 ng/mL LPS. Rn18s and βactin were used as reference genes. Bars are means + SEM of 4 - 5 independent experiments. *p<0.05, **p<0.01 and ***p<0.001 vs. CD200 +/+ control (C); #p<0.05 and ##p<0.01 vs. CD200 +/+ LPS; two-way ANOVA (repeated measures) and Newman-Keuls post-test.

We then analysed the role of CD200-CD200R1 interaction in the anti-inflammatory response of glial cells. To this end, mixed glial and microglial cultures from CD200 +/+ and CD200 -/- mice were treated with 50 ng/mL IL4 for 24 h, and the mRNA expression of anti-inflammatory markers (IL10, TGFβ, Fizz1, Ym1 Arg1 and MR) was determined. Fizz1, Ym1, Arg1 and MR were induced in mixed glial cultures and Arg1 and MR in microglial cultures after IL4 treatment. No differences between CD200 +/+ and CD200 -/- cultures were found (Fig. 1.11).

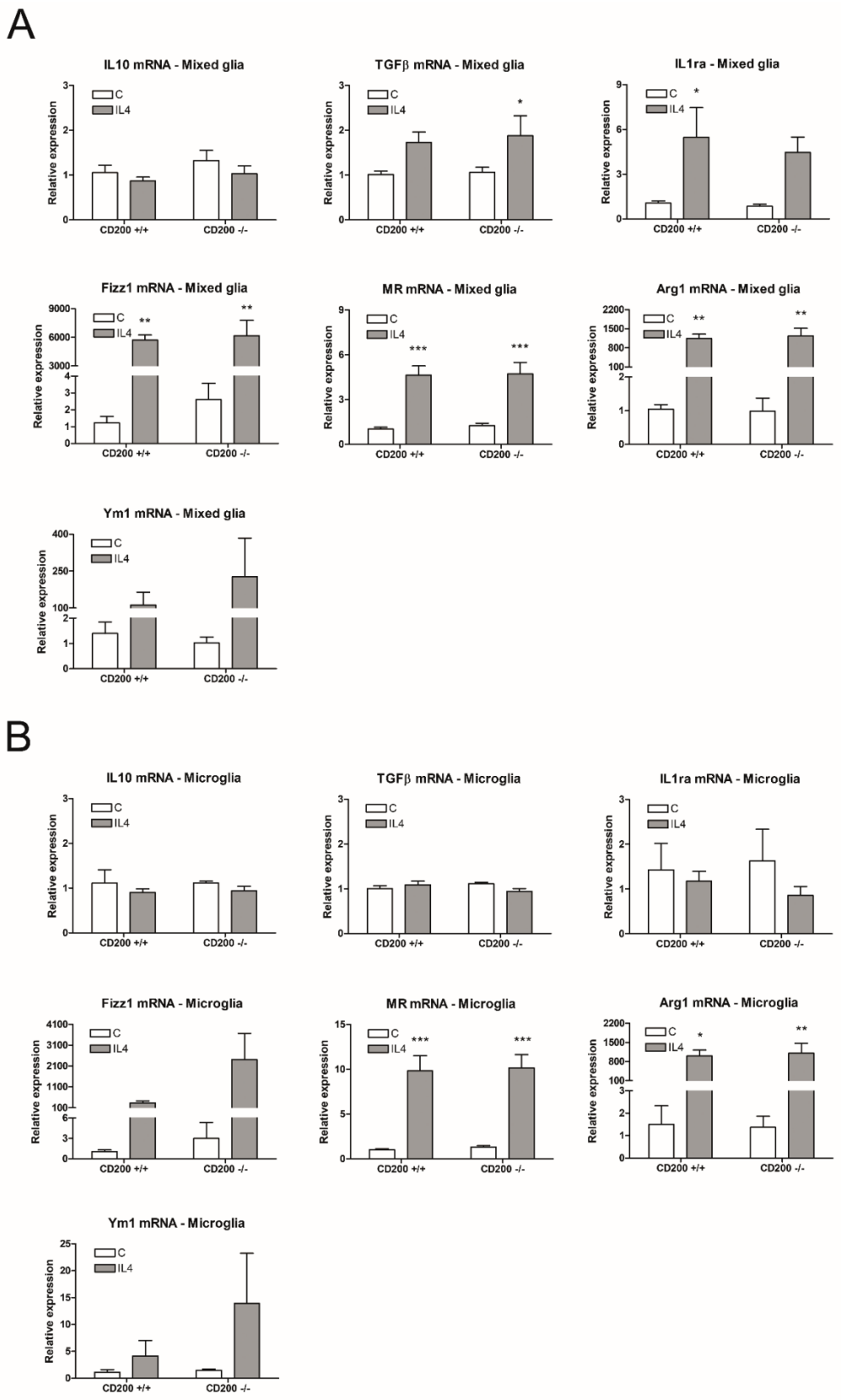

Figure 1.11. Anti-inflammatory response in mixed glial or microglial cultures from CD200-deficient mice treated with IL4. mRNA expression of anti-inflammatory markers (IL10, TGFβ, IL1ra, Fizz1, Ym1 Arg1 and MR) in primary mixed glial (**A**) and microglial (**B**) cultures from CD200 +/+ and CD200 -/- mice treated for 24 h with IL4 (50 ng/mL). Rn18s and βactin were used as reference genes. Bars are means + SEM of 4 - 5 independent experiments. *p<0.05, **p<0.01 and ***p<0.001 vs. control (C); two-way ANOVA (repeated measures) and Newman-Keuls post-test.

1.3 EFFECT OF CD200-DEFICIENCY ON THE INDUCTION OF NEURONAL DEATH

The effect of the absence of CD200 in the sensitivity of neuronal cells to neurotoxic stimuli was investigated *in vitro* using primary mesencephalic neuron-glia cultures (Fig. 1.12). When compared with cortical cultures, mesencephalic cultures are enriched in dopaminergic neurons, the main neuronal cell type affected in PD (Fig. 1.13) (Chen, Oyarzabal, and Hong 2013). Dopaminergic neuronal death was induced in primary mesencephalic cultures with the parkinsonian toxins MPP+ or rotenone, and the role of CD200 in this neurodegeneration was studied using CD200 knock-out mice.

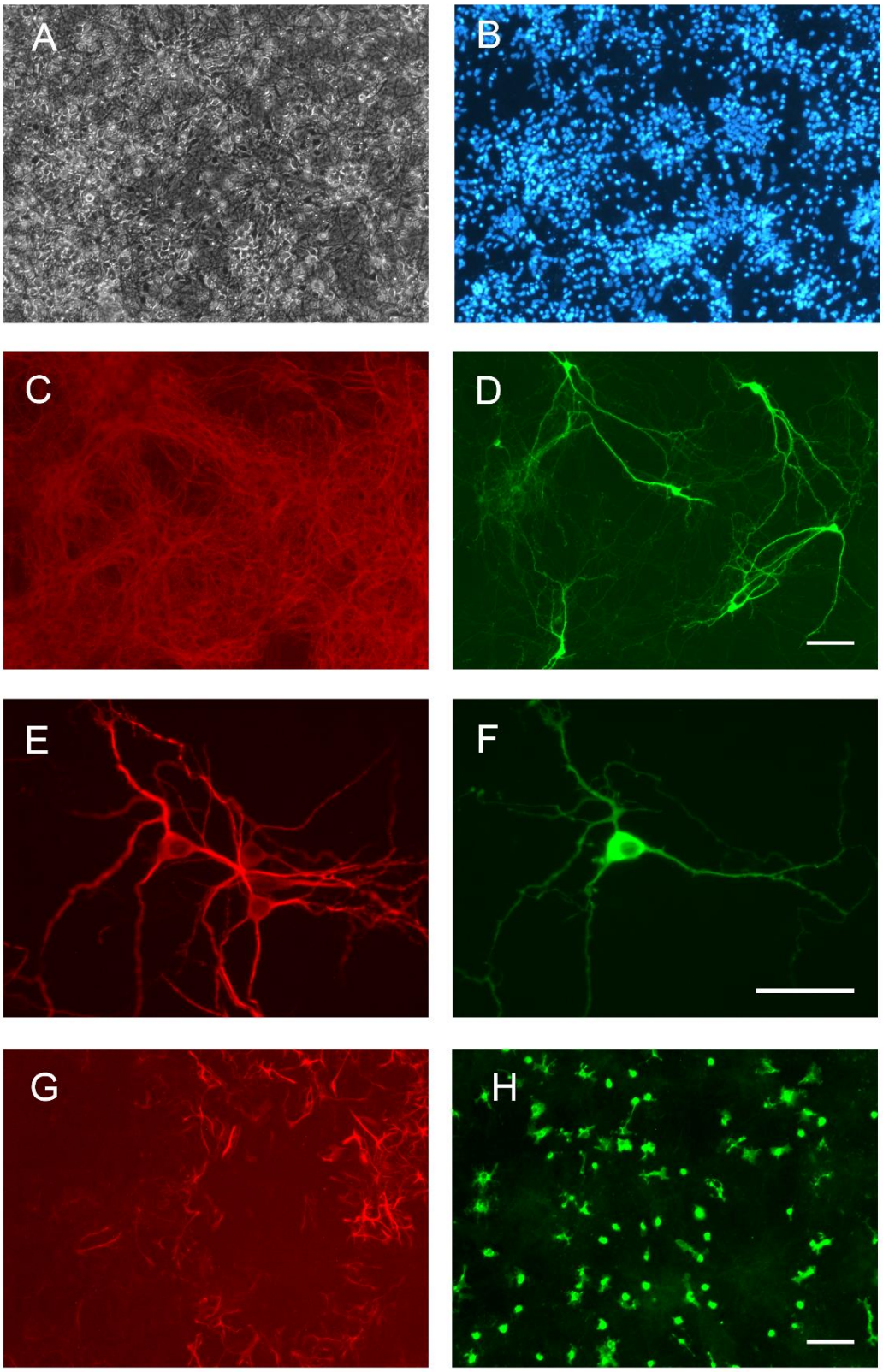

Figure 1.12. Characterisation of mesencephalic cultures. Representative immunocytochemistry and phase-contrast images of cell populations in 10 DIV mesencephalic cultures. **A** Phase-contrast image. **B** Nuclei detected with DAPI. **C, E** Neurons visualised by MAP2 immunostaining **D,F** Dopaminergic neurons visualised by TH immunostaining**. G** Astrocytes visualised by GFAP immunostaining. **H** Microglia visualised by IBA1 + CD68 immunostaining. Scale bars: 100 µm (A-D, G, H) and 50 µm (E,F).

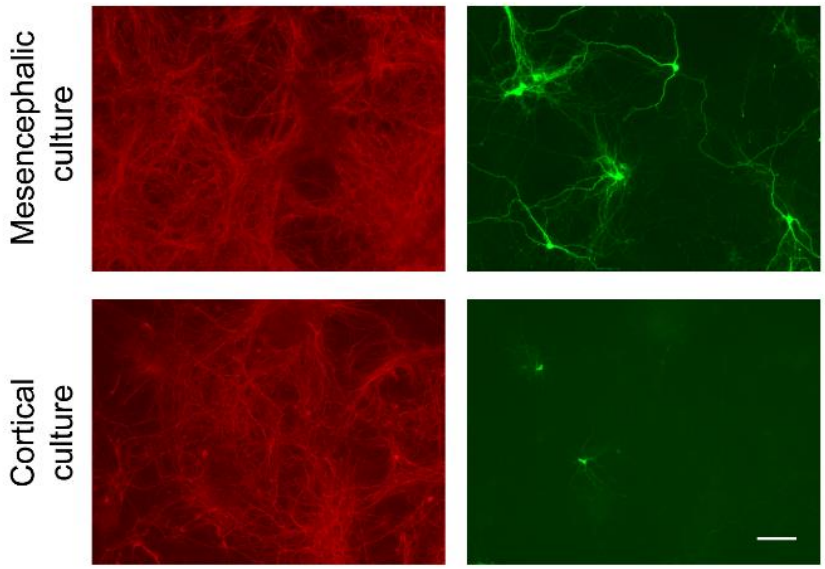

Figure 1.13. Primary mesencephalic cultures are enriched in dopaminergic neurons in comparison with cortical cultures. Immunohistochemistry of TH (green) and MAP2 (red) in 10 DIV primary murine mesencephalic and cortical cultures. Scale bar: 100 µm.

We performed dose-response experiments in order to select working concentrations of MPP+ and rotenone that resulted in the selective death of dopaminergic neurons but maintained the integrity of the rest of the neuronal network (Beck 1991). Mesencephalic neuronal cultures were treated at 10 DIV for 24 h with MPP+ (0.1, 1, 5, 10 µM) or rotenone (0.1, 1, 5, 10 nM). Immunocytochemistry of dopaminergic neurons revealed a minor decrease in the number of TH-positive neurons and shortening of TH-positive neuronal projections caused by 0.1 µM MPP+ and 0.1 nM rotenone, which was higher at 1 µM MPP+ and 1 nM rotenone. At these concentrations, microtubule-associated protein (MAP)2 immunocytochemistry showed that the neuronal network remained unaltered. In contrast, 5 and 10 µM MPP+ treatment and 5 and 10 nM rotenone treatment induced a marked decrease in both the number of TH- and MAP2-positive neurons, as well as shortening of TH- and MAP2-positive neuronal projections (Fig. 1.14). 1 µM MPP+ and 1 nM rotenone were used in subsequent studies.

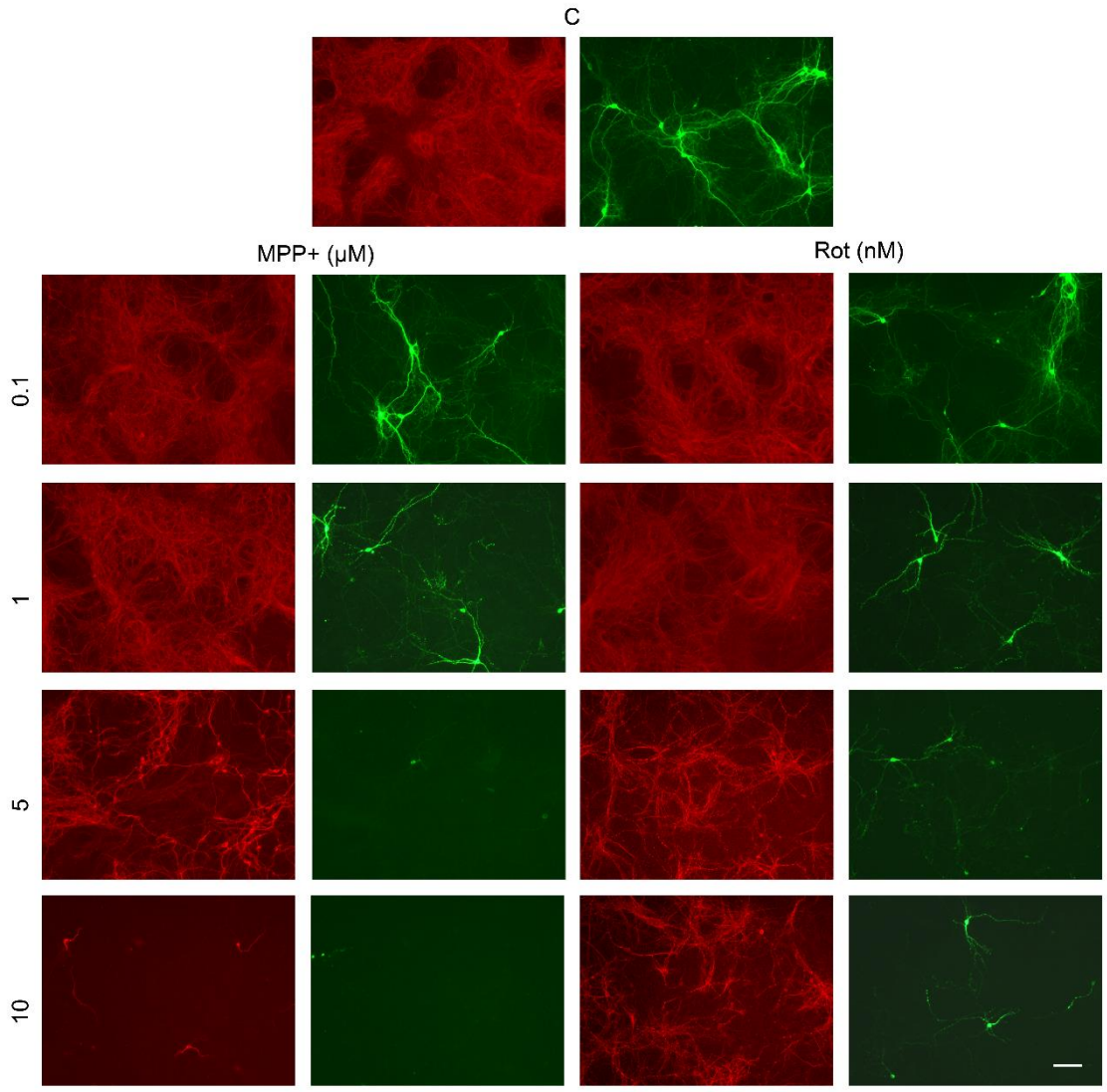

Figure 1.14. Effect of MPP+ and rotenone on neuronal integrity in primary mesencephalic cultures. Immunocytochemistry of MAP2 (red) and TH (green) in control mesencephalic cultures (C), and 24 h after 0.1, 1, 5 and 10 uM MPP+ or 0.1, 1, 5 and 10 nM rotenone (Rot) treatment. Scale bar: 100 µm.

We next studied whether CD200-CD200R1 disruption affected dopaminergic neuronal death induced by parkinsonian neurotoxins. To this end, CD200 +/+ and CD200 -/- primary mesencephalic cultures with the same genetic background were treated with MPP+ or rotenone (Fig. 1.15A,B). Mesencephalic cultures from CD200 +/+ embryos were composed of 2.72% ± 0.39 microglia, 4.14% ± 1.13 of astrocytes and 93.14% ± 1.5 of neurons, 0.20% ± 0.02 of which were dopaminergic neurons. In contrast, mesencephalic cultures from CD200 -/- embryos where composed of 4.82% + 0.58 microglia, 4.31% ± 1.13 of astrocytes and 90.87% ± 0.41 of neurons, 0.18% ± 0.02 of which were dopaminergic neurons. The percentage of IBA1 + CD68- positive cells was significantly increased in CD200 -/- cultures compared to CD200 +/+ cultures (Fig. 1.15C). After MPP+ or rotenone treatment, no effect on neuronal network integrity was observed. CD200 +/+ cultures showed a significant decrease (21.09%) in TH-positive neurons after 1 nM

rotenone treatment whereas CD200 -/- cultures showed a significant decrease after 1 µM MPP+ (24.97%) and 1 nM rotenone (18.23%) treatment (Fig. 1.15D).

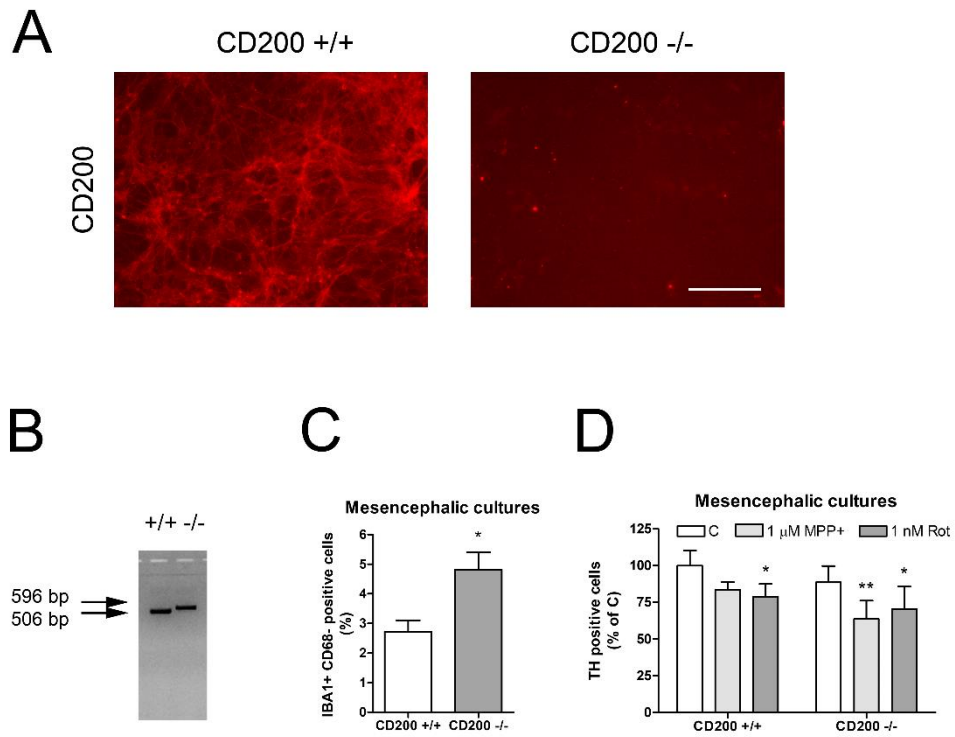

Figure 1.15. MPP+- and rotenone-induced dopaminergic neurotoxicity in mesencephalic cultures. CD200-immunocytochemistry (**A**) and genotyping (**B**) of CD200 +/+ and CD200 -/- primary mesencephalic cultures with the same genetic background. Scale bar: 100 µm. **C** Quantification of IBA1 + CD68 - positive cells (microglial cells). Bars are means + SEM of 3 independent experiments. *p<0.05 vs. CD200 +/+; one-way ANOVA (repeated measures) and Newman-Keuls post-test. **D** Percentage of TH-positive cells (dopaminergic neurons) in primary mesencephalic cultures of CD200 -/- and CD200 +/+ mice with the same genetic background treated for 24 h with 1 µM MPP+ or 1 nM rotenone. Bars are means + SEM of 4 independent experiments. *p<0.05 and **p<0.01 vs. each CD200 +/+; two-way ANOVA and Bonferroni post-test.

2 Effect of MPP+ and rotenone on glial activation and on CD200-CD200R1 system

Since reciprocal communication exists in the CNS between neuronal and glial cells, alterations in neuronal function may affect glial function and *vice versa*. In fact, a possible role of glial activation in the development of neuronal damage in neurodegenerative diseases has been repeatedly proposed (Colonna and Butovsky 2017; Perry, Nicoll, and Holmes 2010) Consequently, alterations in glial function due to exposure to neurotoxic compounds merit study, especially in the context of neurodegenerative diseases in which such exposure is considered a risk factor. The aim of the present work was, therefore, to characterize the effects of MPP+ and rotenone on glial activation using primary mixed glial and microglial cultures. We determined the direct effect of these neurotoxins on glial cell function, and also whether they could interfere with glial activation induced by a classical pro-inflammatory stimulus, such as LPS/IFNγ or by a classical anti-inflammatory stimulus, such as IL4. The chapter “2.1 Pro-inflammatory response” is already published (Rabaneda-Lombarte et al. 2018).

2.1 PRO-INFLAMMATORY RESPONSE

2.1.1 Effects of MPP+ and rotenone on glial cell viability

In a preliminary study, we performed dose-response experiments in order to select working concentrations of MPP+ and rotenone that did not result in significant alterations in cell viability after 24 h exposure. We evaluated glial cell viability after treating the mixed glial or the microglial cultures with increasing concentrations of MPP+ (10, 25, 50 and 100 µM) or rotenone (20, 40, 100 and 150 nM), both in the absence and in the presence of LPS/IFNγ (L/I, 100 ng/mL LPS + 0.1 ng/mL IFNγ), using the MTT assay and PI staining. In mixed glial cell cultures, MPP+ induced a concentration-dependent decrease in MTT reduction that was accentuated in the presence of LPS/IFNγ (Fig. 2.1A). On the contrary, no alterations in MTT reduction were observed in microglial cell cultures treated with MPP+, either in the absence or presence of LPS/IFNγ (Fig. 2.1B). Rotenone-treated mixed glial cell cultures showed a significant decrease in MTT reduction from 100 nM rotenone. In the presence of LPS/IFNγ, there was a significant decrease in MTT reduction even at 20 nM rotenone (Fig. 2.1C). As in the case of MPP+ treatments, no alterations in MTT reduction were observed in microglial cell cultures treated with rotenone or rotenone and LPS/IFNγ (Fig. 2.1D). To determine whether the decrease in MTT reduction in MPP+ and rotenone-treated mixed glial cell cultures was due to a decrease in metabolic activity or to cell death, PI staining was performed. Mixed glial cultures treated with 50 and 100 µM MPP+ showed a significant increase in the percentage of PI positive nuclei. This effect was accentuated in the

presence of LPS/IFNγ, and a significant increase was also detected at 25 μM MPP+ (Fig. 2.1E). No alterations in the percentage of PI-positive nuclei were observed in microglial cultures treated with MPP+ (Fig. 2.1F). In addition, no significant increases in the percentage of PI-positive nuclei were observed in rotenone-treated mixed glial cell cultures or microglial cultures (Fig. 2.1G,H), with the only exception of cells treated with 100 μM rotenone and LPS/IFNγ. Based on these results, the concentrations of 10 and 25 μM MPP+ and 40 and 100 nM rotenone were selected for subsequent studies. Representative images of the cultures in these experimental conditions are shown in Figure 2.2, which corroborate the lack of toxic effect of the selected concentrations of MPP+ (Fig. 2.2A) and rotenone (Fig. 2.2B).

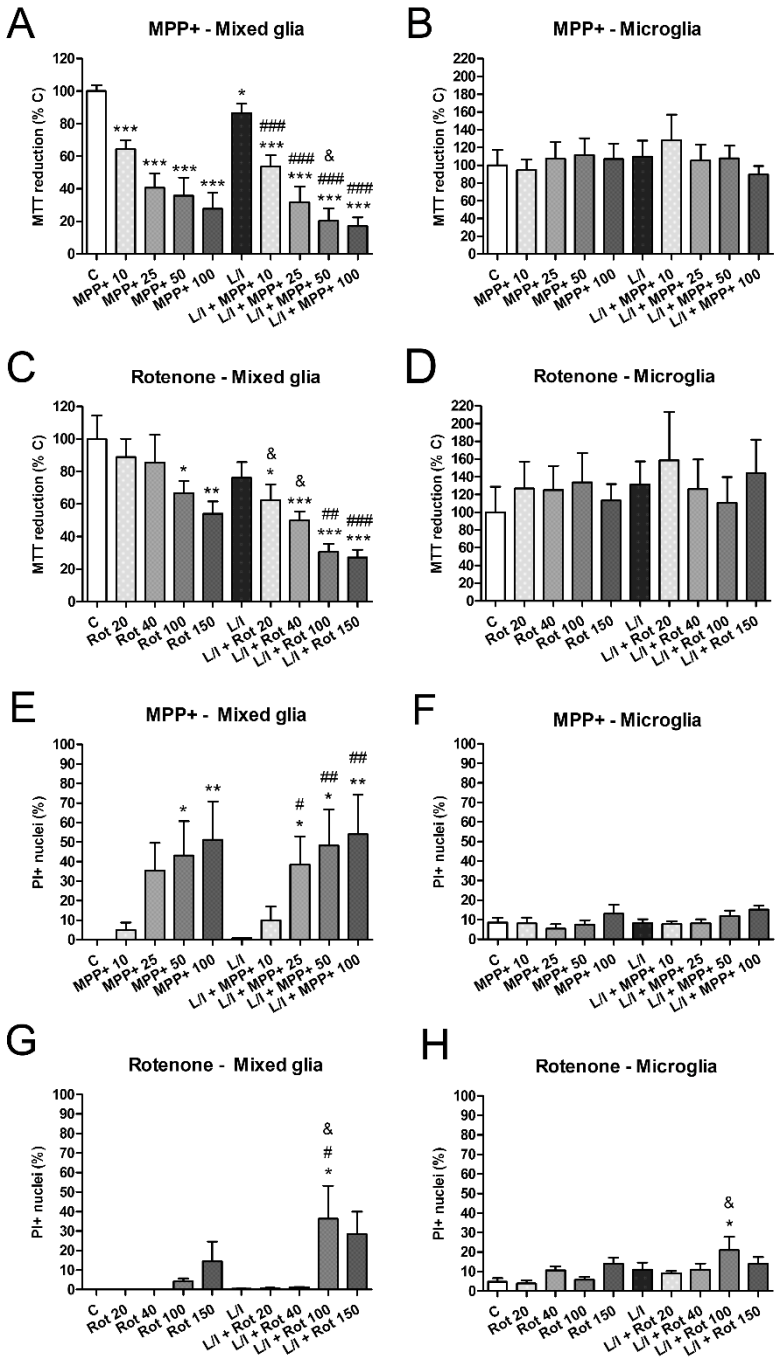

Figure 2.1. Effect of MPP+ and rotenone on glial cell viability. A-D MPP+ and rotenone induced alterations in MTT reduction in primary glial cultures. Effect of 10, 25, 50 and 100 μM MPP+ treatment for 24 h on mixed glial cultures (A) and microglial cultures (B), both in the absence and the presence of LPS/IFNγ (L/I). Effect of 20, 40, 100 and 150 nM rotenone (Rot) treatment for 24 h on mixed glial cultures (C) and microglial cultures (D), both in the absence and the presence of L/I. **E-H** Percentage of propidium iodide (PI) positive nuclei in mixed glial cultures (E) and microglial cultures (F) treated for 24 h with 10, 25, 50 and 100 μM MPP+, both in the absence and the presence of LPS/IFNγ (L/I). Percentage of PI positive nuclei in mixed glial cultures (G) and microglial cultures (H) treated for 24 h with 20, 40, 100 and 150 nM rotenone (Rot), both in the absence and the presence of L/I. Bars are means + SEM of 4 independent experiments. *p<0.05, **p<0.01 and ***p<0.001 vs. control (C); #p<0.05, ##p<0.01 and ###p<0.001 vs. L/I; &p<0.05 vs. MPP+ or Rot alone; one-way ANOVA (repeated measures) and Newman-Keuls post-test.

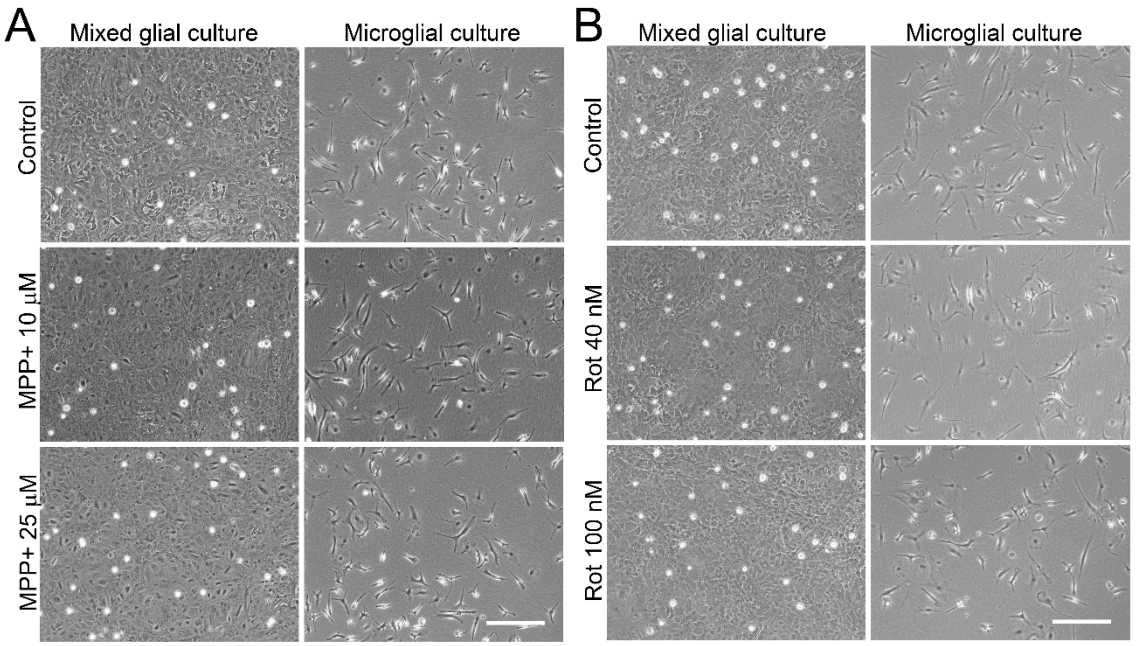

Figure 2.2. Phase contrast images of MPP+- and rotenone-treated primary glial cultures. Images show the appearance of mixed glial cultures and microglial cultures treated for 24 h with 10 and 25 µM MPP+ (A) or 40 and 100 nM rotenone (Rot) (B), the working concentrations used in further studies. Bar = 200 µm.

2.1.2 MPP+ and rotenone induce alterations in the expression of pro-inflammatory genes in LPS/IFNγ-treated primary glial cultures

We next determined whether MPP+ and rotenone induced a pro-inflammatory phenotype in primary glial cell cultures, as well as whether they had any effect on the development of the pro-inflammatory response induced by LPS/IFNγ. We determined the mRNA expression of the cytokines IL1β, IL6 and TNFα and the enzymes iNOS, COX2 and gp91phox, as markers of a pro-inflammatory response. MPP+ (Fig. 2.3) and rotenone (Fig. 2.4) treatment did not significantly induce the mRNA expression of these pro-inflammatory markers in primary glial cell cultures, although a trend towards increased expression was observed for some mRNAs, especially in rotenone-treated mixed glial cultures. On the contrary, 6 h after LPS/IFNγ treatment the mRNA expression of all the pro-inflammatory markers tested was clearly induced (Figs. 2.3 and 2.4). However, MPP+ and especially rotenone induced alterations in the pattern of expression of these markers in LPS/IFNγ treated cultures. When glial cell cultures were treated with LPS/IFNγ in the presence of MPP+, the induction of IL1β mRNA expression was significantly inhibited in mixed glial and microglial cultures (Fig. 2.3A,B), while COX2 mRNA expression was further increased in mixed glial cultures (Fig. 2.3A) and gp91phox mRNA was induced in microglial cultures (Fig. 2.3B). More importantly, rotenone exposure significantly abrogated LPS/IFNγ induction of the mRNA expression of all pro-inflammatory markers in mixed glial cultures (Fig. 2.4A), as well as IL1β, IL6 and COX2 mRNA expression in microglial cultures (Fig. 2.4B).

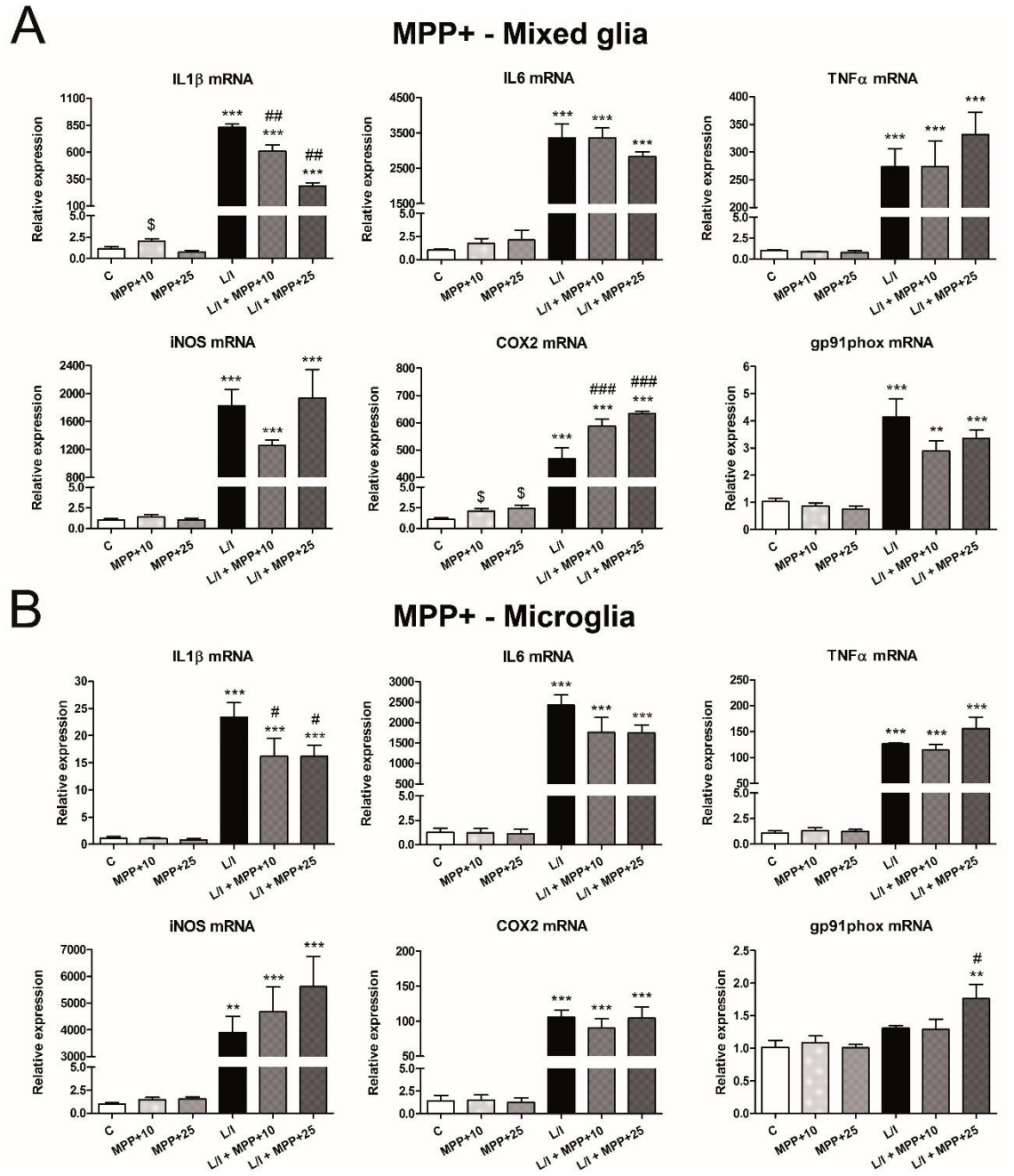

Figure 2.3. Effect of MPP+ treatment on the mRNA expression of pro-inflammatory markers. mRNA expression of pro-inflammatory cytokines (IL-1β, IL-6 and TNFα) and enzymes (iNOS, COX2, gp91phox) in primary mixed glial cultures (A) and microglial cultures (B) treated for 6 h with 10 and 25 μM MPP+, both in the absence and the presence of LPS/IFNγ (L/I). Rn18s and βactin were used as reference genes. Bars are means + SEM of 4 independent experiments. **p<0.01 and ***p<0.001 vs. C; #p<0.05, ##p<0.01 and ###p<0.001 vs. L/I; one-way ANOVA and Newman-Keuls post-test. $p<0.05 MPP+ alone vs. C, one-way ANOVA and Newman-Keuls post-test only considering the L/I-free groups. This latter analysis was performed to detect whether the high values observed in the L/I group may hinder the detection of statistical significance of the effects of MPP+ and Rot alone.

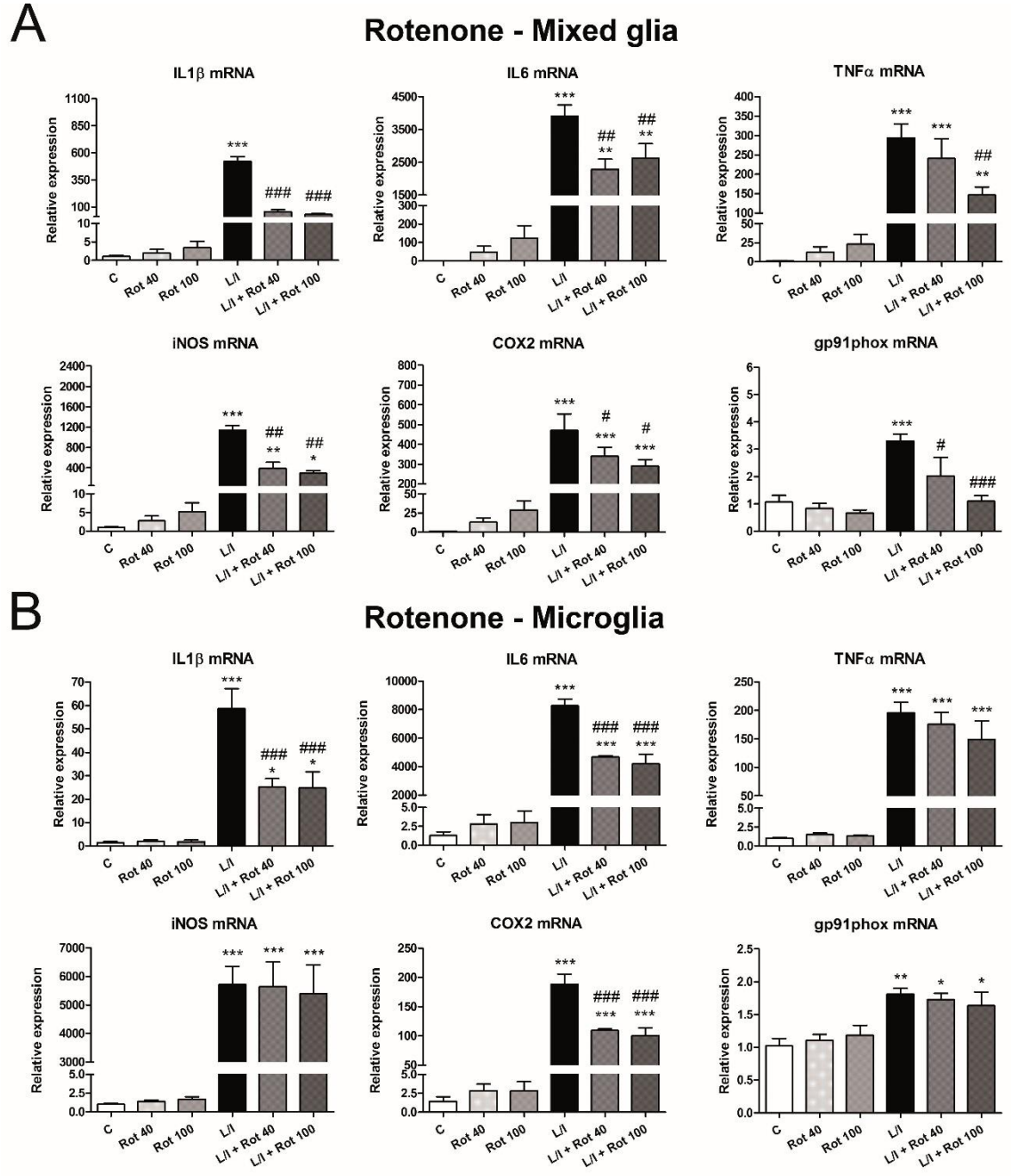

Figure 2.4. Effect of rotenone treatment on the mRNA expression of pro-inflammatory markers. mRNA expression of pro-inflammatory cytokines (IL-1β, IL-6 and TNFα) and enzymes (iNOS, COX-2, gp91phox) in primary mixed glial cultures (A) and microglial cultures (B) treated for 6 h with 40 and 100 nM rotenone (Rot), both in the absence and the presence of LPS/IFNγ (L/I). Rn18s and βactin were used as reference genes. Bars are means + SEM of 4 independent experiments. *p<0.5, **p<0.01 and ***p<0.001 vs. control (C); #p<0.05, ##p<0.01 and ###p<0.001 vs. L/I; one-way ANOVA and Newman-Keuls post-test.

2.1.3 MPP+ and rotenone inhibit LPS/IFNγ-induced NO and pro-inflammatory cytokine production in primary glial cultures

We also analysed the effect of MPP+ and rotenone on NO, IL1β, IL6 and TNFα release into the culture medium. MPP+ alone induced a decrease in NO production and an increase in IL6 release into the culture medium in mixed glial cell cultures 24 h after treatment (Fig. 2.5A). The latter effect was also observed in MPP+-treated microglial cultures (Fig. 2.5B), as well as in rotenone-treated mixed glial (Fig. 2.5C) and microglial cultures (Fig. 2.5D). LPS/IFNγ-treatment clearly increased NO production in mixed glial cultures, and MPP+ (25 μM) and rotenone (40 and 100 nM) significantly inhibited this effect (Fig. 2.5A,C). Significant NO production was not detected in microglial cultures treated with LPS/IFNγ for 24 h (Fig. 2.5B,D). However, an increase in NO production was observed when microglial cultures were treated with LPS/IFNγ for 48 h, but MPP+ and rotenone did not modify this effect (data not shown). With regards to cytokine release, LPS/IFNγ-treatment resulted in drastic increases in IL1β, IL6 and TNFα levels in mixed glial (Fig. 5A,C) and microglial (Fig. 2.5B,D) cultures. MPP+ exposure (25 μM) significantly inhibited LPS/IFNγ-induced release of IL1β and IL6, but not TNFα, in mixed glia (Fig. 2.5A), while it had no significant effect on the production of these cytokines in microglial cell cultures (Fig. 2.5B). Interestingly, rotenone (40 and 100 nM) significantly inhibited IL1β, IL6 and TNFα release induced by LPS/IFNγ in both mixed glial (Fig. 2.5C) and microglial cultures (Fig. 2.5D).

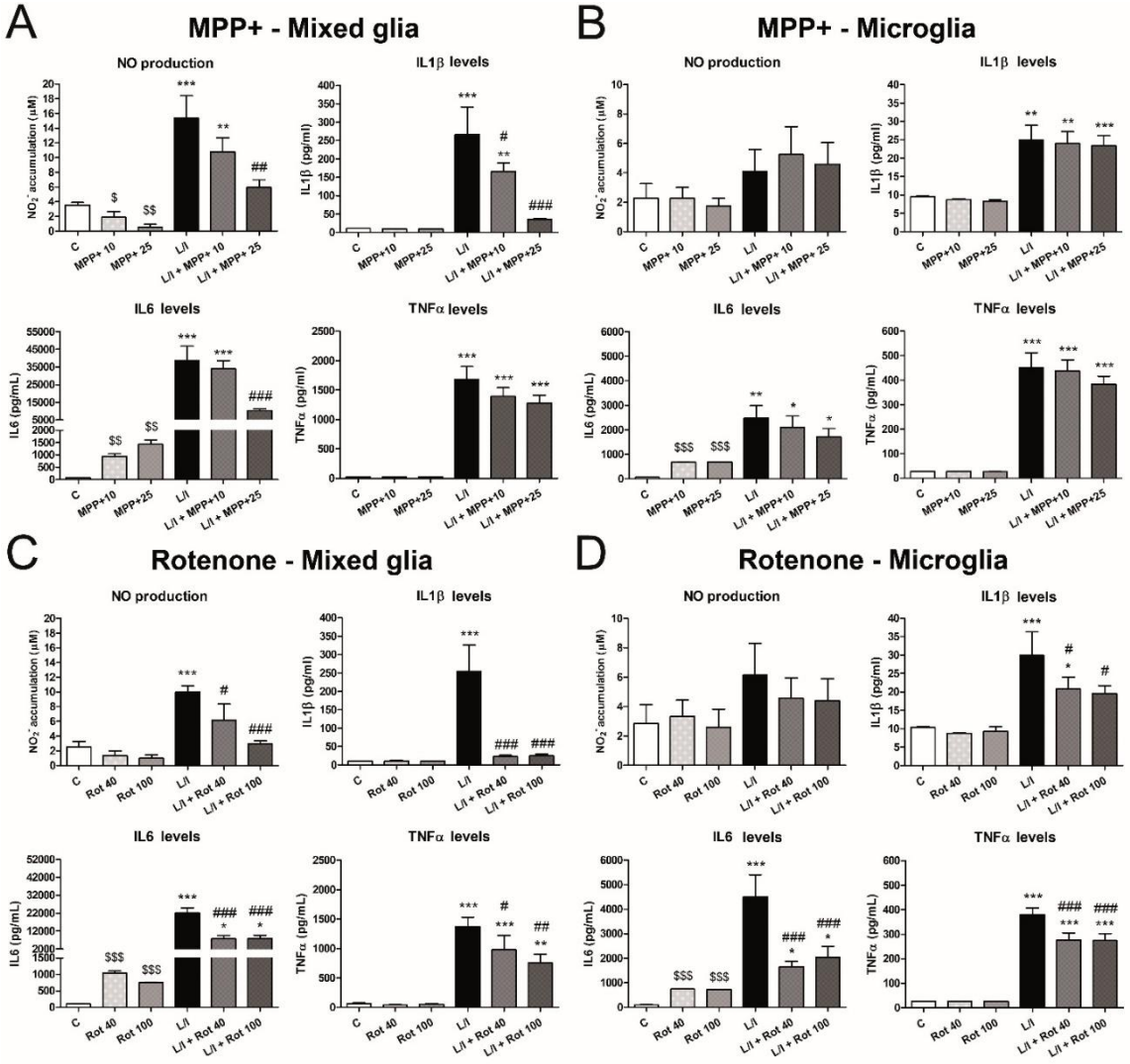

Figure 2.5. NO and pro-inflammatory cytokine production in primary glial cell cultures treated with MPP+ and rotenone. NO production was estimated from NO_2^- accumulation by the Griess method and IL1β, IL6 and TNFα levels were determined by ELISA in the culture medium of MPP+-treated mixed glial (A) and microglial (B) cultures, and rotenone (Rot)-treated mixed glial (C) and microglial (D) cultures. The cell cultures were treated with 10 and 25 µM MPP+ or 40 and 100 nM Rot for 24 h, in the absence or in the presence of LPS/IFNγ (L/I). Bars are means + SEM of 4 independent experiments. *p<0.5, **p<0.01 and ***p<0.001 vs. control (C); #p<0.05, ##p<0.01 and ###p<0.001 vs. L/I; one-way ANOVA and Newman-Keuls post-test. $p<0.05, $$p<0.01 and $$$p<0.001 MPP+ and Rot alone vs. C, one-way ANOVA and Newman-Keuls post-test only considering the L/I-free groups. This latter analysis was performed to detect whether the high values observed in the L/I group may hinder the detection of statistical significance of the effects of MPP+ and Rot alone.

2.1.4 MPP+ and rotenone treatment inhibit the phagocytic activity of microglial cells

We then evaluated whether MPP+ and rotenone modify the phagocytic activity of microglial cells, another important parameter used to characterize the microglial activation phenotype. Both MPP+ and rotenone treatment showed a tendency to decrease the percentage of phagocytic microglial

cells that was statistically significant when the cells were also treated with LPS/IFNγ (Fig. 2.6A). In addition, MPP+ and rotenone treatment resulted in a significant increase in the percentage of microglial cells showing low phagocytic activity (number of microspheres per cell equal or lower than control) and a subsequent significant decrease in the percentage of cells showing high phagocytic activity (number of microspheres per cell higher than control) (Fig. 2.6B). These effects were accentuated in the presence of LPS/IFNγ.

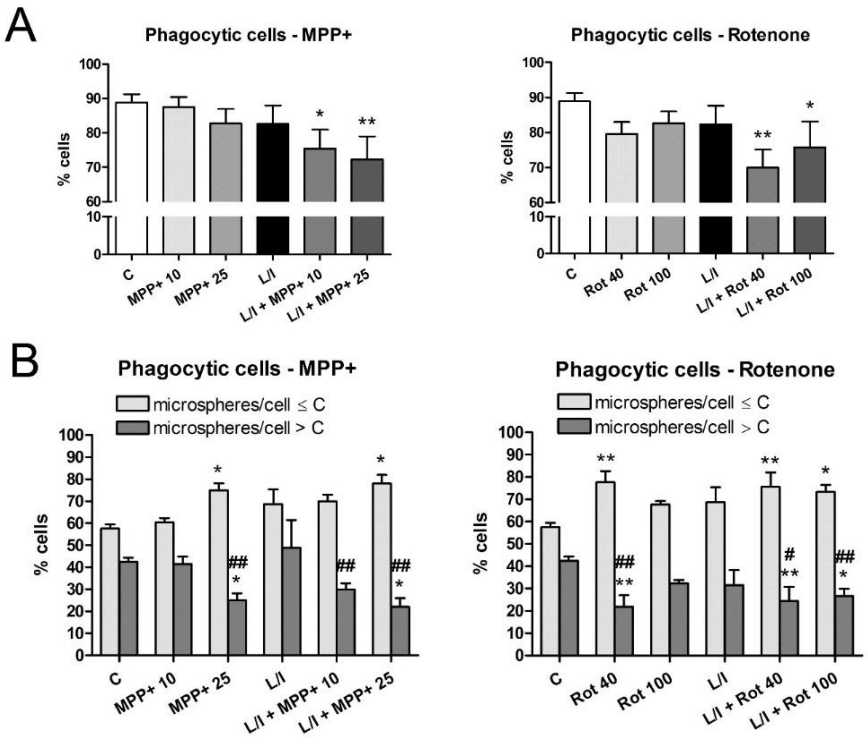

Figure 2.6. Effect of MPP+ and rotenone treatment on microglial cell phagocytosis in primary microglial cell cultures. Phagocytic activity was evaluated through the ingestion of fluorescent microspheres after treating the cell cultures with 10 and 25 μM MPP+ or 40 and 100 nM rotenone (Rot) for 24 h, in the absence and in the presence of LPS/IFNγ (L/I). Internalization of microspheres was quantified after immunofluorescence labelling of microglial cells using an anti-IBA1 antibody. **A** Percentage of cells with microspheres. Bars are means + SEM of 4 independent experiments. *p<0.05 and **p<0.01 vs. control (C); one-way ANOVA and Newman -Keuls post-test. **B** Percentage of cells with low phagocytic activity (number of microspheres/cell equal < C) and cells with high phagocytic activity (number of microspheres/cell > C). Bars are means + SEM of 4 independent experiments. *p<0.05 and **p<0.01 vs. corresponding C; #p<0.05 and ##p<0.01 vs. low-phagocytic cells; two-way ANOVA and Bonferroni post-test.

2.1.5 Intracellular ATP levels are decreased by MPP+ and rotenone in the absence or presence of LPS/IFNγ in glial cell cultures

In an attempt to better characterize the metabolic status of the cells, we determined the intracellular ATP levels in response to MPP+, rotenone and LPS/IFNγ treatments. In general, intracellular ATP levels were modified in mixed glial cultures in our MPP+ and rotenone experimental models (p<0.001, one-way ANOVA) (Fig. 2.7). In particular, ATP levels were significantly decreased after 25 μM MPP+ treatment (Fig. 2.7A). On the contrary, a significant

increase in ATP levels was detected in LPS/IFNγ-treated mixed glial cultures, which was abrogated in the presence of MPP+ and rotenone (Fig. 2.7A,B). ATP levels were also modified in microglial cultures in the MPP+ and rotenone experimental models ($p<0.05$, one-way ANOVA), but to a lesser extent than in mixed glial cultures (Fig. 2.7C,D).

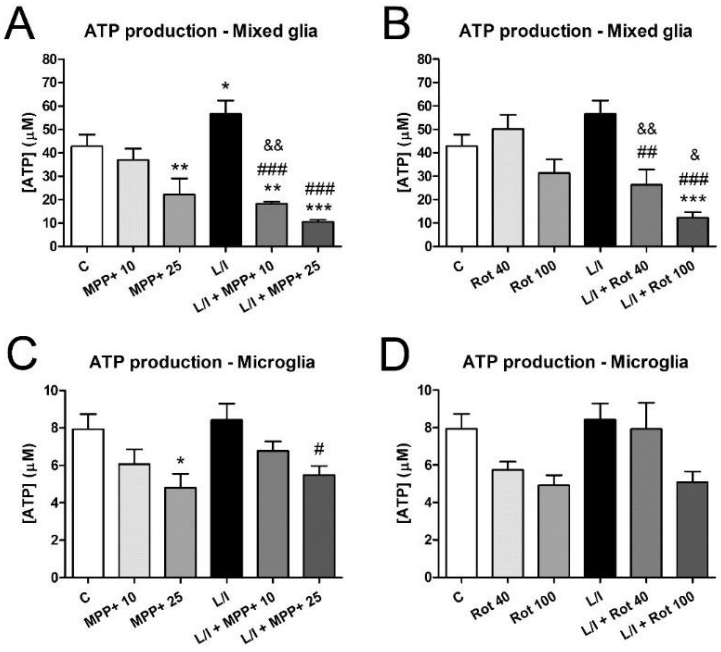

Figure 2.7. ATP levels in primary glial cell cultures treated with MPP+ or rotenone. Intracellular ATP levels were determined in mixed glial cultures and microglial cultures treated with 10 and 25 μM MPP+ (A and B) or 40 and 100 nM rotenone (Rot) (C and D) for 24 h, in the absence and in the presence of LPS/IFNγ (L/I). Bars are means + SEM of 5 independent experiments. *p<0.5, **p<0.01 and ***p<0.001 vs. control (C); ##p<0.01 and ###p<0.001 vs. L/I; one-way ANOVA and Newman-Keuls post-test.

2.1.6 Metabolic changes in LPS/IFNγ-treated glial cultures: effect of MPP+ and rotenone

In immune cells, the development of specific immune responses is associated with specific metabolic changes. Increased glycolysis and potentiation of the pentose phosphate pathway, together with the inhibition of oxidative phosphorylation has been reported for immune cells showing a pro-inflammatory phenotype. We checked whether this was the case in our glial cultures treated with LPS/IFNγ and whether MPP+ and rotenone were able to modify it. We determined the mRNA expression of genes encoding critical proteins for the switch to glycolysis: glucose transporter (Glut) 1 (glucose entrance into the cell), key glycolytic enzymes such as hexokinase (Hk)1 (glycolysis initial rate limiting step) and phosphofructokinase (PFK)1 (master regulator of glycolysis), the glycolysis activator hypoxia-inducible factor (Hif)1α and Carkl, involved in the control of the pentose phosphate pathway. In microglial cell cultures, MPP+ and rotenone alone did not modify per se the expression of these genes (Fig. 2.8). On the contrary, as expected, LPS/IFNγ treatment induced an increase in their expression (Fig. 2.8), with the exception of Carkl mRNA (Fig. 2.8I,J), which showed a decrease. MPP+ treatment further increased LPS/IFNγ-induced Glut1 mRNA expression (Fig. 2.8A), while rotenone inhibited LPS/IFNγ-induced Pfk1 (Fig. 2.8F) and Hif1α (Fig. 2.8H) mRNA expression. We also evaluated the expression of these mRNAs in mixed glial cultures. MPP+ and rotenone alone increased Glut1

mRNA (Fig. 2.9A,B), MPP+ and Hif1α mRNA expression (Fig. 2.9G). LPS/IFNγ treatment inhibited the expression of the glycolytic genes Glut 1 (Fig. 2.9A,B), Hk1 (Fig. 2.9C,D) and Pfk1 (Fig. 2.9E,F), as well as Carkl mRNA expression (Fig. 2.9I,J), and increased the expression of Hif1α (Fig. 2.9G,H). Rotenone inhibited LPS/IFNγ-induced Hif1α mRNA expression (Fig. 2.9H).

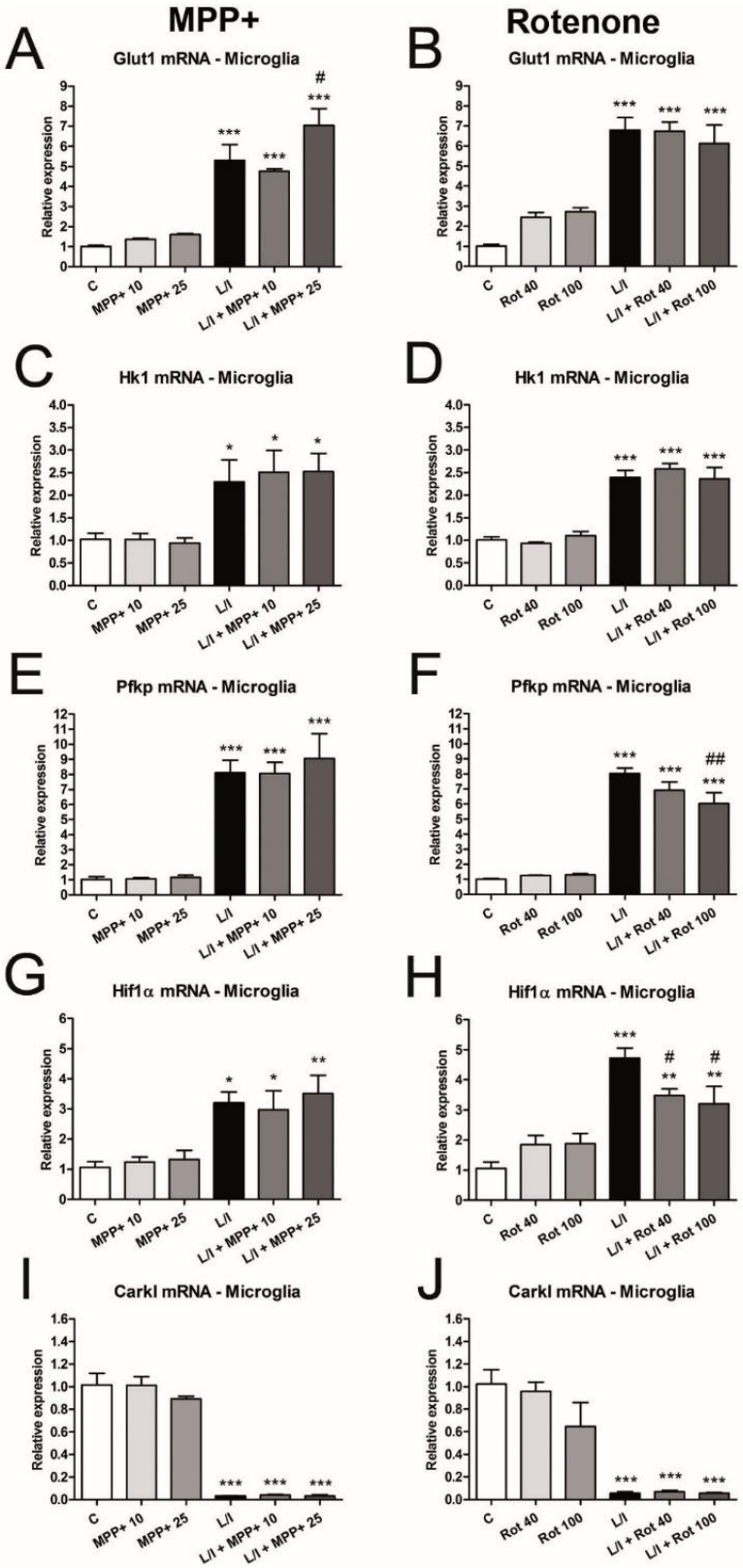

Figure 2.8. Effect of MPP+ and rotenone treatment on the expression of genes involved in the control of glycolysis in microglial cell cultures. mRNA expression of the glucose transporter Glut1 (A and B) and the glycolytic enzymes Hk1 (C and D) and Pfk1 (E and F), as well as Hif1α (G and H) and Carkl (I and J). Primary microglial cultures were treated for 6 h with 10 and 25 μM MPP+ or 40 and 100 nM rotenone (Rot), both in the absence and the presence of LPS/IFNγ (L/I). Rn18s and βactin were used as reference genes. Bars are means + SEM of 4 independent experiments. *p<0.05, **p<0.01 and ***p<0.001 vs. control (C); #p<0.05 and ##p<0.01 vs. L/I; one-way ANOVA and Newman-Keuls post-test.

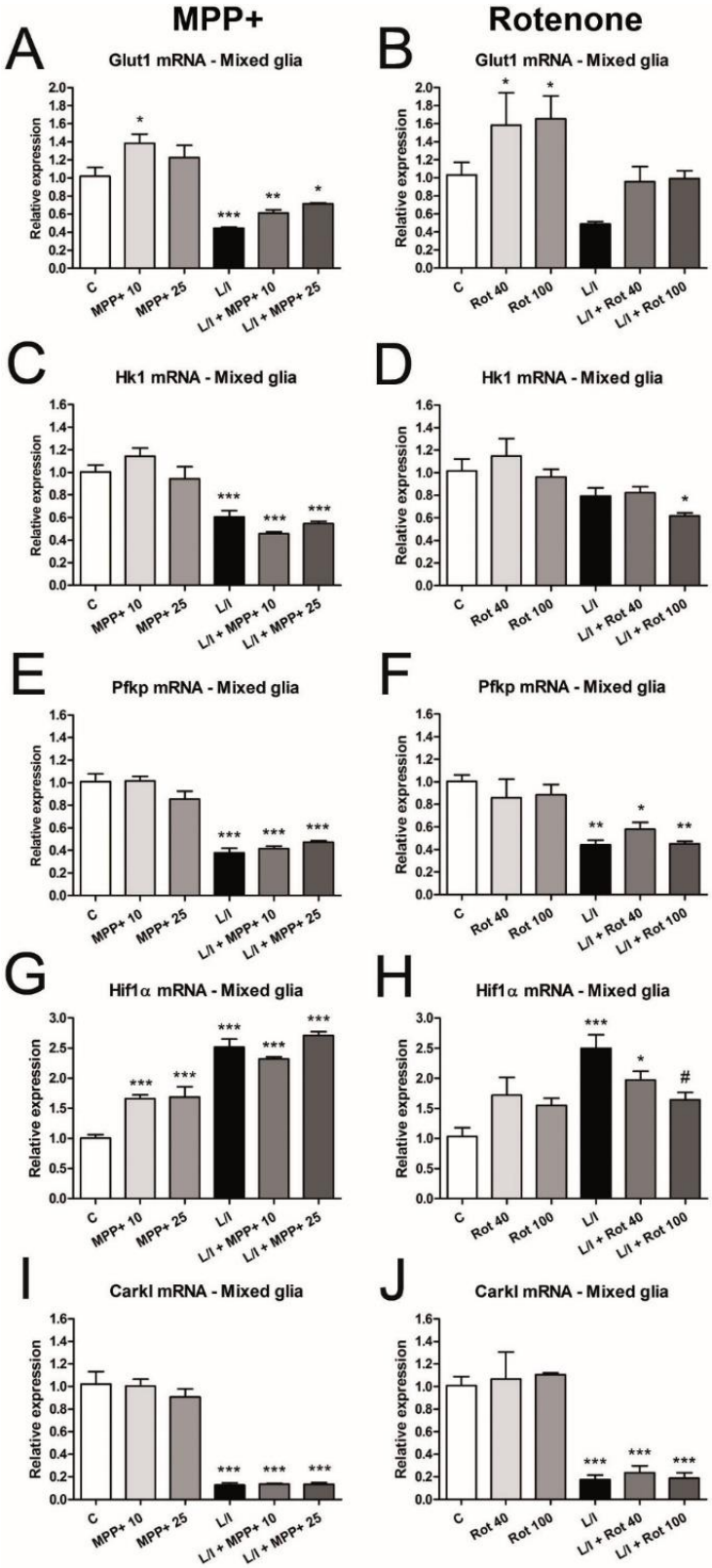

Figure 2.9. Effect of MPP+ and rotenone treatment on the expression of genes involved in the control of glycolysis in mixed glial cell cultures. mRNA expression of the glucose transporter Glut1 (A and B) and the glycolytic enzymes Hk1 (C and D) and Pfk1 (E and F), as well as Hif1α (G and H) and Carkl (I and J). Primary mixed glial cultures were treated for 6 h with 10 and 25 µM MPP+ or 40 and 100 nM rotenone (Rot), both in the absence and the presence of LPS/IFNγ (L/I). Rn18s and βactin were used as reference genes. Bars are means + SEM of 4 independent experiments. *p<0.05, **p<0.01 and ***p<0.001 vs. control (C); #p<0.05 vs. L/I; one-way ANOVA and Newman-Keuls post-test.

2.2 ANTI-INFLAMMATORY RESPONSE

After having shown that MPP+ and rotenone impair the pro-inflammatory response of glial cells, we were interested to study whether these parkinsonian neurotoxins also disturb the glial anti-inflammatory response. To this end, we determined the effects of MPP+ and rotenone exposure on the response of primary glial cell cultures to the anti-inflammatory cytokine IL4.

2.2.1 Effects of MPP+, rotenone and IL4 on glial cell viability

We first evaluated whether the treatment of glial cells with MPP+ or rotenone in the presence of IL4 could result in alterations in cell viability. We treated mixed glial cultures and microglial cultures with the same concentrations of MPP+ (10, 25 µM) and rotenone (40, 100 nM) used in the pro-inflammatory study, but in this case in the absence and in the presence of 50 ng/mL IL4. We evaluated glial cell viability using the MTT assay and PI staining. In mixed glial cell cultures, MPP+ induced a decrease in MTT reduction at 24 h of treatment, in the absence and presence of IL4 (Fig. 2.10A). On the contrary, a tendency to increase MTT reduction was observed in microglial cell cultures treated with MPP+ in the absence or presence of IL4 (Fig. 2.10B). Rotenone-treated mixed glial cell cultures showed a significant decrease in MTT reduction in the absence and presence of IL4 at 24 h of treatment (Fig. 2.10C). An increase in MTT reduction was observed in microglial cell cultures treated for 24 h with rotenone or rotenone plus IL4 (Fig. 2.10D).

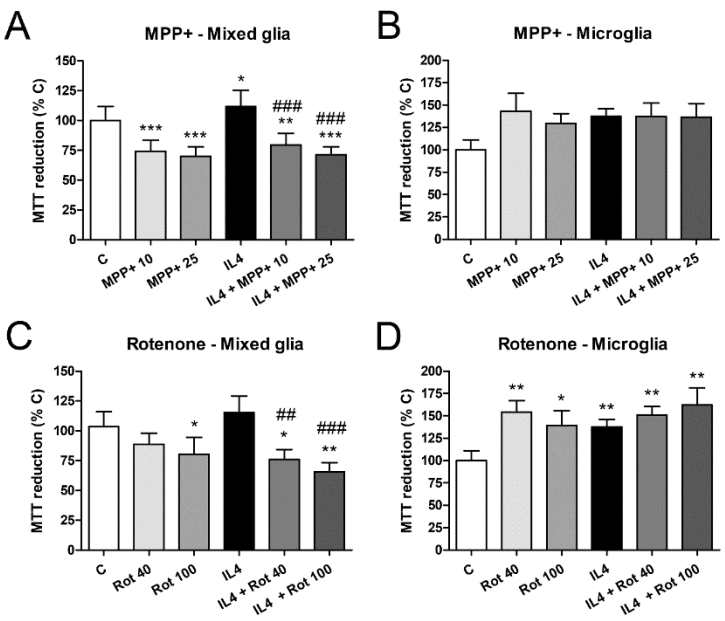

Figure 2.10. MPP+ and rotenone induce alterations in MTT reduction in primary glial cultures. Effect of 10 and 25 µM MPP+ treatment for 24 h on mixed glial cultures (**A**) and microglial cultures (**B**), both in the absence and the presence of IL4. Effect of 40 and 100 nM rotenone (Rot) treatment for 24 h on mixed glial cultures (**C**) and microglial cultures (**D**), both in the absence and the presence of IL4. Bars are means + SEM of 4 independent experiments. *p<0.05, **p<0.01 and ***p<0.001 vs. control (C); ##p<0.01 and ###p<0.001 vs. IL4; one-way ANOVA (repeated measures) and Newman-Keuls post-test.

According to PI labelling, no cell death was observed after treatments in mixed or microglial cell cultures (Fig. 2.11A-D). To determine whether the increase in MTT reduction in MPP+ and rotenone-treated microglial cell cultures was due to an increase in cell number, Hoechst positive

nuclei were counted. The results showed no differences in cell number among experimental conditions (Fig. 2.11E,F).

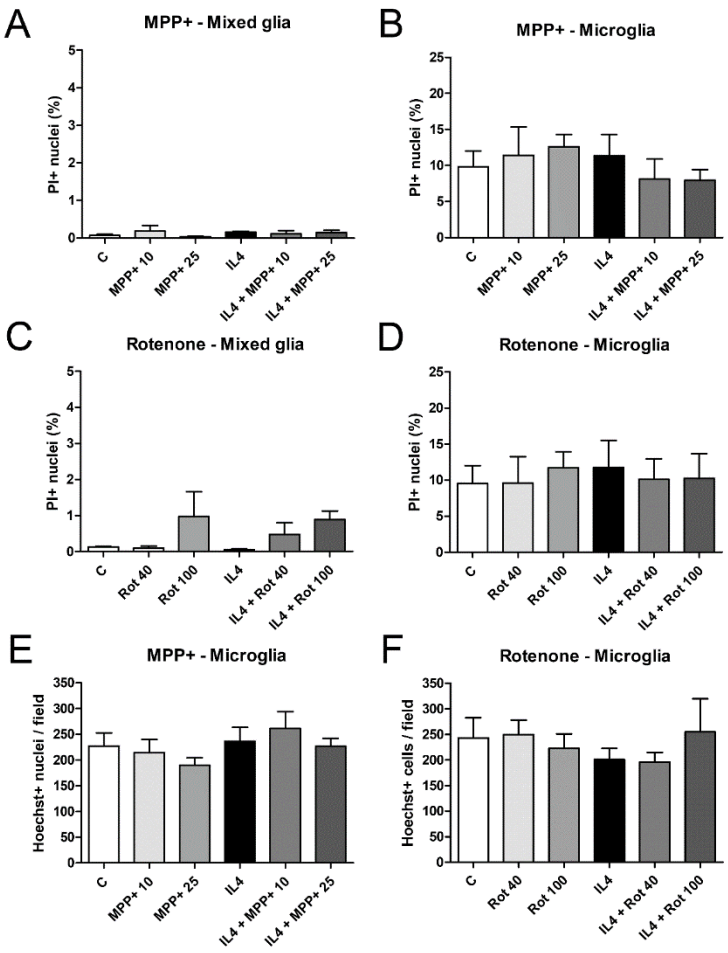

Figure 2.11. Effect of MPP+ and rotenone on glial cell viability and cell number. Percentage of propidium iodide (PI) positive nuclei in mixed glial cultures (**A**) and microglial cultures (**B**) treated for 24 h with 10 and 25 μM MPP+, both in the absence and the presence of IL4. Percentage of PI positive nuclei in mixed glial cultures (**C**) and microglial cultures (**D**) treated for 24 h with 40 and 100 nM rotenone (Rot), both in the absence and the presence of IL4. Number of Hoechst positive cells per microscopic field in microglial cultures treated for 24 h with 10 and 25 μM MPP+ (**E**) or with 40 and 100 nM rotenone (Rot) (**F**), both in the absence and the presence of IL4. Bars are means + SEM of 4 independent experiments. One-way ANOVA (repeated measures) and Newman-Keuls post-test.

2.2.2 MPP+ and rotenone induce alterations in the expression of anti-inflammatory genes in IL4-treated primary glial cultures

We then evaluated the effect of MPP+ and rotenone on the expression of anti-inflammatory markers in primary mixed glial cultures and microglial cultures in the presence or the absence of IL4. As markers of an anti-inflammatory response, we determined the mRNA expression of IL10, TGFβ, IL1β receptor antagonist (IL1ra), Fizz1, MR, Arg1 and Ym1.

After 24 h of treatment, MPP+-treated mixed glial cultures (Fig. 2.12A) showed a decrease in IL10, TGFβ, IL1ra and MR mRNA expression. In contrast, MPP+-treated microglial cultures (Fig. 2.12B) showed a decrease in IL10 and MR mRNA expression but an increase in IL1ra mRNA. Regarding rotenone treatment, this neurotoxin induced a decrease in IL10 mRNA expression in mixed glial cultures (Fig. 2.13A), but no effects were observed in microglial cultures. After IL4 treatment, the mRNA expression of most of the anti-inflammatory markers analysed was markedly

induced in mixed glial and microglial cultures (Figs. 2.12 and 2.13). Both neurotoxins, especially MPP+, induced alterations in the pattern of expression of these markers in IL4-treated cultures. Specifically, in mixed glial cell cultures, all the IL4-induced mRNA expression of anti-inflammatory markers were significantly inhibited by MPP+ and rotenone (Figs. 2.12A and 2.13A). In contrast, in microglial cultures, MPP+ treatment only inhibited the IL4 induction of Fizz1 and MR mRNA expression (Fig. 2.12B) and both MPP+ and rotenone treatment potentiated IL4-induced IL1ra mRNA expression (Fig. 2.13B).

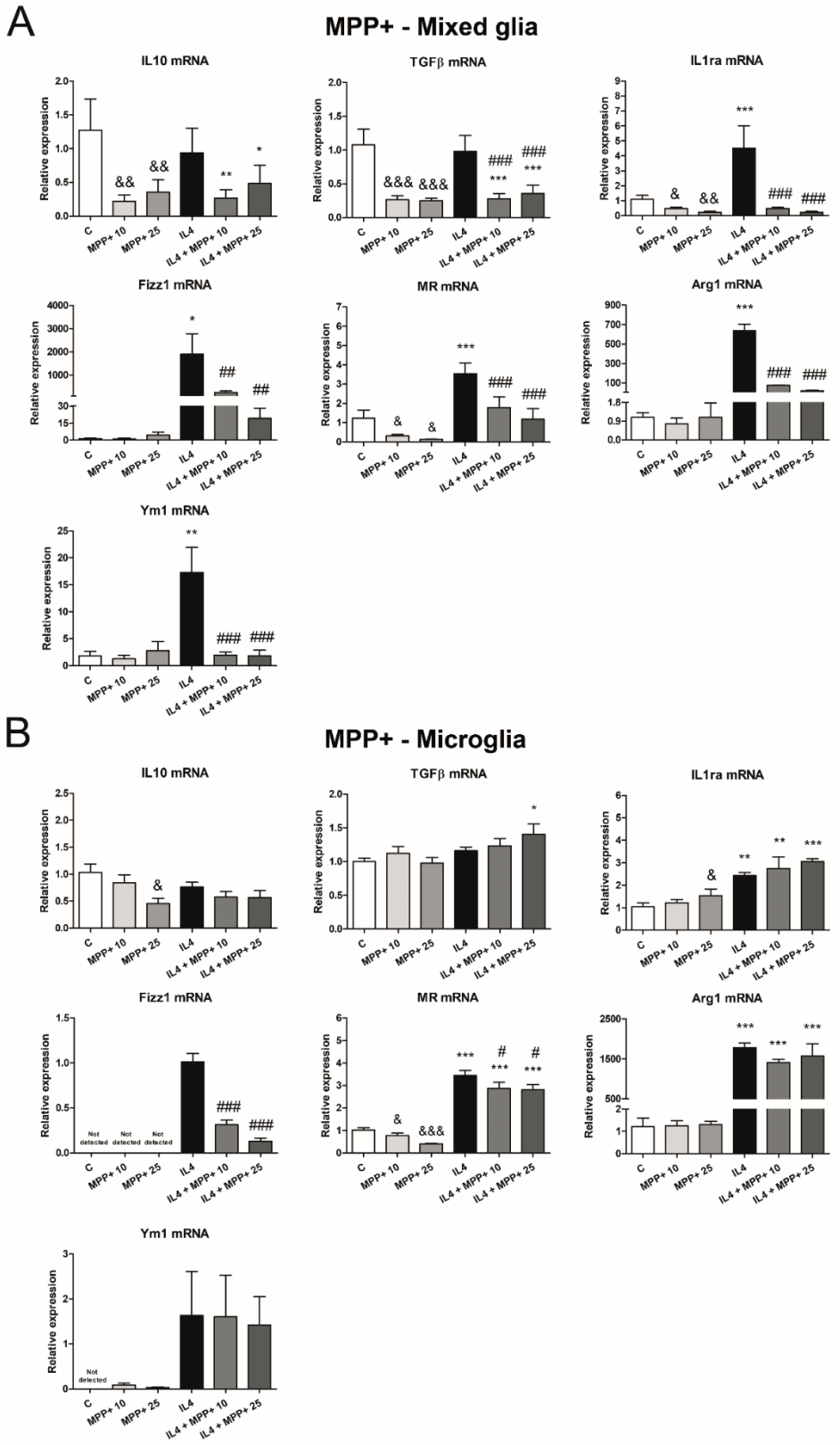

Figure 2.12. Effect of MPP+ treatment on mRNA expression of anti-inflammatory markers in glial cultures. mRNA expression of IL10, TGFβ, IL1ra, Fizz1, MR, Arg1, Ym1 in primary mixed glial cultures (**A**) and microglial cultures (**B**) treated for 24 h with 10 and 25 µM MPP+, both in the absence and the presence of IL4. Rn18s and βactin were used as reference genes. Bars are means + SEM of 4 independent experiments. *p<0.05, **p<0.01 and ***p<0.001 vs. control (C); #p<0.05, ##p<0.01 and ###p<0.001 vs. IL4; one-way ANOVA and Newman-Keuls post-test. &p<0.05, &&p<0.01 and &&&p<0.001 MPP+ alone vs. C; one-way ANOVA and Newman-Keuls post-test.

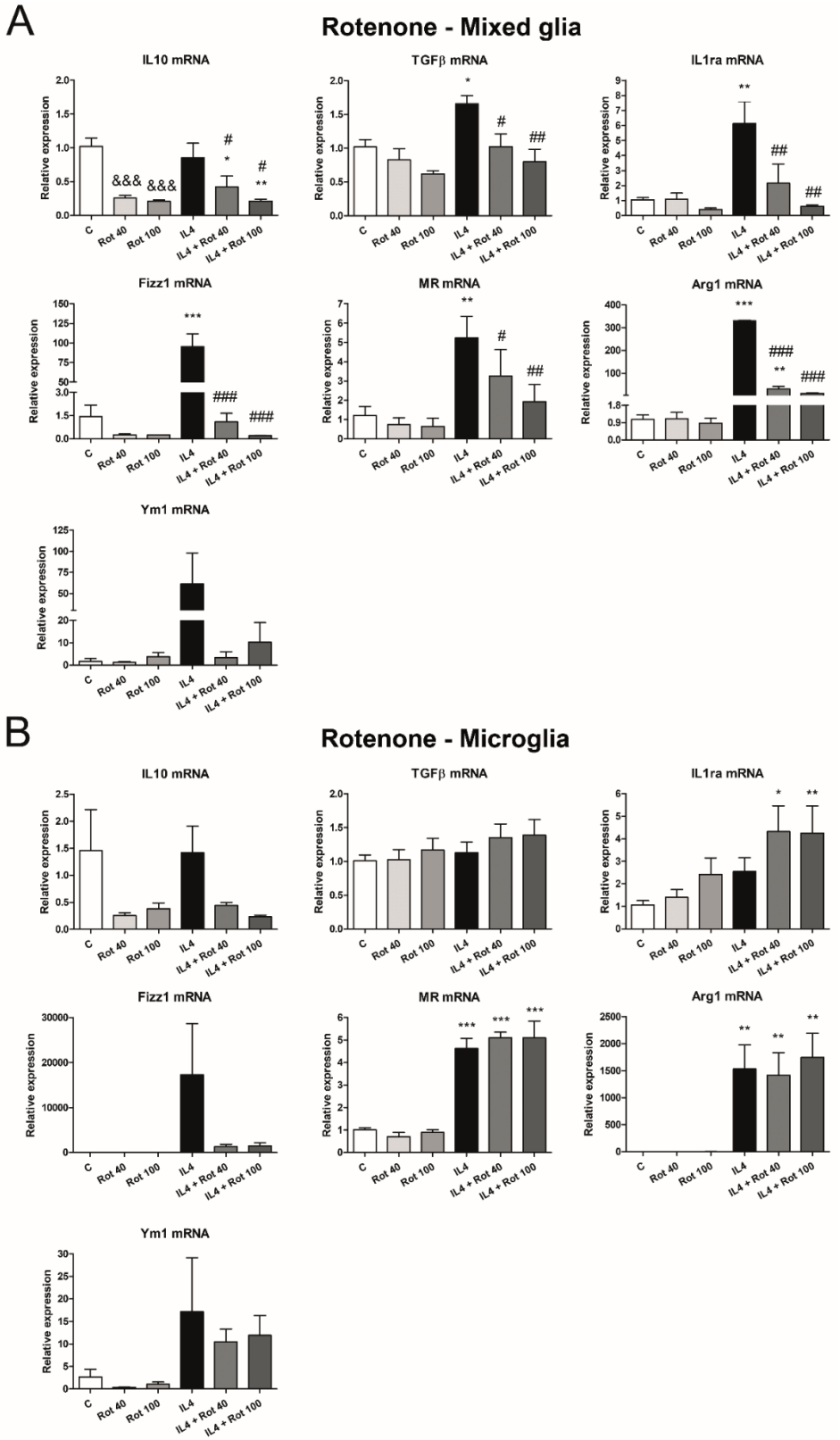

Figure 2.13. Effect of rotenone treatment on mRNA expression of anti-inflammatory markers in glial cultures. mRNA expression of IL10, TGFβ, IL1ra, Fizz1, MR, Arg1, Ym1 in primary mixed glial cultures (**A**) and microglial cultures (**B**) treated for 24 h with 40 and 100 nM rotenone (Rot), both in the absence and the presence of IL4. Rn18s and βactin were used as reference genes. Bars are means + SEM of 4 independent experiments. *p<0.5, **p<0.01 and ***p<0.001 vs. control (C); #p<0.05, ##p<0.01 and ###p<0.001 vs. IL4; one-way ANOVA and Newman-Keuls post-test. &&&p<0.001 MPP+ alone vs. C, one-way ANOVA and Newman-Keuls post-test.

2.2.3 MPP+ and rotenone inhibit IL4-induced expression of anti-inflammatory enzymes in primary glial cultures

We also analysed the protein levels of MR and Arg1 after MPP+ and rotenone treatment in the presence or absence of IL4 in primary glial cultures. After 24 h of treatment, MPP+ and rotenone did not modify protein levels of ARG1 and MR in mixed glial cultures. On the contrary, IL4 treatment induced both ARG1 and MR protein expression, which was inhibited by MPP+ (Fig. 2.14A) and rotenone (Fig. 2.14B). When treating microglial cells with MPP+ or rotenone, no effect was observed on ARG1 and MR protein levels. Induction of the expression of these two proteins was observed following IL4 treatment, and MPP+ (Fig. 2.14C), but not rotenone (Fig. 2.14D), prevented this effect.

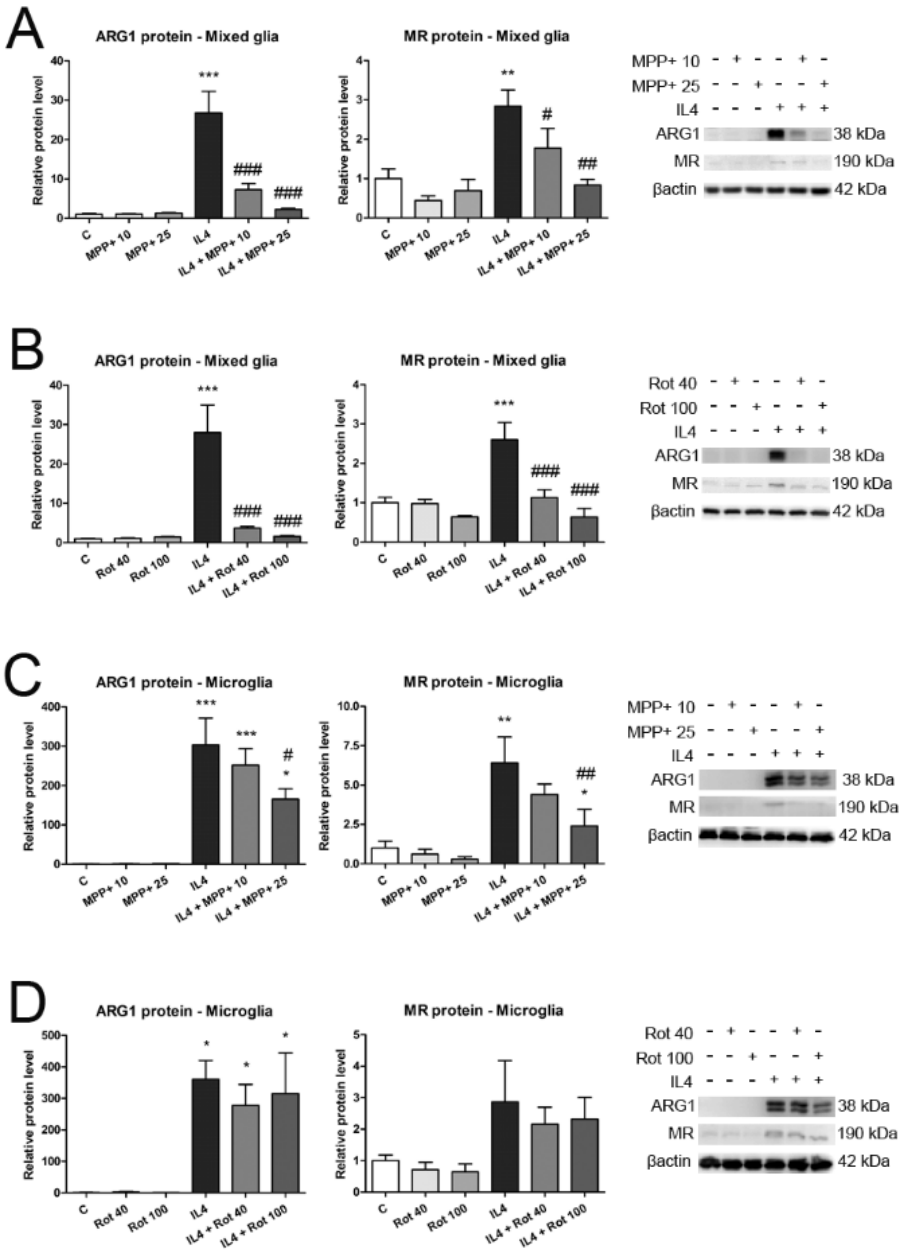

Figure 2.14. Effect of MPP+ and rotenone on IL4-induced ARG1 and MR protein expression in glial cultures. ARG1 and MR protein levels were determined by western blot in mixed glial (**A,B**) and microglial cultures (**C,D**) treated for 24 h with MPP+ (10 or 25 µM) (**A,C**) or rotenone (Rot) (40 or 100 nM) (**B,D**), in the absence and the presence of IL4. Results are presented as fold change to control condition (C). Representative immunoblots are shown. βactin was used as loading control. Bars are means + SEM of 4 independent experiments. *p<0.05, **p<0.01 and ***p<0.001 vs. C; #p<0.05, ##p<0.01 and ###p<0.001 vs. IL4; one-way ANOVA and Newman-Keuls post-test.

2.2.4 MPP+ and rotenone inhibit the phagocytic activity of microglial cells

We then evaluated whether MPP+ and rotenone modified the phagocytic activity of microglial cells in the presence of IL4. As observed in the study of the pro-inflammatory response, both MPP+ and rotenone treatment alone showed a tendency to decrease the percentage of phagocytic microglial cells. In the case of MPP+, this tendency was statistically significant in the presence of IL4 (Fig. 2.15A). When classifying the phagocytic cells as cells showing low- or high-phagocytic activity, both MPP+ and rotenone treatment decreased the percentage of cells showing high phagocytic activity (number of microspheres per cell higher than control) and increased the percentage of microglial cells showing low phagocytic activity (number of microspheres per cell lower than control; Fig. 2.15B). These effects were also observed after IL4 treatment, but no additive effect was observed in microglial cultures treated with MPP+ or rotenone in the presence of IL4.

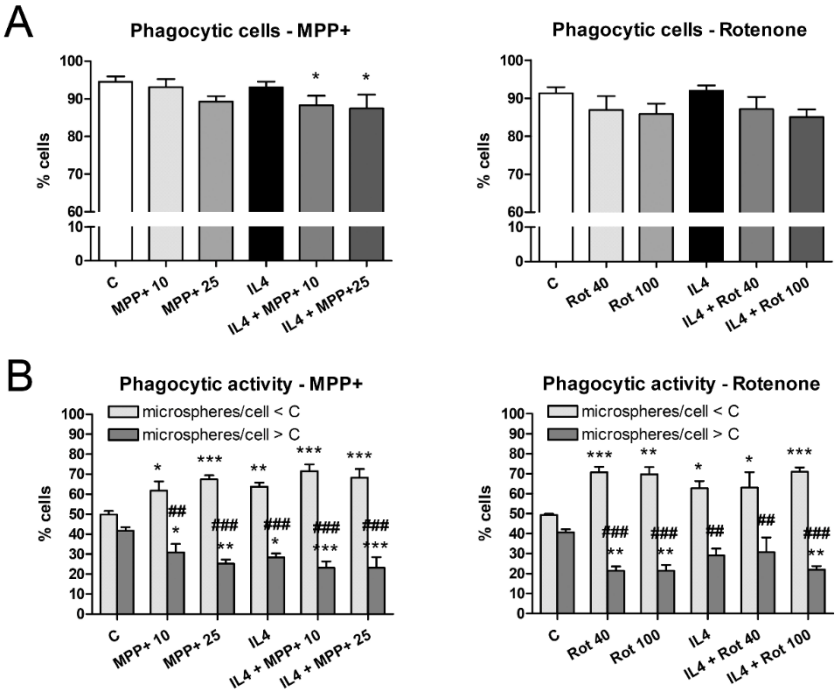

Figure 2.15. Effect of MPP+ and rotenone treatment on microglial cell phagocytosis in the absence or presence of IL4. Cell cultures were treated with 10 and 25 µM MPP+ or 40 and 100 nM rotenone (Rot) for 24 h, in the absence and in the presence of IL4 and the phagocytosis of fluorescent microspheres by microglial cells was quantified after the IBA1-immunofluorescence. **A** Percentage of cells with microspheres. Bars are means + SEM of 4 independent experiments. *p<0.05 vs. control (C); one-way ANOVA (repeated measures) and Newman-Keuls post-test. **B** Percentage of cells with low phagocytic activity (number of microspheres/cell < C) and cells with

high phagocytic activity (number of microspheres/cells > C). Bars are means + SEM of 5 independent experiments. *p<0.05, **p<0.01 and ***p<0.001 vs. corresponding C; ##p<0.01 and ###p < 0.001 vs. low-phagocytic cells; two-way ANOVA and Bonferroni post-test.

2.2.5 MPP+ and rotenone decrease intracellular ATP levels in glial cell cultures

As MPP+ and rotenone are inhibitors of the mitochondrial respiratory chain and given that IL4 increases oxidative phosphorylation, we determined whether ATP production was modified in glial cells under our experimental conditions. In general, intracellular ATP levels tended to decrease in MPP+- and rotenone-treated cultures (Fig. 2.16), with this decrease being statistically significant in the mixed glial cells treated with the higher concentration of MPP+ (Fig. 2.16A). By contrast, ATP levels were significantly increased in IL4-treated mixed glial cell cultures (Fig. 2.16A,B). However, this increase was significantly abrogated by 10 and 25 μM MPP+ and 100 nM rotenone (Fig. 2.16A,B). ATP levels were not significantly affected in the microglial cultures, although ATP levels tended to decrease in response to MPP+ or rotenone exposure (Fig. 2.16C,D).

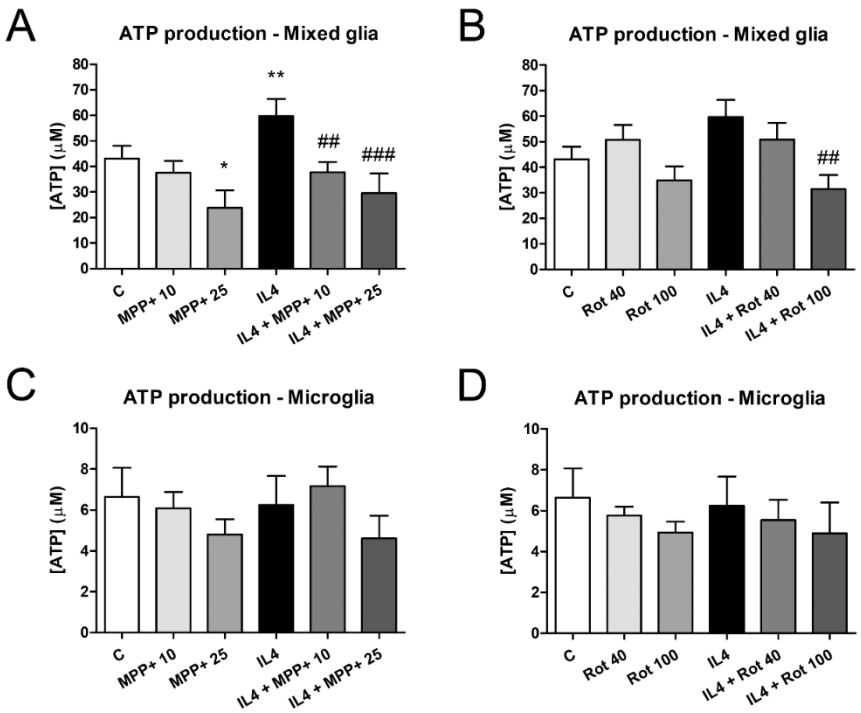

Figure 2.16. ATP levels in primary glial cell cultures treated with IL4, MPP+ and rotenone. Intracellular ATP levels were determined in mixed glial cultures and microglial cultures treated with 10 and 25 μM MPP+ (**A and B**) or 40 and 100 nM rotenone (Rot) (**C and D**) for 24 h, in the absence and in the presence of IL4. Bars are means + SEM of 5 independent experiments. *p<0.5 and **p<0.01 vs. control (C); ##p<0.01 and ###p<0.001 vs. IL4; one-way ANOVA and Newman-Keuls post-test.

2.2.6 Metabolic changes in IL4-treated glial cultures: effect of MPP+ and rotenone

Macrophages/microglia developing a pro-inflammatory phenotype switch to glycolysis to obtain energy supply, where lactate production from pyruvate and the pentose phosphate pathway are potentiated. On the contrary, when displaying an anti-inflammatory phenotype these cells increase oxidative phosphorylation. However, MPP+ and rotenone inhibit complex I of the mitochondrial respiratory chain, and the ATP production by this metabolic pathway is compromised. In order to obtain some clues about how glial cells may adapt their cellular metabolism to be able to respond to IL4 in the presence of MPP+ or rotenone, we determined the mRNA expression of several genes encoding critical proteins for the glycolytic or the oxidative pathways. We focused on a) molecules critical for reprogramming in M1 and M2 polarisation, such as PGC1β, a regulator of beta-oxidation and oxidative phosphorylation, and CARKL, involved in the control of the pentose phosphate pathway, and b) molecules playing a central role in glycolysis, such as the glucose transporter GLUT1 (glucose entrance into the cell), the glycolytic enzyme phosphofructokinase PFKP (one of the most important regulatory enzymes of the glycolysis) and the glycolysis activator HIF1α. Pgc1β mRNA was significantly increased in microglial cultures stimulated with IL4 in the presence of MPP+, and a trend to increase was observed in microglial cultures treated with IL4, both in the absence and in the presence of rotenone (Fig. 2.17A,B). Carkl mRNA was not modified in our experimental conditions (Fig. 2.17C,D). As regards the expression molecules involved in glycolysis, we detected an increase in Glut1 mRNA expression in microglial cells treated with MPP+ or IL4, and a further increase in cells treated with IL4 in the presence of MPP+ (Fig. 2.17E,F). An increase in Pfkp mRNA levels was also observed in cultures treated with IL4 in the presence of MPP+ (Fig. 2.17G,H). Microglial cells treated with MPP+ showed a trend to increased Hif1α mRNA levels (Fig. 2.17I,J). Alterations in the expression of these metabolic enzymes were much more apparent in mixed glial cultures (Fig. 1.18), mainly after MPP+-treatment. Thus, Pgc1β (Fig. 2.18A,B) and Carkl mRNAs (Fig. 1.18C,D) were significantly decreased in MPP+-treated mixed glia, both in the absence and the presence of IL4. Carkl mRNA expression was also inhibited by rotenone in IL4-treated mixed glial cultures (Fig. 2.18C,D). A trend to decreased Pfkp mRNA levels was observed in all the experimental conditions (Fig. 2.18G,H). On the contrary, MPP+ increased Glut1 mRNA (Fig. 2.18E,F) expression in mixed glia, and this effect was potentiated in the presence of IL4. No alterations were detected in Hif1α mRNA levels (Fig. 2.18I,J).

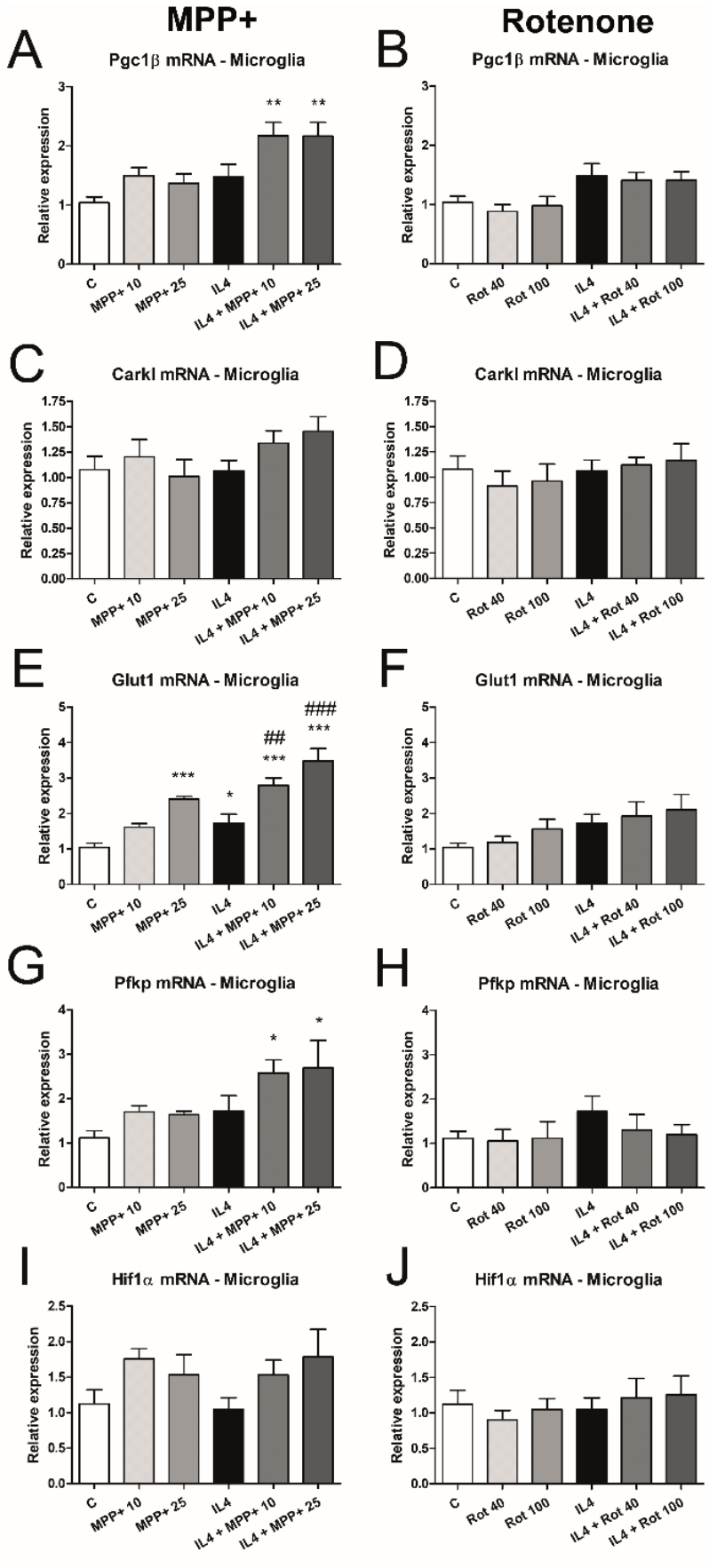

Figure 2.17. Effects of MPP+ and rotenone on the expression of genes involved in the control of energy metabolism in microglial cell cultures. mRNA expression of Pgc1β (A and B), Carkl (C and D), glucose transporter (Glut1) (E and F), the glycolytic enzyme Pfkp (G and H), as well as Hif1α (I and J). Cell cultures were treated for 24 h with 10 and 25 µM MPP+ or 40 and 100 nM rotenone (Rot), both in the absence and the presence of IL4 (50 ng/mL). Rn18s and βactin were used as reference genes. Bars are means + SEM of 4 independent experiments. *p<0.05, **p<0.01 and ***p<0.001 vs. control (C); ##p<0.01 and ###p<0.001 vs. IL4; one-way ANOVA and Newman-Keuls post-test.

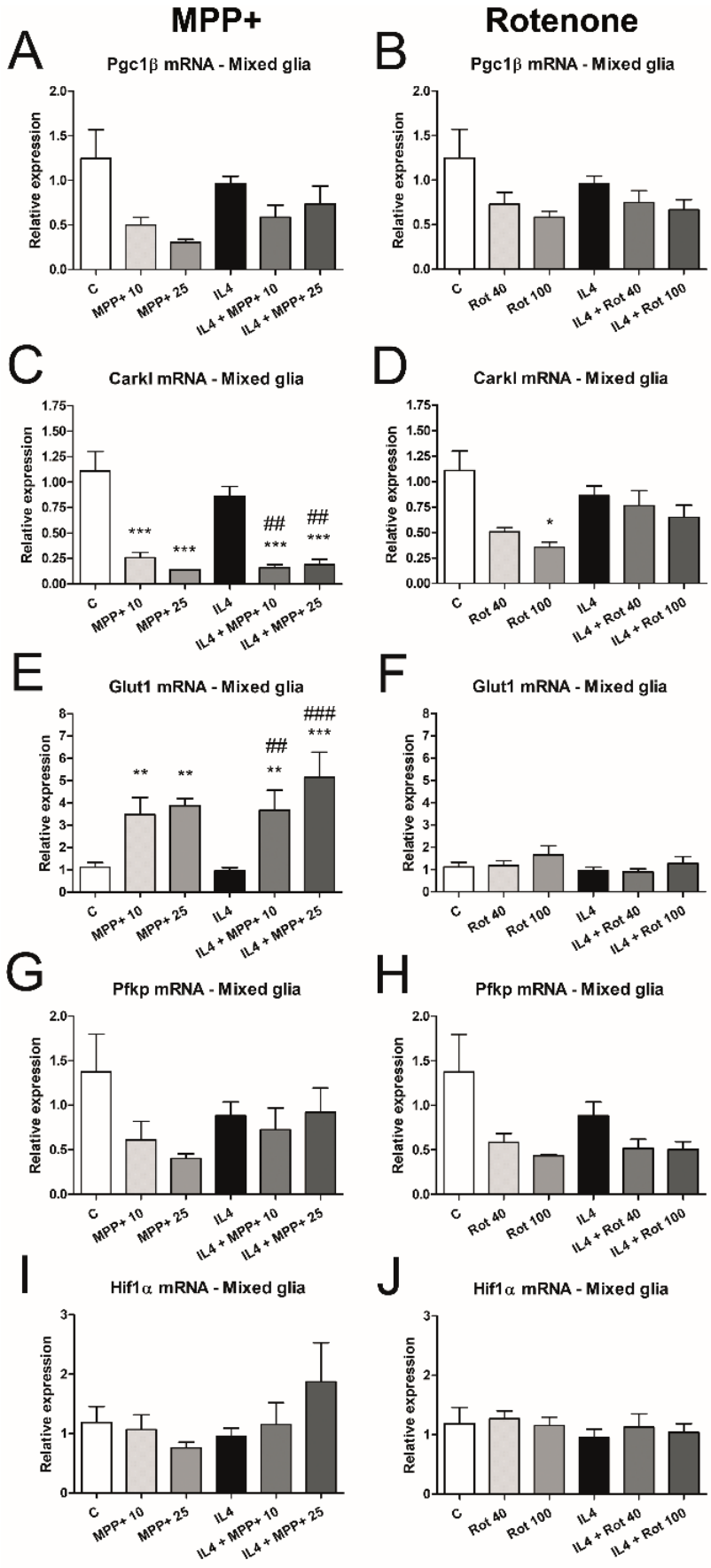

Figure 2.18. Effects of MPP+ and rotenone on the expression of genes involved in the control of energy metabolism in mixed glial cell cultures. mRNA expression of Pgc1β (A and B), Carkl (C and D), glucose transporter (Glut1) (E and F), the glycolytic enzyme Pfkp (G and H), as well as Hif1α (I and J). Cell cultures were treated for 24 h with 10 and 25 µM MPP+ or 40 and 100 nM rotenone (Rot), both in the absence and the presence of IL4 (50 ng/mL). Rn18s and βactin were used as reference genes. Bars are means + SEM of 4 independent experiments. **p<0.01 and ***p<0.001 vs. control (C); ##p<0.01 and ###p<0.001 vs. IL4; one-way ANOVA and Newman-Keuls post-test.

2.3 EFFECT OF MPP+ AND ROTENONE ON THE CD200-CD200R1 SYSTEM IN THE ABSENCE AND PRESENCE OF A PRO- OR ANTI-INFLAMMATORY STIMULUS

As the CD200-CD200R1 system is involved in the control of the inflammatory response of microglial cells, we also studied the effect of MPP+ and rotenone on CD200R1, CD200full and CD200tr mRNA expression on glial cultures.

In mixed glial cultures, the CD200R1 mRNA expression was not modified 6 h after MPP+ treatment (Fig 2.19A), but it was decreased 6 h after rotenone exposure (Fig 2.19B). The mRNA expression levels from both astrocytic forms of CD200 (full and tr) showed a decrease 6 h after exposure to MPP+ (Fig 2.19A), whereas rotenone at 6 h produced a reduction on CD200tr mRNA expression (Fig 2.19B). In microglial cultures, there was an increase in CD200R1 expression 6 h after MPP+ or rotenone treatment (Fig 2.19). Six hours after LPS/IFNγ treatment, the CD200R1 and CD200full mRNA expression were decreased whereas the CD200tr mRNA expression was increased in mixed glial cells, and the CD200R1 mRNA was also decreased in microglial cultures (Fig 2.19). Co-treatment of MPP+ or rotenone with LPS/IFNγ did not modify the effect of LPS/IFNγ treatment (Fig 2.19).

When analysing the mRNA expression at 24 h, MPP+ decreased the CD200R1 mRNA levels (Fig 2.20A) in mixed glial cultures, but rotenone had no effect (Fig 2.20B). CD200full and CD200tr mRNA levels showed a decrease 24 h after both MPP+ and rotenone treatment in mixed glial cultures (Fig 2.20). IL4 induced an increase in CD200R1 and a decrease in CD200full and CD200tr mRNA expression (Fig 2.20). MPP+ inhibited the CD200R1 mRNA expression induced by IL4 (Fig. 2.20A). In microglial cell cultures, an increase in CD200R1 mRNA expression after rotenone plus IL4 treatment was observed (Fig. 2.20B).

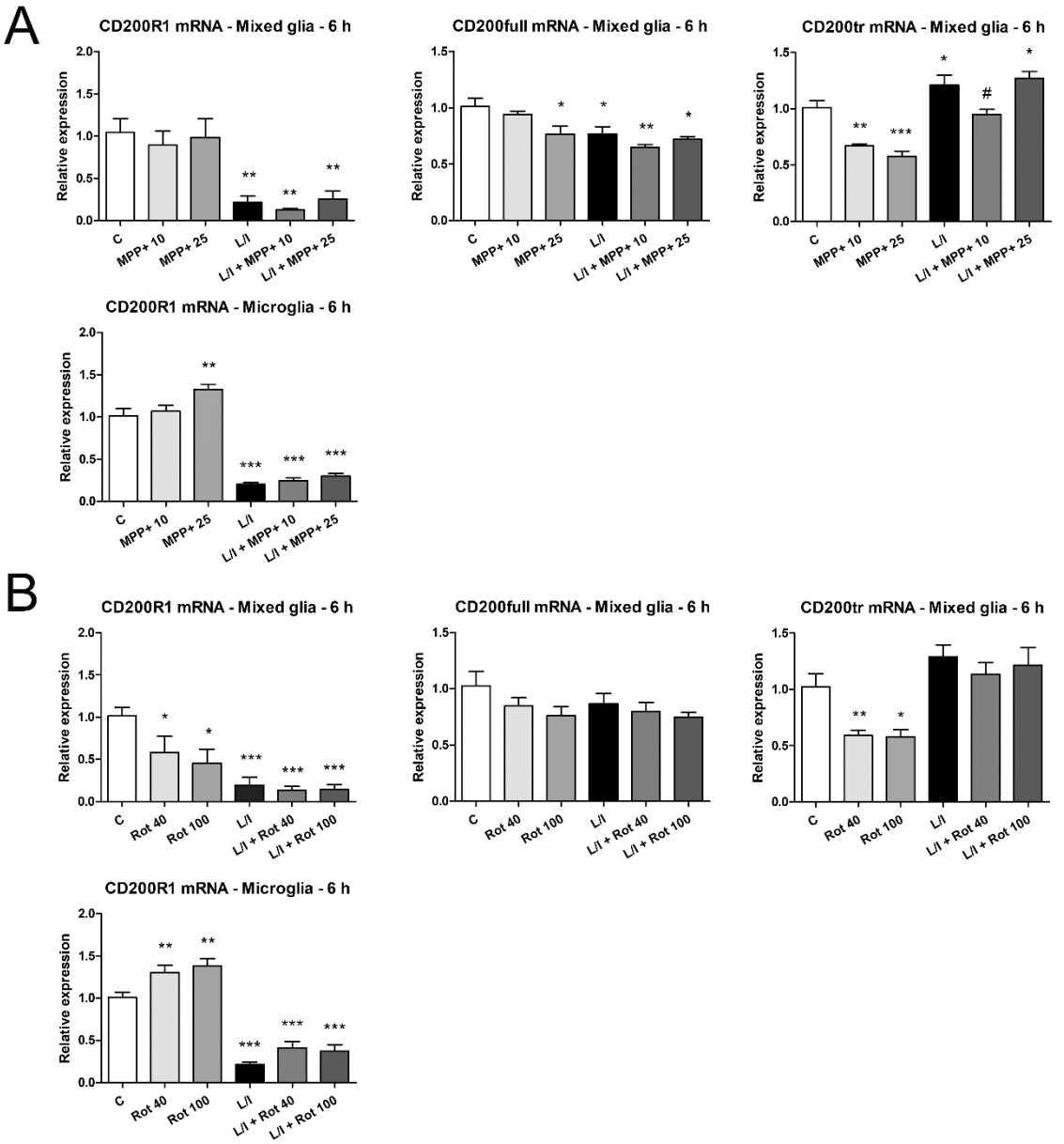

Figure 2.19. Effect of 6 h MPP+, rotenone and L/I treatment on the CD200 and CD200R1 mRNA expression in glial cultures. The mRNA expression of CD200R1, CD200full and CD200tr in primary mixed glial cultures and microglial cultures treated for 6 h with 10 and 20 µM MPP+ (**A**) or 40 and 100 nM rotenone (Rot) (**B**), both in the absence and the presence of LPS/IFNγ (L/I). Rn18s and βactin were used as reference genes. Bars are means + SEM of four independent experiments. *p<0.5, **p<0.01 and ***p<0.001 vs control (C); #p<0.05, ##p<0.01 and ###p<0.001 vs L/I; one-way ANOVA and Newman-Keuls post-test.

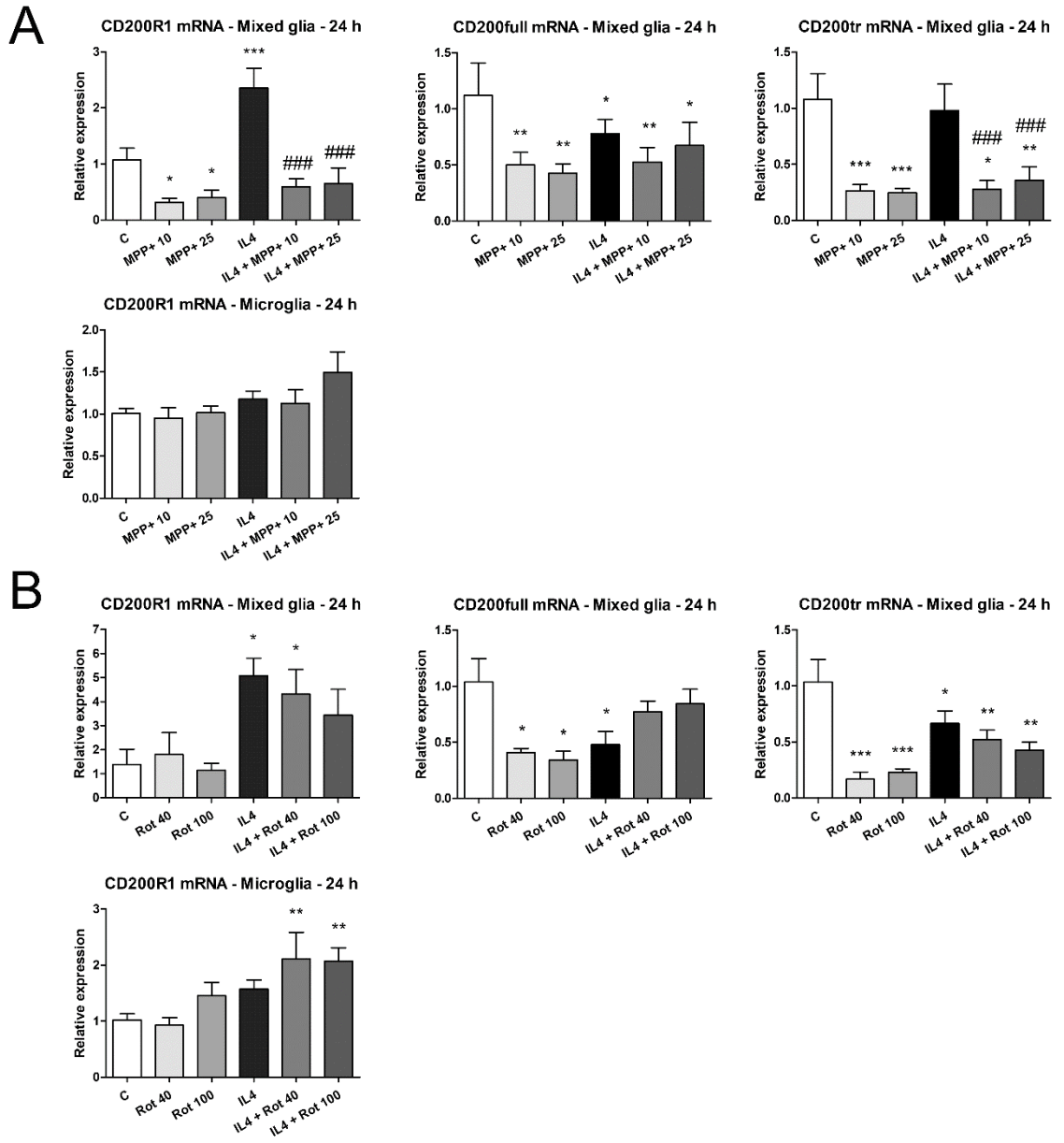

Figure 2.20. Effect of 24 h MPP+, rotenone and IL4 treatment on the CD200 and CD200R1 mRNA expression in glial cultures. The mRNA expression of CD200R1, CD200full and CD200tr in primary mixed glial cultures and microglial cultures treated for 24 h with 10 and 20 µM MPP+ (**A**) or 40 and 100 nM rotenone (Rot) (**B**), both in the absence and the presence of IL4. Rn18s and βactin were used as reference genes. Bars are means + SEM of four independent experiments. *p<0.5, **p<0.01 and ***p<0.001 vs control (C); #p<0.05, ##p<0.01 and ###p<0.001 vs IL4; one-way ANOVA and Newman-Keuls post-test.

3 Evaluation of the effect of CD200-CD200R1 modulation in the MPTP mouse model of PD

We studied the involvement of the CD200-CD200R1 system in the development of neurodegeneration in a mouse model of PD, the acute MPTP model. We first characterized the temporal pattern of dopaminergic neuronal death and neuroinflammation and the change in CD200 and CD200R1 expression occurring after MPTP administration. Then, we evaluated the involvement of the CD200-CD200R1 system using two different approaches: the potentiation of CD200R1 signalling with a CD200R1 agonist and the disruption of CD200-CD200R1 function using CD200 knock-out mice.

3.1 CHARACTERIZATION OF THE MPTP EXPERIMENTAL MODEL OF PD. ALTERATIONS IN CD200 AND CD200R1 EXPRESSION

Adult male C57BL6NCrl mice (Charles River, Lyon, France) were administered with saline or MPTP and killed at 2 hours, 1, 2, 4 and 7 days after the last MPTP injection (Jackson-Lewis and Przedborski 2007) (n = 8 mice per group) (Fig. 3.1A). We chose 7 days as the last time point because it has been previously reported that loss of dopaminergic cell bodies in the SNpc is stable at this time (Jackson-Lewis et al. 1995). Dopaminergic neurodegeneration and glial reactivity in the striatum and SNpc, as well as the expression of inflammatory mediators in the striatum, ventral midbrain and cerebral cortex were analysed. We determined the correlation between these phenomena and the pattern of CD200 and CD200R1 expression.

Only 1 mouse out of a total of 40 died after MPTP administration (2.5%). The extent of striatal dopaminergic denervation induced by MPTP administration was measured by optical densitometry of striatal TH-positive fibers, and the total number of TH-positive SNpc neurons was determined by stereological cell counts of SNpc TH-positive cells, as previously described (Recasens et al. 2014). Saline-injected controls showed abundant TH-positive terminals in the striatum and a dense network of cell bodies and fibers in the SNpc. Administration of MPTP led to a gradual reduction in striatal dopaminergic terminals and dopaminergic neurons in SNpc, starting at 2 hours and 2 days after the MPTP challenge, respectively (Fig. 3.1B,C). At day 2 after MPTP administration, mice exhibited a dramatic 73% reduction in striatal dopaminergic terminals, which were reduced by 79% at day 7 (Fig. 3.1B). In the SNpc, MPTP induced a 41% and 54% of dopaminergic neuronal loss at day 2 and 7, respectively (Fig. 3.1C).

Microglial (IBA1-immunolabelling) and astroglial (GFAP-immunolabelling) activation was observed throughout the striatum (Fig. 3.1D) and SNpc (Fig. 3.1E) in MPTP-injected mice as

increased number of positive cells, hypertrophied morphology and intensified IBA1 or GFAP staining. Although SNpc was the main area of the SN where glial activation was induced by MPTP administration, the entire SN displayed glial activation. Microglia displayed a reactive phenotype as early as 2 hours post-MPTP in the striatum and from day 1 after treatment in the SNpc. In contrast, astroglial reactivity was not evident until day 1 after treatment in both striatum and SNpc. In addition, microglial activation was more intense than astroglial activation in the SNpc at day 1 after MPTP administration. Microglial activation peaked at day 1 - 2 after MPTP injection in the striatum and day 2 - 4 after MPTP injection in the SNpc. Astroglial activation peaked at day 2 - 4 after MPTP injection in the striatum and SNpc. Both microglia and astroglial activation were attenuated, but still remained higher than in controls, at day 7 after MPTP treatment.

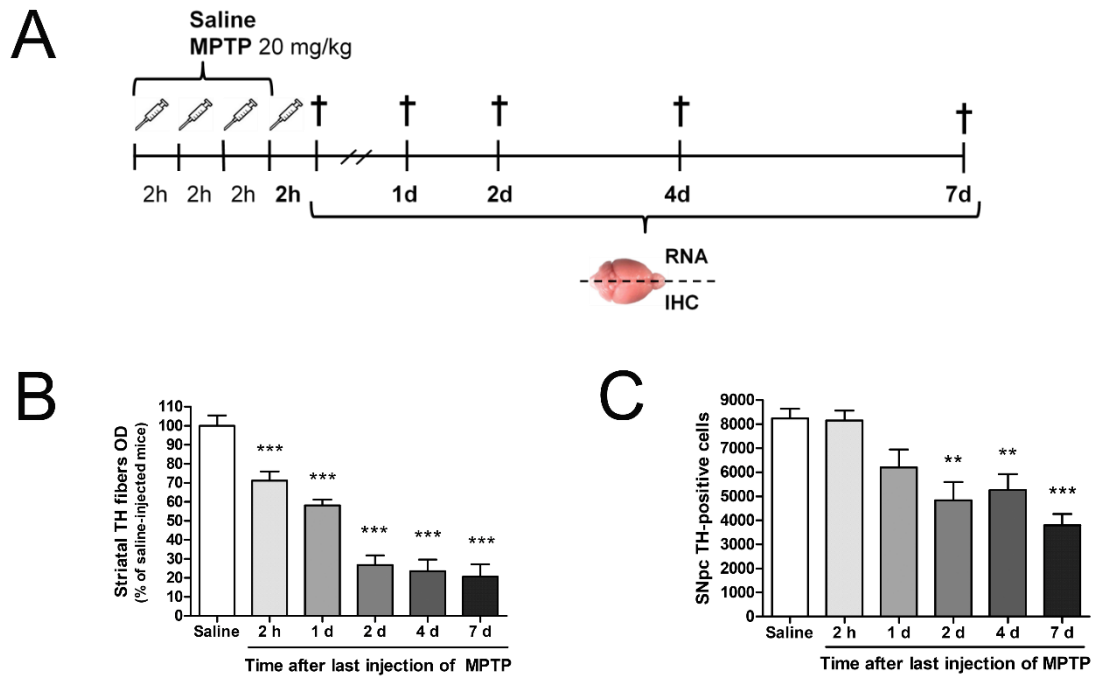

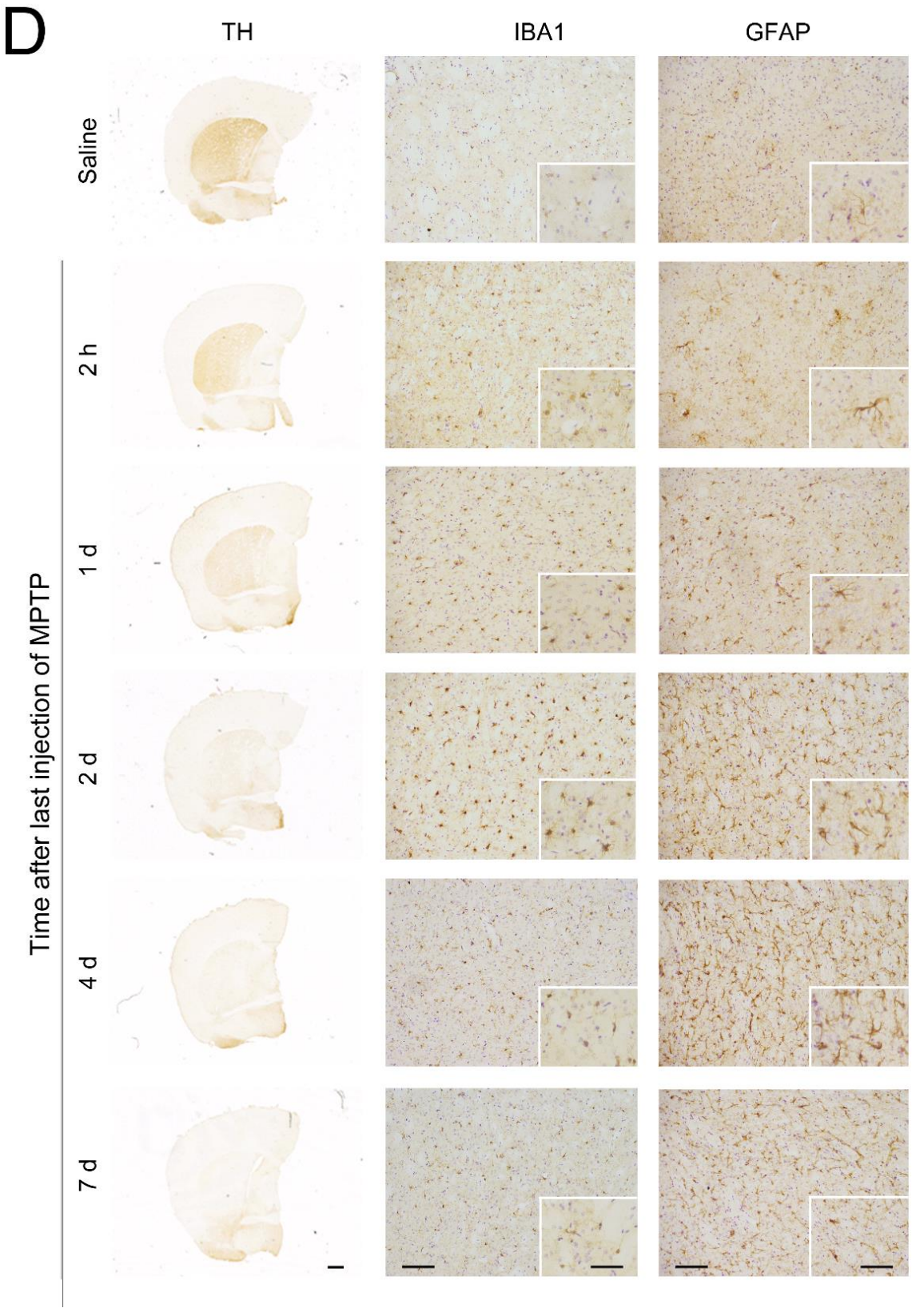
D
TH
IBA1
GFAP
Saline
2 h
1 d
2 d
4 d
7 d
Time after last injection of MPTP

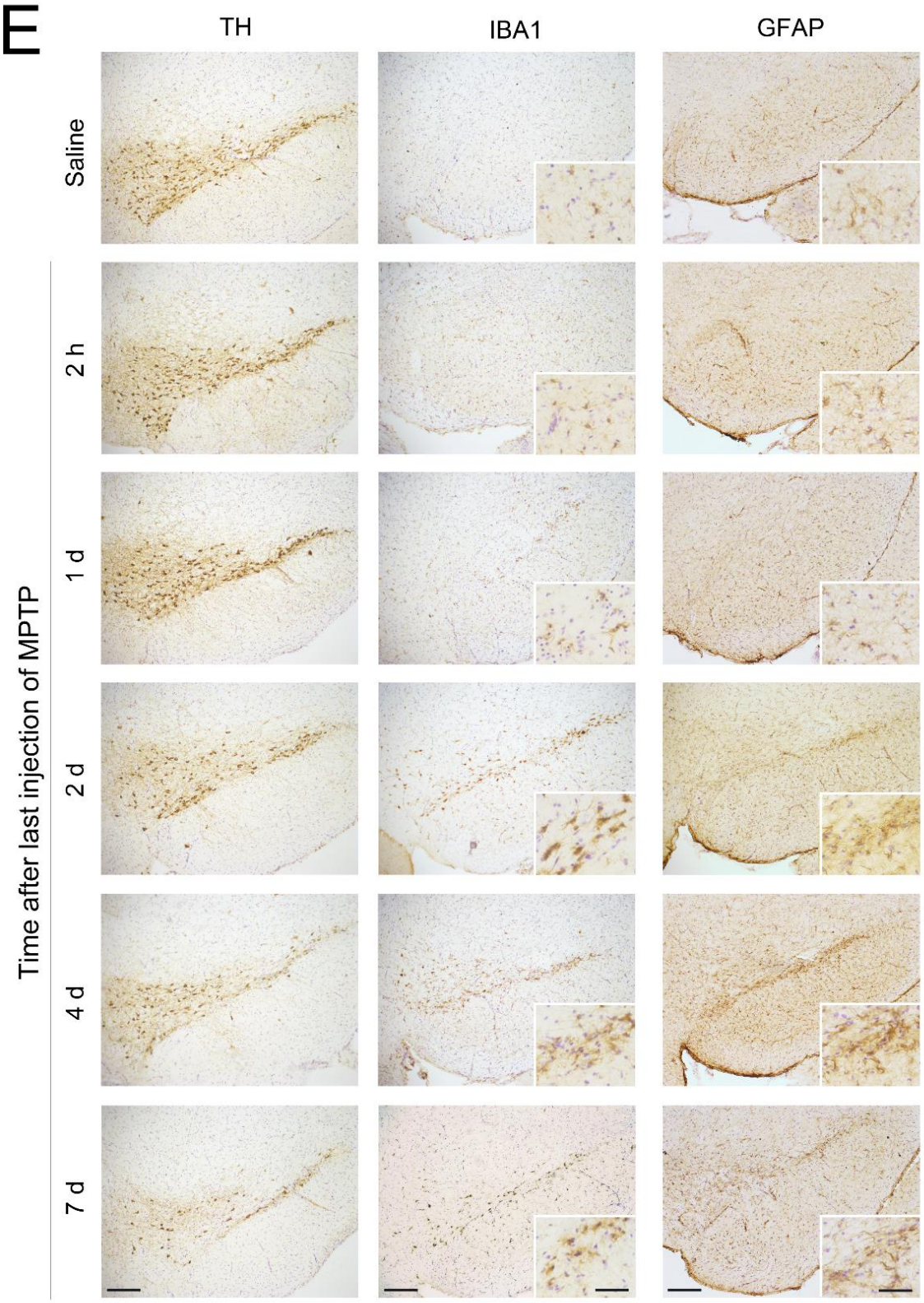
E
TH
IBA1
GFAP
Saline
2 h
1 d
2 d
4 d
7 d
Time after last injection of MPTP

Figure 3.1. Loss of striatal dopaminergic fibers and dopaminergic neurons in the SNpc after MPTP administration is accompanied by microglial and astroglial reactivity. **A** Experimental design. Mice were injected intraperitoneally with saline or MPTP (20 mg/kg) every 2 hours for a total of 4 doses in one day. Animals were killed at 2 h, 1, 2, 4, and 7 days after the last injection. Right hemispheres were fixed for immunohistochemistry (IHC) and left hemispheres were processed for gene expression analysis (RNA). **B** Optical densitometry of striatal TH-positive dopaminergic fibers. **C** Stereological cell counts of dopaminergic neurons in SNpc. Bars are means + SEM of 7 - 8 mice per group. **p<0.01 and ***p<0.001 vs. saline; one-way ANOVA and Newman-Keuls post-test. **D** Representative photomicrographs of TH-, IBA1- and GFAP-immunostained striatum of control mice administered with saline and MPTP-injected mice killed at the indicated time points after MPTP injections. Scale bars: 500 µm (TH), 100 µm (IBA1, GFAP) and 50 µm in the insets. **E** Representative photomicrographs of TH-, IBA1- and GFAP-immunostained SNpc of control mice administered with saline and MPTP-injected mice at the indicated time points after MPTP injection. Scale bars: 200 µm (TH, IBA1, GFAP) and 50 µm in the insets (IBA1, GFAP).

To better characterize the neurodegeneration and neuroinflammation observed, mRNA levels of pro-inflammatory cytokines (IL1β, IL6 and TNFα) and enzymes (COX2, iNOS and gp91phox) were measured in the striatum, ventral midbrain and cerebral cortex of the same saline- and MPTP-injected mice in which TH-, IBA1- and GFAP-immunostaining were analysed. We also determined the mRNA expression of anti-inflammatory cytokines (IL10, TGFβ), enzymes (Arg1), receptors (MR) and transcription factors (nuclear factor erythroid 2-related factor (Nrf2)). Glial-specific markers (Gfap, Iba1, CD11b) were also determined.

Pro-inflammatory cytokine mRNA levels in the striatum showed two peaks after MPTP administration: TNFα mRNA increased as early as 2 hours, whereas IL1β and IL6 mRNAs were not increased until day 4 (Fig. 3.2A). In contrast, ventral midbrain mRNA levels of the three cytokines increased between 2 hours and 1 day. In the cerebral cortex no significant changes in the mRNA levels of these cytokines were observed (Fig. 3.2A).

Surprisingly, down-regulation of the expression of pro-inflammatory enzymes gp91phox and iNOS was observed after MPTP administration: gp91phox mRNA levels decreased at 2 hours and day 1 in the three areas analysed, and iNOS mRNA levels decreased in the ventral midbrain at 2 hours and day 2 after MPTP administration (Fig. 3.2B). In contrast, COX2 mRNA levels increased dramatically in the striatum, while no significant changes were observed in the ventral midbrain and cerebral cortex (Fig. 3.2B).

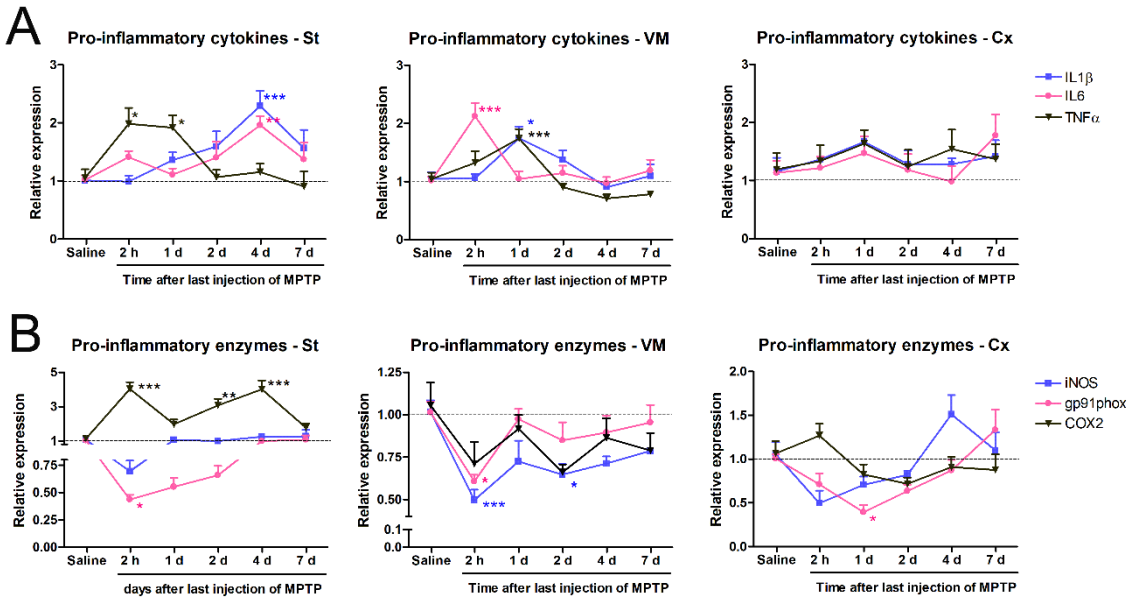

Figure 3.2. Time course of the mRNA expression of pro-inflammatory markers in the striatum, ventral midbrain and cortex after MPTP administration. IL1β, IL6 and TNFα mRNA expression (**A**) and iNOS, gp91phox and COX2 mRNA expression (**B**) in the striatum (St), ventral midbrain (VM) and cerebral cortex (Cx) of saline- and MPTP-injected mice. GAPDH and βactin were used as reference genes. Bars are means + SEM of 7 - 8 mice per experimental group. *p<0.05, **p<0.01 and ***p<0.001 vs. saline; one-way ANOVA and Newman-Keuls post-test.

Regarding anti-inflammatory markers, TGFβ mRNA levels increased at day 1 and 2 in the striatum and at day 2 in the ventral midbrain whereas they decreased at 2 hours in the cerebral cortex (Fig. 3.3A). IL10 mRNA was significantly increased at day 4 in the cerebral cortex. The mRNA levels of Arg1 were significantly increased at day 1 in the ventral midbrain and decreased at 2 hours in the cerebral cortex (Fig. 3.3B). MR mRNA levels increased at 2 hours in both the striatum and cerebral cortex but also at day 4 in the striatum. In the ventral midbrain, MR mRNA levels decreased at day 1 after MPTP administration. Finally, Nrf2 mRNA levels decreased at 2 hours and increased at day 4 in the striatum and decreased at day 4 in the cerebral cortex.

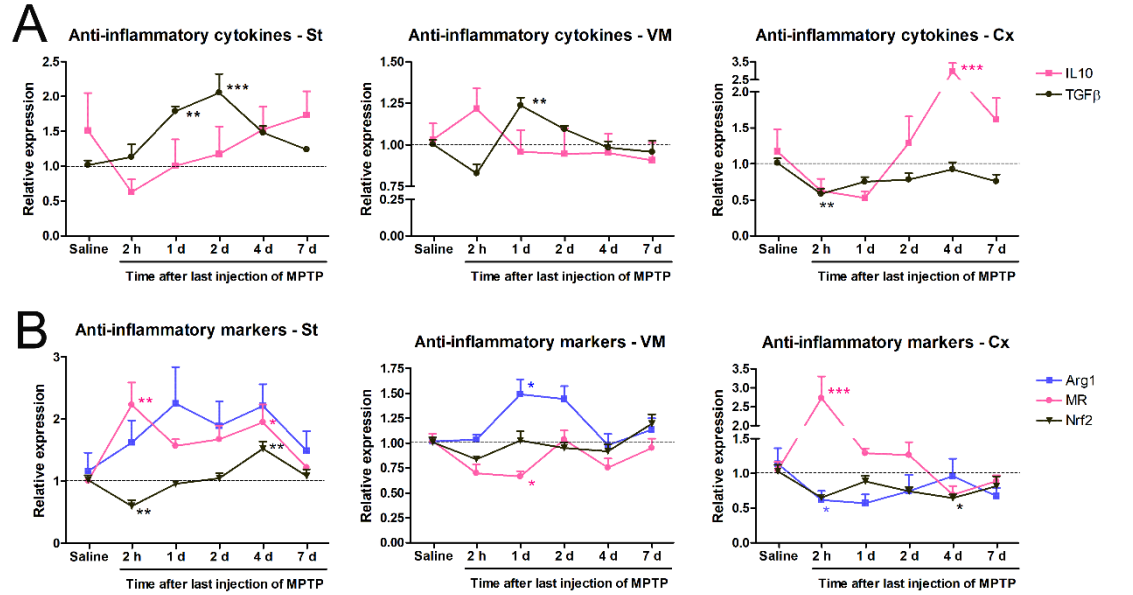

Figure 3.3. Time course of the mRNA expression of anti-inflammatory markers in the striatum, ventral midbrain and cortex after MPTP administration. IL10 and TGFβ mRNA expression (**A**) and Arg1, MR and Nrf2 mRNA expression (**B**) in the striatum (St), ventral midbrain (VM) and cerebral cortex (Cx) of saline- and MPTP-injected mice. GAPDH and βactin were used as reference genes. Bars are means + SEM of 7 - 8 mice per experimental group. *p<0-05, **p<0.01 and ***p<0.001 vs. saline; one-way ANOVA and Newman-Keuls post-test.

Regarding glial markers, Gfap mRNA levels increased dramatically in the striatum following MPTP administration and returned to basal levels at day 7 post MPTP injection (Fig. 3.4A). Increased in Gfap mRNA levels were also observed in the ventral midbrain, but not in the cerebral cortex (Fig. 3.4A). Strikingly, mRNA expression of microglial markers (Iba1, CD11b) showed an irregular pattern with a down-regulation predominance after MPTP administration: Iba1 mRNA decreased at 2 hours in the ventral midbrain and cerebral cortex and increased at day 1 in the ventral midbrain (Fig. 3.4B). CD11b mRNA in the striatum decreased at day 1 and increased at day 2, whereas ventral midbrain CD11b mRNA was decreased at all the time points analysed. In the cerebral cortex a decrease in CD11b mRNA was observed at 2 hours after the last MPTP injection (Fig. 3.4C).

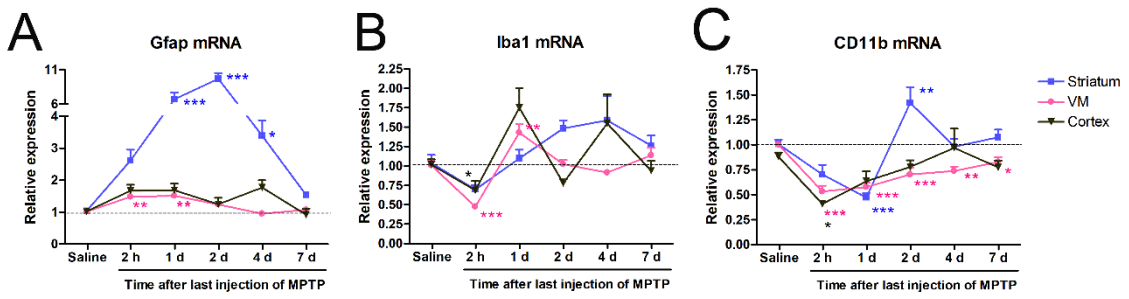

Figure 3.4. Time course of the mRNA expression of glial markers in the striatum, ventral midbrain and cortex after MPTP administration. Gfap (**A**), Iba1 (**B**) and CD11b (**C**) mRNA expression in the striatum (St), ventral midbrain (VM) and cerebral cortex (Cx) of saline- and MPTP-injected mice. GAPDH and βactin were used as reference genes. Bars are means + SEM of 7 - 8 mice per experimental group. *p<0.05, **p<0.01 and ***p<0.001 vs. saline; one-way ANOVA and Newman-Keuls post-test.

Interestingly, all changes observed in the mRNA expression of pro-inflammatory, anti-inflammatory and glial markers analysed after MPTP administration were transient and mRNA expression returned to basal levels at day 7 post MPTP injection (Figs. 3.1-3.4).

Dopaminergic degeneration and neuroinflammation observed after MPTP challenge were accompanied by alterations in CD200 and CD200R1 expression. In the striatum (Fig. 3.5A), CD200full mRNA expression was not modified by MPTP administration, while CD200tr mRNA levels showed a significant increase at 4 days after MPTP administration. In striking contrast, CD200R1 mRNA levels were increased dramatically at 2 and 4 days after treatment. In the ventral midbrain (Fig. 3.5B), a rapid and long-lasting decrease in CD200full was observed, beginning at 2 hours after MPTP administration and sustained until at least 7 days of treatment. CD200tr and

CD200R1 mRNAs were transiently decreased 2 hours after MPTP injection. Curiously, CD200R1 mRNA also showed a transient decrease at day 4 after MPTP injection while levels were equivalent to saline-injected animals at days 1, 2 and 7. In the cortex (Fig. 3.5C), only a transient decrease in CD200tr mRNA at 2 hours after MPTP administration was observed. The expression of CD200full, CD200tr and CD200R1 mRNA in the three brain areas analysed returned to basal levels at day 7 after MPTP administration, with the exception of CD200 mRNA in the ventral midbrain, which remained decreased.

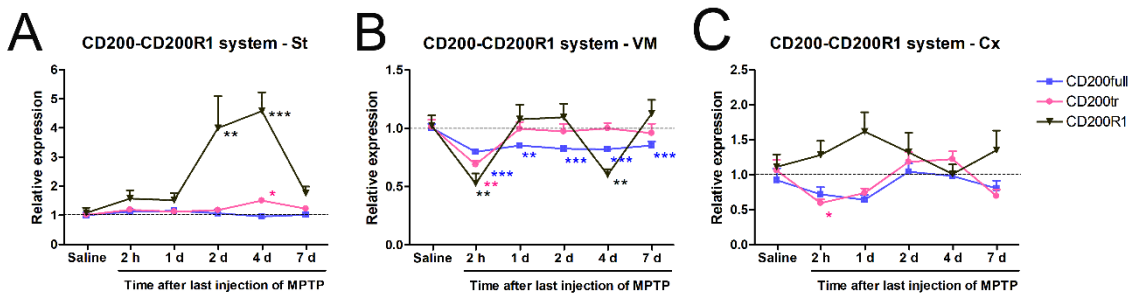

Figure 3.5. Time course of CD200full, CD200tr and CD200R1 mRNA expression in the striatum, ventral midbrain and cortex after MPTP administration. CD200full, CD200tr and CD200R1 mRNA expression in the striatum (St) (**A**), ventral midbrain (VM) (**B**) and cerebral cortex (Cx) (**C**) of saline- and MPTP-injected mice. GAPDH and βactin were used as reference genes. Bars are means + SEM of 7 - 8 mice per group. *p<0.05, **p<0.01 and ***p<0.001 vs. saline; one-way ANOVA and Newman-Keuls post-test.

3.2 EFFECT OF A CD200R1 AGONIST ADMINISTRATION ON MICROGLIAL ACTIVATION AND DOPAMINERGIC NEURODEGENERATION IN THE MPTP MODEL OF PD

To study the effect of the CD200-CD200R1 modulation in the context of PD, a CD200R1 agonist (CD200Fc) or its negative control (isotype) was intraperitoneally administered to MPTP-injected male C57BL6NCrl mice (Charles River, Lyon, France) (Fig. 3.6A), and we studied their effects on the nigrostriatal dopaminergic neurodegeneration induced by MPTP. Six groups of n=8 mice were administered with: 1) saline, 2) MPTP, 3) 1.8 mg/kg CD200Fc and MPTP, 4) 1.8 mg/kg isotype control and MPTP, 5) 3.6 mg/kg CD200Fc and MPTP, and 6) 3.6 mg/kg isotype control and MPTP. Animals were injected with MPTP following the acute regimen and killed at day 7 after the last MPTP injection.

One mice from the 1.8 mg/kg CD200Fc + MPTP group (12.5%), 3 from the 1.8 mg/kg isotype + MPTP group (37.5%), 2 from the 3.6 mg/kg CD200Fc + MPTP group (25%), and 1 from the 3.6 mg/kg isotype + MPTP group (12.5%) died after MPTP administration.

Optical densitometry of striatal TH-positive terminals showed that MPTP injection produced an 86% depletion of dopaminergic terminals (Fig. 3.6B,C,F). The administration of CD200Fc did not prevent this effect. Isotype injection also had no effect on the MPTP-induced striatal degeneration. When analysing neuronal cell bodies of the SNpc, stereological TH-positive cell counts showed that MPTP toxicity induced a significant loss of dopaminergic neurons (51% decrease) (Fig. 3.6D,E,F). The administration of two doses of 1.8 mg/kg of CD200Fc (Fig. 3.6D,F) had no effect on MPTP-induced dopaminergic neuronal loss. However, this loss was attenuated in MPTP-injected mice that received two doses of 3.6 mg/kg CD200Fc (30% decrease) (Fig. 3.6E,F). A significant decrease in TH positive neurons was still observed in isotype + MPTP injected-mice (Fig. 3.6D,E,F).

We next evaluated whether the dopaminergic neuroprotection observed in MPTP-injected mice treated with 3.6 mg/kg CD200Fc was accompanied by effects on microglial cells. The SNpc of MPTP-treated mice exhibited increased microglial cell number, with hypertrophied morphology and intensified IBA1 staining (Fig. 3.6G). CD200Fc treatment, and not the isotype treatment, decreased the MPTP-induced microglial activation at the level of SNpc (Fig. 3.6G).

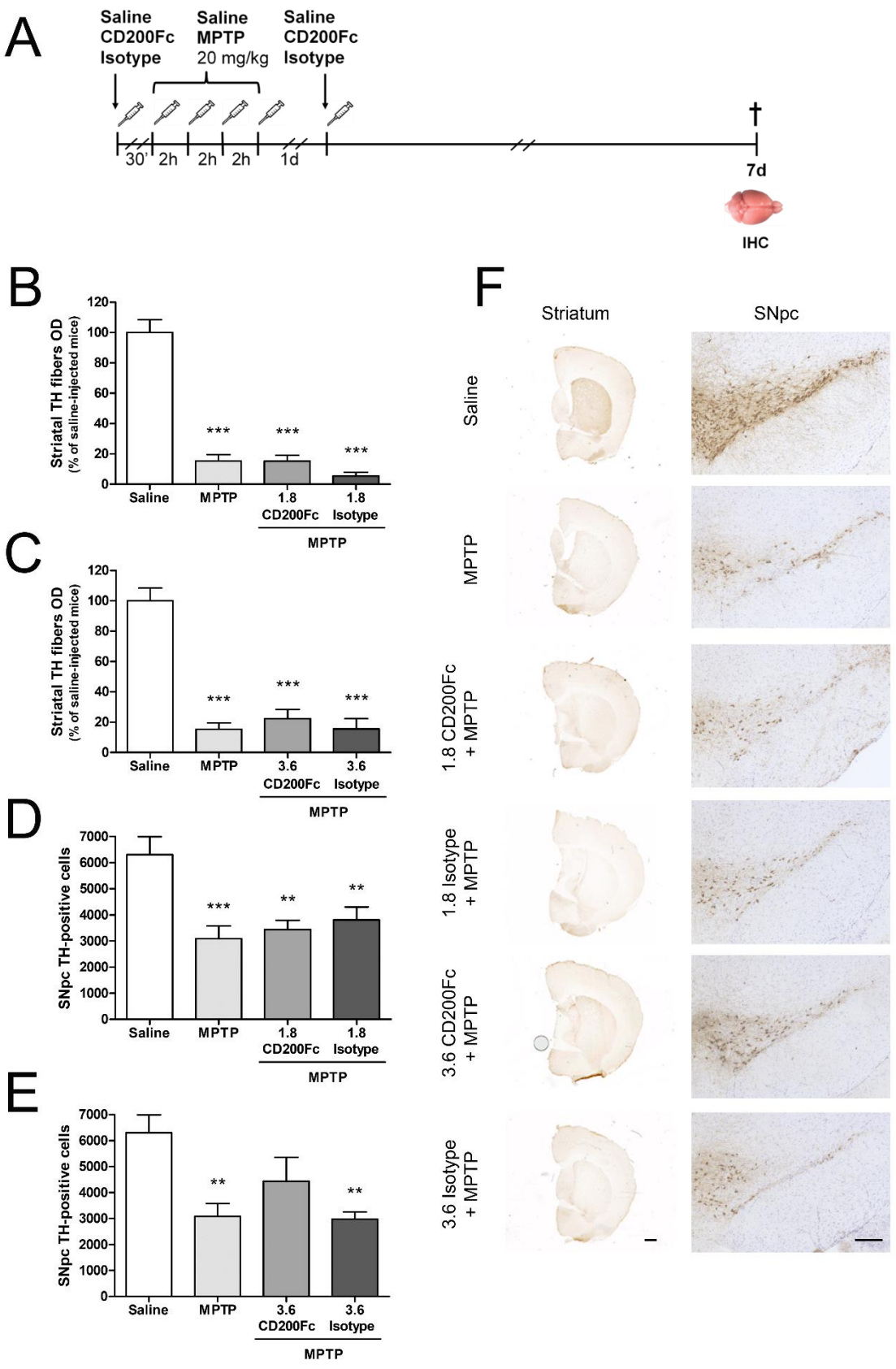
A
Saline
CD200Fc
Isotype
Saline
MPTP
20 mg/kg
Saline
CD200Fc
Isotype
30'
2h
2h
2h
1d
7d
IHC
B
Striatal TH fibers OD
(% of saline-injected mice)
Saline
MPTP
1.8
CD200Fc
1.8
Isotype
MPTP
C
Striatal TH fibers OD
(% of saline-injected mice)
Saline
MPTP
3.6
CD200Fc
3.6
Isotype
MPTP
D
SNpc TH-positive cells
Saline
MPTP
1.8
CD200Fc
1.8
Isotype
MPTP
E
SNpc TH-positive cells
Saline
MPTP
3.6
CD200Fc
3.6
Isotype
MPTP
F
Striatum
SNpc
Saline
MPTP
1.8 CD200Fc
+ MPTP
1.8 Isotype
+ MPTP
3.6 CD200Fc
+ MPTP
3.6 Isotype
+ MPTP

G

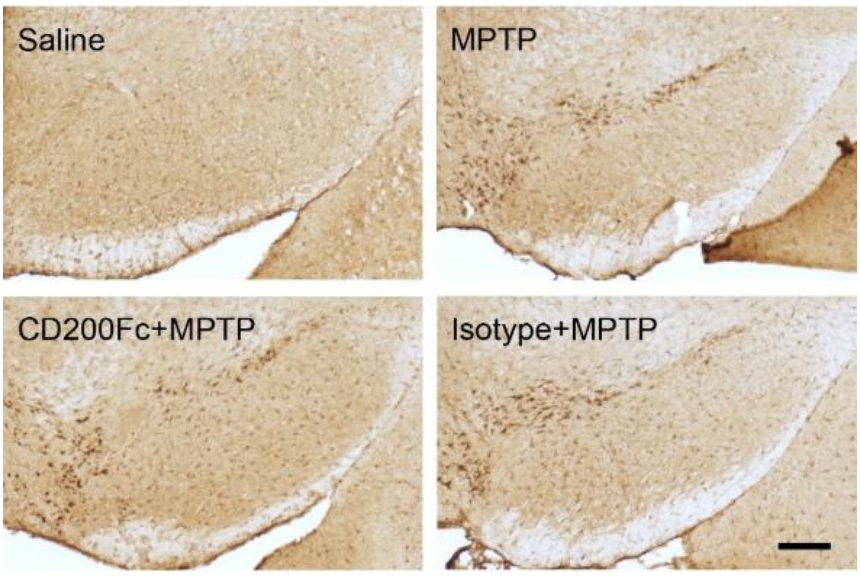

Figure 3.6. Pharmacological stimulation of CD200R1 in MPTP-injected mice attenuates dopaminergic neuronal loss in SNpc. **A** Experimental design. Male C57Bl/6 mice were injected intraperitoneally with MPTP (20 mg/kg) every 2 h for a total of 4 doses in 1 day. In mice treated with the CD200R1 agonist, 1.8 or 3.6 mg/kg CD200Fc was intraperitoneally administered twice, 30 minutes before the first MPTP injection and 24 h after the last one. Isotype administration regimen was the same as for CD200Fc. Mice were killed 7 days following the last MPTP injection and brains were fixed for immunohistochemistry (IHC). **B** Optical densitometry of striatal TH-positive dopaminergic fibers of saline, MPTP, 1.8 mg/kg CD200Fc and MPTP and 1.8 mg/kg isotype and MPTP. **C** Optical densitometry of striatal TH-positive dopaminergic fibers of saline, MPTP, 3.6 mg/kg CD200Fc and MPTP and 3.6 mg/kg isotype and MPTP. **D** Stereological cell counts of dopaminergic neurons in SNpc of saline, MPTP, 1.8 mg/kg CD200Fc and MPTP and 1.8 mg/kg isotype and MPTP. **E** Stereological cell counts of dopaminergic neurons in SNpc of saline, MPTP, 3.6 mg/kg CD200Fc and MPTP and 3.6 mg/kg isotype and MPTP. Bars are means + SEM of 5 - 8 mice per experimental group. *p<0.05, **p<0.01 and ***p<0.001 vs. saline; one-way ANOVA and Newman-Keuls post-test. **F** Representative photomicrographs of TH-immunostained striatum and SNpc sections of mice treated with saline, MPTP, 1.8 mg/kg CD200Fc and MPTP, 1.8 mg/kg isotype and MPTP, 3.6 mg/kg CD200Fc and MPTP or 3.6 µg isotype and MPTP. Scale bars: 500 µm (striatum) and 200 µm (SNpc). **G** Representative photomicrographs of IBA1-immunostained SN of saline- and MPTP-injected mice administered or not with 3.6 CD200Fc or 3.6 isotype. Scale bar: 200 µm (SNpc).

3.3 EFFECT OF CD200-DEFICIENCY ON THE ACUTE MPTP MODEL OF PD

In order to further study the involvement of the CD200-CD200R1 system in the development of dopaminergic neurodegeneration in the acute MPTP model of PD, we used CD200-deficient mice.

The genetic background of the mice is important for MPTP sensitivity. Although C57BL6 mice are usually used in the MPTP model, increased toxicity of MPTP is observed in certain substrains, such as C57BL/6J mice (Jackson-Lewis and Przedborski 2007). We submitted the CD200 knock-out mice to background strain characterisation (Jackson Laboratories) and they were identified to be 67% C57BL/6J and 33% C57BL/6NJ. As the MPTP experiments reported above were performed with C57BL/6N mice, we generated a colony by crossing CD200 knock-out mice with wild-type C57BL/6N mice to yield F1 offspring with an enriched C57BL/6N background. Male and

female heterozygous mice (CD200 +/-) of the F1 offspring were crossed to obtain CD200 -/-, CD200 +/- and CD200 +/+ genotypes. CD200 -/- and CD200 +/+ mice were used henceforth. The genotype of mice used in the experiments was further corroborated by genotyping tail tissue (Fig 3.7A) and CD200 immunohistochemistry of brain sections (Fig 3.7B). The MPTP doses were reduced from 20 to 18 mg/kg because in a preliminary study we detected a higher MPTP sensitivity in mice of the CD200 colony (66% N and 33% J) than in the mice used in the previous experiments (100% N).

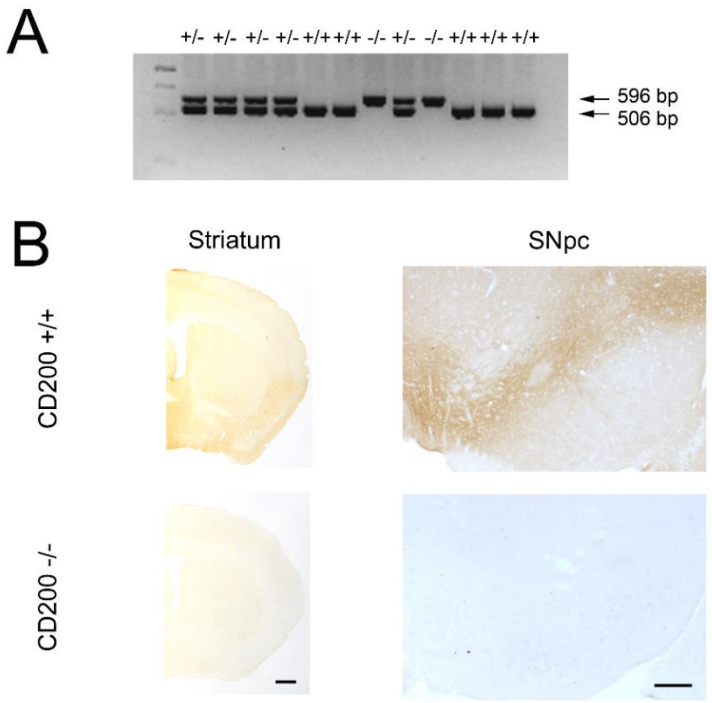

Figure 3.7. Genotype of CD200 +/+, CD200 +/- and CD200 -/- mice. A Representative agarose gel analysis after genotyping tail tissue of CD200 +/+, CD200 +/- and CD200 -/- mice. **B** Representative photomicrographs of CD200-immunostained striatum and SNpc of CD200 -/- mice and their CD200 +/+ littermates. Scale bars: 500 µm (striatum) and 200 µm (SNpc).

Four groups of mice were treated as follows: 1) control group of CD200 +/+ mice with saline (n=8), 2) CD200 +/+ mice with MPTP(n=12), 3) CD200 -/- mice with saline (n=8), 4) CD200 -/- mice with MPTP (n=11). Female mice were used in the saline groups because we did not obtain enough male mice to complete all experimental groups. Mice were killed 7 days after the last administration of MPTP (Fig. 3.8A).

In total, 7 mice died in the MPTP-injected CD200 +/+ group (4, 1 and 2 mice died at day 1, 5 and 7 post MPTP injection, respectively) (58%) and 5 from the MPTP-injected CD200 -/- group (1, 1, 2 and 1 mice died at day 1, 2, 5 and 7 post MPTP injection, respectively) (45.5%). In MPTP-injected CD200 +/+ mice, we observed a significant reduction of the density of dopaminergic fibers in the striatum (90% decrease) and the number of TH-positive cell bodies in the SNpc (42% decrease) at day 7 after MPTP administration (Fig. 3.8B,C). In CD200 -/- mice, similar striatal TH loss (90% decrease vs. saline CD200 -/-) and dopaminergic cell death (33% decrease vs. saline CD200 -/-) 7 days after MPTP injections were observed when compared with their CD200 +/+ littermates (Fig. 3.8B,C).

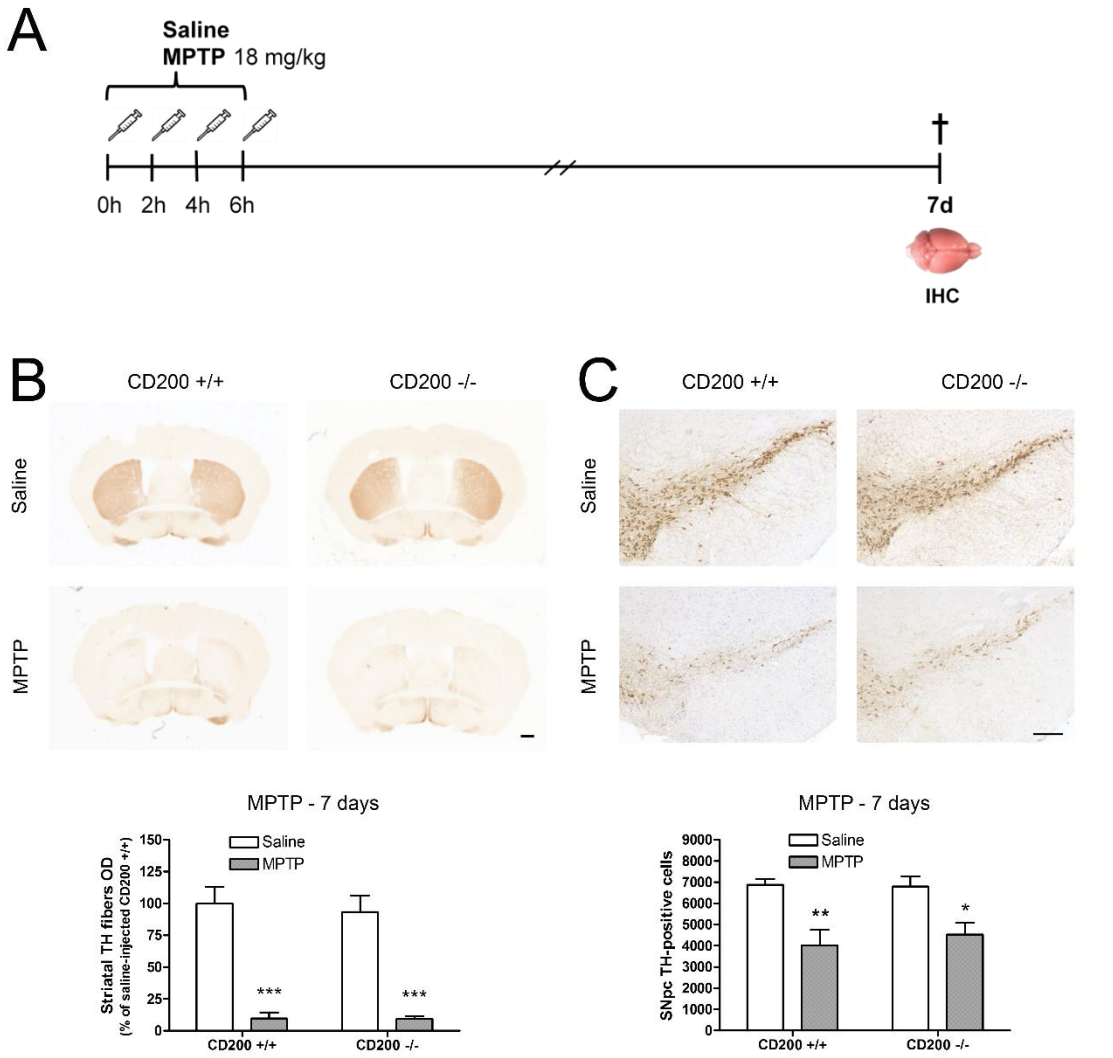

Figure 3.8. CD200-deficiency does not modify the dopaminergic neuronal damage in the striatum and SNpc 7 days after the last MPTP injection. **A** Experimental design. CD200 -/- mice and their CD200 +/+ littermates were injected intraperitoneally with MPTP (18 mg/kg) every 2 hours for a total of 4 doses in one day. Animals were killed 7 days after the last injection and brains were fixed for immunohistochemistry (IHC). **B** TH immunohistochemistry and optical densitometry of TH-positive dopaminergic fibers in the striatum of CD200 -/- mice and their CD200 +/+ littermates injected with saline or MPTP. Scale bar: 500 µm. **C** TH immunohistochemistry and stereological cell counts of dopaminergic neurons in SNpc of CD200 -/- mice and their CD200 +/+ littermates injected with saline or MPTP. Scale bar: 200 µm. Bars are means + SEM of 5 - 8 mice per group. *p<0.05, **p<0.01 and ***p0.001 vs. corresponding saline; two-way ANOVA and Bonferroni post-test.

As shown in Figure 3.9, the IBA1-labelled area in the SN from CD200 -/- mice and their CD200 +/+ littermates showed a tendency to increase 7 days after MPTP administration (Fig. 3.9A,B). When analysing SNpc and SNpr, we observed that the IBA1-labelled area in SNpc but not in SNpr increased (~2.75 times) after MPTP administration in both CD200 -/- and CD200 +/+ mice (Fig. 3.9B). The intensity of the immunolabelling in IBA1-positive cells in total SN and SNpc showed no difference between saline and after MPTP administration in CD200 -/- and CD200 +/+ mice (Fig. 3.9C).

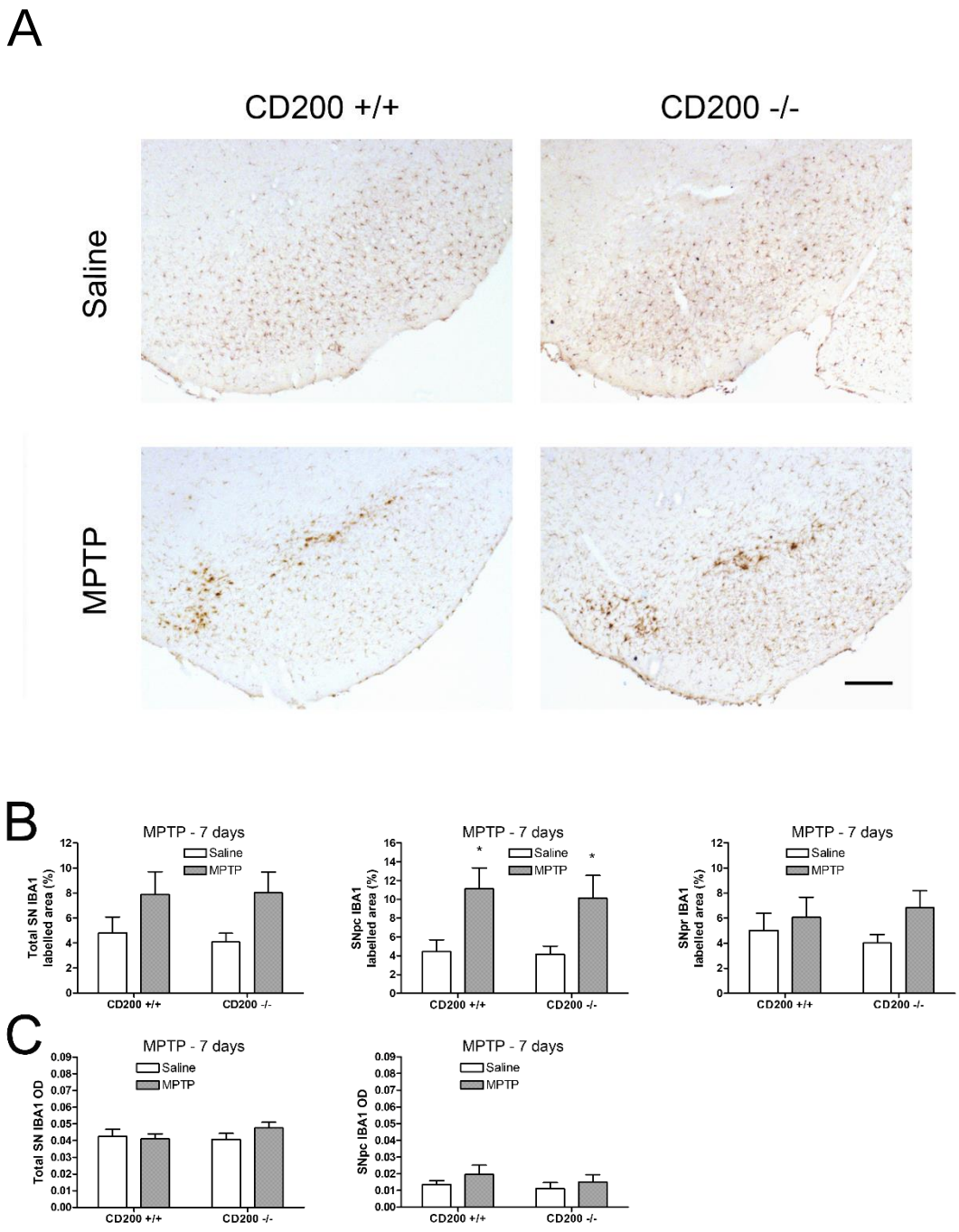

Figure 3.9. CD200-deficiency does not modify the microglial reactivity in the SN 7 days after the last MPTP injection. **A** Representative photomicrographs of IBA1-immunohistochemistry in SN of CD200 -/- mice and their CD200 +/+ littermates injected with saline or MPTP and killed at day 7 after the last injection. Scale bar: 200 µm. **B** Quantification of IBA1-labelled area in total SN, SNpc and SNpr. **C** Intensity of immunolabelling in IBA1-positive cells in total SN and SNpc of all groups of animals. Bars are means + SEM of 5 - 8 mice per group. *p<0.05 vs. corresponding saline; two-way ANOVA and Bonferroni post-test.

To further investigate the effect of CD200-deficiency on glial activation and dopaminergic neurodegeneration in the MPTP model, we designed a second experiment where CD200 -/- mice and CD200 +/+ with matched genetic background were injected with MPTP and killed at an earlier time point, 1 day after the last MPTP injection (Fig. 3.10A). This experimental approach led us to

test the following hypothesis: 1) whether CD200-deficiency accelerates the neuronal dopaminergic decline in the striatum and SNpc after MPTP administration, even though levels of dopaminergic neuronal cell loss at day 7 are the same in CD200 wild-type and null mice; 2) whether CD200-deficiency accelerates microglial activation after MPTP administration.

The same four groups were used as before, with female mice (CD200 +/+ and CD200 -/-, n=8 for both groups) again used for the saline controls, while male mice (CD200 +/+, n=11 and CD200 -/-, n=9) were injected with MPTP. Four CD200 -/- mice died after MPTP administration (20% of death). In wild-type mice, MPTP administration produced 86.6% depletion of striatal dopaminergic terminals and 44.9% loss of dopaminergic neurons at day 1 post MPTP injection (Fig. 3.10B,C). In CD200-deficient mice, we did not observe further striatal TH loss (80.1% decrease vs. saline CD200 -/-). As regards dopaminergic cells in the SN, no differences in the number of TH-positive neurons in SNpc were observed between CD200-deficient mice (57.2% decrease vs. saline CD200 -/-) and wild-type mice 1 day after MPTP injections (Fig. 3.10B,C).

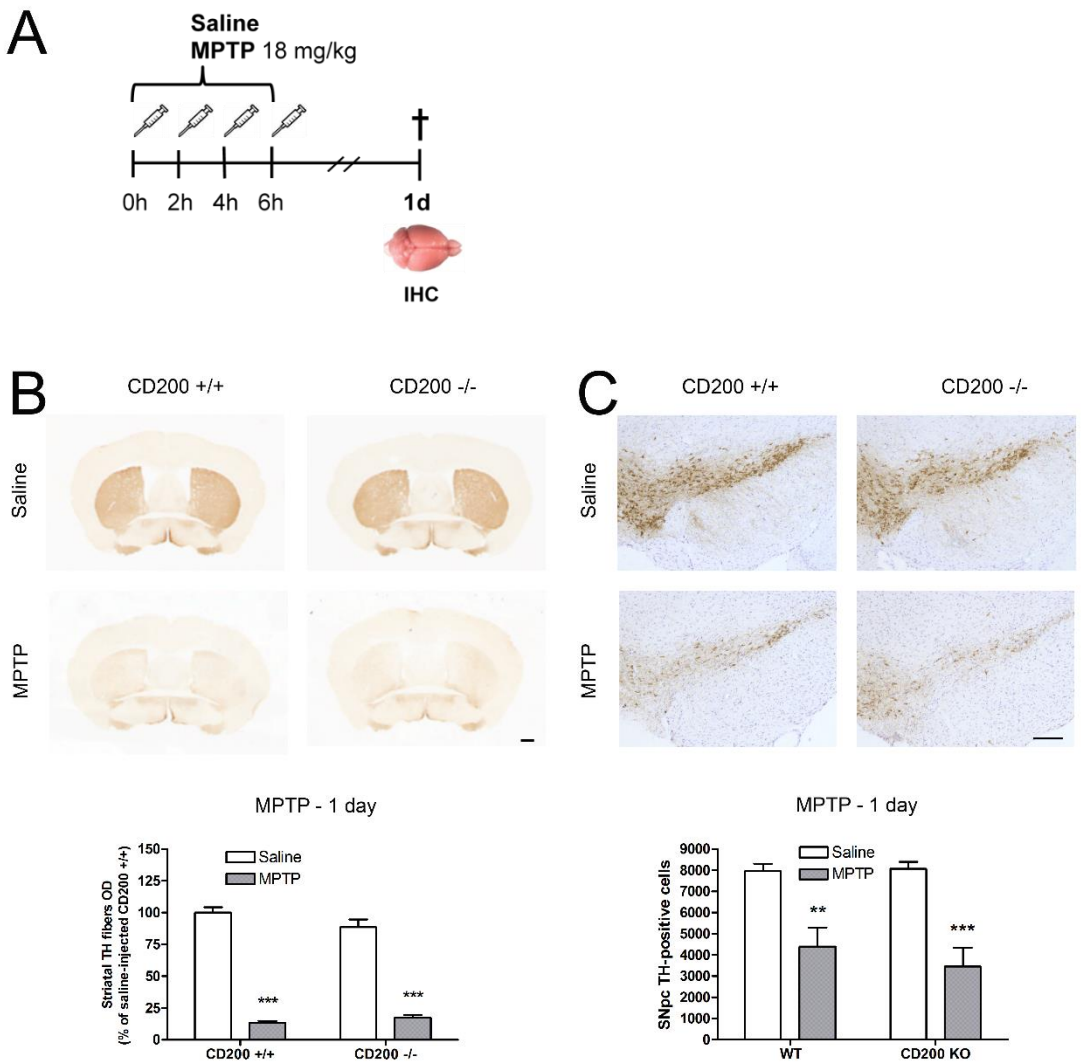

Figure 3.10. CD200-deficiency does not accelerate the dopaminergic neuronal degeneration in the striatum and SNpc 1 day after the last MPTP injection. A Experimental design. CD200 -/- and CD200 +/+ mice with matched background were injected intraperitoneally with MPTP (18 mg/kg) every 2 hours for a total of 4 doses in a single day. Animals were killed at day 1 after the last injection and brains were fixed for immunohistochemistry (IHC). **B** TH-immunohistochemistry and optical densitometry of TH-positive dopaminergic fibers in the striatum of CD200 -/- and CD200 +/+ mice injected with saline or MPTP. Scale bar: 500 µm. **C** TH-immunohistochemistry and stereological cell counts of dopaminergic neurons in SNpc of CD200 -/- and CD200 +/+ mice injected with saline or MPTP. Scale bar: 200 µm. Bars are means + SEM of 5 - 11 mice per group. **p<0.01 and ***p<0.001 vs. corresponding saline; two-way ANOVA and Bonferroni post-test.

Some differences were found, however, when looking at microglial activation 1 day after MPTP administration. The IBA1-labelled area was reduced in the total SN (28% decrease) and SNpr (33% decrease) 1 day after MPTP administration in CD200 -/- mice but not in CD200 +/+ mice (Fig. 3.11A,B). However, the intensity of the immunolabelling in IBA1-positive cells in total SN increased after MPTP administration in both CD200 +/+ (2.3 times) and CD200 -/- (2.6 times) mice (Fig. 3.11C). Interestingly, when analysing SNpc from CD200 -/- mice a greater increase in the intensity of the immunolabelling in IBA1-positive cells (2.6 times) was observed after MPTP administration in comparison with CD200 +/+ mice (1.9 times) (Fig. 3.11C). Moreover, an increase in the number of IBA1-positive cells was observed in CD200 +/+ (1.4 times) and CD200 -/- (1.2 times) mice in the SN total and SNpc after MPTP injections (Fig. 3.11D).

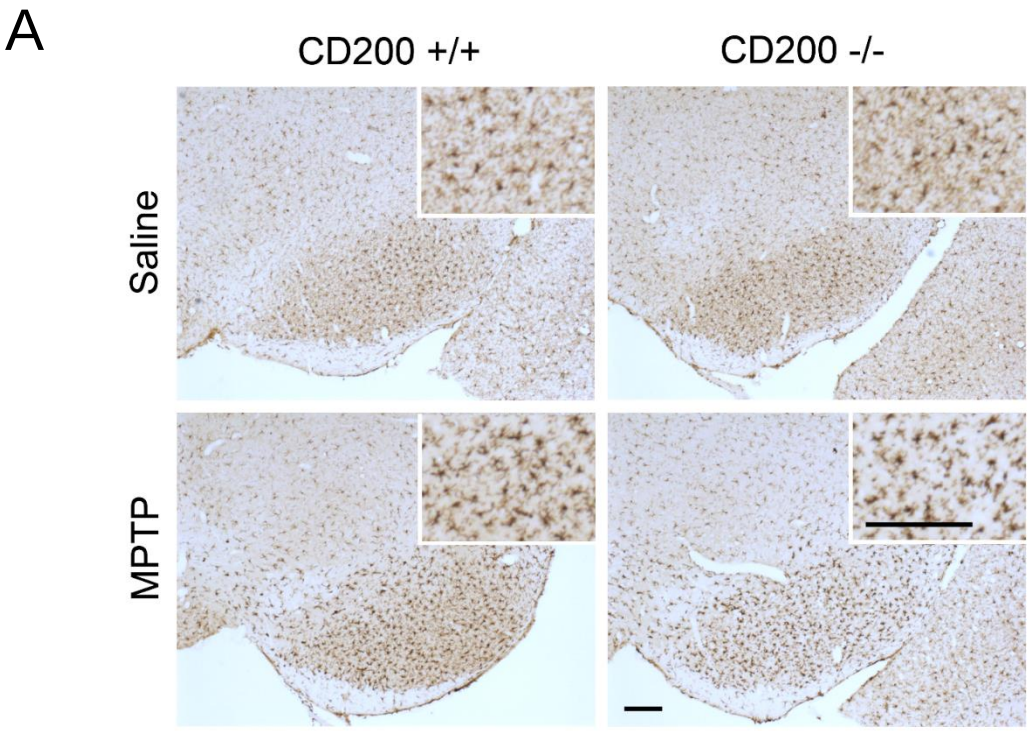

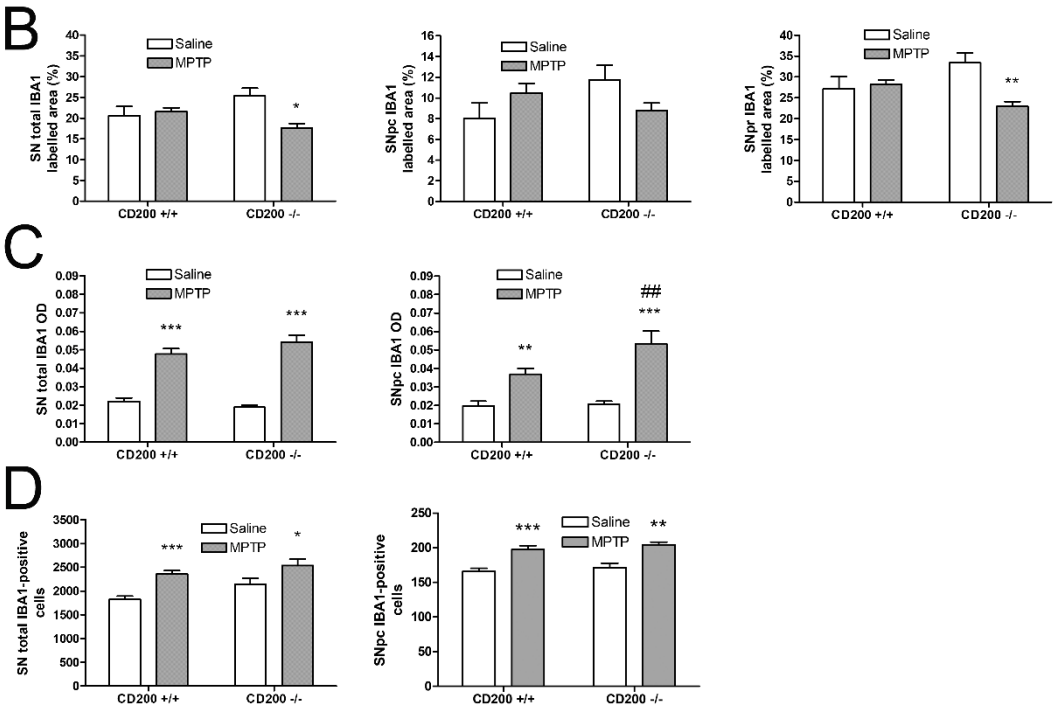

Figure 3.11. CD200-deficiency modify the microglial reactivity in the SN 1 day after the last MPTP injection. **A** Representative photomicrographs of IBA1-immunohistochemistry in SN of CD200 -/- and CD200 +/+ mice with matched background injected with saline or MPTP and killed at day 1 after the last injection. Scale bar: 200 µm. **B** Quantification analysis of IBA1-labelled area in SN total, SNpc and SNpr of all groups of animals. **C** Optical densitometry of IBA1-positive cells in SN total and SNpc of all groups of animals. **D** Cell counts of IBA1-positive cells in SN total and SNpc of all groups of animals. Bars are means + SEM of 5 - 11 mice per group. *p<0.05, **p<0.01 and ***p<0.001 vs. corresponding saline; ##p<0.01 vs. MPTP CD200 +/+; two-way ANOVA and Bonferroni post-test.

4 Expression of CD200-CD200R1 system in human samples

In homeostasis, several inhibitory mechanisms maintain microglia in a surveillant phenotype in the CNS. The presence of chronic microglial activation in the brain of patients with PD suggests that these inhibitory mechanisms are altered (Croisier et al. 2005; McGeer et al. 1988; Mosley et al. 2012; Imamura et al. 2003; Nagatsu and Sawada 2005; Long-Smith, Sullivan, and Nolan 2009). With the aim of studying possible alterations in the CD200-CD200R1 system in the context of PD, we determined the expression of CD200 and CD200R1 in *post-mortem* brain samples of PD patients, identifying mRNA variants and protein isoforms.

The murine CD200R1 gene encodes a single CD200R1 protein (Wright et al. 2000), while the human CD200R1 gene can generate four mRNA variants through alternative splicing (Vieites et al. 2003). Variants 1 and 4 (long variants) encode protein isoforms 1 and 4, which are transmembrane proteins. Variants 2 and 3 (short variants) encode protein isoforms 2 and 3, which are soluble truncated proteins that lack the transmembrane and the cytoplasmic domains. CD200R1 isoform 4 is the equivalent to the murine CD200R1 (Vieites et al. 2003). Regarding CD200, both mouse and human CD200 genes generate CD200full and CD200tr mRNA variants through alternative splicing. In both species, CD200full interacts with CD200R1 and inhibits microglial activation. CD200tr is a physiologic antagonist of CD200full (Chen et al. 2008; Vieites et al. 2003).

4.1 CD200R1 mRNA EXPRESSION IN HUMAN MONOCYTES AND MICROGLIA-LIKE CELLS

Because of their overlapping sequences (Fig. 4.2), optimal primers cannot be designed (75-200 pb amplicon) to quantify individually the four CD200R1 mRNA variants by qPCR after random primer retrotranscription. We designed an alternative approach based on gene-specific primer retrotranscription to quantify the expression of each variant (Fig. 4.1), which consists of specific primer pairs for the retrotranscription of a) V1 and V4 variants (long variants) or b) V2 and V3 variants (short variants), and primer pairs for qPCR that generate short amplicons (75-200 pb) to amplify V1 or V4 in a) and V2 or V3 in b) (Figs. 4.1 and 4.2, Tables 4.1-4.3). We validated this approach using human monocyte primary cell cultures, which express CD200R1, obtained from peripheral blood samples from healthy adult volunteers. We confirmed the presence of CD200R1 transmembrane proteins by immunofluorescence (antibodies commercially available detect only long isoforms) (Fig. 4.3A) and the expression of the four CD200R1 mRNA variants by random

primer retrotranscription followed by conventional PCR (Fig. 4.3A). Then, we determined the expression of each CD200R1 mRNA by qPCR (Fig. 4.3C).

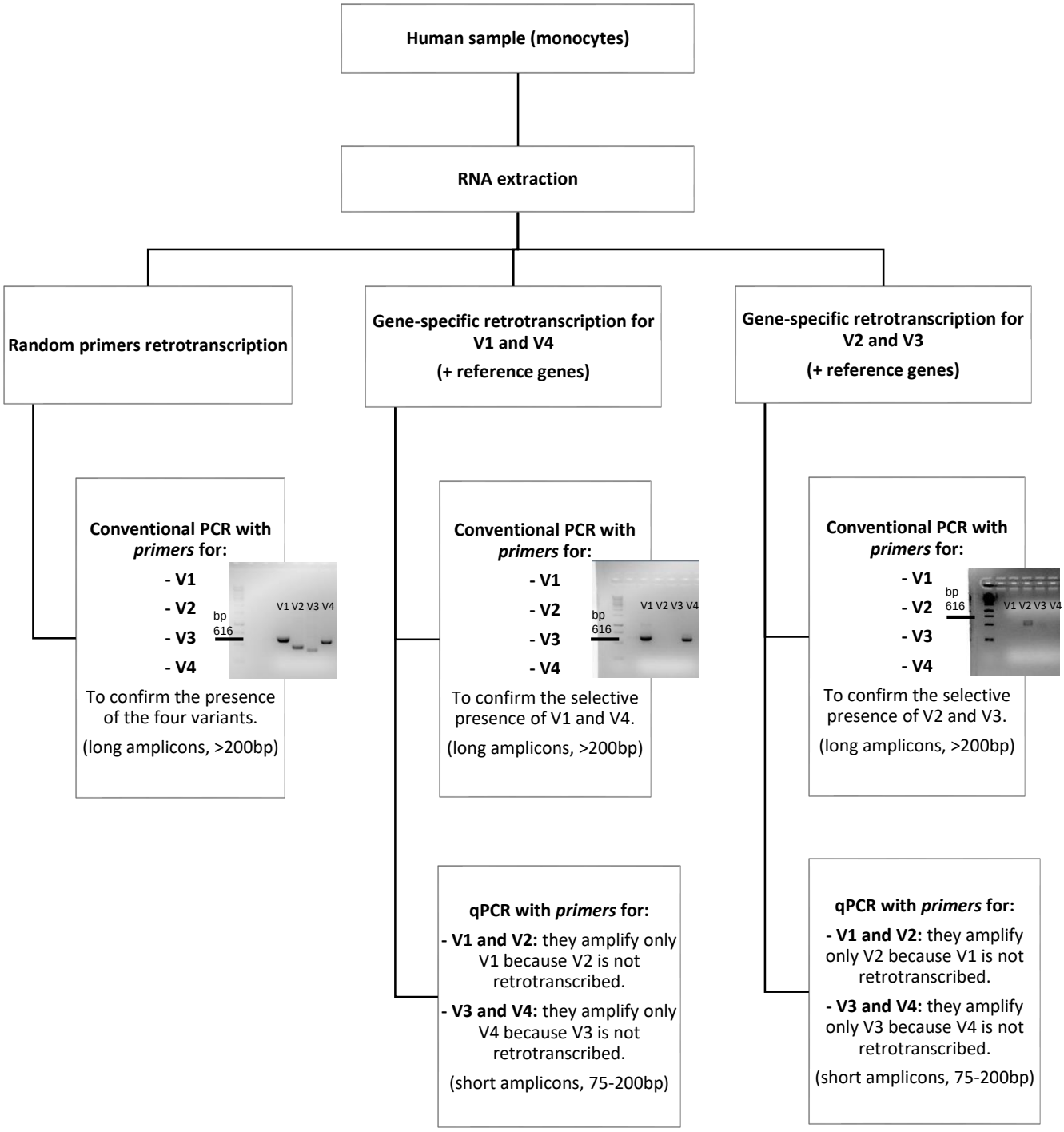

Figure 4.1. Algorithm for the analysis of CD200R1 expression in human samples.

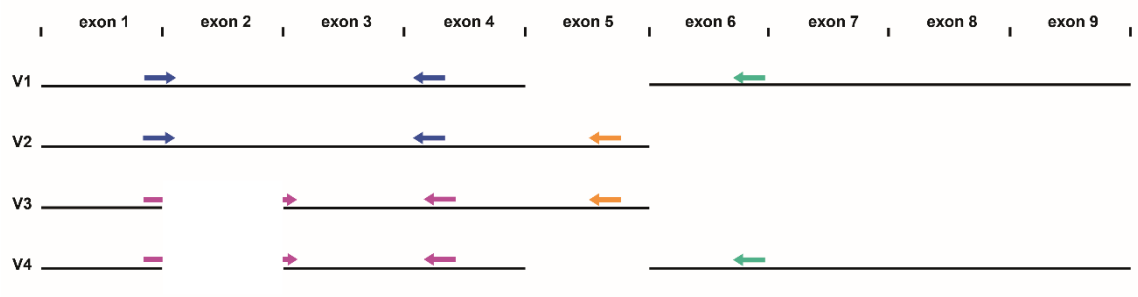

Figure 4.2. Localization of primers used for the quantification of each human CD200R1 variant mRNA. Specific primer pairs for the gene-specific retrotranscription of a) V1 and V4 variants (in green) or b) V2 and V3 variants (in orange), and primer pairs for qPCR that generate short amplicons to amplify V1 (in blue) or V4 (in pink) in a) and V2 (in blue) or V3 (in pink) in b). Exons are not depicted on scale and are represented as thin horizontal lines. The relative positions of primers are indicated by arrows.

Table 4.1 Primers used for gene-specific retrotranscription.

Species: *Homo sapiens*		
Target mRNA	**Accession number**	**Primer (5'→3')**
V1 and V4 CD200R1	NM_138806.4 NM_170780.2	AACTGGAGTAGATTCTG
V2 and V3 CD200R1	NM_138939.2 NM_138940.2	CTGGTGATGTGAAATAC
Reference genes:		
GAPDH	NM_002046.7	CATACTTCTCATGGTTC
RPS18	NM_022551.3	CACGAAGGCCCCAGAA

V1 and V4 CD200R1, variant 1 and 4 CD200 receptor 1; V2 and V3 CD200R1, variant 2 and 3 CD200 receptor 1; GAPDH, glyceraldehyde-3-phosphate dehydrogenase; RPS18, ribosomal protein S18.

Table 4.2 Primers used for qPCR.

Species: *Homo sapiens*				
Target mRNA	**Accession number**	**Forward primer (5'→3')**	**Reverse primer (5'→3')**	**Ampli-con**
V1 and V2 CD200R1	NM_138806.4 NM_138939.2	ATCTTCTTAGTGGCCGAAGC	GCACAGCATTTGTAGCCATC	193 bp
V3 and V4 CD200R1	NM_138940.2 NM_170780.2	CTTCTTAGTGGCCGCTTCAA	TAGGAGGGCAACAAAGCACA	137 bp
V1 and V4 CD200R1	NM_138806.4 NM_170780.2	GTTGTTGAAAGTCAATGGCTGC	CACTTTGTAATGCCTCAGATGCC	164 bp
V2 and V3 CD200R1	NM_138939.2 NM_138940.2	TTCAGATTCGTACCGTGGCC	CCTCAATATATGATGCTCCT	125 bp
Reference genes:				
GAPDH	NM_002046.7	GAAGGTGAAGGTCGGAGTCA	GTTAAAAGCAGCCCTGGTGA	67 bp
RPS18	NM_022551.3	GATGGGCGGCGGAAAAT	CTTGTACTGGCGTGGATTCTGC	174 bp

V1 and V2 CD200R1, variant 1 and 2 CD200 receptor 1; V3 and V4 CD200R1, variant 3 and 4 CD200 receptor 1; V1 and V4 CD200R1, variant 1 and 4 CD200 receptor 1; V2 and V3 CD200R1, variant 2 and 3 CD200 receptor 1; GAPDH, glyceraldehyde-3-phosphate dehydrogenase; RPS18, ribosomal protein S18.

Table 4.3 Primers used for conventional PCR.

Specie: *Homo sapiens*				
Target mRNA	**Accession number**	**Forward primer (5'→3')**	**Reverse primer (5'→3')**	**Ampli-con**
V1 CD200R1	NM_138806.4	GGTGCTGCTCAACCAAACAA	CCTCCCAGTGGCATGTACTCT	616 bp
V2 CD200R1	NM_138939.2	GGTGCTGCTCAACCAAACAA	CCTCAATATATGATGCTCCT	468 bp
V3 CD200R1	NM_138940.2	TTAGTGGCCGCTTCAAGCAG	CCTCAATATATGATGCTCCT	417 bp
V4 CD200R1	NM_170780.2	TTAGTGGCCGCTTCAAGCAG	CCTCCCAGTGGCATGTACTCT	565 bp
Reference genes:				
RPS18	NM_022551.3	CCTGAAAAGTTCCAGCATATTTTGC	TTTATTAACAGACAAGGCCTACAGAC	470 bp

V1 CD200R1, variant 1 CD200 receptor 1; V2 CD200R1, variant 2 CD200 receptor 1; V3 CD200R1, variant 3 CD200 receptor 1; V4 CD200R1, variant 4 CD200 receptor 1; RPS18, ribosomal protein S18.

Next, we also studied the expression of CD200R1 mRNA variants in induced human microglia-like cells obtained by differentiation of peripheral blood monocytes using the protocol of Ohgidani and collaborators (Ohgidani et al. 2014). We detected the presence of CD200R1 transmembrane proteins by immunofluorescence (Fig 4.3B), and we analysed each CD200R1 mRNA variant by random primer retrotranscription followed by conventional PCR. We detected the expression of V1 and V4, but not V2 and V3 in microglia-like cells (Fig. 4.3B). Using the gene-specific retrotranscription strategy mentioned above, we compared the expression of each variant by qPCR in microglia-like cells and monocytes. Induced microglia-like cells showed lower expression of V2 and V3 than monocytes (Fig. 4.3C). Altogether, these results suggest that CD200R1 is differentially expressed in peripheral blood monocytes and microglia.

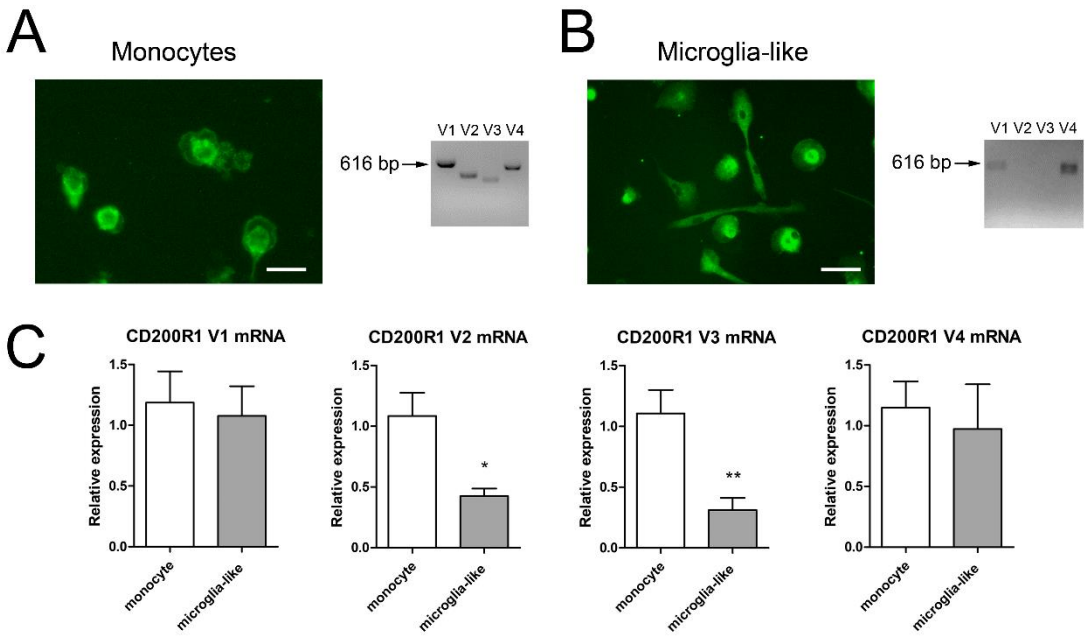

Figure 4.3. CD200R1 variants in human monocytes and microglia-like cells. Representative images of CD200R1 expression by immunofluorescence (isoforms 1 and 4) and agarose gel electrophoresis illustrating conventional PCR products for CD200R1 mRNA variants (V1, 616 bp; V2, 468 bp; V3, 417 bp; V4, 565 bp) after random primer ratrotranscription in human monocytes cultured for 24 h (**A**) and microglia-like cells cultured for 14 days (**B**). Scale bar: 50 µm. **C** mRNA expression of each CD200R1 variant by qPCR after gene-specific retrotranscription in monocytes and microglia-like cells. GAPDH and RPS18 were used as reference genes. Bars are means + SEM of 5 - 7 independent experiments. *p<0.05 and **p<0.01 vs. monocytes; Student's t test.

4.2 EXPRESSION OF CD200R1 mRNA VARIANTS IN HUMAN MICROGLIA-LIKE CELLS IN RESPONSE TO DIFFERENT STIMULUS

We studied the possible differential expression of the four CD200R1 mRNA variants in induced microglia-like cell cultures exposed to pro-inflammatory (LPS and LPS/IFNγ) or anti-inflammatory (IL4) stimuli. We observed that the mRNA expression of V3 and V4, but not V1 and V2, decreased upon LPS treatment in microglia-like cell cultures (Fig. 4.4A). No differences were observed after LPS/IFNγ exposure in comparison to control. After IL4 treatment, the mRNA expression of V1 increased in microglia-like cell cultures (Fig. 4.4C).

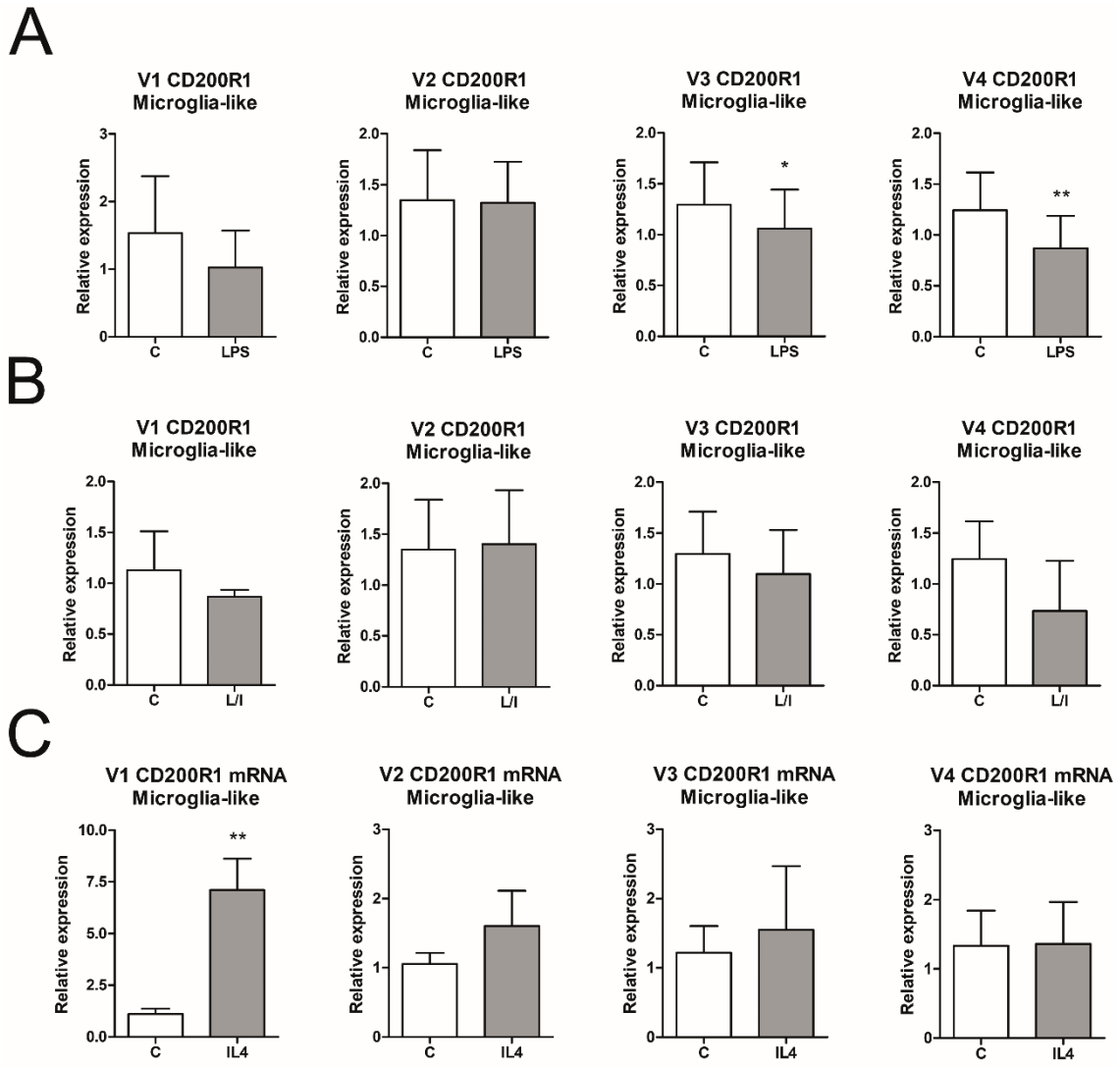

Figure 4.4. Expression of CD200R1 mRNA variants in human microglia-like cells after pro- or anti-inflammatory stimuli. Expression of the four CD200R1 mRNA variants by qPCR 24 h after LPS (100 ng/mL) (**A**), LPS/IFNγ (L/I, 100 ng/mL LPS + 1 ng/mL IFNγ) (**B**) or IL4 (50 ng/mL) (**C**) in microglia-like cells. GAPDH and RPS18 were used as reference genes. Bars are means + SEM of 3 - 5 independent experiments. *p<0.05 and **p<0.01 vs. control (C); Student's t test.

4.3 CD200 AND CD200R1 EXPRESSION IN *post-mortem* BRAIN TISSUE OF PD PATIENTS

We evaluated the mRNA and protein expression of CD200full, CD200tr and CD200R1 in *post-mortem* brain samples of SN, frontal cortex and hippocampus of PD patients and age-matched controls (*Banc de Teixits Neurològics*, SCT-University of Barcelona).

When analysing each CD200R1 mRNA variant by conventional PCR, we detected V1 and V2 but not V3 and V4 mRNA variants in *post-mortem* human brain tissue (Fig. 4.5).

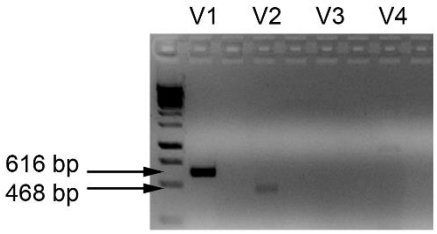

Figure 4.5. CD200R1 mRNA variants in *post-mortem* human brain. Representative agarose gel electrophoresis illustrating conventional PCR products for CD200R1 mRNA variants (V1, 616 bp; V2, 468 bp; V3, 417 bp; V4, 565 bp) after random primer retrotranscription in the frontal cortex of control individuals.

Using the same strategy as in monocytes and microglia-like cells, in *post-mortem* human brain tissue we did not detect the four CD200R1 mRNA variants by qPCR, but only V1 mRNA variant, probably because of a dilution effect of microglial mRNAs in the whole human brain lysates. Given the singularity of CD200R1 expression in humans, where unlike the murine gene the CD200R1 gene generates four variants, we considered important to study the expression of long and short variants. To this end, we used random primer retrotranscription followed by qPCR with primers for long or short mRNA variants (Table 4.2). With this methodology, we could detect long and short variants in the agarose gel electrophoresis and quantify them by qPCR. Long and short mRNA variants were not differentially expressed in the SN of PD subjects compared to age-matched controls (Fig. 4.6A). On the contrary, short mRNA variants showed a significant increase in the frontal cortex of PD patients (Fig. 4.6B), and both long and short mRNA variants were increased in the hippocampus of PD patients (Fig. 4.6C). Protein expression of CD200R1 by western blot with antibodies that only detect long isoforms (the antibodies commercially available) showed higher levels in the SN and hippocampus, but not in the frontal cortex, of PD patients than of age-matched controls (Fig. 4.7). As regards CD200, when analysing CD200full mRNA no difference between control individuals and PD patients was detected in any of the three areas analysed (Fig. 4.6). On the contrary, CD200tr mRNA levels were strongly increased in the hippocampus from PD patients compared to control individuals (Fig. 4.6C). CD200 protein levels were not modified (antibodies commercially available detect CD200full and probably CD200tr as well) in the SN, frontal cortex or hippocampus of PD patients (Fig. 4.7).

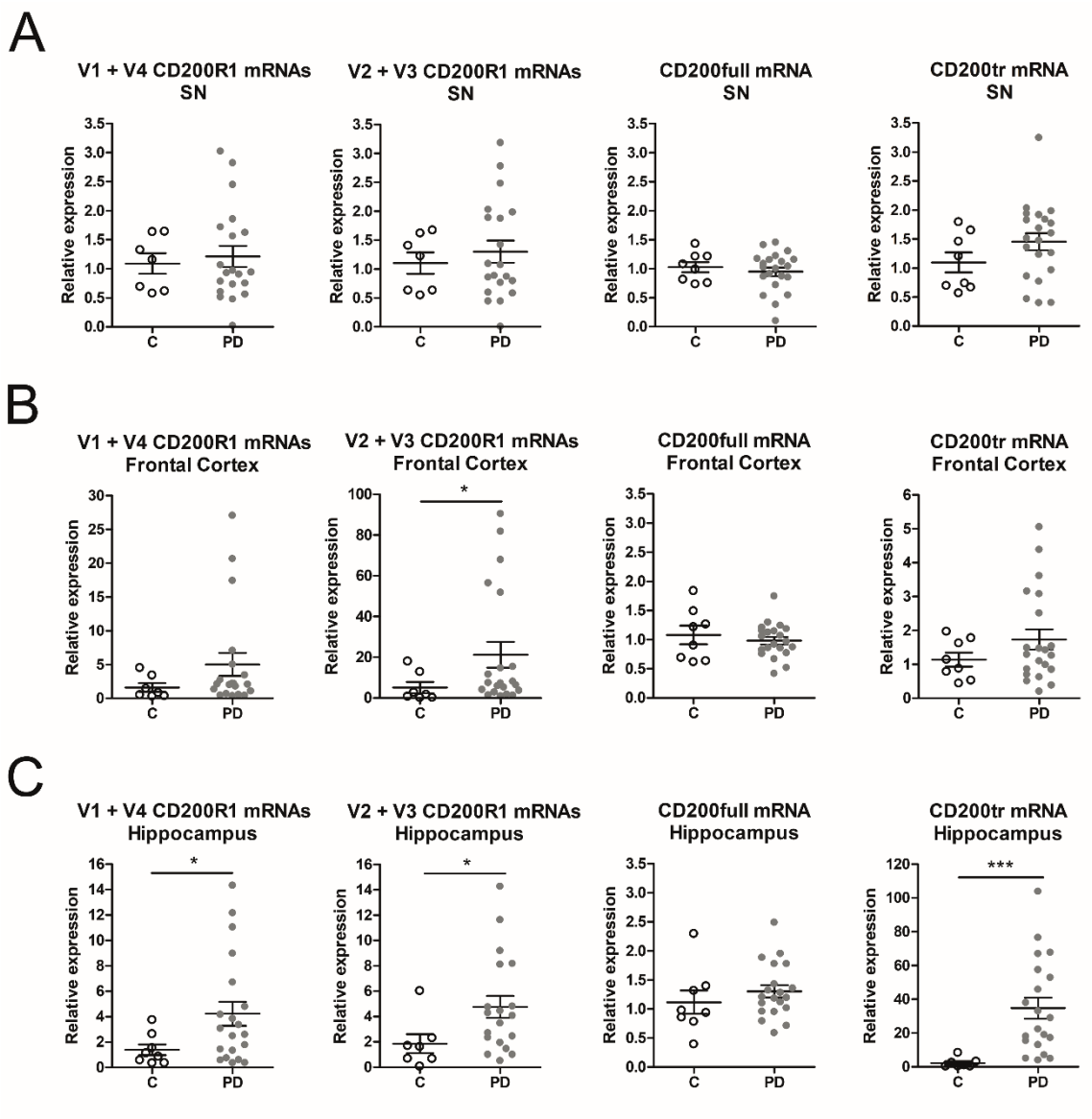

Figure 4.6. CD200R1 and CD200 mRNA expression in human *post-mortem* PD brain. Expression of long (V1+V4) and short (V2+V3) CD200R1 mRNA variants, and CD200full and CD200tr mRNAs in the substantia nigra (SN) (**A**), frontal cortex (**B**) and hippocampus (**C**) homogenates from control individuals (C, n=7-8) and Parkinson's disease patients (PD, n=19-21). GAPDH and RPS18 were used as reference genes. Data are expressed as fold change to C and are depicted as individual points with bars showing means ± SEM. *p<0.05, ***p<0.001 vs. C; unpaired t test with Welch's correction.

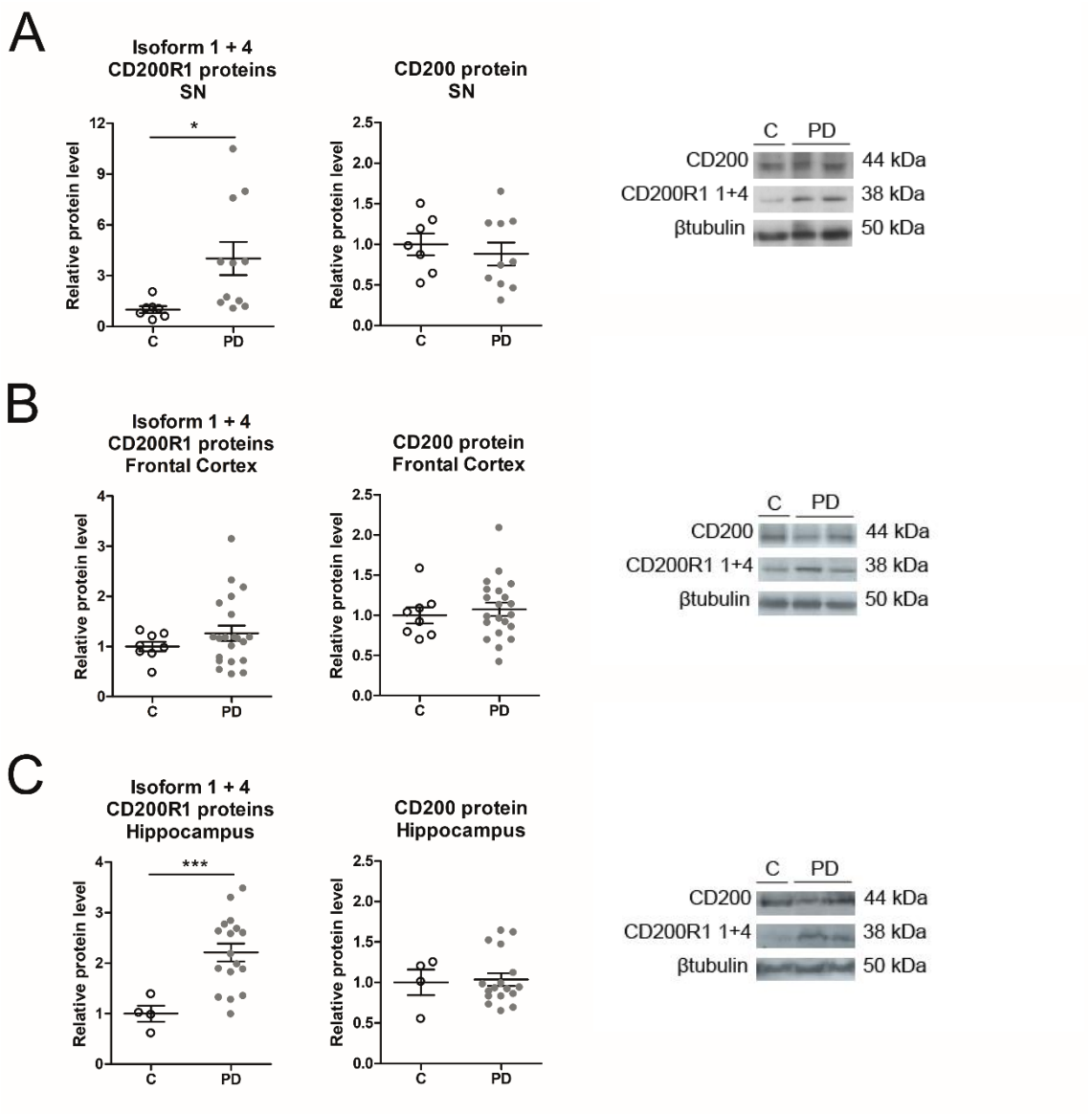

Figure 4.7. CD200R1 and CD200 protein levels in human *post-mortem* PD brain. Expression of isoform 1 and 4 CD200R1 and CD200 protein in the substantia nigra (SN) (**A**), frontal cortex (**B**) and hippocampus (**C**) homogenates from control individuals (C, n=4-8) and PD patients (n=11-21). Representative immunoblots are presented. Protein levels were normalized relative to βtubulin. Data are expressed as fold change to C and are depicted as individual points with bars showing means ± SEM. *p<0.05 and ***p<0.001 vs. C; unpaired t test with Welch's correction.

The results obtained were further analysed taking into account the clinical and the anatomopathological data available (Table 4.4).

Table 4.4. Clinical and anatomopathological data of cases. Information provided by the *Banc de Teixits Neurològics* (Biobanc, Hospital Clínic de Barcelona, IDIBAPS).

Case No.	Gender	Age (yrs)	PMD (h)	AP diagnosis	Clinical diagnosis	Age of onset (yrs)
C1	Male	78	6:00	Multi-infarct Leukoencephalopathy		
C2	Male	83	13:00	AgD I (mild)		
C3	Female	56	14:00	Brain metastasis oat cell lung cancer + NFT I-II		
C4	Female	86	4:00	Right vertebral thrombosis + cerebellar bulbar ictus + NFT III		
C5	Female	82	20:00	AgD III + NFT III + vascular encephalopathy		
C6	Female	90	12:20	Brainstem haemorrhage + SVD + ARP IIIB + TDP43 CA1		
C7	Male	78	6:00	iLBD Braak 1 + NFT I-II + SVD		
C8	Male	76	11:30	AgD I (minimal)		
PD1	Male	85	12:15	LP 5 + capillary CAA + glial tau	PD + dementia	Unknown
PD2	Male	82	7:15	LP 4-5 + AgD III + ARP IV B + microinfarcts	PD + dementia	Unknown
PD3	Male	76	17:10	LP 5 + ARP IVB	PD + dementia, DBS	51
PD4	Female	86	16:04	LP 6 + ARP IIIB	Parkinsonism	81
PD5	Female	82	13:10	LP 4 + ARP IB	PD	54
PD6	Male	79	11:30	LP 3 + NFT II	PD	Unknown
PD7	Male	50	16:30	LP 5 + hypoxic neuronal damage	PD, pallidum and subthalamic nucleus DBS	27
PD8	Male	81	5:00	LP 5 + AgD I	RBD + PD + dementia	71 (RBD) 74 (PD)
PD9	Female	87	7:00	LP 6 + ARP IVB	PD + dementia	67
PD10	Male	77	12:00	LP 4 + NFT II	RBD + PD + mild cognitive impairment	74
PD11	Female	78	18:00	LP 5 + glial tau + diffuse hypoxia	PD + Arnold Chiari I + IBM	56
PD12	Male	74	8:00	LP 5 + ARP IIIB + moderate CAA	PD	55
PD13	Male	87	15:15	LP 5 + ARP IIA	PD + dementia	71
PD14	Male	78	5:15	LP 5 + ARP IIB	PD + dementia	Unknown
PD15	Male	71	5:00	LP 4 + ARP IB	PD + dementia	Unknown
PD16	Male	74	14:03	Mild LP 5 + complex tauopathy	PD + dementia + hallucinations, Right pallidotomy	39
PD17	Male	81	7:20	LP 4-5 + ARP IIA + capillary CAA	PD	Unknown
PD18	Female	83	4:00	LP 4-5 + ARP IIA	PD + dementia + hallucinations	60 (right hand tremor) 76 (hallucinations + cognitive impairment)
PD19	Male	80	16:30	LP 4 + ARP II	PD + bilateral subthalamic nucleus DBS	40

PD20	Male	62	13:30	LP 5 + ARP IIA	PD + dementia	49-50 (PD) 58 (dementia)
PD21	Male	92	16:40	LP 4-5 + ARP IIIA + SVD	PD	76 (motor symptoms)

AP diagnosis: anatomopathological diagnosis; AgD: Argyrophilic grain disease; ARP: Alzheimer's disease-related pathology: classification of neurofibrillary tangle (NFT) pathology based on Braak staging (Braak et al. 2006) (I-VI) and classification of neuritic plaques based on CERAD criteria (A-C) (Mirra et al. 1991); CAA: Cerebral amyloid angiopathy; CT: control; DBS: deep brain stimulation; h, hours; IBM: Inclusion body myositis; LP: Lewy-pathology staging, studies based on the classification of Braak (Braak et al. 2003) (1-6); iLBD: incidental Lewy body disease; PD: Parkinson's disease; RBD: REM sleep behaviour disorder; PMD: *post-mortem* delay; SVD: small vessel disease; TDP43 CA1: TAR DNA binding protein 43 in hippocampal CA1 region; yrs: years.

When analysing our cohort according to the clinical data available, we examined whether parameters such as gender, age at death, age of onset of the disease, duration of the disease or the presence of dementia had any influence on the effects observed. We observed that the changes in the expression of CD200R1, CD200full and CD200tr were independent on the gender or the presence of dementia (data not shown). We observed that the younger the patient when diagnosed with PD, the longer the duration of the disease, although the earlier the age at death (Fig. 4.8).

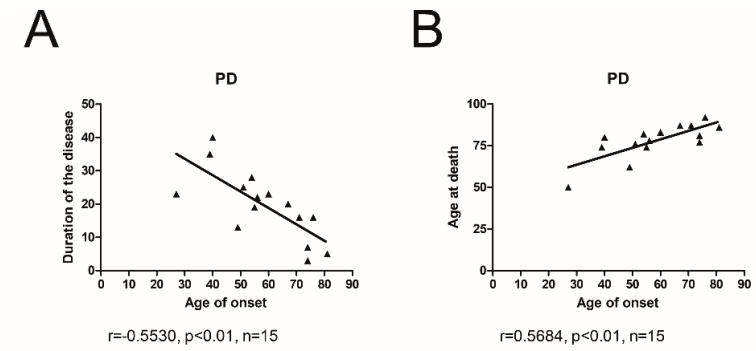

Figure 4.8. Correlations between age of PD onset and duration of the disease or age at death A Significant correlation between duration of the disease and age of onset in PD patients (n=15). **B** Significant correlation between age at death and age of onset in PD patients (n=15). Pearson's correlation coefficient (r) and corresponding p value are indicated in the panel.

Furthermore, the younger the patient was when diagnosed with PD, which correlated with longer disease duration, the lower the CD200tr mRNA levels were in the frontal cortex in the *post-mortem* analysis (Fig. 4.9).

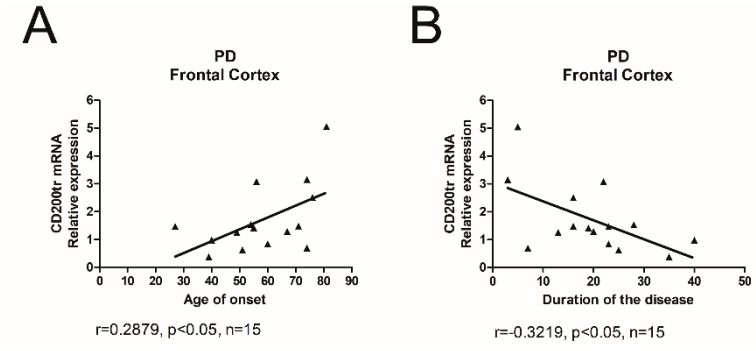

Figure 4.9. Correlation between CD200tr expression and age of onset or duration of the disease in the frontal cortex of PD patients. Significant correlation between CD200tr mRNA levels and age of onset (**A**) or duration of the disease (**B**) in the frontal cortex in PD patients (n=15). Pearson's correlation coefficient (r) and corresponding p value are indicated in the panel.

In control individuals, we observed a positive correlation between CD200R1 protein levels (isoform 1 and 4) and age in the SN (Fig. 4.10A), which was not found in PD patients (Fig. 4.10A). Moreover, negative correlations between V1 and V4 CD200R1 mRNA and age at death in the hippocampus (Fig. 4.10B), and CD200 protein and age at death in the frontal cortex (Fig. 4.10C) were observed in control individuals but not in PD patients (Fig. 4.10B,C).

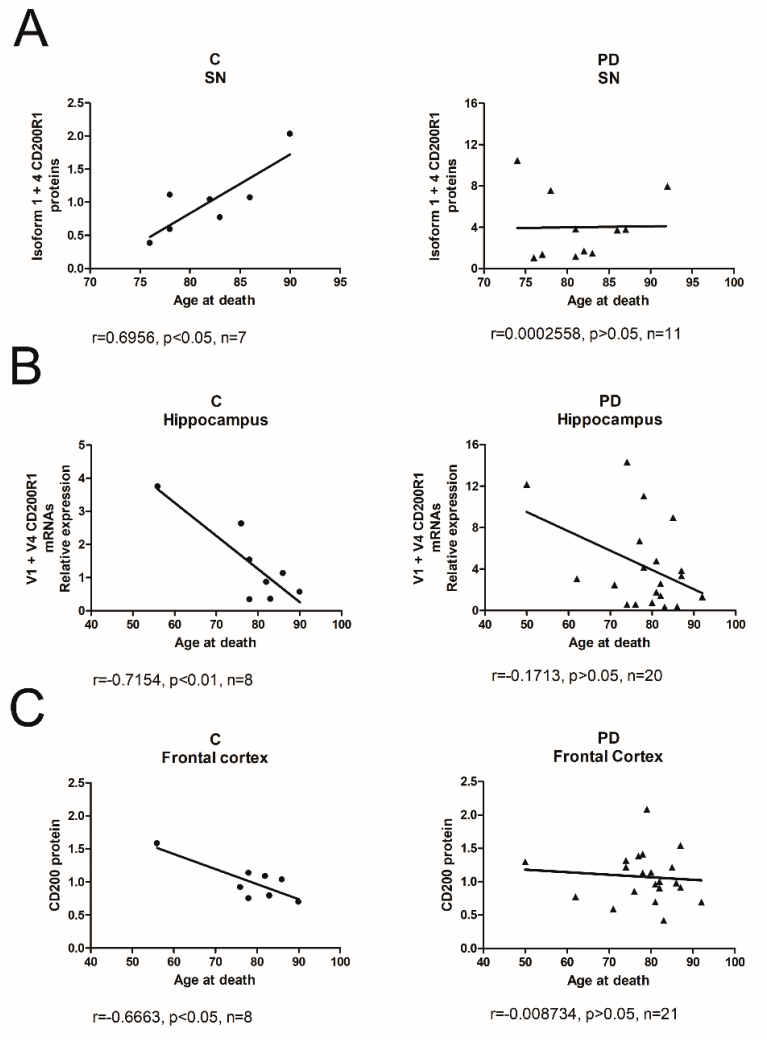

Figure 4.10. Correlation between CD200R1 and CD200 expression and age at death in PD. Significant correlation between CD200R1 protein levels (isoform 1 and 4) in the substantia nigra (SN) (**A**), significant correlation between V1 and V4 CD200R1 mRNA levels and age at death in the hippocampus (**B**) and significant correlation between CD200 protein levels and age at death in the frontal cortex (**C**) in control individuals (C, n=7-8) but not in PD patients (n=11-21). Pearson's correlation coefficient (r) and corresponding p value are indicated in the panel.

We examined whether the changes observed in CD200R1 and CD200 expression were influenced by the Lewy-pathology (LP) stage or the presence of Alzheimer's disease -related pathology such as neurofibrillary tangles (NFT) degeneration and neuritic plaques (NP).

Concerning LP staging [LP 1 (medulla oblongata), 2 (medulla oblongata and pontine tegmentum), 3 (midbrain), 4 (basal prosencephalon and mesocortex), 5 and 6 (neocortex) stage] (Braak et al. 2003), higher levels of V2 and V3 CD200R1 (Fig. 4.11A) and CD200tr (Fig. 4.11B) mRNA were observed in the hippocampus of PD patients at advanced LP stages (4-5, 5) than at early LP stages (4). In the SN and frontal cortex no differences in the expression of long and short

CD200R1 variants, CD200full or CD200tr were found among the different LP stages (data not shown).

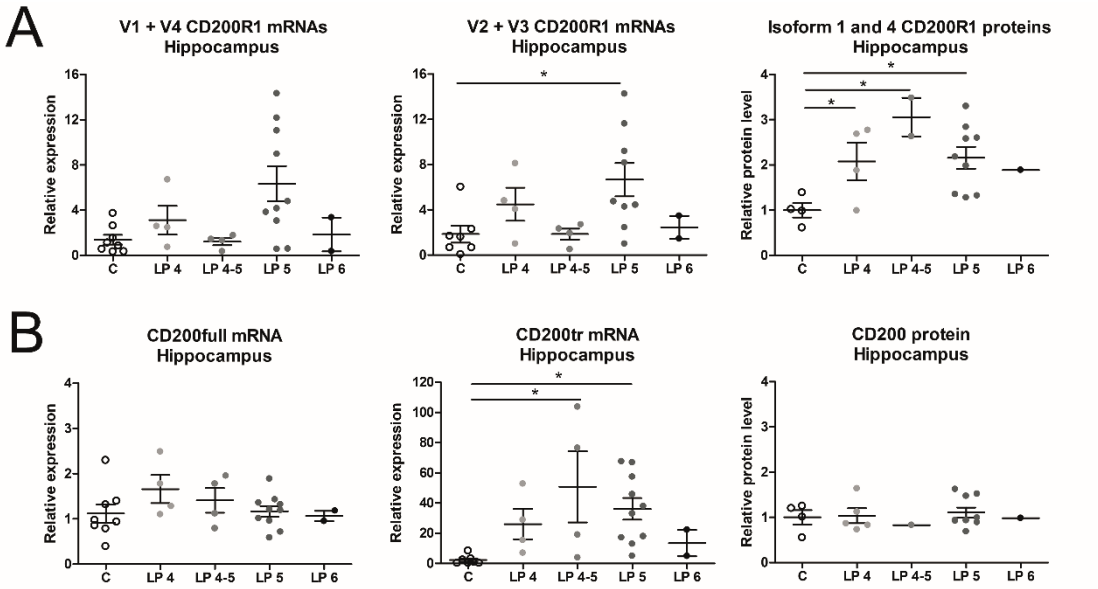

Figure 4.11. CD200R1 and CD200 expression in the hippocampus of PD patients according to LP stage. CD200R1 mRNAs and protein expression (**A**) and CD200 mRNAs and protein expression (**B**) in control (C, n=4-8) and PD patients grouped according to the Lewy-pathology (LP) stage (LP 4, LP 4-6, n=1-10). GAPDH and RPS18 were used as reference genes in mRNA analysis. Protein levels were normalized relative to βtubulin. Data are expressed as fold change to C and are depicted as individual points with bars showing means ± SEM. *p<0.05 vs. C; one-way ANOVA and Newman-Keuls post-test.

As regards AD-related pathology in PD patients, we analysed the changes observed in CD200R1 and CD200 expression according to the neurofibrillary stage (NFT I, II (transentorhinal areas), III, IV (limbic areas), V and VI (isocortical areas) stage) (Braak et al. 2006) or the neuritic plaque score (score A (sparse), score B (moderate) and frequent neuritic plaques (score C)) (CERAD criteria (Mirra et al. 1991) of the PD patients.

We observed that the CD200R1 and CD200 expression in the SN and hippocampus changed with NFT stage. In the SN, the highest level of CD200R1 protein was found in NFT III stage (Fig. 4.12A), and in the hippocampus the highest levels of CD200tr mRNA and CD200R1 protein were observed in NFT II stage (Fig. 4.12B). No correlation between CD200 or CD200R1 levels of expression and neurofibrillary degeneration stage in the frontal cortex was detected (data not shown).

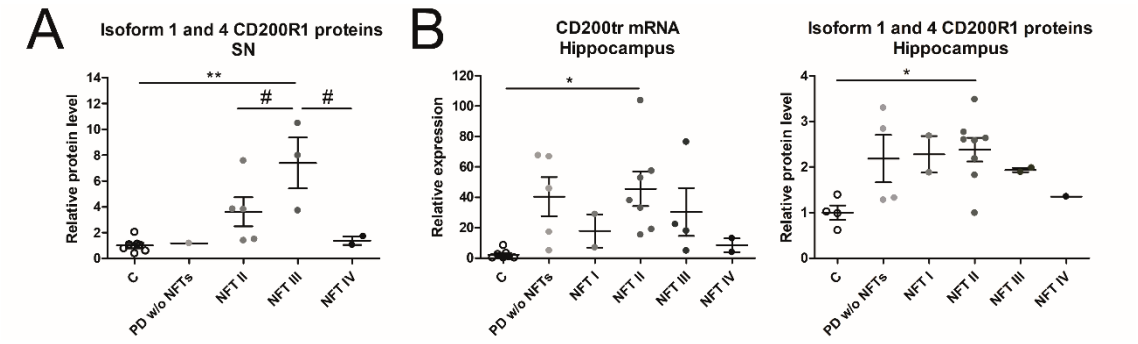

Figure 4.12. CD200R1 and CD200 expression in the SN and hippocampus of PD patients according to AD-related neurofibrillary pathology. Expression of CD200R1 protein in the substantia nigra (SN) (**A**), and CD200tr mRNA and CD200R1 protein in the hippocampus (**B**) of control individuals (C, n=4-7) and PD patients grouped according to the AD-related neurofibrillary tangle (NFT) pathology (PD patients without NFT (PD w/o NFTs, n=1-8) and PD patients with neurofibrillary tangles (NFT I-VI stage, n=1-7). GAPDH and RPS18 were used as reference genes in mRNA analysis. Protein levels were normalized relative to βtubulin Data are expressed as fold change to C and are depicted as individual points with bars showing means ± SEM. *p<0.05 and **p<0.01 vs. C and #p<0.05 vs. NFT III; one-way ANOVA and Newman-Keuls post-test.

With regard to the neuritic plaques score, we observed that in the hippocampus of PD patients, the highest increases of CD200tr and CD200R1 protein were detected in cases without Alzheimer's disease-related pathology or with sparse neuritic plaques (score A) (Fig. 4.13).

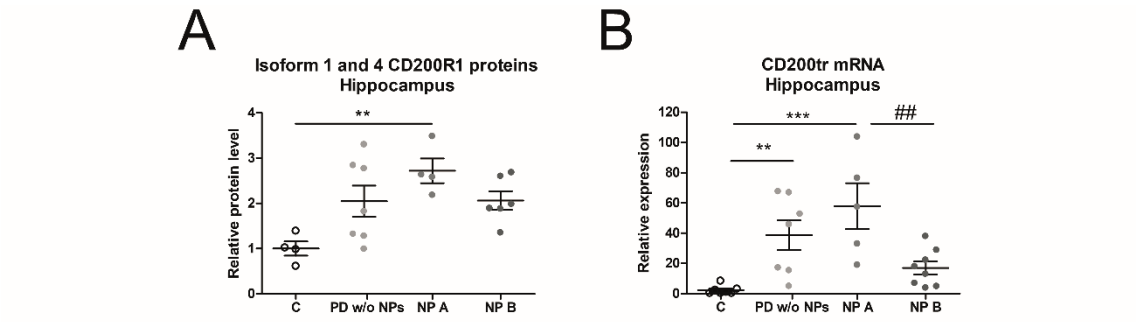

Figure 4.13. CD200R1 and CD200 expression in the hippocampus of PD patients according to neuritic plaque score. Expression of CD200R1 protein (**A**) and CD200tr mRNA (**B**) in the hippocampus of control individuals (C, n=4-7) and PD patients grouped according to the neuritic plaque (NP) score (PD patients without NPs (PD w/o NPs, n=4-8) and PD patients with neuritic plaques (NP A, NP B, NP C, n=4-6). GAPDH and RPS18 were used as reference genes in mRNA analysis. Protein levels were normalized relative to βtubulin. Data are expressed as fold change to C and are depicted as individual points with bars showing means ± SEM. **p<0.01 and ***p<0.001 vs. C and ##p<0.01 vs. NP A; one-way ANOVA and Newman-Keuls post-test.

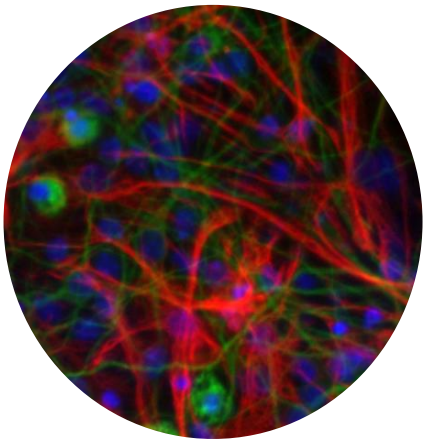

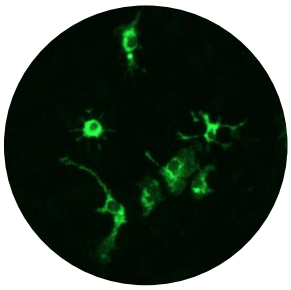

Discussion

1 Effect of CD200-CD200R1 alterations on glial activation and dopaminergic neurodegeneration using *in vitro* approaches

1.1 INHIBITION OF CD200-CD200R1 SYSTEM IN GLIAL CELL CULTURES USING AN ANTI-CD200 BLOCKING ANTIBODY. EFFECT ON GLIAL ACTIVATION

In this study, we aimed at characterizing the implication of the CD200-CD200R1 system on the modulation of the microglial inflammatory response in mixed glial cultures. Firstly, we determined the expression pattern of CD200R1, CD200full and CD200tr under a pro-inflammatory stimulus (LPS/IFNγ). Upon LPS/IFNγ treatment, we observed a decreased CD200R1 and an increased CD200tr expression. Hence, in response to a pro-inflammatory stimulus, microglial cells down-regulate the CD200R1 receptor and astroglial cells do not modify the expression of CD200full ligand but up-regulate its antagonist, CD200tr, which blocks CD200R1. Altogether, these effects may facilitate the pro-inflammatory response.

Previous reports from our laboratory already showed that basal CD200R1 expression is observed in microglial cells from microglial and mixed glial cultures and that it is inhibited in response to LPS or LPS/IFNγ (Dentesano et al. 2014; Dentesano et al. 2012). One of these reports also demonstrated that CD200 is constitutively expressed in astrocytes from mixed glial cultures and that LPS/IFNγ increases CD200 expression in astrocytes but not in neurons (Dentesano et al. 2014). In this study, the increased CD200 expression upon LPS/IFNγ was interpreted as an unsuccessful compensatory response to recover CD200-CD200R1 function alterations. However, the qPCR primers and the WB antibody used in the article detected both CD200full and CD200tr (Dentesano et al. 2014). In the present study, we have demonstrated that the increase in CD200 expression induced by LPS/IFNγ is due to an increase in CD200tr and not to CD200full expression. In consequence, glial cells clearly respond to LPS/IFNγ by increasing CD200tr, decreasing CD200R1 whereas CD200full expression is not modified. All these effects point to the same direction, the inhibition of the CD200-CD200R1 system upon a pro-inflammatory stimulus.

A previous report described a decreased CD200 mRNA expression in the hippocampus of mice 4 hours after intraperitoneal injection of LPS (Lyons et al. 2009), again with no specification on whether CD200full, CD200tr or both mRNA variants were analysed. Another report studying CD200 mRNA expression in brains of mice injected with LPS intraperitoneally showed an increase, no alterations and a decrease in CD200 mRNA levels at 4 hours, 1 day and 1 year post inoculation, respectively (Masocha 2009). In this case, the primers used detected both CD200full

and CD200tr and this was not taken into account in the discussion. In general, most studies do not specify which CD200 is analysed and caution must be taken in the interpretation of the results obtained, as CD200full and CD200tr have opposite functions.

Low levels of CD200 and CD200R1 have been observed in *post-mortem* human brain from Alzheimer's disease (Walker et al. 2009) and multiple sclerosis patients (Koning et al. 2007; Koning et al. 2009) and inflammatory activation of microglia has been extensively described in these diseases (McGeer and McGeer 1998; Lassmann et al. 1998; Bitsch et al. 2000; Sastre, Klockgether, and Heneka 2006; Xiang et al. 2006), suggesting a possible role of the CD200-CD200R1 system in this chronic inflammation. Specifically, Walker and collaborators reported a decreased CD200R1 mRNA expression and a decreased CD200 mRNA and protein expression in Alzheimer's disease hippocampus, inferior temporal gyrus but not cerebellum, although they did not specify which CD200 isoform was analysed (Walker et al. 2009). Koning and collaborators demonstrated no changes in CD200R1 mRNA expression, decreased CD200 mRNA expression (CD200full, deduced from qPCR primers) and decreased CD200-immunostiaining in the center of chronic multiple sclerosis white matter lesions (Koning et al. 2007; Koning et al. 2009). Since CD200full and CD200tr have opposite functions, together with the results we obtained in mixed glial cultures after LPS/IFNγ treatment, suggest that identifying whether CD200full or CD200tr is altered in these diseases would be interesting in order to know the functional consequences of these alterations.

With the aim of further understanding the consequences of the decreased CD200 and/or CD200R1 expression observed in Alzheimer's disease and multiple sclerosis (Walker et al. 2009; Koning et al. 2007; Koning et al. 2009), we evaluated the effect of CD200-CD200R1 disruption using two complementary *in vitro* strategies (anti-CD200 blocking antibody and CD200-deficient mice) in different *in vitro* scenarios (microglial, mixed glial and mesencephalic neuronal cultures).

We have found that concentrations of anti-CD200 blocking antibody, that did not affect cell viability in primary mixed glial cultures, did not result in the induction of a pro-inflammatory response *per se* but it potentiated IL1β, COX2 and IL6 mRNA expression induced by LPS/IFNγ. Despite no effects at protein level or NO production, the mRNA results indicate that CD200R1 may be a potential target to modulate neuroinflammation. Supporting this, previous studies have demonstrated that anti-CD200 blocking antibodies potentiate the pro-inflammatory response. An *in vitro* study showed that amyloid β-induced glial cell activation was attenuated by the addition of CD200-expressing neurons, and this effect was inhibited by an anti-CD200 blocking antibody (Lyons et al. 2007). In *in vivo* studies, anti-CD200 blocking antibody increased CNS inflammation and neurodegeneration in an experimental mouse model of multiple sclerosis (Chitnis et al. 2007) and aggravated the pathology in an experimental auto-immune uveoretinitis rat model (Banerjee and Dick 2004). In all these studies, neuronal CD200 is present and the level of expression of CD200 in neurons is much higher than in astrocytes (Dentesano et al. 2014). Consequently, anti-

CD200 blocking antibody is expected to have a more relevant effect on microglia activation when neurons are present. We can hypothesize that the potentiation by an anti-CD200 blocking antibody of LPS/IFNγ-induced effects at mRNA, but not at protein level, may be attributed to the absence of neuronal CD200 in our experimental model. In this conditions, astrocytic CD200 might not be enough to potentiate microglial activation at protein level. Interestingly, the use of anti-CD200 blocking antibody is also being studied in cancer research in order to potentiate the immune system to fight against tumours, such as acute myeloid leukemia (Pallasch et al. 2009; Coles et al. 2011). Regarding this, clinical trials with Samalizumab, an anti-CD200 blocking antibody, for cancer therapy are in study (Alexion Pharmaceuticals). All these data point out the potential therapeutic effects of anti-CD200 blocking antibodies to modulate the CD200-CD200R1 system.

1.2 GLIAL CELL CULTURES FROM CD200-DEFICIENT MICE. EFFECT ON GLIAL ACTIVATION

In the present study, we set out to evaluate *in vitro* the changes on glial activation that accompany the loss of CD200 in astrocytes to better understand the mechanisms that modulate microglial function. Firstly, we showed that mixed glial cultures from CD200 -/- mice had the same cellular composition as that from CD200 +/+ mice. Then, we observed that CD200-deficiency had no repercussion *per se* in the basal levels of pro- or anti-inflammatory markers neither in mixed glial nor in microglial cultures. Furthermore, pro- (IFNγ, LPS, LPS/IFNγ) and anti- (IL4) inflammatory stimuli had the same effect on mixed glial cultures from CD200 -/- and CD200 +/+ mice. Similarly, IFNγ and IL4 had the same effect in microglial cultures prepared from CD200 -/- or CD200 +/+ mice. However, CD200 -/- microglial cultures exhibited a greater LPS-induced TNFα, COX2 and IL10 mRNA expression and LPS/IFNγ-induced TNFα mRNA expression.

There are previous reports studying the glial cells from CD200 -/- mice under resting conditions. The CD200 knock-out murine colony used in the following articles from the literature has the same origin as the one used in the present thesis. Regarding cell number, *in vivo* studies have shown an increase in the number of microglial cells in the retina of CD200 -/- mice (Broderick et al. 2002). The few *in vitro* studies using CD200 -/- mice did not show increased proportion of microglial cells in glial mixed cultures from CD200 -/- mice supporting our observations (Costello et al. 2011). Regarding basal microglial activation, *in vivo* studies have described that microglia from CD200 -/- mice exhibit features of activation under resting conditions including morphological changes and up-regulation of pro-inflammatory markers (Hoek et al. 2000; Denieffe et al. 2013). However, *in vitro* studies failed to demonstrate this basal activation phenotype in mixed glial or microglial cultures (Costello et al. 2011; Lyons et al. 2017), according to our findings.

Strikingly, we have observed that CD200 inhibition with an anti-CD200 blocking antibody potentiates the pro-inflammatory response of glial cells to LPS/IFNγ whereas knocking-out CD200 had no repercussion on this response. This may be explained because in CD200 knock-out mice CD200 has never been present and the function of the CD200-CD200R1 pathway could be compensated by alternative mechanisms. In contrast, the sudden inhibition elicited by an anti-CD200 blocking antibody may have stronger effects. Regarding the response to other pro-inflammatory stimuli, previous studies reported a more pronounced increase in LPS-induced IL1β, IL6 and TNFα cytokine levels (Costello et al. 2011) and IFNγ-induced TNFα protein (but not mRNA) expression (Denieffe et al. 2013) in mixed glial cultures from CD200 -/- mice compared to wild-type cultures. However, in our experiments, LPS and IFNγ increased the mRNA expression of pro-inflammatory markers to the same extent in mixed glia prepared from CD200 -/- and CD200 +/+ mice. Differences in LPS treatment duration (6 h in our study vs. 24 h) and in IFNγ concentration and treatment duration (0.1 ng/mL for 6 h in our study vs. 50 ng/mL for 24 h) could underlie different outcomes. Also, these articles did not explain which wild-type mice were used as controls, what can be a source of bias. Note that we used wild-type mice on a matched genetic background.

In contrast to glial mixed cultures, in microglial cultures we have found a potentiation of the pro-inflammatory response to LPS/IFNγ and LPS in CD200 -/- cultures. This leads to the hypothesis that knock-out mice may have primed microglial cells but unaltered astrocytic response, which makes mixed glial cultures not sensitive enough to measure specifically microglial alterations that are only detected in a purified microglial culture. This is supported by a previous study reporting no differences in the pro-inflammatory response to IFNγ treatment between purified astrocytic cultures from CD200 +/+ and CD200 -/- mice (Denieffe et al. 2013). Since in microglial cultures CD200 ligand is not present, the results obtained suggest an intrinsic microglial alteration in CD200 -/- mice that does not depend on the presence of CD200. Previous studies also showed an effect of CD200 -/- in microglial cultures (Denieffe et al. 2013; Lyons et al. 2017), or even a greater effect in microglial than mixed glial cultures (Denieffe et al. 2013). However, some of our results are not in agreement with previous findings. It has been reported no potentiation of LPS-induced IL1β, IL6 and TNFα mRNA expression in microglial cells from CD200 -/- mice (Costello et al. 2011). Whereas we obtained the same findings for IL1β and IL6, we did observe a potentiation of the LPS-induced increase in TNFα mRNA levels in CD200 -/- microglia. Another study described no alterations in IFNγ-induced iNOS and a potentiation of IFNγ-induced TNFα mRNA expression in microglial cells from CD200 -/- mice (Denieffe et al. 2013) while we did not observe any differential IFNγ effect in CD200 -/- microglia. Again, differences in LPS and IFNγ concentration and duration of the treatment, as well as, the genetic background of the wild-type mice used could explain these discrepancies.

Since the up-regulation of CD200 expression on neurons has been suggested to mediate IL4 modulation of microglial activation (Lyons et al. 2007; Lyons et al. 2009), we studied whether

CD200-deficiency had an effect on IL4-induced anti-inflammatory markers in glial cultures. IL4 increased the expression of anti-inflammatory markers to the same extent in mixed glial and microglial cultures prepared from CD200 -/- or CD200 +/+ mice. These results suggest a differential role of neuronal and astrocytic CD200 on the modulation of microglial activation by IL4. These results are in concordance with a previous study (Denieffe et al. 2013) that reported no differences in the induction of arginase1 and MR mRNA expression between CD200 +/+ and CD200 -/- mixed glial cultures. However, Yi and collaborators reported that inhibition of CD200R1 prevents from IL4-induced IL10 in BV2 cultures (Yi et al. 2016).

1.3 EFFECT OF CD200-DEFICIENCY ON THE INDUCTION OF NEURONAL DEATH

Mounting evidence supports that innate immunity, especially microglial cells, may contribute to neurodegeneration in PD (Dauer and Przedborski 2003; Hirsch and Hunot 2009) and mesencephalic cultures have been increasingly used to analyse the mechanisms by which microglia facilitate dopaminergic neuronal death. Epidemiologic studies have implicated the exposure to pesticides including rotenone as a risk factor for PD (Betarbet, Sherer, and Greenamyre 2002; Langston 2002). Moreover, mitochondria may also participate in cell death in PD (Orth and Schapira 2002; Swerdlow et al. 1996). Here, the mitochondrial complex I inhibitors rotenone and MPP+ were used to trigger dopaminergic cell death in mesencephalic cultures. We studied whether the disruption of the CD200-CD200R1 system in mesencephalic cultures had an effect on MPP+- or rotenone-induced neuronal death.

We have shown that MPP+ or rotenone reduced dose-dependently the number of TH-positive cells in primary mesencephalic cultures and that this toxicity was selective for TH-positive cells at lower doses. Previous reports also showed that midbrain dopaminergic neurons are selectively sensitive to MPP+ and rotenone (Koutsilieri et al. 1995; Michel et al. 1989; Mytilineou, Cohen, and Heikkila 1985; Sanchez-Ramos et al. 1986; Saporito et al. 1992; Gao et al. 2002). We found that rotenone killed dopaminergic neurons with higher potency than MPP+ in mesencephalic cultures. This result confirmed previous reports and may be attributed to the higher lipophilic properties of rotenone and/or to the fact that rotenone, in contrast ot MPP+, is not sequestered into synaptic vesicles (Ahmadi et al. 2003; Lannuzel et al. 2003; Ren et al. 2005; Dauer et al. 2002).

We found that the CD200-deficiency in mesencephalic cultures was associated with higher microglial content and increased MPP+-induced neurotoxicity. It has been reported that, adding microglial cells to mesencephalic cultures, MPP+ induces a stronger loss of dopaminergic neurons (Kinugawa et al. 2013; Gao et al. 2002). We hypothesise that CD200-deficiency may

lead to a higher number of microglial cells and more primed microglia in mesencephalic cultures, both contributing to neurotoxicity. Further studies are required to fully elucidate the inflammatory properties of CD200-deficiency in mesencephalic cultures.

2 Effect of MPP+ and rotenone on glial activation and on the CD200 - CD200R1 system

In the present study, we show that the response of glial cells to a pro- and anti-inflammatory stimulus was modified by the neurotoxic agents MPP+ and rotenone. In general, MPP+ and rotenone treatment did not induce *per se* a significant pro- or anti-inflammatory phenotype in primary mixed glial and microglial cultures. However, these neurotoxic agents did impair the development of a pro- and anti-inflammatory phenotype in LPS/IFNγ and IL4-treated glial cultures. This effect was observed in the absence of significant cell death but in the presence of impaired metabolic activity.

The toxic effects of MPP+ and rotenone on neurons have been repeatedly demonstrated using primary neuronal cultures, with dopaminergic neurons showing the highest sensitivity to the toxic effects of these compounds. In mouse primary cultures, dopaminergic neuron death is observed at concentrations from 0.1 µM MPP+ (one week exposure) (Kinugawa et al. 2013) or 3 µM MPP+ (48 h exposure) (Henze et al. 2005), and 10 nM (one week exposure) (Gao et al. 2003a) or 5 nM rotenone (48 h exposure) (Radad, Rausch, and Gille 2006). Exposure to higher concentrations of these neurotoxins is necessary to induce the death of non-dopaminergic neurons (Gao et al. 2003a; Henze et al. 2005). The presence of microglial cells in neuronal cultures has been associated to increased MPP+ and rotenone neurotoxicity (Emmrich et al. 2013; Gao et al. 2002; Gao et al. 2003a; Kinugawa et al. 2013). However, as MPP+- and rotenone-damaged neurons induce microglial activation, which has a neurotoxic effect, it is difficult to establish the contribution of a direct effect of the toxins on glial cells in the neurotoxicity observed.

In fact, although the neurotoxic effect of MPP+ and rotenone has been widely described using *in vivo* and *in vitro* experimental approaches, their direct effects on glial cells remain poorly characterized (Bournival et al. 2012; Chen et al. 2015; Du et al. 2014; Gao et al. 2003a; Klintworth, Garden, and Xia 2009; Zhou et al. 2016). Most of the studies performed until now using glial cell cultures have tested whether these neurotoxins induce a pro-inflammatory phenotype in microglial cells, and the results obtained are controversial. The range of concentrations used in these studies is higher than that used in neuronal cultures (0.1-500 µM MPP+ and 10 nM-1 µM rotenone) (Bournival et al. 2012; Du et al. 2014; Gao et al. 2003a; Henze et al. 2005; Jin et al. 2012; Klintworth, Garden, and Xia 2009). Some authors have reported no alterations (Ferger et al. 2010; Jin et al. 2012; Klintworth, Garden, and Xia 2009), but others have shown the induction of pro-inflammatory markers in MPP+- and rotenone-treated microglial cultures (Du et al. 2014; Liang et al. 2015; Zhang et al. 2014; Zhou et al. 2016). Differences in the pattern of neurotoxin treatment (concentration and duration of the treatment) and the cell types used (primary cultures

and cell lines from different species) may partially account for the differences observed. Most studies have considered microglial cell lines, while studies using primary microglial cultures are scarce.

2.1 PRO-INFLAMMATORY RESPONSE

In the present study, we show that concentrations of MPP+ and rotenone that did not affect cell viability in primary glial cultures at 24 h did not result in the induction of a significant pro-inflammatory phenotype (with the exception of IL6 production), but they interfered with the development of the pro-inflammatory phenotype induced by LPS/IFNγ. Thus, MPP+ and rotenone inhibited pro-inflammatory cytokine production induced by LPS/IFNγ in glial cells (IL1β in the case of MPP+, and also IL6 and TNFα in the case of rotenone). They also modified the expression of pro-inflammatory enzymes (iNOS, COX 2 and/or gp91phox). In general, the alterations observed were more pronounced in mixed glia than in microglial cell cultures. In addition, the effect of rotenone was stronger than that of MPP+, although the concentrations of rotenone used were three orders of magnitude below those of MPP+. MPP+ and rotenone treatment also interfered in the phagocytic activity of microglial cells, which was clearly inhibited after neurotoxin treatment, especially in the presence of LPS/IFNγ. Altogether, these results suggest that MPP+ and rotenone directly impair the ability of glial cells to respond to a pro-inflammatory insult. In this sense, exposure to stimuli that affect mitochondrial activity, such as hypoxia or respiratory chain inhibitors, has been suggested to alter the immune response of macrophages (Wiese et al. 2012).

At the cellular level, the main target of both MPP+ and rotenone is the mitochondrial electron transport chain, where they selectively inhibit complex I (Dauer and Przedborski 2003). As a consequence, ATP production is compromised, O_2^- levels increase, and subsequent oxidative stress occurs. This is critical in neuronal cells, where energy production mainly depends on ATP synthesis through oxidative phosphorylation (Belanger, Allaman, and Magistretti 2011a). In contrast, astrocytes are mainly glycolytic (Belanger, Allaman, and Magistretti 2011a). In addition, astrocytes can generate lactate from glycogen via glycolysis under metabolic activation (Hertz, Peng, and Dienel 2007). Macrophages/microglia have the capacity to generate ATP by both glycolytic and oxidative pathways (although in the case of microglial cells the field is still underexplored) (Ghosh et al. 2018; Van den Bossche, O'Neill, and Menon 2017). Indeed, they are able to shift from oxidative phosphorylation to aerobic glycolysis (production of lactate in the presence of oxygen) to obtain ATP from different pathways according to the metabolic demands of their activation status (Galvan-Pena and O'Neill 2014; Haschemi et al. 2012; Orihuela, McPherson, and Harry 2016). The classical activation or M1/pro-inflammatory phenotype is associated with inhibition of the respiratory chain and the potentiation of aerobic glycolysis, which results in more rapid ATP production to satisfy the metabolic demands associated with the quick pro-inflammatory response of the M1 phenotype. In this situation, the glycolytic and pentose

phosphate pathways are potentiated and oxidative phosphorylation is inhibited (Haschemi et al. 2012). A metabolic-epigenetic crosstalk is suggested to control macrophage activation (Baardman et al. 2015). In contrast, pro-inflammatory stimuli increase tricarboxylic acid activity in astrocytes (Gavillet, Allaman, and Magistretti 2008).

In mixed glial cultures, LPS/IFNγ treatment increased intracellular ATP levels, an effect that was clearly inhibited by MPP+ and rotenone. These results suggest that MPP+- and rotenone-treated cultures suffer metabolic stress that is aggravated when the cells increase their energetic demands after LPS/IFNγ treatment. Consequently, activated glial cells may not fulfill their metabolic demands in the presence of MPP+ and rotenone, which would explain why mixed glial cultures exposed to these toxicants were not able to give an appropriate pro-inflammatory response to LPS/IFNγ. The effects of MPP+ and rotenone on intracellular ATP levels were less drastic in LPS/IFNγ-treated microglial than mixed glial cultures. ATP levels were not significantly compromised in LPS/IFNγ-treated microglial cultures exposed to MPP+ and rotenone, with the exception of 25 μM MPP+ treatment. In addition, the response to LPS/IFNγ was also impaired to a lesser extent in microglial cultures than in mixed glial cultures. Altogether, these results suggest that microglial cells can better cope with the metabolic alterations induced by MPP+ and rotenone than astrocytes, which account for 75% of cells in mixed glial cultures. A possible explanation is that while microglial cells developing a pro-inflammatory phenotype switch to glycolysis (Galvan-Pena and O'Neill 2014; Haschemi et al. 2012; Orihuela, McPherson, and Harry 2016), astrocytes exposed to pro-inflammatory stimuli increase the activity of the tricarboxylic acid cycle (Gavillet, Allaman, and Magistretti 2008), which in the presence of MPP+ and rotenone will encounter truncated oxidative phosphorylation. However, the involvement of a differential response of activated microglial cells to the toxins in the presence of astrocytes (or impaired astrocytes) cannot be ruled out.

To assess whether the glycolytic switch mentioned above was behind the ATP production in activated glial cultures, we evaluated the expression of genes encoding critical proteins for the glycolytic pathway. In microglial cultures, a switch to the glycolytic pathway in LPS/IFNγ-activated microglial cultures was suggested by the observed increase in expression of Glut1, HK1, Pfk1 and Hif1α mRNA and the decreased expression of Carkl mRNA. Increased expression of the glucose transporter Glut1 may result in more glucose uptake, while the increased expression of Hk1 and Pfk1, which regulate critical steps in glycolysis, may increase the glycolytic rate. It has been suggested that hypoxia-inducible factor activation contributes to macrophage polarisation, and that Hifα-dependent glycolysis favors polarisation to an M1 phenotype (Palazon et al. 2014; Taylor et al. 2016). In addition, metabolic intermediates such as succinate play a role in Hif1α stabilization and subsequent IL1β expression in LPS-treated macrophages (Tannahill et al. 2013). Inhibition of Carkl expression potentiates the flux through the pentose phosphate pathway (Haschemi et al. 2012). Whereas MPP+ exposure resulted in a further increase in Glut1 expression in LPS/IFN-γ-treated microglial cultures, rotenone exposure partially inhibited

LPS/IFNγ-induced Pfk and Hifα mRNA expression. Consequently, in the case of microglial cultures, the attenuated pro-inflammatory response to LPS/IFNγ mostly observed in the presence of rotenone may result from some alterations to the glycolytic switch. In addition, it cannot be ruled out that ATP production through oxidative phosphorylation may also partially contribute to the energy demand required to develop a pro-inflammatory response, even in situations where the switch to glycolysis occurs. In this sense, Wang and collaborators showed that 2-deoxyglucose, which blocks glycolysis and partially inhibits glycolytic-dependent oxidative phosphorylation, has a stronger inhibitory effect on the IFNγ-induced inflammatory response in macrophages than inhibiting glycolysis when replacing glucose in the cell culture medium with galactose, which reduces glycolytic flux without interfering with oxidative phosphorylation (Wang et al. 2018). Interestingly, control of the pro-inflammatory macrophage response through metabolic reprogramming has been suggested as a potential therapeutic strategy to promote remission in chronic inflammatory diseases (Mills and O'Neill 2016).

We observed contrasting effects in LPS/IFNγ treated mixed glia and microglial cultures in terms of the mRNA expression of the glycolytic enzymes Glut1, Hk1, and Pfk1. Their expression was inhibited in mixed glia, suggesting the contribution of astrocytes to the effects observed. Although astrocytes are mainly glycolytic and have preference for the production of lactate (Belanger, Allaman, and Magistretti 2011a), pro-inflammatory stimuli increase tricarboxylic acid activity in astrocytes (Gavillet, Allaman, and Magistretti 2008). The decreased expression of the glycolytic enzymes we observed may reflect this switch. Consequently, the impaired response of mixed glial cultures to LPS/IFNγ in the presence of MPP+ and rotenone may be explained by the fact that oxidative phosphorylation, which would be responsible for the main ATP production from products of the tricarboxylic acid cycle, is inhibited by MPP+ and rotenone. However, the involvement of microglial cells in the response of mixed glial cultures to MPP+ and rotenone plus LPS/IFNγ cannot be ruled out.

Finally, some studies show that MPP+ causes DNA damage (Zhang, Pieper, and Snyder 1995) and oxidative DNA damage in neuronal cells (Chen et al. 2005). In addition, rotenone-induced DNA damage (Goswami et al. 2016) and DNA methylation (Scola et al. 2014) in neurons have also been described. Although there are no reports on MPP+- and rotenone-induced DNA alterations on glial cells, we cannot discard that these alterations may be behind the decreased expression of inflammatory markers we detected in LPS/IFNγ-treated glial cultures exposed to the neurotoxins.

2.2 ANTI-INFLAMMATORY RESPONSE

We have not only characterized the effect of parkinsonian neurotoxins on the glial pro-inflammatory response but also on the anti-inflammatory response. Here, we demonstrate that

the same concentrations of MPP+ and rotenone used in the study of the pro-inflammatory response resulted *per se* in the reduction of anti-inflammatory markers in glial cultures. Furthermore, these neurotoxins also impaired the development of the anti-inflammatory phenotype in IL4-treated glial cultures. MPP+- and rotenone-induced changes in the metabolic activity of glial cells may be responsible for the impairment of the immune response observed.

Interestingly, in contrast to what we observed in the study of the pro-inflammatory response, where rotenone had a stronger effect than MPP+ even though the concentrations of rotenone were three orders of magnitude below those of MPP+, here MPP+ showed the strongest effect. Thus, we can hypothesize that, although both MPP+ and rotenone are inhibitors of mitochondrial complex I, they differ in the way they impair the pro- and anti-inflammatory responses. As observed in the study of the pro-inflammatory response, these effects were more pronounced in mixed glial than in microglial cell cultures.

Previous studies reported that rotenone had no effect on LPS-induced pro-inflammatory cytokine production in primary microglial cells, but it did inhibit IL4-induced arginase activity and expression (Ferger et al. 2010). The authors also demonstrated that rotenone inhibited IL4-induced reduction of LPS-stimulated cytokine secretion. In the present study, we did not detect changes in IL4-induced Arg1 expression in microglial cultures exposed to rotenone, but we did observe a marked reduction in the expression of Arg1 and other anti-inflammatory markers in IL4-treated mixed glial cultures exposed to rotenone and MPP+. The differences between our results and those of Ferger and collaborators could be due to the lower concentration of IL4 (10 ng/mL) and the higher concentration of rotenone (200 nM) used by Ferger and collaborators (Ferger et al. 2010).

MPP+ and rotenone tended to decrease the percentage of phagocytic microglial cells, with a significant decrease observed in cells treated with both IL4 and MPP+. Regarding phagocytic activity (number of microspheres/cell), MPP+, rotenone and IL4 increased the percentage of cells showing lower phagocytic activity than control, but no additive effect was observed in the IL4-treated cultures exposed to the neurotoxins. Increased phagocytosis in BV2 cells treated with rotenone, at a concentration lower than the one used in the present study, has been reported (Zhang et al. 2014; Chang et al. 2013). Different sensitivity of this murine cell line to the effect of rotenone could account for the differences observed.

Significant changes in intracellular ATP levels were observed in mixed glial cultures treated with MPP+ or rotenone: decreased ATP levels were observed for 25 µM MPP+, while 10 and 25 µM MPP+ inhibited IL4-increased ATP levels. ATP levels were also decreased in mixed glial cultures treated with IL4 and 100 nM rotenone. These results suggest that IL4-treated mixed glial cultures do not meet the metabolic demand needed to develop an anti-inflammatory phenotype in the presence of the neurotoxins. In contrast, in the microglial cultures there were no significant changes in any of our experimental conditions, although ATP levels tended to decrease after

MPP+ or rotenone treatment. In addition, the response of microglial cultures to IL4 in the presence of the neurotoxins was not as affected as that of mixed glial cultures. Thus, microglial cells appear to be more resistant to the toxic effects of MPP+ and rotenone. Curiously, our MTT results showed that metabolic activity was reduced in the mixed glial cultures, but increased in the microglial cultures exposed to MPP+ or rotenone, suggesting that microglial cells activate alternative but less productive ATP-generating pathways or have a higher rate of ATP consumption in response to the presence of the neurotoxins.

When microglia/macrophages are activated by IL4, they acquire an anti-inflammatory or M2 phenotype. In contrast to the M1 program, in which the rapid energy requirements make glycolysis the best metabolic pathway, the M2 program requires a maintained and long-lasting energy supply, in which oxidative metabolism better cope with these energetic requirements. In contrast to the M1 phenotype, M2 macrophages have low glycolysis rates, a reduced pentose phosphate pathway and high rates of fatty acid oxidation and oxidative phosphorylation. Oxidative metabolism provides sustained energy for angiogenesis, tissue remodelling, repair and wound healing (Ghesquiere et al. 2014; Biswas and Mantovani 2012; Odegaard and Chawla 2011). The vast majority of studies describing these metabolic states of immune cells are in peripheral macrophages (O'Neill and Hardie 2013; Pearce and Pearce 2013) and very few studies have been done in microglial cells (Durafourt et al. 2012; Orihuela, McPherson, and Harry 2016; Bernhart et al. 2010; Chenais, Morjani, and Drapier 2002; Gimeno-Bayon et al. 2014; Moss and Bates 2001; Volobouéva et al. 2013; Sohn 2012). Although still underexplored, some metabolic differences are thought to exist between microglia and peripheral macrophages. Thus, while studies on microglial cells have reported increased glycolysis after an M1 stimulus similar to that observed in macrophages, no increased oxidative phosphorylation has been observed in microglial cells after an M2 stimulus (Orihuela, McPherson, and Harry 2016). Indeed, Durafourt and collaborators comparing the polarisation of human microglia and macrophages, suggested that microglial cells are more reluctant to adopt an M2 phenotype than macrophages (Durafourt et al. 2012),

After an M2 stimulus, microglial cells may be less dependent on oxidative metabolism than astrocytes and/or microglial cells exposed to complex I inhibitors may display alternative mechanisms to better handle the effect of MPP+ and rotenone than astrocytes. In this regard, in primary astrocyte cultures, the anti-inflammatory cytokines IL4 and IL10 decrease glucose utilization and enhancement of oxidation of fatty acids and ketone bodies are suggested to occur (Belanger, Allaman, and Magistretti 2011b). Therefore, a possible explanation for the highest susceptibility of mixed glial cells to complex I inhibitors after IL4 treatment could be the requirement of the respiratory chain in astrocytes as a principal source of energy under IL4 stimulus. In contrast, although a switch to oxidative metabolism has been described in macrophages (Ghesquiere et al. 2014), microglial cells do not increase the oxidative metabolism after IL4 treatment (Durafourt et al. 2012; Orihuela, McPherson, and Harry 2016). This suggests

that microglial cells are not as dependent as macrophages on oxidative metabolism to produce an M2 response and may explain the weak impairment of microglial response to IL4 when exposed to complex I inhibitors. Nevertheless, the involvement of a differential response of activated microglial cells to the toxins in the presence of astrocytes (or impaired astrocytes) cannot be discarded.

To further characterize the metabolic changes underlying MPP+ and rotenone treatment, the mRNA expression of key enzymes related to M1 and M2 phenotypes were evaluated. As microglial metabolism is still rather unexplored, we considered macrophage metabolism as a point of reference to study microglial cells.

Vats and collaborators demonstrated that PGC1β, a regulator of the beta-oxidation of fatty acids and oxidative phosphorylation, is critical for M2 macrophage polarisation, inducing fatty acid oxidation and mitochondrial biogenesis and inhibiting pro-inflammatory cytokine production in IL4-treated macrophages (Vats et al. 2006). In microglial cultures, Pgc1β mRNA levels tended to increase in response to MPP+ or IL4 alone. This tendency was also observed in IL4-treated cultures exposed to rotenone, but a significant increase was observed in IL4-treated cultures exposed to MPP+. These results suggest that although MPP+ and rotenone inhibit oxidative phosphorylation, microglial cells treated with both MPP+ and IL4 increase their PGC1β expression to increase oxidative metabolism as a compensatory response.

In macrophages, CARKL, which is involved in regulating the pentose phosphate pathway, is required for metabolic reprogramming during M1 and M2 polarisation (Haschemi et al. 2012). CARKL catalyzes the production of sedoheptulose-7-phosphate, an intermediate in the pentose phosphate pathway, which limits the flux into the pentose phosphate pathway (Haschemi et al. 2012). The expression of CARKL in macrophages is rapidly down-regulated in response to LPS stimulation and it is slightly increased in response to IL4 treatment (Haschemi et al. 2012). CARKL down-regulation appears to be critical for M1 polarisation, given that pro-inflammatory gene expression is repressed by CARKL (O'Neill and Hardie 2013). In microglial cultures, Carkl mRNA expression was not affected in our experimental conditions. Consequently, the pentose phosphate pathway was not potentiated in contrast to what we observed after LPS/IFNγ treatment, which induced a strong inhibition of Carkl mRNA expression. In agreement with these results, Orihuela and collaborators reported that although macrophages and microglia increase glycolysis in response to pro-inflammatory stimuli, macrophages increase oxidative phosphorylation in response to IL4, but microglial cells have an oxidative metabolic state that is similar to that of non-stimulated cells following IL4 treatment (Orihuela, McPherson, and Harry 2016). IL4 stimulation of microglial cells elicits decreased glucose consumption and lactate production (Gimeno-Bayon et al. 2014). However, we observed significantly increased Glut1 mRNA levels in IL4-treated microglial cultures. MPP+ also increased Glut1 mRNA expression, further increasing the IL4-induced rise in expression. Glut1 mRNA expression levels also tended

to increase after rotenone treatment. These increases suggest that an additional uptake of glucose is promoted to compensate for the reduced oxidative metabolism elicited by the parkinsonian neurotoxins. In agreement with this, the mRNA expression of Pfpk, one of the most important regulatory enzymes of glycolysis, was also increased in IL4-treated cultures exposed to MPP+. The expression of Hif1α, which potentiates glycolysis (Palazon et al. 2014; Taylor et al. 2016), showed a trend to increase in MPP+-treated microglial cultures. Altogether, these results indicate that IL4-stimulated microglial cells exposed to MPP+ or rotenone tended to increase both oxidative metabolism and the glycolytic flux to compensate for the inhibition of oxidative phosphorylation by the complex I inhibitors. Interestingly, MPP+ had a greater effect than rotenone both at altering the expression of metabolic enzymes and at inhibiting the anti-inflammatory response.

Regarding mixed glial cultures, down-regulation of Carkl and up-regulation of Glut1 mRNA expression were observed after MPP+ treatment. Reduced Carkl mRNA expression was also observed in rotenone-treated mixed glial cultures. These changes may reflect a preference for the glycolytic and pentose phosphate pathways when oxidative metabolism is inhibited by the neurotoxins. However, this shift may not be enough to fulfil the energy requirements to respond to IL4 in the presence of the neurotoxins.

2.3 EFFECT OF MPP+ AND ROTENONE ON THE CD200-CD200R1 SYSTEM IN THE ABSENCE AND PRESENCE OF A PRO- OR ANTI-INFLAMMATORY STIMULUS

Since the CD200-CD200R1 system is one of the mechanisms of control of microglial activation, we analysed whether changes in the CD200-CD200R1 system were associated with the inhibitory effect of MPP+ and rotenone on the pro- and anti-inflammatory responses of glial cells.

Corroborating the results exposed in the first section, we found that 6 h after LPS/IFNγ treatment CD200R1 mRNA expression dramatically decreased both in mixed glial and microglial cells, and that CD200tr mRNA expression increased in mixed glial cultures. These results suggest that the disruption of the CD200-CD200R1 system facilitates the development of the pro-inflammatory response of microglia to LPS/IFNγ, as previously discussed.

Several studies have shown that CD200R1 stimulation inhibits the expression of pro-inflammatory cytokines, but it also induces the expression of the anti-inflammatory markers IL10 and ARG1 in glial cells treated with pro-inflammatory stimuli (Hernangomez et al. 2012; Liu et al. 2010; Lyons et al. 2012; Yi et al. 2016). In addition, Yi and collaborators reported that CD200R1 is necessary for the IL4-induction of an anti-inflammatory phenotype in microglial cells (Yi et al. 2016). We observed that CD200R1 mRNA levels were increased and CD200tr mRNA levels were decreased

in IL4-treated mixed glial cultures, indicating that the inhibitory function of CD200R1 is enhanced to promote an anti-inflammatory phenotype. However, CD200full mRNA expression was inhibited by IL4. As IL4 has been demonstrated to increase CD200 expression in neurons (Lyons et al. 2007) and since CD200 expression has been reported to be decreased in neuronal cultures from IL4 -/- mice (Lyons et al. 2009), our results suggest a differential CD200 regulation by IL4 in neurons and astrocytes. Nevertheless, there is no specification on which CD200 isoform, full or tr, was determined in these articles.

When treating mixed glial cultures with MPP+ or rotenone, we observed a reduction of CD200R1, CD200full and CD200tr mRNA expression. CD200-CD200R1 impairment may be involved in the increased expression of pro-inflammatory markers (IL1β, IL6, COX2) and the decreased expression of anti-inflammatory markers (IL10, TGFβ, IL1ra, MR) observed after MPP+ or rotenone treatment. Previous studies reported that the potentiation of the CD200-CD200R1 system by recombinant CD200 increased Arg1 and IL10 expression in microglial cells (Yi et al. 2016), supporting that the disruption of the CD200-CD200R1 system we observed following MPP+ and rotenone may lead to a decrease in the expression of anti-inflammatory markers.

The effect of LPS/IFNγ on CD200 and CD200R1 mRNA expression in mixed glial cultures was similar in the absence and presence of MPP+ or rotenone. Therefore, the dominant effect seems to be the one produced by LPS/IFNγ. As mentioned before, following LPS/IFNγ treatment, the dramatic decrease in CD200R1, the decrease in CD200full and the increase in CD200tr mRNA expression may contribute to the pro-inflammatory activation of glial cells. However, in the presence of MPP+ or rotenone, the pro-inflammatory response of glial cells to LPS/IFNγ was inhibited, although the CD200-CD200R1 system remained disrupted. This observation suggests that the CD200-CD200R1 system is not implicated in the inhibition of LPS/IFNγ-induced pro-inflammatory markers by MPP+ and rotenone and that additional mechanisms are probably involved.

In contrast, MPP+ and rotenone treatment inhibited the IL4-induced expression of CD200R1 mRNA in mixed glial cultures. CD200R1 is necessary for the induction of the anti-inflammatory phenotype elicited by IL4 in microglia (Yi et al. 2016). Therefore, MPP+ inhibition of IL4-induced CD200R1 mRNA expression may be one of the mechanisms by which MPP+ inhibits the IL4-induced expression of anti-inflammatory markers. Rotenone inhibited the IL4-induced CD200R1 mRNA expression to a lesser extent than MPP+ and interestingly, the inhibitory effect of rotenone on the IL4-induced anti-inflammatory response was also lower than that of MPP+.

Regarding microglial cultures, we have to take into account that CD200 is not present in these cultures. However, changes in CD200R1 expression were also observed. In microglial cultures, CD200R1 mRNA expression was increased 6 h after MPP+ and rotenone treatment, in contrast to what we observed in mixed glial cultures. Similar to IL4, that requires CD200R1 for the induction

of anti-inflammatory markers (Yi et al. 2016), MPP+ and rotenone may increase CD200R1 and induce the expression of anti-inflammatory markers. Although we did not analyse the expression of anti-inflammatory markers at 6 h, an increase in IL1ra mRNA expression was interestingly observed 24 h after MPP+ treatment. In addition, no increase in anti-inflammatory markers was observed after MPP+ or rotenone in mixed glial cultures where, in contrast to microglial cultures, CD200R1 mRNA expression was decreased after neurotoxin exposure.

In mixed glial cultures, MPP+ and rotenone inhibited IL4-induced CD200R1 mRNA expression, which could explain the inhibition in the expression of anti-inflammatory markers observed. On the contrary, CD200R1 mRNA expression was increased in IL4-treated microglial cultures exposed to MPP+ or rotenone, which showed few changes in the expression of anti-inflammatory markers. Nevertheless, as mentioned above, CD200 was not present in microglial cultures, suggesting that although changes were observed in CD200R1 expression in microglial cells in response to treatments, CD200R1 cannot activate the downstream signalling pathway and consequently, other systems may be responsible for the changes observed in the inflammatory response. CD200R1 mRNA expression was dramatically inhibited by LPS/IFNγ in microglial cultures, indicating that despite the absence of the ligand, CD200R1 expression is regulated. However, other mechanisms may be responsible for the pro-inflammatory response observed after LPS/IFNγ in microglial cultures.

Altogether, the results of the present section indicate that MPP+ and rotenone impair the pro- and anti-inflammatory responses of glial cells to LPS/IFNγ and IL4 *in vitro*. Furthermore, astroglial cells appear to be more sensitive than microglial cells to these neurotoxins, or at least, when both cell types are together the repercussion of MPP+ and rotenone exposure is stronger than when analysing microglial cells alone. In addition, alterations in CD200R1 expression may be involved in the impairment of the anti-, but not the pro-inflammatory response, elicited by MPP+ and rotenone. This suggests that the immune response of glial cells is compromised by neurotoxins that inhibit the mitochondrial electron transport chain. Although the involvement of glial cells in the development of neurodegenerative diseases is widely accepted, the precise role they play in every neurodegenerative disorder remains to be established. As many genetic and environmental factors are probably involved in the etiopathogenesis of neurodegenerative diseases, many factors may also determine when and how glial cells take part in the pathological process. In the case of pathologies where the exposure to certain neurotoxicants is a risk factor, such as PD, the direct effect of the toxic agents on glial cell function may be an additional factor to take into account, as alterations in glial function will have an effect on neuronal function and CNS homeostasis. In this context, our results suggest that glial metabolic alterations induced by neurotoxin exposure compromise the brain immune response. This impaired immune response may imply a more vulnerable brain, which can be a further aspect contributing to the development of PD.

3 Evaluation of the effect of CD200-CD200R1 modulation in the MPTP mouse model of PD

Neuroinflammation has been described in the context of PD, but little is known concerning the role of microglial activation in this neurodegenerative disorder (Gelders, Baekelandt, and Van der Perren 2018; Hirsch and Hunot 2009; McGeer et al. 1988; Barcia 2013).

In this study, dopaminergic neurodegeneration after MPTP administration was accompanied by a transient glial activation both in the striatum and SN, especially in the SNpc. Glial activation and dopaminergic degeneration occurred earlier in the striatum than in the SNpc. In addition, microglial activation occurred before astroglial activation, at least in the striatum. We also observed transient up- and down-regulation of inflammatory markers in these brain areas. These effects were accompanied by changes in CD200 and CD200R1 expression, mainly a transient increase in striatal CD200R1 and a sustained decrease in CD200full in the ventral midbrain. The administration of a CD200R1 agonist attenuated the MPTP-induced microglial activation and dopaminergic neurodegeneration. Inversely, CD200-deficient mice showed a more activated microglial phenotype at early stages after MPTP administration, but did not present an increase in the MPTP-induced dopaminergic neurodegeneration.

TH-positive striatal fibers were dramatically reduced to 29% of the control level as soon as 2 hours after the last MPTP injection. At this time point, 99% of the TH-positive neurons in the SNpc remained intact. Thus, striatal TH-positive fibers show a more rapid response to MPTP compared to TH-positive cell bodies in the SNpc. Seven days after MPTP-injection, when dopaminergic neurodegeneration is established (Jackson-Lewis et al. 1995), TH-positive striatal fibers were reduced to 21% of the control level, while 46% of the TH-positive neurons still remained. These results suggest that striatal TH-positive fibers are more sensitive to MPTP toxicity than TH-positive neuronal bodies. This data is corroborated by previous studies (Bian et al. 2012; Costa et al. 2013; Gibrat et al. 2009; Teismann et al. 2003).

There are previous reports that have studied whether glial activation precedes the dopaminergic neurodegeneration after MPTP administration using the same MPTP mouse model we have used here (Brochard et al. 2009; Czlonkowska et al. 1996; Kohutnicka et al. 1998; Liberatore et al. 1999). However, some effects occur so rapidly that it is difficult to determine what occurs first. From our data, we can say that microglial activation precedes astroglial activation in the striatum. Liberatore and collaborators reported that a similar glial activation can be found in the striatum and ventral midbrain after acute MPTP administration, however, no mention on whether microglial preceded astroglial activation in the striatum was given (Liberatore et al. 1999). Liu and collaborators showed that microglial activation was already detected in the striatum 90 minutes

after MPTP administration (Liu et al. 2015), and Suo and collaborators 2015 reported that astroglial activation was not yet detected in the striatum at day 1 after MPTP administration (Suo et al. 2015). Here, we corroborated that microglial activation in the striatum occurred before astroglial activation and to our knowledge, it is the first time that this has been determined in the same animals. Regarding SNpc, microglial and astroglial activation were detected simultaneously from day 1 after MPTP administration. However, microglial immunostaining was more intense than astroglial immunostaining, suggesting that microglial activation also preceded astroglial activation in the SNpc. This idea is supported by previous reports where glial activation was quantified (Brochard et al. 2009; Kohutnicka et al. 1998; Liberatore et al. 1999).

We observed that glial activation appeared in the striatum before than in the SNpc. In agreement with our observations, a previous report showed microglial activation as early as 90 minutes in the striatum, but not in the SN (Liu et al. 2015). Liberatore and collaborators reported similar glial activation in the striatum and ventral midbrain, but without specifying where it occurred first (Liberatore et al. 1999). Studies that did not analyse time points earlier than 1 day missed this observation (Czlonkowska et al. 1996).

Previous reports have shown that microglial activation occurs before significant dopaminergic neurodegeneration in the SNpc (Liberatore et al. 1999) whereas astroglial activation occurs concomitant to TH-neuronal loss in SNpc (Czlonkowska et al. 1996; Kohutnicka et al. 1998; Liberatore et al. 1999). We provided further evidence that a similar pattern occurs in the striatum, at least for astroglial activation. Striatal microglial activation and loss of TH-positive fibers occurred so rapidly and dramatically that earlier time points should be analysed to determine whether microglial activation precedes striatal dopaminergic denervation. However, astroglial activation did appear after the striatal TH-fiber loss. Therefore, the astrocytic reaction may be secondary to the neurodegeneration but microglial activation may appear early enough to play a role in the pathogenicity of the neurodegeneration. Nevertheless, we observed that the mRNA expression of inflammatory markers where changed as soon as 2 hours in both the striatum and ventral midbrain, indicating that, at mRNA level, inflammatory cytokines and enzymes are already displaying alterations at the very beginning of the MPTP-induced toxicity in both areas.

It is important to take into account that we used the same animals to determine the TH-positive neuronal loss, the microglial and astroglial reactivity and the mRNA expression profile. In contrast, Liberatore and collaborators, who described the microglial and astroglial dynamics, referred to a previous study (Jackson-Lewis et al. 1995) to compare the temporal patterns of SNpc neurodegeneration and glial activation (Liberatore et al. 1999). Other studies in the SNpc (Czlonkowska et al. 1996; Kohutnicka et al. 1998) did not consider time points earlier than day 1, missing whether microglial activation preceded neuronal loss in the SNpc.

We observed that glial activation was transient and once it reached a peak, IBA1- and GFAP-immunostaining started to decrease showing a tendency to return to control levels by 7 days after MPTP administration. This has been previously described (Czlonkowska et al. 1996; Kohutnicka et al. 1998; Liberatore et al. 1999; Liu et al. 2015) and may be due to the stabilisation of the lesion (Jackson-Lewis et al. 1995).

Glial activation and dopaminergic neuronal death after MPTP administration were accompanied by changes in the mRNA expression of pro- and anti-inflammatory markers in the striatum, ventral midbrain and cerebral cortex. Although the cerebral cortex was the least affected area, some changes were also observed, suggesting a widespread pathology. We detected changes in the expression of inflammatory markers as soon as 2 hours after the last MPTP injection. Interestingly, the expression of all the markers analysed returned to basal levels at day 7 after MPTP administration, suggesting a resolution of the inflammatory process.

The dynamic profile of pro- and anti-inflammatory markers has been previously studied in the acute MPTP mouse model mainly in the SN, but little is known about the changes in the striatum and cerebral cortex. In the ventral midbrain, the mRNA expression of IL1β, IL6 and TNFα were increased in concordance with mRNA and protein increases described previously using the acute MPTP regimen (Chung, Kim, and Jin 2010; Khan et al. 2013; Kim et al. 2016; Suo et al. 2015; Chung et al. 2011; Wu et al. 2002). We also observed increased IL1β, IL6 and TNFα mRNA expression in the striatum. In the SN of PD patients, increased density of glial cells expressing IL1β and TNFα, as assessed by immunohistochemistry, has been described (Hunot et al. 1999). Regarding pro-inflammatory enzymes, iNOS and gp91phox mRNA expression was surprisingly decreased in the ventral midbrain and striatum, in contrast to previous observations using the same MPTP regimen (Chung, Kim, and Jin 2010; Liberatore et al. 1999; Wu et al. 2003; Chung et al. 2011; L'Episcopo et al. 2012). The reason for this divergence is unknown and further studies are required to clarify the temporal pattern of iNOS and gp91phox expression after MPTP administration. COX2 mRNA expression was increased in the striatum and previous studies reported that COX2 mediates microglial activation and dopaminergic cell death in the MPTP mouse model (Teismann et al. 2003; Vijitruth et al. 2006). Interestingly enough, some anti-inflammatory markers were up-regulated (TGFβ, IL10) whereas others were down-regulated (Nrf2) and interestingly, others (MR, Arg1) showed up- or down-regulations in a region-specific manner. In *post-mortem* and serum human PD samples, alterations both in pro- and anti-inflammatory markers have been also described (Gelders, Baekelandt, and Van der Perren 2018). This suggests a complex pattern of glial activation. Previous reports showed down-regulation of anti-inflammatory markers after MPTP administration (Rojo et al. 2010; Yao and Zhao 2018).

Regarding glial markers, Gfap mRNA expression showed a robust increase in the striatum and, to a lesser extent, in the ventral midbrain. Although at 2 hours after MPTP administration no

changes in GFAP-immunostaining were observed in the ventral midbrain, changes at the mRNA level were already detected at this time point. Increased GFAP expression in the ventral midbrain (Kuroiwa et al. 2010; Liberatore et al. 1999) and striatum (Francis et al. 1995; Suo et al. 2015) has also been reported in the same MPTP regimen. Strikingly, the temporal pattern of Iba1 and CD11b mRNA expression in the ventral midbrain, striatum and cerebral cortex was complex with up- and down-regulations, in contrast to the increased IBA1-immunostaining we observed or the results of previous reports (Liberatore et al. 1999; Kinugawa et al. 2013; L'Episcopo et al. 2012; Yuan et al. 2018). Further studies are required to clarify these observations.

We demonstrated that MPTP administration induced changes in the CD200-CD200R1 system. In the ventral midbrain, a marked decrease in the expression of CD200R1 mRNA was observed as soon as 2 hours after MPTP injection, suggesting that microglial activation is facilitated. The sustained down-regulation in the ventral midbrain of CD200full mRNA expression, which is mainly expressed by neurons, may reflect the early neuronal damage and the final neurodegeneration. A different explanation may be applied to CD200tr. CD200tr mRNA expression decreased at 2 hours after MPTP administration in the ventral midbrain as a possible consequence of the early neuronal damage; however, from day 1 CD200tr mRNA levels returned to the basal expression. This observation suggests that astrocytes may contribute to CD200tr expression. A different scenario was observed in the striatum, where CD200R1 mRNA was dramatically increased at day 2 and 4 after MPTP administration, suggesting a mechanism to return microglial activation to basal levels. Decreased CD200 and CD200R1 protein expression was previously reported in the whole brain of mice injected with MPTP subacute regimen, together with increased levels of IL1β, TNFα and IFNγ transcripts in the midbrain (Ren, Zhao, et al. 2016).

Since glial activation may play a role in the development of dopaminergic degeneration in the MPTP model and the CD200-CD200R1 system is an inhibitory mechanism involved in the control of the inflammatory response, we further assessed whether CD200full and CD200R1 decreased mRNA levels observed in the ventral midbrain of MPTP-injected mice had a role in the induced neuroinflammation and neurodegeneration. The administration of a CD200R1 agonist attenuated the MPTP-induced dopaminergic neurodegeneration. In fact, MPTP or isotype + MPTP administration produced a significant loss of TH-positive neurons and the administration of two doses of 3.6 mg/kg CD200Fc + MPTP did not, although the value of the CD200Fc + MPTP treatment was not significantly different from that of MPTP or isotype + MPTP treatment. However, the fact that a lower dose of CD200R1 agonist had undoubtedly no effect on the MPTP-induced neurodegeneration give further support to the potential neuroprotective effect observed after the highest dose of CD200R1 agonist and suggests that this effect is concentration-dependent. In addition, microglial activation in SNpc was less apparent in CD200Fc-injected mice, as revealed by IBA1-immunostaining. The MPTP-induced loss of striatal dopaminergic nerve terminals was not modified by the CD200R1 agonist, but, as exposed above, striatal terminals are more

sensitive to MPTP than SNpc dopaminergic cell bodies and it may be more difficult to prevent their loss. These results give further evidence to the role of the CD200-CD200R1 system in PD.

In line with these results, previous studies demonstrated that a CD200R1 agonist stimulated the production of neurotrophic factors involved in the protection of dopaminergic neurons in microglial cultures (Varnum et al. 2015). When CD200R1 is blocked, an exacerbation of microglial activation and dopaminergic neurodegeneration in 6-OHDA-treated rats has been described (Zhang, Wang, et al. 2011). Several *in vitro* and *in vivo* studies showed that the CD200R1 agonist exerts its effect by suppressing the pro-inflammatory microglial activation (Copland et al. 2007; Costello et al. 2011; Cox et al. 2012; Denieffe et al. 2013; Jiang et al. 2016). The potentiation of the CD200-CD200R1 system through a CD200R1 agonist has also protective effects on other experimental models of brain diseases such as the LPS model of PD (Xie et al. 2017), experimental autoimmune encephalitis (Liu et al. 2010) and experimental autoimmune uveoretinitis (Copland et al. 2007). Other immunomodulatory agents have also been described to exert neuroprotection in experimental models of PD (Gao et al. 2003a; Hou et al. 2017; Martinez and Peplow 2018; Wu et al. 2003; Lee, Kim, and Lee 2017). Importantly enough, we have included an experimental group with the isotype as a negative control, something that many previous studies did not consider (Cox et al. 2012; Hernangomez et al. 2016; Gorczynski, Yu, and Clark 2000; Sarangi, Woo, and Rouse 2009; Yue et al. 2012). Our results provide further evidence that alterations in the CD200-CD200R1 system may contribute to neurodegeneration in PD. We believe that modulating simultaneously microglial activation through different mechanisms of control may have a greater impact.

The CD200-deficient mice presented the same levels of MPTP-induced microglial activation and dopaminergic neurodegeneration as their wild-type littermates at day 7 after the last MPTP injection, when the lesion is stabilized (Jackson-Lewis et al. 1995). However, at day 1 microglial cells presented a more activated phenotype in MPTP-injected CD200-deficient mice, including a decreased IBA1-labelled area with larger cell bodies and shortened projections, as well as increased intensity of the IBA1-immunolabelling in SNpc without an increase in the number of microglial cells. However, this increased microglial activation was not accompanied by an increase in MPTP-induced dopaminergic neurodegeneration. It may be that the MPTP dose administered was too high to observe any difference in the dopaminergic neurodegeneration between CD200-deficient mice and their wild-type littermates. In fact, the mice used in the present experiment (CD200 +/+ and CD200 -/- colony) presented a higher peripheral sensitivity to MPTP toxicity than the mice we used in the previous studies (commercial mice): they showed a higher mortality after MPTP injection, which led us to reduce the MPTP dosage. In addition, the dopaminergic neurons degenerated more rapidly in response to MPTP. Even in the wild-type group, at day 1 post-MPTP injection there was already a 90% decrease in TH-positive fibers in the striatum and a 42% decrease in TH-positive cells in the SNpc, values that we did not obtain until 7 days after MPTP administration in the time course experiment. These differences, could

be due to the different genetic background of the two substrains used in the experiments with commercial mice (100% C57BL/6N) and in the experiments with CD200-deficient mice (66% C57BL/6NJ - 33% C57BL/6J), as previous studies showed that different substrains had different peripheral sensitivity and dopaminergic neuronal response to MPTP (Giovanni et al. 1991; Hamre et al. 1999; Jackson-Lewis and Przedborski 2007). Interestingly, it has been reported that dopaminergic neuronal sensitivity depends on glial cell number in the SNpc (Smeyne et al. 2005). Therefore, it is extremely important to use wild-type and knock-out mice with the same genetic background (Jackson-Lewis and Przedborski 2007), something that in previous reports using the CD200-deficient mice has either not been taken into account or no data is provided (Broderick et al. 2002; Copland et al. 2007; Denieffe et al. 2013; Costello et al. 2011).

Previous reports using the same CD200-deficient mouse line we have used here have shown that in the spleen CD11b+ cells doubled in size and macrophage and dendritic cells showed increased activation, whereas lymph nodes were slightly enlarged with expanded and activated macrophages (Hoek et al. 2000). Furthermore, microglia of CD200 -/- mice spontaneously exhibited many features of activation (less ramified, shorter glial processes, disordered arrangement, increased CD11b and CD45 expression) and formed aggregates, especially in the spinal cord (Hoek et al. 2000). In this line, CD200-deficiency dramatically accelerated the microglial response to nerve damage, as described in a facial nerve transection model (Hoek et al. 2000), advanced and enhanced macrophage and microglia activation in EAE model (Hoek et al. 2000), increased the susceptibility to the development of experimental rheumatoid arthritis (collagen-induced arthritis (CIA)) model (Hoek et al. 2000), and accelerated experimental autoimmune uveoretinitis (Broderick et al. 2002; Taylor et al. 2005). Although in some of these pathologies the role of the peripheral immune system has been well documented, Hoek and collaborators reported no evidence of T cell deregulation in CD200-deficient mice (Hoek et al. 2000) and consequently, the effects observed appeared to be directly related to a deregulation of the myeloid lineage, the main inflammatory effector in PD (Prinz and Priller 2017).

Altogether, our results suggest that the absence of CD200 leads to a more activated microglial phenotype, and that CD200R1 activation may attenuate the progression of neuronal damage in PD. Therapeutic interventions aimed at preventing microglial activation through potentiation of CD200-CD200R1 signalling may be a novel approach for PD treatment.

4 Expression of CD200-CD200R1 system in human samples

Microglial activation has been identified in *post-mortem* samples of PD patients and interpreted as the presence of an innate immune response with an inflammatory profile that could take part in the neurodegenerative process (Croisier et al. 2005; Imamura et al. 2003; Long-Smith, Sullivan, and Nolan 2009; Nagatsu and Sawada 2005; McGeer et al. 1988; Mosley et al. 2012). This suggests that changes in the mechanisms of control of microglial activation may contribute to the pathological features observed in PD. We focused our interest on the CD200-CD200R1 system as one of these mechanisms of control of microglial activation.

Both in mouse and human, CD200 ligand is represented by the CD200full isoform, which interacts with CD200R1 to inhibit pro-inflammatory microglial activation, and the CD200tr isoform, which acts as an antagonist of CD200full. However, the murine CD200R1 gene encodes a single CD200R1 protein, while the human CD200R1 gene can generate four mRNA variants through alternative splicing: V1 and V4, encoding two transmembrane protein-isoforms, and V2 and V3, encoding two soluble protein-isoforms.

Decreased expression of CD200 and/or CD200R1 in Alzheimer's disease hippocampus, inferior temporal gyrus but not cerebellum (Walker et al. 2009) and in multiple sclerosis white matter lesions (Koning et al. 2007; Koning et al. 2009) has been described. These studies do not discriminate between CD200full and CD200tr or among the different CD200R1 mRNA variants and the resulting protein isoforms.

To our knowledge, this is the first time that the mRNA expression of all the components described in the human CD200-CD200R1 system (CD200full, CD200tr and the four CD200R1 variants) is analysed. As the quantification of the mRNA expression of each CD200R1 variant is not possible using random primer retrotranscription followed of qPCR because of their overlapping sequences, we designed a method based on gene-specific retrotranscription.

We observed differences in the relative expression of the four CD200R1 mRNA variants among human monocytes, induced microglia-like cells and brain tissue. Monocytes expressed the four CD200R1 mRNA variants. Microglia-like cells presented V1 and V4 mRNA levels similar to monocytes but V2 and V3 mRNA levels were dramatically lower than in monocytes. This indicates that myeloid cell types differ on the relative expression of CD200R1 variants.

The function of each CD200R1 mRNA variant remains to be elucidated. Because of its amino acid sequence identity with murine CD200R1 (Vieites et al. 2003), V4 is the variant that most

likely plays similar functions to murine CD200R1. In microglia-like cultures, we found that not all the CD200R1 variants respond equally to stimuli. While V1 may be responsible for IL4 functions, V3 and V4 decreased after a pro-inflammatory stimulus. Therefore, different functions can be attributed to different CD200R1 variants.

In *post-mortem* brain tissue (frontal cortex), where cells expressing CD200R1 include microglia but also meningeal, perivascular and choroid plexus macrophages and blood monocytes and lymphocytes, we only detected individually the mRNA expression of V1 and V2. The V3 and V4 variants may be present but the methodology not be sensitive enough to detect them individually. We have to take into account that CD200R1 is a gene that is weakly expressed and by cells that are not the predominant ones in the brain. Isolation of microglia from brain tissue to obtain pure microglia mRNA would be of relevance to study the expression of the CD200R1 variants in these cells. However, the relative expression of the CD200R1 variants in brain tissue was different than in monocytes and microglia-like cells. This suggests that the mRNAs of the CD200R1 variants detected in monocytes and microglia-like cells may be diluted in the large amount of different mRNAs found in the brain tissue and it may also reflect a differential expression in microglia and microglia-like cells. Differential CD200R1 expression in meningeal, perivascular and choroid plexus macrophages, monocytes and lymphocytes may also contribute to the different relative expression of CD200R1 variants detected in brain tissue.

Despite we only detected V1 and V2 in the frontal cortex, Vieites and collaborators described the presence of the four variants in different human tissues including the brain (Vieites et al. 2003). These authors did not specify which region of the brain was analysed. Differential expression of each CD200R1 variant in different brain regions could explain these discordances. Furthermore, the methodology used by Vieites and collaborators was different allowing only the detection, but not the quantification, of each mRNA variant.

Not discarding the possible presence of the four CD200R1 mRNA variants in the brain tissue and not being able to quantify individually the four variants (only V1), we decided to quantify the long variants together (V1 + V4) and the short variants together (V2 + V3) in the *post-mortem* brain of PD patients. Considering the singularity of CD200R1 expression in humans, where the CD200R1 gene encodes not only long transmembrane isoforms but also short soluble isoforms, we considered of relevance to study the possible differences between the mRNA expression of long vs. short variants. Probably, at least in the frontal cortex, the results obtained when analysing long variants may correspond mainly to V1 and when analysing short variants to V2.

In this study we determined for the first time CD200 and CD200R1 expression in *post-mortem* brain samples of SN, hippocampus and frontal cortex of PD patients, identifying mRNA variants and protein isoforms. We observed an increase in the expression of CD200tr and CD200R1 transmembrane and soluble forms in PD samples. The pattern of changes differed among brain

regions, probably reflecting different degrees of neural damage and inflammatory response. An increase in the expression of CD200tr may be associated with an inhibition of the CD200-CD200R1 system. As regards CD200R1, an increase in the expression of the membrane forms could be interpreted as a potentiation of the CD200-CD200R1 system in the context of inflammation resolution and reparative response. Although the physiological meaning of the CD200R1 soluble forms is still unknown, an increase in the CD200R1 soluble forms may result in the inhibition of the CD200-CD200R1 system.

In control individuals, we observed lower levels of V1 and V4 CD200R1 mRNA expression in the hippocampus and lower levels of CD200 protein in the frontal cortex with aging. This could indicate more primed microglia with aging, as observed in previous studies (Norden, Muccigrosso, and Godbout 2015; Niraula, Sheridan, and Godbout 2017; Norden and Godbout 2013). However, in SN of control individuals, we observed higher levels of CD200R1 protein isoforms 1 and 4 with aging. Importantly, these correlations were lost in PD patients, suggesting a dysregulation of the CD200-CD200R1 system in PD patients.

In general, the changes we found in the CD200-CD200R1 system were mainly observed in advanced LP stage patients, a typical feature of PD. In contrast, characteristic features of Alzheimer's disease including neurofibrillary degeneration or neuritic plaques did not present this association to the same degree. Indeed, PD patients with non or sparse neuritic plaques had more changes in the CD200-CD200R1 system. Walker and collaborators described no differences in the protein levels of CD200 in temporal and cingulate cortex of PD patients, independently of the presence of dementia (Walker et al. 2017). At protein level, we did not detect changes in CD200 either, neither in the presence nor absence of dementia. However, when we distinguished by mRNA analysis the two variants of CD200, we detected a robust increase in CD200tr expression in the hippocampus whereas these authors did not specify which CD200 was analysed (Walker et al. 2017).

Although *post-mortem* samples reflect an end-state of the disease, these results suggest an involvement of the mechanisms of control of the inflammatory response in PD development. More studies are needed to clarify the functional role of each CD200 and CD200R1 isoform in different brain areas in PD. To sum up, the results here obtained show that alterations in the CD200-CD200R1 system in PD differ from those observed in Alzheimer's disease (Walker et al. 2009) and multiple sclerosis (Koning et al. 2007; Koning et al. 2009), suggesting that mechanisms associated with neuroinflammation differ among neurological disorders. The differences observed between CD200full and CD200tr expression and between long and short CD200R1 variants emphasize the importance of taking into account the different variants separately when analysing CD200 and CD200R1 expression, something that has not been considered to date in the literature.

5 General discussion

Neuroinflammation is a common feature of neurodegenerative diseases and is emerging as a key process in their pathophysiology. Activated glial cells, mainly microglia, are involved in neuroinflammation. Microglia are the main representatives of the endogenous immune system of the brain and microglial activation is a well-established hallmark of these diseases. Glial activation is a physiological reaction; however, in the context of chronic brain pathology without resolution, it becomes perpetuated and it may result in harmful effects (Glass et al. 2010; Heneka, Kummer, and Latz 2014). From the histopathological point of view, PD is characterized by the loss of dopaminergic neurons and abnormal intracellular accumulations of α-synuclein protein, but also chronic glial activation (Hirsch, Vyas, and Hunot 2012).

In the present thesis, we focused our attention on the study of one of the mechanisms of control of microglial activation, the CD200-CD200R1 system, in the context of PD. We used different experimental approaches including *in vivo* and *in vitro* studies as well as *post-mortem* human samples, to determine the involvement of the CD200-CD200R1 system in the modulation of neuroinflammation and its potential as a therapeutic target in PD.

The CD200-CD200R1 system inhibits the pro-inflammatory response of microglia and contributes to maintaining microglia in a quiescent state in homeostatic conditions. We have shown that *in vitro* disruption of the CD200-CD200R1 system, using an anti-CD200 blocking antibody or cultures from CD200-deficient mice, potentiated the pro-inflammatory response in glial cultures. Previous studies have shown that neuronal CD200 is necessary to induce the IL4 anti-inflammatory response in neuronal/glial cultures (Lyons et al. 2007; Lyons et al. 2009). However, we did not observe that the absence of CD200 in astrocytes modified the IL4 anti-inflammatory response in primary mixed glial cultures, maybe because the levels of CD200 expression are much lower in astrocytes than in neurons. Mesencephalic cultures from CD200-deficient mice had a higher proportion of microglial cells and were more sensitive to the neurotoxin MPP+, suggesting an association between the absence of CD200, microglial cell number and neurodegeneration.

Exposure to pesticides such as rotenone is a risk factor for PD (Goldman 2014). Moreover, the neurotoxin MPTP was shown to provoke parkinsonism in humans after an accidental exposure (Langston et al. 1983). Both rotenone and MPTP are neurotoxins that inhibit complex I of the mitochondrial respiratory chain and induce deleterious effects on neuronal cells, especially dopaminergic neurons (Dauer and Przedborski 2003). However, their direct effect on glial cells is poorly studied. Here, we have shown that MPP+ and rotenone impair the response of glial cells to pro- and anti-inflammatory stimuli and induce alterations in the CD200-CD200R1 system.

These results highlight that glial cell function is directly affected by this kind of neurotoxins, what can additionally contribute to their neurotoxic effects and the development of PD.

We also tested the involvement of the CD200-CD200R1 system in an experimental model of PD: the acute MPTP mouse model. We first characterized the MPTP model revealing a progressive dopaminergic neuronal death and a transient glial activation, as well as alterations in the mRNA expression of inflammatory markers and components of the CD200-CD200R1 system. In the ventral midbrain, we observed an early and persistent down-regulation of CD200 expression, which directed us to potentiate this mechanism of control of microglial activation by administering a CD200R1 agonist before and after MPTP administration. The CD200R1 agonist partially protected dopaminergic neurons and attenuated the microglial activation in the SNpc of MPTP-injected mice. Then, we studied whether disruption of the CD200-CD200R1 system had the opposite effect. Strikingly, its disruption using CD200-deficient mice was not able to aggravate the dopaminergic neurodegeneration induced by MPTP. However, CD200-deficient mice showed a more activated microglial phenotype at early time points after MPTP administration than wild-type mice. The dramatic reduction of striatal TH-fibers and dopaminergic neurodegeneration induced by MPTP in these CD200-deficient and wild-type mice may explain the absence of a greater effect in the CD200-deficient mice. It is important to point out that we used wild-type mice on a matched genetic background in all experiments with CD200-deficient mice in order to minimise genetic variability in both experimental groups since response to MPTP depends on the mouse genetic background (Jackson-Lewis and Przedborski 2007; Giovanni et al. 1991; Hamre et al. 1999).

The murine CD200R1 gene encodes a single CD200R1 transmembrane protein, while the human CD200R1 gene can generate four mRNA variants through alternative splicing, which encode transmembrane and soluble proteins. We have designed an approach based on gene-specific primer retrotranscription to quantify the expression of each human CD200R1 mRNA variant. In response to pro- and anti-inflammatory stimuli, the expression of the four CD200R1 mRNA variants was differently regulated in human (monocyte-derived) microglia-like cells, suggesting distinct functions for each variant. In *post-mortem* brain tissue of PD patients, CD200 and CD200R1 expression was modified. The hippocampus was the area where more changes were observed, mainly an increase in CD200R1 and CD200tr expression. The SN, frontal cortex and hippocampus showed different patterns of changes in the CD200-CD200R1 system components, which may reflect different degrees of neural damage and inflammatory response.

In summary, our results demonstrate that the CD200-CD200R1 system controls neuroinflammation, and that inhibition of microglia activation through potentiation of the CD200-CD200R1 system has neuroprotective effects in the MPTP mouse model of PD. Moreover, changes in CD200 and CD200R1 expression are observed in human PD brain samples. Therefore, targeting the CD200-CD200R1 system has therapeutic potential for preventing

neurodegeneration in PD. Further studies are needed to characterize the potential of the mechanisms of control of microglial activation as possible therapeutic targets to control neuroinflammation and the derived neurotoxicity in PD.

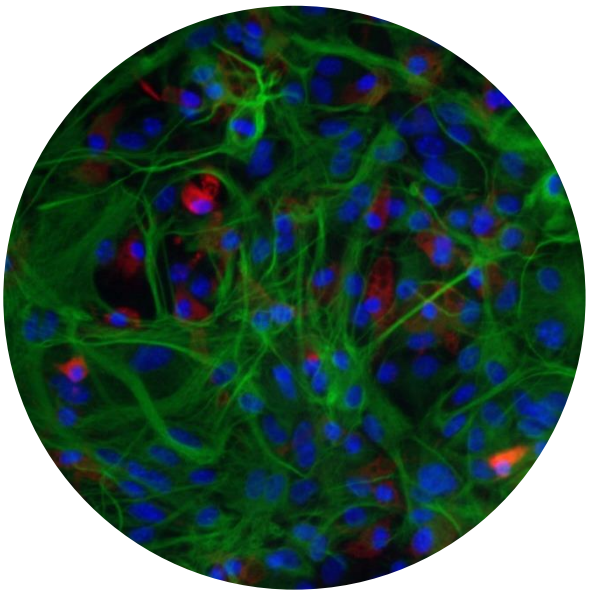

Conclusions

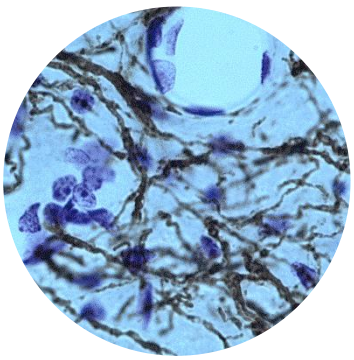

Conclusions

1. *In vitro*, disruption of the CD200-CD200R1 system potentiates glial response to pro-inflammatory stimuli and increases the sensitivity of dopaminergic neuronal cells to a neurotoxic stimulus (MPP+).

2. The parkinsonian neurotoxins MPP+ and rotenone inhibit the pro-inflammatory response induced by LPS/IFNγ in mouse primary glial cell cultures. This effect is more pronounced in mixed glial cultures, where both astrocytes and microglia are present, than in microglial cultures.

3. MPP+ and rotenone also inhibit the anti-inflammatory response induced by IL4 in mouse primary glial cell cultures, more markedly in mixed glial cultures than in microglial cultures.

4. MPP+ and rotenone decrease CD200 and CD200R1 mRNA expression in mixed glial cultures and increase CD200R1 mRNA expression in microglial cultures. These effects do not explain the inhibition of the pro-inflammatory response induced by the neurotoxins in LPS/IFNγ-treated cultures. However, the inhibition of the anti-inflammatory response induced by the neurotoxins in IL4-treated cultures could involve the CD200-CD200R1 system.

5. In the acute MPTP mouse model of PD, dopaminergic neuronal loss and glial activation are associated with alterations in the mRNA expression of CD200 and CD200R1, mainly a transient increase in striatal CD200R1 and a sustained decrease in CD200full in the ventral midbrain.

6. The administration of a CD200R1 agonist partially prevents microglial activation and attenuates dopaminergic neuronal loss in the SNpc of MPTP-injected mice.

7. C57BL/6 mice with a mixed N and J genetic background (66% N – 33% J) show a higher sensitivity to the toxic action of MPTP than C57BL/6 mice with pure N background, with increased dopaminergic neurodegeneration and mortality.

8. Dopaminergic neurodegeneration induced by MPTP in CD200 knock-out mice is similar to that in wild-type mice with a matched genetic background, but a stronger microglial activation is observed at early time points in CD200 knock-out mice.

9. The four CD200R1 mRNA variants are present in human monocytes and monocyte-derived microglia-like cell cultures, but the mRNA expression of the soluble CD200R1 variants (V2 and V3) is lower in microglia-like cells than in monocytes.

10. The expression of each CD200R1 mRNA variant is differentially regulated in response to pro- or anti-inflammatory stimulus in human microglia-like cell cultures.

11. CD200 and CD200R1 expression is modified in *post-mortem* brain tissue from PD patients. From the three analysed brain regions (SN, frontal cortex and hippocampus), the hippocampus is the area showing more significant changes, mainly an increase in CD200tr and CD200R1.

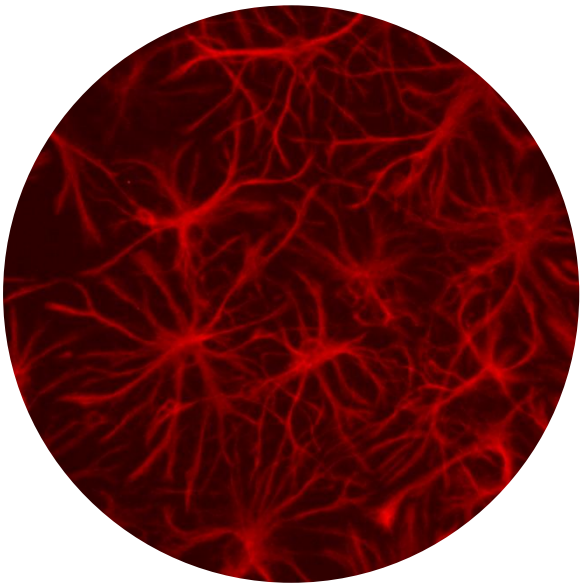

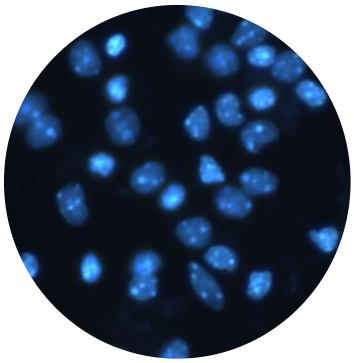

Bibliography

Bibliography

A

Ahlskog, J. E. 2011. 'Does vigorous exercise have a neuroprotective effect in Parkinson disease?', *Neurology*, 77: 288-94.

Ahmadi, F. A., D. A. Linseman, T. N. Grammatopoulos, S. M. Jones, R. J. Bouchard, C. R. Freed, K. A. Heidenreich, and W. M. Zawada. 2003. 'The pesticide rotenone induces caspase-3-mediated apoptosis in ventral mesencephalic dopaminergic neurons', *J Neurochem*, 87: 914-21.

Ajami, B., J. L. Bennett, C. Krieger, K. M. McNagny, and F. M. Rossi. 2011. 'Infiltrating monocytes trigger EAE progression, but do not contribute to the resident microglia pool', *Nat Neurosci*, 14: 1142-9.

Ajami, B., J. L. Bennett, C. Krieger, W. Tetzlaff, and F. M. Rossi. 2007. 'Local self-renewal can sustain CNS microglia maintenance and function throughout adult life', *Nat Neurosci*, 10: 1538-43.

Akkaya, M., and A. N. Barclay. 2010. 'Heterogeneity in the CD200R paired receptor family', *Immunogenetics*, 62: 15-22.

Akman-Karakas, A., A. D. Yalcin, S. Koc, S. Gumuslu, E. Ergun, G. E. Genc, G. Ongut, S. Uzun, and E. Alpsoy. 2014. 'Serum soluble CD200 level was higher in patients with bullous pemphigoid during the active phase of the disease than for healthy individuals', *Clin Lab*, 60: 1237-40.

Alcalay, R. N., E. Caccappolo, H. Mejia-Santana, M. X. Tang, L. Rosado, B. M. Ross, M. Verbitsky, S. Kisselev, E. D. Louis, C. Comella, A. Colcher, D. Jennings, M. A. Nance, S. B. Bressman, W. K. Scott, C. Tanner, S. Mickel, H. Andrews, C. Waters, S. Fahn, L. Cote, S. Frucht, B. Ford, M. Rezak, K. Novak, J. H. Friedman, R. Pfeiffer, L. Marsh, B. Hiner, A. Siderowf, R. Ottman, K. Marder, and L. N. Clark. 2010. 'Frequency of known mutations in early-onset Parkinson disease: implication for genetic counseling: the consortium on risk for early onset Parkinson disease study', *Arch Neurol*, 67: 1116-22.

Annese, V., C. Barcia, F. Ros-Bernal, A. Gomez, C. M. Ros, V. De Pablos, E. Fernandez-Villalba, M. E. De Stefano, and M. T. Herrero. 2013. 'Evidence of oligodendrogliosis in 1-methyl-4-phenyl-1,2,3,6-tetrahydropyridine (MPTP)-induced Parkinsonism', *Neuropathol Appl Neurobiol*, 39: 132-43.

Appel, S. H., D. R. Beers, and J. S. Henkel. 2010. 'T cell-microglial dialogue in Parkinson's disease and amyotrophic lateral sclerosis: are we listening?', *Trends Immunol*, 31: 7-17.

Ara, J., S. Przedborski, A. B. Naini, V. Jackson-Lewis, R. R. Trifiletti, J. Horwitz, and H. Ischiropoulos. 1998. 'Inactivation of tyrosine hydroxylase by nitration following exposure to peroxynitrite and 1-methyl-4-phenyl-1,2,3,6-tetrahydropyridine (MPTP)', *Proc Natl Acad Sci U S A*, 95: 7659-63.

Ascherio, A., and M. A. Schwarzschild. 2016. 'The epidemiology of Parkinson's disease: risk factors and prevention', *Lancet Neurol*, 15: 1257-72.

Aspelund, A., S. Antila, S. T. Proulx, T. V. Karlsen, S. Karaman, M. Detmar, H. Wiig, and K. Alitalo. 2015. 'A dural lymphatic vascular system that drains brain interstitial fluid and macromolecules', *J Exp Med*, 212: 991-9.

B

Baardman, J., I. Licht, M. P. de Winther, and J. Van den Bossche. 2015. 'Metabolic-epigenetic crosstalk in macrophage activation', *Epigenomics*, 7: 1155-64.

Banerjee, D., and A. D. Dick. 2004. 'Blocking CD200-CD200 receptor axis augments NOS-2 expression and aggravates experimental autoimmune uveoretinitis in Lewis rats', *Ocul Immunol Inflamm*, 12: 115-25.

Barcia, C. 2013. 'Glial-mediated inflammation underlying parkinsonism', *Scientifica (Cairo)*, 2013: 357805.

Barcia, C., C. M. Ros, V. Annese, M. A. Carrillo-de Sauvage, F. Ros-Bernal, A. Gomez, J. E. Yuste, C. M. Campuzano, V. de Pablos, E. Fernandez-Villalba, and M. T. Herrero. 2012. 'ROCK/Cdc42-mediated microglial motility and gliapse formation lead to phagocytosis of degenerating dopaminergic neurons in vivo', *Sci Rep*, 2: 809.

Barcia, C., C. M. Ros, V. Annese, A. Gomez, F. Ros-Bernal, D. Aguado-Yera, M. E. Martinez-Pagan, V. de Pablos, E. Fernandez-Villalba, and M. T. Herrero. 2011. 'IFN-gamma signaling, with the synergistic contribution of TNF-alpha, mediates cell specific microglial and astroglial activation in experimental models of Parkinson's disease', *Cell Death Dis*, 2: e142.

Barclay, A. N., G. J. Wright, G. Brooke, and M. H. Brown. 2002. 'CD200 and membrane protein interactions in the control of myeloid cells', *Trends Immunol*, 23: 285-90.

Bartels, A. L., A. T. Willemsen, J. Doorduin, E. F. de Vries, R. A. Dierckx, and K. L. Leenders. 2010. '[11C]-PK11195 PET: quantification of neuroinflammation and a monitor of anti-inflammatory treatment in Parkinson's disease?', *Parkinsonism Relat Disord*, 16: 57-9.

Bartolome, M. V., M. A. Ibanez-Olias, and P. Gil-Loyzaga. 2002. 'Transitional expression of OX-2 and GAP-43 glycoproteins in developing rat cochlear nerve fibers', *Histol Histopathol*, 17: 83-95.

Batchelor, P. E., M. J. Porritt, P. Martinello, C. L. Parish, G. T. Liberatore, G. A. Donnan, and D. W. Howells. 2002. 'Macrophages and Microglia Produce Local Trophic Gradients That Stimulate Axonal Sprouting Toward but Not beyond the Wound Edge', *Mol Cell Neurosci*, 21: 436-53.

Beck, K. D., B. Knusel, G. Pasinetti, PP. Michel, H. Zawadzka, M. Goldstein and F. Hefti. 1991. 'Tyrosine hydroxylase mRNA expression by dopaminergic neurons in culture: effect of 1-methyl-4-pyridinium treatment.', *J. Neurochem.*, 57: 527-32.

Belanger, M., I. Allaman, and P. J. Magistretti. 2011a. 'Brain energy metabolism: focus on astrocyte-neuron metabolic cooperation', *Cell Metab*, 14: 724-38.

Belanger, M., I. Allaman, and P. J. Magistretti. 2011b. 'Differential effects of pro- and anti-inflammatory cytokines alone or in combinations on the metabolic profile of astrocytes', *J Neurochem*, 116: 564-76.

Berg, D., C. H. Adler, B. R. Bloem, P. Chan, T. Gasser, C. G. Goetz, G. Halliday, A. E. Lang, S. Lewis, Y. Li, I. Liepelt-Scarfone, I. Litvan, K. Marek, C. Maetzler, T. Mi, J. Obeso, W. Oertel, C. W. Olanow, W. Poewe, S. Rios-Romenets, E. Schaffer, K. Seppi, B. Heim, E. Slow, M. Stern, I. O. Bledsoe, G. Deuschl, and R. B. Postuma. 2018. 'Movement disorder society criteria for clinically established early Parkinson's disease', *Mov Disord*, 33: 1643-46.

Berg, D., R. B. Postuma, C. H. Adler, B. R. Bloem, P. Chan, B. Dubois, T. Gasser, C. G. Goetz, G. Halliday, L. Joseph, A. E. Lang, I. Liepelt-Scarfone, I. Litvan, K. Marek, J. Obeso, W. Oertel, C. W. Olanow, W. Poewe, M. Stern, and G. Deuschl. 2015. 'MDS research criteria for prodromal Parkinson's disease', *Mov Disord*, 30: 1600-11.

Bernhart, E., M. Kollroser, G. Rechberger, H. Reicher, A. Heinemann, P. Schratl, S. Hallstrom, A. Wintersperger, C. Nusshold, T. DeVaney, K. Zorn-Pauly, R. Malli, W. Graier, E. Malle, and W. Sattler. 2010. 'Lysophosphatidic acid receptor activation affects the C13NJ microglia cell line proteome leading to alterations in glycolysis, motility, and cytoskeletal architecture', *Proteomics*, 10: 141-58.

Betarbet, R., T. B. Sherer, and J. T. Greenamyre. 2002. 'Animal models of Parkinson's disease', *Bioessays*, 24: 308-18.

Bian, M., J. Liu, X. Hong, M. Yu, Y. Huang, Z. Sheng, J. Fei, and F. Huang. 2012. 'Overexpression of parkin ameliorates dopaminergic neurodegeneration induced by 1- methyl-4-phenyl-1,2,3,6-tetrahydropyridine in mice', *PLoS One*, 7: e39953.

Biber, K., H. Neumann, K. Inoue, and H. W. Boddeke. 2007. 'Neuronal 'On' and 'Off' signals control microglia', *Trends Neurosci*, 30: 596-602.

Bilkei-Gorzo, A. 2014. 'Genetic mouse models of brain ageing and Alzheimer's disease', *Pharmacol Ther*, 142: 244-57.

Biswas, S. K., M. Chittezhath, I. N. Shalova, and J. Y. Lim. 2012. 'Macrophage polarization and plasticity in health and disease', *Immunol Res*, 53: 11-24.

Biswas, S. K., and A. Mantovani. 2012. 'Orchestration of metabolism by macrophages', *Cell Metab*, 15: 432-7.

Bitsch, A., J. Schuchardt, S. Bunkowski, T. Kuhlmann, and W. Bruck. 2000. 'Acute axonal injury in multiple sclerosis. Correlation with demyelination and inflammation', *Brain*, 123 (Pt 6): 1174-83.

Block, M. L., L. Zecca, and J. S. Hong. 2007. 'Microglia-mediated neurotoxicity: uncovering the molecular mechanisms', *Nat Rev Neurosci*, 8: 57-69.

Blum-Degen, D., T. Muller, W. Kuhn, M. Gerlach, H. Przuntek, and P. Riederer. 1995. 'Interleukin-1 beta and interleukin-6 are elevated in the cerebrospinal fluid of Alzheimer's and de novo Parkinson's disease patients', *Neurosci Lett*, 202: 17-20.

Bohlen, C. J., F. C. Bennett, A. F. Tucker, H. Y. Collins, S. B. Mulinyawe, and B. A. Barres. 2017. 'Diverse Requirements for Microglial Survival, Specification, and Function Revealed by Defined-Medium Cultures', *Neuron*, 94: 759-73 e8.

Boje, K. M., and P. K. Arora. 1992. 'Microglial-produced nitric oxide and reactive nitrogen oxides mediate neuronal cell death', *Brain Res*, 587: 250-6.

Boka, G., P. Anglade, D. Wallach, F. Javoy-Agid, Y. Agid, and E. C. Hirsch. 1994. 'Immunocytochemical analysis of tumor necrosis factor and its receptors in Parkinson's disease', *Neurosci Lett*, 172: 151-4.

Bolmont, T., F. Haiss, D. Eicke, R. Radde, C. A. Mathis, W. E. Klunk, S. Kohsaka, M. Jucker, and M. E. Calhoun. 2008. 'Dynamics of the microglial/amyloid interaction indicate a role in plaque maintenance', *J Neurosci*, 28: 4283-92.

Borriello, F., R. Tizard, E. Rue, and R. Reeves. 1998. 'Characterization and localization of Mox2, the gene encoding the murine homolog of the rat MRC OX-2 membrane glycoprotein', *Mamm Genome*, 9: 114-8.

Bournival, J., M. Plouffe, J. Renaud, C. Provencher, and M. G. Martinoli. 2012. 'Quercetin and sesamin protect dopaminergic cells from MPP+-induced neuroinflammation in a microglial (N9)-neuronal (PC12) coculture system', *Oxid Med Cell Longev*, 2012: 921941.

Bove, J., and C. Perier. 2012. 'Neurotoxin-based models of Parkinson's disease', *Neuroscience*, 211: 51-76.

Braak, H., I. Alafuzoff, T. Arzberger, H. Kretzschmar, and K. Del Tredici. 2006. 'Staging of Alzheimer disease-associated neurofibrillary pathology using paraffin sections and immunocytochemistry', *Acta Neuropathol*, 112: 389-404.

Braak, H., K. Del Tredici, U. Rub, R. A. de Vos, E. N. Jansen Steur, and E. Braak. 2003. 'Staging of brain pathology related to sporadic Parkinson's disease', *Neurobiol Aging*, 24: 197-211.

Braak, H., E. Ghebremedhin, U. Rub, H. Bratzke, and K. Del Tredici. 2004. 'Stages in the development of Parkinson's disease-related pathology', *Cell Tissue Res*, 318: 121-34.

Bradford, M. M. 1976. 'A rapid and sensitive method for the quantitation of microgram quantities of protein utilizing the principle of protein-dye binding', *Anal Biochem*, 72: 248-54.

Brendecke, S. M., and M. Prinz. 2015. 'Do not judge a cell by its cover--diversity of CNS resident, adjoining and infiltrating myeloid cells in inflammation', *Semin Immunopathol*, 37: 591-605.

Brochard, V., B. Combadiere, A. Prigent, Y. Laouar, A. Perrin, V. Beray-Berthat, O. Bonduelle, D. Alvarez-Fischer, J. Callebert, J. M. Launay, C. Duyckaerts, R. A. Flavell, E. C. Hirsch, and S. Hunot. 2009. 'Infiltration of CD4+ lymphocytes into the brain contributes to neurodegeneration in a mouse model of Parkinson disease', *J Clin Invest*, 119: 182-92.

Broderick, C., R. M. Hoek, J. V. Forrester, J. Liversidge, J. D. Sedgwick, and A. D. Dick. 2002. 'Constitutive retinal CD200 expression regulates resident microglia and activation state of inflammatory cells during experimental autoimmune uveoretinitis', *Am J Pathol*, 161: 1669-77.

Brooke, G., J. D. Holbrook, M. H. Brown, and A. N. Barclay. 2004. 'Human lymphocytes interact directly with CD47 through a novel member of the signal regulatory protein (SIRP) family', *J Immunol*, 173: 2562-70.

Brown, G. C., and J. J. Neher. 2014. 'Microglial phagocytosis of live neurons', *Nat Rev Neurosci*, 15: 209-16.

Burch, D., and F. Sheerin. 2005. 'Parkinson's disease', *Lancet*, 365: 622-7.

Burguillos, M. A., T. Deierborg, E. Kavanagh, A. Persson, N. Hajji, A. Garcia-Quintanilla, J. Cano, P. Brundin, E. Englund, J. L. Venero, and B. Joseph. 2011. 'Caspase signalling controls microglia activation and neurotoxicity', *Nature*, 472: 319-24.

Burke, R. E., and K. O'Malley. 2013. 'Axon degeneration in Parkinson's disease', *Exp Neurol*, 246: 72-83.

Burns, R. S., C. C. Chiueh, S. P. Markey, M. H. Ebert, D. M. Jacobowitz, and I. J. Kopin. 1983. 'A primate model of parkinsonism: selective destruction of dopaminergic neurons in the pars compacta of the substantia nigra by N-methyl-4-phenyl-1,2,3,6-tetrahydropyridine', *Proc Natl Acad Sci U S A*, 80: 4546-50.

Burnstock, G. 2016. 'P2X ion channel receptors and inflammation', *Purinergic Signal*, 12: 59-67.

C

Calsolaro, V., and P. Edison. 2016. 'Neuroinflammation in Alzheimer's disease: Current evidence and future directions', *Alzheimers Dement*, 12: 719-32.

Cao, X. Z., H. Ma, J. K. Wang, F. Liu, B. Y. Wu, A. Y. Tian, L. L. Wang, and W. F. Tan. 2010. 'Postoperative cognitive deficits and neuroinflammation in the hippocampus triggered by surgical trauma are exacerbated in aged rats', *Prog Neuropsychopharmacol Biol Psychiatry*, 34: 1426-32.

Carare, R. O., M. Bernardes-Silva, T. A. Newman, A. M. Page, J. A. Nicoll, V. H. Perry, and R. O. Weller. 2008. 'Solutes, but not cells, drain from the brain parenchyma along basement membranes of capillaries and arteries: significance for cerebral amyloid angiopathy and neuroimmunology', *Neuropathol Appl Neurobiol*, 34: 131-44.

Carballo-Carbajal, I., A. Laguna, J. Romero-Gimenez, T. Cuadros, J. Bove, M. Martinez-Vicente, A. Parent, M. Gonzalez-Sepulveda, N. Penuelas, A. Torra, B. Rodriguez-Galvan, A. Ballabio, T. Hasegawa, A. Bortolozzi, E. Gelpi, and M. Vila. 2019. 'Brain tyrosinase overexpression implicates age-dependent neuromelanin production in Parkinson's disease pathogenesis', *Nat Commun*, 10: 973.

Cardona, A. E., P. A. Gonzalez, and J. M. Teale. 2003. 'CC chemokines mediate leukocyte trafficking into the central nervous system during murine neurocysticercosis: role of gamma delta T cells in amplification of the host immune response', *Infect Immun*, 71: 2634-42.

Carrillo-de Sauvage, M. A., A. Gomez, C. M. Ros, F. Ros-Bernal, E. D. Martin, A. Perez-Valles, J. M. Gallego-Sanchez, E. Fernandez-Villalba, C. Barcia, Sr., C. Barcia, Jr., and M. T. Herrero. 2012. 'CCL2-expressing astrocytes mediate the extravasation of T lymphocytes in the brain. Evidence from patients with glioma and experimental models in vivo', *PLoS One*, 7: e30762.

Carter, D. A., and A. D. Dick. 2004. 'CD200 maintains microglial potential to migrate in adult human retinal explant model', *Curr Eye Res*, 28: 427-36.

Chan, P., L. E. DeLanney, I. Irwin, J. W. Langston, and D. Di Monte. 1991. 'Rapid ATP loss caused by 1-methyl-4-phenyl-1,2,3,6-tetrahydropyridine in mouse brain', *J Neurochem*, 57: 348-51.

Chang, C. Y., D. K. Choi, D. K. Lee, Y. J. Hong, and E. J. Park. 2013. 'Resveratrol confers protection against rotenone-induced neurotoxicity by modulating myeloperoxidase levels in glial cells', *PLoS One*, 8: e60654.

Chang, G. D., and V. D. Ramirez. 1986. 'The mechanism of action of MPTP and MPP+ on endogenous dopamine release from the rat corpus striatum superfused in vitro', *Brain Res*, 368: 134-40.

Chen, L. C., A. Smith, Y. Ben, B. Zukic, S. Ignacio, D. Moore, and N. Lee. 2004. 'Temporal gene expression patterns in G93A/SOD1 mouse', *Amyotroph Lateral Scler Other Motor Neuron Disord*, 5: 164-71.

Chen, L. J., Y. Q. Gao, X. J. Li, D. H. Shen, and F. Y. Sun. 2005. 'Melatonin protects against MPTP/MPP+ -induced mitochondrial DNA oxidative damage in vivo and in vitro', *J Pineal Res*, 39: 34-42.

Chen, L. W., K. L. Yung, and Y. S. Chan. 2005. 'Reactive astrocytes as potential manipulation targets in novel cell replacement therapy of Parkinson's disease', *Curr Drug Targets*, 6: 821-33.

Chen, S. H., E. A. Oyarzabal, and J. S. Hong. 2013. 'Preparation of rodent primary cultures for neuron-glia, mixed glia, enriched microglia, and reconstituted cultures with microglia', *Methods Mol Biol*, 1041: 231-40.

Chen, T., R. Hou, S. Xu, and C. Wu. 2015. 'Donepezil Regulates 1-Methyl-4-phenylpyridinium-Induced Microglial Polarization in Parkinson's Disease', *ACS Chem Neurosci*, 6: 1708-14.

Chen, Z., D. X. Chen, Y. Kai, I. Khatri, B. Lamptey, and R. M. Gorczynski. 2008. 'Identification of an expressed truncated form of CD200, CD200tr, which is a physiologic antagonist of CD200-induced suppression', *Transplantation*, 86: 1116-24.

Chen, Z., A. Kapus, I. Khatri, O. Kos, F. Zhu, and R. M. Gorczynski. 2018. 'Cell membrane-bound CD200 signals both via an extracellular domain and following nuclear translocation of a cytoplasmic fragment', *Leuk Res*, 69: 72-80.

Chen, Z., X. Ma, J. Zhang, J. Hu, and R. M. Gorczynski. 2010. 'Alternative splicing of CD200 is regulated by an exonic splicing enhancer and SF2/ASF', *Nucleic Acids Res*, 38: 6684-96.

Chen, Z., Y. Yang, X. Yang, C. Zhou, F. Li, P. Lei, L. Zhong, X. Jin, and G. Peng. 2013. 'Immune effects of optimized DNA vaccine and protective effects in a MPTP model of Parkinson's disease', *Neurol Sci*, 34: 1559-70.

Chenais, B., H. Morjani, and J. C. Drapier. 2002. 'Impact of endogenous nitric oxide on microglial cell energy metabolism and labile iron pool', *J Neurochem*, 81: 615-23.

Cheng, H. C., C. M. Ulane, and R. E. Burke. 2010. 'Clinical progression in Parkinson disease and the neurobiology of axons', *Ann Neurol*, 67: 715-25.

Cherry, J. D., J. A. Olschowka, and M. K. O'Banion. 2014a. 'Are "resting" microglia more "m2"?', *Front Immunol*, 5: 594.

Cherry, J. D., J. A. Olschowka, and M. K. O'Banion. 2014b. 'Neuroinflammation and M2 microglia: the good, the bad, and the inflamed', *J Neuroinflammation*, 11: 98.

Chesselet, M. F., F. Richter, C. Zhu, I. Magen, M. B. Watson, and S. R. Subramaniam. 2012. 'A progressive mouse model of Parkinson's disease: the Thy1-aSyn ("Line 61") mice', *Neurotherapeutics*, 9: 297-314.

Chhor, V., T. Le Charpentier, S. Lebon, M. V. Ore, I. L. Celador, J. Josserand, V. Degos, E. Jacotot, H. Hagberg, K. Savman, C. Mallard, P. Gressens, and B. Fleiss. 2013. 'Characterization of phenotype markers and neuronotoxic potential of polarised primary microglia in vitro', *Brain Behav Immun*, 32: 70-85.

Chin, J. H., and N. Vora. 2014. 'The global burden of neurologic diseases', *Neurology*, 83: 349-51.

Chitnis, T., J. Imitola, Y. Wang, W. Elyaman, P. Chawla, M. Sharuk, K. Raddassi, R. T. Bronson, and S. J. Khoury. 2007. 'Elevated neuronal expression of CD200 protects Wlds mice from inflammation-mediated neurodegeneration', *Am J Pathol*, 170: 1695-712.

Choi, D. K., S. Pennathur, C. Perier, K. Tieu, P. Teismann, D. C. Wu, V. Jackson-Lewis, M. Vila, J. P. Vonsattel, J. W. Heinecke, and S. Przedborski. 2005. 'Ablation of the inflammatory enzyme myeloperoxidase mitigates features of Parkinson's disease in mice', *J Neurosci*, 25: 6594-600.

Chung, Y. C., E. Bok, S. H. Huh, J. Y. Park, S. H. Yoon, S. R. Kim, Y. S. Kim, S. Maeng, S. H. Park, and B. K. Jin. 2011. 'Cannabinoid receptor type 1 protects nigrostriatal dopaminergic neurons against MPTP neurotoxicity by inhibiting microglial activation', *J Immunol*, 187: 6508-17.

Chung, Y. C., S. R. Kim, and B. K. Jin. 2010. 'Paroxetine prevents loss of nigrostriatal dopaminergic neurons by inhibiting brain inflammation and oxidative stress in an experimental model of Parkinson's disease', *J Immunol*, 185: 1230-7.

Cicchetti, F., A. L. Brownell, K. Williams, Y. I. Chen, E. Livni, and O. Isacson. 2002. 'Neuroinflammation of the nigrostriatal pathway during progressive 6-OHDA dopamine degeneration in rats monitored by immunohistochemistry and PET imaging', *Eur J Neurosci*, 15: 991-8.

Clark, D. A., A. Keil, Z. Chen, U. Markert, J. Manuel, and R. M. Gorczynski. 2003. 'Placental trophoblast from successful human pregnancies expresses the tolerance signaling molecule, CD200 (OX-2)', *Am J Reprod Immunol*, 50: 187-95.

Clark, M. J., J. Gagnon, A. F. Williams, and A. N. Barclay. 1985. 'MRC OX-2 antigen: a lymphoid/neuronal membrane glycoprotein with a structure like a single immunoglobulin light chain', *EMBO J*, 4: 113-8.

Cohen, M., H. Ben-Yehuda, Z. Porat, C. Raposo, S. Gordon, and M. Schwartz. 2017. 'Newly Formed Endothelial Cells Regulate Myeloid Cell Activity Following Spinal Cord Injury via Expression of CD200 Ligand', *J Neurosci*, 37: 972-85.

Coles, S. J., E. C. Wang, S. Man, R. K. Hills, A. K. Burnett, A. Tonks, and R. L. Darley. 2011. 'CD200 expression suppresses natural killer cell function and directly inhibits patient anti-tumor response in acute myeloid leukemia', *Leukemia*, 25: 792-9.

Colonna, M., and O. Butovsky. 2017. 'Microglia Function in the Central Nervous System During Health and Neurodegeneration', *Annu Rev Immunol*, 35: 441-68.

Cooper, J. F., and J. M. Van Raamsdonk. 2018. 'Modeling Parkinson's Disease in C. elegans', *J Parkinsons Dis*, 8: 17-32.

Copland, D. A., C. J. Calder, B. J. Raveney, L. B. Nicholson, J. Phillips, H. Cherwinski, M. Jenmalm, J. D. Sedgwick, and A. D. Dick. 2007. 'Monoclonal antibody-mediated CD200 receptor signaling suppresses macrophage activation and tissue damage in experimental autoimmune uveoretinitis', *Am J Pathol*, 171: 580-8.

Costa, G., L. Frau, J. Wardas, A. Pinna, A. Plumitallo, and M. Morelli. 2013. 'MPTP-induced dopamine neuron degeneration and glia activation is potentiated in MDMA-pretreated mice', *Mov Disord*, 28: 1957-65.

Costello, D. A., A. Lyons, S. Denieffe, T. C. Browne, F. F. Cox, and M. A. Lynch. 2011. 'Long term potentiation is impaired in membrane glycoprotein CD200-deficient mice: a role for Toll-like receptor activation', *J Biol Chem*, 286: 34722-32.

Cottler, L. B., J. Zunt, B. Weiss, A. K. Kamal, and K. Vaddiparti. 2015. 'Building global capacity for brain and nervous system disorders research', *Nature*, 527: S207-13.

Cox, F. F., D. Carney, A. M. Miller, and M. A. Lynch. 2012. 'CD200 fusion protein decreases microglial activation in the hippocampus of aged rats', *Brain Behav Immun*, 26: 789-96.

Croisier, E., L. B. Moran, D. T. Dexter, R. K. Pearce, and M. B. Graeber. 2005. 'Microglial inflammation in the parkinsonian substantia nigra: relationship to alpha-synuclein deposition', *J Neuroinflammation*, 2: 14.

Cserr, H. F., C. J. Harling-Berg, and P. M. Knopf. 1992. 'Drainage of brain extracellular fluid into blood and deep cervical lymph and its immunological significance', *Brain Pathol*, 2: 269-76.

Czlonkowska, A., M. Kohutnicka, I. Kurkowska-Jastrzebska, and A. Czlonkowski. 1996. 'Microglial reaction in MPTP (1-methyl-4-phenyl-1,2,3,6-tetrahydropyridine) induced Parkinson's disease mice model', *Neurodegeneration*, 5: 137-43.

D

Daeron, M., S. Jaeger, L. Du Pasquier, and E. Vivier. 2008. 'Immunoreceptor tyrosine-based inhibition motifs: a quest in the past and future', *Immunol Rev*, 224: 11-43.

Dauer, W., N. Kholodilov, M. Vila, A. C. Trillat, R. Goodchild, K. E. Larsen, R. Staal, K. Tieu, Y. Schmitz, C. A. Yuan, M. Rocha, V. Jackson-Lewis, S. Hersch, D. Sulzer, S. Przedborski, R. Burke, and R. Hen. 2002. 'Resistance of alpha -synuclein null mice to the parkinsonian neurotoxin MPTP', *Proc Natl Acad Sci U S A*, 99: 14524-9.

Dauer, W., and S. Przedborski. 2003. 'Parkinson's disease: mechanisms and models', *Neuron*, 39: 889-909.

Davalos, D., J. Grutzendler, G. Yang, J. V. Kim, Y. Zuo, S. Jung, D. R. Littman, M. L. Dustin, and W. B. Gan. 2005. 'ATP mediates rapid microglial response to local brain injury in vivo', *Nat Neurosci*, 8: 752-8.

de Lau, L. M., and M. M. Breteler. 2006. 'Epidemiology of Parkinson's disease', *Lancet Neurol*, 5: 525-35.

Deckert, M., J. D. Sedgwick, E. Fischer, and D. Schluter. 2006. 'Regulation of microglial cell responses in murine Toxoplasma encephalitis by CD200/CD200 receptor interaction', *Acta Neuropathol*, 111: 548-58.

Dendrou, C. A., G. McVean, and L. Fugger. 2016. 'Neuroinflammation - using big data to inform clinical practice', *Nat Rev Neurol*, 12: 685-98.

Denieffe, S., R. J. Kelly, C. McDonald, A. Lyons, and M. A. Lynch. 2013. 'Classical activation of microglia in CD200-deficient mice is a consequence of blood brain barrier permeability and infiltration of peripheral cells', *Brain Behav Immun*, 34: 86-97.

Dentesano, G., J. Serratosa, J. M. Tusell, P. Ramon, T. Valente, J. Saura, and C. Sola. 2014. 'CD200R1 and CD200 expression are regulated by PPAR-gamma in activated glial cells', *Glia*, 62: 982-98.

Dentesano, G., M. Straccia, A. Ejarque-Ortiz, J. M. Tusell, J. Serratosa, J. Saura, and C. Sola. 2012. 'Inhibition of CD200R1 expression by C/EBP beta in reactive microglial cells', *J Neuroinflammation*, 9: 165.

Dick, A. D., C. Broderick, J. V. Forrester, and G. J. Wright. 2001. 'Distribution of OX2 antigen and OX2 receptor within retina', *Invest Ophthalmol Vis Sci*, 42: 170-6.

Dickson, D. W. 2012. 'Parkinson's disease and parkinsonism: neuropathology', *Cold Spring Harb Perspect Med*, 2.

Dickson, D. W., H. Braak, J. E. Duda, C. Duyckaerts, T. Gasser, G. M. Halliday, J. Hardy, J. B. Leverenz, K. Del Tredici, Z. K. Wszolek, and I. Litvan. 2009. 'Neuropathological assessment of Parkinson's disease: refining the diagnostic criteria', *Lancet Neurol*, 8: 1150-7.

Dorfman, D. M., and A. Shahsafaei. 2011. 'CD200 (OX-2 membrane glycoprotein) is expressed by follicular T helper cells and in angioimmunoblastic T-cell lymphoma', *Am J Surg Pathol*, 35: 76-83.

Dorsey, E. R., R. Constantinescu, J. P. Thompson, K. M. Biglan, R. G. Holloway, K. Kieburtz, F. J. Marshall, B. M. Ravina, G. Schifitto, A. Siderowf, and C. M. Tanner. 2007. 'Projected number of people with Parkinson disease in the most populous nations, 2005 through 2030', *Neurology*, 68: 384-6.

Du, C., M. Jin, Y. Hong, Q. Li, X. H. Wang, J. M. Xu, F. Wang, Y. Zhang, J. Jia, C. F. Liu, and L. F. Hu. 2014. 'Downregulation of cystathionine beta-synthase/hydrogen sulfide contributes to rotenone-induced microglia polarization toward M1 type', *Biochem Biophys Res Commun*, 451: 239-45.

Durafourt, B. A., C. S. Moore, D. A. Zammit, T. A. Johnson, F. Zaguia, M. C. Guiot, A. Bar-Or, and J. P. Antel. 2012. 'Comparison of polarization properties of human adult microglia and blood-derived macrophages', *Glia*, 60: 717-27.

Dzamko, N., C. L. Geczy, and G. M. Halliday. 2015. 'Inflammation is genetically implicated in Parkinson's disease', *Neuroscience*, 302: 89-102.

E

Ecker, J., G. Liebisch, M. Englmaier, M. Grandl, H. Robenek, and G. Schmitz. 2010. 'Induction of fatty acid synthesis is a key requirement for phagocytic differentiation of human monocytes', *Proc Natl Acad Sci U S A*, 107: 7817-22.

Edison, P., I. Ahmed, Z. Fan, R. Hinz, G. Gelosa, K. Ray Chaudhuri, Z. Walker, F. E. Turkheimer, and D. J. Brooks. 2013. 'Microglia, amyloid, and glucose metabolism in Parkinson's disease with and without dementia', *Neuropsychopharmacology*, 38: 938-49.

ElAli, A., and N. Jean LeBlanc. 2016. 'The Role of Monocytes in Ischemic Stroke Pathobiology: New Avenues to Explore', *Front Aging Neurosci*, 8: 29.

Emborg, M. E. 2007. 'Nonhuman primate models of Parkinson's disease', *ILAR J*, 48: 339-55.

Emmrich, J. V., T. C. Hornik, J. J. Neher, and G. C. Brown. 2013. 'Rotenone induces neuronal death by microglial phagocytosis of neurons', *FEBS J*, 280: 5030-8.

Engelhardt, B., R. O. Carare, I. Bechmann, A. Flugel, J. D. Laman, and R. O. Weller. 2016. 'Vascular, glial, and lymphatic immune gateways of the central nervous system', *Acta Neuropathol*, 132: 317-38.

Engelhardt, B., P. Vajkoczy, and R. O. Weller. 2017. 'The movers and shapers in immune privilege of the CNS', *Nat Immunol*, 18: 123-31.

Escartin, C., and G. Bonvento. 2008. 'Targeted activation of astrocytes: a potential neuroprotective strategy', *Mol Neurobiol*, 38: 231-41.

F

Fabre, E., J. Monserrat, A. Herrero, G. Barja, and M. L. Leret. 1999. 'Effect of MPTP on brain mitochondrial H2O2 and ATP production and on dopamine and DOPAC in the striatum', *J Physiol Biochem*, 55: 325-31.

Farkas, E., G. I. De Jong, R. A. de Vos, E. N. Jansen Steur, and P. G. Luiten. 2000. 'Pathological features of cerebral cortical capillaries are doubled in Alzheimer's disease and Parkinson's disease', *Acta Neuropathol*, 100: 395-402.

Faucheux, B. A., A. M. Bonnet, Y. Agid, and E. C. Hirsch. 1999. 'Blood vessels change in the mesencephalon of patients with Parkinson's disease', *Lancet*, 353: 981-2.

Fenn, B., A. T. Bulti, T. Nduna, A. Duffield, and F. Watson. 2012. 'An evaluation of an operations research project to reduce childhood stunting in a food-insecure area in Ethiopia', *Public Health Nutr*, 15: 1746-54.

Ferger, A. I., L. Campanelli, V. Reimer, K. N. Muth, I. Merdian, A. C. Ludolph, and A. Witting. 2010. 'Effects of mitochondrial dysfunction on the immunological properties of microglia', *J Neuroinflammation*, 7: 45.

Ferreira, S. A., and M. Romero-Ramos. 2018. 'Microglia Response During Parkinson's Disease: Alpha-Synuclein Intervention', *Front Cell Neurosci*, 12: 247.

Ferrer, I., R. Blanco, B. Cutillas, and S. Ambrosio. 2000. 'Fas and Fas-L expression in Huntington's disease and Parkinson's disease', *Neuropathol Appl Neurobiol*, 26: 424-33.

Filardy, A. A., D. R. Pires, M. P. Nunes, C. M. Takiya, C. G. Freire-de-Lima, F. L. Ribeiro-Gomes, and G. A. DosReis. 2010. 'Proinflammatory clearance of apoptotic neutrophils induces an IL-12(low)IL-10(high) regulatory phenotype in macrophages', *J Immunol*, 185: 2044-50.

Forno, L. S., J. W. Langston, L. E. DeLanney, I. Irwin, and G. A. Ricaurte. 1986. 'Locus ceruleus lesions and eosinophilic inclusions in MPTP-treated monkeys', *Ann Neurol*, 20: 449-55.

Forsyth, C. B., K. M. Shannon, J. H. Kordower, R. M. Voigt, M. Shaikh, J. A. Jaglin, J. D. Estes, H. B. Dodiya, and A. Keshavarzian. 2011. 'Increased intestinal permeability correlates with sigmoid mucosa alpha-synuclein staining and endotoxin exposure markers in early Parkinson's disease', *PLoS One*, 6: e28032.

Frade, J. M., and Y. A. Barde. 1998. 'Microglia-derived nerve growth factor causes cell death in the developing retina', *Neuron*, 20: 35-41.

Francis, J. W., J. Von Visger, G. J. Markelonis, and T. H. Oh. 1995. 'Neuroglial responses to the dopaminergic neurotoxicant 1-methyl-4-phenyl-1,2,3,6-tetrahydropyridine in mouse striatum', *Neurotoxicol Teratol*, 17: 7-12.

Franco, R., and D. Fernandez-Suarez. 2015. 'Alternatively activated microglia and macrophages in the central nervous system', *Prog Neurobiol*, 131: 65-86.

Frank, M. G., R. M. Barrientos, J. C. Biedenkapp, J. W. Rudy, L. R. Watkins, and S. F. Maier. 2006. 'mRNA up-regulation of MHC II and pivotal pro-inflammatory genes in normal brain aging', *Neurobiol Aging*, 27: 717-22.

Frank, M. G., L. K. Fonken, J. L. Annis, L. R. Watkins, and S. F. Maier. 2018. 'Stress disinhibits microglia via down-regulation of CD200R: A mechanism of neuroinflammatory priming', *Brain Behav Immun*, 69: 62-73.

G

Gadani, S. P., J. C. Cronk, G. T. Norris, and J. Kipnis. 2012. 'IL-4 in the brain: a cytokine to remember', *J Immunol*, 189: 4213-9.

Galvan-Pena, S., and L. A. O'Neill. 2014. 'Metabolic reprograming in macrophage polarization', *Front Immunol*, 5: 420.

Gao, H. M., and J. S. Hong. 2008. 'Why neurodegenerative diseases are progressive: uncontrolled inflammation drives disease progression', *Trends Immunol*, 29: 357-65.

Gao, H. M., J. S. Hong, W. Zhang, and B. Liu. 2002. 'Distinct role for microglia in rotenone-induced degeneration of dopaminergic neurons', *J Neurosci*, 22: 782-90.

Gao, H. M., P. T. Kotzbauer, K. Uryu, S. Leight, J. Q. Trojanowski, and V. M. Lee. 2008. 'Neuroinflammation and oxidation/nitration of alpha-synuclein linked to dopaminergic neurodegeneration', *J Neurosci*, 28: 7687-98.

Gao, H. M., B. Liu, W. Zhang, and J. S. Hong. 2003a. 'Critical role of microglial NADPH oxidase-derived free radicals in the in vitro MPTP model of Parkinson's disease', *FASEB J*, 17: 1954-6.

o, H. M., B. Liu, W. Zhang, and J. S. Hong. 2003b. 'Novel anti-inflammatory therapy for Parkinson's disease', *Trends Pharmacol Sci*, 24: 395-401.

o, H. M., B. Liu, W. Zhang, and J. S. Hong. 2003c. 'Synergistic dopaminergic neurotoxicity of MPTP and inflammogen lipopolysaccharide: relevance to the etiology of Parkinson's disease', *FASEB J*, 17: 1957-9.

Gavillet, M., I. Allaman, and P. J. Magistretti. 2008. 'Modulation of astrocytic metabolic phenotype by proinflammatory cytokines', *Glia*, 56: 975-89.

Gelb, D. J., E. Oliver, and S. Gilman. 1999. 'Diagnostic criteria for Parkinson disease', *Arch Neurol*, 56: 33-9.

Gelders, G., V. Baekelandt, and A. Van der Perren. 2018. 'Linking Neuroinflammation and Neurodegeneration in Parkinson's Disease', *J Immunol Res*, 2018: 4784268.

Gemma, C., and A. D. Bachstetter. 2013. 'The role of microglia in adult hippocampal neurogenesis', *Front Cell Neurosci*, 7: 229.

Gerhard, A., N. Pavese, G. Hotton, F. Turkheimer, M. Es, A. Hammers, K. Eggert, W. Oertel, R. B. Banati, and D. J. Brooks. 2006. 'In vivo imaging of microglial activation with [11C](R)-PK11195 PET in idiopathic Parkinson's disease', *Neurobiol Dis*, 21: 404-12.

Ghesquiere, B., B. W. Wong, A. Kuchnio, and P. Carmeliet. 2014. 'Metabolism of stromal and immune cells in health and disease', *Nature*, 511: 167-76.

Ghosh, S., E. Castillo, E. S. Frias, and R. A. Swanson. 2018. 'Bioenergetic regulation of microglia', *Glia*, 66: 1200-12.

Giasson, B. I., J. E. Duda, I. V. Murray, Q. Chen, J. M. Souza, H. I. Hurtig, H. Ischiropoulos, J. Q. Trojanowski, and V. M. Lee. 2000. 'Oxidative damage linked to neurodegeneration by selective alpha-synuclein nitration in synucleinopathy lesions', *Science*, 290: 985-9.

Gibb, W. R., and A. J. Lees. 1988. 'The relevance of the Lewy body to the pathogenesis of idiopathic Parkinson's disease', *J Neurol Neurosurg Psychiatry*, 51: 745-52.

Gibrat, C., M. Saint-Pierre, M. Bousquet, D. Levesque, C. Rouillard, and F. Cicchetti. 2009. 'Differences between subacute and chronic MPTP mice models: investigation of dopaminergic neuronal degeneration and alpha-synuclein inclusions', *J Neurochem*, 109: 1469-82.

Gimeno-Bayon, J., A. Lopez-Lopez, M. J. Rodriguez, and N. Mahy. 2014. 'Glucose pathways adaptation supports acquisition of activated microglia phenotype', *J Neurosci Res*, 92: 723-31.

Ginhoux, F., and S. Garel. 2018. 'The mysterious origins of microglia', *Nat Neurosci*, 21: 897-99.

Ginhoux, F., M. Greter, M. Leboeuf, S. Nandi, P. See, S. Gokhan, M. F. Mehler, S. J. Conway, L. G. Ng, E. R. Stanley, I. M. Samokhvalov, and M. Merad. 2010. 'Fate mapping analysis reveals that adult microglia derive from primitive macrophages', *Science*, 330: 841-5.

Giovanni, A., B. A. Sieber, R. E. Heikkila, and P. K. Sonsalla. 1991. 'Correlation between the neostriatal content of the 1-methyl-4-phenylpyridinium species and dopaminergic neurotoxicity following 1-methyl-4-phenyl-1,2,3,6-tetrahydropyridine administration to several strains of mice', *J Pharmacol Exp Ther*, 257: 691-7.

Glass, C. K., K. Saijo, B. Winner, M. C. Marchetto, and F. H. Gage. 2010. 'Mechanisms underlying inflammation in neurodegeneration', *Cell*, 140: 918-34.

Goetz, C. G. 2011. 'The history of Parkinson's disease: early clinical descriptions and neurological therapies', *Cold Spring Harb Perspect Med*, 1: a008862.

Goldman, S. M. 2014. 'Environmental toxins and Parkinson's disease', *Annu Rev Pharmacol Toxicol*, 54: 141-64.

Goldmann, J., E. Kwidzinski, C. Brandt, J. Mahlo, D. Richter, and I. Bechmann. 2006. 'T cells traffic from brain to cervical lymph nodes via the cribroid plate and the nasal mucosa', *J Leukoc Biol*, 80: 797-801.

Gomez-Nicola, D., and V. H. Perry. 2015. 'Microglial dynamics and role in the healthy and diseased brain: a paradigm of functional plasticity', *Neuroscientist*, 21: 169-84.

Gomez-Nicola, D., S. T. Schetters, and V. H. Perry. 2014. 'Differential role of CCR2 in the dynamics of microglia and perivascular macrophages during prion disease', *Glia*, 62: 1041-52.

Gorczynski, R., Z. Chen, Y. Kai, L. Lee, S. Wong, and P. A. Marsden. 2004. 'CD200 is a ligand for all members of the CD200R family of immunoregulatory molecules', *J Immunol*, 172: 7744-9.

Gorczynski, R., Z. Chen, I. Khatri, and K. Yu. 2013. 'sCD200 present in mice receiving cardiac and skin allografts causes immunosuppression in vitro and induces Tregs', *Transplantation*, 95: 442-7.

Gorczynski, R. M., Z. Chen, D. A. Clark, Y. Kai, L. Lee, J. Nachman, S. Wong, and P. Marsden. 2004. 'Structural and functional heterogeneity in the CD200R family of immunoregulatory molecules and their expression at the feto-maternal interface', *Am J Reprod Immunol*, 52: 147-63.

Gorczynski, R. M., Z. Chen, J. Diao, I. Khatri, K. Wong, K. Yu, and J. Behnke. 2010. 'Breast cancer cell CD200 expression regulates immune response to EMT6 tumor cells in mice', *Breast Cancer Res Treat*, 123: 405-15.

Gorczynski, R. M., Z. Chen, L. Lee, K. Yu, and J. Hu. 2002. 'Anti-CD200R ameliorates collagen-induced arthritis in mice', *Clin Immunol*, 104: 256-64.

Gorczynski, R. M., K. Yu, and D. Clark. 2000. 'Receptor engagement on cells expressing a ligand for the tolerance-inducing molecule OX2 induces an immunoregulatory population that inhibits alloreactivity in vitro and in vivo', *J Immunol*, 165: 4854-60.

Gosselin, D., D. Skola, N. G. Coufal, I. R. Holtman, J. C. M. Schlachetzki, E. Sajti, B. N. Jaeger, C. O'Connor, C. Fitzpatrick, M. P. Pasillas, M. Pena, A. Adair, D. D. Gonda, M. L. Levy, R. M. Ransohoff, F. H. Gage, and C. K. Glass. 2017. 'An environment-dependent transcriptional network specifies human microglia identity', *Science*, 356.

Goswami, P., S. Gupta, J. Biswas, N. Joshi, S. Swarnkar, C. Nath, and S. Singh. 2016. 'Endoplasmic Reticulum Stress Plays a Key Role in Rotenone-Induced Apoptotic Death of Neurons', *Mol Neurobiol*, 53: 285-98.

H

Halliday, G., A. Lees, and M. Stern. 2011. 'Milestones in Parkinson's disease--clinical and pathologic features', *Mov Disord*, 26: 1015-21.

Hallman, H., L. Olson, and G. Jonsson. 1984. 'Neurotoxicity of the meperidine analogue N-methyl-4-phenyl-1,2,3,6-tetrahydropyridine on brain catecholamine neurons in the mouse', *Eur J Pharmacol*, 97: 133-6.

Hamre, K., R. Tharp, K. Poon, X. Xiong, and R. J. Smeyne. 1999. 'Differential strain susceptibility following 1-methyl-4-phenyl-1,2,3,6-tetrahydropyridine (MPTP) administration acts in an autosomal dominant fashion: quantitative analysis in seven strains of Mus musculus', *Brain Res*, 828: 91-103.

Hanisch, U. K., and H. Kettenmann. 2007. 'Microglia: active sensor and versatile effector cells in the normal and pathologic brain', *Nat Neurosci*, 10: 1387-94.

Harms, A. S., S. Cao, A. L. Rowse, A. D. Thome, X. Li, L. R. Mangieri, R. Q. Cron, J. J. Shacka, C. Raman, and D. G. Standaert. 2013. 'MHCII is required for alpha-synuclein-induced activation of microglia, CD4 T cell proliferation, and dopaminergic neurodegeneration', *J Neurosci*, 33: 9592-600.

Haschemi, A., P. Kosma, L. Gille, C. R. Evans, C. F. Burant, P. Starkl, B. Knapp, R. Haas, J. A. Schmid, C. Jandl, S. Amir, G. Lubec, J. Park, H. Esterbauer, M. Bilban, L. Brizuela, J. A. Pospisilik, L. E. Otterbein, and O. Wagner. 2012. 'The sedoheptulose kinase CARKL directs macrophage polarization through control of glucose metabolism', *Cell Metab*, 15: 813-26.

Hatherley, D., H. M. Cherwinski, M. Moshref, and A. N. Barclay. 2005. 'Recombinant CD200 protein does not bind activating proteins closely related to CD200 receptor', *J Immunol*, 175: 2469-74.

Hatherley, D., S. M. Lea, S. Johnson, and A. N. Barclay. 2013. 'Structures of CD200/CD200 receptor family and implications for topology, regulation, and evolution', *Structure*, 21: 820-32.

Hawkes, C. H., K. Del Tredici, and H. Braak. 2007. 'Parkinson's disease: a dual-hit hypothesis', *Neuropathol Appl Neurobiol*, 33: 599-614.

Hayakawa, K., X. Wang, and E. H. Lo. 2016. 'CD200 increases alternatively activated macrophages through cAMP-response element binding protein - C/EBP-beta signaling', *J Neurochem*, 136: 900-6.

Hayley, S., S. J. Crocker, P. D. Smith, T. Shree, V. Jackson-Lewis, S. Przedborski, M. Mount, R. Slack, H. Anisman, and D. S. Park. 2004. 'Regulation of dopaminergic loss by Fas in a 1-

methyl-4-phenyl-1,2,3,6-tetrahydropyridine model of Parkinson's disease', *J Neurosci*, 24: 2045-53.

Hebert, G., J. Arsaut, R. Dantzer, and J. Demotes-Mainard. 2003. 'Time-course of the expression of inflammatory cytokines and matrix metalloproteinases in the striatum and mesencephalon of mice injected with 1-methyl-4-phenyl-1,2,3,6-tetrahydropyridine, a dopaminergic neurotoxin', *Neurosci Lett*, 349: 191-5.

Heneka, M. T. 2019. 'Microglia take centre stage in neurodegenerative disease', *Nat Rev Immunol*, 19: 79-80.

Heneka, M. T., M. J. Carson, J. El Khoury, G. E. Landreth, F. Brosseron, D. L. Feinstein, A. H. Jacobs, T. Wyss-Coray, J. Vitorica, R. M. Ransohoff, K. Herrup, S. A. Frautschy, B. Finsen, G. C. Brown, A. Verkhratsky, K. Yamanaka, J. Koistinaho, E. Latz, A. Halle, G. C. Petzold, T. Town, D. Morgan, M. L. Shinohara, V. H. Perry, C. Holmes, N. G. Bazan, D. J. Brooks, S. Hunot, B. Joseph, N. Deigendesch, O. Garaschuk, E. Boddeke, C. A. Dinarello, J. C. Breitner, G. M. Cole, D. T. Golenbock, and M. P. Kummer. 2015. 'Neuroinflammation in Alzheimer's disease', *Lancet Neurol*, 14: 388-405.

Heneka, M. T., M. P. Kummer, and E. Latz. 2014. 'Innate immune activation in neurodegenerative disease', *Nat Rev Immunol*, 14: 463-77.

Henze, C., A. Hartmann, T. Lescot, E. C. Hirsch, and P. P. Michel. 2005. 'Proliferation of microglial cells induced by 1-methyl-4-phenylpyridinium in mesencephalic cultures results from an astrocyte-dependent mechanism: role of granulocyte macrophage colony-stimulating factor', *J Neurochem*, 95: 1069-77.

Hernangomez, M., F. J. Carrillo-Salinas, M. Mecha, F. Correa, L. Mestre, F. Loria, A. Feliu, F. Docagne, and C. Guaza. 2014. 'Brain innate immunity in the regulation of neuroinflammation: therapeutic strategies by modulating CD200-CD200R interaction involve the cannabinoid system', *Curr Pharm Des*, 20: 4707-22.

Hernangomez, M., I. Klusakova, M. Joukal, I. Hradilova-Svizenska, C. Guaza, and P. Dubovy. 2016. 'CD200R1 agonist attenuates glial activation, inflammatory reactions, and hypersensitivity immediately after its intrathecal application in a rat neuropathic pain model', *J Neuroinflammation*, 13: 43.

Hernangomez, M., L. Mestre, F. G. Correa, F. Loria, M. Mecha, P. M. Inigo, F. Docagne, R. O. Williams, J. Borrell, and C. Guaza. 2012. 'CD200-CD200R1 interaction contributes to neuroprotective effects of anandamide on experimentally induced inflammation', *Glia*, 60: 1437-50.

Herrera, A. J., A. Castano, J. L. Venero, J. Cano, and A. Machado. 2000. 'The single intranigral injection of LPS as a new model for studying the selective effects of inflammatory reactions on dopaminergic system', *Neurobiol Dis*, 7: 429-47.

Hertz, L., L. Peng, and G. A. Dienel. 2007. 'Energy metabolism in astrocytes: high rate of oxidative metabolism and spatiotemporal dependence on glycolysis/glycogenolysis', *J Cereb Blood Flow Metab*, 27: 219-49.

Hickman, S., S. Izzy, P. Sen, L. Morsett, and J. El Khoury. 2018. 'Microglia in neurodegeneration', *Nat Neurosci*, 21: 1359-69.

Hirsch, E. C. 2006. 'Altered regulation of iron transport and storage in Parkinson's disease', *J Neural Transm Suppl*: 201-4.

Hirsch, E. C., T. Breidert, E. Rousselet, S. Hunot, A. Hartmann, and P. P. Michel. 2003. 'The role of glial reaction and inflammation in Parkinson's disease', *Ann N Y Acad Sci*, 991: 214-28.

Hirsch, E. C., and S. Hunot. 2009. 'Neuroinflammation in Parkinson's disease: a target for neuroprotection?', *Lancet Neurol*, 8: 382-97.

Hirsch, E. C., S. Hunot, P. Damier, and B. Faucheux. 1998. 'Glial cells and inflammation in Parkinson's disease: a role in neurodegeneration?', *Ann Neurol*, 44: S115-20.

Hirsch, E. C., S. Vyas, and S. Hunot. 2012. 'Neuroinflammation in Parkinson's disease', *Parkinsonism Relat Disord*, 18 Suppl 1: S210-2.

Hoek, R. M., S. R. Ruuls, C. A. Murphy, G. J. Wright, R. Goddard, S. M. Zurawski, B. Blom, M. E. Homola, W. J. Streit, M. H. Brown, A. N. Barclay, and J. D. Sedgwick. 2000. 'Down-regulation of the macrophage lineage through interaction with OX2 (CD200)', *Science*, 290: 1768-71.

Holmannova, D., M. Kolackova, K. Kondelkova, P. Kunes, J. Krejsek, and C. Andrys. 2012. 'CD200/CD200R paired potent inhibitory molecules regulating immune and inflammatory responses; Part I: CD200/CD200R structure, activation, and function', *Acta Medica (Hradec Kralove)*, 55: 12-7.

Holmqvist, S., O. Chutna, L. Bousset, P. Aldrin-Kirk, W. Li, T. Bjorklund, Z. Y. Wang, L. Roybon, R. Melki, and J. Y. Li. 2014. 'Direct evidence of Parkinson pathology spread from the gastrointestinal tract to the brain in rats', *Acta Neuropathol*, 128: 805-20.

Hong, S., V. F. Beja-Glasser, B. M. Nfonoyim, A. Frouin, S. Li, S. Ramakrishnan, K. M. Merry, Q. Shi, A. Rosenthal, B. A. Barres, C. A. Lemere, D. J. Selkoe, and B. Stevens. 2016. 'Complement and microglia mediate early synapse loss in Alzheimer mouse models', *Science*, 352: 712-16.

Hornykiewicz, O. 2008. 'Basic research on dopamine in Parkinson's disease and the discovery of the nigrostriatal dopamine pathway: the view of an eyewitness', *Neurodegener Dis*, 5: 114-7.

Hou, L., X. Zhou, C. Zhang, K. Wang, X. Liu, Y. Che, F. Sun, H. Li, Q. Wang, D. Zhang, and J. S. Hong. 2017. 'NADPH oxidase-derived H2O2 mediates the regulatory effects of microglia on astrogliosis in experimental models of Parkinson's disease', *Redox Biol*, 12: 162-70.

Houser, M. C., and M. G. Tansey. 2017. 'The gut-brain axis: is intestinal inflammation a silent driver of Parkinson's disease pathogenesis?', *NPJ Parkinsons Dis*, 3: 3.

Hu, X., P. Li, Y. Guo, H. Wang, R. K. Leak, S. Chen, Y. Gao, and J. Chen. 2012. 'Microglia/macrophage polarization dynamics reveal novel mechanism of injury expansion after focal cerebral ischemia', *Stroke*, 43: 3063-70.

Huang, R., Q. Lan, L. Chen, H. Zhong, L. Cui, L. Jiang, H. Huang, L. Li, S. Zeng, M. Li, X. Zhao, and F. Xu. 2018. 'CD200Fc Attenuates Retinal Glial Responses and RGCs Apoptosis After Optic Nerve Crush by Modulating CD200/CD200R1 Interaction', *J Mol Neurosci*, 64: 200-10.

Hunot, S., F. Boissiere, B. Faucheux, B. Brugg, A. Mouatt-Prigent, Y. Agid, and E. C. Hirsch. 1996. 'Nitric oxide synthase and neuronal vulnerability in Parkinson's disease', *Neuroscience*, 72: 355-63.

Hunot, S., N. Dugas, B. Faucheux, A. Hartmann, M. Tardieu, P. Debre, Y. Agid, B. Dugas, and E. C. Hirsch. 1999. 'FcepsilonRII/CD23 is expressed in Parkinson's disease and induces, in vitro, production of nitric oxide and tumor necrosis factor-alpha in glial cells', *J Neurosci*, 19: 3440-7.

Hutchings, M., and R. O. Weller. 1986. 'Anatomical relationships of the pia mater to cerebral blood vessels in man', *J Neurosurg*, 65: 316-25.

I

Iacono, D., M. Geraci-Erck, M. L. Rabin, C. H. Adler, G. Serrano, T. G. Beach, and R. Kurlan. 2015. 'Parkinson disease and incidental Lewy body disease: Just a question of time?', *Neurology*, 85: 1670-9.

Iannaccone, S., C. Cerami, M. Alessio, V. Garibotto, A. Panzacchi, S. Olivieri, G. Gelsomino, R. M. Moresco, and D. Perani. 2013. 'In vivo microglia activation in very early dementia with Lewy bodies, comparison with Parkinson's disease', *Parkinsonism Relat Disord*, 19: 47-52.

Iliff, J. J., M. Wang, Y. Liao, B. A. Plogg, W. Peng, G. A. Gundersen, H. Benveniste, G. E. Vates, R. Deane, S. A. Goldman, E. A. Nagelhus, and M. Nedergaard. 2012. 'A paravascular

pathway facilitates CSF flow through the brain parenchyma and the clearance of interstitial solutes, including amyloid beta', *Sci Transl Med*, 4: 147ra11.

Imamura, K., N. Hishikawa, M. Sawada, T. Nagatsu, M. Yoshida, and Y. Hashizume. 2003. 'Distribution of major histocompatibility complex class II-positive microglia and cytokine profile of Parkinson's disease brains', *Acta Neuropathol*, 106: 518-26.

J

Jackson-Lewis, V., J. Blesa, and S. Przedborski. 2012. 'Animal models of Parkinson's disease', *Parkinsonism Relat Disord*, 18 Suppl 1: S183-5.

Jackson-Lewis, V., M. Jakowec, R. E. Burke, and S. Przedborski. 1995. 'Time course and morphology of dopaminergic neuronal death caused by the neurotoxin 1-methyl-4-phenyl-1,2,3,6-tetrahydropyridine', *Neurodegeneration*, 4: 257-69.

Jackson-Lewis, V., and S. Przedborski. 2007. 'Protocol for the MPTP mouse model of Parkinson's disease', *Nat Protoc*, 2: 141-51.

Jang, H., D. A. Boltz, R. G. Webster, and R. J. Smeyne. 2009. 'Viral parkinsonism', *Biochim Biophys Acta*, 1792: 714-21.

Javitch, J. A., R. J. D'Amato, S. M. Strittmatter, and S. H. Snyder. 1985. 'Parkinsonism-inducing neurotoxin, N-methyl-4-phenyl-1,2,3,6 -tetrahydropyridine: uptake of the metabolite N-methyl-4-phenylpyridine by dopamine neurons explains selective toxicity', *Proc Natl Acad Sci U S A*, 82: 2173-7.

Jenmalm, M. C., H. Cherwinski, E. P. Bowman, J. H. Phillips, and J. D. Sedgwick. 2006. 'Regulation of myeloid cell function through the CD200 receptor', *J Immunol*, 176: 191-9.

Jiang, L., F. Xu, W. He, L. Chen, H. Zhong, Y. Wu, S. Zeng, L. Li, and M. Li. 2016. 'CD200Fc reduces TLR4-mediated inflammatory responses in LPS-induced rat primary microglial cells via inhibition of the NF-kappaB pathway', *Inflamm Res*, 65: 521-32.

Jin, M., B. W. Kim, S. Koppula, I. S. Kim, J. H. Park, H. Kumar, and D. K. Choi. 2012. 'Molecular effects of activated BV-2 microglia by mitochondrial toxin 1-methyl-4-phenylpyridinium', *Neurotoxicology*, 33: 147-55.

K

Kacerovsky, M., M. Drahosova, J. Krejsek, I. Musilova, H. Hornychova, V. Matula, O. Simetka, B. Jacobsson, and C. Andrys. 2013. 'Amniotic fluid CD200 levels in pregnancies complicated by preterm prelabor rupture of the membranes', *J Matern Fetal Neonatal Med*, 26: 1416-24.

Kalia, L. V., and A. E. Lang. 2015. 'Parkinson's disease', *Lancet*, 386: 896-912.

Kamel, F., S. M. Goldman, D. M. Umbach, H. Chen, G. Richardson, M. R. Barber, C. Meng, C. Marras, M. Korell, M. Kasten, J. A. Hoppin, K. Comyns, A. Chade, A. Blair, G. S. Bhudhikanok, G. Webster Ross, J. William Langston, D. P. Sandler, and C. M. Tanner. 2014. 'Dietary fat intake, pesticide use, and Parkinson's disease', *Parkinsonism Relat Disord*, 20: 82-7.

Kaminski, M., I. Bechmann, M. Pohland, J. Kiwit, R. Nitsch, and J. Glumm. 2012. 'Migration of monocytes after intracerebral injection at entorhinal cortex lesion site', *J Leukoc Biol*, 92: 31-9.

Keener, A. M., and Y. M. Bordelon. 2016. 'Parkinsonism', *Semin Neurol*, 36: 330-4.

Kettenmann, H., U. K. Hanisch, M. Noda, and A. Verkhratsky. 2011. 'Physiology of microglia', *Physiol Rev*, 91: 461-553.

Kettenmann, H., F. Kirchhoff, and A. Verkhratsky. 2013. 'Microglia: new roles for the synaptic stripper', *Neuron*, 77: 10-8.

Khan, M. M., D. Kempuraj, R. Thangavel, and A. Zaheer. 2013. 'Protection of MPTP-induced neuroinflammation and neurodegeneration by Pycnogenol', *Neurochem Int*, 62: 379-88.

Khatri, I., I. Boudakov, B. Lamptey, A. Taseva, K. Wong, A. Podnos and R. M. Gorczynski. 2012. 'Structural and functional consequences of switching carboxy terminal domains in mouse CD200 receptors', *Open Journal of Immunology*, 2: 168-86.

Kida, S., A. Pantazis, and R. O. Weller. 1993. 'CSF drains directly from the subarachnoid space into nasal lymphatics in the rat. Anatomy, histology and immunological significance', *Neuropathol Appl Neurobiol*, 19: 480-8.

Kim, B. W., K. H. Jeong, J. H. Kim, M. Jin, J. H. Kim, M. G. Lee, D. K. Choi, S. Y. Won, C. McLean, M. T. Jeon, H. W. Lee, S. R. Kim, and K. Suk. 2016. 'Pathogenic Upregulation of Glial Lipocalin-2 in the Parkinsonian Dopaminergic System', *J Neurosci*, 36: 5608-22.

Kinugawa, K., Y. Monnet, C. Bechade, D. Alvarez-Fischer, E. C. Hirsch, A. Bessis, and S. Hunot. 2013. 'DAP12 and CD11b contribute to the microglial-induced death of dopaminergic neurons in vitro but not in vivo in the MPTP mouse model of Parkinson's disease', *J Neuroinflammation*, 10: 82.

Kirschner, P. B., B. G. Jenkins, J. B. Schulz, S. P. Finkelstein, R. T. Matthews, B. R. Rosen, and M. F. Beal. 1996. 'NGF, BDNF and NT-5, but not NT-3 protect against MPP+ toxicity and oxidative stress in neonatal animals', *Brain Res*, 713: 178-85.

Kivisakk, P., B. Tucky, T. Wei, J. J. Campbell, and R. M. Ransohoff. 2006. 'Human cerebrospinal fluid contains CD4+ memory T cells expressing gut- or skin-specific trafficking determinants: relevance for immunotherapy', *BMC Immunol*, 7: 14.

Klein, C., and A. Westenberger. 2012. 'Genetics of Parkinson's disease', *Cold Spring Harb Perspect Med*, 2: a008888.

Klintworth, H., G. Garden, and Z. Xia. 2009. 'Rotenone and paraquat do not directly activate microglia or induce inflammatory cytokine release', *Neurosci Lett*, 462: 1-5.

Knott, C., G. Stern, and G. P. Wilkin. 2000. 'Inflammatory regulators in Parkinson's disease: iNOS, lipocortin-1, and cyclooxygenases-1 and -2', *Mol Cell Neurosci*, 16: 724-39.

Kohutnicka, M., E. Lewandowska, I. Kurkowska-Jastrzebska, A. Czlonkowski, and A. Czlonkowska. 1998. 'Microglial and astrocytic involvement in a murine model of Parkinson's disease induced by 1-methyl-4-phenyl-1,2,3,6-tetrahydropyridine (MPTP)', *Immunopharmacology*, 39: 167-80.

Koning, N., L. Bo, R. M. Hoek, and I. Huitinga. 2007. 'Downregulation of macrophage inhibitory molecules in multiple sclerosis lesions', *Ann Neurol*, 62: 504-14.

Koning, N., D. F. Swaab, R. M. Hoek, and I. Huitinga. 2009. 'Distribution of the immune inhibitory molecules CD200 and CD200R in the normal central nervous system and multiple sclerosis lesions suggests neuron-glia and glia-glia interactions', *J Neuropathol Exp Neurol*, 68: 159-67.

Kordower, J. H., C. W. Olanow, H. B. Dodiya, Y. Chu, T. G. Beach, C. H. Adler, G. M. Halliday, and R. T. Bartus. 2013. 'Disease duration and the integrity of the nigrostriatal system in Parkinson's disease', *Brain*, 136: 2419-31.

Kos, O., R. L. Hughson, D. A. Hart, G. Clement, P. Frings-Meuthen, D. Linnarsson, W. H. Paloski, J. Rittweger, F. Wuyts, J. Zange, and R. M. Gorczynski. 2014. 'Elevated serum soluble CD200 and CD200R as surrogate markers of bone loss under bed rest conditions', *Bone*, 60: 33-40.

Koutsilieri, E., T. S. Chen, P. Kruzik, and W. D. Rausch. 1995. 'A morphometric analysis of bipolar and multipolar TH-IR neurons treated with the neurotoxin MPP+ in co-cultures from mesencephalon and striatum of embryonic C57BL/6 mice', *J Neurosci Res*, 41: 197-205.

Kovacs, G. G. 2016. 'Molecular Pathological Classification of Neurodegenerative Diseases: Turning towards Precision Medicine', *Int J Mol Sci*, 17.

Krasemann, S., C. Madore, R. Cialic, C. Baufeld, N. Calcagno, R. El Fatimy, L. Beckers, E. O'Loughlin, Y. Xu, Z. Fanek, D. J. Greco, S. T. Smith, G. Tweet, Z. Humulock, T. Zrzavy, P. Conde-Sanroman, M. Gacias, Z. Weng, H. Chen, E. Tjon, F. Mazaheri, K. Hartmann, A. Madi, J. D. Ulrich, M. Glatzel, A. Worthmann, J. Heeren, B. Budnik, C. Lemere, T.

Ikezu, F. L. Heppner, V. Litvak, D. M. Holtzman, H. Lassmann, H. L. Weiner, J. Ochando, C. Haass, and O. Butovsky. 2017. 'The TREM2-APOE Pathway Drives the Transcriptional Phenotype of Dysfunctional Microglia in Neurodegenerative Diseases', *Immunity*, 47: 566-81 e9.

Kurkowska-Jastrzebska, I., A. Wronska, M. Kohutnicka, A. Czlonkowski, and A. Czlonkowska. 1999. 'The inflammatory reaction following 1-methyl-4-phenyl-1,2,3, 6-tetrahydropyridine intoxication in mouse', *Exp Neurol*, 156: 50-61.

Kuroiwa, H., H. Yokoyama, H. Kimoto, H. Kato, and T. Araki. 2010. 'Biochemical alterations of the striatum in an MPTP-treated mouse model of Parkinson's disease', *Metab Brain Dis*, 25: 177-83.

L

L'Episcopo, F., C. Tirolo, N. Testa, S. Caniglia, M. C. Morale, M. Deleidi, M. F. Serapide, S. Pluchino, and B. Marchetti. 2012. 'Plasticity of subventricular zone neuroprogenitors in MPTP (1-methyl-4-phenyl-1,2,3,6-tetrahydropyridine) mouse model of Parkinson's disease involves cross talk between inflammatory and Wnt/beta-catenin signaling pathways: functional consequences for neuroprotection and repair', *J Neurosci*, 32: 2062-85.

Laemmli, U. K. 1970. 'Cleavage of structural proteins during the assembly of the head of bacteriophage T4', *Nature*, 227: 680-5.

Laemmli, U. K., and M. Favre. 1973. 'Maturation of the head of bacteriophage T4. I. DNA packaging events', *J Mol Biol*, 80: 575-99.

Lago, N., B. Pannunzio, J. Amo-Aparicio, R. Lopez-Vales, and H. Peluffo. 2018. 'CD200 modulates spinal cord injury neuroinflammation and outcome through CD200R1', *Brain Behav Immun*, 73: 416-26.

Langston, J. W. 2002. 'Parkinson's disease: current and future challenges', *Neurotoxicology*, 23: 443-50.

Langston, J. W., P. Ballard, J. W. Tetrud, and I. Irwin. 1983. 'Chronic Parkinsonism in humans due to a product of meperidine-analog synthesis', *Science*, 219: 979-80.

Lannuzel, A., P. P. Michel, G. U. Hoglinger, P. Champy, A. Jousset, F. Medja, A. Lombes, F. Darios, C. Gleye, A. Laurens, R. Hocquemiller, E. C. Hirsch, and M. Ruberg. 2003. 'The mitochondrial complex I inhibitor annonacin is toxic to mesencephalic dopaminergic neurons by impairment of energy metabolism', *Neuroscience*, 121: 287-96.

Lassmann, H., C. S. Raine, J. Antel, and J. W. Prineas. 1998. 'Immunopathology of multiple sclerosis: report on an international meeting held at the Institute of Neurology of the University of Vienna', *J Neuroimmunol*, 86: 213-7.

Lawson, L. J., V. H. Perry, and S. Gordon. 1992. 'Turnover of resident microglia in the normal adult mouse brain', *Neuroscience*, 48: 405-15.

Lee, L., J. Liu, J. Manuel, and R. M. Gorczynski. 2006. 'A role for the immunomodulatory molecules CD200 and CD200R in regulating bone formation', *Immunol Lett*, 105: 150-8.

Lee, Y., M. S. Kim, and J. Lee. 2017. 'Neuroprotective strategies to prevent and treat Parkinson's disease based on its pathophysiological mechanism', *Arch Pharm Res*, 40: 1117-28.

Li, Q., and B. A. Barres. 2018. 'Microglia and macrophages in brain homeostasis and disease', *Nat Rev Immunol*, 18: 225-42.

Li, T., S. Pang, Y. Yu, X. Wu, J. Guo, and S. Zhang. 2013. 'Proliferation of parenchymal microglia is the main source of microgliosis after ischaemic stroke', *Brain*, 136: 3578-88.

Liang, Y., X. Jing, Z. Zeng, W. Bi, Y. Chen, X. Wu, L. Yang, J. Liu, S. Xiao, S. Liu, D. Lin, and E. Tao. 2015. 'Rifampicin attenuates rotenone-induced inflammation via suppressing NLRP3 inflammasome activation in microglia', *Brain Res*, 1622: 43-50.

Liberatore, G. T., V. Jackson-Lewis, S. Vukosavic, A. S. Mandir, M. Vila, W. G. McAuliffe, V. L. Dawson, T. M. Dawson, and S. Przedborski. 1999. 'Inducible nitric oxide synthase

stimulates dopaminergic neurodegeneration in the MPTP model of Parkinson disease', *Nat Med*, 5: 1403-9.

Liddelow, S. A., and B. A. Barres. 2017. 'Reactive Astrocytes: Production, Function, and Therapeutic Potential', *Immunity*, 46: 957-67.

Liddelow, S. A., K. A. Guttenplan, L. E. Clarke, F. C. Bennett, C. J. Bohlen, L. Schirmer, M. L. Bennett, A. E. Munch, W. S. Chung, T. C. Peterson, D. K. Wilton, A. Frouin, B. A. Napier, N. Panicker, M. Kumar, M. S. Buckwalter, D. H. Rowitch, V. L. Dawson, T. M. Dawson, B. Stevens, and B. A. Barres. 2017. 'Neurotoxic reactive astrocytes are induced by activated microglia', *Nature*, 541: 481-87.

Lin, L. F., D. H. Doherty, J. D. Lile, S. Bektesh, and F. Collins. 1993. 'GDNF: a glial cell line-derived neurotrophic factor for midbrain dopaminergic neurons', *Science*, 260: 1130-2.

Liu, B., H. M. Gao, and J. S. Hong. 2003. 'Parkinson's disease and exposure to infectious agents and pesticides and the occurrence of brain injuries: role of neuroinflammation', *Environ Health Perspect*, 111: 1065-73.

Liu, J., D. Huang, J. Xu, J. Tong, Z. Wang, L. Huang, Y. Yang, X. Bai, P. Wang, H. Suo, Y. Ma, M. Yu, J. Fei, and F. Huang. 2015. 'Tiagabine Protects Dopaminergic Neurons against Neurotoxins by Inhibiting Microglial Activation', *Sci Rep*, 5: 15720.

Liu, J., and F. Wang. 2017. 'Role of Neuroinflammation in Amyotrophic Lateral Sclerosis: Cellular Mechanisms and Therapeutic Implications', *Front Immunol*, 8: 1005.

Liu, M., and G. Bing. 2011. 'Lipopolysaccharide animal models for Parkinson's disease', *Parkinsons Dis*, 2011: 327089.

Liu, Y., Y. Bando, D. Vargas-Lowy, W. Elyaman, S. J. Khoury, T. Huang, K. Reif, and T. Chitnis. 2010. 'CD200R1 agonist attenuates mechanisms of chronic disease in a murine model of multiple sclerosis', *J Neurosci*, 30: 2025-38.

Livak, K. J., and T. D. Schmittgen. 2001. 'Analysis of relative gene expression data using real-time quantitative PCR and the 2(-Delta Delta C(T)) Method', *Methods*, 25: 402-8.

Loh, K. H., P. S. Stawski, A. S. Draycott, N. D. Udeshi, E. K. Lehrman, D. K. Wilton, T. Svinkina, T. J. Deerinck, M. H. Ellisman, B. Stevens, S. A. Carr, and A. Y. Ting. 2016. 'Proteomic Analysis of Unbounded Cellular Compartments: Synaptic Clefts', *Cell*, 166: 1295-307 e21.

Long-Smith, C. M., A. M. Sullivan, and Y. M. Nolan. 2009. 'The influence of microglia on the pathogenesis of Parkinson's disease', *Prog Neurobiol*, 89: 277-87.

Louveau, A., I. Smirnov, T. J. Keyes, J. D. Eccles, S. J. Rouhani, J. D. Peske, N. C. Derecki, D. Castle, J. W. Mandell, K. S. Lee, T. H. Harris, and J. Kipnis. 2015. 'Structural and functional features of central nervous system lymphatic vessels', *Nature*, 523: 337-41.

Luchtman, D. W., D. Shao, and C. Song. 2009. 'Behavior, neurotransmitters and inflammation in three regimens of the MPTP mouse model of Parkinson's disease', *Physiol Behav*, 98: 130-8.

Lui, H., J. Zhang, S. R. Makinson, M. K. Cahill, K. W. Kelley, H. Y. Huang, Y. Shang, M. C. Oldham, L. H. Martens, F. Gao, G. Coppola, S. A. Sloan, C. L. Hsieh, C. C. Kim, E. H. Bigio, S. Weintraub, M. M. Mesulam, R. Rademakers, I. R. Mackenzie, W. W. Seeley, A. Karydas, B. L. Miller, B. Borroni, R. Ghidoni, R. V. Farese, Jr., J. T. Paz, B. A. Barres, and E. J. Huang. 2016. 'Progranulin Deficiency Promotes Circuit-Specific Synaptic Pruning by Microglia via Complement Activation', *Cell*, 165: 921-35.

Luo, X. G., J. J. Zhang, C. D. Zhang, R. Liu, L. Zheng, X. J. Wang, S. D. Chen, and J. Q. Ding. 2010. 'Altered regulation of CD200 receptor in monocyte-derived macrophages from individuals with Parkinson's disease', *Neurochem Res*, 35: 540-7.

Lyons, A., E. J. Downer, D. A. Costello, N. Murphy, and M. A. Lynch. 2012. 'Dok2 mediates the CD200Fc attenuation of Abeta-induced changes in glia', *J Neuroinflammation*, 9: 107.

Lyons, A., E. J. Downer, S. Crotty, Y. M. Nolan, K. H. Mills, and M. A. Lynch. 2007. 'CD200 ligand receptor interaction modulates microglial activation in vivo and in vitro: a role for IL-4', *J Neurosci*, 27: 8309-13.

Lyons, A., K. McQuillan, B. F. Deighan, J. A. O'Reilly, E. J. Downer, A. C. Murphy, M. Watson, A. Piazza, F. O'Connell, R. Griffin, K. H. Mills, and M. A. Lynch. 2009. 'Decreased neuronal CD200 expression in IL-4-deficient mice results in increased neuroinflammation in response to lipopolysaccharide', *Brain Behav Immun*, 23: 1020-7.

Lyons, A., A. M. Minogue, R. S. Jones, O. Fitzpatrick, J. Noonan, V. A. Campbell, and M. A. Lynch. 2017. 'Analysis of the Impact of CD200 on Phagocytosis', *Mol Neurobiol*, 54: 5730-39.

M

Maasz, G., Z. Zrinyi, D. Reglodi, D. Petrovics, A. Rivnyak, T. Kiss, A. Jungling, A. Tamas, and Z. Pirger. 2017. 'Pituitary adenylate cyclase-activating polypeptide (PACAP) has a neuroprotective function in dopamine-based neurodegeneration in rat and snail parkinsonian models', *Dis Model Mech*, 10: 127-39.

Madore, C., C. Baufeld, and O. Butovsky. 2017. 'Microglial confetti party', *Nat Neurosci*, 20: 762-63.

Mahmood, T., and P. C. Yang. 2012. 'Western blot: technique, theory, and trouble shooting', *N Am J Med Sci*, 4: 429-34.

Makhija, D. T., and A. G. Jagtap. 2014. 'Studies on sensitivity of zebrafish as a model organism for Parkinson's disease: Comparison with rat model', *J Pharmacol Pharmacother*, 5: 39-46.

Manich, G., M. Recasens, T. Valente, B. Almolda, B. Gonzalez, and B. Castellano. 2019. 'Role of the CD200-CD200R Axis During Homeostasis and Neuroinflammation', *Neuroscience*, 405: 118-36.

Mantovani, A., S. K. Biswas, M. R. Galdiero, A. Sica, and M. Locati. 2013. 'Macrophage plasticity and polarization in tissue repair and remodelling', *J Pathol*, 229: 176-85.

Mantovani, A., A. Sica, S. Sozzani, P. Allavena, A. Vecchi, and M. Locati. 2004. 'The chemokine system in diverse forms of macrophage activation and polarization', *Trends Immunol*, 25: 677-86.

Marder, K. 2010. 'Cognitive impairment and dementia in Parkinson's disease', *Mov Disord*, 25 Suppl 1: S110-6.

Marin-Teva, J. L., M. A. Cuadros, D. Martin-Oliva, and J. Navascues. 2011. 'Microglia and neuronal cell death', *Neuron Glia Biol*, 7: 25-40.

Markey, S. P., J. N. Johannessen, C. C. Chiueh, R. S. Burns, and M. A. Herkenham. 1984. 'Intraneuronal generation of a pyridinium metabolite may cause drug-induced parkinsonism', *Nature*, 311: 464-7.

Martin, E., C. Boucher, B. Fontaine, and C. Delarasse. 2017. 'Distinct inflammatory phenotypes of microglia and monocyte-derived macrophages in Alzheimer's disease models: effects of aging and amyloid pathology', *Aging Cell*, 16: 27-38.

Martinez, B., and P. V. Peplow. 2018. 'Neuroprotection by immunomodulatory agents in animal models of Parkinson's disease', *Neural Regen Res*, 13: 1493-506.

Masocha, W. 2009. 'Systemic lipopolysaccharide (LPS)-induced microglial activation results in different temporal reduction of CD200 and CD200 receptor gene expression in the brain', *J Neuroimmunol*, 214: 78-82.

Mayer, R. A., M. V. Kindt, and R. E. Heikkila. 1986. 'Prevention of the nigrostriatal toxicity of 1-methyl-4-phenyl-1,2,3,6-tetrahydropyridine by inhibitors of 3,4-dihydroxyphenylethylamine transport', *J Neurochem*, 47: 1073-9.

McCaughan, G. W., M. J. Clark, and A. N. Barclay. 1987. 'Characterization of the human homolog of the rat MRC OX-2 membrane glycoprotein', *Immunogenetics*, 25: 329-35.

McGeer, P. L., S. Itagaki, B. E. Boyes, and E. G. McGeer. 1988. 'Reactive microglia are positive for HLA-DR in the substantia nigra of Parkinson's and Alzheimer's disease brains', *Neurology*, 38: 1285-91.

McGeer, P. L., and E. G. McGeer. 1998. 'Glial cell reactions in neurodegenerative diseases: pathophysiology and therapeutic interventions', *Alzheimer Dis Assoc Disord*, 12 Suppl 2: S1-6.

McMaster, W. R., and A. F. Williams. 1979. 'Identification of Ia glycoproteins in rat thymus and purification from rat spleen', *Eur J Immunol*, 9: 426-33.

Mecha, M., F. J. Carrillo-Salinas, L. Mestre, A. Feliu, and C. Guaza. 2013. 'Viral models of multiple sclerosis: neurodegeneration and demyelination in mice infected with Theiler's virus', *Prog Neurobiol*, 101-102: 46-64.

Meredith, G. E., P. K. Sonsalla, and M. F. Chesselet. 2008. 'Animal models of Parkinson's disease progression', *Acta Neuropathol*, 115: 385-98.

Meredith, G. E., S. Totterdell, J. A. Potashkin, and D. J. Surmeier. 2008. 'Modeling PD pathogenesis in mice: advantages of a chronic MPTP protocol', *Parkinsonism Relat Disord*, 14 Suppl 2: S112-5.

Meuth, S. G., O. J. Simon, A. Grimm, N. Melzer, A. M. Herrmann, P. Spitzer, P. Landgraf, and H. Wiendl. 2008. 'CNS inflammation and neuronal degeneration is aggravated by impaired CD200-CD200R-mediated macrophage silencing', *J Neuroimmunol*, 194: 62-9.

Michel, P. P., B. K. Dandapani, J. Sanchez-Ramos, S. Efange, B. C. Pressman, and F. Hefti. 1989. 'Toxic effects of potential environmental neurotoxins related to 1-methyl-4-phenylpyridinium on cultured rat dopaminergic neurons', *J Pharmacol Exp Ther*, 248: 842-50.

Michelucci, A., T. Cordes, J. Ghelfi, A. Pailot, N. Reiling, O. Goldmann, T. Binz, A. Wegner, A. Tallam, A. Rausell, M. Buttini, C. L. Linster, E. Medina, R. Balling, and K. Hiller. 2013. 'Immune-responsive gene 1 protein links metabolism to immunity by catalyzing itaconic acid production', *Proc Natl Acad Sci U S A*, 110: 7820-5.

Mihrshahi, R., A. N. Barclay, and M. H. Brown. 2009. 'Essential roles for Dok2 and RasGAP in CD200 receptor-mediated regulation of human myeloid cells', *J Immunol*, 183: 4879-86.

Mihrshahi, R., and M. H. Brown. 2010. 'Downstream of tyrosine kinase 1 and 2 play opposing roles in CD200 receptor signaling', *J Immunol*, 185: 7216-22.

Mildner, A., B. Schlevogt, K. Kierdorf, C. Bottcher, D. Erny, M. P. Kummer, M. Quinn, W. Bruck, I. Bechmann, M. T. Heneka, J. Priller, and M. Prinz. 2011. 'Distinct and non-redundant roles of microglia and myeloid subsets in mouse models of Alzheimer's disease', *J Neurosci*, 31: 11159-71.

Mildner, A., H. Schmidt, M. Nitsche, D. Merkler, U. K. Hanisch, M. Mack, M. Heikenwalder, W. Bruck, J. Priller, and M. Prinz. 2007. 'Microglia in the adult brain arise from Ly-6ChiCCR2+ monocytes only under defined host conditions', *Nat Neurosci*, 10: 1544-53.

Mills, E. L., and L. A. O'Neill. 2016. 'Reprogramming mitochondrial metabolism in macrophages as an anti-inflammatory signal', *Eur J Immunol*, 46: 13-21.

Mirra, S. S., A. Heyman, D. McKeel, S. M. Sumi, B. J. Crain, L. M. Brownlee, F. S. Vogel, J. P. Hughes, G. van Belle, and L. Berg. 1991. 'The Consortium to Establish a Registry for Alzheimer's Disease (CERAD). Part II. Standardization of the neuropathologic assessment of Alzheimer's disease', *Neurology*, 41: 479-86.

Mittelbronn, M., K. Dietz, H. J. Schluesener, and R. Meyermann. 2001. 'Local distribution of microglia in the normal adult human central nervous system differs by up to one order of magnitude', *Acta Neuropathol*, 101: 249-55.

Moertel, C. L., J. Xia, R. LaRue, N. N. Waldron, B. M. Andersen, R. M. Prins, H. Okada, A. M. Donson, N. K. Foreman, M. A. Hunt, C. A. Pennell, and M. R. Olin. 2014. 'CD200 in CNS tumor-induced immunosuppression: the role for CD200 pathway blockade in targeted immunotherapy', *J Immunother Cancer*, 2: 46.

Mogi, M., M. Harada, T. Kondo, H. Narabayashi, P. Riederer, and T. Nagatsu. 1995. 'Transforming growth factor-beta 1 levels are elevated in the striatum and in ventricular cerebrospinal fluid in Parkinson's disease', *Neurosci Lett*, 193: 129-32.

Mogi, M., M. Harada, T. Kondo, P. Riederer, H. Inagaki, M. Minami, and T. Nagatsu. 1994. 'Interleukin-1 beta, interleukin-6, epidermal growth factor and transforming growth factor-alpha are elevated in the brain from parkinsonian patients', *Neurosci Lett*, 180: 147-50.

Mogi, M., M. Harada, H. Narabayashi, H. Inagaki, M. Minami, and T. Nagatsu. 1996. 'Interleukin (IL)-1 beta, IL-2, IL-4, IL-6 and transforming growth factor-alpha levels are elevated in ventricular cerebrospinal fluid in juvenile parkinsonism and Parkinson's disease', *Neurosci Lett*, 211: 13-6.

Mogi, M., M. Harada, P. Riederer, H. Narabayashi, K. Fujita, and T. Nagatsu. 1994. 'Tumor necrosis factor-alpha (TNF-alpha) increases both in the brain and in the cerebrospinal fluid from parkinsonian patients', *Neurosci Lett*, 165: 208-10.

Mosley, R. L., J. A. Hutter-Saunders, D. K. Stone, and H. E. Gendelman. 2012. 'Inflammation and adaptive immunity in Parkinson's disease', *Cold Spring Harb Perspect Med*, 2: a009381.

Moss, D. W., and T. E. Bates. 2001. 'Activation of murine microglial cell lines by lipopolysaccharide and interferon-gamma causes NO-mediated decreases in mitochondrial and cellular function', *Eur J Neurosci*, 13: 529-38.

Mosser, D. M., and J. P. Edwards. 2008. 'Exploring the full spectrum of macrophage activation', *Nat Rev Immunol*, 8: 958-69.

Mostafalou, S., and M. Abdollahi. 2013. 'Pesticides and human chronic diseases: evidences, mechanisms, and perspectives', *Toxicol Appl Pharmacol*, 268: 157-77.

Mott, R. T., G. Ait-Ghezala, T. Town, T. Mori, M. Vendrame, J. Zeng, J. Ehrhart, M. Mullan, and J. Tan. 2004. 'Neuronal expression of CD22: novel mechanism for inhibiting microglial proinflammatory cytokine production', *Glia*, 46: 369-79.

Mount, M. P., A. Lira, D. Grimes, P. D. Smith, S. Faucher, R. Slack, H. Anisman, S. Hayley, and D. S. Park. 2007. 'Involvement of interferon-gamma in microglial-mediated loss of dopaminergic neurons', *J Neurosci*, 27: 3328-37.

Muthane, U. B., H. S. Swamy, P. Satishchandra, M. N. Subhash, S. Rao, and D. Subbakrishna. 1994. 'Early onset Parkinson's disease: are juvenile- and young-onset different?', *Mov Disord*, 9: 539-44.

Mytilineou, C., G. Cohen, and R. E. Heikkila. 1985. '1-Methyl-4-phenylpyridine (MPP+) is toxic to mesencephalic dopamine neurons in culture', *Neurosci Lett*, 57: 19-24.

N

Nagatsu, T., M. Mogi, H. Ichinose, and A. Togari. 2000. 'Cytokines in Parkinson's disease', *J Neural Transm Suppl*: 143-51.

Nagatsu, T., and M. Sawada. 2005. 'Inflammatory process in Parkinson's disease: role for cytokines', *Curr Pharm Des*, 11: 999-1016.

Niehaus, I., and J. H. Lange. 2003. 'Endotoxin: is it an environmental factor in the cause of Parkinson's disease?', *Occup Environ Med*, 60: 378.

Nimmerjahn, A., F. Kirchhoff, and F. Helmchen. 2005. 'Resting microglial cells are highly dynamic surveillants of brain parenchyma in vivo', *Science*, 308: 1314-8.

Niraula, A., J. F. Sheridan, and J. P. Godbout. 2017. 'Microglia Priming with Aging and Stress', *Neuropsychopharmacology*, 42: 318-33.

Nizet, V., and R. S. Johnson. 2009. 'Interdependence of hypoxic and innate immune responses', *Nat Rev Immunol*, 9: 609-17.

Norden, D. M., and J. P. Godbout. 2013. 'Review: microglia of the aged brain: primed to be activated and resistant to regulation', *Neuropathol Appl Neurobiol*, 39: 19-34.

Norden, D. M., M. M. Muccigrosso, and J. P. Godbout. 2015. 'Microglial priming and enhanced reactivity to secondary insult in aging, and traumatic CNS injury, and neurodegenerative disease', *Neuropharmacology*, 96: 29-41.

O

O'Neill, L. A., and D. G. Hardie. 2013. 'Metabolism of inflammation limited by AMPK and pseudo-starvation', *Nature*, 493: 346-55.

Odegaard, J. I., and A. Chawla. 2011. 'Alternative macrophage activation and metabolism', *Annu Rev Pathol*, 6: 275-97.

Ogata, A., K. Tashiro, S. Nukuzuma, K. Nagashima, and W. W. Hall. 1997. 'A rat model of Parkinson's disease induced by Japanese encephalitis virus', *J Neurovirol*, 3: 141-7.

Ohgidani, M., T. A. Kato, D. Setoyama, N. Sagata, R. Hashimoto, K. Shigenobu, T. Yoshida, K. Hayakawa, N. Shimokawa, D. Miura, H. Utsumi, and S. Kanba. 2014. 'Direct induction of ramified microglia-like cells from human monocytes: dynamic microglial dysfunction in Nasu-Hakola disease', *Sci Rep*, 4: 4957.

Orihuela, R., C. A. McPherson, and G. J. Harry. 2016. 'Microglial M1/M2 polarization and metabolic states', *Br J Pharmacol*, 173: 649-65.

Orth, M., and A. H. Schapira. 2002. 'Mitochondrial involvement in Parkinson's disease', *Neurochem Int*, 40: 533-41.

Ouchi, Y., E. Yoshikawa, Y. Sekine, M. Futatsubashi, T. Kanno, T. Ogusu, and T. Torizuka. 2005. 'Microglial activation and dopamine terminal loss in early Parkinson's disease', *Ann Neurol*, 57: 168-75.

Ovadia, A., Z. Zhang, and D. M. Gash. 1995. 'Increased susceptibility to MPTP toxicity in middle-aged rhesus monkeys', *Neurobiol Aging*, 16: 931-7.

Owens, T., I. Bechmann, and B. Engelhardt. 2008. 'Perivascular spaces and the two steps to neuroinflammation', *J Neuropathol Exp Neurol*, 67: 1113-21.

P

Palazon, A., A. W. Goldrath, V. Nizet, and R. S. Johnson. 2014. 'HIF transcription factors, inflammation, and immunity', *Immunity*, 41: 518-28.

Pallasch, C. P., S. Ulbrich, R. Brinker, M. Hallek, R. A. Uger, and C. M. Wendtner. 2009. 'Disruption of T cell suppression in chronic lymphocytic leukemia by CD200 blockade', *Leuk Res*, 33: 460-4.

Palmer, S. S., J. A. Mortimer, D. D. Webster, R. Bistevins, and G. L. Dickinson. 1986. 'Exercise therapy for Parkinson's disease', *Arch Phys Med Rehabil*, 67: 741-5.

Pankratova, S., H. Bjornsdottir, C. Christensen, L. Zhang, S. Li, O. Dmytriyeva, E. Bock, and V. Berezin. 2016. 'Immunomodulator CD200 Promotes Neurotrophic Activity by Interacting with and Activating the Fibroblast Growth Factor Receptor', *Mol Neurobiol*, 53: 584-94.

Paolicelli, R. C., G. Bolasco, F. Pagani, L. Maggi, M. Scianni, P. Panzanelli, M. Giustetto, T. A. Ferreira, E. Guiducci, L. Dumas, D. Ragozzino, and C. T. Gross. 2011. 'Synaptic pruning by microglia is necessary for normal brain development', *Science*, 333: 1456-8.

Parkhurst, C. N., G. Yang, I. Ninan, J. N. Savas, J. R. Yates, 3rd, J. J. Lafaille, B. L. Hempstead, D. R. Littman, and W. B. Gan. 2013. 'Microglia promote learning-dependent synapse formation through brain-derived neurotrophic factor', *Cell*, 155: 1596-609.

Parkinson, J. 2002. 'An essay on the shaking palsy. 1817', *J Neuropsychiatry Clin Neurosci*, 14: 223-36; discussion 22.

Pascual, O., S. Ben Achour, P. Rostaing, A. Triller, and A. Bessis. 2012. 'Microglia activation triggers astrocyte-mediated modulation of excitatory neurotransmission', *Proc Natl Acad Sci U S A*, 109: E197-205.

Pearce, E. L., and E. J. Pearce. 2013. 'Metabolic pathways in immune cell activation and quiescence', *Immunity*, 38: 633-43.

Perier, C., A. Bender, E. Garcia-Arumi, M. J. Melia, J. Bove, C. Laub, T. Klopstock, M. Elstner, R. B. Mounsey, P. Teismann, T. Prolla, A. L. Andreu, and M. Vila. 2013. 'Accumulation of

mitochondrial DNA deletions within dopaminergic neurons triggers neuroprotective mechanisms', *Brain*, 136: 2369-78.

Perry, V. H. 2016. 'Microglia', *Microbiol Spectr*, 4.

Perry, V. H., and C. Holmes. 2014. 'Microglial priming in neurodegenerative disease', *Nat Rev Neurol*, 10: 217-24.

Perry, V. H., J. A. Nicoll, and C. Holmes. 2010. 'Microglia in neurodegenerative disease', *Nat Rev Neurol*, 6: 193-201.

Pileblad, E., H. Nissbrandt, and A. Carlsson. 1984. 'Biochemical and functional evidence for a marked dopamine releasing action of N-methyl-4-phenyl-1,2,3,6-tetrahydropyridine (NMPTP) in mouse brain', *J Neural Transm*, 60: 199-203.

Pinter, B., A. Diem-Zangerl, G. K. Wenning, C. Scherfler, W. Oberaigner, K. Seppi, and W. Poewe. 2015. 'Mortality in Parkinson's disease: a 38-year follow-up study', *Mov Disord*, 30: 266-9.

Pocock, J. M., and H. Kettenmann. 2007. 'Neurotransmitter receptors on microglia', *Trends Neurosci*, 30: 527-35.

Poewe, W., and P. Mahlknecht. 2009. 'The clinical progression of Parkinson's disease', *Parkinsonism Relat Disord*, 15 Suppl 4: S28-32.

Poewe, W., K. Seppi, C. M. Tanner, G. M. Halliday, P. Brundin, J. Volkmann, A. E. Schrag, and A. E. Lang. 2017. 'Parkinson disease', *Nat Rev Dis Primers*, 3: 17013.

Postuma, R. B., D. Berg, M. Stern, W. Poewe, C. W. Olanow, W. Oertel, J. Obeso, K. Marek, I. Litvan, A. E. Lang, G. Halliday, C. G. Goetz, T. Gasser, B. Dubois, P. Chan, B. R. Bloem, C. H. Adler, and G. Deuschl. 2015. 'MDS clinical diagnostic criteria for Parkinson's disease', *Mov Disord*, 30: 1591-601.

Preston, S., G. J. Wright, K. Starr, A. N. Barclay, and M. H. Brown. 1997. 'The leukocyte/neuron cell surface antigen OX2 binds to a ligand on macrophages', *Eur J Immunol*, 27: 1911-8.

Pringsheim, T., N. Jette, A. Frolkis, and T. D. Steeves. 2014. 'The prevalence of Parkinson's disease: a systematic review and meta-analysis', *Mov Disord*, 29: 1583-90.

Prinz, M., D. Erny, and N. Hagemeyer. 2017. 'Ontogeny and homeostasis of CNS myeloid cells', *Nat Immunol*, 18: 385-92.

Prinz, M., and J. Priller. 2017. 'The role of peripheral immune cells in the CNS in steady state and disease', *Nat Neurosci*, 20: 136-44.

Procaccini, C., V. De Rosa, V. Pucino, L. Formisano, and G. Matarese. 2015. 'Animal models of Multiple Sclerosis', *Eur J Pharmacol*, 759: 182-91.

Przedborski, S., and M. Vila. 2001. 'MPTP: a review of its mechanisms of neurotoxicity', *Clinical Neuroscience Research*, 1: 407-18.

Przedborski, S., Q. Chen, M. Vila, B. I. Giasson, R. Djaldatti, S. Vukosavic, J. M. Souza, V. Jackson-Lewis, V. M. Lee, and H. Ischiropoulos. 2001. 'Oxidative post-translational modifications of alpha-synuclein in the 1-methyl-4-phenyl-1,2,3,6-tetrahydropyridine (MPTP) mouse model of Parkinson's disease', *J Neurochem*, 76: 637-40.

Przedborski, S., V. Jackson-Lewis, A. B. Naini, M. Jakowec, G. Petzinger, R. Miller, and M. Akram. 2001. 'The parkinsonian toxin 1-methyl-4-phenyl-1,2,3,6-tetrahydropyridine (MPTP): a technical review of its utility and safety', *J Neurochem*, 76: 1265-74.

Q

Qin, L., X. Wu, M. L. Block, Y. Liu, G. R. Breese, J. S. Hong, D. J. Knapp, and F. T. Crews. 2007. 'Systemic LPS causes chronic neuroinflammation and progressive neurodegeneration', *Glia*, 55: 453-62.

R

Rabaneda-Lombarte, N., E. Xicoy-Espaulella, J. Serratosa, J. Saura, and C. Sola. 2018. 'Parkinsonian Neurotoxins Impair the Pro-inflammatory Response of Glial Cells', *Front Mol Neurosci*, 11: 479.

Racette, B. A., A. Gross, S. M. Vouri, A. Camacho-Soto, A. W. Willis, and S. Searles Nielsen. 2018. 'Immunosuppressants and risk of Parkinson disease', *Ann Clin Transl Neurol*, 5: 870-75.

Radad, K., W. D. Rausch, and G. Gille. 2006. 'Rotenone induces cell death in primary dopaminergic culture by increasing ROS production and inhibiting mitochondrial respiration', *Neurochem Int*, 49: 379-86.

Ransohoff, R. M. 2016. 'How neuroinflammation contributes to neurodegeneration', *Science*, 353: 777-83.

Ransohoff, R. M., and A. E. Cardona. 2010. 'The myeloid cells of the central nervous system parenchyma', *Nature*, 468: 253-62.

Ransohoff, R. M., and B. Engelhardt. 2012. 'The anatomical and cellular basis of immune surveillance in the central nervous system', *Nat Rev Immunol*, 12: 623-35.

Ransohoff, R. M., and V. H. Perry. 2009. 'Microglial physiology: unique stimuli, specialized responses', *Annu Rev Immunol*, 27: 119-45.

Ransom, B. R., D. M. Kunis, I. Irwin, and J. W. Langston. 1987. 'Astrocytes convert the parkinsonism inducing neurotoxin, MPTP, to its active metabolite, MPP+', *Neurosci Lett*, 75: 323-8.

Rayaprolu, S., B. Mullen, M. Baker, T. Lynch, E. Finger, W. W. Seeley, K. J. Hatanpaa, C. Lomen-Hoerth, A. Kertesz, E. H. Bigio, C. Lippa, K. A. Josephs, D. S. Knopman, C. L. White, 3rd, R. Caselli, I. R. Mackenzie, B. L. Miller, M. Boczarska-Jedynak, G. Opala, A. Krygowska-Wajs, M. Barcikowska, S. G. Younkin, R. C. Petersen, N. Ertekin-Taner, R. J. Uitti, J. F. Meschia, K. B. Boylan, B. F. Boeve, N. R. Graff-Radford, Z. K. Wszolek, D. W. Dickson, R. Rademakers, and O. A. Ross. 2013. 'TREM2 in neurodegeneration: evidence for association of the p.R47H variant with frontotemporal dementia and Parkinson's disease', *Mol Neurodegener*, 8: 19.

Recasens, A., B. Dehay, J. Bove, I. Carballo-Carbajal, S. Dovero, A. Perez-Villalba, P. O. Fernagut, J. Blesa, A. Parent, C. Perier, I. Farinas, J. A. Obeso, E. Bezard, and M. Vila. 2014. 'Lewy body extracts from Parkinson disease brains trigger alpha-synuclein pathology and neurodegeneration in mice and monkeys', *Ann Neurol*, 75: 351-62.

Reinhard, J. F., Jr., E. J. Diliberto, Jr., O. H. Viveros, and A. J. Daniels. 1987. 'Subcellular compartmentalization of 1-methyl-4-phenylpyridinium with catecholamines in adrenal medullary chromaffin vesicles may explain the lack of toxicity to adrenal chromaffin cells', *Proc Natl Acad Sci U S A*, 84: 8160-4.

Ren, Y., W. Liu, H. Jiang, Q. Jiang, and J. Feng. 2005. 'Selective vulnerability of dopaminergic neurons to microtubule depolymerization', *J Biol Chem*, 280: 34105-12.

Ren, Y., M. Ye, S. Chen, and J. Ding. 2016. 'CD200 Inhibits Inflammatory Response by Promoting KATP Channel Opening in Microglia Cells in Parkinson's Disease', *Med Sci Monit*, 22: 1733-41.

Ren, Z. X., Y. F. Zhao, T. Cao, and X. C. Zhen. 2016. 'Dihydromyricetin protects neurons in an MPTP-induced model of Parkinson's disease by suppressing glycogen synthase kinase-3 beta activity', *Acta Pharmacol Sin*, 37: 1315-24.

Rijkers, E. S., T. de Ruiter, A. Baridi, H. Veninga, R. M. Hoek, and L. Meyaard. 2008. 'The inhibitory CD200R is differentially expressed on human and mouse T and B lymphocytes', *Mol Immunol*, 45: 1126-35.

Rio-Hortega, P. Del. 1932. *Microglia. In: Cytology and Cellular Pathology of the Nervous System* (Penfield W: New York).

Rodriguez-Prados, J. C., P. G. Traves, J. Cuenca, D. Rico, J. Aragones, P. Martin-Sanz, M. Cascante, and L. Bosca. 2010. 'Substrate fate in activated macrophages: a comparison between innate, classic, and alternative activation', *J Immunol*, 185: 605-14.

Rojo, A. I., N. G. Innamorato, A. M. Martin-Moreno, M. L. De Ceballos, M. Yamamoto, and A. Cuadrado. 2010. 'Nrf2 regulates microglial dynamics and neuroinflammation in experimental Parkinson's disease', *Glia*, 58: 588-98.

Roodveldt, C., J. Christodoulou, and C. M. Dobson. 2008. 'Immunological features of alpha-synuclein in Parkinson's disease', *J Cell Mol Med*, 12: 1820-9.

Rose, S., M. Nomoto, E. A. Jackson, W. R. Gibb, P. Jaehnig, P. Jenner, and C. D. Marsden. 1993. 'Age-related effects of 1-methyl-4-phenyl-1,2,3,6-tetrahydropyridine treatment of common marmosets', *Eur J Pharmacol*, 230: 177-85.

Rosenblum, M. D., E. B. Olasz, K. B. Yancey, J. E. Woodliff, Z. Lazarova, K. A. Gerber, and R. L. Truitt. 2004. 'Expression of CD200 on epithelial cells of the murine hair follicle: a role in tissue-specific immune tolerance?', *J Invest Dermatol*, 123: 880-7.

S

Salter, M. W., and B. Stevens. 2017. 'Microglia emerge as central players in brain disease', *Nat Med*, 23: 1018-27.

Sampson, T. R., J. W. Debelius, T. Thron, S. Janssen, G. G. Shastri, Z. E. Ilhan, C. Challis, C. E. Schretter, S. Rocha, V. Gradinaru, M. F. Chesselet, A. Keshavarzian, K. M. Shannon, R. Krajmalnik-Brown, P. Wittung-Stafshede, R. Knight, and S. K. Mazmanian. 2016. 'Gut Microbiota Regulate Motor Deficits and Neuroinflammation in a Model of Parkinson's Disease', *Cell*, 167: 1469-80 e12.

Sanchez-Ramos, J., J. N. Barrett, M. Goldstein, W. J. Weiner, and F. Hefti. 1986. '1-Methyl-4-phenylpyridinium (MPP+) but not 1-methyl-4-phenyl-1,2,3,6-tetrahydropyridine (MPTP) selectively destroys dopaminergic neurons in cultures of dissociated rat mesencephalic neurons', *Neurosci Lett*, 72: 215-20.

Saporito, M. S., R. E. Heikkila, S. K. Youngster, W. J. Nicklas, and H. M. Geller. 1992. 'Dopaminergic neurotoxicity of 1-methyl-4-phenylpyridinium analogs in cultured neurons: relationship to the dopamine uptake system and inhibition of mitochondrial respiration', *J Pharmacol Exp Ther*, 260: 1400-9.

Sarangi, P. P., S. R. Woo, and B. T. Rouse. 2009. 'Control of viral immunoinflammatory lesions by manipulating CD200:CD200 receptor interaction', *Clin Immunol*, 131: 31-40.

Sastre, M., T. Klockgether, and M. T. Heneka. 2006. 'Contribution of inflammatory processes to Alzheimer's disease: molecular mechanisms', *Int J Dev Neurosci*, 24: 167-76.

Saura, J., J. M. Tusell, and J. Serratosa. 2003. 'High-yield isolation of murine microglia by mild trypsinization', *Glia*, 44: 183-9.

Schafer, D. P., E. K. Lehrman, A. G. Kautzman, R. Koyama, A. R. Mardinly, R. Yamasaki, R. M. Ransohoff, M. E. Greenberg, B. A. Barres, and B. Stevens. 2012. 'Microglia sculpt postnatal neural circuits in an activity and complement-dependent manner', *Neuron*, 74: 691-705.

Schapira, A. H. V., K. R. Chaudhuri, and P. Jenner. 2017. 'Non-motor features of Parkinson disease', *Nat Rev Neurosci*, 18: 435-50.

Schildknecht, S., H. R. Gerding, C. Karreman, M. Drescher, H. A. Lashuel, T. F. Outeiro, D. A. Di Monte, and M. Leist. 2013. 'Oxidative and nitrative alpha-synuclein modifications and proteostatic stress: implications for disease mechanisms and interventions in synucleinopathies', *J Neurochem*, 125: 491-511.

Schintu, N., L. Frau, M. Ibba, A. Garau, E. Carboni, and A. R. Carta. 2009. 'Progressive dopaminergic degeneration in the chronic MPTPp mouse model of Parkinson's disease', *Neurotox Res*, 16: 127-39.

Scola, G., H. K. Kim, L. T. Young, M. Salvador, and A. C. Andreazza. 2014. 'Lithium reduces the effects of rotenone-induced complex I dysfunction on DNA methylation and hydroxymethylation in rat cortical primary neurons', *Psychopharmacology (Berl)*, 231: 4189-98.

Sedel, F., C. Bechade, S. Vyas, and A. Triller. 2004. 'Macrophage-derived tumor necrosis factor alpha, an early developmental signal for motoneuron death', *J Neurosci*, 24: 2236-46.

Sekar, A., A. R. Bialas, H. de Rivera, A. Davis, T. R. Hammond, N. Kamitaki, K. Tooley, J. Presumey, M. Baum, V. Van Doren, G. Genovese, S. A. Rose, R. E. Handsaker, Consortium Schizophrenia Working Group of the Psychiatric Genomics, M. J. Daly, M. C. Carroll, B. Stevens, and S. A. McCarroll. 2016. 'Schizophrenia risk from complex variation of complement component 4', *Nature*, 530: 177-83.

Sepulveda-Diaz, J. E., M. O. Ouidja, S. B. Socias, S. Hamadat, S. Guerreiro, R. Raisman-Vozari, and P. P. Michel. 2016. 'A simplified approach for efficient isolation of functional microglial cells: Application for modeling neuroinflammatory responses in vitro', *Glia*, 64: 1912-24.

Shen, R. S., C. W. Abell, W. Gessner, and A. Brossi. 1985. 'Serotonergic conversion of MPTP and dopaminergic accumulation of MPP+', *FEBS Lett*, 189: 225-30.

Shimohama, S., H. Sawada, Y. Kitamura, and T. Taniguchi. 2003. 'Disease model: Parkinson's disease', *Trends Mol Med*, 9: 360-5.

Shimoji, M., F. Pagan, E. B. Healton, and I. Mocchetti. 2009. 'CXCR4 and CXCL12 expression is increased in the nigro-striatal system of Parkinson's disease', *Neurotox Res*, 16: 318-28.

Shrivastava, K., P. Gonzalez, and L. Acarin. 2012. 'The immune inhibitory complex CD200/CD200R is developmentally regulated in the mouse brain', *J Comp Neurol*, 520: 2657-75.

Sica, A., and A. Mantovani. 2012. 'Macrophage plasticity and polarization: in vivo veritas', *J Clin Invest*, 122: 787-95.

Sieger, D., C. Moritz, T. Ziegenhals, S. Prykhozhij, and F. Peri. 2012. 'Long-range Ca2+ waves transmit brain-damage signals to microglia', *Dev Cell*, 22: 1138-48.

Singh, A., M. K. Falk, T. V. Hviid, and T. L. Sorensen. 2013. 'Increased expression of CD200 on circulating CD11b+ monocytes in patients with neovascular age-related macular degeneration', *Ophthalmology*, 120: 1029-37.

Sipe, G. O., R. L. Lowery, M. E. Tremblay, E. A. Kelly, C. E. Lamantia, and A. K. Majewska. 2016. 'Microglial P2Y12 is necessary for synaptic plasticity in mouse visual cortex', *Nat Commun*, 7: 10905.

Smeyne, M., Y. Jiao, K. R. Shepherd, and R. J. Smeyne. 2005. 'Glia cell number modulates sensitivity to MPTP in mice', *Glia*, 52: 144-52.

Smeyne, R. J., and V. Jackson-Lewis. 2005. 'The MPTP model of Parkinson's disease', *Brain Res Mol Brain Res*, 134: 57-66.

Sofroniew, M. V. 2015. 'Astrocyte barriers to neurotoxic inflammation', *Nat Rev Neurosci*, 16: 249-63.

Sohn, S. H., J. H. Lee, H. S. Chung, H. E. Lee, J. M. Lee, H. Bae 2012. 'The effects of Foxp3 on gene expression profiles in activated microglial cells', *Molecular & Cellular Toxicology*, 8: 139–48.

Song, W. M., and M. Colonna. 2018. 'The identity and function of microglia in neurodegeneration', *Nat Immunol*, 19: 1048-58.

Spector, R., S. Robert Snodgrass, and C. E. Johanson. 2015. 'A balanced view of the cerebrospinal fluid composition and functions: Focus on adult humans', *Exp Neurol*, 273: 57-68.

Stevens, B., N. J. Allen, L. E. Vazquez, G. R. Howell, K. S. Christopherson, N. Nouri, K. D. Micheva, A. K. Mehalow, A. D. Huberman, B. Stafford, A. Sher, A. M. Litke, J. D. Lambris, S. J. Smith, S. W. John, and B. A. Barres. 2007. 'The classical complement cascade mediates CNS synapse elimination', *Cell*, 131: 1164-78.

Suo, H., P. Wang, J. Tong, L. Cai, J. Liu, D. Huang, L. Huang, Z. Wang, Y. Huang, J. Xu, Y. Ma, M. Yu, J. Fei, and F. Huang. 2015. 'NRSF is an essential mediator for the neuroprotection

of trichostatin A in the MPTP mouse model of Parkinson's disease', *Neuropharmacology*, 99: 67-78.

Swerdlow, R. H., J. K. Parks, S. W. Miller, J. B. Tuttle, P. A. Trimmer, J. P. Sheehan, J. P. Bennett, Jr., R. E. Davis, and W. D. Parker, Jr. 1996. 'Origin and functional consequences of the complex I defect in Parkinson's disease', *Ann Neurol*, 40: 663-71.

T

Tannahill, G. M., A. M. Curtis, J. Adamik, E. M. Palsson-McDermott, A. F. McGettrick, G. Goel, C. Frezza, N. J. Bernard, B. Kelly, N. H. Foley, L. Zheng, A. Gardet, Z. Tong, S. S. Jany, S. C. Corr, M. Haneklaus, B. E. Caffrey, K. Pierce, S. Walmsley, F. C. Beasley, E. Cummins, V. Nizet, M. Whyte, C. T. Taylor, H. Lin, S. L. Masters, E. Gottlieb, V. P. Kelly, C. Clish, P. E. Auron, R. J. Xavier, and L. A. O'Neill. 2013. 'Succinate is an inflammatory signal that induces IL-1beta through HIF-1alpha', *Nature*, 496: 238-42.

Tanner, C. M., F. Kamel, G. W. Ross, J. A. Hoppin, S. M. Goldman, M. Korell, C. Marras, G. S. Bhudhikanok, M. Kasten, A. R. Chade, K. Comyns, M. B. Richards, C. Meng, B. Priestley, H. H. Fernandez, F. Cambi, D. M. Umbach, A. Blair, D. P. Sandler, and J. W. Langston. 2011. 'Rotenone, paraquat, and Parkinson's disease', *Environ Health Perspect*, 119: 866-72.

Tansey, M. G., and M. S. Goldberg. 2010. 'Neuroinflammation in Parkinson's disease: its role in neuronal death and implications for therapeutic intervention', *Neurobiol Dis*, 37: 510-8.

Tatton, N. A., and S. J. Kish. 1997. 'In situ detection of apoptotic nuclei in the substantia nigra compacta of 1-methyl-4-phenyl-1,2,3,6-tetrahydropyridine-treated mice using terminal deoxynucleotidyl transferase labelling and acridine orange staining', *Neuroscience*, 77: 1037-48.

Tay, T. L., D. Mai, J. Dautzenberg, F. Fernandez-Klett, G. Lin, Sagar, M. Datta, A. Drougard, T. Stempfl, A. Ardura-Fabregat, O. Staszewski, A. Margineanu, A. Sporbert, L. M. Steinmetz, J. A. Pospisilik, S. Jung, J. Priller, D. Grun, O. Ronneberger, and M. Prinz. 2017. 'A new fate mapping system reveals context-dependent random or clonal expansion of microglia', *Nat Neurosci*, 20: 793-803.

Taylor, C. T., G. Doherty, P. G. Fallon, and E. P. Cummins. 2016. 'Hypoxia-dependent regulation of inflammatory pathways in immune cells', *J Clin Invest*, 126: 3716-24.

Taylor, N., K. McConachie, C. Calder, R. Dawson, A. Dick, J. D. Sedgwick, and J. Liversidge. 2005. 'Enhanced tolerance to autoimmune uveitis in CD200-deficient mice correlates with a pronounced Th2 switch in response to antigen challenge', *J Immunol*, 174: 143-54.

Teismann, P., K. Tieu, D. K. Choi, D. C. Wu, A. Naini, S. Hunot, M. Vila, V. Jackson-Lewis, and S. Przedborski. 2003. 'Cyclooxygenase-2 is instrumental in Parkinson's disease neurodegeneration', *Proc Natl Acad Sci U S A*, 100: 5473-8.

Tenreiro, S., V. Franssens, J. Winderickx, and T. F. Outeiro. 2017. 'Yeast models of Parkinson's disease-associated molecular pathologies', *Curr Opin Genet Dev*, 44: 74-83.

Tomac, A., E. Lindqvist, L. F. Lin, S. O. Ogren, D. Young, B. J. Hoffer, and L. Olson. 1995. 'Protection and repair of the nigrostriatal dopaminergic system by GDNF in vivo', *Nature*, 373: 335-9.

Tremblay, M. E., R. L. Lowery, and A. K. Majewska. 2010. 'Microglial interactions with synapses are modulated by visual experience', *PLoS Biol*, 8: e1000527.

Tural Onur, S., A. D. Yalcin, B. Celik, and S. Gumuslu. 2015. 'Evaluation of d-dimer, CXCL8, homocysteine, eosinophil cationic peptide, 25(OH)-vitamin D and immunomodulatory OX-2 levels in allergic patients', *J Asthma*, 52: 123-7.

Turner, C. A., E. Eren-Kocak, E. G. Inui, S. J. Watson, and H. Akil. 2016. 'Dysregulated fibroblast growth factor (FGF) signaling in neurological and psychiatric disorders', *Semin Cell Dev Biol*, 53: 136-43.

Twelves, D., K. S. Perkins, and C. Counsell. 2003. 'Systematic review of incidence studies of Parkinson's disease', *Mov Disord*, 18: 19-31.

U

Upton, M. L., and R. O. Weller. 1985. 'The morphology of cerebrospinal fluid drainage pathways in human arachnoid granulations', *J Neurosurg*, 63: 867-75.

V

Valente, T., J. Serratosa, U. Perpina, J. Saura, and C. Sola. 2017. 'Alterations in CD200-CD200R1 System during EAE Already Manifest at Presymptomatic Stages', *Front Cell Neurosci*, 11: 129.

Van den Bossche, J., L. A. O'Neill, and D. Menon. 2017. 'Macrophage Immunometabolism: Where Are We (Going)?', *Trends Immunol*, 38: 395-406.

Van Den Eeden, S. K., C. M. Tanner, A. L. Bernstein, R. D. Fross, A. Leimpeter, D. A. Bloch, and L. M. Nelson. 2003. 'Incidence of Parkinson's disease: variation by age, gender, and race/ethnicity', *Am J Epidemiol*, 157: 1015-22.

Van Eldik, L. J., W. L. Thompson, H. Ralay Ranaivo, H. A. Behanna, and D. Martin Watterson. 2007. 'Glia proinflammatory cytokine upregulation as a therapeutic target for neurodegenerative diseases: function-based and target-based discovery approaches', *Int Rev Neurobiol*, 82: 277-96.

Varnum, M. M., and T. Ikezu. 2012. 'The classification of microglial activation phenotypes on neurodegeneration and regeneration in Alzheimer's disease brain', *Arch Immunol Ther Exp (Warsz)*, 60: 251-66.

Varnum, M. M., T. Kiyota, K. L. Ingraham, S. Ikezu, and T. Ikezu. 2015. 'The anti-inflammatory glycoprotein, CD200, restores neurogenesis and enhances amyloid phagocytosis in a mouse model of Alzheimer's disease', *Neurobiol Aging*, 36: 2995-3007.

Vats, D., L. Mukundan, J. I. Odegaard, L. Zhang, K. L. Smith, C. R. Morel, R. A. Wagner, D. R. Greaves, P. J. Murray, and A. Chawla. 2006. 'Oxidative metabolism and PGC-1beta attenuate macrophage-mediated inflammation', *Cell Metab*, 4: 13-24.

Viceconte, N., M. A. Burguillos, A. J. Herrera, R. M. De Pablos, B. Joseph, and J. L. Venero. 2015. 'Neuromelanin activates proinflammatory microglia through a caspase-8-dependent mechanism', *J Neuroinflammation*, 12: 5.

Vieites, J. M., R. de la Torre, M. A. Ortega, T. Montero, J. M. Peco, A. Sanchez-Pozo, A. Gil, and A. Suarez. 2003. 'Characterization of human cd200 glycoprotein receptor gene located on chromosome 3q12-13', *Gene*, 311: 99-104.

Vijitruth, R., M. Liu, D. Y. Choi, X. V. Nguyen, R. L. Hunter, and G. Bing. 2006. 'Cyclooxygenase-2 mediates microglial activation and secondary dopaminergic cell death in the mouse MPTP model of Parkinson's disease', *J Neuroinflammation*, 3: 6.

Vila, M., and S. Przedborski. 2003. 'Targeting programmed cell death in neurodegenerative diseases', *Nat Rev Neurosci*, 4: 365-75.

Voehringer, D., K. Shinkai, and R. M. Locksley. 2004. 'Type 2 immunity reflects orchestrated recruitment of cells committed to IL-4 production', *Immunity*, 20: 267-77.

Voloboueva, L. A., J. F. Emery, X. Sun, and R. G. Giffard. 2013. 'Inflammatory response of microglial BV-2 cells includes a glycolytic shift and is modulated by mitochondrial glucose-regulated protein 75/mortalin', *FEBS Lett*, 587: 756-62.

von Bernhardi, R., L. Eugenin-von Bernhardi, and J. Eugenin. 2015. 'Microglial cell dysregulation in brain aging and neurodegeneration', *Front Aging Neurosci*, 7: 124.

W

Wakabayashi, K., S. Hayashi, M. Yoshimoto, H. Kudo, and H. Takahashi. 2000. 'NACP/alpha-synuclein-positive filamentous inclusions in astrocytes and oligodendrocytes of Parkinson's disease brains', *Acta Neuropathol*, 99: 14-20.

Wakabayashi, K., and H. Takahashi. 1997. 'Neuropathology of autonomic nervous system in Parkinson's disease', *Eur Neurol*, 38 Suppl 2: 2-7.

Wakselman, S., C. Bechade, A. Roumier, D. Bernard, A. Triller, and A. Bessis. 2008. 'Developmental neuronal death in hippocampus requires the microglial CD11b integrin and DAP12 immunoreceptor', *J Neurosci*, 28: 8138-43.

Walker, D. G., J. E. Dalsing-Hernandez, N. A. Campbell, and L. F. Lue. 2009. 'Decreased expression of CD200 and CD200 receptor in Alzheimer's disease: a potential mechanism leading to chronic inflammation', *Exp Neurol*, 215: 5-19.

Walker, D. G., and L. F. Lue. 2013. 'Understanding the neurobiology of CD200 and the CD200 receptor: a therapeutic target for controlling inflammation in human brains?', *Future Neurol*, 8.

Walker, D. G., L. F. Lue, T. M. Tang, C. H. Adler, J. N. Caviness, M. N. Sabbagh, G. E. Serrano, L. I. Sue, and T. G. Beach. 2017. 'Changes in CD200 and intercellular adhesion molecule-1 (ICAM-1) levels in brains of Lewy body disorder cases are associated with amounts of Alzheimer's pathology not alpha-synuclein pathology', *Neurobiol Aging*, 54: 175-86.

Wallace, R. A., R. Boldry, T. Schmittgen, D. Miller, and N. Uretsky. 1984. 'Effect of 1-methyl-4-phenyl-1,2,3,6 tetrahydropyridine (MPTP) on monoamine neurotransmitters in mouse brain & heart', *Life Sci*, 35: 285-91.

Wang, F., S. Zhang, R. Jeon, I. Vuckovic, X. Jiang, A. Lerman, C. D. Folmes, P. D. Dzeja, and J. Herrmann. 2018. 'Interferon Gamma Induces Reversible Metabolic Reprogramming of M1 Macrophages to Sustain Cell Viability and Pro-Inflammatory Activity', *EBioMedicine*, 30: 303-16.

Wang, Q., Y. Liu, and J. Zhou. 2015. 'Neuroinflammation in Parkinson's disease and its potential as therapeutic target', *Transl Neurodegener*, 4: 19.

Wang, X. J., S. Zhang, Z. Q. Yan, Y. X. Zhao, H. Y. Zhou, Y. Wang, G. Q. Lu, and J. D. Zhang. 2011. 'Impaired CD200-CD200R-mediated microglia silencing enhances midbrain dopaminergic neurodegeneration: roles of aging, superoxide, NADPH oxidase, and p38 MAPK', *Free Radic Biol Med*, 50: 1094-106.

Webb, M., and A. N. Barclay. 1984. 'Localisation of the MRC OX-2 glycoprotein on the surfaces of neurones', *J Neurochem*, 43: 1061-7.

Weller, C., A. Charlett, N. L. Oxlade, S. M. Dobbs, R. J. Dobbs, D. W. Peterson, and I. T. Bjarnason. 2005. 'Role of chronic infection and inflammation in the gastrointestinal tract in the etiology and pathogenesis of idiopathic parkinsonism. Part 3: predicted probability and gradients of severity of idiopathic parkinsonism based on H. pylori antibody profile', *Helicobacter*, 10: 288-97.

Wes, P. D., I. R. Holtman, E. W. Boddeke, T. Moller, and B. J. Eggen. 2016. 'Next generation transcriptomics and genomics elucidate biological complexity of microglia in health and disease', *Glia*, 64: 197-213.

Whedon, J. M., and D. Glassey. 2009. 'Cerebrospinal fluid stasis and its clinical significance', *Altern Ther Health Med*, 15: 54-60.

Whitworth, A. J. 2011. 'Drosophila models of Parkinson's disease', *Adv Genet*, 73: 1-50.

WHO. 2006. 'Neurological disorders: public health challenges, ISBN 978 92 4 156336 9 '.

Wiese, M., R. G. Gerlach, I. Popp, J. Matuszak, M. Mahapatro, K. Castiglione, D. Chakravortty, C. Willam, M. Hensel, C. Bogdan, and J. Jantsch. 2012. 'Hypoxia-mediated impairment of the mitochondrial respiratory chain inhibits the bactericidal activity of macrophages', *Infect Immun*, 80: 1455-66.

Wohleb, E. S. 2016. 'Neuron-Microglia Interactions in Mental Health Disorders: "For Better, and For Worse"', *Front Immunol*, 7: 544.

Wolf, S. A., H. W. Boddeke, and H. Kettenmann. 2017. 'Microglia in Physiology and Disease', *Annu Rev Physiol*, 79: 619-43.

Wong, K. K., F. Brenneman, A. Chesney, D. E. Spaner, and R. M. Gorczynski. 2012. 'Soluble CD200 is critical to engraft chronic lymphocytic leukemia cells in immunocompromised mice', *Cancer Res*, 72: 4931-43.

Wong, K. K., I. Khatri, S. Shaha, D. E. Spaner, and R. M. Gorczynski. 2010. 'The role of CD200 in immunity to B cell lymphoma', *J Leukoc Biol*, 88: 361-72.

Wong, K. K., F. Zhu, I. Khatri, Q. Huo, D. E. Spaner, and R. M. Gorczynski. 2016. 'Characterization of CD200 Ectodomain Shedding', *PLoS One*, 11: e0152073.

Wright, G. J., H. Cherwinski, M. Foster-Cuevas, G. Brooke, M. J. Puklavec, M. Bigler, Y. Song, M. Jenmalm, D. Gorman, T. McClanahan, M. R. Liu, M. H. Brown, J. D. Sedgwick, J. H. Phillips, and A. N. Barclay. 2003. 'Characterization of the CD200 receptor family in mice and humans and their interactions with CD200', *J Immunol*, 171: 3034-46.

Wright, G. J., M. J. Puklavec, A. C. Willis, R. M. Hoek, J. D. Sedgwick, M. H. Brown, and A. N. Barclay. 2000. 'Lymphoid/neuronal cell surface OX2 glycoprotein recognizes a novel receptor on macrophages implicated in the control of their function', *Immunity*, 13: 233-42.

Wu, D. C., V. Jackson-Lewis, M. Vila, K. Tieu, P. Teismann, C. Vadseth, D. K. Choi, H. Ischiropoulos, and S. Przedborski. 2002. 'Blockade of microglial activation is neuroprotective in the 1-methyl-4-phenyl-1,2,3,6-tetrahydropyridine mouse model of Parkinson disease', *J Neurosci*, 22: 1763-71.

Wu, D. C., P. Teismann, K. Tieu, M. Vila, V. Jackson-Lewis, H. Ischiropoulos, and S. Przedborski. 2003. 'NADPH oxidase mediates oxidative stress in the 1-methyl-4-phenyl-1,2,3,6-tetrahydropyridine model of Parkinson's disease', *Proc Natl Acad Sci U S A*, 100: 6145-50.

X

Xiang, Z., V. Haroutunian, L. Ho, D. Purohit, and G. M. Pasinetti. 2006. 'Microglia activation in the brain as inflammatory biomarker of Alzheimer's disease neuropathology and clinical dementia', *Dis Markers*, 22: 95-102.

Xie, X., X. Luo, N. Liu, X. Li, F. Lou, Y. Zheng, and Y. Ren. 2017. 'Monocytes, microglia, and CD200-CD200R1 signaling are essential in the transmission of inflammation from the periphery to the central nervous system', *J Neurochem*, 141: 222-35.

Y

Yamada, E., and D. W. McVicar. 2008. 'Paired receptor systems of the innate immune system', *Curr Protoc Immunol*, Chapter 1: Appendix 1X.

Yamada, T., P. L. McGeer, E. G. McGeer 1991. 'Relationship of complement-activated oligodendrocytes to reactive microglia and neuronal pathology in neurodegenerative disease', *Dement Geriatr Cogn Disord*, 2: 71–77.

Yao, K., and Y. F. Zhao. 2018. 'Aging modulates microglia phenotypes in neuroinflammation of MPTP-PD mice', *Exp Gerontol*, 111: 86-93.

Yeh, F. L., D. V. Hansen, and M. Sheng. 2017. 'TREM2, Microglia, and Neurodegenerative Diseases', *Trends Mol Med*, 23: 512-33.

Yi, M. H., E. Zhang, J. W. Kang, Y. N. Shin, J. Y. Byun, S. H. Oh, J. H. Seo, Y. H. Lee, and D. W. Kim. 2012. 'Expression of CD200 in alternative activation of microglia following an excitotoxic lesion in the mouse hippocampus', *Brain Res*, 1481: 90-6.

Yi, M. H., E. Zhang, J. J. Kim, H. Baek, N. Shin, S. Kim, S. R. Kim, H. R. Kim, S. J. Lee, J. B. Park, Y. Kim, O. Y. Kwon, Y. H. Lee, S. H. Oh, and D. W. Kim. 2016. 'CD200R/Foxp3-mediated signalling regulates microglial activation', *Sci Rep*, 6: 34901.

Yuan, Y. Q., Y. L. Wang, B. S. Yuan, X. Yuan, X. O. Hou, J. S. Bian, C. F. Liu, and L. F. Hu. 2018. 'Impaired CBS-H2S signaling axis contributes to MPTP-induced neurodegeneration in a mouse model of Parkinson's disease', *Brain Behav Immun*, 67: 77-90.

Yue, X., D. Qiao, A. Wang, X. Tan, Y. Li, C. Liu, and H. Wang. 2012. 'CD200 attenuates methamphetamine-induced microglial activation and dopamine depletion', *J Huazhong Univ Sci Technolog Med Sci*, 32: 415-21.

Z

Zecca, L., H. Wilms, S. Geick, J. H. Claasen, L. O. Brandenburg, C. Holzknecht, M. L. Panizza, F. A. Zucca, G. Deuschl, J. Sievers, and R. Lucius. 2008. 'Human neuromelanin induces neuroinflammation and neurodegeneration in the rat substantia nigra: implications for Parkinson's disease', *Acta Neuropathol*, 116: 47-55.

Zeng, X. S., W. S. Geng, and J. J. Jia. 2018. 'Neurotoxin-Induced Animal Models of Parkinson Disease: Pathogenic Mechanism and Assessment', *ASN Neuro*, 10: 1759091418777438.

Zhang, J., A. Pieper, and S. H. Snyder. 1995. 'Poly(ADP-ribose) synthetase activation: an early indicator of neurotoxic DNA damage', *J Neurochem*, 65: 1411-4.

Zhang, S., H. Cherwinski, J. D. Sedgwick, and J. H. Phillips. 2004. 'Molecular mechanisms of CD200 inhibition of mast cell activation', *J Immunol*, 173: 6786-93.

Zhang, S., X. J. Wang, L. P. Tian, J. Pan, G. Q. Lu, Y. J. Zhang, J. Q. Ding, and S. D. Chen. 2011. 'CD200-CD200R dysfunction exacerbates microglial activation and dopaminergic neurodegeneration in a rat model of Parkinson's disease', *J Neuroinflammation*, 8: 154.

Zhang, W., K. Phillips, A. R. Wielgus, J. Liu, A. Albertini, F. A. Zucca, R. Faust, S. Y. Qian, D. S. Miller, C. F. Chignell, B. Wilson, V. Jackson-Lewis, S. Przedborski, D. Joset, J. Loike, J. S. Hong, D. Sulzer, and L. Zecca. 2011. 'Neuromelanin activates microglia and induces degeneration of dopaminergic neurons: implications for progression of Parkinson's disease', *Neurotox Res*, 19: 63-72.

Zhang, W., T. Wang, Z. Pei, D. S. Miller, X. Wu, M. L. Block, B. Wilson, W. Zhang, Y. Zhou, J. S. Hong, and J. Zhang. 2005. 'Aggregated alpha-synuclein activates microglia: a process leading to disease progression in Parkinson's disease', *FASEB J*, 19: 533-42.

Zhang, X. Y., L. Chen, Y. Yang, D. M. Xu, S. R. Zhang, C. T. Li, W. Zheng, S. Y. Yu, E. Q. Wei, and L. H. Zhang. 2014. 'Regulation of rotenone-induced microglial activation by 5-lipoxygenase and cysteinyl leukotriene receptor 1', *Brain Res*, 1572: 59-71.

Zhou, P., R. Weng, Z. Chen, R. Wang, J. Zou, X. Liu, J. Liao, Y. Wang, Y. Xia, and Q. Wang. 2016. 'TLR4 Signaling in MPP(+)-Induced Activation of BV-2 Cells', *Neural Plast*, 2016: 5076740.

Zlokovic, B. V. 2008. 'The blood-brain barrier in health and chronic neurodegenerative disorders', *Neuron*, 57: 178-201.

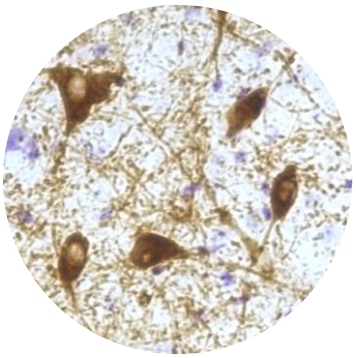

Annex

frontiers in Molecular Neuroscience

ORIGINAL RESEARCH
published: 10 January 2019
doi: 10.3389/fnmol.2018.00479

Parkinsonian Neurotoxins Impair the Pro-inflammatory Response of Glial Cells

*Neus Rabaneda-Lombarte[1,2], Efren Xicoy-Espaulella[1], Joan Serratosa[1], Josep Saura[2] and Carme Solà[1]**

[1]*Department of Brain Ischemia and Neurodegeneration, Institut d'Investigacions Biomèdiques de Barcelona (IIBB)—Consejo Superior de Investigaciones Científicas (CSIC), Institut d'Investigacions Biomèdiques August-Pi i Sunyer (IDIBAPS), Barcelona, Spain,* [2]*Biochemistry and Molecular Biology Unit, School of Medicine, Institut d'Investigacions Biomèdiques August-Pi i Sunyer (IDIBAPS), University of Barcelona, Barcelona, Spain*

In the case of Parkinson's disease (PD), epidemiological studies have reported that pesticide exposure is a risk factor for its pathology. It has been suggested that some chemical agents, such as rotenone and paraquat, that inhibit the mitochondrial respiratory chain (in the same way as the PD mimetic toxin 1-methyl-4-phenylpyridinium, MPP+) are involved in the development of PD. However, although the neurotoxic effect of such compounds has been widely reported using *in vivo* and *in vitro* experimental approaches, their direct effect on the glial cells remains poorly characterized. In addition, the extent to which these toxins interfere with the immune response of the glial cells, is also underexplored. We used mouse primary mixed glial and microglial cultures to study the effect of MPP+ and rotenone on glial activation, in the absence and the presence of a pro-inflammatory stimulus (lipopolysaccharide plus interferon-γ, LPS+IFN-γ). We determined the mRNA expression of the effector molecules that participate in the inflammatory response (pro-inflammatory cytokines and enzymes), as well as the nitric oxide (NO) and cytokine production. We also studied the phagocytic activity of the microglial cells. In addition, we evaluated the metabolic changes associated with the observed effects, through the measurement of adenosine triphosphate (ATP) production and the expression of genes involved in the control of metabolic pathways. We observed that exposure of the glial cultures to the neurotoxins, especially rotenone, impaired the pro-inflammatory response induced by LPS/IFN-γ. MPP+ and rotenone also impaired the phagocytic activity of the microglial cells, and this effect was potentiated in the presence of LPS/IFN-γ. The deficit in ATP production that was detected, mainly in MPP+ and rotenone-treated mixed glial cultures, may be responsible for the effects observed. These results show that the response of glial cells to a pro-inflammatory challenge is altered in the presence of toxins inhibiting mitochondrial respiratory chain

OPEN ACCESS

Edited by:
Yolanda Diz-Chaves, University of Vigo, Spain

Reviewed by:
Tarja Maarit Malm, University of Eastern Finland, Finland
Hong Qing, Beijing Institute of Technology, China

****Correspondence:***
Carme Solà
carme.sola@iibb.csic.es

Received: *02 October 2018*
Accepted: *07 December 2018*
Published: *10 January 2019*

Citation:
Rabaneda-Lombarte N, Xicoy-Espaulella E, Serratosa J, Saura J and Solà C (2019) Parkinsonian Neurotoxins Impair the Pro-inflammatory Response of Glial Cells. Front. Mol. Neurosci. 11:479. doi: 10.3389/fnmol.2018.00479

Abbreviations: ATP, adenosine triphosphate; BSA, bovine serum albumin; (COX-2), cyclooxygenase-2; Carkl, carbohydrate kinase-like protein; CNS, central nervous system; Glut, glucose transporter; gp91phox, NADPH oxidase, catalytic subunit; Hif, hypoxia-inducible factor; Hk, hexokinase; IL, interleukin; IFN-γ, interferon-γ; iNOS, inducible nitric oxide synthase; LPS, lipopolysaccharide; MPP+, 1-methyl-4-phenylpyridinium; MPTP, 1-methyl-4-phenyl-1,2,3,6-tetrahydropyridine; MTT, 3-(4,5-dimethylthiazol-2-yl)-2,5-diphenyltetrazolium bromide; NO, nitric oxide; PBS, Phosphate-buffered saline; PCR, polymerase chain reaction; PFK-P, phosphofructokinase; PI, propidium iodide; PD, Parkinson's disease; qRT-PCR, quantitative real time PCR; Rot, rotenone; TNF, tumor necrosis factor.

activity, suggesting that the glial immune response is impaired by such agents. This may have relevant consequences for brain function and the central nervous system's (CNS's) response to insults.

Keywords: glial activation, mixed glia, microglia, immune response, MPP+, rotenone, glial metabolism, Parkinson's disease

INTRODUCTION

Microglia are the main endogenous immune cells of the central nervous system (CNS). Under physiological conditions, they constantly patrol the CNS parenchyma, ready to detect alterations that could interfere with normal brain function. In response to noxious stimuli, microglial cells develop a wide range of reactive phenotypes aimed at re-establishing cerebral homeostasis and minimizing neuronal damage. In this way, they can respond to alterations in the CNS homeostasis due to the presence of exogenous pathogens or anomalous protein aggregates resulting from pathological processes. In addition, they are also able to respond to neuronal damage resulting from brain lesions, brain ischemia, neurodegenerative diseases or exposure to neurotoxic agents (Salter and Stevens, 2017).

In fact, exposure to neurotoxic agents, such as pesticides, may contribute to the development of some neurodegenerative diseases (Mostafalou and Abdollahi, 2013). In 1982, the accidental exposure to 1-methyl-4-phenyl-1,2,3,6-tetrahydropyridine (MPTP) in drug abusers caused parkinsonism (Langston et al., 1983). Epidemiological studies show that exposure to the pesticides rotenone and paraquat, which are functional and structural analogs of MPTP respectively, as well as to other pesticides, is a risk factor for Parkinson's disease (PD; Tanner et al., 2011; Goldman, 2013; Kamel, 2013). MPTP and its analogs are inhibitors of the mitochondrial respiratory chain and it has been suggested that mitochondrial dysfunction is involved in the induction of oxidative damage in dopaminergic neurons in parkinsonism (Dauer and Przedborski, 2003; Goldman, 2013). Due to the particular sensitivity of dopaminergic neurons to the effect of these neurotoxins, experimental models of PD have been developed by exposing neuronal cell cultures or laboratory animals to these agents (Bové and Perier, 2012). These experimental models are useful for studying mechanisms of dopaminergic neuronal cell degeneration and testing potential therapeutic approaches. However, although the toxic effect of MPTP [or its active metabolite 1-methyl-4-phenylpyridinium (MPP+)] and rotenone on dopaminergic neurons has been widely described using both *in vivo* and *in vitro* approaches, reports of their direct effect on glial cells are scarce. In addition, there is some controversy regarding the results already obtained. Either no direct effect of MPP+ on microglial cell function (Gao et al., 2003; Jin et al., 2012), or an increase in the expression of pro-inflammatory markers in microglial cells after MPP+ exposure (Bournival et al., 2012; Chen et al., 2015) has been reported. Similarly, either an increase in the expression of pro-inflammatory factors (Gao et al., 2013; Yuan et al., 2013; Du et al., 2014) or no direct effect on the production of inflammatory factors (Klintworth et al., 2009) has been observed in rotenone-treated microglial cell cultures.

Since reciprocal communication exists in the CNS between neuronal and glial cells, alterations in neuronal function may affect glial function and vice versa. In fact, a possible role of glial activation in the development of neuronal damage in neurodegenerative diseases has been repeatedly proposed (Perry et al., 2010; Colonna and Butovsky, 2017). In addition, communication also exists between glial cells, and alterations in a given cell type may affect the function of other glial cell types. Consequently, alterations in glial function due to exposure to neurotoxic compounds merit study, especially in the context of neurodegenerative diseases in which such exposure is considered a risk factor. The aim of this study was therefore to characterize the effects of MPP+ and rotenone on glial activation using primary mixed glial cultures, (mainly composed of astrocytes and microglia) and microglial cultures. We determined the direct effect of these neurotoxins on glial cell function, and also whether they could interfere with glial activation induced by a classical pro-inflammatory stimulus such as lipopolysaccharide (LPS)/interferon-γ (IFN-γ). We observed that MPP+ and rotenone did not induce the expression of pro-inflammatory markers by glial cells *per se*. However, the LPS/IFN-γ-induced pro-inflammatory response was modified in glial cultures in the presence of MPP+ and rotenone. These neurotoxins induced modifications in the mRNA expression of pro-inflammatory genes and phagocytic activity. Alterations in adenosine triphosphate (ATP) production could account for the effects observed. These results show that insults affecting the metabolic activity of glial cells, result in an altered immune response, which may have relevant consequences for normal brain function and the CNS response to insults.

MATERIALS AND METHODS

Experiments were carried out in accordance with European Union directives (86/609/EU) and Spanish regulations (BOE 67/8509-12, 1988) on the use of laboratory animals, and were approved by the Ethics and Scientific Committees of the University of Barcelona and CSIC.

Cell Cultures

Primary mixed glial cultures were prepared from the cerebral cortex of 1–3-day old C57Bl/6 mice as previously described (Gresa-Arribas et al., 2010). The culture medium used was the Dulbecco's modified Eagle medium-F12 nutrient mixture (GIBCO) supplemented with 10% heat-inactivated fetal bovine serum (FBS, Invitrogen, Molecular Probes, Eugene, OR, USA),

20 U/mL penicillin-20 μg/mL streptomycin (Invitrogen), and 0.5 μg/mL amphotericin B (Fungizone®, Invitrogen). The cells were seeded at a density of 3.5×10^5 cells/mL (100 μL, 300 μL and 2.5 mL per well into 96-, 48- and 6-well culture plates) and cultured at 37°C in a humidified 5% CO_2 atmosphere. The medium was replaced once a week. The cultures were used at 21 DIV.

Primary microglia enriched cultures were obtained from 21 DIV mixed glial cultures using the mild trypsinization method as previously described (Saura et al., 2003). Microglia enriched cultures were used 24 h after isolation by this procedure.

Cell Culture Treatments

LPS and IFN-γ treatment: Cells were treated with 100 ng/ml LPS (*E. coli* 026:B6, Sigma-Aldrich, St. Louis, MO, USA) and 0.1 ng/ml IFN-γ (Sigma-Aldrich) for 6 h or 24 h. Stock solutions of 1 mg/mL LPS in a serum-free culture medium and 10 μg/mL IFN-γ in a serum-containing culture medium, were prepared and stored at −20°C.

MPP+ and rotenone treatment: Cells were treated with 10, 25, 50 and 100 μM MPP+ or 20, 40, 100 and 150 nM rotenone (both from Sigma-Aldrich) for 6 h or 24 h, in the absence or presence of LPS/IFN-γ. Stock solutions of 50 mM MPP+ in milliQ H_2O and 10 mM rotenone in DMSO were freshly prepared on the day of treatment. DMSO in the cell cultures was always below 1/1,000.

Treatments were added directly to the culture medium.

Nitric Oxide Production

Nitric oxide (NO) production was estimated from the nitrite accumulation in the culture supernatant using the colorimetric Griess reaction. Briefly, the culture supernatant from the glial cells seeded into 96-well culture plates, was collected 24 and 48 h after treatments and stored at −20°C until used. Fifty microliter aliquots of the culture supernatant were incubated with equal volumes of the Griess reagent for 10 min at 20–25°C. Optical density at 540 nm was measured using a microplate reader (Multiskan Spectrum, Thermo Fisher Scientific, Vantaa, Finland). Nitrite concentration was determined from a sodium nitrate standard curve.

Cell Viability Measurements

Glial cells seeded into 96-well culture plates were used to estimate cell viability from the metabolic activity by a 3-(4,5-dimethylthiazol-2-yl)-2,5-diphenyl tetrazolium bromide (MTT) colorimetric assay, 24 h after treatments. Briefly, MTT (Sigma-Aldrich) was added to the cell cultures to reach a final concentration of 1 mg/mL. After incubation for 30 min (mixed glial cultures) or 90 min (microglial cultures) at 37°C, the medium was removed and 200 μL of DMSO was added to each well. The optical density of the resulting blue formazan was measured at 570 nm using a microplate reader (Multiskan Spectrum, Thermo Fisher Scientific). Readings were taken at 650 nm to obtain background levels. Results were expressed as percentages of the control.

Propidium iodide (PI) and Hoechst labeling were performed to corroborate data obtained in the MTT assay. Briefly, cells were incubated with PI (7.5 μg/ml, Molecular Probes, Eugene, OR, USA) and Hoechst 33342 (3 μg/ml, Molecular Probes) for 10 min. Microscopy images were obtained using an Olympus IX70 microscope (Olympus, Okoya, Japan) and a digital camera (CC-12, Olympus Soft Imaging Solutions GmbH, Hamburg, Germany). The extent of cell death was calculated from the ratio between PI positive nuclei, corresponding to dead cells, vs. Hoechst positive total nuclei.

RNA Extraction and Quantitative Real Time PCR

Glial cells seeded into six-well culture plates were used (one or two wells per experimental condition for mixed glia and microglia, respectively) to assess the mRNA expression of pro-inflammatory markers by quantitative real time polymerase chain reaction (PCR) 6 h after treatments. A High Pure RNA Isolation Kit (Roche Diagnostics Scheiwz AG, Rotkreuz, Switzerland) was used to isolate the total RNA from the mixed glial cultures. A PureLink RNA micro kit (Invitrogen) was used to isolate the total RNA from the primary microglial cultures. The RNA (0.5–1 μg) was reverse transcribed with random primers using the Transcriptor Reverse Transcriptase Kit (Roche Diagnostics). Three nanograms of cDNA were used to perform quantitative real time PCR (qRT-PCR) with the IQ SYBRGREEN SuperMix (Bio-Rad Laboratories, Hercules, CA, USA) using an iCycler MyIQ apparatus (Bio-Rad Laboratories) as previously described (Dentesano et al., 2014). The primers used (Integrated DNA Technology, IDT, Skokie, IL, USA) are shown in **Table 1**. Samples were run for 40 cycles (95°C for 15 s, 60°C for 30 s, and 72°C for 15 s). The amplification specificity was confirmed by the analysis of melting curves. Relative gene expression values were calculated using the ΔΔCt method (Livak and Schmittgen, 2001). β-Actin and 18S ribosomal RNA (Rn18s) were used as the reference genes.

ELISAs

The interleukin (IL) 1β, IL6 and tumor necrosis factor α (TNFα) release in the culture supernatant was determined using ELISA kits specific for each cytokine (mouse IL1-β ELISA Ready-SET-GO!, mouse IL6 ELISA Ready-SET-GO! and mouse TNFα ELISA Ready-SET-GO!, eBioscience-Affimetrix, Inc., San Diego, CA, USA), following the manufacturer's instructions. The culture supernatant from 48-well culture plates was collected 24 h after treatments and stored at −80°C until use. IL1β, IL6 and TNFα concentrations were determined from the standard curves.

Phagocytosis Assay

The phagocytic activity of the microglial cells was assessed 24 h after treatments. Briefly, the microglial cell cultures in 48-well plates were incubated for 1 h at 37°C with fluorescent latex beads (FluoSpheres, carboxylate-modified microspheres, 2.0 μm, red fluorescent (580/605), 2% solids; Thermofisher Scientific; 1/1,000) 23 h after treatments. Then, the cells were washed three times with a phosphate-buffered saline (PBS) and fixed with 4% paraformaldehyde for 15 min.

Immunocytochemistry was performed using a rabbit polyclonal anti-Iba1 primary antibody (1/500, WAKO; Japan), a specific marker for microglial cells. Cells were first incubated with 0.3% Triton-X-100 in PBS containing 1% bovine serum

TABLE 1 | Primers used for quantitative real time polymerase chain reaction (qRT-PCR).

Target mRNA	Accession number	Forward primer (5′→3′)	Reverse primer (5′→3′)
Carkl	NM_029031.3	CAGGCCAAGGCTGTGAAT	GCCAGCTGCATCATAGGACT
COX2	NM_011198.4	TGCAGAATTGAAAGCCCTCT	CCCCAAAGATAGCATCTGGA
Glut1	NM_011400.3	CATCCTTATTGCCCAGGTGTTT	GAAGATGACACTGAGCAGCAGA
gp91phox	NM_007807.5	ACTCCTTGGGTCAGCACTGGCT	GCAACACGCACTGGAACCCCT
Hifα	NM_010431.2	ACAAGTCACCACAGGACAG	AGGGAGAAAATCAAGTCG
Hk1	NM_010438.3	GATGGAGGTGAAGAAGAAGC	GGAAACGAGAAGGTGAAGC
Hk2	NM_013820.3	CGGTACACTCAATGACATCC	GTAGACAGAGCCATCCACG
IL1β	NM_008361.4	TGGTGTGTGACGTTCCCATTA	CAGCACGAGGCTTTTTTGTTG
IL6	NM_031168.2	CCAGTTTGGTAGCATCCATC	CCGGAGAGGAGACTTCACAG
iNOS	NM_010927.3	GGCAGCCTGTGAGACCTTTG	GCATTGGAAGTGAAGCGTTTC
Pfkp	NM_019703.4	AAGCTATCGGTGTCCTGACC	TCCCACCCACTTGCAGAAT
TNFα	NM_013693.3	TGATCCGCGACGTGGAA	ACCGCCTGGAGTTCTGGAA
Reference genes:			
β-Actin	NM_007393.5	CAACGAGCGGTTCCGATG	GCCACAGGATTCCATACCCA
Rn18s	NR_003278.3_	GTAACCCGTTGAACCCCATT	CCATCCAATCGGTAGTAGCG

β-Actin, Actin, beta; Carkl, sedoheptulokinase; COX2, cyclooxygenase-2; Glut1, Glucose transporter 1; gp91phox, catalytic subunit of NAPH oxidase; Hifα, hypoxia inducible factor 1, alpha subunit; Hk1, hexokinase 1, Hk2, hexokinase 2; IL1β, interleukin 1, beta; IL6, interleukin 6; iNOS, inducible nitric oxide synthase; Pfkp, phosphofructokinase, platelet; TNFα, tumor necrosis factor alpha; Rn18s, 18S ribosomal RNA.

albumin (BSA) and 10% normal donkey serum for 20 min at room temperature, and then overnight at 4°C with the primary antibody. Once they had been rinsed in PBS, cells were incubated for 1 h at room temperature with an ALEXA 488 donkey anti-rabbit secondary antibody (1/1,000; Invitrogen). Antibodies were diluted in 0.3% Triton X-100 in PBS containing 1% BSA and 10% normal donkey serum.

Images of three microscopic fields using a 20× objective were obtained with an Olympus IX70 fluorescence microscope and a digital camera (CC-12, Olympus Soft Imaging Solutions GmbH). Two to three wells per experimental condition were processed and each experimental condition was repeated at least four times. Visual counting of the FluoSpheres was performed. The percentage of phagocytic cells and the average number of fluorescent microspheres per microglial cell were calculated. To further characterize the phagocytic activity, we also calculated the percentage of cells showing lower phagocytic activity (microspheres/cell) than the controls and the percentage of cells showing higher phagocytic activity than the controls.

ATP Production

The intracellular production of ATP was determined using a luminescence assay kit (ATPlite Luminescence ATP Detection Assay System, PerkinElmer, Waltham, MA, USA) following the manufacturer's instructions. Briefly, cells in 96-well plates (mixed glia) or 6-well-plates (microglia) were lysed 24 h after treatments and the ATP concentration was measured based on the production of light, caused by the reaction of the ATP with added luciferase and D-luciferin. The emitted light was quantified using a luminometer (Orion Microplate Luminometer, Berthold Detection System, Germany). The ATP concentration in the samples was calculated from an ATP standard curve.

Data Presentation and Statistical Analysis

The results are presented as the mean + SEM. At least three independent experiments were performed for analysis. Data were statistically analyzed with the GraphPad Prism software. Statistical analyses were performed using the one-way analysis of variance (ANOVA) followed by the Newman-Keuls post-test, and a two-way ANOVA followed by the Bonferroni post-test. Values of $p < 0.05$ were considered statistically significant.

RESULTS

Effects of MPP+ and Rotenone on Glial Cell Viability

In a preliminary study, we performed dose-response experiments in order to select working concentrations of MPP+ and rotenone that did not result in significant alterations in cell viability after 24 h exposure. We evaluated glial cell viability after treating the mixed glial or the microglial cultures with increasing concentrations of MPP+ (10, 25, 50 and 100 μM) or rotenone (20, 40, 100 and 150 nM), both in the absence and in the presence of LPS/IFN-γ, considering the MTT assay and PI staining. In mixed glial cell cultures, MPP+ induced a concentration-dependent decrease in MTT reduction that was accentuated in the presence of LPS/IFN-γ (**Figure 1A**). On the contrary, no alterations in MTT reduction were observed in microglial cell cultures treated with MPP+, both in the absence and presence of LPS/IFN-γ (**Figure 1B**). Rotenone-treated mixed glial cell cultures showed a significant decrease in MTT reduction from 100 nM rotenone. In the presence of LPS/IFN-γ, there was a significant decrease in MTT reduction even at 20 nM rotenone (**Figure 1C**). As in the case of MPP+ treatments, no alterations in MTT reduction were observed in microglial cell cultures treated with rotenone or rotenone and LPS/IFN-γ (**Figure 1D**). To determine whether the decrease in MTT reduction in MPP+ and rotenone-treated mixed glial cell cultures was due to a decrease in metabolic activity or due to cell death, PI staining was performed. Mixed glial cultures treated with 50 and 100 μM MPP+ showed a significant increase in the percentage of PI positive nuclei. This effect was accentuated in the presence

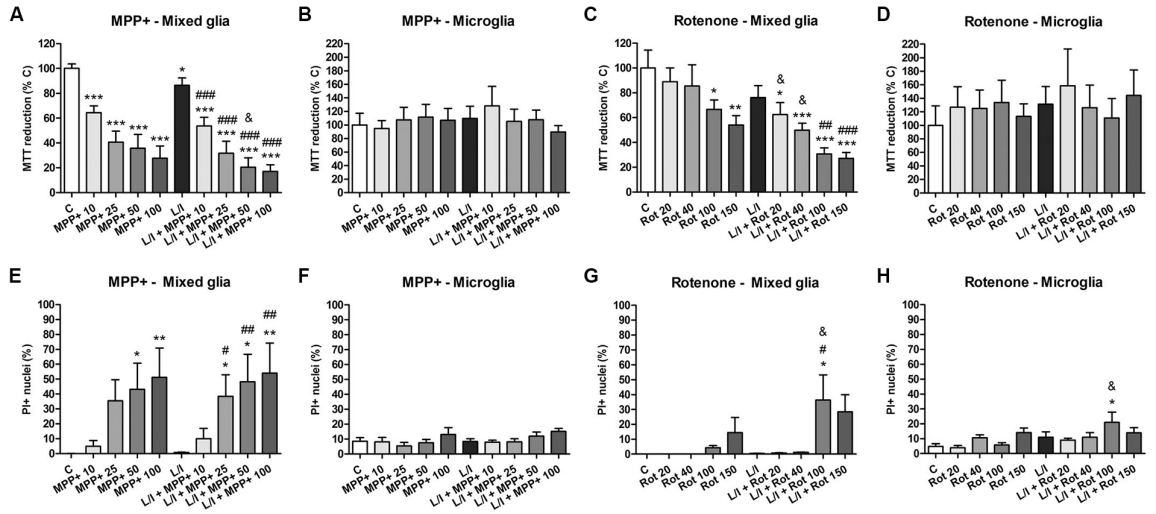

FIGURE 1 | Effect of 1-methyl-4-phenylpyridinium (MPP+) and rotenone on glial cell viability. **(A–D)** MPP+ and rotenone induced alterations in 3-(4,5-dimethylthiazol-2-yl)-2,5-diphenyltetrazolium bromide (MTT) reduction in the primary glial cultures. Effect of 10, 25, 50 and 100 μM MPP+ treatment for 24 h on the mixed glial cultures **(A)** and microglial cultures **(B)**, both in the absence and the presence of lipopolysaccharide (LPS)/interferon-γ (IFN-γ; L/I). Effect of 20, 40, 100 and 150 nM rotenone (Rot) treatment for 24 h on the mixed glial cultures **(C)** and microglial cultures **(D)**, both in the absence and the presence of L/I. **(E–H)** Percentage of propidium iodide (PI) positive nuclei in the mixed glial cultures **(E)** and microglial cultures **(F)** treated for 24 h with 10, 25, 50 and 100 μM MPP+, both in the absence and the presence of LPS/IFN-γ (L/I). Percentage of PI positive nuclei in the mixed glial cultures **(G)** and microglial cultures **(H)** treated for 24 h with 20, 40, 100 and 150 nM rotenone (Rot), both in the absence and the presence of L/I. Bars are means ± SEM of four independent experiments. $^{*}p < 0.05$, $^{**}p < 0.01$ and $^{***}p < 0.001$ vs. control (C); $^{\#}p < 0.05$, $^{\#\#}p < 0.01$ and $^{\#\#\#}p < 0.001$ vs. L/I; $^{\&}p < 0.05$ vs. MPP+ or Rot alone; one-way analysis of variance (ANOVA; repeated measures) and Newman-Keuls post-test.

of LPS/IFN-γ, and a significant increase was also detected at 25 μM MPP+ (**Figure 1E**). No alterations in the percentage of PI-positive nuclei were observed in microglial cultures treated with MPP+ (**Figure 1F**). In addition, no significant increases in the percentage of PI-positive nuclei were observed in rotenone-treated mixed glial cell cultures or microglial cultures (**Figures 1G,H**), with the exception of cells treated with 100 μM rotenone and LPS/IFN-γ.

The concentrations of 10 and 25 μM MPP+ and 40 and 100 nM rotenone were used in subsequent studies. Representative images of the cultures in these experimental conditions are shown in **Figure 2**, which corroborate the lack of a toxic effect of the concentrations of MPP+ (**Figure 2A**) and rotenone (**Figure 2B**) selected for further experiments.

MPP+ and Rotenone Induce Alterations in the Expression of Pro-inflammatory Genes in LPS/IFN-γ-Treated Primary Glial Cultures

We next determined whether MPP+ and rotenone induced a pro-inflammatory phenotype in primary glial cell cultures, as well as whether they had some effect on the development of the pro-inflammatory response induced by LPS/IFN-γ. We determined the mRNA expression of the cytokines IL1β, IL6 and TNFα and the enzymes inducible NO synthase (iNOS), cyclooxygenase 2 (COX2) and gp91phox (the catalytic subunit of NADPH oxidase), as markers of a pro-inflammatory response. In general, MPP+ (**Figure 3**) and rotenone (**Figure 4**) treatment did not significantly induce the mRNA expression of these pro-inflammatory markers in the primary glial cell cultures, although a trend towards increased expression was observed for some mRNAs, especially in rotenone-treated mixed glial cultures. On the contrary, 6 h after LPS/IFN-γ treatment, the mRNA expression of all the pro-inflammatory markers tested was clearly induced (**Figures 3**, **4**). However, MPP+ and especially rotenone induced alterations in the pattern of expression of these markers in LPS/IFN-γ treated cultures. When glial cell cultures were treated with LPS/IFN-γ in the presence of MPP+, the induction of IL1β mRNA expression was significantly inhibited in the mixed glial and microglial cultures (**Figures 3A,B**), while COX2 mRNA expression was further increased in the mixed glial cultures (**Figure 3A**) and gp91phox mRNA was induced in the microglial cultures (**Figure 3B**). More importantly, rotenone exposure significantly abrogated LPS/IFN-γ induction of the mRNA expression of all pro-inflammatory markers in the mixed glial cultures (**Figure 4A**), as well as IL1β, IL6 and COX2 mRNA expression in microglial cultures (**Figure 4B**).

MPP+ and Rotenone Inhibit LPS/IFN-γ-Induced NO and Pro-inflammatory Cytokine Production in Primary Glial Cultures

We also analyzed the effect of MPP+ and rotenone on NO, IL1β, IL6 and TNFα release into the culture medium. MPP+ alone induced a decrease in NO production and an increase

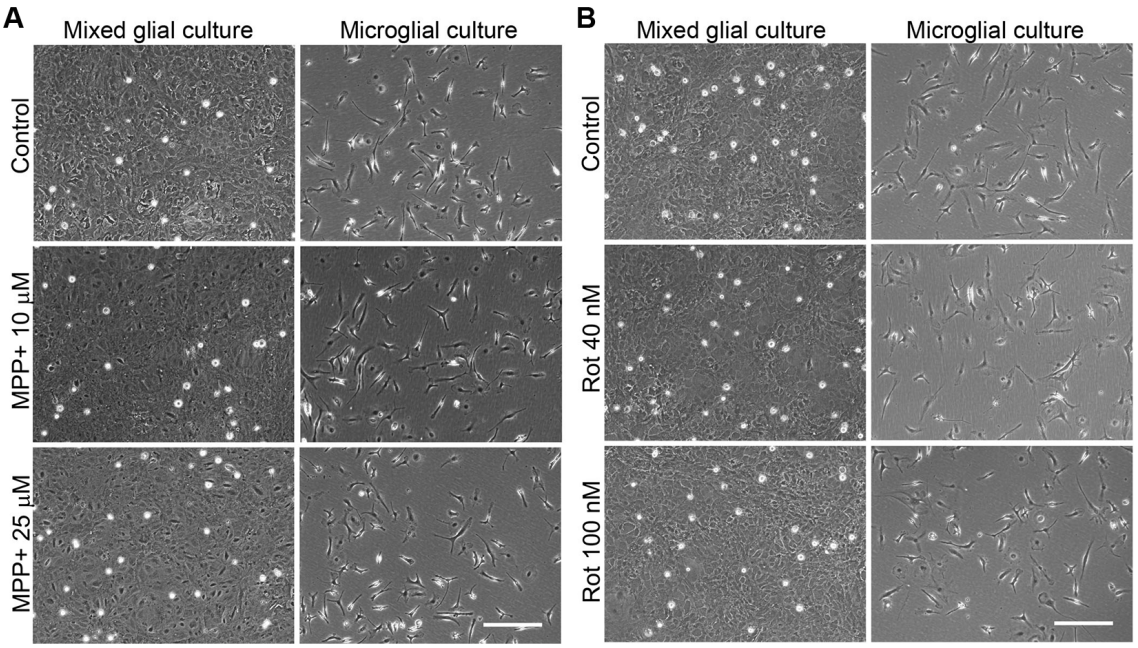

FIGURE 2 | Phase contrast images of the MPP+- and rotenone-treated primary glial cultures. Images show the appearance of the mixed glial cultures and microglial cultures treated for 24 h with 10 and 25 μM MPP+ **(A)** or 40 and 100 nM rotenone (Rot; **B**), the working concentrations used in further studies. Bar = 200 μm.

in IL6 release into the culture medium in mixed glial cell cultures 24 h after treatment (**Figure 5A**). The latter effect was also observed in the MPP+-treated microglial cultures (**Figure 5B**), as well as in the rotenone-treated mixed glial (**Figure 5C**) and microglial cultures (**Figure 5D**). LPS/IFN-γ-treatment clearly increased NO production in the mixed glial cultures, and MPP+ (25 μM) and rotenone (40 and 100 nM) significantly inhibited this effect (**Figures 5A,C**). Significant NO production was not detected in the microglial cultures treated with LPS/IFN-γ for 24 h (**Figures 5B,D**). However, an increase in NO production was observed when the microglial cultures were treated with LPS/IFN-γ for 48 h, but MPP+ and rotenone did not modify this effect (data not shown). With regards to cytokine release, LPS/IFN-γ-treatment resulted in drastic increases in IL1β, IL6 and TNFα levels in the mixed glial (**Figures 5A,C**) and microglial (**Figures 5B,D**) cultures. MPP+ exposure (25 μM) significantly inhibited LPS/IFN-γ-induced release of IL1β and IL6, but not TNFα, in the mixed glia (**Figure 5A**), while it had no significant effect on the production of these cytokines in the microglial cell cultures (**Figure 5B**). Interestingly, rotenone (40 and 100 nM) significantly inhibited IL1β, IL6 and TNFα release induced by LPS/IFN-γ in both the mixed glial (**Figure 5C**) and microglial cultures (**Figure 5D**).

MPP+ and Rotenone Treatment Inhibit the Phagocytic Activity of Microglial Cells

We then evaluated whether MPP+ and rotenone modified the phagocytic activity of the microglial cells, another important parameter used to characterize the microglial activation phenotype. Both MPP+ and rotenone treatment showed a tendency to decrease the percentage of phagocytic microglial cells that were statistically significant when the cells were also treated with LPS/IFN-γ (**Figure 6A**). In addition, MPP+ and rotenone treatment resulted in a significant increase in the percentage of microglial cells showing low phagocytic activity (number of microspheres per cell lower than control) and a subsequent significant decrease in the percentage of cells showing high phagocytic activity (number of microspheres per cell higher than control; **Figure 6B**). These effects were accentuated in the presence of LPS/IFN-γ.

ATP Production Is Compromised in MPP+- and Rotenone-Treated Glial Cell Cultures

In an attempt to better characterize the metabolic status of the cells, we determined the intracellular ATP production in response to MPP+, rotenone and LPS/IFN-γ treatments. In general, ATP production was modified in the mixed glial cultures in our MPP+ and rotenone experimental models ($p < 0.001$, one-way ANOVA; **Figure 7**). In particular, ATP production was significantly decreased after 25 μM MPP+ treatment (**Figure 7A**). On the contrary, a significant increase in ATP production was detected in the LPS/IFN-γ-treated mixed glial cultures, which was abrogated in the presence of MPP+ and rotenone (**Figures 7A,B**). ATP production was also modified in the microglial cultures in the MPP+ and rotenone experimental models ($p < 0.05$, one-way ANOVA), but to a lesser extent than in the mixed glial cultures (**Figures 7C,D**).

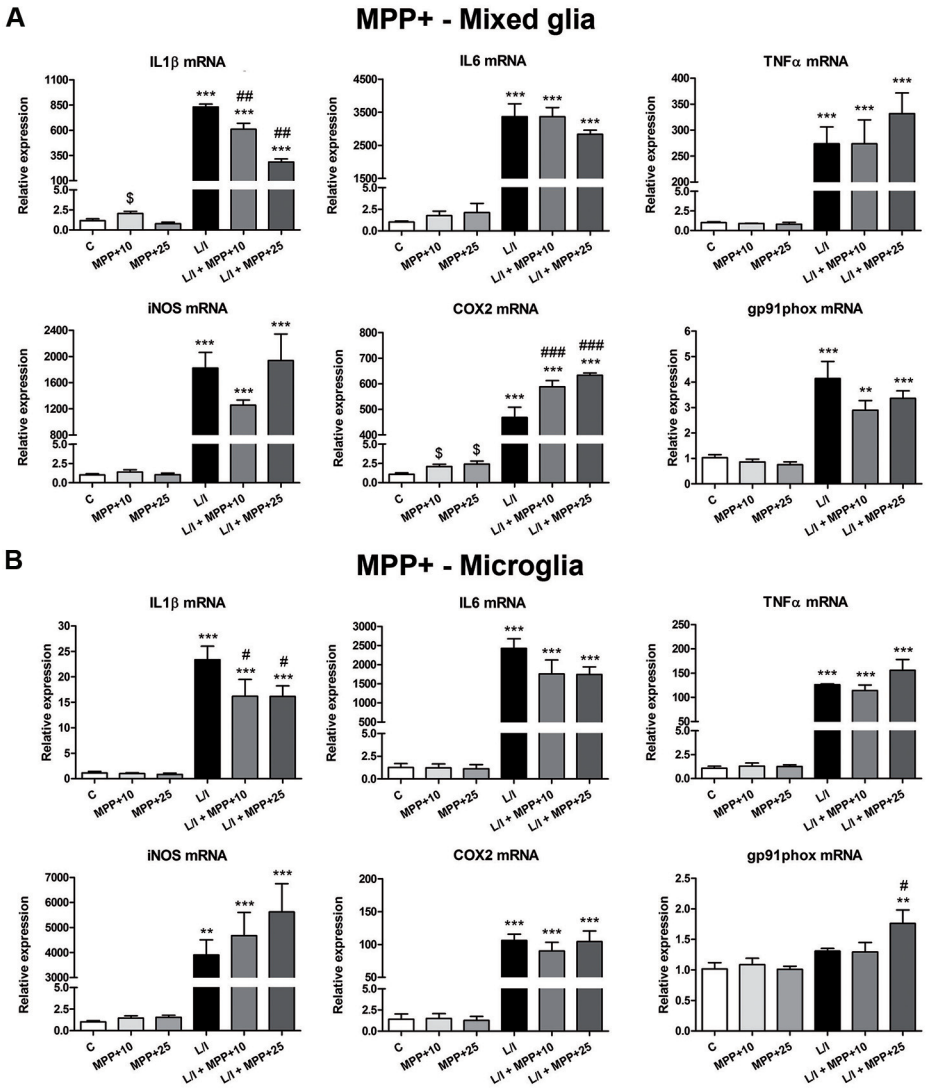

FIGURE 3 | Effect of MPP+ treatment on the mRNA expression of pro-inflammatory markers. mRNA expression of pro-inflammatory cytokines [interleukin-1β (IL-1β), IL-6 and tumor necrosis factor-α (TNF-α)] and enzymes [inducible nitric oxide synthase (iNOS), cyclooxygenase-2 (COX-2), gp91phox] in the primary mixed glial cultures **(A)** and microglial cultures **(B)** treated for 6 h with 10 and 25 μM MPP+, both in the absence and the presence of LPS/IFN-γ (L/I). 18S ribosomal RNA (Rn18s) and β-actin were used as housekeeping genes. Bars are means ± SEM of four independent experiments. $^{**}p < 0.01$ and $^{***}p < 0.001$ vs. C; $^{\#}p < 0.05$, $^{\#\#}p < 0.01$ and $^{\#\#\#}p < 0.001$ vs. L/I; one-way ANOVA and Newman-Keuls post-test. $^{\$}p < 0.05$ MPP+ alone vs. C, one-way ANOVA and Newman-Keuls post-test only considering the L/I-free groups. This latter analysis was performed to detect whether the high values observed in the L/I group may hinder the detection of statistical significance of the effects of MPP+ alone.

Metabolic Changes in LPS/IFN-γ-Treated Glial Cultures: Effect of MPP+ and Rotenone

In immune cells, the development of specific immune responses is associated with specific metabolic changes. Increased glycolysis and potentiation of the pentose phosphate pathway, together with the inhibition of oxidative phosphorylation has been reported for immune cells showing a pro-inflammatory phenotype. We checked whether this was the case in our glial cultures treated with LPS/IFN-γ and whether MPP+ and rotenone were able to modify it. We determined the mRNA expression of genes encoding critical proteins for the switch to glycolysis: glucose transporter 1 (Glut1; glucose entrance into the cell), key glycolytic enzymes such as hexokinase 1 (Hk1) (glycolysis initial rate limiting step) and phosphofructokinase 1 (PFK1) (master regulator of glycolysis), the glycolysis activator hypoxia-inducible factor 1α (Hif1α) and carbohydrate kinase-like protein (Carkl), involved in the control of the pentose phosphate pathway. In the microglial cell cultures, MPP+ and rotenone alone did not modify the expression of these genes *per se* (**Figure 8**). On the contrary, as expected, LPS/IFN-γ treatment induced an increase in their

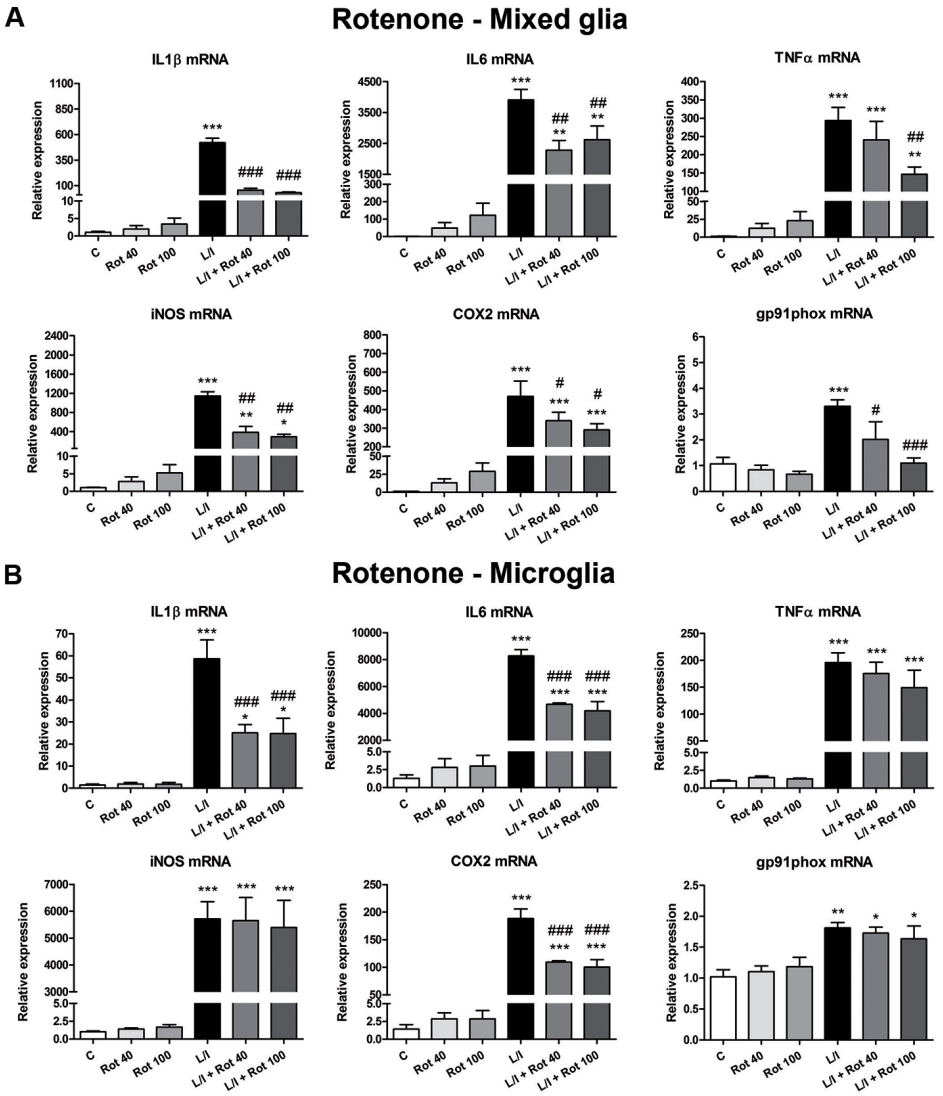

FIGURE 4 | Effect of rotenone treatment on the mRNA expression of pro-inflammatory markers. mRNA expression of pro-inflammatory cytokines (IL-1β, IL-6 and TNF-α) and enzymes (iNOS, COX-2, gp91phox) in the primary mixed glial cultures **(A)** and microglial cultures **(B)** treated for 6 h with 40 and 100 nM rotenone (Rot), both in the absence and the presence of LPS/IFN-γ (L/I). Rn18s and β-actin were used as housekeeping genes. Bars are means ± SEM of four independent experiments. $^{*}p < 0.5$, $^{**}p < 0.01$ and $^{***}p < 0.001$ vs. control (C); $^{\#}p < 0.05$, $^{\#\#}p < 0.01$ and $^{\#\#\#}p < 0.001$ vs. L/I; one-way ANOVA and Newman-Keuls post-test.

expression (**Figure 8**), with the exception of Carkl mRNA (**Figures 8I,J**), which showed a decrease. MPP+ treatment further increased LPS-IFN-γ-induced Glut1 mRNA expression (**Figure 8A**), while rotenone inhibited LPS-IFN-γ-induced Pfk1 (**Figure 8F**) and Hif1α (**Figure 8H**) mRNA expression. We also evaluated the expression of these mRNAs in the mixed glial cultures. MPP+ and rotenone alone increased the Glut1 mRNA (**Figures 9A,B**), MPP+ and Hif1α mRNA expression (**Figure 9G**). LPS/IFN-γ treatment inhibited the expression of the glycolytic genes Glut1 (**Figures 9A,B**), Hk1 (**Figures 9C,D**) and Pfk1 (**Figures 9E,F**), as well as Carkl mRNA expression (**Figures 9I,J**), and increased the expression of Hif1α (**Figures 9G,H**). Rotenone inhibited LPS/IFN-γ-induced Hif1α mRNA expression (**Figure 9H**).

DISCUSSION

In this study, we show that the response of glial cells to a pro-inflammatory stimulus is modified by the neurotoxic agents MPP+ and rotenone. MPP+ and rotenone treatment did not induce a significant pro-inflammatory phenotype in the primary mixed glial and microglial cultures *per se*. However, these neurotoxic agents, mainly rotenone, did impair the development of a pro-inflammatory phenotype in the LPS/IFN-γ-treated glial cultures. This effect was observed in the absence of significant cell death but in the presence of impaired metabolic activity.

The toxic effects of MPP+ and rotenone on neurons have repeatedly been demonstrated using primary neuronal cultures, with dopaminergic neurons showing the highest sensitivity to

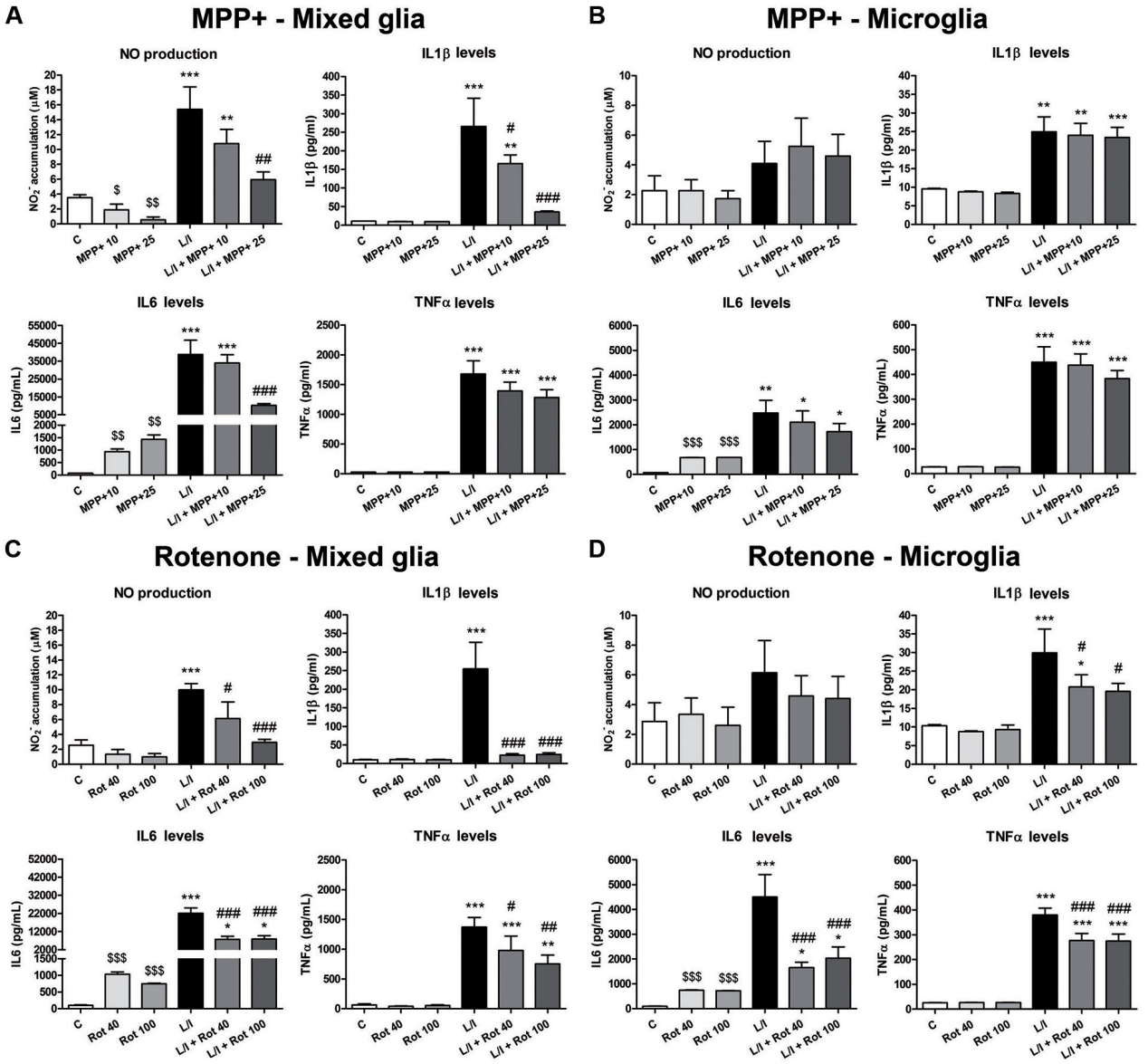

FIGURE 5 | Nitric oxide (NO) and pro-inflammatory cytokine production in the primary glial cell cultures treated with MPP+ and rotenone. NO production was estimated from nitrite accumulation and IL1β, IL6 and TNFα levels were determined by ELISA in the culture medium of the MPP+-treated mixed glial **(A)** and microglial **(B)** cultures, and the rotenone (Rot)-treated mixed glial **(C)** and microglial **(D)** cultures. The cell cultures were treated with 10 and 25 μM MPP+ or 40 and 100 nM Rot for 24 h, in the absence or in the presence of LPS/IFN-γ (L/I). Bars are means ± SEM of four independent experiments. $^{*}p < 0.5$, $^{**}p < 0.01$ and $^{***}p < 0.001$ vs. control (C); $^{\#}p < 0.05$, $^{\#\#}p < 0.01$ and $^{\#\#\#}p < 0.001$ vs. L/I; one-way ANOVA and Newman-Keuls post-test. $^{\$}p < 0.05$, $^{\$\$}p < 0.01$ and $^{\$\$\$}p < 0.001$ MPP+ and Rot alone vs. C, one-way ANOVA and Newman-Keuls post-test only considering the L/I-free groups. This latter analysis was performed to detect whether the high values observed in the L/I group may hinder the detection of a statistical significance of the effects of MPP+ and Rot alone.

the toxic effects of these compounds. In mouse primary cultures, dopaminergic neuron death is observed at concentrations from 0.1 μM MPP+ (1-week exposure; Kinugawa et al., 2013) or 3 μM MPP+ (48 h exposure; Henze et al., 2005), and 10 nM (1-week exposure; Gao et al., 2003) or 5 nM rotenone (48 h exposure; Radad et al., 2006). Exposure to higher concentrations of these neurotoxins is necessary to induce the death of non-dopaminergic neurons (Gao et al., 2003; Henze et al., 2005). The presence of microglial cells in neuronal cultures has been associated to the increased neurotoxicity of MPP+ and rotenone (Gao et al., 2002, 2003; Emmrich et al., 2013; Kinugawa et al., 2013). However, as MPP+- and rotenone-damaged neurons induce reactive microgliosis, which has a neurotoxic effect, it is difficult to establish the contribution of a direct effect of the toxins on glial cells in the neurotoxicity observed. In fact, although the neurotoxic effect of MPP+ and rotenone has been widely described using *in vivo* and *in vitro* experimental approaches, their direct effects on glial cells remain

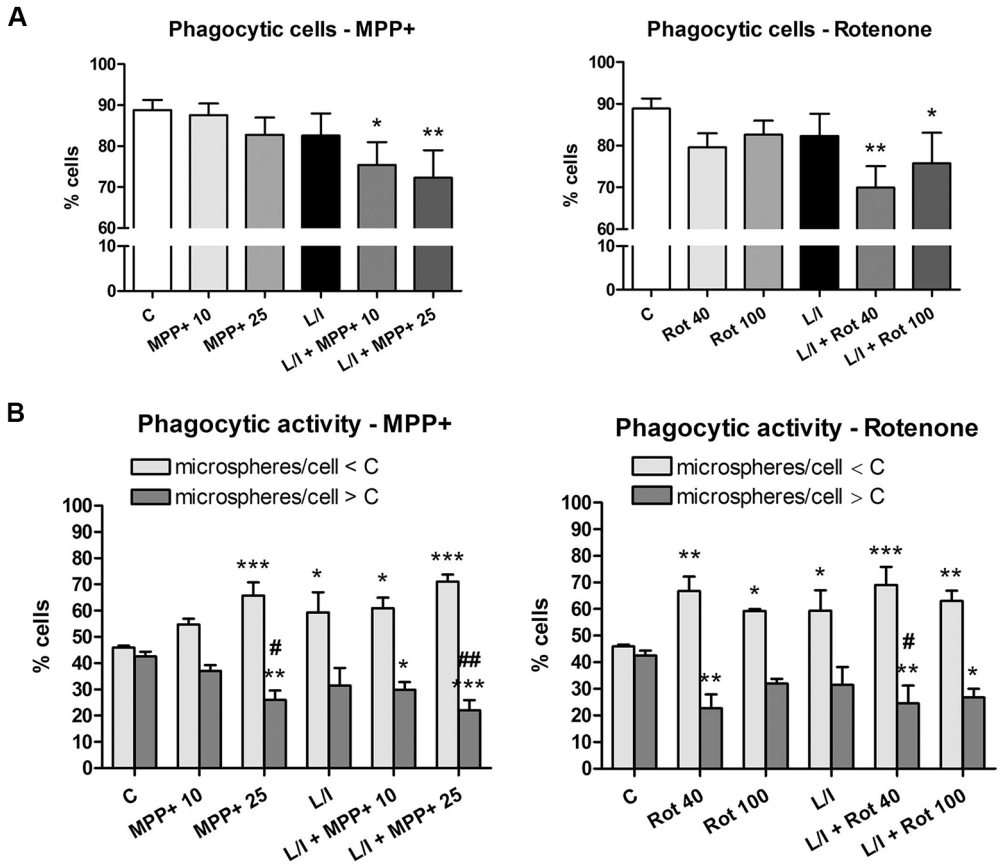

FIGURE 6 | Effect of MPP+ and rotenone treatment on the microglial cell phagocytosis in the primary microglial cell cultures. Phagocytic activity was evaluated through the ingestion of fluorescent microspheres after treating the cell cultures with 10 and 25 μM MPP+ or 40 and 100 nM rotenone (Rot) for 24 h, in both the absence and presence of LPS/IFN-γ (L/I). Internalization of microspheres was quantified after immunofluorescence labeling of the microglial cells using an anti-Iba1 antibody. **(A)** Percentage of cells with microspheres. Bars are means ± SEM of four independent experiments. $^{*}p < 0.05$ and $^{**}p < 0.01$ vs. control (C); one-way ANOVA and Newman-Keuls post-test. **(B)** Percentage of cells with low phagocytic activity (number of microspheres/cell < C) and cells with high phagocytic activity (number of microspheres/cells > C). Bars are means ± SEM of four independent experiments. $^{*}p < 0.05$, $^{**}p < 0.01$ and $^{***}p < 0.001$ vs. corresponding C; $^{\#}p < 0.05$ and $^{\#\#}p < 0.01$ vs. low-phagocytic cells; two-way ANOVA and Bonferroni post-test.

poorly characterized (Gao et al., 2003; Klintworth et al., 2009; Bournival et al., 2012; Du et al., 2014; Chen et al., 2015; Zhou et al., 2016). Most of the studies performed until now using glial cell cultures have tested whether these neurotoxins induce a pro-inflammatory phenotype in the microglial cells, and the results obtained are controversial. The range of concentrations used in these studies are higher than that used in neuronal cultures (0.1–500 μM MPP+ and 10 nM-1 μM rotenone; Gao et al., 2003; Henze et al., 2005; Klintworth et al., 2009; Bournival et al., 2012; Jin et al., 2012; Du et al., 2014). Some authors have reported no alterations (Klintworth et al., 2009; Ferger et al., 2010; Jin et al., 2012), but others have shown the induction of pro-inflammatory markers in the MPP+- and rotenone-treated microglial cultures (Du et al., 2014; Zhang et al., 2014; Liang et al., 2015; Zhou et al., 2016). Differences in the pattern of neurotoxin treatment (concentration and duration of the treatment) and the cell types used (primary cultures and cell lines from different species) may partially account for the differences observed. Most studies have considered microglial cell lines, while studies using primary microglial cultures are scarce. In this study, we show that concentrations of MPP+ and rotenone that did not affect cell viability in primary glial cultures at 24 h did not result in the induction of a significant pro-inflammatory phenotype (with the exception of IL6 production), but they interfered with the development of the pro-inflammatory phenotype induced by LPS/IFN-γ. Thus, MPP+ and rotenone inhibited pro-inflammatory cytokine production induced by LPS/IFN-γ in glial cells (IL1β in the case of MPP+, and also IL6 and TNFα in the case of rotenone). They also modified the expression of pro-inflammatory enzymes (iNOS, COX2 and/or gp91phox). In general, the alterations observed were more pronounced in the mixed glia than in the microglial cell cultures. In addition, the effect of rotenone was stronger than that of MPP+, although the concentrations of rotenone used were three orders of magnitude below those of MPP+. MPP+ and rotenone treatment also interfered in the phagocytic activity of the microglial cells, which was clearly inhibited after neurotoxin treatment, especially in the presence of LPS/IFN-γ. Altogether, these results suggest

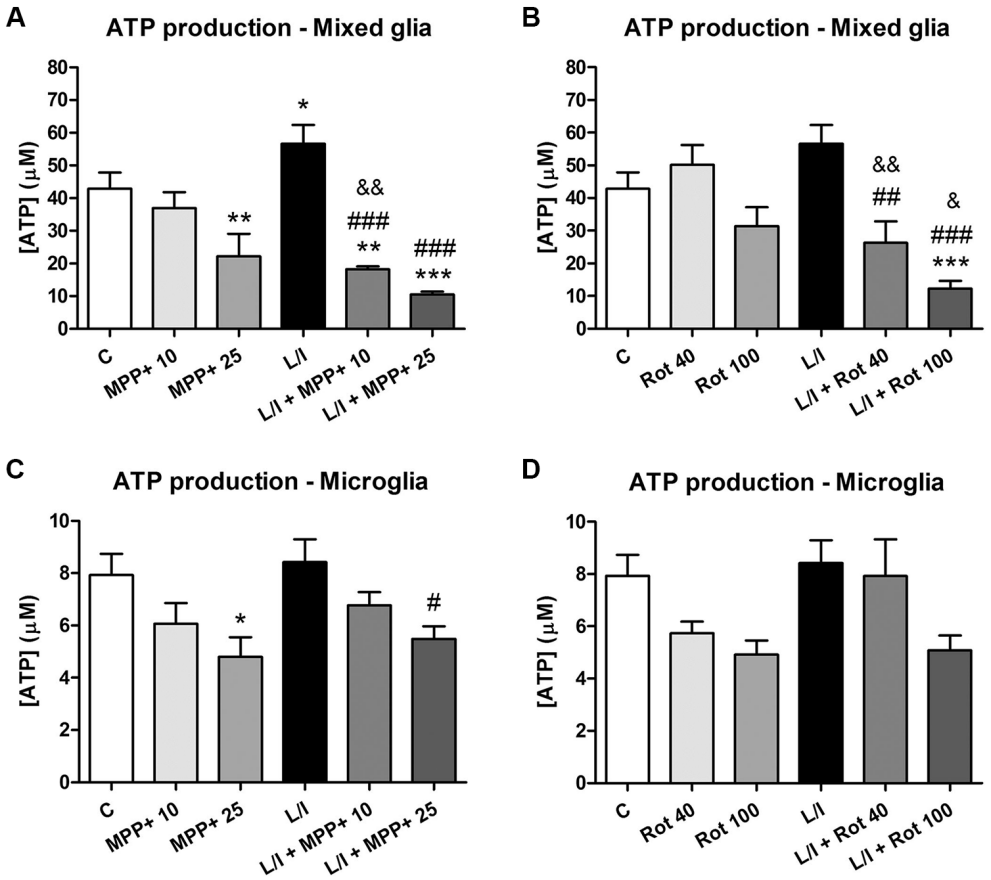

FIGURE 7 | Adenosine triphosphate (ATP) production in the primary glial cell cultures treated with MPP+ and rotenone. Intracellular ATP production was determined in the mixed glial cultures and microglial cultures treated with 10 and 25 μM MPP+ **(A,B)** or 40 and 100 nM rotenone (Rot; **C,D**) for 24 h, in the absence and in the presence of LPS/IFN-γ (L/I). Bars are means ± SEM of five independent experiments. $^{*}p < 0.5$, $^{**}p < 0.01$ and $^{***}p < 0.001$ vs. control **(C)**; $^{\#}p < 0.05$, $^{\#\#}p < 0.01$ and $^{\#\#\#}p < 0.001$ vs. L/I; $^{\&}p < 0.05$ and $^{\&\&}p < 0.01$ vs. MPP+ or Rot alone; one-way ANOVA and Newman-Keuls post-test.

that MPP+ and rotenone directly impair the ability of the glial cells to respond to a pro-inflammatory insult. In this sense, exposure to stimuli that affect the mitochondrial activity, such as hypoxia or respiratory chain inhibitors, has been suggested to alter the immune response of macrophages (Wiese et al., 2012).

At the cellular level, the main target of both MPP+ and rotenone is the mitochondrial electron transport chain, where they selectively inhibit complex I (Dauer and Przedborski, 2003). As a consequence, ATP production is compromised, O_2^- levels increase, and subsequent oxidative stress occurs. This is critical in neuronal cells, where energy production depends mainly on ATP synthesis through oxidative phosphorylation (reviewed in Bélanger et al., 2011). In contrast, astrocytes are mainly glycolytic (reviewed in Bélanger et al., 2011). In addition, astrocytes can generate lactate from glycogen *via* glycolysis under metabolic activation (Hertz et al., 2007). Macrophages/microglia have the capacity to generate ATP by both glycolytic and oxidative pathways (although in the case of microglial cells the field is still underexplored; Van den Bossche et al., 2017; Ghosh et al., 2018). Indeed, they are able to shift from oxidative phosphorylation to aerobic glycolysis (production of lactate in the presence of oxygen) to obtain ATP from different pathways according to the metabolic demands of their activation status (Haschemi et al., 2012; Galván-Peña and O'Neill, 2014; Orihuela et al., 2016). The classical activation or M1/pro-inflammatory phenotype is associated with inhibition of the respiratory chain and the potentiation of aerobic glycolysis, which results in more rapid ATP production to satisfy the metabolic demands associated with the quick pro-inflammatory response of the M1 phenotype. In this situation, the glycolytic and pentose phosphate pathways are potentiated, and oxidative phosphorylation is inhibited (Haschemi et al., 2012). A metabolic-epigenetic crosstalk is suggested to control macrophage activation (Baardman et al., 2015). In contrast, pro-inflammatory stimuli increase tricarboxylic acid activity in astrocytes (Gavillet et al., 2008). In mixed glial cultures, LPS/IFN-γ treatment increased ATP production, an effect that was clearly inhibited by MPP+ and rotenone. These results suggest that MPP+- and rotenone-treated cultures suffer metabolic stress that is aggravated when the cells increase their energetic demands after LPS/IFN-γ treatment. Consequently, activated glial cells may not fulfill their

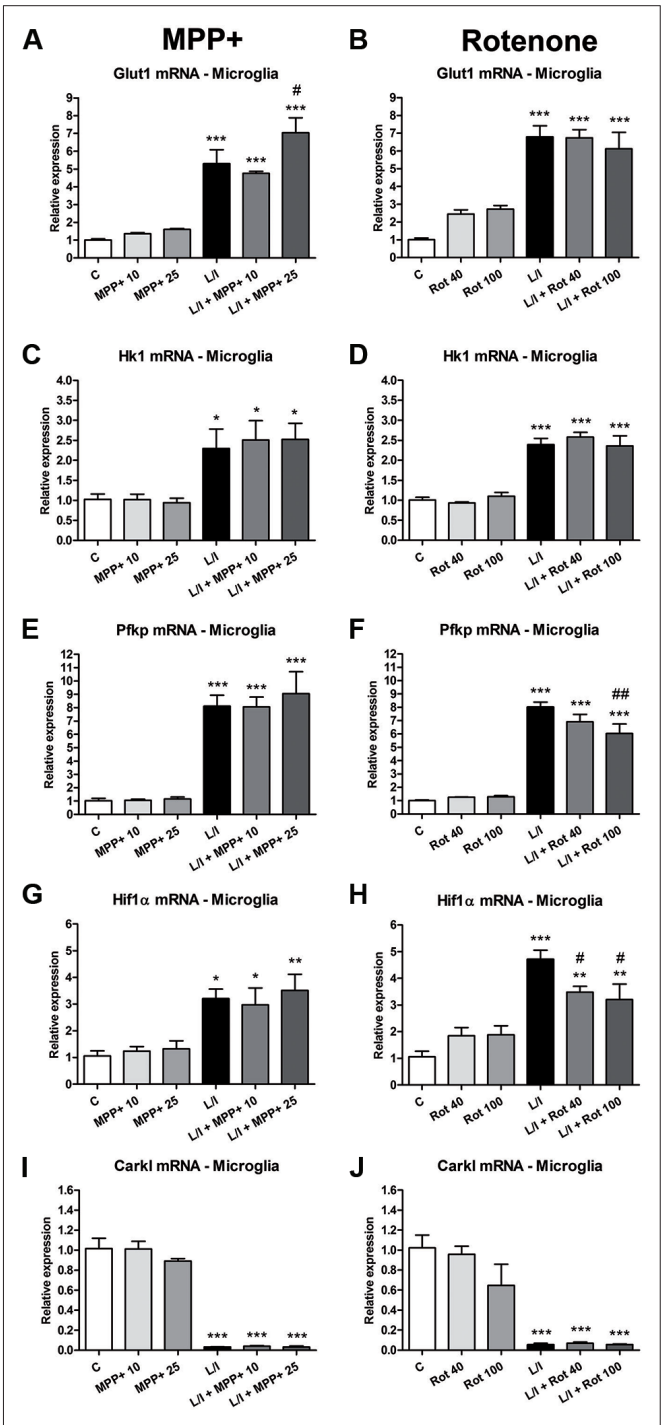

FIGURE 8 | Effect of MPP+ and rotenone treatment on the expression of genes involved in the control of the glycolysis in the microglial cell cultures. mRNA expression of the glucose transporter (Glut1; **A,B**) and the glycolytic enzymes hexokinase 1 (Hk1; **C,D**) and phosphofructokinase 1 (Pfk1; **E,F**), as well as Hif1α **(G,H)** and carbohydrate kinase-like protein 1 (Carkl; **I,J**). The primary microglial cultures were treated for 6 h with 10 and 25 μM MPP+ or 40 and 100 nM rotenone (Rot), both in the absence and the presence of LPS/IFN-γ (L/I). Rn18s and β-actin were used as housekeeping genes. Bars are means ± SEM of four independent experiments. $^{*}p < 0.05$, $^{**}p < 0.01$ and $^{***}p < 0.001$ vs. control (C); $^{\#}p < 0.05$ and $^{\#\#}p < 0.01$ vs. L/I; one-way ANOVA and Newman-Keuls post-test.

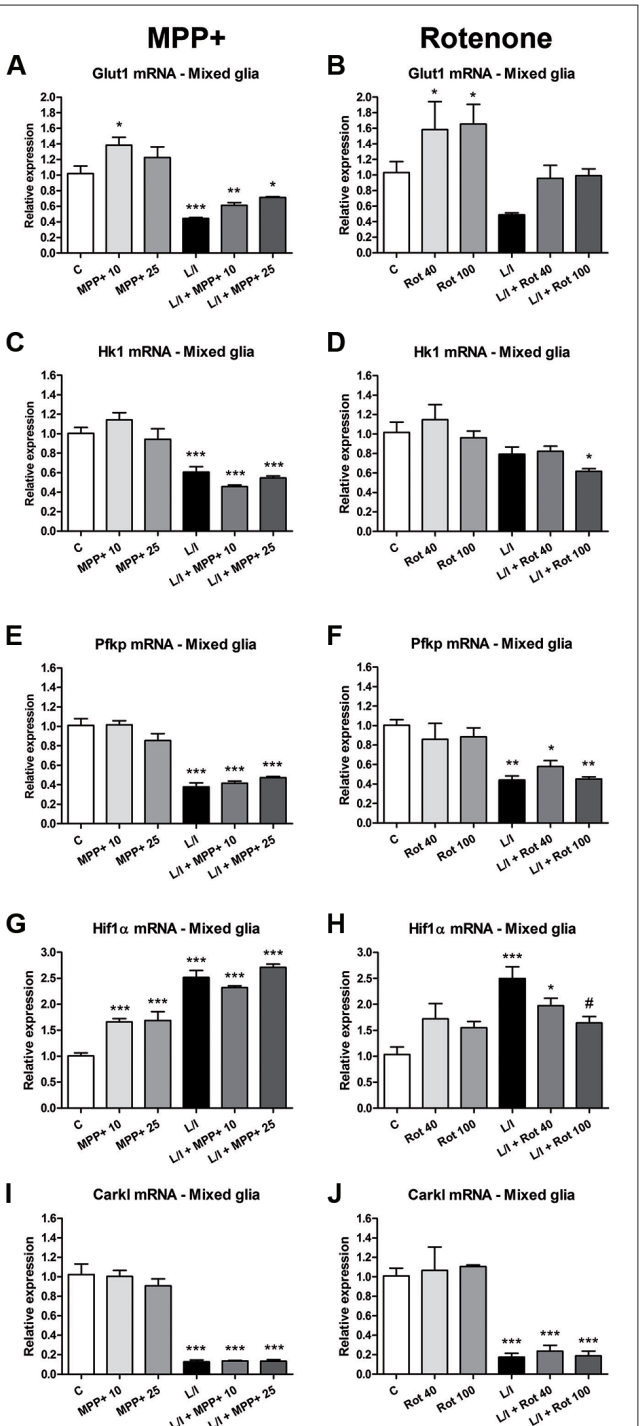

FIGURE 9 | Effect of MPP+ and rotenone treatment on the expression of genes involved in the control of glycolysis in the mixed glial cell cultures. mRNA expression of the glucose transporter Glut1 **(A,B)** and the glycolytic enzymes Hk1 **(C,D)** and Pfk1 **(E,F)**, as well as Hif1α **(G,H)** and Carkl **(I,J)**. The primary mixed glial cultures were treated for 6 h with 10 and 25 μM MPP+ or 40 and 100 nM rotenone (Rot), both in the absence and the presence of LPS/IFN-γ (L/I). Rn18s and β-actin were used as housekeeping genes. Bars are means ± SEM of four independent experiments. $^{*}p < 0.05$, $^{**}p < 0.01$ and $^{***}p < 0.001$ vs. control (C); $^{\#}p < 0.05$ vs. L/I; one-way ANOVA and Newman-Keuls post-test.

metabolic demands in the presence of MPP+ and rotenone, which would explain why mixed glial cultures exposed to these toxicants were not able to produce an appropriate pro-inflammatory response to LPS/IFN-γ. The effects of MPP+ and rotenone on ATP production were less drastic in the LPS-IFN-γ-treated microglial than the mixed glial cultures. ATP production was not significantly compromised in the LPS/IFN-γ-treated microglial cultures exposed to MPP+ and rotenone, with the exception of 25 μM MPP+ treatment. In addition, the response to LPS/IFN-γ was also impaired, to a lesser extent, in the microglial cultures than in the mixed glial cultures. Altogether, these results suggest that the microglial cells can better cope with the metabolic alterations induced by MPP+ and rotenone than astrocytes can, which accounts for 75% of the cells in the mixed glial cultures. A possible explanation is that while microglial cells developing a pro-inflammatory phenotype switch to glycolysis (Haschemi et al., 2012; Galván-Peña and O'Neill, 2014; Orihuela et al., 2016), astrocytes exposed to pro-inflammatory stimuli increase the activity of the tricarboxylic acid cycle (Gavillet et al., 2008), which in the presence of MPP+ and rotenone will encounter truncated oxidative phosphorylation. However, the involvement of a differential response of the activated microglial cells to the toxins in the presence of astrocytes (or impaired astrocytes) cannot be ruled out.

To assess whether the glycolytic switch mentioned above was behind the ATP production in activated glial cultures, we evaluated the expression of genes encoding critical proteins for the glycolytic pathway. In the microglial cultures, a switch to the glycolytic pathway in the LPS/IFN-γ-activated microglial cultures was suggested by the observed increase in the expression of Glut1, HK1, Pfk1 and Hif1α mRNA and the decreased expression of the Carkl mRNA. Increased expression of the glucose transporter Glut1 may result in more glucose uptake, while the increased expression of Hk1 and Pfk1, which regulate critical steps in glycolysis, may increase the glycolytic rate. It has been suggested that Hif activation contributes to macrophage polarization, and that Hifα-dependent glycolysis favors polarization to a M1 phenotype (Palazon et al., 2016; Taylor et al., 2016). In addition, metabolic intermediates such as succinate play a role in Hif1α stabilization and subsequent IL1β expression in LPS-treated macrophages (Tannahill et al., 2013). Inhibition of the Carkl expression potentiates the flux through the pentose phosphate pathway (Haschemi et al., 2012). Whereas MPP+ exposure resulted in a further increase in Glut1 expression in the LPS/IFN-γ-treated microglial cultures, rotenone exposure partially inhibited the LPS/IFN-γ-induced Pfk and Hifα mRNA expression. Consequently, in the case of microglial cultures, the attenuated pro-inflammatory response to LPS-IFN-γ mostly observed in the presence of rotenone may result from some alterations to the glycolytic switch. In addition, it cannot be ruled out that ATP production through oxidative phosphorylation may also partially contribute to the energy demand required to develop a pro-inflammatory response, even in situations where the switch to glycolysis occurs. In this sense, Wang et al. (2018) showed that 2-deoxyglucose, which blocks glycolysis and partially inhibits glycolytic-dependent oxidative phosphorylation, has a stronger inhibitory effect on the IFN-γ-induced inflammatory response in macrophages than inhibiting glycolysis when replacing glucose in the cell culture medium with galactose, which reduces glycolytic flux without interfering with oxidative phosphorylation. Interestingly, control of the pro-inflammatory macrophage response, through metabolic reprogramming, has been suggested as a potential therapeutic strategy to promote remission in chronic inflammatory diseases (Mills and O'Neill, 2016).

We observed contrasting effects in the LPS/IFN-γ-treated mixed glia and microglial cultures in terms of the mRNA expression of the glycolytic enzymes Glut1, Hk1, and Pfk1. Their expression was inhibited in the mixed glia, suggesting the contribution of astrocytes to the effects observed. Although astrocytes are mainly glycolytic (Bélanger et al., 2011), pro-inflammatory stimuli increase tricarboxylic acid activity in astrocytes (Gavillet et al., 2008). The decreased expression of the glycolytic enzymes we observed may reflect this switch. Consequently, the impaired response of the mixed glial cultures to LPS/IFN-γ in the presence of MPP+ and rotenone may be explained by the fact that oxidative phosphorylation, which would be responsible for the main ATP production from products of the tricarboxylic acid cycle, is inhibited by MPP+ and rotenone. However, the involvement of the microglial cells in the response of the mixed glial cultures to MPP+ and rotenone plus LPS/IFN-γ cannot be ruled out.

Finally, some studies show that MPP+ causes DNA damage (Zhang et al., 1995) and oxidative DNA damage in neuronal cells (Chen et al., 2005). In addition, rotenone-induced DNA damage (Goswami et al., 2016) and DNA methylation (Scola et al., 2014) in neurons have also been described. Although there are no reports on MPP+- and rotenone-induced DNA alterations on glial cells, we cannot discard that these alterations may be behind the decreased expression of inflammatory markers we detected in LPS/IFN-γ–treated glial cultures exposed to the neurotoxins.

CONCLUSION

In summary, the results of the present study show that the pro-inflammatory response induced by LPS/IFN-γ in mouse primary glial cell cultures, is impaired under MPP+ and rotenone exposure, mainly when both the astrocytes and microglia are present. This suggests that the immune response of the glial cells is compromised in the presence of neurotoxins that inhibit the mitochondrial electron transport chain. We are currently studying the possible effects of MPP+ and rotenone on the development of an anti-inflammatory phenotype by the glial cells. Although the involvement of the glial cells in the development of neurodegenerative diseases is widely accepted, the precise role they play in every neurodegenerative disorder remains to be established. As many genetic and environmental factors are probably involved in the etiopathogenesis of neurodegenerative diseases, many factors may also determine when and how the glial cells take part in the pathological process. In the case of pathologies where the exposure to certain neurotoxicants is a risk factor, such as PD, the direct effect of the toxic agents on glial cell function may be

an additional factor to take into account, as alterations in glial function will have an effect on neuronal function and CNS homeostasis. In this context, our results suggest that glial metabolic alterations induced by neurotoxin exposure compromises the brain's immune response. This impaired immune response may imply a more vulnerable brain, which can be a further aspect contributing to the development of PD.

DATA AVAILABILITY

All data generated or analyzed during this study are included in this published article.

AUTHOR CONTRIBUTIONS

NR-L and EX-E performed most of the experiments and analyzed the data. JSe participated in the processing of the samples and quantified the phagocytosis assay. JSa provided critical guidance and contributed to the final version of the manuscript. CS conceived and coordinated the experiments, provided guidance in the production of data and drafted the manuscript. All authors provided input and ideas throughout the process, and critically revised and approved the final manuscript.

FUNDING

NR-L was recipient of an FPU grant (FPU13/05491) from the Spanish *Ministerio de Educación, Cultura y Deporte*. This study was supported by grants PI14/00302 and PI15/00033 from the *Instituto de Salud Carlos III* (Spain) with joint financing by FEDER funds from the European Union.

ACKNOWLEDGMENTS

We thank Lucas Blasco and Andrés Jurado for their technical assistance. We acknowledge support for the publication fee, by the CSIC Open Access Publication Support Initiative through its Unit of Information Resources for Research (URICI).

REFERENCES

Baardman, J., Licht, I., de Winther, M. P. J., and Van den Bossche, J. (2015). Metabolic-epigenetic crosstalk in macrophage activation. *Epigenomics* 7, 1155–1164. doi: 10.2217/epi.15.71

Bélanger, M., Allaman, I., and Magistretti, P. J. (2011). Brain energy metabolism: focus on astrocyte-neuron metabolic cooperation. *Cell Metab.* 14, 724–738. doi: 10.1016/j.cmet.2011.08.016

Bournival, J., Plouffe, M., Renaud, J., Provencher, C., and Martolini, M. G. (2012). Quercetin and sesamin protect dopaminergic cells from MPP^+-induced neuroinflammation in a microglial (N9)-neuronal (PC12) coculture system. *Oxid. Med. Cell Longev.* 2012:921941. doi: 10.1155/2012/921941

Bové, J., and Perier, C. (2012). Neurotoxin-based models of Parkinson's disease. *Neuroscience* 211, 51–76. doi: 10.1016/j.neuroscience.2011.10.057

Chen, L. J., Gao, Y. Q., Li, X. J., Shen, D. H., and Sun, F. J. (2005). Melatonin protects against MPTP/MPP^+-induced mitochondrial DNA oxidative damage *in vivo* and *in vitro*. *J. Pineal Res.* 39, 34–42. doi: 10.1111/j.1600-079X.2005.00209.x

Chen, T., Hou, R., Xu, S., and Wu, C. (2015). Donepezil regulates 1-methyl-4-phenylpyridinium-induced microglial polarization in Parkinson's disease. *ACS Chem. Neurosci.* 6, 1708–1714. doi: 10.1021/acschemneuro.5b00026

Colonna, M., and Butovsky, O. (2017). Microglia function in the central nervous system during health and neurodegeneration. *Annu. Rev. Immunol.* 35, 441–468. doi: 10.1146/annurev-immunol-051116-052358

Dauer, W., and Przedborski, S. (2003). Parkinson's disease: mechanisms and models. *Neuron* 39, 889–909. doi: 10.1016/S0896-6273(03)00568-3

Dentesano, G., Serratosa, J., Tusell, J. M., Ramón, P., Valente, T., Saura, J., et al. (2014). CD200R1 and CD200 expression are regulated by PPAR-γ in activated glial cells. *Glia* 62, 982–998. doi: 10.1002/glia.22656

Du, C., Jin, M., Hong, Y., Li, Q., Wang, X. H., Xu, J. M., et al. (2014). Downregulation of cystathione β-synthase/hydrogen sulfide contributes to rotenone-induced microglia polarization toward M1 type. *Biochem. Biophys. Res. Commun.* 451, 239–245. doi: 10.1016/j.bbrc.2014.07.107

Emmrich, J. V., Hornik, T. C., Neher, J. J., and Brown, G. C. (2013). Rotenone induces neuronal death by microglial phagocytosis of neurons. *FEBS J.* 280, 5030–5038. doi: 10.1111/febs.12401

Ferger, A. I., Campanelli, L., Reimer, V., Muth, K. N., Merdian, I., Ludolph, A. C., et al. (2010). Effects of mitochondrial dysfunction on the immunological properties of microglia. *J Neuroinflammation* 7:45. doi: 10.1186/1742-2094-7-45

Galván-Peña, S., and O'Neill, L.A.J. (2014). Metabolic reprograming in macrophage polarization. *Front. Immunol.* 5:420. doi: 10.3389/fimmu.2014.00420

Gao, F., Chen, D., Hu, Q., and Wang, G. (2013). Rotenone directly induces BV2 cell activation via the p38 MAPK pathway. *PLos One* 8:e722046. doi: 10.1371/journal.pone.0072046

Gao, H.-M., Hong, J.-S., Zhang, W., and Liu, B. (2002). Distinct role for microglia in rotenone-induced degeneration of dopaminergic neurons. *J. Neurosci.* 22, 782–790. doi: 10.1523/JNEUROSCI.22-03-00782.2002

Gao, H.-M., Liu, B., Zhang, W., and Hong, J.-S. (2003). Critical role of microglial NADPH oxidase-derived free radicals in the *in vitro* MPTP model of Parkinson's disease. *FASEB J.* 17, 1954–1956. doi: 10.1096/fj.03-0109fje

Gavillet, M., Allaman, I., and Magistretti, P. J. (2008). Modulation of astrocytic metabolic phenotype by proinflammatory cytokines. *Glia* 56, 975–989. doi: 10.1002/glia.20671

Ghosh, S., Castillo, E., Frias, E. S., and Swanson, R. A. (2018). Bioenergetic regulation of microglia. *Glia* 66, 1200–1212. doi: 10.1002/glia.23271

Goldman, S. M. (2013). Environmental toxins and Parkinson's disease. *Annu. Rev. Pharmacol. Toxicol.* 54, 141–164. doi: 10.1146/annurev-pharmtox-011613-135937

Goswami, P., Gupta, S., Biswas, J., Joshi, N., Swarnkar, S., Nath, C., et al. (2016). Endoplasmic reticulum stress plays a key role in rotenone-induced apoptotic death of neurons. *Mol. Neurobiol.* 53, 285–298. doi: 10.1007/s12035-014-9001-5

Gresa-Arribas, N., Serratosa, J., Saura, J., and Solà, C. (2010). Inhibition of CCAAT/enhancer binding protein δ expression by chrysin in microglial cells results in anti-inflammatory and neuroprotective effects. *J. Neurochem.* 115, 526–536. doi: 10.1111/j.1471-4159.2010.06952.x

Haschemi, A., Kosma, P., Gille, L., Evans, C. R., Burant, C. F., Starkl, P., et al. (2012). The sedoheptulose kinase CARKL directs macrophage polarization through control of glucose metabolism. *Cell Metab.* 15, 813–826. doi: 10.1016/j.cmet.2012.04.023

Henze, C., Hartmann, A., Lescot, T., Hirsch, E. C., and Michel, P. P. (2005). Proliferation of microglial cells induced by 1-methyl-4-phenylpyridinium in mesencephalic cultures results from an astrocyte-dependent mechanism: role of granulocyte macrophage colony-stimulating factor. *J. Neurochem.* 95, 1069–1077. doi: 10.1111/j.1471-4159.2005.03416.x

Hertz, L., Peng, L., and Dienel, G. A. (2007). Energy metabolism in astrocytes: high rate of oxidative metabolism and spatiotemporal dependence on glycolysis/glycogenolysis. *J. Cereb. Blood Flow Metab.* 27, 219–249. doi: 10.1038/sj.jcbfm.9600343

Jin, M., Kim, B. W., Koppula, S., Kim, I. S., Park, J. H., Kumar, H., et al. (2012). Molecular effects of activated BV-2 microglia by mitochondrial toxin 1-methyl-4-phenylpyridinium. *Neurotoxicology* 33, 147–155. doi: 10.1016/j.neuro.2011.12.019

Kamel, F. (2013). Paths from pesticides to Parkinson's. *Science* 341, 722–723. doi: 10.1126/science.1243619

Kinugawa, K., Monnet, Y., Béchade, C., Alvarez-Fisher, D., Hirsch, E., Bessis, A., et al. (2013). DAP12 and CD11b contribute to the microglial-induced death of dopaminergic neurons *in vitro* but not *in vivo* in the MPTP mouse model of Parkinson's disease. *J. Neuroinflammation* 10:82. doi: 10.1186/1742-2094-10-82

Klintworth, H., Garden, G., and Xia, Z. (2009). Rotenone and paraquat do not directly activate microglia or induce inflammatory cytokine release. *Neurosci. Lett.* 462, 1–5. doi: 10.1002/jcp.27938

Langston, J. W., Ballard, P. A., Tetrud, J. W., and Irwin, I. (1983). Chronic parkinsonism in humans due to a product of meperidine-analog synthesis. *Science* 219, 979–980. doi: 10.1126/science.6823561

Liang, Y., Jing, X., Zeng, Z., Bi, W., Chen, Y., Wu, X., et al. (2015). Rifampicin attenuates rotenone-induced inflammation via suppressing NLRP3 inflammasome activation in microglia. *Brain Res.* 1622, 43–50. doi: 10.1016/j.brainres.2015.06.008

Livak, K. J., and Schmittgen, T. D. (2001). Analysis of relative gene expression data using real-time quantitative PCR and the $2^{-\Delta\Delta CT}$ method. *Methods* 25, 402–408. doi: 10.1006/meth.2001.1262

Mills, E. L., and O'Neill, L. A. (2016). Reprogramming mitochondrial metabolism in macrophages as an anti-inflammatory signal. *Eur. J. Immunol.* 46, 13–21. doi: 10.1002/eji.201445427

Mostafalou, S., and Abdollahi, M. (2013). Pesticides and human chronic diseases: evidences, mechanisms, and perspectives. *Toxicol. Appl. Pharmacol.* 268, 157–177. doi: 10.1016/j.taap.2013.01.025

Orihuela, R., McPherson, C. A., and Harry, G. J. (2016). Microglial M1/M2 polarization and metabolic states. *Br. J. Pharmacol.* 173, 649–665. doi: 10.1111/bph.13139

Palazon, A., Goldrath, A. W., Nizet, V., and Johnson, R. S. (2016). HIF transcription factors, inflammation, and immunity. *Immunity* 41, 518–528. doi: 10.1016/j.immuni.2014.09.008

Perry, V. H., Nicoll, J. A. R., and Clive, H. (2010). Microglia in neurodegenerative disease. *Nature Rev.* 6, 193–201. doi: 10.1038/nrneurol.2010.17

Radad, K., Rausch, W. D., and Gille, G. (2006). Rotenone induces cell death in primary dopaminergic culture by increasing ROS production and inhibiting mitochondrial respiration. *Neurochem. Int.* 49, 379–386. doi: 10.1016/j.neuint.2006.02.003

Salter, M. W., and Stevens, B. (2017). Microglia emerge as central players in brain disease. *Nat. Med.* 9, 1018–1027. doi: 10.1038/nm.4397

Saura, J., Tusell, J. M., and Serratosa, J. (2003). High-yield isolation of murine microglia by mild trypsinization. *Glia* 44, 183–189. doi: 10.1002/glia.10274

Scola, G., Kim, H. K., Young, L. T., Salvador, M., and Andreazza, A. C. (2014). Lithium reduces the effects of rotenone-induced complex I dysfunction on DNA methylation and hydroxymethylation in rat cortical primary neurons. *Psychopharmacology* 231, 4189–4198. doi: 10.1007/s00213-014-3565-7

Tannahill, G. M., Curtis, A. M., Adamik, J., Palsson-McDermott, E. M., McGettrick, A. F., Goel, G., et al. (2013). Succinate is an inflammatory signal that induces IL-1β through HIF-1α. *Nature* 496, 238–242. doi: 10.1038/nature11986

Tanner, C. M., Kamel, F., Ross, G. W., Hoppin, J. A., Goldman, S. M., Korell, M., et al. (2011). Rotenone, Paraquat, and Parkinson's disease. *Environm. Health Perspect.* 6, 866–872. doi: 10.1289/ehp.1002839

Taylor, C. T., Doherty, G., Fallon, P. G., and Cummins, E. P. (2016). Hypoxia-dependent regulation of inflammatory pathways in immune cells. *J. Clin. Invest.* 126, 3716–3724. doi: 10.1172/JCI84433

Van den Bossche, J., O'Neill, L. A., and Menon, D. (2017). Macrophage immunometabolism: where are we (going)? *Trends Immunol.* 38, 395–406. doi: 10.1016/j.it.2017.03.001

Wang, F., Zhang, S., Jeon, R., Vuckovic, I., Jiang, X., Lerman, A., et al. (2018). Interferon gamma induces reversible metabolic reprogramming of M1 macrophages to sustain cell viability and pro-inflammatory activity. *EBioMedicine* 30, 303–316. doi: 10.1016/j.ebiom.2018.02.009

Wiese, M., Gerlach, R. G., Popp, I., Matuszak, J., Mahapatro, M., Castiglione, K., et al. (2012). Hypoxia-mediated impairment of the mitochondrial respiratory chain inhibits the bactericidal activity of macrophages. *Infect. Immun.* 80, 1455–1466. doi: 10.1128/IAI.05972-11

Yuan, Y., Sun, J., Wu, M., Hu, J., Peng, S., and Chen, N. (2013). Rotenone could activate microglia through NFκB associated pathway. *Neurochem. Res.* 38, 1553–1560. doi: 10.1007/s11064-013-1055-7

Zhang, J., Pieper, A., and Snyder, S. H. (1995). Poly(ADP-ribose) synthetase activation: an early indicator of neurotoxic DNA damage. *J. Neurochem.* 65, 1411–1414. doi: 10.1046/j.1471-4159.1995.65031411.x

Zhang, X. Y., Chen, L., Yang, Y., Xu, D. M., Zhang, S. R., Li, C. T., et al. (2014). Regulation of rotenone-induced microglial activation by 5-lipoxygenase and cysteinyl leukotriene receptor 1. *Brain Res.* 1572, 59–71. doi: 10.1016/j.brainres.2014.05.026

Zhou, P., Weng, R., Chen, Z., Wang, R., Zou, J., Liu, X., et al. (2016). TLR4 signaling in MPP^+-induced activation of BV-2 cells. *Neural Plast.* 2016:5076740. doi: 10.1155/2016/5076740

Conflict of Interest Statement: The authors declare that the research was conducted in the absence of any commercial or financial relationships that could be construed as a potential conflict of interest.